VOL. 694 NO. 1 3 MARCH 1995

**International Symposium on Molecular Chirality Kyoto, 24–27 May 1994**

JOURNAL OF

# CHROMATOGRAPHY A

## INCLUDING ELECTROPHORESIS AND OTHER SEPARATION METHODS



ELSEVIER

# JOURNAL OF CHROMATOGRAPHY A

INCLUDING ELECTROPHORESIS AND OTHER SEPARATION METHODS

**Scope.** The *Journal of Chromatography A* publishes papers on all aspects of **chromatography, electrophoresis** and related methods. Contributions consist mainly of research papers dealing with chromatographic theory, instrumental developments and their applications. In the *Symposium volumes*, which are under separate editorship, proceedings of symposia on chromatography, electrophoresis and related methods are published. *Journal of Chromatography B: Biomedical Applications* —This journal, which is under separate editorship, deals with the following aspects: developments in and applications of chromatographic and electrophoretic techniques related to clinical diagnosis or alterations during medical treatment; screening and profiling of body fluids or tissues related to the analysis of active substances and to metabolic disorders; drug level monitoring and pharmacokinetic studies; clinical toxicology; forensic medicine; veterinary medicine; occupational medicine; results from basic medical research with direct consequences in clinical practice.

**Submission of Papers.** The preferred medium of submission is on disk with accompanying manuscript (see *Electronic manuscripts* in the Instructions to Authors, which can be obtained from the publisher, Elsevier Science B.V., P.O. Box 330, 1000 AH Amsterdam, Netherlands). Manuscripts (in English; *four* copies are required) should be submitted to: Editorial Office of *Journal of Chromatography A*, P.O. Box 681, 1000 AR Amsterdam, Netherlands, Telefax (+31-20) 485 2304, or to: The Editor of *Journal of Chromatography B: Biomedical Applications*, P.O. Box 681, 1000 AR Amsterdam, Netherlands. Review articles are invited or proposed in writing to the Editors who welcome suggestions for subjects. An outline of the proposed review should first be forwarded to the Editors for preliminary discussion prior to preparation. Submission of an article is understood to imply that the article is original and unpublished and is not being considered for publication elsewhere. For copyright regulations, see below.

**Publication information.** *Journal of Chromatography A* (ISSN 0021-9673): for 1995 Vols. 683–714 are scheduled for publication. *Journal of Chromatography B: Biomedical Applications* (ISSN 0378-4347): for 1995 Vols. 663–674 are scheduled for publication. Subscription prices for *Journal of Chromatography A*, *Journal of Chromatography B: Biomedical Applications* or a combined subscription are available upon request from the publisher. Subscriptions are accepted on a prepaid basis only and are entered on a calendar year basis. Issues are sent by surface mail except to the following countries where air delivery via SAL is ensured: Argentina, Australia, Brazil, Canada, China, Hong Kong, India, Israel, Japan, Malaysia, Mexico, New Zealand, Pakistan, Singapore, South Africa, South Korea, Taiwan, Thailand, USA. For all other countries airmail rates are available upon request. Claims for missing issues must be made within six months of our publication (mailing) date. Please address all your requests regarding orders and subscription queries to: Elsevier Science B.V., Journal Department, P.O. Box 211, 1000 AE Amsterdam, Netherlands. Tel.: (+31-20) 485 3642; Fax: (+31-20) 485 3598. Customers in the USA and Canada wishing information on this and other Elsevier journals, please contact Journal Information Center, Elsevier Science Inc., 655 Avenue of the Americas, New York, NY 10010, USA, Tel. (+1-212) 633 3750, Telefax (+1-212) 633 3764.

**Abstracts/Contents Lists** published in Analytical Abstracts, Biochemical Abstracts, Biological Abstracts, Chemical Abstracts, Chemical Titles, Chromatography Abstracts, Current Awareness in Biological Sciences (CABS), Current Contents/Life Sciences, Current Contents/Physical, Chemical & Earth Sciences, Deep-Sea Research/Part B: Oceanographic Literature Review, Excerpta Medica, Index Medicus, Mass Spectrometry Bulletin, PASCAL-CNRS, Referativnyi Zhurnal, Research Alert and Science Citation Index.

**US Mailing Notice.** *Journal of Chromatography A* (ISSN 0021-9673) is published weekly (total 52 issues) by Elsevier Science B.V., (Sara Burgerhartstraat 25, P.O. Box 211, 1000 AE Amsterdam, Netherlands). Annual subscription price in the USA US$ 5389.00 (US$ price valid in North, Central and South America only) including air speed delivery. Second class postage paid at Jamaica, NY 11431. **USA POSTMASTERS**: Send address changes to *Journal of Chromatography A*, Publications Expediting, Inc., 200 Meacham Avenue, Elmont, NY 11003. Airfreight and mailing in the USA by Publications Expediting.

**See inside back cover** for Publication Schedule, Information for Authors and information on Advertisements.

---



0021-9673/95/$09.50



Printed in the Netherlands

---

**For Contents see p. VII.**

# Chiral HPLC Column

## Application Guide for Chiral HPLC Column Selection

## *SECOND EDITION!*

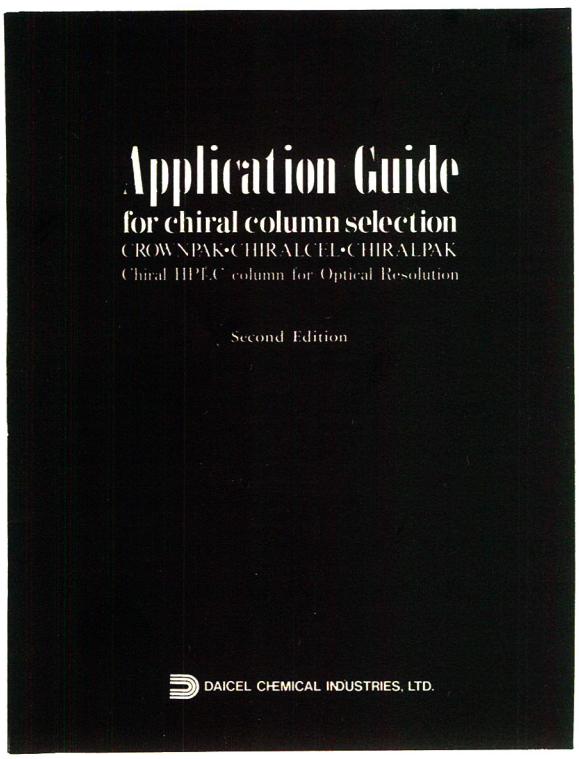


**FREE OF CHARGE**

**The 112-page green book contains chromatographic resolutions of over 350 chiral separations, cross-indexed by chemical compound class, structure, and the type of chiral column respectively. This book also lists chromatographic data together with analytical conditions and structural information. A quick reference guide for column selection from a wide range of DAICEL chiral HPLC columns is included.**

---

*To request this book, please let us know by fax or mail.*

## DAICEL CHEMICAL INDUSTRIES, LTD.


**AMERICA**

**CHIRAL TECHNOLOGIES, INC.**

730 Springdale Drive, P.O. Box 564
Exton, PA 19341
Phone: 800-624-4725
Facsimile: 610-594-2325

**EUROPE**

**DAICEL (EUROPA) GmbH**

Oststr. 22
D-40211 Düsseldorf, Germany
Phone: +49-211-369848
Facsimile: +49-211-364429

**ASIA/OCEANIA**

**DAICEL CHEMICAL INDUSTRIES, LTD.**
CHIRAL CHEMICALS NDD
8-1, Kasumigaseki 3-chome,
Chiyoda-ku, Tokyo 100, JAPAN
Phone: +81-3-3507-3151
Facsimile: +81-3-3507-3193

# FOR ADVERTISING INFORMATION PLEASE CONTACT OUR ADVERTISING REPRESENTATIVES

USA/CANADA

**Weston Media Associates**

Mr. Daniel S. Lipner
P.O. Box 1110, GREENS FARMS, CT 06436-1110
Tel: (203) 261-2500, Fax: (203) 261-0101

GREAT BRITAIN

**T.G. Scott & Son Ltd.**

Vanessa Bird
Portland House, 21 Narborough Road
COSBY, Leicestershire LE9 5TA
Tel: (0116) 2750.521, Fax: (0116) 2750-522

JAPAN

**ES - Tokyo Branch**

Ms. Noriko Kodama
20-12 Yushima, 3 chome, Bunkyo-Ku
TOKYO 113
Tel: (03) 3836 0810, Fax: (03) 3839-4344
Telex: 02657617


REST OF WORLD

**ELSEVIER SCIENCE**

Ms. W. van Cattenburch
Advertising Department
P.O.Box 211, 1000 AE AMSTERDAM
The Netherlands
Tel: (20) 485.3796, Fax: 485.3810



Please note our new phone & fax nos.!

JOURNAL OF CHROMATOGRAPHY A

VOL. 694 (1995)

# JOURNAL OF CHROMATOGRAPHY A

INCLUDING ELECTROPHORESIS AND OTHER SEPARATION METHODS



ELSEVIER

Amsterdam – Lausanne – New York – Oxford – Shannon – Tokyo

*J. Chromatogr. A*, Vol. 694 (1995)

*Katsura Imperial Villa, Kyoto*



0021-9673/95/$09.50

SYMPOSIUM VOLUME

# INTERNATIONAL SYMPOSIUM ON MOLECULAR CHIRALITY

*Kyoto (Japan), 24–27 May 1994*

*Guest Editors*


SHOJI HARA
(Tokyo, Japan)

TERUMICHI NAKAGAWA
(Kyoto, Japan)

SHIGERU TERABE
(Hyogo, Japan)

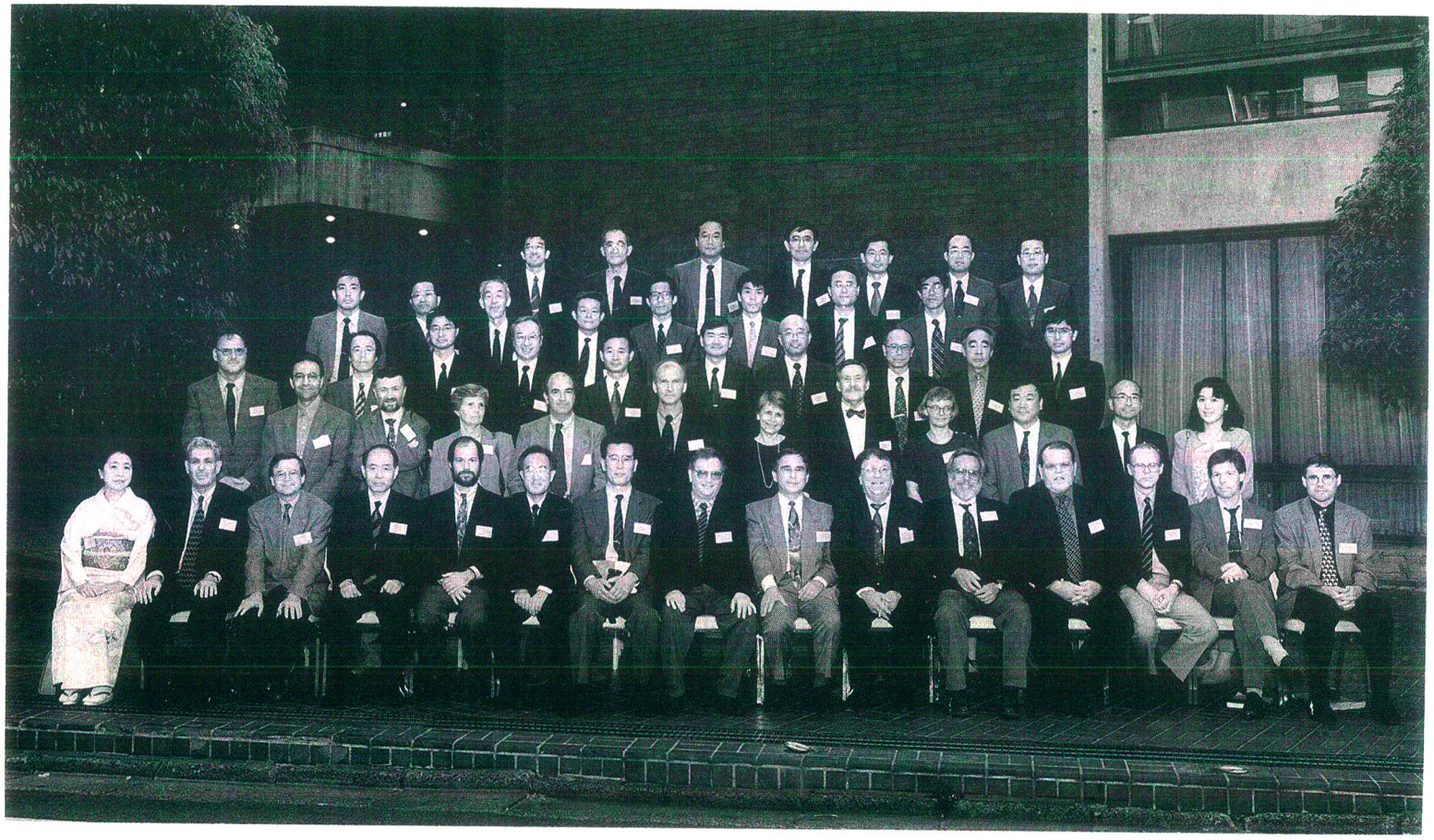

The International Advisory Board and Organizing Committee.

VOL. 694, NO. 1 JOURNAL OF CHROMATOGRAPHY A 3 MARCH 1995

# CONTENTS

*(Abstracts/Contents Lists published in Analytical Abstracts, Biochemical Abstracts, Biological Abstracts, Chemical Abstracts, Chemical Titles, Chromatography Abstracts, Current Awareness in Biological Sciences (CABS), Current Contents/Life Sciences, Current Contents/Physical, Chemical & Earth Sciences, Deep-Sea Research/Part B: Oceanographic Literature Review, Excerpta Medica, Index Medicus, Mass Spectrometry Bulletin, PASCAL-CNRS, Referativnyi Zhurnal, Research Alert and Science Citation Index)*

## INTERNATIONAL SYMPOSIUM ON MOLECULAR CHIRALITY, KYOTO, 24–27 MAY 1995



## GENERAL



## LIQUID CHROMATOGRAPHY

*Columns*

ELSEVIER

Journal of Chromatography A, 694 (1995) 1–2

JOURNAL OF CHROMATOGRAPHY A

# Foreword

The word "chiral" comes from the Greek word *cheir*, which means "hand". A pair of isomers representing mutual reflections are said to have handedness. They are optically active and are called "enantiomers". A mixture of equal parts of enantiomers, called a "racemate", obtained by some ordinary chemical reaction (in a non-chiral environment) from non-chiral precursors is optically inactive, because the rotation caused by a molecule of one enantiomer is neatly cancelled by the opposite rotation caused by a molecule of its antipode. In "asymmetric synthesis" a non-chiral compound can be converted into a chiral compound by the introduction of a chiral molecule.

The enantiomer ratio in the products of an asymmetric synthesis can be determined by measuring the optical rotation with a polarimeter and reference to optically pure standard material, but this is not sufficiently accurate. Chromatographic techniques based on chiral stationary phases have been developed, and this new methodology provides a high degree of accuracy for the measurement of "enantiomeric excess". Efforts have been directed towards finding new types of chiral stationary phases, based on stereochemical considerations and on the technical evolution of high-performance liquid chromatography. Systematic studies on chiral stationary phases for liquid chromatography began in 1979. A molecular design derived from hydrogen bond interactions, which is now widely used for chiral separations by liquid chromatography, gave the first successful results. Since then, extensive research soon established the superiority of the method of determining optical purity directly. Liquid chromatography is now accepted not only as a useful analytical method but also as an essential technology for preparative chiral separations.

Direct optical resolution by chromatography is associated with diastereomeric interactions between selector and selectand molecules. Thus, molecular complexes dynamically formed in chromatographic columns serve to produce a means for expressing the enantioselectivity of a system. In this respect, mechanistic considerations are indispensable for developing new chiral recognition systems. In recent years, capillary zone electrophoresis and micellar electrokinetic chromatography with chiral additives have become most important technologies for chiral separations. It should be stressed that the elucidation of chiral recognition phenomena is of cardinal interest in stereochemistry. The probing of chiral molecules is finding extensive use in studies of supramolecular chemistry.

The *Symposium on Molecular Chirality* was organized to integrate knowledge recently developed by using novel technologies, in particular chromatographic methods, for optical resolution and to exploit new functions of chiral molecules. The meeting was intitiated in 1992 in Tokyo by the Pharmaceutical Society of Japan to promote progress in the pharmaceutical sciences dealing with chiral drugs. It was held under the auspices of the Chemical Society of Japan and six additional scientific societies in Japan. In continuation of the second meeting, which took place in Tokyo in 1993, the third one was

*SSDI* 0021-9673(94)00961-9

expanded to an international scale and was held in Kyoto from 24 to 27 May 1994.

The *International Symposium on Molecular Chirality* opened with a session entitled: "International regulatory issues for chiral drugs". During the meeting, three plenary lectures and twenty-eight keynote lectures were presented by internationally recognized scientists. The scientific program included over 60 poster presentations. The contributions covered a wide range of scientific topics as follows: Generation of molecular chirality, Chiral discrimination and chiral separation, Crystal, surface and interfacial chirality, Functions of chiral compounds in chemistry, Dynamic aspects of chiral compounds in bio-systems, Drug metabolism, Pharmacokinetics and toxicokinetics, Stereochemical drug regulation and Industrial applications of molecular chirality.

More than 400 registered delegates attended. The symposium was preceded by a workshop for younger active scientists, entitled "Supramolecular Chemistry Basics for Probing Molecular Chirality". A social program was organized which brought the participants together in the evenings and gave them an opportunity to exchange information and ideas.

Kyoto was founded in 794 A.D. as *Heian-kyo –the Capital of Peace*. In 1994 the city celebrated its 1200th anniversary. Kyoto, the ancient capital of Japan, nestles among picturesque mountains and calm streams. There are hundreds of temples and shrines in Kyoto. With its innumerable cultural treasures and traditional crafts, Kyoto has always attracted both domestic and foreign visitors. The climate in May is mild and warm. We believe that the participants staying there had a pleasant time, enjoying both the historic traditions and the cultural atmosphere.

This proceedings volume collects review articles and original contributions presented at the symposium. We hope that the articles contributed to this issue will serve to promulgate the state of the art in this fast-growing area of research and to stimulate further progress in this new frontier of science. We look forward to the *4th National Meeting on Molecular Chirality*, to be held in May 1995 in Tokyo.

We would like to thank the international advisory boards and organizing committees for their kind suggestions and generous help. Special recognition is due to Dr. Erich Heftmann of the *Journal of Chromatography A* for serving as Editor of this volume.

*Tokyo, Japan* Shoji Hara

*Kyoto, Japan* Terumichi Nakagawa

*Hyogo, Japan* Shigeru Terabe

ELSEVIER

Journal of Chromatography A, 694 (1995) 3–13

JOURNAL OF CHROMATOGRAPHY A

Review

# Molecular imprinting used for chiral separations

Maria Kempe[1], Klaus Mosbach*

*Pure and Applied Biochemistry, Chemical Center, University of Lund, P.O. Box 124, S-221 00 Lund, Sweden*

**Abstract**

Molecular imprinting is a promising technique for the preparation of synthetic polymers of predetermined specificity. Functional monomers are copolymerized with crosslinkers in the presence of the desired molecule, the imprint molecule. The use of these polymers as chiral stationary phases is discussed. Other applications, such as antibody-mimics, enzyme-like catalysts and sensors, are also focused upon.

## Contents



## 1. Introduction

The idea to create a host, specific for a desired molecule, by coordinating the assembly of functional monomers around the molecule of interest (the imprint molecule) has been considered and discussed for quite some time. It is only recently, however, that the techniques required have been sufficiently developed to allow a realization of this dream [1]. Two essentially different approaches have been developed: covalent and non-covalent molecular imprinting. In both cases, the functional monomers, chosen so as to allow interactions with the functional groups of

* Corresponding author.
[1] Present address: Department of Chemistry, University of Minnesota, 207 Pleasant Street S.E., Minneapolis, MN 55455, USA.

0021-9673/95/$09.50 
*SSDI* 0021-9673(94)01070-6

the imprint molecule, are polymerized in the presence of the imprint molecule.

In the covalent approach, the imprint molecule is covalently coupled to a polymerizable molecule. After copolymerization with a crosslinker, the imprint molecule is chemically cleaved from the highly crosslinked polymer. The binding of this type of polymer relies on reversible covalent bonds. Covalent imprinting has been used in the preparation of polymers selective for derivatized and free sugars [2–4], glyceric acid and its derivatives [5–7], amino acids and amino acid derivatives [8–10], mandelic acid [11], aromatic ketones [12,13], dialdehydes [14], transferrin [15] and bis-NAD [16].

In the non-covalent approach, the imprint molecules are mixed with functional monomers capable of interacting non-covalently with the imprint molecules. The functional monomers are copolymerized with crosslinkers to yield a highly crosslinked and rigid polymer. The imprint molecules are subsequently removed from the polymer, leaving recognition sites complementary to the imprint species in shape and in the positioning of the functional groups. The recognition of the polymer constitutes an induced molecular memory, which makes the recognition sites capable of selectively recognizing the imprint species. The imprint molecules interact, during both the imprinting procedure and the rebinding, with the polymer via non-covalent interactions, e.g. ionic, hydrophobic and hydrogen bonding (Fig. 1). Non-covalent molecular imprinting has been applied to the preparation of polymers selective for dyes [15,17,18], diamines [17,19], vitamins [20], amino acid derivatives [21–44], peptides [33,44,45], β-adrenergic blockers [46], theophylline [47], diazepam [47], nucleotide bases [48] and naproxen [49]. A combination of covalent and non-covalent molecular imprinting has also been reported [50], where the monomers and the imprint molecules were covalently coupled during the polymerization, whereas the subsequent rebinding took place by non-covalent interactions.

Over a relatively short period, molecularly imprinted polymers (MIPs) have been developed for a broad range of potential applications. Three main areas can be foreseen for the MIPs: (i) as tailor-made separation materials, (ii) as

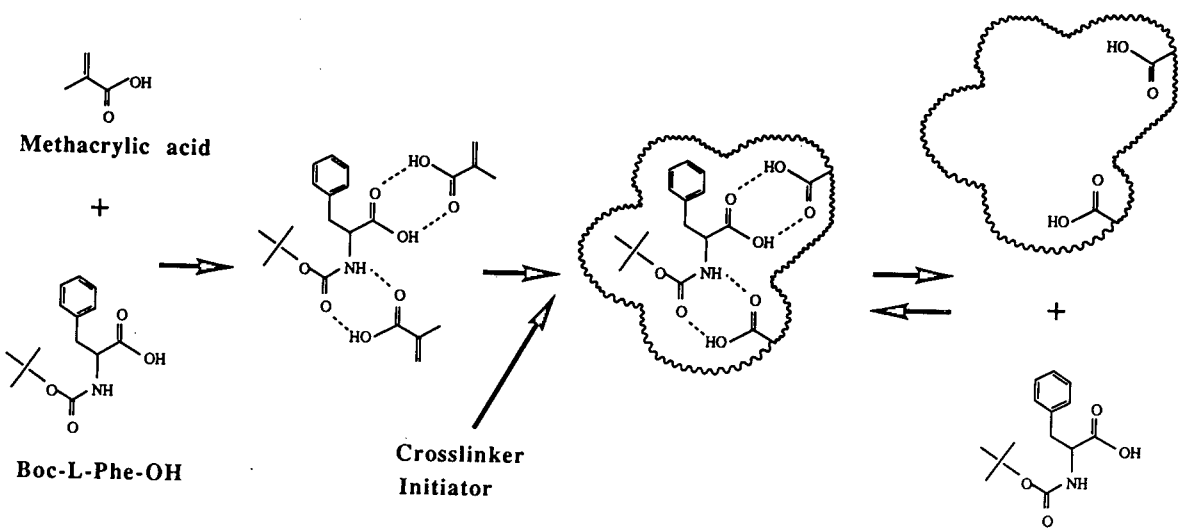


Fig. 1. Schematic representation of the concept of non-covalent molecular imprinting with an amino acid derivative (Boc-L-Phe-OH) as the imprint molecule and methacrylic acid as the functional monomer. Methacrylic acid interacts, via hydrogen bonds, with the carboxyl and carbamate functionalities of the imprint molecule. Crosslinker is added and the polymerization is initiated. The interactions are maintained in the rigid bulk polymer formed. The imprint molecule is extracted from the polymer, leaving a recognition site selective for the imprint molecule. The polymer is able to recognize and rebind the imprint molecule.

enzyme mimics or catalytically active polymers in enzyme technology and organic synthesis, and (iii) as sensors in biosensor-like configurations, whereby the polymers are used as substitutes for the biological materials normally employed. Most of the following examples are taken from work utilizing the non-covalent approach, as this seems to be a more direct approach for the applications to be discussed, especially those involving chiral separation. For more details on covalent imprinting we refer to reviews on this topic [51,52].

## 2. Molecularly imprinted separation materials

Molecular imprinting has become a simple and straightforward technique for preparing synthetic polymers of predetermined selectivity. Normally, the polymers are produced by bulk polymerization of a mixture of functional monomers and crosslinking monomers arranged around the imprint molecule, followed by grinding to particles and extraction of the imprint species. The particle size is usually in the 25 $\mu$m range, suitable for use as stationary phases in high-performance liquid chromatography (HPLC) [24–38,40,42–46,48,49] and thin-layer chromatography (TLC) [53]. Alternative approaches include the preparation of continuous polymer rods [41], the preparation of polymer beads by suspension polymerization and the preparation of composite materials, e.g. polymer-coated silica particles [15,18] and polymer beads grafted with imprinted polymers [54]. Figs. 2 and 3 show the functional monomers and the crosslinkers that have been utilized in non-covalent molecular imprinting.

A number of non-covalent molecularly imprinted copolymers have been reported (Table 1). The functional monomers were in general chosen so as to facilitate specific interactions

Table 1
Non-covalently molecularly imprinted polymers prepared by copolymerization of functional monomers and crosslinkers

| Functional monomer | Crosslinker | Ref. |
|---|---|---|
| Methyl methacrylate (**3**) | N,N′-Methylenediacrylamide (**11**), N,N′-phenylenediacrylamide (**12**), 3,5-bis(acryloylamido)benzoic acid (**13**) | [17] |
| Methyl methacrylate (**3**) | N,N′-Methylenediacrylamide (**11**), N,N′-phenylenediacrylamide (**12**) | [18] |
| *p*-Vinylbenzoic acid (**4**), ethylstyrene (**5**) | Divinylbenzene (**15**) | [21] |
| Acrylic acid (**1**) | Ethylene glycol dimethacrylate (**14**) | [21,41] |
| Acrylic acid (**1**) | N,O-Bisacryloyl-L-phenylalaninol (**16**) | [22] |
| Methacrylic acid (**2**) | Ethylene glycol dimethacrylate (**14**) | [24–39,42–47,53] |
| Itaconic acid (**6**) | Ethylene glycol dimethacrylate (**14**) | [46] |
| 2-Acrylamido-2-methyl-1-propane-sulphonic acid (**7**) | Ethylene glycol dimethacrylate (**14**) | [19] |
| Methacrylic acid (**2**) | Ethylene glycol dimethacrylate (**14**), N,N′-1,3-phenylene-diacrylamide | [48] |
| 1-Vinylimidazole (**8**) | Ethylene glycol dimethacrylate (**14**) | [40] |
| 4-Vinylpyridine (**9**) | Ethylene glycol dimethacrylate (**14**) | [40,49] |
| 2-Vinylpyridine (**10**) | Ethylene glycol dimethacrylate (**14**) | [42] |
| Methacrylic acid (**2**), 2-vinylpyridine (**10**) | Ethylene glycol dimethacrylate (**14**) | [42] |
| Methacrylic acid (**2**) | Trimethylolpropane trimethacrylate (**18**) | [44] |
| Methacrylic acid (**2**) | pentaerythritol triacrylate (**17**) | [44] |
| Methacrylic acid (**2**) | pentaerythritol tetraacrylate (**19**) | [44] |

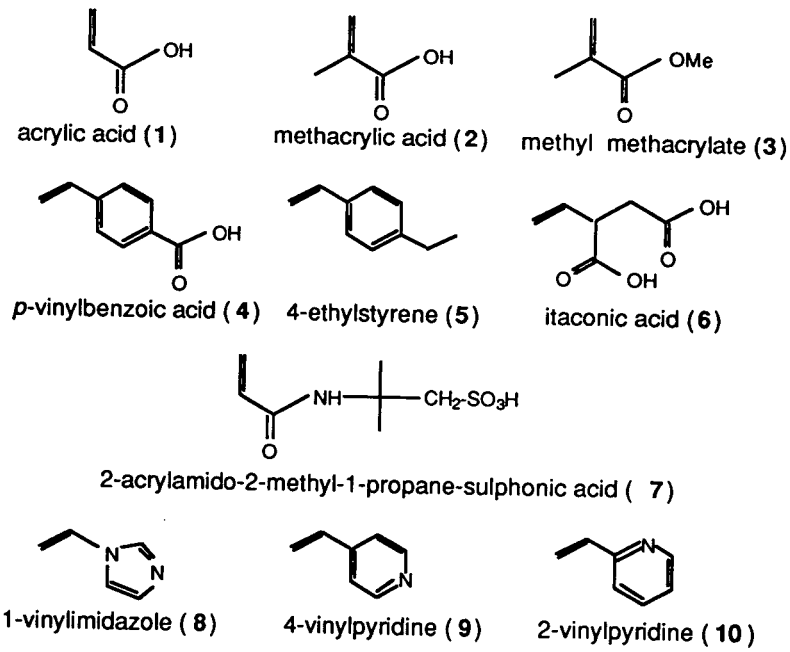


Fig. 2. Functional monomers used in non-covalent molecular imprinting.

with the functional groups of the imprint molecules. The most widely used functional monomer is methacrylic acid (MAA) (**2**, Fig. 2). It is assumed to interact via ionic interactions with amines and via hydrogen bonds with amides, carbamates and carboxyls.

The ionic interaction is stronger than the hydrogen bonding interaction, a fact which is reflected in better selectivities of polymers interacting with the imprint molecules via ionic bonds than of polymers interacting only via hydrogen bonds. The introduction of 4-vinylpyridine (**9**, Fig. 2) as a functional monomer in non-covalent MIPs made the ionic interactions possible between the recognition sites of the polymers and the imprint molecules containing the carboxyl functionality [40,49]. This resulted in better selectivities for such imprint species compared to the selectivities that have been achieved with polymers prepared with methacrylic acid [35]. The related monomer 2-vinylpyridine (**10**, Fig. 2) has also been shown to be useful for this purpose, either as sole functional monomer or in conjunction with methacrylic acid [42].

Ethylene glycol dimethacrylate (EDMA) (**14**, Fig. 3) has been extensively used as crosslinker in non-covalent MIPs. Recently, crosslinkers containing three or four vinyl groups have also been investigated [44]. Pentaerythritol triacrylate (PETRA) (**17**, Fig. 3) and trimethylolpropane trimethacrylate (TRIM) (**18**, Fig. 3), both being pentaerythritol derivatives with three vinyl groups, were shown to be superior to EDMA (**14**, Fig. 3), in that the resulting polymers exhibited better load capacities, selectivities and resolving capabilities when used as stationary phases in liquid chromatography.

### *2.1. Chiral separations*

More than half of all drugs on the market are asymmetric molecules [55]. Some 90% of these are administered as racemates. Since all biological systems in nature are based on optically active molecules (proteins, enzymes, receptors, sugars, etc.), it is no surprise that the two enantiomers of a racemic drug might interact with the biological system differently. One of the enantiomers may have pharmacologically different or unwanted side effects [56–58]. The same

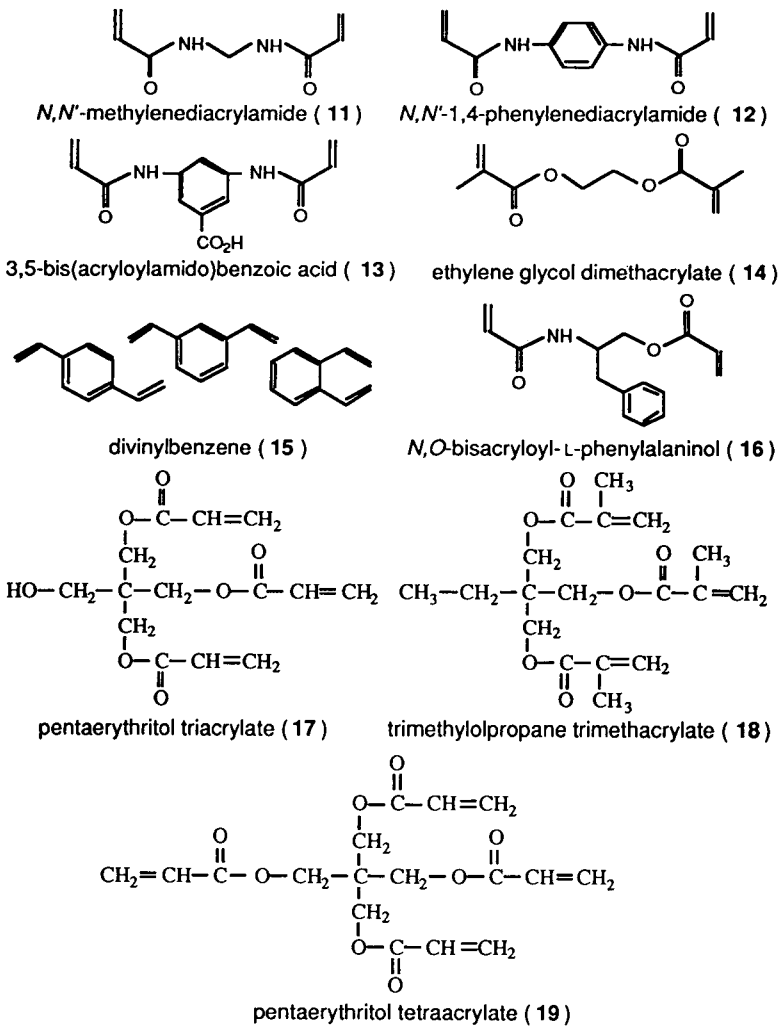


Fig. 3. Crosslinking monomers used in non-covalent molecular imprinting.

is true for racemic pesticides and herbicides; often only one of the enantiomers possesses the desired activity.

These facts moved the Food and Drug Administration in 1992 to issue a *Policy Statement for the Development of New Stereoisomeric Drugs*, stating that for every new racemic drug, the two enantiomers must be treated as separate substances in pharmacokinetic and toxicological profiling. The European Community has also recently issued statements about chiral active substances. This increasing demand for optically pure compounds has resulted in an interest in asymmetric synthesis and development of tools for efficient chiral separations. There is a need for both preparative methods to purify optically active compounds, as well as analytical methods to be able to perform pharmacokinetic studies and to control the enantiomeric excess and the optical purity of chiral precursors and final products of asymmetric syntheses.

Chiral separation by liquid chromatography is a widely studied area. Four main approaches have been developed: (i) derivatization with a

chiral reagent and separation of the resulting diastereomers on a non-chiral stationary phase, (ii) direct separation on a non-chiral stationary phase with the use of a chiral mobile phase additive, (iii) derivatization with a non-chiral reagent and separation on a chiral stationary phase (CSP) and (iv) direct separation on a CSP. The CSP consists of a chiral selector, sometimes immobilized to a stationary phase to improve its stability. A broad range of CSPs have been developed, e.g. the 'Blaschke-type CSPs' [59–61], the 'Pirkle-type CSPs' [62–64], polysaccharides, such as cellulose [65,66], amylose [67] and cyclodextrins [68,69], and immobilized proteins and enzymes [70–74].

With all due respect to the current methods for asymmetric synthesis, enzymatic resolution and techniques for the separation of enantiomers including the more traditional CSPs, the field of chirotechnology demands more. When an optically active compound is successfully imprinted, the polymer formed is able to discriminate between the imprint molecule and its antipode. Non-covalent MIPs have therefore proven useful as CSPs. We feel that the technique of molecular imprinting has a great potential in this context as the concept permits, at least in principle, the manufacturing of specific tailor-made polymers for a given separation process.

*2.1.1. Chromatographic conditions*

In general, the MIPs are packed into analytical HPLC columns. The applied flow-rates are in the range of 0.1–1.0 ml/min. The eluents, consisting of neat solvents or mixtures of solvents such as acetonitrile, chloroform and heptane, with or without added acetic acid, are chosen so as to give appropriate retentions. It is considered to be advantageous if the eluent is identical with the polymerization solvent, in order to resemble the conditions during the formation of the recognition sites as much as possible, but it is not a prerequisite. There are usually no chromatographic problems due to swelling or shrinking of the polymers when the eluents are changed, since the polymers are highly crosslinked. The elutions are generally performed at ambient temperature. In some cases, however, elevated temperatures have been applied [23,28].

*2.1.2. Load capacity*

Typically, the resolution of up to 500 $\mu$g of racemic amino acid derivatives or short peptides requires approximately 1 g of dry polymer. This is fine for analytical separations or if one wishes to carry out enantiopolishing on a commercial scale, i.e. the removal of small amounts of a contaminating optical isomer. Recently, however, we have developed a new polymer system in our laboratory which is superior to previously reported MIPs [44]. Considerably higher load capacities and selectivities were observed (1 mg of racemate per g polymer leading to baseline separation), making large-scale processes soon realistic.

*2.1.3. Column efficiency*

The last eluting peak, i.e. the enantiomer used as imprint molecule, is usually broadened due to tailing. This is likely due to the slow kinetics of the binding and the dissociation and to the fact that the recognition sites are heterogeneous. Some of the sites possess very good recognition for the imprint molecule, whereas others are less specific. The elution rate of the last eluting compound can, however, be enhanced with gradient elution, which results in sharper peaks [44].

It is important to have in mind that the polymer particles are prepared by grinding the bulk polymers. The particles are therefore highly irregular and not of uniform size, which also affects the column efficiency. New methods for the preparation of spherical beads of uniform size are, however, under development in our laboratory. This will most likely improve the column efficiency.

*2.1.4. Selectivity*

A characteristic feature of CSPs prepared by molecular imprinting is that the elution order of the enantiomers is easily predicted, because this is solely dependent on which enantiomer is used as imprint molecule. One is thus not confined to the trial and error approach inherent with the

old CSPs. This was demonstrated, for example, with copolymers of 4-vinylpyridine and ethylene glycol dimethacrylate imprinted with Z-aspartic acid [40]. When the imprint molecule was of L-configuration, the L-enantiomer was more retarded than the D-enantiomer, and vice versa when the imprint molecule was of D-configuration. In this context it should be mentioned that when the racemate was present during the polymerization, no chiral resolution could be achieved on the resulting polymer. Hence, the chiral information is introduced during the imprinting procedure and is not inherent to the polymer as such.

Chiral resolution of various racemic amino acid derivatives, peptides, other organic acids and some drugs has been studied on non-covalent molecularly imprinted stationary phases. Some examples are given in Table 2. The first reported drugs separated by this technique were β-blockers. For example, (*R,S*)-timolol was separated with baseline separation [46]. Another drug that was recently separated into its optical antipodes is naproxen, a non-steroidal anti-inflammatory drug (NSAID) [49].

In some cases, an extremely high selectivity for the imprint molecule was achieved. For example, racemic Z-aspartic acid, but not racemic Z-glutamic acid, was resolved on a Z-L-aspartic acid-imprinted 4-vinylpyridine–EDMA copolymer, and vice versa when a polymer imprinted with Z-L-glutamic acid was investigated [40]. Despite the small difference between Z-aspartic acid and Z-glutamic acid, the polymers were able to discriminate between these two species. The same high selectivity has also been shown on Z-L-aspartic acid- and Z-L-glutamic acid-imprinted methacrylic acid–EDMA copolymers [35].

High selectivity towards the imprint species was also observed on methacrylic acid–EDMA copolymers imprinted with some other $N^{\alpha}$-protected amino acids [43]. The resolving capabilities of various racemic $N^{\alpha}$-protected amino acids were tested and it was concluded that the separation factors were in all cases highest for the racemate of the molecule present during the polymerization. For example, separation of racemic Boc-phenylalanine, Fmoc-phenylalanine and Z-alanine on a Z-L-phenylalanine-imprinted CSP resulted in lower separation factors than when racemic Z-phenylalanine was separated.

Noteworthy are the recently reported extremely high separation factor (α) of 17.8 obtained for

Table 2
Chromatographic resolution on non-covalently molecularly imprinted CSPs (N.S. means not specified)

| Imprint molecule | α | $R_s$[a] | f/g[b] | Ref. |
|---|---|---|---|---|
| Z-L-Ala-OH | 1.93 | N.S. | N.S. | [43] |
| H-L-Arg-OEt | 1.5 | N.S. | N.S. | [32] |
| Z-L-Asp-OH | 2.81 | 1.22 | 0.81 | [40] |
| Z-L-Glu-OH | 2.45 | 3.10 | 1.00 | [44] |
| H-L-Leu-βNA | 3.8 | N.S. | N.S. | [33] |
| H-L-Phe-OEt | 1.3 | 0.3 | N.S. | [29] |
| H-L-*p*-$NH_2$Phe-OEt | 1.8 | 0.8 | N.S. | [29] |
| H-L-Phe-NHEt | 2.0 | 0.5 | N.S. | [29] |
| H-L-Phe-NHPh | 13 | N.S. | N.S. | [38] |
| H-L-*p*-$NH_2$Phe-NHPh | 8.38 | N.S. | N.S. | [31] |
| H-D-*p*-$NH_2$Phe-NHPh | 15 | N.S. | N.S. | [32] |
| H-L-Phe-NMePh | 2.03 | N.S. | N.S. | [30] |
| H-L-$Me_2$Phe-NHPh | 3.7 | N.S. | N.S. | [33] |
| Boc-L-Phe-OH | 2.14 | N.S. | N.S. | [36] |
| Dansyl-L-Phe-OH | 3.15 | 1.6 | 0.96 | [42] |
| Fmoc-L-Phe-OH | 1.36 | N.S. | N.S. | [43] |
| Z-L-Phe-OH | 2.29 | 3.14 | 1.00 | [44] |
| Boc-L-Phe-NHPh | 2.95 | N.S. | N.S. | [43] |
| Pyridoxyl-L-Phe-NHPh | 2.50 | N.S. | N.S. | [87] |
| Pyridylmethyl-L-Phe-NHPh | 8.4 | N.S. | N.S. | [33] |
| H-L-Pro-NHPh | 4.5 | N.S. | N.S. | [33] |
| Boc-L-Pro-OSu | 1.25 | 0.8 | N.S. | [35] |
| H-L-Trp-OEt | 1.8 | 0.5 | N.S. | [29] |
| Ac-D-Trp-OMe | 3.92 | 2.2 | 1.0 | [42] |
| Boc-L-Trp-OH | 4.35 | 1.9 | 1.0 | [42] |
| Z-L-Trp-OH | 1.67 | 0.1 | N.S. | [35] |
| Z-L-Trp-OMe | 1.28 | 0.2 | N.S. | [35] |
| Z-L-Tyr-OH | 2.86 | 5.47 | 1.00 | [44] |
| H-L-Phe-Gly-NHPh | 5.1 | N.S. | N.S. | [33] |
| Boc-L-Phe-Gly-OEt | 3.04 | 3.44 | 1.00 | [44] |
| Z-L-Ala-L-Ala-OMe | 3.19 | 4.50 | 1.00 | [44] |
| Ac-L-Phe-L-Trp-OMe | 17.8 | N.S. | 1.00 | [45] |
| Z-L-Ala-Gly-L-Phe-OMe | 3.60 | 4.15 | 1.00 | [44] |
| (*S*)-(−)-timolol | 2.9 | 2.0 | N.S. | [46] |
| (*S*)-naproxen | 1.65 | N.S. | 0.83 | [49] |
| (*R*)-phenylsuccinic acid | 3.61 | 2.0 | 1.0 | [42] |
| L-mandelic acid | 1.41 | N.S. | 0.70 | [40] |

[a] The resolution factors ($R_s$) were calculated according to Ref. [85].
[b] The resolution factors (*f/g*) were calculated according to Ref. [86].

the racemic system of Ac–Phe–Trp–OMe [45] and the high resolution factors obtained when various racemic amino acid derivatives and peptides were resolved [44].

### 2.2. Separation of macromolecules

Most imprinting studies, involving both the imprinting and the separation steps, have been performed in organic solvents. Efforts are now being made to accomplish this also in aqueous systems. Likewise, the majority of imprinting studies have been carried out with small molecules. An important extension would be the use of macromolecules such as proteins, an area of increasing interest in the scientific community. For these studies we use a variant of molecular imprinting which we have named surface imprinting [75,76].

## 3. Other areas of application

### 3.1. Antibody mimics

Another area for which imprints have been tested is their suitability as antibody mimics. Imprints against the bronchodilating drug theophylline and against the tranquillizer diazepam have shown astonishingly specific recognition. In fact, when these MIPs were tested in competitive radioimmuno-style assays, their recognition of related structures was either non-existent or far below that of the original imprint molecule [47,77]. Amazingly, the cross-reactivity profiles of these MIPs were practically identical to those reported for monoclonal antibodies against these drugs. The anti-theophylline MIPs were used for the determination of theophylline concentrations in patient serum samples, pointing towards their use as stable alternatives to antibodies in conventional immunoassays. The measured dissociation constants were in the micromolar range. Some of our more recent studies have involved the successful preparation of imprints against morphine and Leu-enkephalin, leading to what could be considered as an artificial opioid receptor. It will be interesting to study and compare molecular recognition in these receptor binding site mimics.

### 3.2. Enzyme mimics

Scientists have long attempted to create synthetic polymers with enzyme-like properties, i.e. polymers expressing substrate-selective catalytic behaviour, although progress until now has been extremely modest. In light of the impressive results obtained in mimicking enzyme and antibody binding sites by molecular imprinting, an obvious extension would be to utilize the same technique to develop polymer systems possessing various catalytic functionalities in the binding sites [78,79]. In one of the earliest studies on this topic (in parallel with the ongoing work on catalytically active antibodies [80]), imprints were prepared against a transition-state analogue. A polymer was prepared with sites selective for *p*-nitrophenol methylphosphonate, a transition-state analogue for the hydrolysis of *p*-nitrophenyl acetate [78]. The MIP demonstrated preferential binding of the transition-state analogue and induced a small increase in the rate of hydrolysis of *p*-nitrophenyl acetate to *p*-nitrophenol and acetate. This rate enhancement was specifically inhibited by the transition-state analogue, providing evidence that the catalysis achieved was taking place in the sites selective for the transition state analogue.

Attempts to direct organic reactions using MIPs are obviously related in nature to the more enzyme-like systems described above. The most impressive study to date, in terms of mediating reaction selectivity, demonstrated the selective reduction of a 3,17-diketo steroid. In this case, the reaction could be directed, almost exclusively, to reduction at a predetermined keto group on the steroid. A reactive $LiAlH_2$ group was selectively positioned in the surrounding imprinted polymer, thus leaving the other keto group unreduced [81].

More recently, efforts in two laboratories [82,83] have led to the development of polymer systems showing modest catalytic activity for the $\beta$-elimination of HF from 4-fluoro-4(*p*-nitrophenyl)-2-butanone. In one system [82], a car-

boxylic group was positioned opposite to the fluorine. This was achieved by imprinting with a corresponding molecule containing a base, in order to direct the positioning of the carboxylic group in the active site. This is similar to the studies on catalytic antibodies in which aspartate and glutamate residues in the antibody combining sites were aligned to catalyze the elimination of HF from a $\beta$-fluoroketone by abstraction of an $\alpha$-carbon proton [88]. We believe that the complementarity obtained allows the negatively charged carboxylate monomer residue to function as a general base.

In summary, the results obtained so far from catalytically active polymers are modest. However, the stability of such preparations, along with the possibility of introducing totally new catalytic properties, suggests this as an area worthy of intense effort [84]. The chance of success utilizing the imprint as a model for directing catalytic stereo- and regioselective reactions is not too remote. It is quite conceivable that with such catalytic systems chiral discriminations might be achieved.

### 3.3. Substrate-selective sensors

With the refinement of molecular imprinting as demonstrated in the successful chiral separation of compounds or in the preparation of antibody or receptor binding-site mimics, an obvious additional application would be the use of such substrate-selective polymers as sensor components. Despite the current wide range of biosensor applications, there is much room for improvement. On substituting the bio-part in an enzyme or antibody-based sensor with catalytically active or ligand-specific polymers prepared from specific molecular imprints, a more robust sensing element system would be obtained. Furthermore, in many cases no suitable biomolecule is available and it is here that molecular imprinting has its great potential, namely creating the custom-tailored binding site for a given molecule. Work in this area has recently begun to show success, and only few published data are available. In one example, a separation process differentiated optical isomers of amino acid derivatives on a column containing molecular imprints made against one enantiomer using streaming potential measurements [34]. Finally, in studies using imprinted polymer membranes as a sensing layer in a field effect device, a lowering of the capacitance was observed on specific binding of the original imprint molecule [39].

All these studies are preliminary but there is no doubt that we will see, in the near future, many such sensoring systems utilizing synthetic binding sites. The systems discussed above can also be considered as high-specificity chemical sensors. The potential for such devices as a kind of artificial nose in single- and multiple-compound determinations appears promising and should constitute a valuable extension to existing chemical and bio-sensor systems.

## 4. Concluding remarks

We believe that the possibility of making stereospecific polymers by the technique of molecular imprinting will be extended further and find increasing application. The remarkable stability of the acrylic polymers, expressing unimpaired molecular memory after repeated use (100-fold) and over extended periods of time (several years), strongly support this notion.

## References

[1] K. Mosbach, *Trends Biochem. Sci.*, 19 (1994) 9.
[2] G. Wulff, A. Sarhan and K. Zabrocki, *Tetrahedron Lett.*, (1973) 4329.
[3] G. Wulff and S. Schauhoff, *J. Org. Chem.*, 56 (1991) 395.
[4] G. Wulff and J. Haarer, *Makromol. Chem.*, 192 (1991) 1329.
[5] G. Wulff, A. Sarhan, J. Gimpel and E. Lohmar, *Chem. Ber.*, 107 (1974) 3364.
[6] G. Wulff and E. Lohmar, *Isr. J. Chem.*, 18 (1979) 279.
[7] A. Sarhan and G. Wulff, *Makromol. Chem.*, 183 (1982) 85.
[8] J. Damen and D.C. Neckers, *Tetrahedron Lett.*, 21 (1980) 1913.
[9] G. Wulff, W. Best and A. Akelah, *Reactive Polymers*, 2 (1984) 167.

[10] G. Wulff and J. Vietmeier, *Makromol. Chem.*, 190 (1989) 1717.
[11] A. Sarhan, *Makromol. Chem. Rapid Commun.*, 3 (1982) 489.
[12] K.J. Shea and T.K. Dougherty, *J. Am. Chem. Soc.*, 108 (1986) 1091.
[13] K.J. Shea and D.Y. Sasaki, *J. Am. Chem. Soc.*, 111 (1989) 3442.
[14] G. Wulff, B. Heide and G. Helfmeier, *J. Am. Chem. Soc.*, 108 (1986) 1089.
[15] M. Glad, O. Norrlöw, B. Sellergren, N. Siegbahn and K. Mosbach, *J. Chromatogr.*, 347 (1985) 11.
[16] O. Norrlöw, M.-O. Månsson and K. Mosbach, *J. Chromatogr.*, 396 (1987) 374.
[17] R. Arshady and K. Mosbach, *Makromol. Chem.*, 182 (1981) 687.
[18] O. Norrlöw, M. Glad and K. Mosbach, *J. Chromatogr.*, 299 (1984) 29.
[19] I.R. Dunkin, J. Lenfeld and D.C. Sherrington, *Polymer*, 34 (1993) 77.
[20] L.I. Andersson, C.F. Mandenius and K. Mosbach, *Tetrahedron Lett.*, 29 (1988) 5437.
[21] L. Andersson, B. Sellergren and K. Mosbach, *Tetrahedron Lett.*, 25 (1984) 5211.
[22] L. Andersson, B. Ekberg and K. Mosbach, *Tetrahedron Lett.*, 26 (1985) 3623.
[23] B. Sellergren, B. Ekberg and K. Mosbach, *J. Chromatogr.*, 347 (1985) 1.
[24] B. Sellergren, M. Lepistö and K. Mosbach, *J. Am. Chem. Soc.*, 110 (1988) 5853.
[25] D.J. O'Shannessy, B. Ekberg and K. Mosbach, *Anal. Biochem.*, 177 (1989) 144.
[26] D.J. O'Shannessy, L.I. Andersson and K. Mosbach, *J. Mol. Recogn.*, 2 (1989) 1.
[27] D.J. O'Shannessy, B. Ekberg, L.I. Andersson and K. Mosbach, *J. Chromatogr.*, 470 (1989) 391.
[28] B. Sellergren, *Makromol. Chem.*, 190 (1989) 2703.
[29] B. Sellergren, *Chirality*, 1 (1989) 63.
[30] M. Lepistö and B. Sellergren, *J. Org. Chem.*, 54 (1989) 6010.
[31] A. Moradian and K. Mosbach, *J. Mol. Recogn.*, 2 (1989) 167.
[32] B. Sellergren and K. Nilsson, *Methods Mol. Cell. Biol.*, 1 (1989) 59.
[33] L.I. Andersson, D.J. O'Shannessy and K. Mosbach, *J. Chromatogr.*, 513 (1990) 167.
[34] L.I. Andersson, A. Miyabayashi, D.J. O'Shannessy and K. Mosbach, *J. Chromatogr.*, 516 (1990) 323.
[35] L.I. Andersson and K. Mosbach, *J. Chromatogr.*, 516 (1990) 313.
[36] M. Kempe and K. Mosbach, *Anal. Lett.*, 24 (1991) 1137.
[37] B. Sellergren and K.J. Shea, *J. Chromatogr.*, 635 (1993) 31.
[38] B. Sellergren and K.J. Shea, *J. Chromatogr. A*, 654 (1993) 17.
[39] E. Hedborg, F. Winquist, I. Lundström, L.I. Andersson and K. Mosbach, *Sens. Act. A*, 37-38 (1993) 796.
[40] M. Kempe, L. Fischer and K. Mosbach, *J. Mol. Recogn.*, 6 (1993) 25.
[41] J. Matsui, T. Kato, T. Takeuchi, M. Suzuki, K. Yokoyama, E. Tamiya and I. Karube, *Anal. Chem.*, 65 (1993) 2223.
[42] O. Ramström, L.I. Andersson and K. Mosbach, *J. Org. Chem.*, 58 (1993) 7562.
[43] M. Kempe and K. Mosbach, *Int. J. Pept. Prot. Res.*, (1994) in press.
[44] M. Kempe, *Chiral Recognition. Studies on Chiral Discrimination in Enzymatic Peptide Synthesis and Noncovalent Molecular Imprinting*, Doctoral thesis, University of Lund, Lund, 1994.
[45] O. Ramström, I.A. Nicholls and K. Mosbach, *Tetrahedron: Asymmetry*, 5 (1994) 649.
[46] L. Fischer, R. Müller, B. Ekberg and K. Mosbach, *J. Am. Chem. Soc.*, 113 (1991) 9358.
[47] G. Vlatakis, L.I. Andersson, R. Müller and K. Mosbach, *Nature*, 361 (1993) 645.
[48] K.J. Shea, D.A. Spivak and B. Sellergren, *J. Am. Chem. Soc.*, 115 (1993) 3368.
[49] M. Kempe and K. Mosbach, *J. Chromatogr. A*, 664 (1994) 276.
[50] B. Sellergren and L. Andersson, *J. Org. Chem.*, 55 (1990) 3381.
[51] G. Wulff, in W.T. Ford (Editor), *Polymeric Reagents and Catalysts* (*ACS Symposium Series*, No. 308), American Chemical Society, Washington DC, 1986, p. 186.
[52] G. Wulff, *Trends Biotechnol.*, 11 (1993) 85.
[53] D. Kriz, C. Berggren Kriz, L.I. Andersson and K. Mosbach, *Anal. Chem.*, 66 (1994) 2636.
[54] M. Glad, P. Reinholdsson and K. Mosbach, (1994) submitted for publication.
[55] S.C. Stinson, *Chem. Eng. News*, September 27 (1993) 38.
[56] D.E. Drayer, in I.W. Wainer and D.E. Drayer (Editors), *Drug Stereochemistry. Analytical Methods and Pharmacology*, Marcel Dekker, New York, 1988, p. 209.
[57] W.E. Müller, in I.W. Wainer and D.E. Drayer (Editors), *Drug Stereochemistry. Analytical Methods and Pharmacology*, Marcel Dekker, New York, 1988, p.227.
[58] J.R. Powell, J.J. Ambre and T.I. Ruo, in I.W. Wainer and D.E. Drayer (Editors), *Drug Stereochemistry. Analytical Methods and Pharmacology*, Marcel Dekker, New York, 1988, p. 245.
[59] G. Blaschke, *J. Liq. Chromatogr.*, 9 (1986) 341.
[60] G. Blaschke and J. Maibaum, *J. Chromatogr.*, 366 (1986) 329.
[61] G. Blaschke, W. Bröker and W. Fraenkel, *Angew. Chem. Int. Ed. Engl.*, 25 (1986) 830.
[62] W.H. Pirkle, D.W. House and J.M. Finn, *J. Chromatogr.*, 192 (1980) 143.
[63] W.H. Pirkle, T.C. Pochapsky, G.S. Mahler, D.E. Corey, D.S. Reno and D.M. Alessi, *J. Org. Chem.*, 51 (1986) 4991.
[64] W.H. Pirkle and J.E. McCune, *J. Chromatogr.*, 471 (1989) 271.

[65] T. Shibata, I. Okamoto and K. Ishii, *J. Liq. Chromatogr.*, 9 (1986) 313.
[66] F. Westhoff and G. Blaschke, *J. Chromatogr.*, 578 (1992) 265.
[67] Th. Hollenhorst and G. Blaschke, *J. Chromatogr.*, 585 (1991) 329.
[68] K. Fujimura, M. Kitagawa, H. Takayanagi and T. Ando, *J. Liq. Chromatogr.*, 9 (1986) 607.
[69] T.J. Ward and D.W. Armstrong, *J. Liq. Chromatogr.*, 9 (1986) 407.
[70] S. Allenmark, *J. Liq. Chromatogr.*, 9 (1986) 425.
[71] H. Fieger and G. Blaschke, *J. Chromatogr.*, 575 (1992) 255.
[72] I. Marle, P. Erlandsson, L. Hansson, R. Isaksson and G. Pettersson, *J. Chromatogr.*, 586 (1991) 233.
[73] S. Thelohan, Ph. Jadaud and I.W. Wainer, *Chromatographia*, 28 (1989) 551.
[74] P. Jadaud, S. Thelohan, G.R. Schonbaum and I.W. Wainer, *Chirality*, 1 (1989) 38.
[75] M. Glad, M. Kempe and K. Mosbach, Patent application PCT/SE92/00610 (1992).
[76] M. Kempe, M. Glad and K. Mosbach, *J. Mol. Recogn.*, (1994) in press.
[77] K. Mosbach, *US Pat.*, 5 110 833.
[78] D.K. Robinson and K. Mosbach, *J. Chem. Soc., Chem. Commun.*, 14 (1989) 969.
[79] A. Leonhardt and K. Mosbach, *React. Polym.*, 6 (1987) 285.
[80] R. Lerner, S.J. Benkovic and P.G. Schultz, *Science*, 252 (1991) 659.
[81] S.E. Byström, A. Börje and B. Åkermark, *J. Am. Chem. Soc.*, 115 (1993) 2081.
[82] R. Müller, L.I. Andersson and K. Mosbach, *Makromol. Chem. Rapid Commun.*, 14 (1993) 637.
[83] J.V. Beach and K.J. Shea, *J. Am. Chem. Soc.*, 116 (1994) 379.
[84] K. Mosbach, I.A. Nicholls and O. Ramström, *Swedish Pat.*, Appl. No. 92-30914-0 (1992).
[85] G. Wulff, H.-G. Poll and M. Minarik, *J. Liq. Chromatogr.*, 9 (1986) 385.
[86] V.R. Meyer, *Chromatographia* 24 (1987) 639.
[87] L.I. Andersson and K. Mosbach, *Makromol. Chem. Rapid Commun.*, 10 (1989) 491.
[88] K.M. Shokat, C.J. Leumann, R. Sugasawara and P.G. Schultz, *Nature*, 338 (1989) 269.

ELSEVIER

Journal of Chromatography A, 694 (1995) 15–37

JOURNAL OF CHROMATOGRAPHY A

Review

# Theoretical studies of type II–V chiral stationary phases

Kenny B. Lipkowitz

*Department of Chemistry, Indiana University–Purdue University Indianapolis, Indianapolis, IN 46202-3274, USA*

**Abstract**

A review of atomic-level molecular modeling in chiral chromatography is given. The focus of this review is on non-brush-like stationary phases with emphasis on cyclodextrin and cellulosic stationary phases. Most of the theoretical papers reviewed invoke regression models to understand where and how chiral discrimination takes place.

## Contents



## 1. Introduction

Separation scientists have long been interested in resolving enantiomers without having to prepare diastereomers as intermediates. This concept of direct enantiomer separation by using chiral mobile or stationary phases has, until recently, eluded the separation scientist. During the last decade, however, advances in both the science and technology of direct enantiomer resolution have been made, and one can now routinely separate a wide range of enantiomers [1–9]. Understanding where and how chiral selection takes place in chromatography is important because it allows one to design improved chromatographic systems and it addresses fundamental concepts in chiral recognition for disciplines outside separation science. Although the intermolecular forces (hydrogen bonding, multipolar association, dispersion forces, charge-

0021-9673/95/$09.50 
*SSDI* 0021-9673(94)00956-2

transfer complexation, hydrophobic association, etc.) have been thoroughly studied and are well documented, precisely how these forces work in concert to promote binding is not clear. Indeed, a major effort made by research scientists in the past decade has been in the area of molecular recognition, where the goals have been to sort out how substrates bind to natural and non-natural receptors [10]. One of the difficulties in understanding how chiral recognition takes place is that the forces responsible for one enantiomer binding to a chiral surface are the same as those for its optical antipode. What one would like to have, then, is a method that allows us not only to determine which forces are at play, but also to quantitate them so that differences between mirror image isomers can be assessed. One approach that shows promise in this regard is computational chemistry [11].

In this paper, we review computational approaches that have been applied toward understanding where and how chiral recognition takes place on type II–V chiral stationary phases (CSPs). This is a follow-up to a previous review on the molecular modeling done on type I or brush-type chiral stationary phases [12]. Wainer [13] categorizes existing HPLC CSPs as follows:

*Type I.* Where the solute–CSP complexes are formed by attractive interactions, hydrogen bonding, $\pi-\pi$ interactions, dipole stacking, etc., between the solute and CSP.

*Type II.* Where the primary mechanism for the formation of the solute–CSP complex is through attractive interactions, but where inclusion complexes also play an important role.

*Type III.* Where the solute enters into chiral cavities within the CSP to form inclusion complexes.

*Type IV.* Where the solute is part of a diastereomeric metal complex (chiral ligand-exchange chromatography).

*Type V.* Where the CSP is a protein and the solute–CSP complexes are based on combinations of hydrophobic and polar interactions.

The major difference between the first three categories, irrespective of the type of intermolecular attractions, is the extent of inclusion. Type I has no inclusion complexation, type II has partial inclusion and type III uses as the "primary mechanism" inclusion complexation. For this review, a greater line of demarcation between type II and type III CSPs is created by considering type III to be exclusively guest–host complexes as found in crown ethers, cyclodextrins and related systems, whereas type II uses only partial guest–host complexation. Hence, whereas Wainer considers polymethacrylate polymers and microcrystalline cellulose triacetate as type III CSPs, we shall consider them as type II along with the other cellulose-based CSPs.

## 2. Molecular modeling

A model is a representation of reality. It is a likeness or a semblance, and means different things to different people. There are two categories of chemical models: macroscopic and microscopic. Macroscopic models describe coarse-grain features of a system or process. They consider, e.g., relative rates of uptake, kinetics of transport and rates of depletion of entities involved in a process without consideration of structural features of the individual molecules. Microscopic models, sometimes called atomistic models, usually take full account of all the atoms in the system.

Microscopic, atomistic modeling is done in two ways: using fitting procedures or applying theory. The fitting procedures are an attempt to rationalize connections between molecular structure and physico-chemical properties (quantitative structure–property relationships, QSPR) or with biological response (quantitative structure–activity relationships, QSAR). Usually the response is regressed onto a set of molecular descriptors, e.g., $\log (1/C) = b_0 + \Sigma_i b_i D_i$, where $C$ is the concentration of a compound needed to elicit a response, $b_0$ is a constant, $b_i$ are the least-squares multiple regression coefficients and $D_i$ are molecular descriptors. One can very accurately predict an unknown molecule's property or anticipated response by computing its molecular descriptors and substituting those values into the model. There are no rules about what kind of descriptors are to be used, but

descriptors often include information about molecular size and shape, electronic effects and lipophilicity. This type of modeling requires the use of existing data to create the model and then allows one to interpolate or extrapolate new properties/activities of as yet unknown molecules within that same class of compounds. QSARs and QSPRs have been a major influence on the design of drugs and materials.

The second kind of atomistic, molecular modeling applies theory. The major tools implemented are as follows.

### 2.1. Quantum mechanics (QM)

The objective of quantum mechanics is to describe the spatial positions of electrons and nuclei. Most commonly implemented is the molecular orbital theory (MOT), where electrons are allowed to flow around fixed nuclei until they reach a self-consistent field (SCF). This is where the attractive and repulsive forces of all particles are in a steady state. The nuclei are iteratively moved followed by SCF calculations until the energy can go no lower. This is called energy minimization or geometry optimization and allows one to predict structural and electronic features of molecules.

### 2.2. Molecular mechanics (MM)

Molecular mechanics is a non-quantum mechanical method of computing structures, energies and some properties of molecules. Molecular mechanics uses an empirical force field (EFF), which is a recipe for reproducing a molecule's potential energy surface (the location and motion of nuclei on such surfaces dictate a molecule's structure and dynamic properties). A molecule is viewed as a collection of particles (nuclei) held together by elastic forces (electrons). These forces are defined in terms of potential energy functions of internal coordinates such as bond lengths, bond angles and torsion angles. Once all the potential functions and associated force constants have been determined, the internal energy is minimized by moving the particles toward their equilibrium positions (geometry optimization). Since EFFs treat electrons implicitly rather than explicitly, molecular mechanics is much faster than quantum mechanics.

### 2.3. Molecular dynamics (MD)

In molecular dynamics the motion of atoms is described by Newtonian laws: $F_i(t) = m_i a_i = m_i \partial^2 r_i(t)/\partial t^2$, where $F_i(t)$, $a_i(t)$ and $r_i(t)$ are the force, acceleration and position of atom $i$ at time $t$, respectively. The force on atom $i$ is the negative gradient of the potential function which is obtained from the same EFF as used in molecular mechanics. To integrate the equations of motion, position vectors are determined using these forces and the previous positions of atoms. From this, atom velocities and temperature are evaluated. With these ingredients a trajectory, which is a history of the motion of the system over the time period of interest, can be generated. Simulation time periods are typically in the picosecond ($10^{-12}$ s) range, so that only very fast processes such as low-energy bond rotations can be studied.

### 2.4. Monte Carlo simulations (MC)

This method uses the same EFFs as in MM and MD. One starts with a collection of particles and computes the system's energy, $E_1$, for that initial configuration. One or more of the particles is then randomly moved to create a second configuration. The energy of this configuration, $E_2$, is computed and that new configuration is deemed "acceptable" if $E_2 < E_1$ or $E_2 > E_1$ with some probability, $p = \exp[(E_2 - E_1)/kT]$. A large number of energetically feasible states are thus obtained, providing averaged energies or properties. A common application is in the assessment of the distribution of solvent molecules around solutes in solvation studies.

### 2.5. Molecular graphics

QM, MM, MD and MC calculations all generate enormous quantities of data; graphics or visualization methods render the data manage-

able and assimilable. The pictures may be graphs or simple chemical structures or they may be highlighted, three-dimensional images emphasizing structural, electronic or reactivity features of interest. With cleverness, four or five attributes of the system can be shown in a single image. Motion pictures can be created to illustrate dynamic processes. Molecular graphics temporarily uncouples the scientist from the underlying theories and equations being implemented so as to focus on the science at hand. It is an aid that helps the chemist to perceive relationships more easily and is now a standard feature of most computational programs.

Most of the molecular modeling tools are themselves models, often used in tandem to compute structures, energies and properties of molecules. Such tools along with statistics programs, relational databases and other methods for generating data are fully integrated into sophisticated molecular modeling programs. These modeling programs allow one to put together bits and pieces of seemingly unrelated, atomic-level data and create a simplified view of reality that has predictive power. This simplified representation is a molecular model and the act of creating such models is molecular modeling. Applications of molecular modeling to discern where and how chiral discrimination takes place on Type II–V CSPs are now considered.

## 3. Type II CSPs

The first application of atomistic molecular modeling in the area of chiral chromatography was carried out by Weinstein et al. [14]. Earlier, chiral secondary amides (**1**) were found to be suitable chiral stationary phases in gas–liquid chromatography [15]. To begin rationalizing how this melt acted as a CSP, especially for (*R*)-N-lauroyl-α-(1-naphthyl)ethylamine, Gil-Av's chromatography group began working with Leiserowitz' crystallography group to carry out a series of X-ray crystallographic studies on the molecular packing modes of mono-N-substituted primary amides [16].

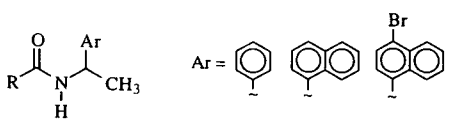


**1**

R = –$CH_3$, $CF_3$, *n*-$C_3H_7$, *n*-$C_{11}H_{23}$, *tert.*-Bu

Of thirteen amides in which R is unbranched, nine form H-bonded stacks with an inter-strand spacing of 5 Å. Two other packing modes are possible: a two-fold screw axis or a glide plane, which were also observed. However, the 5 Å translational mode is the dominant motif found for these amides and it forms the basis for a model that accounts for discrimination of enantiomers.

The model is an intercalative one that assumes the bound analyte intercalates within the H-bonded array of the CSP matrix without disrupting that 5 Å, H-bonded motif. An example of the (*S*)-N-trifluoroacetyl-α-phenylethylamine inserted in the 5 Å stack of (*R*)-N-lauroyl-α-(1-naphthyl)ethylamine is shown in Fig. 1 (top) and that for the *R*-enantiomer is shown in Fig. 1 (bottom).

It was found experimentally and verified computationally that analytes with the same configuration as the CSP have longer retention times than the analytes with inverted stereocenters. Hence the example in Fig. 1 (top) corresponds to the intercalation of the first-eluted analyte. Throughout these studies, the QCFF/PI force field, developed at the Weizmann Institute, was used to determine which conformations and packing modes were most favorable. The variation in energy of the diastereomeric inclusion complexes between the guest analyte and host CSP were examined. Both intermolecular energies and intramolecular energies, given as contour plots, were evaluated, confirming the proposed model.

The collaboration between Gil-Av and Leiserowitz provides an example of atomistic molecular modeling where interaction energies between analyte and CSP are computed. To accomplish this one must have some knowledge of the shape of the CSP which, for these authors,

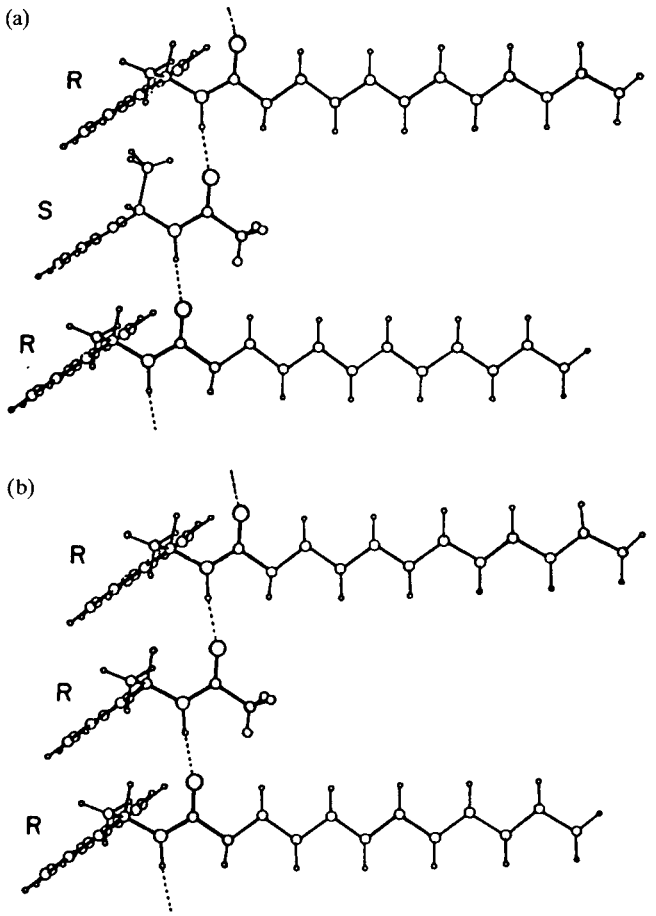


Fig. 1. Weinstein et al.'s intercalation model for chiral recognition on chiral secondary amide CSPs in gas chromatography. (a) (*S*)-N-Trifluoracetyl-α-phenylethylamine inserted into the 5 Å stack of (*R*)-N-lauroyl-α-(1-naphthyl)ethylamine; (b) the more retained *R*-enantiomer intercalated into the same stack.

was derived from X-ray crystallography. In the case of cellulose-based phases, however, little information concerning the structure of the polymer is known and, consequently, modeling of the enantiorecognition is not feasible. Nonetheless, molecular modeling studies directed toward understanding the molecular recognition process of cellulose-based CSPs have been carried out.

For example, Isaksson et al. [17] considered analyte binding to cellulose triacetate (CTA) with statistical theories to assess the relationships between chiral recognition and symmetry of the analyte. This study was precipitated by their finding that small changes in analytes, such as biphenyls, often led to unexpected retention times. Rather than attempt to compute the actual binding constants, they addressed how symmetry influences differential binding constants for chemically similar compounds. Their conclusion is that there is a higher probability of obtaining a good resolution for symmetrical molecules containing a proper axis of rotation ($C_n$ axis) than for asymmetric enantiomer pairs. Further, the higher the order and number of symmetry axes, the better the separation is expected to be.

To test this theory, a set of separations were considered. Of the 216 chiral compounds consid-

ered, 36 had a least one $C_n$ axis of symmetry and four had more than one ($D_2$ symmetry). A plot of the number of compounds, $n$, as a function of the $\alpha$ values, grouped in intervals of $0.2\alpha$ units, was made (Fig. 2, top). Comparison of the complete set with that of a subset containing only symmetrical compounds (Fig. 2, bottom) indicated that these two distributions are different. In general, the symmetrical compounds show consistently good separations whereas the unsymmetrical compounds show poorer separations.

Another example of applying computational chemistry to understand how CTA I works was carried out by Wolf's group at Ciba-Geigy [18]. They investigated the influence of the chemical

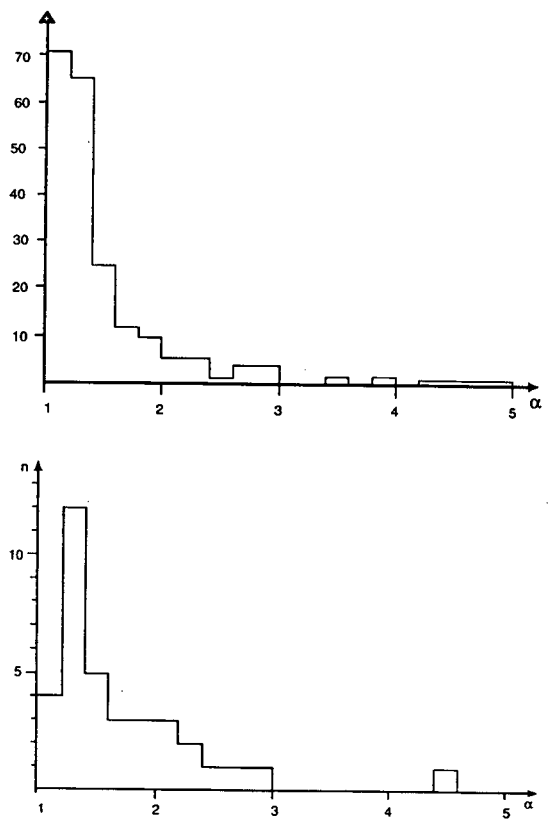


Fig. 2. Top: histogram of the number of analytes resolved on cellulose triacetate vs. their separability factors. A total of 216 compounds are represented. Bottom: the distribution of a subset (36 compounds) containing at least one $C_n$ axis of symmetry.

Table 1
Chromatographic results: capacity factors $k_1'$ and $k_2'$ and separation factor $\alpha$

| Racemate | $k_1'$ | $k_2'$ | $\alpha$ |
|---|---|---|---|
| 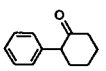 | 1.2 | 2.6 | 2.2 |
| 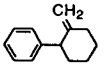 | 0.8 | 0.8 | 1.0 |
| 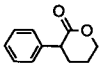 | 1.3 | 4.2 | 3.3 |
| 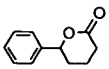 | 1.3 | 29.7 | 23.3 |
| 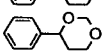 | 2.4 | 11.1 | 4.6 |
| 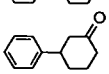 | 1.2 | 1.6 | 1.4 |
| 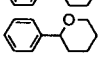 | 1.0 | 3.3 | 3.3 |
| 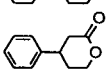 | 1.7 | 1.7 | 1.0 |
| 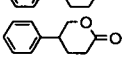 | 1.5 | 1.5 | 1.0 |
| 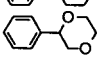 | 2.2 | 12.0 | 5.4 |
| 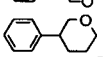 | 0.8 | 0.8 | 1.0 |
| 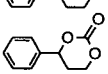 | 1.4 | 9.5 | 6.8 |

structure for a series of related racemates. The molecules, capacity factors and separability factors are presented in Table 1. It should be noted that the capacity factors for the first-eluted enantiomer are about the same whereas those of the second-eluted enantiomer span a large range. On CTA I a large $k_2'$ value almost always leads to a high $\alpha$. Hence these authors decided to use $k_2'$ as the important experimental parameter to be correlated with their computed molecular descriptors. They attempted to find quantitative molecular descriptors for these twelve analytes and to correlate those descriptors with their chromatographic data. These molecular properties, it must be emphasized, are independent of the configuration of the analyte so no stereochemical arguments can be made.

Two criteria seemed important in the chiral separations. First, as had been noted by many

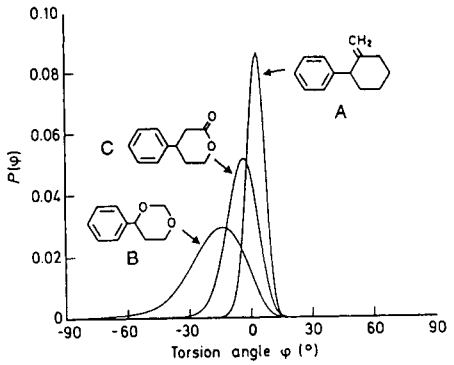


Fig. 3. Boltzmann distribution of the conformational states of the three classes of compounds displaying very restricted, intermediate and high conformational freedom.

authors, the shape of the analyte seems important, and second, all compounds containing an oxygen adjacent to the stereogenic center have large $k_2'$ values indicating that negative charge adjacent to that center enhances resolution. These two effects are, experimentally, inexorably linked; placing an $sp^3$ oxygen $\alpha$ to the stereogenic center provides the requisite electron density but, by replacing the *exo*-methylene or carbonyl groups with this oxygen, it makes the analyte more flexible owing to easy rotation around the phenyl group.

Conformational studies (shape descriptor) were carried out with molecular mechanics and atomic charges used to create molecular electrostatic potential maps (electronic descriptor) were done with quantum mechanics. The authors examined the rigidity of the analyte by Boltzmann weighting the conformational energies for all analytes. They found that the twelve analytes could be partitioned into three categories, depicted in Fig. 3. One grouping, represented by A in Fig. 3, has a very narrow probability distribution and may be considered "rigid". In Fig. 3 a 0° dihedral angle means that the phenyl ring is orthogonal to the saturated ring. Hence these rigid molecules will never become planar (it is presumed that flat molecules generally fit better into the chiral cavities or crevices of CTA I than do non-planar molecules). The second category, represented by molecule B in Fig. 3, has a broad distribution of conformational states and can adopt near-planar shapes. The third category is between the "stiff" and the "flexible" analytes. It turns out that the flatness of the analyte alone is not the only factor responsible for good complexation with CTA. To probe the electronics of these analytes, the authors computed molecular electrostatic maps as in Fig. 4 and extracted from them a normalized electrostatic interaction energy.

The two molecular descriptors thus used were $[\Omega]$, a measure of flatness, and $E_{00}$, a measure of negative charge distribution around the stereogenic carbon. Using these two simple descriptors, a regression model was developed:

$$\ln k_2'^{(i)} = AE_{00}^{(i)} + B[\Omega]^{(i)} + C \quad (i = 1\text{–}12) \qquad (1)$$

where $A = -0.122$, $B = 0.0211$ and $C = 0.497$.

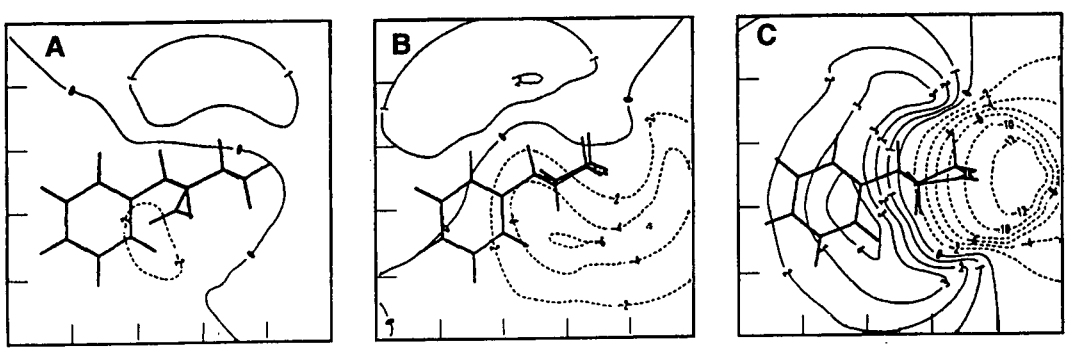


Fig. 4. Molecular electrostatic contour maps for molecules A, B and C in Fig. 3. Contour lines are in units of kcal $mol^{-1}$, full lines represent positive regions and broken lines represent negative regions.

Using this model, the authors predicted $k_2'$ values for comparison with experiment and found a good correlation (correlation coefficient = 0.96).

Other attempts to quantify the effect of structural parameters on the separation of enantiomers of CTA I have been reported. Most notable is the work by Roussel and his group in France, who use full factorial design to quantify the effect of structural parameters (factors) on either the separations or capacity factors (responses) of atropisomeric isomers on CTA I [19]. In this way one can quantitate the variables responsible for retention and separation.

The three structural modifications are shown in Fig. 5. Since there are three changes being made there must be $2^3 = 8$ molecules to explore fully (for three changes at two levels) the recognition process. $X_1$ can be oxygen (level − 1) or sulfur (level + 1); $X_2$ can be hydrogen (level − 1) or methyl (level + 1); $X_3$ can be hydrogen (level − 1) or methyl (level + 1). These eight test probes were synthesized and resolved on CTA I. If one assumes linearization of the influence of substituent patterns for each enantiomer, by difference, one can assess the enantioselectivity. This linearization is expressed by the equation

$$Y = c_0 + c_1X_1 + c_2X_2 + c_3X_3 + c_{12}X_1X_2 + c_{13}X_1X_3 + c_{23}X_2X_3 + c_{123}X_1X_2X_3 \quad (2)$$

where $Y$ is the response, $X_1$, $X_2$, $X_3$ are the primary effects and $X_1X_2$, $X_1X_3$, $X_2X_3$, $X_1X_2X_3$ are the bilinear and trilinear cross-terms. The $c$s are the coefficients for each term determined from solving the eight equations, from eight experiments, by replacing the $X_i$ with +1 or −1 according to the experiment. A positive coefficient means that on going from the low level to the high level of that factor, the response is increased. A negative coefficient, in turn, means the response is decreased. Table 2 lists the molecules studied, their design levels and chromatographic results.

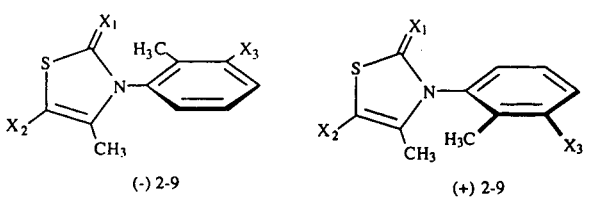


Fig. 5. Structures of the N-arylthiazoline-2-thiones and N-arylthiazolin-2-ones used by Roussel et al. $X_1$ = oxygen or sulphur; $X_2$ = hydrogen or methyl; $X_3$ = hydrogen or methyl.

Table 2
Compounds, design levels and responses

| Compound | Design level | | | Response | | |
|---|---|---|---|---|---|---|
| | $X_1$ | $X_2$ | $X_3$ | $k'(+)$ | $k'(-)$ | $k_2'/k_1'$ |
| 2 | − | − | − | 2.05 | 1.66 | 1.24 |
| 3 | + | − | − | 1.52 | 2.30 | 1.51 |
| 4 | − | + | − | 0.66 | 0.55 | 1.21 |
| 5 | + | + | − | 0.87 | 0.78 | 1.12 |
| 6 | − | − | + | 0.81 | 1.92 | 2.36 |
| 7 | + | − | + | 0.96 | 3.09 | 3.20 |
| 8 | − | + | + | 0.35 | 0.35 | 1.00 |
| 9 | + | + | + | 0.64 | 0.61 | 1.04 |

Eq. 3 is derived for the (+)-enantiomer and Eq. 4 for the (−)-enantiomer:

$$k'(+) = 0.98 + 0.015X_1 - 0.35X_2 - 0.29X_3 + 0.11X_1X_2 + 0.09X_1X_3 + 0.15X_2X_3 - 0.075X_1X_2X_3 \quad (3)$$

$$k'(-) = 1.40 + 0.29X_1 - 0.83X_2 + 0.08X_3 - 0.16X_1X_2 + 0.07X_1X_2 - 0.17X_2X_3 - 0.06X_1X_2X_3 \quad (4)$$

For the dextrorotatory isomer, the primary interactions most dominant are $X_2$ and $X_3$. The sign and the magnitude of these coefficients indicate that on going from a low level (H) to a high level (Me) at either C-5 on the thiazoline or C-3′ on the aryl ring, steric effects between analyte and CSP decrease the capacity factor. The relatively small coefficient for $X_1$ means replacing the ketone with a thione has a minor influence on the dextrorotatory enantiomer retention.

For the levorotatory isomer, the most important primary effects are $X_1$ and $X_2$. Hence for this enantiomer replacement of the carbonyl with a thiocarbonyl has a substantive impact on re-

tention whereas replacing the H with Me on the aryl C-3′ has almost no effect on retention. The dominant primary effect is still due to $X_2$.

From this kind of analysis (a full discussion of the significance of the cross-terms is given in the original paper), Roussel et al. were able to address which parts of the analytes were most sensitive for both enantiomers binding to the CTA I CSP. This type of computational approach is complementary to the work described by Isaksson [17] and by Wolf et al. [18], and it has great promise for unraveling how the complex intermolecular forces responsible for chiral separation work.

An extension of this work was done by Roussel and Popescu [20], who developed a lipophilicity parameter, log $k'_w$, by extrapolating plots of log $k'$ in methanol–water solvents (on an alkyl-bonded stationary phase) to 100% water. Separation of atropisomers **2–9** on CTA I and *tris*(*p*-methylbenzoyl)cellulose beads (CTPB) resulted in five measured responses: log $k'_w$, ln $k'(+)$-CTA, ln $k'(-)$-CTA, ln $k'(+)$-CTPB and ln $k'(-)$-CTPB. The derived coefficients are as follows:

$$\log k'_w = 3.14 + 0.001X_1 + 0.256X_2 + 0.226X_3 - 0.01X_1X_2 - 0.01X_1X_3 - 0.006X_2X_3 + 0.01X_1X_2X_3 \quad (5)$$

$$\ln k'(+)\text{-CTA} = -0.14 + 0.09X_1 - 0.36X_2 - 0.28X_3 + 0.12X_1X_2 + 0.09X_1 + 0.09X_1X_3 + 0.05X_2X_3 - 0.01X_1X_2X_3 \quad (6)$$

$$\ln k'(-)\text{-CTA} = 0.09 + 0.21X_1 - 0.68X_2 - 0.03X_3 + 0.01X_1X_2 + 0.04X_1X_3 - 0.14X_2X_3 + 0.007X_1X_2X_3 \quad (7)$$

$$\ln k'(+)\text{-CTPB} = 0.67 + 0.60X_1 - 0.13X_2 - 0.12X_3 + 0.05X_1X_2 + 0.05X_1X_3 + 0.01X_2X_3 + 0.006X_1X_2X_3 \quad (8)$$

$$\ln k'(-)\text{-CTPB} = 0.62 + 0.74X_1 + 0.11X_2 - 0.91X_3 + 0.09X_1X_2 - 0.18X_1X_3 - 0.01X_2X_3 - 0.04X_1X_2X_3 \quad (9)$$

Using the same kind of analysis as above, the authors were able to explain the relationship between chiral retention of the enantiomers and their lipophilic interactions with the CSPs. Quantification of the influence of structural parameters $X_1$, $X_2$ and $X_3$ was possible. The relationship between lipophilicity and chiral chromatographic behavior was explained for compounds **2–9** and an extension to other alkyl-substituted atropisomers was made along with rationalization for unexpected results. A related study on the resolution of **2–9** on various *p*-methylbenzoylcellulose beads has also been published [21].

Molecular modeling studies of enantiorecognition by the cellulose triphenylcarbamate CSP has been reported by Camilleri et al. [22]. They carried out separations of oxiracetam (**10**) and two related molecules (**11** and **12**) on a Chiracel OC column. For modeling purposes they generated a trisaccharide of β-1,4-linked D-glucoses, end-capped with methyls. Energy minimization with quantum mechanics gave a linear structure with intramolecular H-bonds. The hydroxyls were replaced with phenylcarbamate resides and the resulting trisaccharide was energy minimized again. The phenyl carbamate groups induce a helical twist to the polymer owing to steric repulsions of the phenyls, but the helicity of the CSP was dismissed as being responsible for chiral recognition.

After manual docking of the analyte with CSP, energy minimization with molecular mechanics was performed. It was found that only for the *R*-isomer of **10** could a viable three-point as-

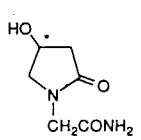

**10**

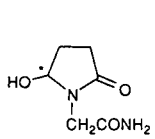

**11**

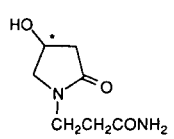

**12**

sociation exist, which explains why the *R*-isomer is retained longer than the *S*-isomer. With the aid of molecular modeling, the authors were able to identify possible interactions leading to stereoselection.

Most of the computational studies of type II CSPs have not considered the CSP directly. Instead, regression models are constructed to explain how a set of probe molecules interact with the CSP. The example above by Camilleri et al. sets forth an explicit treatment of the CSP. Other examples where the CSP is explicitly modeled have been published.

One example is by Alkorta et al. [23]. Here the molecular modeling involved correlating the molecular mechanics binding energies of substituted benzenes, phenols and naphthalene with retention orders on CTA I. Eventually a linear relationship between log $k'$ and the interaction energies was obtained. This study does not explain chiral interactions but it does introduce a picture of what the CSP looks like. Another example of modeling the structure of these type II CSPs is presented by Francotte and Wolf [24]. They prepared and evaluated benzoylcellulose beads in a pure polymeric form as a sorbent for the chromatographic resolution of racemic compounds such as benzylic alcohols and acetates of aliphatic alcohols and diols. Their results implicated multiple interaction sites to be involved in the complexation. A rationalization of the interaction mechanism required a more systematic investigation of the factors influencing separations and, to address the structural features of the cellulose tribenzoate, they carried out molecular modeling with molecular mechanics. The key question being addressed is the extent to which the polysaccharide backbone is exposed to small molecules when sterically encumbered benzoates are attached.

Representative decameric chain segments were generated by excising the third unit of an energy-minimized hexamer as their monomer. This monomer was polymerized, *in computero*, using the glycosidic bridge angles between the two middle segments to create the polymer backbone. In this way the computational artifact of having terminal end-groups is eliminated. Color-coded molecular graphics displays of the decameric strands in two low-energy conformations revealed that the sugar residues are able to interact, at least partially, with small molecules so that the chiral discrimination does not come solely from the benzoyl groups.

Another study is by Lipkowitz' group [25], who repeated an earlier study on the crystal packing of cellulose triacetate reported by Wolf and Scheraga [25]. Similar results were found using different force fields (MM3, AMBER) than that used by Wolf and Scheraga (ECEPP-2). A display of the disaccharide making up the unit cell, a sheet of these polymers and a microcrystallite of CTA I are presented in Fig. 6. Lipkowitz' group is currently examining averaged structural features of the monomers, interstrand geometries and dynamic properties of these microcrystallites from molecular dynamics simulations in an attempt to understand where analytes bind. Eventually, their goal is to simulate the binding of analytes like those in Table 1 to understand enantiodifferentiation based on atomistic modeling.

The helical conformations and conformational stability of isotactic poly(triphenylmethyl methacrylate) have been investigated by Vacatello's group [26] in Italy using an empirical force field. For their preliminary analysis they considered a dimer and omitted several of the phenyl rings to simplify the calculations. The authors acknowledged that not all the conformations for the dimer will be allowed in longer chains and, accordingly, they generated a hexameric unit. It was found that only one backbone conformation is allowed for helical segments with the two-bond repeat unit and that the polymer has approximately 3.6 monomers per turn with a 2.0 Å pitch per monomer unit. Their conclusion is that the polymer is composed of $\ldots|G^+T|G^+T|\ldots$ and $\ldots|TG^-|TG^-|\ldots$ with $G^+ \approx +75°$, $G^- \approx -75°$ and $T \approx \pm 160°$. This motif firmly locks in the side groups and the interconversion between P and M helices is inhibited by a large energy barrier. No analyte binding studies have been reported by this or any other group, however.

Finally, we mention here the work by Ning [27] on salting effects in reversed mobile phases for the chiral separation of both *cis*- and *trans*-benzonaphthazepine enantiomers on cellulose

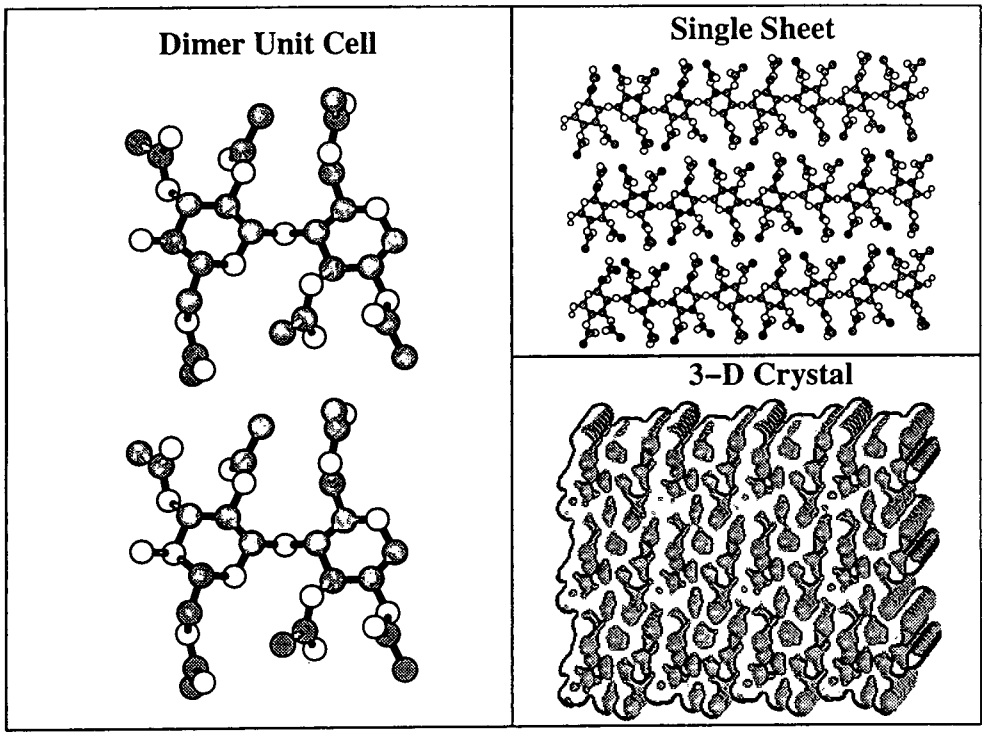


Fig. 6. The unit cell of CTA I consists of two disaccharides. Three strands of crystallite are shown on the top right and a space-filling model of a microcrystallite, with spacings consonant with X-ray data, is shown on the bottom right. Hydrogen atoms are omitted for clarity.

tris(3,5-dimethylphenylcarbamate) CSP. The salting-in effect of $NaClO_4$ makes the analytes more soluble in the mobile phase so that the CSP can selectively retain the four stereoisomers. The salting-out effect of NaCl induces hydrophobic self-association and, accordingly, the author proposed that the NaCl works differently than a conventional ion-pair reagent in non-chiral reversed-phased chromatography.

Experimentally, the retention order is (−)-*trans*, (−)-*cis*, (+)-*trans*, (+)-*cis*. This order is unusual and was rationalized by atomistic molecular modeling. Using molecular mechanics, the lowest energy conformers for both *cis* and *trans* analytes were located. Ning then discovered that the *cis* isomer can be superimposed almost perfectly on top of the *trans* diastereomer. In contrast, two enantiomers do not possess such perfect matching. Hence, when a *cis* diastereomer encounters a *trans* diastereomer they are forced, by hydrophobic effects, to form a dimer that moves into and out of the mobile phase until they become trapped in a suitable cavity of the CSP. There they are further discriminated. By comparison, the enantiomers do not match well when forced together and are proposed to be moving about individually, randomly associating with the CSP and being well resolved. This proposal rationalizes why the corresponding diastereomer rather than the enantiomer follows in the separation. Finally, because the *trans* isomer has a smaller pucker angle by 6° than does the *cis* isomer, it has less steric bulk and should elute less quickly than the *cis* isomer. This is consonant with experiment.

Most of the molecular modeling studies of type II CSPs, as we see from above, do not directly involve interaction of the analyte with the CSP to discern where and how chiral recognition takes place. This is in contrast to modeling of brush-type CSPs previously reviewed [12] and type III CSPs discussed below. The reason for

this is, apparently, the lack of structural information about these CSPs. It is anticipated, however, that one will soon find direct analyte–CSP computations to discern where and how chiral separations take place.

## 4. Type III CSPs

Type III CSPs work by forming inclusion complexes and two main categories of host molecules have been studied computationally. These are cyclodextrins (CDs) and their derivatives and crown ethers. In a series of papers, Armstrong and co-workers used molecular graphics representations of how $\beta$-CD separates diastereomers [28] and enantiomers [29,30]. These graphic images were presented in color to highlight similarities and differences of analyte binding, but these studies did not involve complete energy minimizations. Using rigid cyclodextrin, the authors allowed only the important torsion angles and the location of the analyte in the macrocycle to change. The modeling highlighted the importance of the 2- and 3-hydroxyl groups for the resolution of enantiomers and allowed the authors to design rationally derivatives of CDs to optimize a particular separation.

This led Boehm et al. [31] to formulate a statistical thermodynamic theory of chiral solute retention and separation on models of chemically bonded CSPs. For an infinitely dilute solution, the capacity factor for a distribution of solute molecules between two phases is $k = \exp(-\beta\,\Delta A)$, where $\beta\,\Delta A$ represents the Helmholtz free energy accompanying the transfer of solute from the mobile phase to the stationary phase. When the mobile phase is non-chiral and all the interactions of solvent molecules with individual enantiomers are identical, the equation

$$\alpha = k_{\mathrm{D}}/k_{\mathrm{L}} = \sum_i \exp(-E_{i\mathrm{D}}/kT) \Big/ \sum_j \exp(-E_{j,\mathrm{L}}/kT) \quad (10)$$

holds where $E_{i,\mathrm{D}}$ and $E_{j,\mathrm{L}}$ are the interaction energies of D- and L-enantiomers in their $i$th and $j$th modes of retention on the CSP. In Eq. 10 one must specify the complete set of $E_{i,\mathrm{D}}$ and $E_{j,\mathrm{L}}$ available to the system. This requires introducing a model for both solute and CSP. Models for CDs were provided which consist of truncated conical cavities with three or more binding domains on the periphery of one rim and a fourth site attached to silica.

Chiral tetrahedral analytes with four groups a, b, c and d are presumed to interact with three sites 1, 2 and 3 on the CSP by simultaneous three-site, two-site and one-site interactions. There are twelve three-site CSP–analyte interactions, 36 two-site interactions and twelve one-site interactions, giving 60 possible, distinctly unique types of $E_{i,\mathrm{D}}$ and $E_{j,\mathrm{L}}$ interactions, all of which can contribute to the total interaction energies for D- and L-analytes. Of these possible combinations some are different for the D-enantiomer when compared with the L-enantiomer and these are the interaction modes than can lead to separation. For a tetrahedral analyte with groups abcd embedded in the interior of a CD with domains 1234, there are twelve different four-site, twelve different three-site, 36 different two-site and twelve different one-site interaction modes possible. Only the four- and three-site modes are enantiodiscriminating.

An estimation of the separability factor in Eq. 10 requires evaluation of the ratio of the sums of the two Boltzmann weighted terms, summed over all the interaction modes possible. When one mode of interaction predominates over all others, the summations in Eq. 10 can be approximated by those dominant terms alone. If there is a single dominant mode of retention, denoted by Boehm as $E_{i^*,\mathrm{D}}$ and $E_{j^*,\mathrm{L}}$, Eq. 10 reduces to

$$\alpha = \exp[-\beta(E_{i^*,\mathrm{D}} - E_{j^*,\mathrm{L}})] \quad (11)$$

where $\beta = 1/kT$. When the retention for each enantiomer is dominated by a single chirally discriminating mode of retention, Eq. 11 is approximated by $\alpha = \exp(\beta\,\Delta E)$. Thus $\ln\,\alpha$ is a linear function of both adsorption energy and the reciprocal of temperature. The slope of $\ln\,\alpha$ vs. $1/T$ will provide $\Delta E$ of D- vs. L-analyte in their dominant retention mode and variation from linearity indicates mixed modes.

Rather than dwell on hypothetical interactions, Berthod et al. [32] devised a scheme for attributing individual substituent contributions to chiral recognition by (*R*)-(−)-1(1-naphthylethyl)carbamoylated β-CD CSP (*R*-NEC-β-CD) and the corresponding (*S*)-(+) phase (*S*-NEC-β-CD). The objective was to be able to predict whether or not an analyte with four different substituents connected to the stereogenic center would be resolvable on these CSPs. The separability factor, $\alpha$, is due to the chiral interactions for enantiomer 1 and enantiomer 2 by $\alpha = \exp \Sigma [(\Delta G_{c1} - \Delta G_{c2})/RT]$. The differential free energy due to the chiral interaction of the two enantiomers, $\Delta\Delta G_c$, was divided into four terms, each representing one of the four groups as in the equation

$$\Delta\Delta G_c = (\Delta G_{c11} - \Delta G_{c12}) + (\Delta G_{c21} - \Delta G_{c22}) + (\Delta G_{c31} - \Delta G_{c32}) + (\Delta G_{c41} - \Delta G_{c42}) \quad (12)$$

It is assumed that the chiral interaction contributions are independent of one another and that the interactions are additive and, accordingly, predictive.

A total of 126 compounds were analyzed on these two CSPs. However, only 81 unique groups exist in their data set owing to redundancy. The hydrogen substituent was arbitrarily set equal to 0 cal/mol for a chiral free energy contribution and the authors noted that changing this arbitrary value would influence the sign of some substituents contributions. The authors generated one equation (Eq. 12) for each compound studied, and, setting $\Delta G_H = 0$ cal/mol, solved the equations while the error function $E = \Sigma |\alpha_{calc} - \alpha_{obs}|$ was minimized. If the substituent has a positive value it means an enhanced chiral recognition by the NEC-β-CD CSP exists compared with H, and a negative energy value means the opposite.

Generally, the chiral recognition increased when $sp^2$ carbons are attached to the stereogenic center and decreased when $sp^3$ carbons are attached to the stereogenic carbon. The effects of $\pi-\pi$ stacking, hydrogen bonding and dipole stacking were also assessed. Although this method does not allow one to predict an elution order, the substituent constants (for those CSPs) can be used to make an estimate of the enantioselectivity of an unknown by adding the energy contributions of the four substituents connected to the stereogenic carbon of that unknown compound.

A slightly different approach was taken by Roussel and Favrou [33] toward understanding chiral separations by cyclodextrins and quantifying the effect of substituents. Using compounds (−)-**2–9** and (+)-**2–9**, the authors carried out chiral separations using β- and γ-cyclodextrins as a chiral mobile phase additives. The full factorial design methodology was applied to $k_0'$ (retention without cyclodextrin), $k'(+)$, $k'(-)$ and $\alpha$ for two different achiral stationary phases. In the presence of γ-CD on a non-end-capped phase, the following equations were derived:

$$k_0' = 86.43 - 2.77X_1 + 33.39X_2 + 31.70X_3 - 6.19X_1X_2 - 2.74X_1X_3 + 12.73X_2X_3 - 3.43X_1X_2X_3 \quad (13)$$

$$k'(+) = 20.92 - 6.15X_1 + 7.31X_2 + 8.17X_3 - 2.65X_1X_2 - 2.81X_1X_3 + 3.00X_2X_3 - 1.27X_1X_2X_3 \quad (14)$$

$$k'(-) = 20.65 - 6.25X_1 + 7.14X_2 + 8.44X_3 - 2.65X_1X_2 - 2.71X_1X_3 + 3.17X_2X_3 - 1.27X_1X_2X_3 \quad (15)$$

$$\alpha = 1.024 + 0.016X_1 + 0.008X_2 - 0.024X_3 + 0.008X_1X_2 - 0.016X_1X_3 - 0.008X_2X_3 - 0.008X_1X_2X_3 \quad (16)$$

From Eq. 13, one finds that without γ-CD, two structural features, $X_2$ and $X_3$, have a predominant influence on retention. A change in electrostatics by converting the carbonyl to thiocarbonyl does not have much influence on the capacity factor. In contrast, when γ-CD is present, Eqs. 14 and 15 show $X_1$, $X_2$ and $X_3$ to affect retention similarly for each atropisomer, and these influences are weak. In the presence of the chiral modifier γ-CD, then, the change from carbonyl to thiocarbonyl becomes important with the latter being more retained. Finally, from Eq. 16,

$X_1$ and $X_3$ are most important. Similar analyses for stability constants were addressed and an attempt to assess factors responsible for β-CD as a mobile phase additive were made. Optimization of the separations by varying the EtOH percentage and the nature and pH of the buffer were attempted, but chiral discrimination was mainly influenced by the CD cavity size and strength of the inclusion complex.

The chromatographic behavior of phaclofen (**13**) and its difluoro derivative (**14**), along with the diastereomeric monofluoro species **15** and **16** on acetylated β-CD has been studied. In methanol/aqueous triethylamine–acetic acid, **13** is not resolved but **14** is with $\alpha = 1.11$. Further, **16** is resolved but not **15**. A theoretical model for this behavior, in terms of the asymmetry in the π-facial molecular electrostatic potentials on the phenyl ring, was presented [34]. Using semiempirical molecular orbital theory the electrostatic potentials on the *syn* and *anti* faces of the aryl ring were determined. Those analytes with larger electrostatic differences between *syn* and *anti* faces appear to correlate with separations, but precisely how this electrostatic asymmetry works was not explained.

Most of the aforementioned studies represent quantitative structure–retention relationship studies where a series of analytes are used as probes of enantiodiscrimination. There are, however, a number of atomistic molecular modeling studies where the interactions of chiral guests (analytes) with chiral hosts (CSPs) are explicitly determined. Before reviewing these papers, we point out that most of the published computational studies of cyclodextrins (CDs) involve examination of their structures with MM or MD techniques or, using quantum mechanics, to rationalize their proclivity to bind non-chiral guests in a particular orientation. Also, an analysis of the shapes of cyclodextrins exists [35] and a comparison of α-, β- and γ-CDs in the solid state was made for native and derivatized species. Features of the CD monomer units, including orientations of 1° OH groups and pyran ring pucker, were presented. Macromolecular features described for these host molecules include planarity of the macrocycle, tilt of the pyran rings and deviations from six-, seven- and eightfold symmetry for α-, β- and γ-CDs, respectively. The mean values and standard deviations for these shape descriptors were given, making this an especially valuable reference.

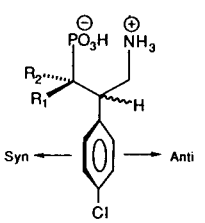


**13** $R_1 = R_2 = H$
**14** $R_1 = R_2 = F$
**15** $R_1 = H, R_2 = F$
**16** $R_1 = F, R_2 = H$

Atomistic molecular modeling studies where guest and host are considered as transient diastereomeric complexes have been published. Both liquid and gas chromatographic studies have been modeled. For example, from work by Armstrong et al. [36] it was known that (*R*)-tryptophan binds more tightly to an α-CD column than does (*S*)-tryptophan with $\alpha = 1.20$. To understand this enantioselection, Lipkowitz et al. [37] used molecular dynamics simulations to answer the following questions: (a) what are the intermolecular forces responsible for analyte binding to the CSP?; (b) where on or in the host does the analyte bind?; (c) what are the differential interactions giving rise to chiral discrimination?; (d) what differences do (*R*)- and (*S*)-tryptophan experience in the CD cavity?; and (e) are existing chiral recognition mechanisms valid?

Using the CHARMM force field for molecular dynamics, the authors' simulations reproduced both the correct retention order and separability factor from chromatography in addition to the intermolecular and intramolecular NOE observations from their NMR experiments. Total averaged energies were partitioned into their component terms. The more tightly bound *R*-enantiomer was favored computationally because its complex had less torsional strain and because the non-bonded interactions are more favorable. Both analytes had similar electrostatic components, however. These component energies were also partitioned into internal energies (intramolecular energies) and external energies (inter-

molecular energies). Both internal and external energies favor the *R*-analyte.

Because intermolecular H-bonding was considered to be important, the authors evaluated the number and kinds of intermolecular H-bonds between guest and host. They found that not only does the more retained *R*-enantiomer form more H-bonds than does the *S*-enantiomer, but also that these H-bonds are usually simultaneous, multiple-contact H-bonds between guest and host. An illustration summarizing their results is depicted in Fig. 7.

Three key features emerge from this illustration. First, both complexes are highly localized on the interior of the CD with the *R*-enantiomer binding to one side of the macrocycle and the *S*-enantiomer to the other. Second, the *R*-enantiomer forms almost twice as many intermolecular H-bonds (2662) than does the *S*-enantiomer (1307) and, as pointed out above, they are of the multiple-contact type. Third, the hydrogen bonding occurs primarily from tryptophan's carboxylate and indole N–H but not the ammonium group. Based on this, the authors confirmed an earlier recognition model proposed by Armstrong but pointed out that a high degree of localization is tantamount to a tight fit in the CD cavity as promulgated by Armstrong.

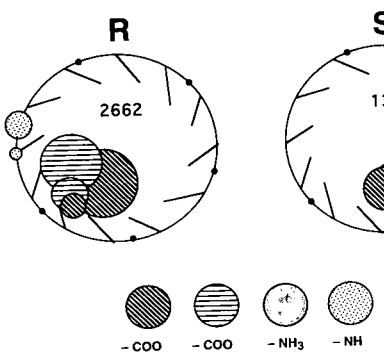


Fig. 7. Graphical representation of the intermolecular hydrogen bonds of (*R*)- and (*S*)-tryptophan with α-cyclodextrin. The large circle represents the macrocyclic host. The small black dots on that circle are the acetal linker oxygens, and the lines attached to the circle represent the unidirectional C-2 and C-3 hydroxyl groups. The cross-hatching indicates the atoms or groups of atoms on the tryptophan that are forming the intermolecular hydrogen bonds. The size of the cross-hatched circle corresponds to the number of hydrogen bonds formed during the simulation. The centers of the cross-hatched circles are placed at the mean positions of the hydrogen bond contacts.

Another paper by this group was published [38]. It does not involve chromatography directly but it does have a direct impact on understanding chiral discrimination in cyclodextrins. In that study the authors searched the crystallographic literature for cyclodextrins with enantiomerically pure *R* and *S* guests. Using molecular mechanics they first computed the binding enthalpy, $\Delta H$, for each guest by comparing the molecular mechanics energy of the guest–host complex with that of the guest and host infinitely separate, i.e., $\Delta H = H_{\text{bound}} - H_{\text{free}}$. Doing this for the (*R*)-CD complex and for the (*S*)-CD complex allowed them to compute $\Delta\Delta H = \Delta H_R - \Delta H_S$, which is the enantiodiscriminating enthalpy. It was found that the dominant force responsible for guest–host complexation is the short-range London force. The enantiodiscriminating forces tended to be very small and are generally, but not always, dominated by the long-range Coulomb force. It was also found that enhanced enantioselectivity occurs in the derivatized CDs compared with the CDs in their native state. It is not clear why this occurs but the following observation was made. The native CDs, when they form guest–host complexes, form stacked or skewed columns of CDs with guests embedded along these stacks. The guest is found on the interior of the host molecule or slightly above/below the interior. This is represented by structure I. In contrast, the derivatized CDs tend to have a guest embedded in the interior (or slightly above the interior) of one host molecule but protruding into the interstitial region between CDs of the next layer. This is depicted in structure II.

In the derivatized examples, then, there is a large amount of intermolecular contact with the *exterior* of the CDs, whereas there is only *interior* contact with the native CDs. The conclusion derived by the authors is that enhanced chiral discrimination can take place on the exterior of the CD compared with the interior. This statement is noteworthy, but remains highly speculative given the limited number of systems studied.

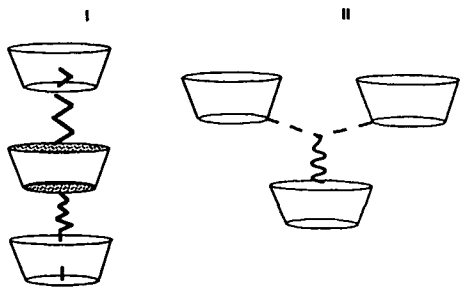


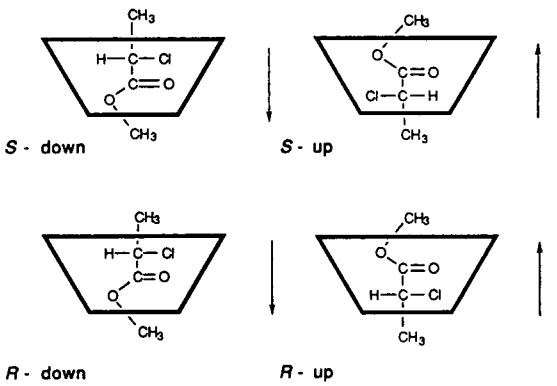


Fig. 8. Initial orientations selected for (*R*)- and (*S*)-2-chloromethylpropionate in Lipodex D for molecular dynamics simulations. The wider rim corresponds to the C-2 and C-3 groups and the narrow rim corresponds to C-6 substituents.

The concept of chiral recognition on the exterior of the CD is especially relevant to gas chromatography. One of the predominant forces for guest–host complexation in aqueous phase liquid chromatography is the hydrophobic force. This is absent in the gas phase and consequently it is not clear what forces induce an analyte to bind as an inclusion complex in CD stationary phases used in gas chromatography. Indeed, from an extrathermodynamic analysis of analyte binding to derivatized cyclodextrins in the gas phase, Berthod et al. [39] suggest that both exterior and interior binding modes are possible. Exterior binding and/or partial inclusion complexation seem consistent with molecular mechanics and dynamics calculations showing these otherwise toroidal macrocycles to collapse upon themselves in the gas phase [40]. However, all publications to date assume that binding takes place in the interior.

The pioneering paper on using molecular dynamics simulations to understand chiral gas chromatographic results was published by König's group [41]. Experimentally they found the *S*-enantiomer of methyl-2-chloropropionate to be more retained on Lipodex D[heptakis-(3-O-acetyl-2,6-di-O-pentyl)-$\beta$-CD] coated on a capillary column at 333 K. A large separability factor, $\alpha = 2.02$, corresponding to $\Delta\Delta G = 2$ kJ mol$^{-1}$, was observed and an attempt to discern the structural features of the transient complexes was made.

Using a known $\beta$-CD neutron diffraction structure, the authors homogeneously fixed the C-2 and C-3 substituents upward and the C-6 pentyl groups downward. The analytes were placed into the interior of the resulting cavity in "up" or "down" orientations as depicted in Fig. 8. Upon providing kinetic energy to the system, the authors found the "down" orientation led to immediate expulsion of guest from the host cavity. The *R*-"up" orientation migrated outside of the cavity but remained near the hydrophobic side-chains and the *S*-"up" complex was found to be most stable. These results are consistent with the GC results and agree with nuclear Overhauser effect results from their NMR studies showing the methyl ester near the C-3 groups of the CSP. The authors indicated that a 5-ps simulation is too short to provide unequivocal results and indicated that longer trajectories would be needed.

In a follow-up study the authors carried out longer simulations [42]. The computed complexation energy difference, favoring the *S*-enantiomer, is 5.75 kcal mol$^{-1}$ at 300 K (experimental $\Delta\Delta G = 0.65$ kcal mol$^{-1}$) and at 333 K it is favored by 1.12 kcal mol$^{-1}$ (experimental $\Delta\Delta G = 0.47$ kcal mol$^{-1}$) (1 cal = 4.184 J). In this paper the authors considered the shape of the host, showing that "self-inclusion" takes place when no host is present, and the shape of the analyte in both the free and complexed states. From their simulations they were also able to

deduce the time-averaged orientation in the CSP host cavity, evaluate the geometry of the guest–host complex and describe intermolecular distances between the enantiomeric analytes and chiral cavity.

Koen de Vries et al. [43] likewise found that a combined molecular mechanics and molecular dynamics approach is a valuable tool for rationalizing qualitative gas chromatographic trends. Experimentally they evaluated the thermodynamic parameters ($\Delta G$, $\Delta\Delta G$, $\Delta H$, $\Delta\Delta H$, etc.) for guest–host complexation of six analytes on a variety of derivatized CD columns. Their interpretation of the results was that one enantiomer fits the CD cavity better than the other, resulting in a larger interaction energy and greater loss of mobility. To help understand this, they studied the binding of one analyte (styrene oxide) to several cyclodextrins including octakis-(3-O-trifluoroacetyl-2,6-di-O-methyl)-γ-CD, octakis-(2,3,6-tri-O-methyl)-γ-CD, octakis-(3-O-acetyl-2,6-di-O-methyl)-γ-CD and heptakis-(3-O-trifluoroacetyl-2,6-di-O-methyl)-β-CD. No interaction energies were reported. Rather, attention was paid to how molecules generally tend to align in the cavity of these CSP analogs.

Kobor et al. [44] also used molecular modeling to examine how polar and non-polar analytes bind to derivatized CDs as selectors in gas chromatography. Their goals are to explore systematically suitable GC-compatible chiral selectors that are more universal with regard to their application. They prepared 2,3-di-O-methyl-6-O-*tert.*-butyldimethylsilyl-β-CD (TBCD) for comparison with the more common permethyl-β-CD (PMCD) CSP. The idea was to narrow the secondary opening of the cavity and block the opening on the primary side of the CSP. The TBCD was dissolved in a lipophilic polysiloxane (OV-1701) and coated on treated and non-pretreated silica capillary surfaces. The test compounds studied were limonene and 1-phenylethanol. (*S*)-limonene is eluted before the *R*-enantiomer and $\alpha = 1.078$ on TBCD and $\alpha = 1.029$ on PMCD. The *R*-enantiomer emerges before the *S*-enantiomer for the polar alcohol with $\alpha = 1.044$ on TBCD and 1.048 on PMCD.

The molecular modeling involved converting the X-ray structure of permethyl-β-CD to TBCD. The structure was energy minimized and subjected to molecular dynamics at high temperatures to probe its conformations. Likewise, the analyte conformations were probed and these conformers were placed in the interior of the CD cavity. A Monte Carlo docking algorithm was used to generate guest–host complexes which were then geometry optimized by molecular mechanics. A distance-dependent dielectric constant was used to simulate the presence of the polysiloxane matrix. In this way a range of energies for each diastereomeric complex were generated as were average energy differences that were in agreement with their experiment. Moreover, from their simulations, they were able to determine the number of inclusion complexes formed between each guest and host; the more stable complex always had the larger number of inclusion complexes. Based on their modeling studies and experimental observations, the authors drew several conclusions about how the analytes bind and fit into the TBCD cavity and the influence of CSP rigidity on chiral discrimination.

Other atomistic molecular modeling studies on molecules that serve as type III CSPs exist. The first, by Gehin et al. [45], used MM and MD to understand how D- and L-phenylglycine methyl esters bind to Cram's macrocycle. A 1.3 kcal $mol^{-1}$ energy difference favoring the L-enantiomer is in agreement with NMR studies but no chromatography on this CSP was done.

Bradshaw et al. [46] constructed new crown ethers that could serve as CSPs, tested their ability to resolve enantiomeric amines and used molecular mechanics to help understand how these potential CSPs work so that better ones could be designed. Chiral polyethers **17–20** were synthesized and their free energies of dissociation with (*R*) vs. (*S*)-1-(1-naphthyl)ethyl ammonium perchlorates (**21**) were determined by NMR methods. The computed enthalpy differences of the lowest energy *R* vs. *S* complexes did not agree very well with the experimental free energy differences, but in all cases the more tightly bound substrate was correctly predicted.

In a later study [47], other pyridine–18-crown-

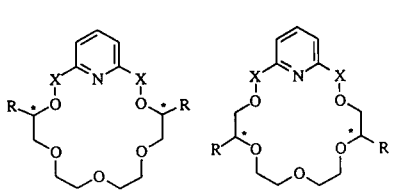

17 X = C=O, R=Me
18 X = C=O, R=phenyl
19 X = $CH_2$, R=Me



20 X = C=O, R=phenyl

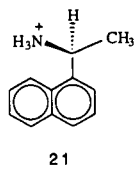

21

6 polyethers were synthesized and their dissociation free energies with chiral alkylammonium salts were measured. The degree of chiral recognition of these chiral crown ethers is substantial. Again using MM, all of conformational space was scanned to find the lowest energy structures of the host and the chiral guest ammonium ions were complexed with these low-energy conformations. These structures were then geometry optimized. The enthalpy differences for nineteen enantiomer pairs were computed in this way. Of these, six have experimental dissociation free energies that compare fairly well with theory. Structural comparisons of the diastereomeric complexes helped elucidate how chiral recognition takes place but, because these macrocyclic hosts have yet to be implemented in chromatographic resolutions, we shall not pursue this.

Finally, we point out a paper by Alvira et al. [48] which, although not involving chromatography, should nonetheless be of interest. In this paper the authors compute the interaction between a helix and amino acids. The helix, consisting of glucose rings, is characterized by its radius, pitch and charge distribution. Intermolecular interactions are computed with a potential energy function as used in molecular mechanics. Various helix characteristics representing helicoidal polysaccharides such as cellulose or chiral cavities such as cyclodextrins were used. The chiral discrimination increases when the analyte molecule is inside the cavity formed by the helix and the chiral discrimination of D- and L-amino acids is 2–8% of the total interaction energy.

## 5. Type IV CSPs

These kinds of stationary phases involve solute association with a metal complex as in chiral ligand-exchange chromatography (CLEC). To our knowledge, there are no reported atomistic computations in this area but there are molecular modeling studies of chiral mobile phase additives which are coordination complexes as well as modeling in chiral ion-pair chromatography that will be discussed here.

In a recent report, Bazylak [49] compared the resolution of underivatized primary and secondary amino alcohols by reversed-phase HPLC using nickel(II) chelates as a mobile phase additive with traditional CLEC. The coordination complexes prepared are depicted in Fig. 9, where the substituents at stereocenters *z* and *q* were modified. These compounds are helically distorted nickel(II) Schiff base chelates derived from condensation of optically pure tetradentate Schiff base ligands with nickel(II) acetate. These coordination complexes work differently from ligand-exchange chelates by virtue of the fact that during association with analytes the chelate structure remains intact. In other words, no coordinating bonds between the nickel and Schiff-base ligand have been broken or formed, and the coordinatively unsaturated nickel(II) only has specific steric and electrostatic interactions with the two analytes. No energy calculations were done. Rather, least-squares superpositions of analyte with chelating reagent were depicted showing where the author believes

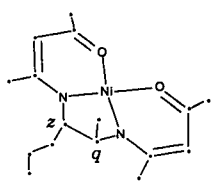

| | z | q |
|---|---|---|
| Ni $L^1$ | H | $CH_3$ |
| Ni $L^2$ | $CH_3$ | $CH_3$ |
| Ni $L^3$ | $C_2H_5$ | H |
| Ni $L^4$ | $C_3H_7$ | $CH_3$ |

Fig. 9. Computer model of $NiL_4$ chelate as an example of the structure of helical nickel(II) chelates used as mobile phase additive. The asymmetric carbon atoms are designated *z* and *q*. The hydrogen atoms have been omitted for clarity.

negatively charged amine groups associate with the metal and how other interactions such as $\pi$-stacking with the chelate rings induce chiral discrimination.

Another report on ion-pair chromatography, where computed molecular descriptors from molecular modeling were nicely correlated with experimented separation factors, was published by Karlsson et al. [50]. They examined factors responsible for separation of aminotetralins **22–27** on achiral stationary phases in the presence of the chiral additive L-ZGP (N-benzyloxycarbonyl-glycyl-L-proline), a protected peptide derivative.

Using the MMX force field, these authors first determined the distribution of conformational states accessible to the analytes and then evaluated the preferred conformations of L-ZGP in the neutral and ionic forms. Then the authors brought these components together to form the various diastereomeric complexes. In their studies their strategy was to implement a flexible docking scheme because it was felt that both molecules of the complex may change their conformations during association.

To put this in perspective, the authors found 40 conformations with energy <3 kcal $mol^{-1}$ from the global minimum (the most stable conformer) for **22** and 243 low-energy conformations for L-ZPG. This would require $40 \times 243$ combinations, each one of which would have a large number of orientations and positions with respect to one another, to consider. Thus a computer-aided docking protocol was used to complement their manual docking results. For each diastereomeric complex, over $10^4$ unique geometries were saved and subjected to molecular mechanics energy minimization which produced, in turn, about 1500 low-energy structures. Stereographic views of L-ZGP with **22**, **23** and **24** are presented in Fig. 10.

These structures are amongst thousands that can participate in the act of chiral discrimination. Accordingly, the authors decided not to use only the lowest energy structures but rather all of their data to derive averaged energies and averaged properties for comparison to experiment. The best molecular descriptor found to correlate with experiment is the averaged non-polar unsaturated surface area of the complex vs. $\alpha$. A more recent paper extending their studies to include 4-hydroxy-2-dipropylaminoindan has appeared [51]. Similar conclusions were derived.

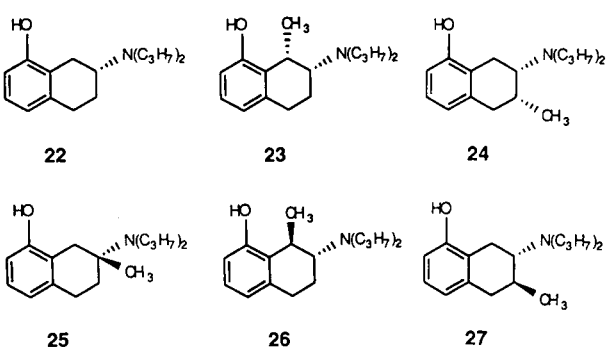


22 23 24

25 26 27

## 6. Type V CSPs

Type V CSPs are protein phases where analytes may adsorb from repulsive hydrophobic forces and attractive polar interactions. It would appear that, with nearly 400 entries in the Brookhaven Protein Databank to select from (X-ray and neutron data), separation scientists would have used one of these proteins to serve as a chiral selector and carry out molecular modeling studies on type V stationary phases whose structures are known. This has not happened. Rather, treating the CSP as an unknown, quantitative structure–enantioselective retention relationships (QSERRs) have been carried out.

Norinder and Hermansson [52] separated 35 N-aminoalkylsuccinimides (**28**) on an $\alpha_1$-acid glycoprotein (AGP) column. To explore the relationship between molecular structure and enantioselectivity, a principal component analysis with partial least-squares projection techniques allowed the authors to determine which of 50 physico-chemical descriptors correlated with separation factors, $\alpha$. A partial list of variables used in the models is given in Table 3. Similar descriptors along with indicator variables for the other R groups on **28** give rise to the

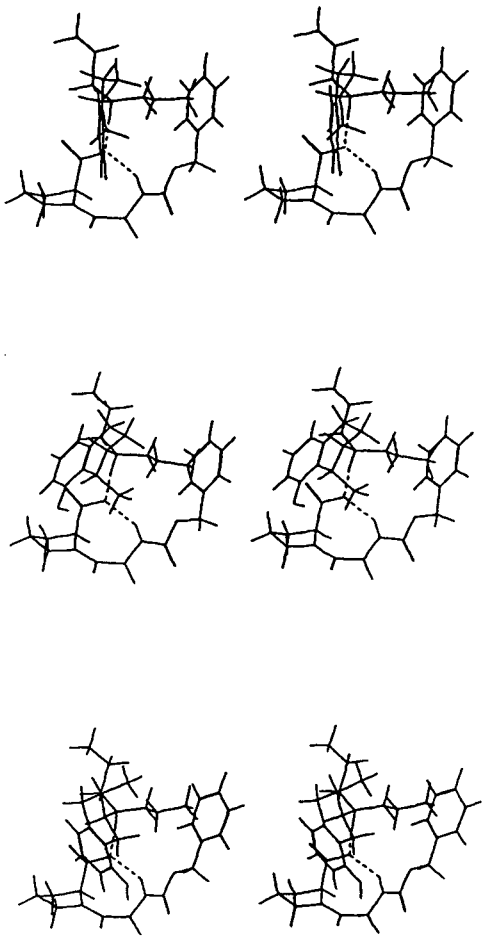

Fig. 10. Stereoscopic representation of changes in complex conformation resulting from the introduction of methyl groups in different positions of the non-aromatic ring of **22**. Energy-minimized (*R*)-**22**–L-ZGP complex (top); energy-minimized complex resulting from the introduction of a *cis*-**1**-methyl group forming the (1*S*,2*R*)-**23**–L-ZGP complex (middle); energy minimized complex resulting from introduction of a *cis*-3-methyl group forming the (2*S*,3*R*)-**24**–L-ZGP complex (bottom). Complexes formed by introduction of methyl groups in the *trans* C-1 and C-3 positions and in the C-2 position did not show significant changes in the complex geometries compared with (*R*)-**22**–L-ZGP.

other variables used. Some variables such as $n$ and $MR$ are obvious, but other terms such as the minimum width ($B_1$) and maximum width ($B_5$) should be looked up in the original literature.

Four significant principal components describing 85% of the variance were found. The most important variables were associated with positions 6 and 7 on the aryl ring. Lipophilic groups containing aromatic character are especially important for enantioselectivity and the length of the aliphatic side chain was also found to be important.

Another QSERR was carried out by Kaliszan et al. [53], who suggested that many of the abstract and arbitrary indicator variables used by Norinder and Hermansson obscure the physical interpretation of the correlations. These authors measured the retentions of 21 chiral and achiral 1,4-benzodiazepine derivatives (**29–32**) on an immobilized human serum albumin CSP. The variables used to determine the QSERR consisted of molecular descriptors derived from computational chemistry. Regression analysis to the data resulted in equations for both enantiomers with these non-empirical molecular descriptors.

Log $k_1'$ and log $k_2'$ were considered as two sets of mutually independent variables. The resulting models were

$$\log k_1' = -1.75 + 0.39 \log f_y - 1.84C_3 - 0.16W + 0.04\beta_{CCN} + 0.17f_x \quad (17)$$

$$\log k_2' = 1.99 + 0.89P_{SM} + 0.48f_y - 4.15C_3 - 0.12W + 0.13f_x \quad (18)$$

where $f_y$ is the hydrophobicity of substituents on position 7, $C_3$ is the atomic charge on carbon 3 derived by semi-empirical molecular orbital calculations, $W$ is the width of the analyte, $\beta_{CNN}$ is the diazepine C-2–C-3–C-4 angle, $f_x$ is the hydrophobicity of substituents at carbon 2′ and $P_{SM}$ is the substructure dipole which is the charge difference between the hydrogen at C-3 and the most negatively charged atom multiplied by the distance ($D$ in Fig. 11) between them. Eqs. 17 and 18 allow one to gain an insight into the retention mechanism. Eq. 17 indicates that the binding site responsible for the first-eluted isomer contains structural and spatial constraints and that the hydrophobicity of group Y at C-7 is most important by anchoring the analyte to the CSP. Counteracting this is the excess charge at C-3 and the width of the binding site, which

Table 3
Partial list of variables used in the Norinder–Hermansson models

| No. | Variable | Position | Explanation |
|---|---|---|---|
| 1 | $n$ | | Chain length, number of $CH_2$ groups |
| 2 | $n^2$ | | Chain length, number of $CH_2$ groups |
| 3 | $MR$ | $R_1$ | Molecular refractivity |
| 4 | $MR^2$ | | Molecular refractivity |
| 5 | $L$ | $R_1$ | Verloop Sterimol parameter |
| 6 | $L^2$ | $R_1$ | Verloop Sterimol parameter |
| 7 | $B_1$ | $R_1$ | Verloop Sterimol parameter |
| 8 | $B^2$ | $R_1$ | Verloop Sterimol parameter |
| 9 | $B_5$ | $R_1$ | Verloop Sterimol parameter |
| 10 | $B^2$ | $R_1$ | Verloop Sterimol parameter |
| 11 | $f$ | $R_1$ | Rekkers aliphatic fragmental constant |
| 12 | $f^2$ | $R_1$ | Rekkers aliphatic fragmental constant |
| 13 | $MR$ | $R_2$ | Molecular refractivity |
| 14 | $MR^2$ | $R_2$ | Molecular refractivity |
| 15 | $L$ | $R_2$ | Verloop Sterimol parameter |
| 16 | $L^2$ | $R_2$ | Verloop Sterimol parameter |
| 17 | $B_1$ | $R_2$ | Verloop Sterimol parameter |
| 18 | $B^2$ | $R_2$ | Verloop Sterimol parameter |
| 19 | $B_5$ | $R_2$ | Verloop Sterimol parameter |
| 20 | $B_5$ | $R_2$ | Verloop Sterimol parameter |
| 21 | $f$ | $R_2$ | Rekkers aliphatic fragmental constant |
| 22 | $f^2$ | $R_2$ | Rekkers aliphatic fragmental constant |

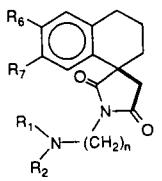

28

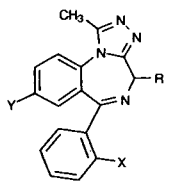

29

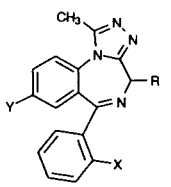

30

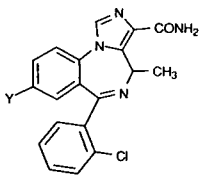

31

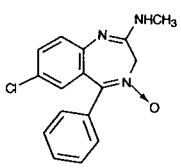

32

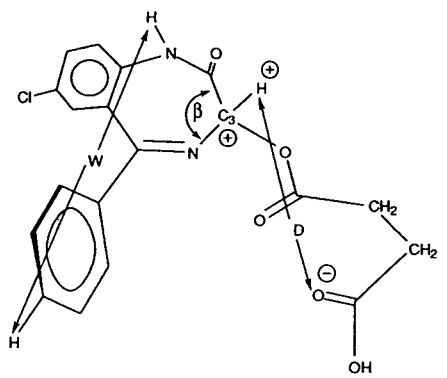


Fig. 11. Several of the molecular descriptors used in a QSERR study of 1,4-benzodiazepine analogues on a human serum albumin-based HPLC chiral stationary phase.

appears to be restricted. Eq. 18 indicates that the second-eluted isomer is influenced by the same structural features as the first-eluted enantiomer, i.e., hydrophobicity, $f_y$, excess charge at C-3 and width. However, the most significant retention descriptor for log $k_2'$ is the local dipole, $P_{SM}$. This indicates that the greatest difference be-

tween binding sites for the enatiomers involves the charge density of the cationic area on the exterior of the CSP. The significant conclusion derived from this computational approach is that there appear to be two distinct binding sites on the protein CSP for chiral benzodiazepines.

## 7. Summary and conclusions

Molecular modeling studies directed toward understanding where and how chiral discrimination takes place in chromatography have been reviewed. This review focused on CSP types II–V and complements an earlier review that focused on type I CSPs [12]. In contrast to type I phases, where intermolecular interactions between selector and selectand were explicitly calculated with quantum or molecular mechanics tools, one finds more regression models for type II–V CSPs. The reason for this is that the shape of these CSPs is, with the exception of cyclodextrin and several synthetic hosts, not well defined or not known at all. Hence all one can do is rely on regression models. These models, albeit lacking a detailed atom-by-atom account of the interactions taking place during chromatography, do provide important information concerning where and how chiral recognition takes place. Moreover, these models are capable of making predictions. That is, once the model has been constructed and validated, one can use those same kinds of molecular descriptors to predict what the separation will be for an as yet unknown analyte.

It is important to realize that molecular modeling is in its infancy. The computational tools available for simulating analyte separation under a variety of chromatographic conditions with various stationary phases, chiral and achiral, gas or liquid, exist. However, we point out that while these computational tools are powerful when used properly, one still would like to use one's experience to determine how best to resolve enantiomers chromatographically. In this regard, then, we point out the enormous research effort by Roussel and Piras [54] and Koppenhoefer et al. [55], who created and maintain CHIRBASE, a graphical molecular database on the separation of enantiomers by gas, liquid and supercritical fluid chromatographies. A more recent and potentially very useful database once it is more complete is CHIRULE, a column selection system using similarity searching, developed by Stauffer and Dessy [56]. Databases such as these together with the computational methodologies described above allow one to make a better selection of the chromatographic tools needed for a resolution and provide insights concerning the mechanism of chiral discrimination. The future of molecular modeling and computational chemistry in the separation sciences looks bright.

## Acknowledgement

This work was carried out under the auspices of a grant from the Petroleum Research Fund administered by the American Chemical Society (25343-AC4) and a grant from the National Science Foundation.

## References

[1] R.W. Souter, *Chromatographic Separations of Stereoisomers*, CRC Press, Boca Raton, FL, 1985.
[2] M. Zeif and L. Crane (Editors), *Chromatographic Chiral Separations* (*Chromatographic Science Series*, Vol. 40), Marcel Dekker, New York, 1987.
[3] W.A. Konig, *The Practice of Enantiomer Separation by Capillary Gas Chromatography*, Hüthig, Heidelberg, 1987.
[4] S.G. Allenmark, *Chromatographic Enantioseparation. Methods and Application*, Ellis Horwood, Chichester, 1988.
[5] D. Stevenson and I.D. Wilson (Editors), *Chiral Separations*, Plenum Press, New York, 1988.
[6] W.J. Lough (Editor), *Chiral Liquid Chromatography*, Blackie, London, 1989.
[7] D. Stevenson and I.D. Wilson (Editors), *Recent Advances in Chiral Separations*, Plenum Press, New York, 1990.
[8] S. Ahuja (Editor), *Chiral Separations by Liquid Chromatography* (*ACS Symposium Series*, No. 471), American Chemical Society, Washington, DC, 1991.
[9] G. Subramanian (Editor), *Chiral Separations by Liquid Chromatography*, VCH, Weinheim 1994.

[10] For a list of books, monographs and reviews on this topic, see the citations in H.J. Schneider, *Angew. Chem., Int. Ed. Engl.*, 30 (1991) 1417.
[11] For a review series covering all aspects of computational chemistry, see K. Lipkowitz and D. Boyd (Editors), *Reviews in Computational Chemistry*, Vols. 1–6, VCH, New York, 1990–95.
[12] K.B. Lipkowitz, *J. Chromatogr. A*, 666 (1994) 493.
[13] I.W. Wainer, *Trends Anal. Chem.*, 6 (1987) 125.
[14] S. Weinstein, L. Leiserowitz and E. Gil-Av, *J. Am. Chem. Soc.*, 102 (1980) 2768.
[15] S. Weinstein, B. Feibush and E. Gil-Av, *J. Chromatogr.*, 126 (1975) 97.
[16] S. Weinstein and L. Leiserowitz, *Acta Crystallogr., Sect. B*, 36 (1980) 1406.
[17] R. Isaksson, H. Wennerstrom and O. Wennerstrom, *Tetrahedron*, 44 (1988) 1697.
[18] R.M. Wolf, E. Francotte and D. Lohmann, *J. Chem. Soc., Perkin Trans. 2*, (1988) 893.
[19] C. Roussel, J.-L. Stein, M. Sergent and R. Phan Tan Luu, in D. Stevenson and I.D. Wilson (Editors), *Recent Advances in Chiral Separations*, Plenum Press, New York, 1990, p. 105.
[20] C. Roussel and C. Popescu, *Chirality*, 6 (1994) 251.
[21] C. Roussel, S. Lehuédé, C. Popescu and J.-L. Stein, *Chirality*, 5 (1993) 207.
[22] P. Camilleri, J.A. Murphy, M.R. Saunders and C.J. Thorpe, *J. Computer-Aided Mol. Design*, 5 (1991) 277.
[23] I. Alkorta, J. Elguero, P. Goya and C. Roussel, *Chromatographia*, 27 (1989) 77.
[24] E. Francotte and R.M. Wolf, *Chirality*, 3 (1991) 43.
[25] K.B. Lipkowitz, G. Pearl and M.A. Peterson, unpublished results, 1994; R.M. Wolf, E. Francotte, L. Glasser, I. Simon and H. Scheraga, *Macromolecules*, 25 (1992) 709.
[26] L. Cavallo, P. Corradini and M. Vacatello, *Polym. Commun.*, 30 (1989) 236.
[27] J.G. Ning, *J. Chromatogr. A*, 659 (1994) 299.
[28] R.D. Armstrong, T.J. Ward, N. Pattabiraman, C. Benz and D.W. Armstrong, *J. Chromatogr.*, 414 (1987) 192.
[29] R.D. Armstrong, in W.L. Hinze and D.W. Armstrong (Editors), *Ordered Media in Chemical Separations* (*ACS Symposium Series*, No. 342), American Chemical Society, Washington, DC, 1987, Ch. 16.
[30] D.W. Armstrong, T.J. Ward, R.D. Armstrong and T.E. Beesley, *Science*, 232 (1986) 1132.
[31] R.E. Boehm, D.E. Martire and D.W. Armstrong, *Anal. Chem.*, 60 (1988) 522.
[32] A. Berthod, S.-C. Chang and D.W. Armstrong, *Anal. Chem.*, 64 (1992) 395.
[33] C. Roussel and A. Favrou, *Chirality*, 5 (1993) 471.
[34] P. Camilleri, A.J. Edwards, H.S. Rzepa and S.M. Green, *J. Chem. Soc., Chem. Commun.*, (1992) 1122.
[35] K.B. Lipkowitz, K. Green and J.-A. Yang, *Chirality*, 4 (1992) 205.
[36] D.W. Armstrong, X. Yang, S.M. Han and R.A. Menges, *Anal. Chem.*, 59 (1987) 2594.
[37] K.B. Lipkowitz, S. Raghothama and J.-A. Yang, *J. Am. Chem. Soc.*, 114 (1992) 1554.
[38] K.B. Lipkowitz, K. Green, J.-A. Yang, G. Pearl and M.A. Peterson, *Chirality*, 5 (1993) 51.
[39] A. Berthod, W. Li and D.W. Armstrong, *Anal. Chem.*, 64 (1992) 873.
[40] K.B. Lipkowitz, *J. Org. Chem.*, 56 (1991) 6357.
[41] J.E.H. Köhler, M. Hohla, M. Richters and W.A. König, *Angew Chem.*, 104 (1992) 362; *Angew. Chem., Int. Ed. Engl.*, 31 (1992) 319.
[42] J.E.H. Köhler, M. Hohla, M. Richters and W.A. König, *Chem. Ber.*, 127 (1994) 119.
[43] N. Koen de Vries, B. Coussens and R.J. Meier, *J. High Resolut. Chromatogr.*, 15 (1992) 499.
[44] F. Kobor, K. Angermund and G. Schomburg, *J. High Resolut. Chromatogr.*, 16 (1993) 299.
[45] D. Gehin, P.A. Kollman and G. Wipff, *J. Am. Chem. Soc.*, 111 (1989) 3011.
[46] J.S. Bradshaw, R.M. Izatt, J.J. Christensen, K.E. Krakowiak, B.J. Tarbet, R.L. Bruening and S. Lifson, *J. Inclus. Phenom. Mol. Recog.*, 7 (1989) 127.
[47] J.S. Bradshaw, P. Huszthy, C.W. McDaniel, C.Y. Zhu, N.K. Dalley, R.M. Izatt and S. Lifson, *J. Org. Chem.*, 55 (1990) 3129.
[48] E. Alvira, J. Breton, J. Plata and C. Girardet, *Chem. Phys.*, 155 (1991) 7.
[49] G. Bazylak, *J. Chromatogr. A*, 665 (1994) 75 and 668 (1994) 519.
[50] A. Karlsson, K. Luthman, C. Pettersson and U. Hacksell, *Acta Chem. Scand.*, 47 (1993) 469.
[51] K. Luthman, A.V. Jensen, U. Hacksell, A. Karlsson and C. Pettersson, *J. Chromatogr. A*, 666 (1994) 527.
[52] U. Norinder and J. Hermansson, *Chirality*, 3 (1991) 422.
[53] R. Kaliszan, T.A.G. Noctor and I.W. Wainer, *Chromatographia*, 33 (1992) 546.
[54] C. Roussel and P. Piras, *Pure Appl. Chem.*, 65 (1993) 235.
[55] B. Koppenhoefer, A. Nothdurft, J. Pierrot-Sanders, P. Piras, C. Popescu, C. Roussel, M. Stiebler and U. Trettin, *Chirality*, 5 (1993) 213.
[56] S.T. Stauffer and R.E. Dessy, *J. Chromatogr. Sci.*, 32 (1994) 228.

ELSEVIER

Journal of Chromatography A, 694 (1995) 39–48

JOURNAL OF CHROMATOGRAPHY A

Review

# Stereochemical determinants of the nature and consequences of drug metabolism

John Caldwell

*Department of Pharmacology and Toxicology, St. Mary's Hospital Medical School, Imperial College of Science, Technology and Medicine, London W2 1PG, UK*

**Abstract**

Enantiomeric discrimination in drug disposition depends on the mechanism of the process under consideration. Absorption, distribution and excretion are generally passive processes which do not differentiate between enantiomers, but enzymic metabolism and protein binding, to plasma or tissue proteins, can show a high degree of stereoselectivity. In terms of metabolism, chiral discrimination occurs at both substrate and product levels, giving rise to five distinct stereochemical courses for drug metabolism, namely (i) prochiral → chiral, (ii) chiral → chiral, (iii) chiral → diastereoisomer, (iv) chiral → non-chiral and (v) chiral inversion. As a result, the metabolic and pharmacokinetic profiles of enantiomers after administration of racemic drugs can be very variable, so that the exposure to the two enantiomers may be very different. There now an enormous number of examples of each of these possibilities. The net result of the interaction of the stereoselectivities of these various processes can obscure the fact that one (or more) shows a marked stereoselectivity. This is particularly the case for metabolism: while the ratios of the total plasma clearance of the enantiomers of a wide range of drugs never exceed 2, individual metabolic pathways often show much greater stereoselectivity. This is particularly evident for those high-affinity, low-capacity enzyme systems which exhibit genetic polymorphism, namely the human cytochromes P450 2C18 and 2D6. This review provides an introduction to the stereoselectivity of drug metabolism.

## Contents



0021-9673/95/$09.50 
*SSDI* 0021-9673(94)00812-4

## 1. Introduction

One in four of all therapeutic agents is marketed and administered to man as mixtures, not drug combinations in the accepted sense of two or more coformulated therapeutic agents, but combinations of isomeric substances whose biological activity may well reside predominantly in one optical form. The majority of these are racemic mixtures of synthetic chiral drugs; mixtures of diastereoisomers are used less frequently. The use of such agents may be regarded as polypharmacy with the proportions of the various optical forms present being dictated by chemical rather than pharmacological or therapeutic criteria. The use of such mixtures may contribute to the toxicity or adverse effects of the material, particularly when these are associated with the pharmacologically less active or inactive isomers, unrelated to the stereochemistry of the compound(s), not associated with the mechanism of action of the material, or idiosyncratic reactions.

It was a matter of early experience in biochemistry and pharmacology that the receptors and enzymes which are the targets of drug action are able to discriminate between stereoisomers. In contrast, the realization of the importance of chiral discrimination for the pharmacokinetic phase of drug action is more recent. The availability of novel analytical modalities has led to substantial growth in our knowledge of the nature, magnitude and consequences of such discrimination. The pharmacokinetic importance of drug stereochemistry depends on the mechanism of the process under consideration: passive processes such as diffusion across membranes do not involve macromolecular interactions and stereochemistry has little influence, but when the drug interacts with an enzyme or a transporter system, then discrimination may be seen. There are now a range of examples showing differences between stereoisomeric forms of numerous drugs in terms of their absorption, distribution, metabolism and excretion. Although often of biological importance, the magnitude of these differences is generally much less than those exhibited by receptor and enzyme targets.

Much currently available metabolic and pharmacokinetic data on racemic mixtures is derived from the non-selective assay of the total drug present in biological media, i.e. the sum of the individual enantiomers. Such data have at best limited value and can be highly misleading, particularly when attempting to relate plasma concentrations to pharmacological effect or therapeutic benefit. The examination of the pharmacokinetics of individual isomers permits the determination of the "true" pharmacokinetic parameters of the active agent and provides a basis for the determination of enantiomeric potency ratios and, if required, rational therapeutic drug monitoring. Enantiospecific pharmacokinetic studies have explained apparent anomalies in drug concentration–effect relationships with route of administration. Toxicity testing of drugs and other xenobiotics is carried out using animal models and there are a number of examples where the disposition of the enantiomers of racemic drugs differ markedly between species (see below). Examination of the pharmacokinetics of the enantiomers of racemic drugs in various species is therefore necessary for the effective extrapolation of preclinical safety data to the human situation.

The significance of stereochemical considerations in drug metabolism and pharamacokinetics has recently become an issue for both the pharmaceutical industry and the regulatory authorities [1]. Recent developments in methodology for both the analytical and preparative resolution of racemic drug mixtures [2–4] have provided a major stimulus for the present considerable interest in stereochemical considerations in drug disposition.

## 2. Stereochemistry of drug metabolism

The interaction of the enantiomers of a chiral drug molecule with a chiral macromolecule, such as an enzyme, results in the formation of a pair of diastereoisomeric complexes, which differ energetically. It is therefore not surprising that the products of enzyme-mediated reactions carried out on a pair of enantiomers may vary in

nature and/or extent. Indeed, as to the nature of the enzyme–substrate complex, it is reasonable to assume that enantioselectivity in metabolism is the rule rather than the exception. Similarly, the binding of a prochiral substrate to an enzyme may well orientate two enantiotopic groups differently with respect to the enzyme catalytic site and hence within the enzyme–substrate complex these two groups become diastereotopic. It is therefore relatively easy to appreciate why the formation of a chiral metabolite from a prochiral substrate may exhibit stereoselectivity for one isomeric product. Enzyme-mediated stereoselectivity, in terms of substrate and product, has been extensively reported and is the subject of a number of reviews [5–9].

Metabolic transformations of xenobiotics show two types of stereoselectivity, at substrate and product levels. They may therefore be classified in terms of their stereoselectivity or, if such selectivity is complete, their stereospecificity. This latter term should be used with some caution as the ability to detect "specificity" obviously depends on the analytical methodology employed. The terms substrate and product "stereospecificity" were first applied by Prelog [10] to the enzyme-mediated reduction of ketones, and were later extended to the reactions of drug metabolism by Jenner and Testa [5]. Substrate stereoselectivity refers to the preferential metabolism of one of a pair of stereoisomers over the other, whilst product stereoselectivity refers to the preferential formation of one particular stereoisomer over that of other possible stereoisomers. These two "selectivities" may be closely linked such that substrate–product stereoselectivity may also be observed, i.e., the selective metabolism of one of a pair of enantiomers to produce one of a number of potentially diastereoisomeric products.

Data obtained from in vivo studies must be treated with some care if the enantiomeric composition of a drug or metabolites determined in excreta is to be used as an indication of stereoselectivity in metabolism. In such cases the observed enantiomeric excess may reflect a number of stereoselective processes, e.g., absorption, protein binding, selective tissue uptake, renal and/or bilary excretion, in addition to metabolism. Hence the enantiomeric composition of metabolites may not be a reflection of enzyme activity.

Metabolic transformations may be categorized in terms of their various stereochemical courses. Reaction types in Sections 2.2–2.4 below and the metabolic chiral inversion differ from the type in Section 2.1 in that the stereochemistry of the substrate, together with that of the enzyme binding site and/or catalytic site, influence the nature of the product formed. Hence in the cases of the reactions in Sections 2.2–2.4 and the chiral inversion, use of an individual enantiomer in place of a racemic mixture may have a significant influence on the properties of a drug. Examples of these various possibilities are now discussed under the headings of the various reaction types.

### 2.1. Prochiral to chiral transformations

A non-chiral compound may become chiral by metabolism of enantiotopic groups, either at a prochiral centre, e.g., oxidation of ethylbenzene to yield 1-phenylethanol and oxidation of 4-tolyl ethyl sulphide to the corresponding sulphoxide, or at a site remote from a prochiral centre, e.g., aromatic oxidation of phenytoin to yield 4-hydroxyphenytoin [5]. The reduction of non-symmetrically substituted ketones gives rise to a new chiral centre in the product secondary alcohols. A considerable number of prochiral ketones have been examined as substrates and their reduction proceeds with high stereoselectivity to give the (*S*)-alcohols in 80% or greater excess [5].

Reactions of this type are potentially the most complex to deal with from a toxicological viewpoint, as the stereochemistry of the product is determined by the binding orientation of the substrate towards the enzyme active site and are not open to control at the level of the stereochemistry of the substrate. The metabolism of prochiral substrates, an example of what has been termed "product enantioselectivity", is of considerable interest. In such cases, the chirality of products is solely a function of the biological

system responsible for the metabolism and obviously cannot be influenced by the drug substrate administered. If the chiral metabolite is biologically active and this activity shows enantioselectivity, a by no means unlikely situation, then inter-species (in animals) and inter-individual (in humans) variation in metabolic enantioselectivity, which is observed with increasing frequency, will have an impact on the drug's action.

### 2.2. Chiral to chiral transformations

There are numerous examples of chiral compounds whose individual enantiomers are transformed at different rates and/or by different routes to metabolites which retain their original chirality.

The enantiomers of a chiral drug may be transformed by different routes and/or at different rates to yield metabolites without alteration of the stereochemistry of the product relative to the substrate, e.g., the oxidation of warfarin in man is stereoselective for the *S*-enantiomer of the drug to yield (*S*)-7-hydroxywarfarin [7]. The carboxylic acid metabolite of primaquine, a drug used to treat malaria, has been identified as the principal plasma metabolite in man. Primaquine has a chiral centre in its alkyl side-chain and studies have shown that there is a stereoselective formation of the carboxylic acid metabolite from (−)-primaquine [11]. Stereoselectivity in ester hydrolysis has been shown for a variety of ester-containing compounds [12–14]. The stereoselectivity of the hydrolysis of the β-blocker esmolol by blood estereases differs markedly between species [15].

### 2.3. Chiral to diastereoisomeric metabolites

Chiral drugs may be metabolized to yield diastereoisomers by transformation of prochiral (diastereotopic) groups or by combination with a conjugating agent derived from the chiral pools of the body (see below).

Many chiral drugs undergo metabolic conversion in which a second chiral centre is introduced, thus producing diastereoisomers, e.g., oxidation of perhexiline and pentobarbitone. This is exemplified by the metabolism of hexobarbital by rat liver microsomes [16]. (+)-Hexobarbital was metabolized 1.5 times faster than the (−)-enantiomer, with both enantiomers exhibiting high stereoselectivity for the formation of the hydroxylated metabolites. (+)-Hexobarbital forms β-3′-hydroxyhexobarbital whereas the (−)-enantiomer is preferentially metabolized to α-3′-hydroxyhexobarbital. Investigations of the metabolic stereochemistry of warfarin have shown that the principal routes of metabolism are aromatic hydroxylation of the 7-position of the coumarin ring and ketone reduction in the side-chain [17]. The latter route produces a new chiral centre which results in the production of diastereoisomers. In the cases of warfarin and its analogues, the *R*-enantiomers are converted into the (*S*)-alcohols [18] by two enzymes present in rat liver cytosol.

The conjugation reactions of drug metabolism are energy-requiring biosyntheses, involving the linkage of the drug or a metabolite to an endogenous conjugating agent to give a characteristic product known as a conjugate. The endogenous conjugating agents, or endocons, are generally derived from activated synthetic intermediates with well defined roles in intermediary metabolism. However, in two cases, the required energy is derived by activation of the drug prior to transfer of the conjugating agent. With glutathione conjugation, this is by oxidation or, rarely, reduction, whereas for amino acid conjugation, there is a link with lipid biochemistry through the formation of high-energy acyl CoA intermediates.

The endocons can be divided into two groups, achiral and chiral. The former include methyl and acetyl groups, sulphate and the amino acids glycine and taurine. Chiral endocons, which are quantitatively more significant, are glucuronic acid, glucose, glutathione and glutamine, derived from chiral pools and of fixed configuration. Conjugation of enantiomeric drugs will give epimeric pairs of diastereoisomeric conjugates, in which the configuration of the endocon is fixed. Two possible stereochemical courses can be discerned for conjugation reactions: enantio-

mers can be conjugated at different rates with an achiral endocon, or with a chiral endocon to give pairs of diastereoisomeric conjugates, perhaps at different rates. The first case shows substrate enantioselectivity whereas the second exhibits substrate/product enantioselectivity. The formation of diastereoisomeric conjugates is of considerable significance since they will have different physico-chemical properties: this underlies their facile chromatographic discrimination without the need for chiral phases. Examples include the glucuronides of 2-phenylpropionic acid [19] and oxazepam, the glutamine conjugate of 4-chlorophenoxypropionic acid and the glutathione conjugates of bromoisovalerylurea and bromovaleric acid [20].

A number of examples can be cited to show the importance of conjugation reactions for discrimination between enantiomers in biological systems. The anti-inflammatory drug carprofen shows enantioselective glucuronidation (Fig. 1), which governs its pharmacokinetic properties. The renal clearance of the (S)-D-glucuronide diastereoisomer is twice that of the (*R*)-D-glucuronide epimer. Since there is preferential conjugation of (*S*)-carprofen, the result is

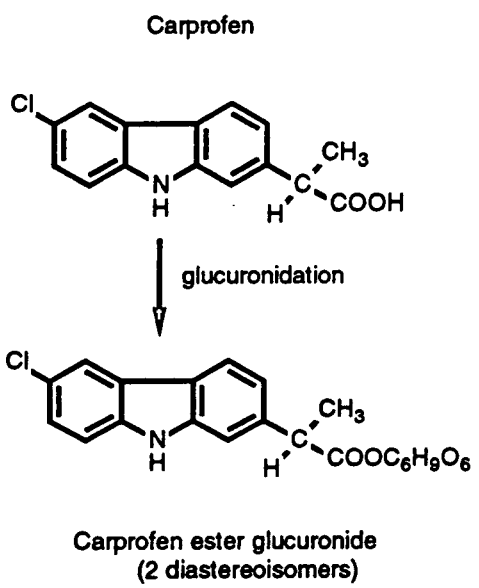


Fig. 1. Conjugation of the anti-inflammatory acid carprofen with glucuronic acid to yield diastereomeric glucuronides.

that the area under the plasma concentration–time curve (AUC) of both (*S*)-carprofen and its glucuronide are lower than those of the *R*-enantiomer [21].

The major biliary metabolites of both (+)- and (−)-menthol are their glucuronides, there being a twofold difference in the rates of their formation by rat liver slices and by rat hepatic microsomes [22]. The plasma elimination half-life of (−)-menthol is 2.4 h compared with 4.0 h for (+)-menthol, with the plasma AUC of (−)-menthol being threefold less than for the (+)-isomer. These pharmacokinetic differences arise from the enormous difference between the isomers in terms of the biliary excretion of their glucuronides: 69% of a dose of the more rapidly cleared (−)-menthol is excreted in the bile in 24 h compared with only 32% for (+)-menthol.

There are numerous other examples of enantioselectivity in the formation of glucuronic acid conjugates with a variety of drug classes, including the 2-arylpropionic acid anti-inflammatory drugs, β-blockers and tricyclic antidepressants.

Many examples can be cited to show the substrate enantioselectivity of glutathione conjugation, notably with epoxides. A well documented example of the importance of the stereochemistry of glutathione conjugation in the metabolism and excretion of a compound is that of bromoisovalerylurea (BIU), which has been systematically studied by Mulders et al. [20]. This now outmoded ureide hypnotic is chiral at the carbon bearing the bromine atom and the major routes of its metabolism are amide hydrolysis to bromoisovaleric acid (BI) and displacement of the bromine atom by glutathione (Fig. 2). The diastereoisomeric isovalerylureide–glutathione (IU–(*S*)-G) conjugates are readily separated by reversed-phase HPLC, allowing the relative rates of the formation and metabolism to be studied. In rat hepatocytes, (*R*)-BIU is converted into both (*R*)-IU–(*S*)-G and (*R*)-BI, but the (*R*)-BI so formed is not conjugated with glutathione (Fig. 3). In contrast, the major pathway of (*S*)-BIU metabolism is hydrolysis, with only small amounts of (*S*)-IU–(*S*)-G formed, but in this case (*S*)-BI is extensively conjugated with glutathione (Fig. 3). The implications of these find-

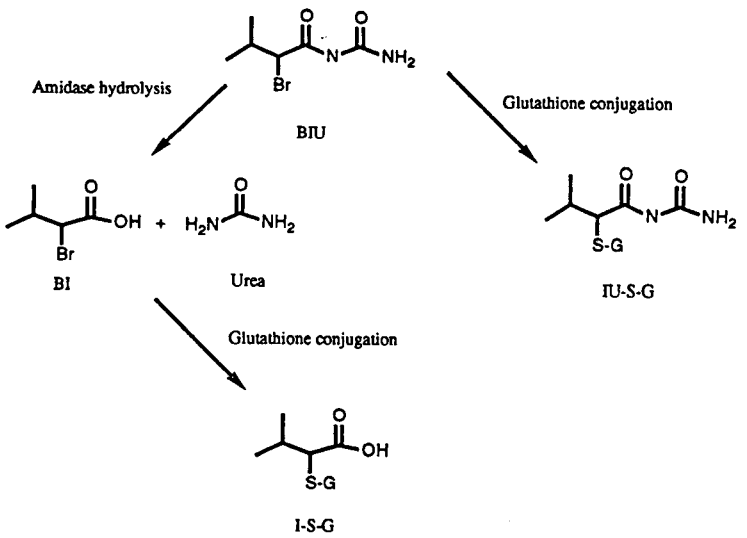


Fig. 2. Metabolic pathways of bromoisoval (2-bromoisovalerylurea).

ings for the eliminations of BIU are harder to discern. Much more (*R*)-IU–(*S*)-G is excreted in rat bile than its *S*-epimer, which agrees with the stereoselectivity of their formation.

Glutathione conjugates undergo extensive further metabolism prior to urinary elimination: in the rat, the major excretion products are mercapturic acids (S-substituted N-acetylcysteine conjugates, produced by hydrolysis and N-acetylation), whose stereochemistry cannot be easily related to that of their parent glutathione conjugates.

### 2.4. Chiral to non-chiral transformations

Chirality may be lost by oxidative metabolism at a chiral centre, e.g., oxidation of secondary alcohols to yield ketones [5], deamination of amphetamine to yield phenylacetone [5,23] and oxidative aromatization of the dihydropyridine calcium channel blocking drugs such as nilvadipine. Such examples are rare, in part owing to the failure to search for them effectively.

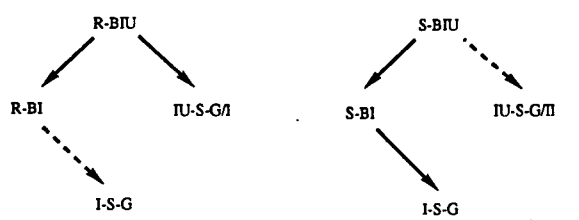


Fig. 3. Stereochemistry of the major metabolic routes of bromoisoval.

### 2.5. Metabolic chiral inversion

Certain drugs, e.g., oxazepam and thalidomide (Fig. 4), undergo rapid and extensive chemical racemization in vivo so that data concerning the biological properties of a single enantiomer should be viewed with some caution [24–26]. In addition, there are significant cases where metabolic chiral inversion can occur which have great impact on the biological properties of the drugs concerned. Indeed, these reactions are the origin of much of the current interest in stereochemistry in drug development.

Studies on the chiral inversion reaction have mainly involved the 2-arylpropionic acid (the "profens") non-steroidal anti-inflammatory drugs (NSAIDs) [27,28]. These agents possess a chiral centre $\alpha$- to the carboxyl group and their pharmacological activity resides mainly in the enantiomers of the *S*-absolute configuration, the *R*-enantiomers being only weakly active or inactive in in vitro test systems [29–31]. These

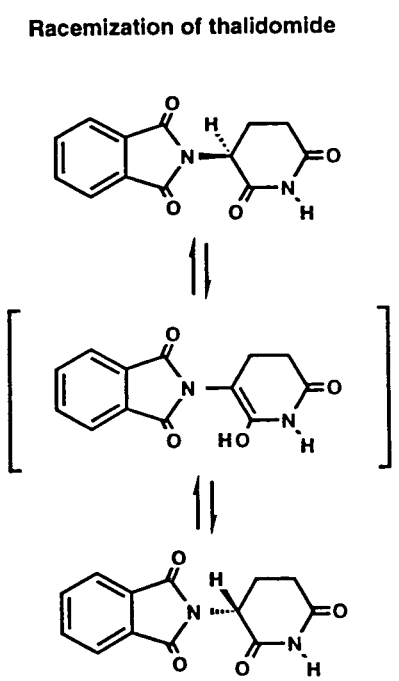


Fig. 4. Chemical racemization of thalidomide in aqueous solution at pH 7.4.

differences in in vitro activity become much less marked in vivo, mainly owing to the metabolic inversion of chirality of the *R*-enantiomers to their active *S*-antipodes [29,30]. The reaction therefore represents a metabolic activation of the *R*-enantiomers, which in some cases may be regarded as pro-drugs for the *S*-isomers.

Since the initial observations with ibuprofen, numerous related 2-arylpropionic acid NSAIDs have been shown to undergo chiral inversion, the extent of which depends on both the structure of the profen and the animal species under investigation.

The mechanism of the inversion reaction is thought to involve the stereospecific formation of a coenzyme A thioester from the *R*-enantiomer of the profen, which undergoes a number of alternative fates:

(i) racemization of the chiral centre in the profen moiety followed by hydrolysis to yield a mixture of enantiomers of the parent molecule;

(ii) hydrolysis with retention of configuration to yield the original (*R*)-2-arylpropionate; or

(iii) acyl transfer of the profen moiety to glycerol resulting in the formation of a hybrid triglyceride.

There are therefore a number of enzymic steps associated with the inversion of these agents, some of which may have toxicological significance.

The involvement of a coenzyme A thioester in the inversion reaction was first shown by Nakamura et al. [32]. Using a rat liver homogenate preparation, they reported that the formation of ibuprofen CoA thioester was dependent on both coenzyme A and ATP. Although synthetic samples of both (−)-(*R*)- and (+)-(*S*)-ibuprofen CoA thioesters were found to undergo racemization and hydrolysis on incubation with rat liver homogenates, only (−)-(*R*)-ibuprofen was converted into a thioester enzymatically. Knadler and Hall [33] examined the enantiomeric composition of the material incorporated into the thioesters and found this to be close to unity irrespective of the form of the compound used, i.e., the *R*-enantiomer or the racemate. Hence the thioesters once formed are racemized readily.

The formation of CoA thioesters of the profens may have considerable toxicological significance. Fears and Richards [34], using racemic mixtures of a number of profens, showed that these compounds were able to inhibit cholesterogenesis and fatty acid synthesis in vitro and that this activity was correlated with their ability to form hybrid triacylglycerols. The formation of such lipid acylglycerols and their incorporation into membranes have the potential to alter membrane structure and may be associated with disordered membrane function [35]. These effects are presumably related to the ability of these compounds to form acyl CoA thioesters with the acyl moiety being transferred to glycerol rather than undergoing hydrolysis to liberate the free profen. If the above is the mechanism, then the stereochemical composition of the profen should influence the incorporation into lipid.

This was first shown to be the case using racemic ibuprofen and its individual enantiomers. Following chronic administration of ibuprofen to rats, samples of fat were collected, the triglycerides were isolated and the stereochem-

istry of the incorporated material was investigated. Incorporation was greatest following administration of the *R*-enantiomer and the levels of both (*R*)- and (*S*)-ibuprofen in lipids were approximately twice those following administration of the racemate. Only trace amounts of drug were found in triglycerides following administration of the *S*-enantiomer [36]. The stereoselective incorporation of (*R*)-fenoprofen into hybrid triacylglycerols has also been reported using hepatocyte and adipocyte preparations [37].

That chiral inversion and lipid incorporation are closely associated is demonstrated by a comparison of the metabolic clearance of the *R*-enantiomers via inversion to the rate of profen incorporation into lipid. Thus fenoprofen undergoes extensive inversion and lipid incorporation, whereas flurbiprofen undergoes no detectable incorporation into lipid and low inversion [38,39].

An example of metabolic inversion which appears to be unrelated to the inversion of the 2-arylpropionic acid derivatives is provided by mandelic acid. This compound has been known to undergo chiral inversion in bacteria, from the *S*-enantiomer to its *R*-antipode, for a number of years [40], but only recently has this reaction been observed in rodents. Following administration of (*S*)-mandelic acid to rats, about 16% of the dose was eliminated in urine in 24 h apparently unchanged. However, an examination of the stereochemical composition of the material the *R*:*S* enantiomeric ratio was found to be 4:1 [41]. The remainder of the dose was recovered as phenylglyoxylic acid. In bacteria, the isomerization of mandelic acid is mediated by mandelate racemase [42], but the mechanism in the rat is unknown.

## 3. Pharmacogenetics and the stereochemistry of metabolism

"Pfeiffer's rule", which generalizes that the more potent a drug is, the more likely it is to show stereoselectivity of action as a consequence of the greater steric demand for tight receptor binding, may have parallels in drug metabolism. However, the drug-metabolizing enzymes have always been regarded as showing little substrate selectivity, making such generalizations difficult. In the past 10 years, it has become clear that the relative lack of substrate specificity of the major drug-metabolizing enzymes is illusory and that it is the net result of the activities of families of isozymes which often have marked, but overlapping, catalytic specificities. It may therefore be the case that an enzyme with marked specificity may well show stereoselectivity, and this is case with two cytochrome P450 isozymes, CYP2D6, which catalyses the 4-hydroxylation of debrisoquine, and CYP2C18, which performs the aromatic hydroxylation of mephenytoin.

The metabolism of mephenytoin in man is highly stereoselective. (*S*)-Mephenytoin is rapidly metabolized by aromatic hydroxylation to 4-hydroxymephenytoin, a phenolic product which is eliminated rapidly in urine as a glucuronide. However, the inability of the liver to hydroxylate (*R*)-mephenytoin in position 4 of the aromatic ring leads to the alternative metabolic pathway of oxidative demethylation to form 5-phenyl-5-ethylhydantoin (PEH) [43]. The elimination kinetics of the two enantiomers are markedly different, with the *S*-isomer having a half-life of around 4 h and about 47% of a dose of mephenytoin eliminated in the urine as its 4-hydroxy metabolite in 24 h. By contrast, the elimination half-life of PEH is 5–6 days, such that it accumulates upon repeated administration, reaching a steady state over 2–3 weeks. CYP 2C18 exhibits a genetic polymorphism, with a deficiency in this activity being inherited as an autosomal recessive trait. This polymorphism also affects the metabolism of diazepam and mephobarbital [44]. The incidence of the poor metabolizer phenotype varies from 4–5% in Caucasians from Switzerland, Canada and the USA to 13% in Canadian Orientals and 29% in Japanese resident in Canada [44].

The best known of the human genetic polymorphisms of drug oxidation is that affecting the metabolism of debrisoquine and arises from the virtual absence of CYP2D6 from the poor metabolizer phenotype. Drugs such as debrisoquine which are subject to this polymor-

phism are substrates almost exclusively metabolized by this isozyme. Debrisoquine itself is achiral but a number of other compounds whose metabolism is influenced by the polymorphism contain chiral centres and in a number of these cases CYP2D6, a high-affinity, low-capacity isozyme, is able to discriminate between the enantiomers [45,46].

A very significant example of the stereoselectivity of the CYP2D isozymes is given by their differential inhibition by the Cinchona alkaloids, quinine and quinidine, which differ in their configuration at C-8 and C-9 (quinine is 8*S*, 9*R* and quinidine is 8*R*, 9*S*). Quinidine inhibits the human isozyme CYP2D6, converting the predominant extensive metabolizer (EM) phenotype for debrisoquine and sparteine into "phenocopies" of the poor metabolizer (PM) phenotype, which are markedly deficient in CYP2D6 activity [47]. In contrast, quinine has no effect on the metabolism of typical CYP2D6 substrates in humans [47]. The rat orthologue of CYP2D6 is CYP2D1, which shows comparable substrate selectivity. The female dark agouti (DA) rat seemingly lacks CYP2D1 and provides a limited animal model of the human debrisoquine PM phenotype. However, in the rat, the stereoselectivity of CYP2D inhibition by the Cinchona alkaloids is reversed, with quinine inhibiting CYP2D1 whereas quinidine has no effect.

## 4. Conclusions

More and more new drugs are designed to interact with targets that can be described in atomic detail and chiral discrimination by these targets has to be taken into account ab initio in the design process. In such cases, enantiomeric discrimination by pharmacokinetic and metabolic processes is of academic interest only, since only the active stereoisomers will be advanced into development and use. However, interest in this area has led to the re-examination of a large number of chiral drugs already under development or in use as racemic mixtures to see if they might be improved if used in stereochemically pure form. It should be noted that recent great advances in chemical- and biotechnology-based synthesis mean that for the first time a very wide range of stereochemically pure drugs can be made available on a commercial scale. The use of stereochemically pure drugs would be expected to be advantageous by (i) reducing the total dose given, (ii) simplifying dose–response relationships, (iii) removing a source of inter-subject variability and (iv) minimizing toxicity due to the inactive isomer. The steeper the dose–response curve, the greater the benefit to be expected. It is important to appreciate that although the differences between the total clearances of stereoisomers of chiral drugs may be small, these are the composite of the many processes of absorption, distribution, metabolism and excretion.

This brief review has highlighted the exquisite stereoselectivities which can occur in the metabolism of drugs and other xenobiotics whose considerable magnitude often belies relatively small differences in total clearance. The decision as to the relative value of racemate or pure enantiomer is multifactorial and is driven by the magnitude and significance of the pharmacodynamic and pharmacokinetic differences and their clinical significance as well as marketing advantages. It is evident that metabolic studies are central to decision making in this area and there is every justification for the most detailed consideration of the stereochemistry of drug metabolism at every stage through drug development and safety evaluation.

## Acknowledgement

I am very grateful to Mrs Sheila Rose for her assistance with the preparation of the manuscript.

## References

[1] B. Testa and J. Caldwell, *Trends Pharm. Sci.*, 9 (1988) 90–96.

[2] S. Allenmark, in S. Allenmark (Editor), *Chromatographic Enantioseparation: Methods and Applications*, Ellis Horwood, Chichester, 1988.
[3] M. Zief and L.J. Crane, in M. Zief and L.J. Crane (Editors), *Chromatographic Chiral Separations*, Marcel Dekker, New York, 1988.
[4] A.M. Krstulovic, in A.M. Krstulovic (Editor), *Chiral Separations by High Performance Liquid Chromatography: Applications to Pharmaceutical Compounds*, Ellis Horwood, Chichester, 1989.
[5] P. Jenner and B. Testa, *Drug Metab. Rev.*, 2 (1973) 117–184.
[6] B. Testa and P. Jenner, in P. Jenner and B. Testa (Editors), *Concepts in Drug Metabolism*, Part A, Marcel Dekker, New York, 1980, Ch. 2, p. 53.
[7] B. Testa and W.F. Trager, in D.D. Breimer and P. Speiser (Editors), *Topics in Pharmaceutical Sciences*, Elsevier, Amsterdam, 1983, p. 99.
[8] W.F. Trager and B. Testa, in G.R. Wilkinson and M.D. Rawlins (Editors), *Drug Metabolism and Disposition: Considerations in Clinical Pharmacology*, MTP Press, Lancaster, 1985, p. 35.
[9] B. Testa, *Trends Pharmacol. Sci.*, 7 (1986) 60–64.
[10] V. Prelog, *Ind. Chim. Belge*, 11 (1962) 1309.
[11] D.D. Nicholl, G. Edwards, S.A. Ward, M.L. Orme and A.M. Breckenridge, *Biochem. Pharmacol.*, 36 (1987) 3365–3369.
[12] M. Salmona, R. Saroma, R. Bianchi, F. Marcucci and E. Mussini, *J. Pharm. Sci.*, 63 (1974) 222–225.
[13] G. Maksay, Z. Tegyey and L. Otvös, *J. Pharm. Sci.*, 67 (1978) 1208–1210.
[14] W.K. Wilson, S.B. Baca, Y.J. Barber, T.J. Scallen and C.J. Marrow, *J. Org. Chem.*, 48 (1983) 3960–3966.
[15] C.Y. Quon, K. Mai, G. Patil and H.F. Stampfli, *Drug Metab. Dispos.*, 16 (1988) 425–428.
[16] K. Miyano, Y. Fujii and S. Toki, *Drug Metab. Dispos.* 8 (1980) 104–110.
[17] R.J. Lewis, W.F. Trager, K.K. Chan, A. Breckenridge, M. L'Orme, M. Rowland and W. Schary, *J. Clin. Invest.*, 53 (1974) 1607–1617.
[18] J.J.R. Hermans and H.H.W. Thijssen, *Drug Metab. Dispos.*, 20 (1992) 268–274.
[19] S. Fournel and J. Caldwell, *Biochem. Pharmacol.*, 35 (1986) 4153–4159.
[20] T.M.T. Mulders, V. Venizelos, R. Schoemaker, A.F. Cohen, D.D. Breimer and G.J. Mulder, *Clin. Pharmacol. Ther.*, 53 (1993) 49–58.
[21] S. Iwakawa, T. Suganuma, S.-F. Lee, H. Spahn, L.Z. Benet and E.T. Lin, *Drug Metab. Dispos.*, 17 (1989) 414–419.
[22] P.J. Eddershaw, T. Yamaguchi and J. Caldwell, in *V International Congress of Toxicology. Basic Science in Toxicology. Abstracts. Proceedings of the 5th International Congress of Toxicology. Brighton, July 1989*, Taylor & Francis, London, 1989, p. 44.
[23] J. Wright, A.K. Cho and J. Gal, *Xenobiotica*, 7 (1977) 257–266.
[24] Y. Aso, S. Yoshioka, T. Shibazaki and M. Uchiyama, *Chem. Pharm. Bull.*, 36 (1988) 1834–1840.
[25] S.K. Yang and X.-L. Lu. *J. Pharm. Sci.*, 78 (1989) 789–795.
[26] B. Testa, P.A. Carrupt and J. Gal, *Chirality*, 5 (1993) 105–111.
[27] A.J. Hutt and J. Caldwell, *J. Pharm. Pharmacol.*, 35 (1983) 693–704.
[28] J. Caldwell, A.J. Hutt and S. Fournel-Gigleux, *Biochem. Pharmacol.*, 37 (1988) 105–114.
[29] S.S. Adams, P. Bresloff and C.G. Mason, *J. Pharm. Pharmacol.*, 28 (1976) 256–257.
[30] A.J. Hutt and J. Caldwell, *Clin. Pharmacokinet.*, 9 (1984) 371–373.
[31] W.F. Kean, C.J.L. Lock, J. Rischke, R. Butt, W.W. Buchanan and H. Howard-Lock, *J. Pharm. Sci.*, 78 (1989) 324–327.
[32] Y. Nakamura, T. Yamaguchi, S. Takahashi, S. Itashimoto, K. Iwatani and Y. Nagagawa, *J. Pharmaco-Biodynam.* 4 (1981) S-1.
[33] M.P. Knadler and S.D. Hall, *Chirality*, 2 (1990) 67–73.
[34] R. Fears and D.H. Richards, *Biochem. Soc. Trans.*, 9 (1981) 572.
[35] J. Caldwell and M.V. Marsh, *Biochem. Pharmacol.*, 32 (1983) 1667–1672.
[36] K. Williams, R.O. Day, R. Knihinicki and A. Duffield, *Biochem. Pharmacol.*, 35 (1986) 3403–3405.
[37] B.S. Sallustio, P.J. Meffin and K.M. Knights, *Biochem. Pharmacol.*, 37 (1988) 1919–1923.
[38] R. Fears, K.H. Baggaley, R. Alexander, B. Morgan and R.M. Hindley, *J. Lipid. Res.*, 19 (1978) 3–11.
[39] K.M. Williams, *Pharmacol. Ther.*, 46 (1990) 273–295.
[40] G.L. Kenyon and G.D. Hegeman, *Biochemistry*, 9 (1970) 4036–4043.
[41] L. Drummond, J. Caldwell and H.K. Wilson, *Xenobiotica*, 20 (1990) 159–168.
[42] G.D. Hegeman, E.Y. Rosenberg and G.L. Kenyon, *Biochemistry*, 9 (1970) 4029–2036.
[43] A. Kupfer, P.V. Desmond, S. Schenker and R.A. Branch, *J. Pharmacol. Exp. Ther.*, 221 (1982) 590–597.
[44] G.R. Wilkinson, F.P. Guengerich and R.A. Branch, in R. Kalow (Editor), *Pharmacogenetics of Drug Metabolism*, Pergamon, New York, 1992, Ch. 23, p. 657.
[45] M.S. Lennard, G.T. Tucker, H.F. Woods, A.O. Iyun and M. Eichelbaum, *Biochem. Pharmacol.*, 37 (1988) 97–98.
[46] L. Koymans, N.P.E. Vermeulen, S.A.B.E. van Acker, J.M. te Koppele, J.J.P. Heykants, K. Lavrijsen, W. Meuldermans and G.M. Donne-Op den Kelder, *Chem. Res. Toxicol.*, 5 (1992) 211–219.
[47] R. Ayesh, S. Dawling, A. Hayler, N.S. Oates, S. Cholerton, B. Widdop, J.R. Idle and R.L. Smith, *Chirality*, 3 (1991) 14–18.

ELSEVIER

Journal of Chromatography A, 694 (1995) 49–56

JOURNAL OF CHROMATOGRAPHY A

# Influence of the method of preparation of chiral stationary phases on enantiomer separations in high-performance liquid chromatography

Toshihide Ihara*, Yoshio Sugimoto, Makoto Asada, Tatsuro Nakagama, Toshiyuki Hobo

*Department of Industrial Chemistry, Faculty of Technology, Tokyo Metropolitan University, 1-1 Minami-Ohsawa, Hachioji, Tokyo 192-03, Japan*

**Abstract**

Various chiral stationary phases were immobilized on supports using suitable alkyl spacers. Aminopropylsilica, which is aminopropylsilylated silica gel, is a typical spacer-carrying support for immobilization. Silanol and aminopropyl groups left unreacted on the support surface disturb the separation of enantiomers through a non-chiral interaction. The following three types of chiral stationary phases were prepared using different preparation methods and the effect of the total structure on the chiral separation was studied: (1) a chiral group was immobilized on aminopropylsilica; (2) a chiral group connected with a spacer was immobilized on silica gel; and (3) a chiral group connected with a spacer was immobilized on dimethylchlorosilane-treated silica gel. It was shown for (1) that when the amount of chiral groups immobilized was lower, free silanol groups and unreacted amino groups would preferentially interact with sample molecules. When the amount immobilized was increased, its interaction with samples became effective, and also aminopropyl groups left unreacted were thought to enhance the interaction. Too many chiral groups, however, resulted in lower separability. In case (2), a similar tendency to that with (1) but lower separabilities were obtained. A more effective performance was found with (3), with lower immobilization. For the preparation of an effective chiral stationary phase, the amount of chiral groups on the support and the structural and topographical conditions of the support material should be assessed.

## 1. Introduction

As an effective method for the separation of optical isomers, high-performance liquid chromatography with various chiral stationary phases (CSPs) has been widely used [1]. The chiral separation is often provided by the differences in the diastereomeric association energy between analytes and a chiral selector introduced to the stationary phase.

The chiral stationary phases are usually prepared by immobilizing chiral molecules on siliceous supports by way of appropriate alkyl spacers. Aminopropylsilica, prepared by aminoalkylation of silica gel [2], has frequently been used as the support material for the immobilization of chiral molecules. Unreacted silanol groups and amino groups remaining on the stationary phase after the immobilization reaction do not work for the chiral separation. The effect of residual silanol groups on the selectivity of the stationary phase has been discussed by many workers [3,4].

* Corresponding author.

0021-9673/95/$09.50 
*SSDI* 0021-9673(94)00753-5

Greater enantioselectivity was observed with end-capped chiral stationary phases, which were investigated by Pirkle and Readnour [5]. We have previously [6] investigated the effect of unreacted alkyl spacers on chiral separations by changing the amount of the chiral selector, and found that the total immobilized structure should be taken into consideration.

In this study, Pirkle type stationary phases [7], with which the separation mechanism has been precisely investigated, were chosen. Three types of stationary phases with the same chiral selector but differing in their total structures were prepared, and the effect of the total structure of the stationary phase including the residual silanol groups on the separation was investigated. Previously, we discussed thirteen chiral diamide-type stationary phases [8], including Pirkle-type phases. The phase that showed the highest separability was the immobilized 3,5-dimethylbenzoyl-L-valine phase for N-3,5-dinitrobenzoyl-O-isopropyl-derivatized amino acids. In this work, 3,5-dimethylbenzoyl-L-valine (DMB-L-Val) chiral selector was immobilized through different routes on the support surface, and the enantiomer separability was examined.

## 2. Experimental

### 2.1. Instrumentation

The chromatographic equipment consisted of a Shimadzu (Kyoto, Japan) Model LC-9A high-pressure pump, a Rheodyne (Cotati, CA, USA) Model 7125 sampling valve with a 25-$\mu$l loop, a Shimadzu Model SPD-6AV variable-wavelength UV–Vis spectrophotometric detector and a Shimadzu C-R4A integrator. The column (150 × 2.1 mm I.D.) was packed with modified silica gel using the slurry packing technique. The mobile phase was chosen to be 2-propanol–hexane (5:95) at a flow-rate of 250 $\mu$l/min. The detection wavelength used was 254 nm. The hold-up time was measured using the peak of 1,3,5-tri-*tert.*-butylbenzene.

### 2.2. Samples

Amino acids were used as test samples. The carboxylic group was esterified with 2 *M* HCl–2-propanol solution at 120°C for 2 h under reflux. The amino group was treated with 3,5-dinitrobenzoyl chloride to give the corresponding benzoylamide. After derivatization, the samples were purified by column chromatography using a silica gel column and hexane–ethyl acetate (10:1) as the mobile phase.

### 2.3. Synthesis of CSP-A

*Preparation of 3,5-dimethylbenzoyl-L-valine*

L-Valine was acylated with 3,5-dimethylbenzoyl chloride by the Schotten–Baumann procedure. The method of preparation in the literature [9] was partly employed.

*Preparation of aminopropyl-functionalized silica*

A porous silica (Develosil silica 100-5, mean particle size 5 $\mu$m, mean pore size 100 Å and specific surface area 350 $m^2/g$) (Nomura Chemical) was dried at 160°C and 20 Pa for 5 h. An excess of aminopropyldimethylethoxysilane (Sinetsu Chemical) in 13.2 ml (70 mmol) of toluene was added to 10 g of dried silica gel. The mixture was heated at reflux until ethanol was no longer removed azeotropically. After cooling, the modified gel was filtered and washed successively with toluene, tetrahydrofuran, methanol, acetone and diethyl ether and finally dried under vacuum. Elemental analysis gave the amount of the aminopropyl groups as 0.987 mmol/g.

*Preparation of CSP-A*

Different amounts of 3,5-dimethylbenzoyl-L-valine(DMB-L-Val) in 100 ml of dry tetrahydrofuran were mixed with 1.2 g of aminopropyl-functionalized silica gel and 1-ethoxycarbonyl-2-ethoxy-1,2-dihydroquinoline (EEDQ) in 1.2 times the molar amount of DMB-L-Val was added [10,11]. The suspension was stirred for 1 day under an argon atmosphere at room temperature. The bonded phase was filtered and washed with tetrahydrofuran, methanol, acetone

and diethyl ether. After drying, the coverage densities of the chiral selector were calculated from the carbon contents obtained by elemental analysis. All of these compounds were confirmed by $^1$H NMR and fast atom bombardment MS.

### 2.4. Synthesis of CSP-B

*Preparation of 3,5-dimethylbenzoyl-L-valine allylamide*

Six grams (24 mmol) of DMB-L-Val were dissolved in 200 ml of dry ethyl acetate. To the solution, stirred and cooled to −18°C by a CTP-100 cooling thermo pump (Tokyo Scientific Chemical), was added 3.3 g (29 mmol) of N-hydroxysuccinimide and 5.9 g (29 mmol) of dicyclohexylcarbodiimide under an argon atmosphere. After stirring the reaction mixture for 24 h at −18°C, the suspension was warmed slowly (12 h) to room temperature under continuous stirring. Subsequently, the white precipitate of dicyclohexylurea thus formed was removed by filtration, and the resulting clear solution was evaporated. To the residual oil were added 200 ml of dry tetrahydrofuran and the mixture was cooled to −18°C under an argon atmosphere. Then, a mixture of 3.7 ml (34 mmol) of N-methylmorpholine and 2.6 ml (34 mmol) of allylamine in 30 ml of dry tetrahydrofuran were dropwise added to the stirred solution over 1 h. After the solution had been kept stirred for 48 h, the solvent was evaporated. The residue was dissolved in chloroform and the solution was washed with 0.1 *M* hydrochloric acid and then with 5% sodium hydrogen carbonate, and finally dried under vacuum.

*Preparation of 3,5-dimethylbenzoyl-L-valine dimethylchlorosilylpropylamide*

To a solution of DMB-L-Val allylamide, 1.8 g (6.4 mmol) and 0.044 g (0.064 mmol) of $H_2PtCl_6$ in 70 ml of chloroform were added 11.3 ml (102 mmol) of dimethylchlorosilane. The mixture was then heated at reflux for 5 h, the solvent and excess silane were removed in vacuo and the residue was used in the next step without purification.

*Preparation of CSP-B*

Different amounts of silylated DMB-L-Val in 50 ml of dry toluene were mixed with 1.6 g of dried silica gel (160°C, 5 h), and a small amount of pyridine was added. The suspension was stirred for 1 day under an argon atmosphere at room temperature. The bonded phase was filtered and washed with chloroform, toluene, tetrahydrofuran, methanol, acetone and diethyl ether.

### 2.5. Synthesis of end-capped CSP-B

CSP-B (0.8 g) was suspended in 50 ml of dry toluene and 1.2 ml (5.6 mmol) of 1,1,1,3,3,3-hexamethyldisilazane were added. After refluxing the mixture for 3 h under an argon atmosphere, the modified gel was collected by filtration and washed successively with toluene, tetrahydrofuran, methanol, acetone and diethyl ether.

### 2.6. Synthesis of CSP-C

*Preparation of silanized silica gel (pre-end-capped silica)*

A 15-ml volume (14 mmol) of dimethylchlorosilane (Sinetsu Chemical) in 150 ml of toluene was added to 10 g of dried silica gel. The mixture was stirred for 24 h under an argon atmosphere at room temperature. Then, the pre-end-capped silica gel was filtered and washed with toluene, tetrahydrofuran, methanol, acetone and diethyl ether and dried under vacuum. The amount of the dimethylchlorosilyl function was determined to be 0.598 mmol/g from elemental analysis.

*Preparation of CSP-C*

Different amounts of DMB-L-Val allylamide in 100 ml of dry tetrahydrofuran were mixed with 0.8 g of pre-end-capped silica gel. After adding a small amount of dicyclopentadienylplatinum dichloride as the platinum catalyst, the mixture was stirred for 5 h under an argon atmosphere at 60°C. The bonded phase was filtered and washed with tetrahydrofuran, methanol, acetone and diethyl ether.

## 3. Results and discussion

In the case of CSP-A type immobilization, the chiral moiety was immobilized after attaching the alkyl spacer to the silica gel. A certain amount of unreacted amino groups was present on the silica gel after reaction as shown in Fig. 1. In order to examine the effects of the extent of bonding of the chiral moiety, and the remaining amount of amino groups, CSPs with different coverage densities of the chiral moiety were prepared by changing the mixing ratio of DMB-L-Val to aminoalkylated silica gel (coverage density 1.70 groups/nm$^2$). The amount of the chiral selector was estimated by elemental analysis of carbon. Then the number of groups per unit surface area of silica gel was calculated. These phases were evaluated mainly by separation factors and capacity factors of the derivatized enantiomer samples. Separation factors on six different CSP-A type phases are shown in Fig. 2. The phases with coverage densities of not more than 0.1 groups/nm$^2$ showed a very low separability of enantiomers. Considering that the remaining aminopropyl groups do not work for the chiral separation, when the amount of the immobilized chiral selector is small, analytes are retained mainly by the residual amino and silanol groups. When the coverage densities were between 0.3 and 0.5 groups/nm$^2$, the residual aminopropyl groups were thought to enhance the enantioselectivity. As in the usual cases, the separation factor of D,L-leucine derivatives is far higher than those of alanine and valine. Coverage densities higher than 0.5 groups/nm$^2$ did not result in a higher separation factor. This result demonstrates that optimum amounts of the chiral selector exist for the separation of enantiomers. When the density of the chiral selector is too high, the interaction between the selector and the analyte might be blocked. We speculate that the self-association, described in a previous paper [12], of the selectors occurs in that region.

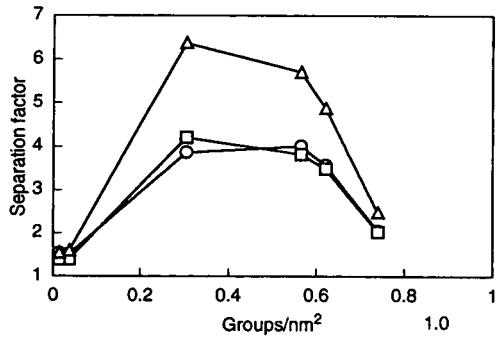


Fig. 2. Relationship between separation factor and the coverage density of CSP-A phase. ○ = N-(3,5-Dinitrobenzoyl)alanine isopropyl ester; □ = N-(3,5-dinitrobenzoyl)-valine isopropyl ester; △ = N-(3,5-dinitrobenzoyl)leucine isopropyl ester. Column, 150 × 2.1 mm I.D.; mobile phase, 2-propanol–*n*-hexane (5:95, v/v); flow-rate, 250 μl/min; column temperature, room temperature; detection, UV at 254 nm.

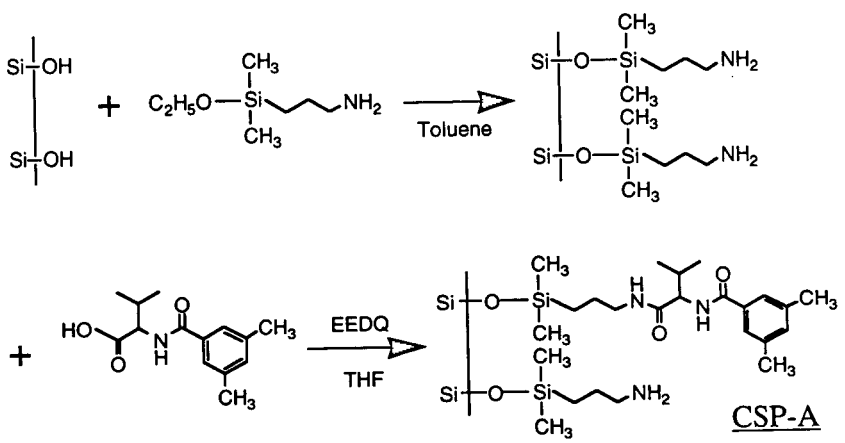


Fig. 1. Preparation scheme for CSP-A phase.

The optimum values of coverage density were different from analyte to analyte, and the reason was considered to be due in part to the difference in the spaces needed for the formation of complexes between the stationary phase and analytes.

With CSP-B type phases, DMB-L-Val was first reacted with the spacer, allylamine, and then the product was reacted with dimethylchlorosilane. This chiral selector was directly reacted with the silica gel, so that the prepared CSP was completely free from residual amino groups. As shown in Fig. 3A, however, this CSP has remaining silanol groups on the silica gel surface. These residual silanol groups show a non-chiral interaction with analytes, and therefore are considered to suppress the enantioselectivity. Thus, end-capped CSP-B type phases were further modified by end-capping, which minimized the number of silanol groups on the surface as shown in Fig. 3B.

The separation factors on five different CSP-Bs and end-capped CSP-Bs with different coverage densities of chiral selector are shown in Figs. 4 and 5. Similarly to CSP-A, the CSP-Bs in Fig. 4 with a coverage density of chiral selector of not

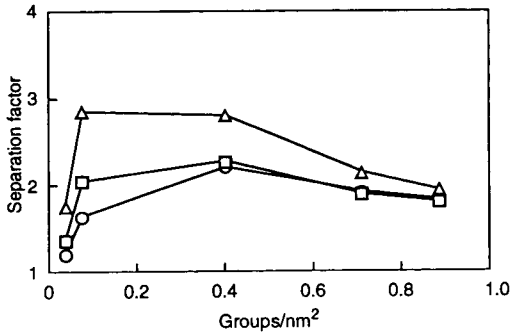


Fig. 4. Relationship between separation factor and the coverage density of CSP-B phase. Conditions as in Fig. 2.

less than 0.4 group/nm$^2$ showed lower separation factors. A low coverage density resulted in an extremely low performance, which was considered to be due to the presence of silanol groups on the silica gel surface. On the end-capped CSP-B with a coverage density not more than 0.2 groups/nm$^2$, a higher selectivity in chiral separation was observed. CSP-Bs with coverage densities higher than 0.3–0.4 groups/nm$^2$ have almost no end-capping effect. Therefore, the silanol groups still remaining were not considered to have a significant effect on the

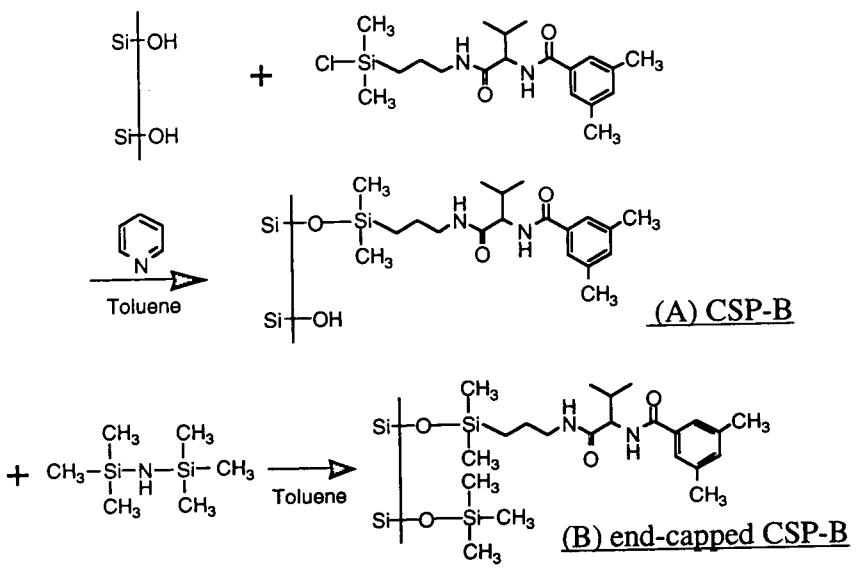


Fig. 3. Preparation schemes for (A) CSP-B and (B) end-capped CSP-B phases.

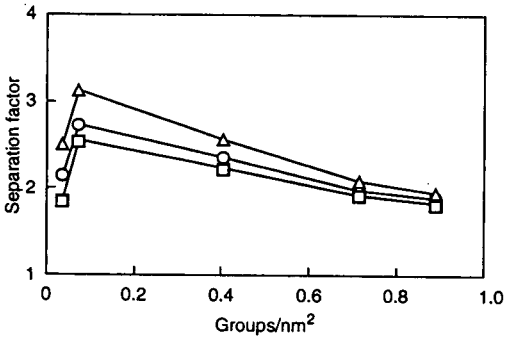


Fig. 5. Relationship between separation factor and the coverage density of end-capped CSP-B phase. Conditions as in Fig. 2.

performance. When the coverage density was extremely low, CSP-B type phases showed a higher performance than CSP-A type stationary phases after end-capping. Previously, Brügger and Arm [13] synthesized urea-linked CSPs, silica gel bonded with different amount of silylurea, with or without end-capped silanol groups. According to Brügger and Arm, silanol groups may interfere with the interactions between the analyte and the chiral selector. For the non-end-capped CSPs, the separation factors decrease with decrease in coverage density. However, on the end-capped CSPs a lower coverage density leads to reduced non-chiral interactions. In this study, with diamide-type CSPs, similar results were obtained.

In order to cover the silanol groups on the surface of silica gel more effectively, we tried another immobilization method, a pre-end-capping method, expecting that the silanol groups on the surface would be more efficiently covered. With the CSP-C type immobilization method shown in Fig. 6, dimethylchlorosilane was first reacted with silica gel (coverage density 1.03 groups/$nm^2$). We chose monochlorosilane as a silylating reagent. Such a type of silane has high reactivity and no possibility of regenerating the silanol groups [14]. Then, DMB-L-Val allylamide was immobilized using a hydrosilylation reaction. By changing the amount of DMB-L-Val allylamide, CSP-Cs with different coverage densities were prepared. Platinum catalyst, $H_2PtCl_6$, is often used in hydrosilylation reactions. It does not work, however, in a highly polar field such as on the silica gel surface, and leads to an extremely low yield of immobilization. Ohtsu et al. [15] synthesized ODS-silica gel by hydrosilylation of Si–H after suppressing the polarity of silica gel by a polysiloxane coating. In this study, however, we found that dicyclopentadienylplatinum dichloride [16] could efficiently catalyse the hydrosilylation of Si–H on the silanized silica gel surface. An immobilization yield as high as about 70% was achieved.

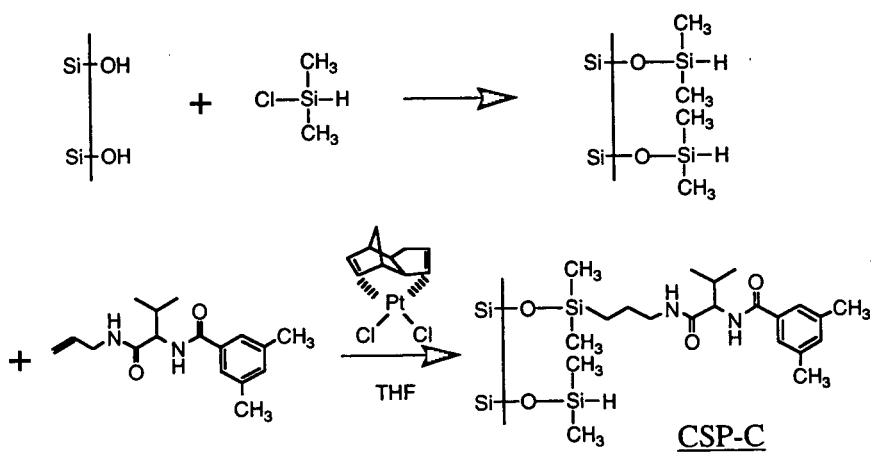


Fig. 6. Preparation scheme for CSP-C phase.

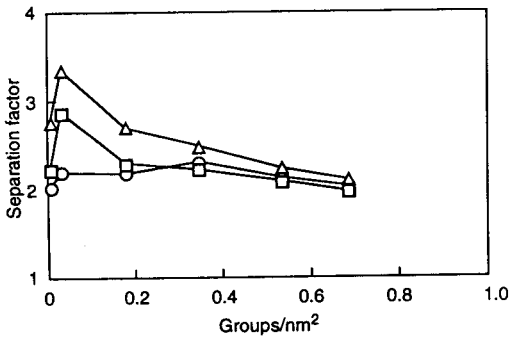


Fig. 7. Relationship between separation factor and the coverage density of CSP-C phase. Conditions as in Fig. 2.

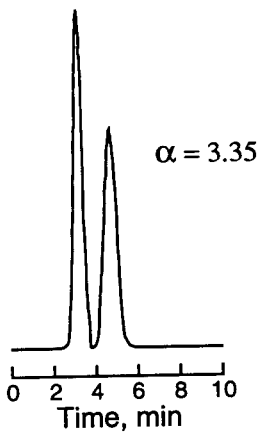


Fig. 8. Chromatogram of N-(3,5-dinitrobenzoyl)leucine isopropyl ester on CSP-C column (coverage density 0.033 groups/nm$^2$). Conditions as in Fig. 2.

The separation factors on six different CSP-Cs with different coverage densities are shown in Fig. 7. The CSP-Cs with a coverage density of not less than 0.3 groups/nm$^2$ showed almost the same properties as CSP-B and end-capped CSP-B, and the pre-end-capping effect was not observed. Therefore, it was concluded that in this instance the chiral separability depends on the coverage density of the chiral selector, and that the effect of the silica gel surface can be neglected. When the coverage density is not higher than 0.2 groups/nm$^2$, however, no decrease in separation factors even at very low coverage density is observed. Even with a coverage density not greater than 0.05 groups/nm$^2$, CSP-C showed a higher enantioselectivity than CSP-A and CSP-B. It could be concluded that the adsorption on silanol groups could be eliminated effectively through the post-end-capping method. The chromatogram shown in Fig. 8 demonstrates a typical separation of D,L-leucine derivatives on CSP-C. It shows a good resolution and small capacity factor.

In Fig. 9, the correlations between the coverage densities and $k'$ values on various CSPs prepared in the present study are shown. On either type of CSPs, the coverage density of the chiral selector showed a positive correlation with capacity factors ($k'$). The increase in $k'$ value with increase in the coverage density of CSPs was similar to those on the non-chiral phases. The decrease in the performance of chiral separation along with the increase in the coverage density of the chiral selector, such as shown in Figs. 2, 4 and 5, means that retention unrelated to the chiral separation occurs predominantly in the interaction between the stationary phase and the analytes. In this study, we used Pirkle-type chiral stationary phases, which utilize hydrogen bonding and the $\pi$-donor–$\pi$-acceptor group interaction. It was considered that the mutual interaction of the selector groups in the stationary phase was increased at higher coverage densities, which leads to a possible inefficiency of the interaction between the analytes and the chiral selector. Therefore, it is necessary to

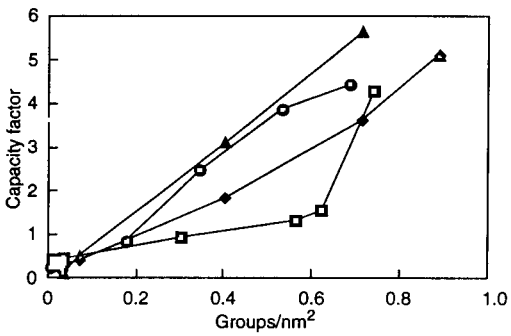


Fig. 9. Capacity factors of N-(3,5-dinitrobenzoyl)-D-leucine isopropyl ester on (□) CSP-A, (◆) CSP-B, (▲) end-capped CSP-B and (●) CSP-C as a function of the coverage density. Conditions as in Fig. 2.

examine the effect of the surface coverage density on the chiral separability of other chiral phases that have different interaction mechanisms.

## 4. Conclusions

The behaviours of the chiral stationary phases were demonstrated to be affected by the method of immobilization of the chiral selector. The chiral separability also varied depending on the coverage density of the chiral selector and the environmental conditions near the chiral selector. Therefore, in order to evaluate a chiral stationary phase, these factors should be taken into consideration. Of the immobilization methods studied, the pre-end-capping method was found to be useful, as it can reduce the amount of chiral selectors required for immobilization. As the time required for analysis is very short owing to the small $k'$ value, this pre-end-capping method could be very suitable for the preparation of other chiral stationary phases. These findings will be applied in our future development of new chiral stationary phases.

## Acknowledgement

The authors acknowledge the support of the Taisho Pharmaceutical (Department of Organic Chemistry of Research Centre).

## References

[1] W.H. Pirkle and T.C. Pochapsky, *Chem. Rev.*, 89 (1989) 347.
[2] R.E. Majors, *J. Chromatogr. Sci.*, 18 (1980) 488.
[3] H. Engelhardt and G. Ahr, *Chromatographia*, 14 (1981) 227.
[4] J. Köhler, D.B. Chase, R.D. Farlee, A.J. Vega and J.J. Kirkland, *J. Chromatogr.*, 352 (1986) 275.
[5] W.H. Pirkle and R.S. Readnour, *Chromatographia*, 31 (1991) 129.
[6] M. Asada, I. Yamada and T. Hobo, in *International Symposium on Molecular Chirality, Tokyo*, 1993, p. 120.
[7] W.H. Pirkle, C.J. Welch and M.H. Hyun, *J. Org. Chem.*, 48 (1983) 5022.
[8] K. Sato, H. Nakano and T. Hobo, *J. Chromatogr.*, 666 (1994) 463.
[9] S.G. Allenmark, *Chromatographic Enantioseparation*, Ellis Horwood, Chichester, 1988, p. 208.
[10] W.H. Pirkle, D.W. House and J.M. Finn, *J. Chromatogr.*, 192 (1980) 143.
[11] S. Hara and Y. Dobashi, *J. Chromatogr.*, 186 (1979) 543.
[12] K. Watabe, E. Gil-Av, T. Hobo and S. Suzuki, *Anal. Chem.*, 61 (1989) 126.
[13] R. Brügger and H. Arm, *J. Chromatogr.*, 592 (1992) 309.
[14] Y. Dobashi and S. Hara, *J. Org. Chem.*, 52 (1987) 2490.
[15] Y. Ohtsu, H. Fukui, T. Kanda, K. Nakamura, O. Nakata and Y. Fujiwara, *Chromatographia*, 24 (1987) 380.
[16] M.A. Apfel, H. Finkelmann, G.M. Janini, R.J. Laub, B.H. Lühmann, A. Price, W.L. Roberts, T.J. Shaw and C.A. Smith, *Anal. Chem.*, 57 (1985) 651.

ELSEVIER

Journal of Chromatography A, 694 (1995) 57–69

JOURNAL OF CHROMATOGRAPHY A

# Optimization of the separation of enantiomers of basic drugs Retention mechanisms and dynamic modification of the chiral bonding properties on an $\alpha_1$-acid glycoprotein column

Jörgen Hermansson*, Anders Grahn

*ChromTech AB, Box 6056, S-129 06 Hägersten, Sweden*

**Abstract**

The chromatographic properties of 29 basic drugs were studied by varying the pH and the concentration of inorganic ions in the mobile phase. It was observed that the chromatographic performance of most hydrophobic basic drug compounds could be strongly enhanced by decreasing the pH in the mobile phase from 7 to 4–6. The enantioselectivity increased and a much faster resolution was obtained. The results indicate that ion exchange and ion-pair distribution may be involved in the retention process of cationic drug enantiomers. Increasing the concentration of acetate and phosphate increases the retention of the enantiomers of the drug compounds. The relative contribution of the two retention processes can be affected by the pH and the nature and the concentration of the ions in the mobile phase. Decreasing the pH reduces the influence of the ion-exchange process since the negative charge of the protein is decreased. The enantioselectivity is also greatly affected by increasing salt concentration.

## 1. Introduction

In many publications it has been demonstrated that $\alpha_1$-acid glycoprotein (AGP) has the ability to achieve stereoselective binding of enantiomers of widely different character [1–10]. Drug compounds can be bound to the binding domain of the protein by interaction with uncharged or charged groups or a combination of both types of interactions. An interesting property of immobilized $\alpha_1$-acid glycoprotein (AGP) is that the character of this chiral selector can be changed by a simple change of the mobile phase composition, such as the nature and the concentration of uncharged modifier or by changing the pH. By such changes drastic effects can be obtained on the enantioselectivity and the retention [4,6]. The fact that the enantioselectivity can be induced by simple changes of the mobile phase composition is one of the reasons for the extremely broad applicability of the AGP column. By changing the pH of the mobile phase the degree of charge of the amino acids, containing free acidic or basic groups, are affected, which can, reversibly, influence the conformation of the protein and also the way the solutes and the mobile phase ions and additives are bound to the protein. In a recent paper the retention mechanisms of anionic drug compounds were discussed [4]. The aim of the present study was to obtain a deeper understanding of the mechanisms in-

* Corresponding author.

0021-9673/95/$09.50 
*SSDI* 0021-9673(94)00936-8

volved in the binding of cationic drug compounds to immobilized AGP.

## 2. Experimental

### 2.1. Chemicals and reagents

2-Propanol of HPLC grade was obtained from Lab-Scan (Dublin, Ireland). All other chemicals were of analytical-reagent grade. The drug compounds were gifts from the manufacturers. Structures of the compounds are shown in Fig. 1A and B.

### 2.2. Apparatus

The chromatographic system consisted of an LKB Model 2150 pump (Pharmacia–LKB Biotechnology, Uppsala, Sweden), a Kontron (Eching/Munich, Germany) Model 360 autosampler equipped with a 20-$\mu$l injection loop and a Spectra 100 variable-wavelength UV detector (Spectra-Physics, San Jose, CA, USA). The experimental data were collected and analysed on a Kontron Model 450 MT2 data system, which also controlled the autosampler. CHIRAL-AGP columns (100 × 4.0 mm I.D., 5 $\mu$m) were obtained from ChromTech (Hägersten, Sweden).

### 2.3. Chromatographic conditions

The experiments were carried out in a thermostated room at 23°C. A flow-rate of 0.9 ml/min was used. The UV detector was set at 225 nm. The sample concentrations were in the range 0.02–0.03 mg/ml. The void volume ($V_0$) was determined by injection of distilled water or mobile phase with a different composition.

### 2.4. Preparation of mobile phases

Mobile phases containing phosphate buffer at pH 6–7 were prepared from sodium dihydrogenphosphate. The phosphate salt was dissolved in 200 ml of distilled water, followed by adjustment of the pH with 2.0 *M* sodium hydroxide solution. When approaching the final pH, 0.1 *M* sodium hydroxide was used, 2-propanol was added and the volume was adjusted to 250.0 ml with distilled water.

The phosphate buffers used at pH 2.1 were prepared from concentrated phosphoric acid dissolved in 440 ml of distilled water. The pH was adjusted with 2.0 *M* sodium hydroxide solution. When approaching the final pH, 0.1 *M* sodium hydroxide was used. Distilled water was added to 500.0 ml. The phosphate concentrations given in the tables refer to the total phosphate concentration.

Acetate buffers were prepared from sodium or ammonium acetate. The acetate salt was dissolved in 200 ml of distilled water. The pH was adjusted with 3.0 *M* acetic acid solution, giving the higher total acetate concentration given in the tables. Then 2-propanol was added before addition of distilled water to 250.0 ml.

## 3. Results and discussion

### 3.1. Binding of solute molecules to $\alpha_1$-acid glycoprotein

AGP is built up of a single peptide chain containing 183 amino acids [11]. Five carbohydrate units are linked to the peptide chain via the asparagine residues and the carbohydrate content is about 45%. At least two different binding sites have been demonstrated on AGP [12]. The main binding site is most likely a hydrophobic pocket which is formed by an enrichment of hydrophobic amino acid residues such as tryptophan, phenylalanine, tyrosine, leucine and isoleucine [13]. In addition to hydrophobic amino acids, the binding site contains numerous hydrogen bonding groups such as the amides and also numerous protolytic groups, both acidic and basic. Schmid [13] determined the amino acid composition and found 26 basic amino acid residues (13 lysine, 3 histidine and 10 arginine) and 51 acidic amino acids (21 asparagine and 30 glutamic acid). The $pK_a$ values for the protolytic groups of AGP have been determined [14]. Two different carboxylic acid groups were observed

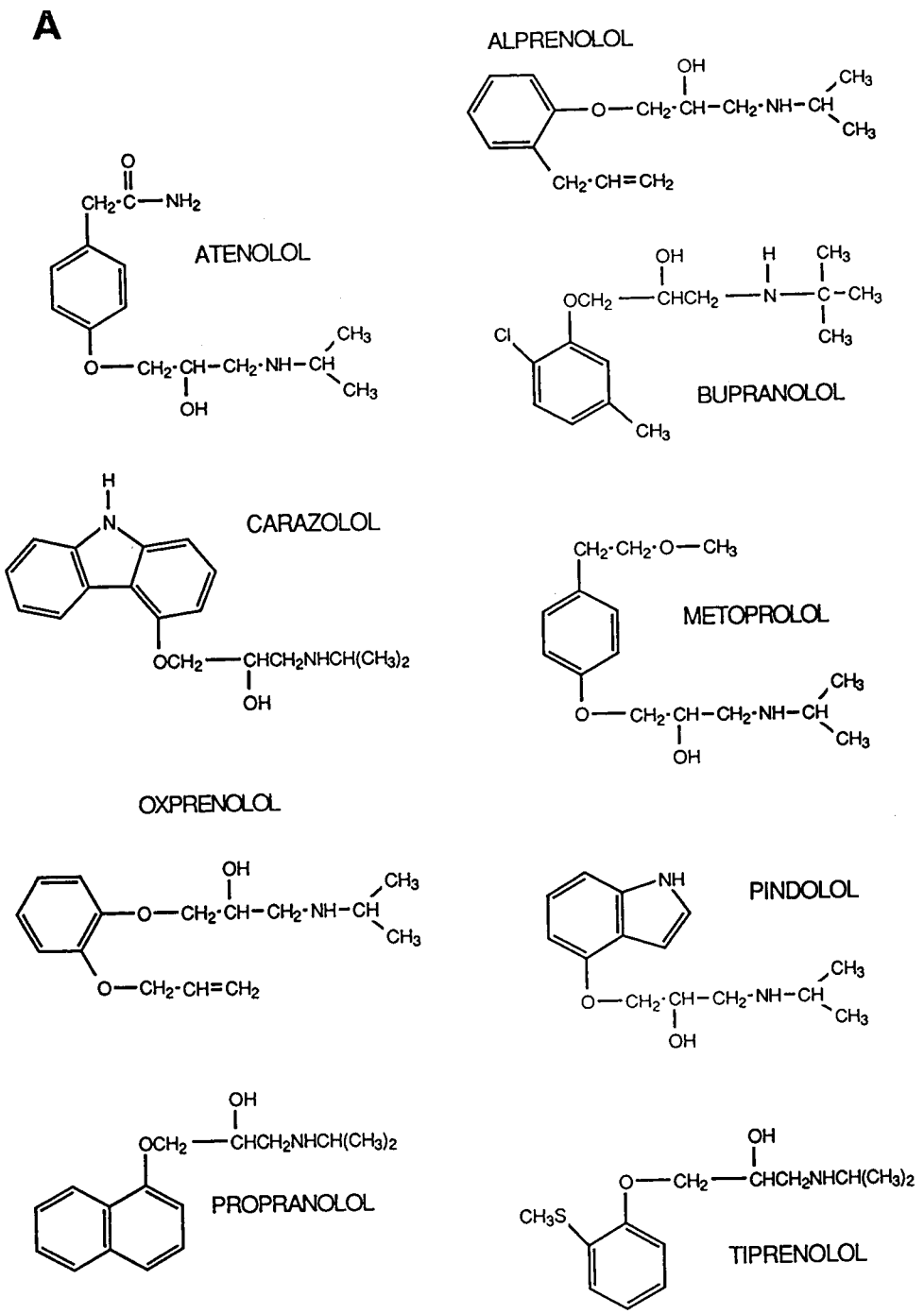


Fig. 1 *(continued on p. 60).*

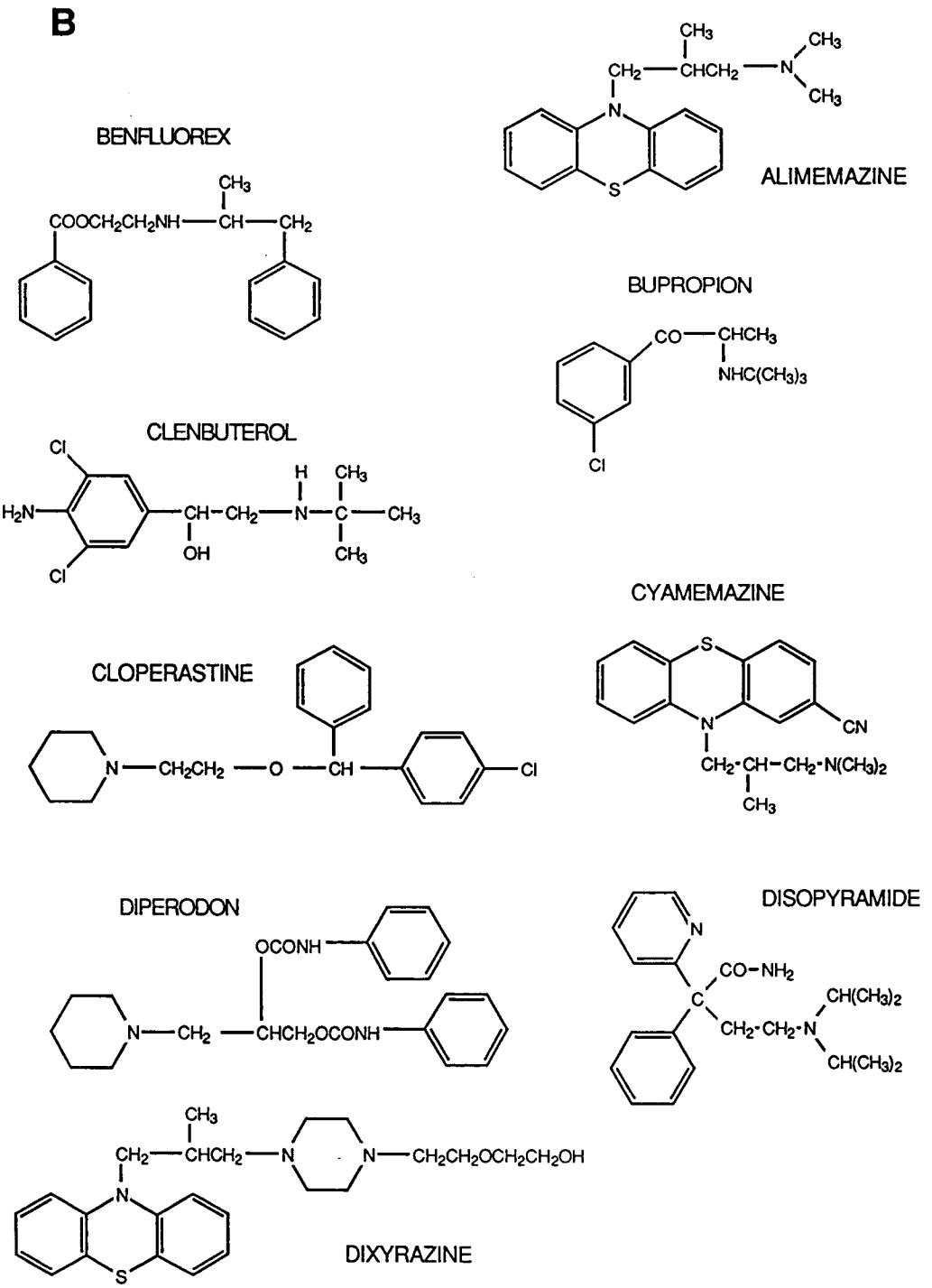


Fig. 1 *(continued)*.

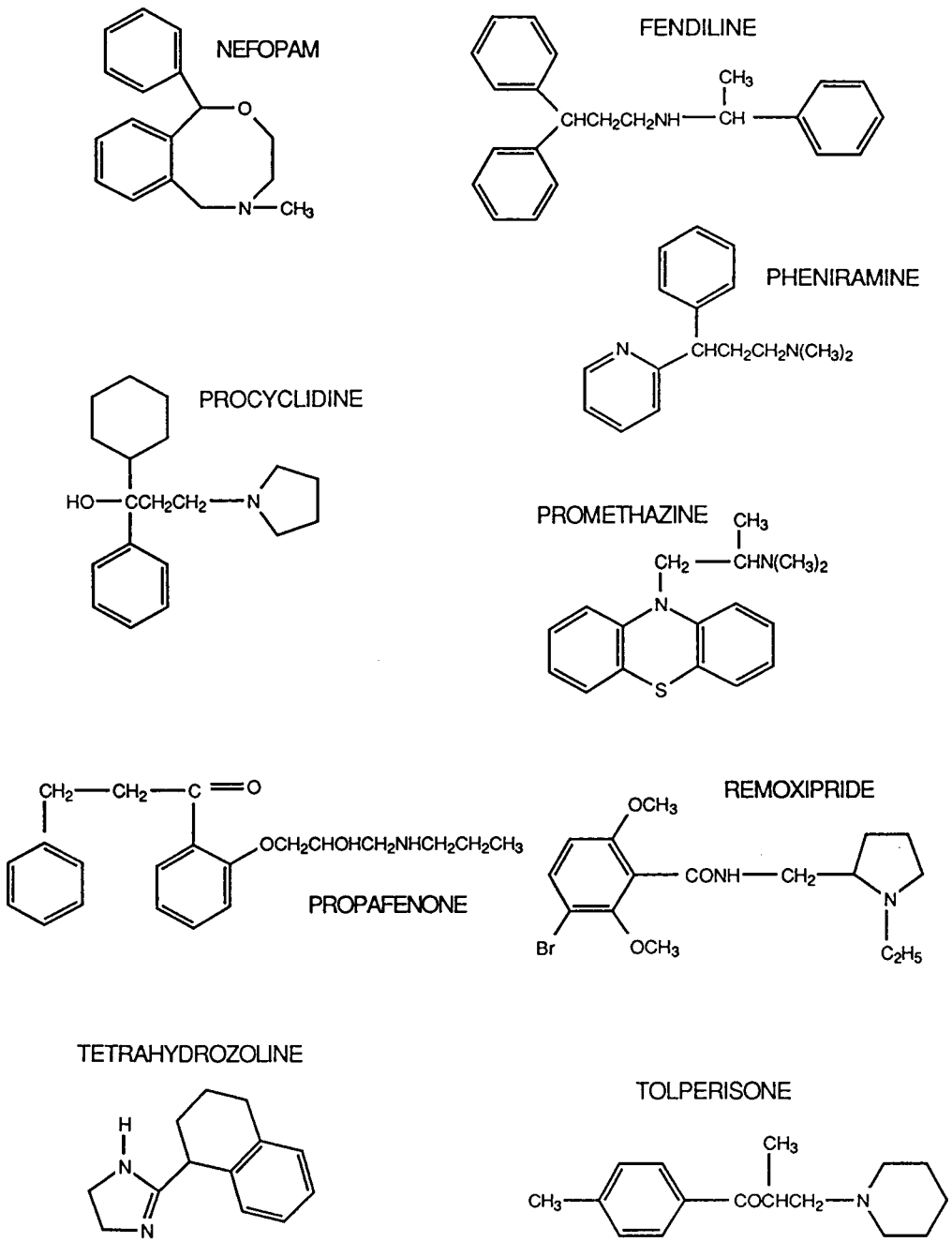


Fig. 1 *(continued on p. 62).*

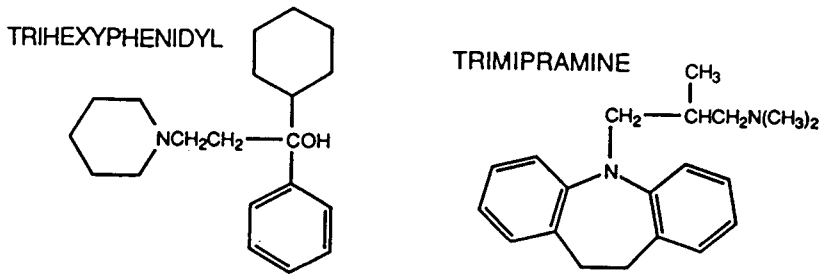


Fig. 1. Structures of (A) β-blockers and (B) other drug compounds.

with p$K_a$ values of 2.95 and 4.14. The p$K_a$ values for the basic groups, imidazole of histidine and the ε-amino groups of lysine, were determined to be 6.57 and 9.70, respectively [14]. The isoelectric point of AGP is 2.5 [13]. Many of the protolytic amino acid residues can most likely be found in the binding sites, allowing ionic binding between the solute and this kind of binding group in the binding sites. Such indications were found in chromatrographic and adsorption isotherm studies on the AGP column, using terodiline, a relatively hydrophobic secondary amine, as a model compound [12]. Normally chromatographic experiments are performed in the pH range 4–7, which means that the protein has a net negative charge. Thus, cationic solutes can be retained by interaction with negatively charged groups in the binding sites. This is supported by the strong effects on the capacity factors, obtained for basic and acidic solutes, by changing the pH of the mobile phase [2,15]. Chromatography of non-protolytic compounds at different pH values results in very small effects on the retention, but the enantioselectvity can be strongly affected [15]. A solute can also be retained by interaction with hydrogen bonding groups and with hydrophobic amino acid residues located in the binding sites. Hence, the solutes can be bound to the binding sites by, in principle, two different kinds of interactions, ionic binding and binding to uncharged groups.

### 3.2. *Influence of pH on chromatographic properties of cationic solutes*

Cationic drugs have traditionally been resolved on the AGP column using a pH of 6–7 [1,2]. The background for using mobile phases with pH in that range for resolution of cationic drugs was due to results of earlier studies where it was observed that the enantioselectivity increases for basic solutes with increasing pH. For example, the enantioselectivity for metoprolol increases from 1.25 to 1.48 on increasing the pH from 4.5 to 7.5 without a modifier in the mobile phase [1]. However, chromatography of cationic solutes at pH ≈ 7 also results in high capacity factors and long retention times and the more hydrophobic the solutes the higher is the retention. Thus, chromatography of hydrophobic basic compounds at pH 7 requires the addition of an uncharged modifier in order to be able to elute the enantiomers within a reasonable time. Addition of uncharged modifiers such as 2-propanol or acetonitrile decreases the enantioselectivity for cationic compounds. This means that the concentration of modifier must be so low that the enantioselectivity is not reduced to such an extent that the resolution is incomplete, i.e., $R_s < 1.5$. The major reason for the high retention obtained for cationic solutes at pH 7 is that the protein has a high degree of negative charge at pH 7 since this is 4.5 pH units higher than the p*I* value of AGP. Chromatography of basic drug compounds with p$K_a$ values higher than 9 at pH 7 means that the enantiomers are fully ionized and can be strongly retained by ionic bonding to the anionic groups in the binding sites of the protein. A decrease in the pH of the mobile phase towards the isoelectric point of the protein gives a lower degree of negative charge of the protein and thus lower retention of cationic drugs.

Table 1 gives results for five different cationic

Table 1
Influence of pH on the chromatographic properties of cationic drugs

| Compound | pH 7.0[a] | | | | pH 4.1[b] | | | |
|---|---|---|---|---|---|---|---|---|
| | $k'_1$ | $k'_2$ | $\alpha$ | $R_s$ | $k'_1$ | $k'_2$ | $\alpha$ | $R_s$ |
| Disopyramide | 18.5 | 53.9 | 2.91 | 5.93 | 2.78 | 8.79 | 3.41 | 3.72 |
| Diperodon | 48.3 | 59.9 | 1.24 | 1.68 | 5.70 | 8.51 | 1.49 | 2.50 |
| Carazolol | 48.9 | 55.6 | 1.14 | 0.90 | 4.64 | 5.98 | 1.29 | 1.63 |
| Bupranolol | 25.0 | 31.4 | 1.25 | 1.58 | 3.04 | 3.81 | 1.25 | 1.39 |
| Propranolol | 48.9 | 56.1 | 1.15 | 1.08 | 7.04 | 10.7 | 1.52 | 2.62 |

For the preparation of the mobile phases, see Experimental.
[a] Mobile phase: 6% 2-propanol in 10 m*M* sodium phosphate buffer (pH 7.0).
[b] Mobile phase: 0.5% 2-propanol in 20 m*M* ammonium acetate buffer (pH 4.1) (total acetate concentration 96 m*M*).

drug compounds chromatographed at two pH values, 7.0 and 4.1. The mobile phase at pH 7 also contained 6% 2-propanol in order to be able to elute the most retained enantiomer within a reasonable time. However, despite this, the capacity factors for the last-eluted enatiomers of the solutes were in the range 31.4–59.9, which are fairly high. It can also be noted that relatively low separation factors, with one exception (disopyramide), were obtained for the compounds at pH 7. On decreasing the pH to 4.1 and the concentration of modifier to 0.5%, 2-propanol gives a higher enantioselectivity for all compounds, except bupranolol, with a separation factor of 1.25 at both pH values. The retention is also greatly reduced on decreasing the pH to 4.1, with capacity factors ranging from 3.8 to 10.7. For example, the capacity factors for the enantiomers of carazolol are reduced about tenfold on decreasing the pH from 7 to 4.1, despite the fact that the 2-propanol concentration was also substantially lowered. The resolution, $R_s$, of carazolol is 0.9 at pH 7 and 1.63 at pH 4.1.

The general rule concerning the uncharged modifier concentration in the mobile phase is that the retention increases with decrease in the concentration of uncharged modifier. From this it can be concluded that the strong decrease in the retention obtained by decreasing the pH is most likely caused by a decrease in the net negative charge of the protein. Figs. 2 and 3 demonstrate the dramatic improvement of the chromatographic performance and the strong decrease in retention time obtained at pH 4.1 compared with pH 7 for two other compounds included in Table 1, diperodon and propranolol.

Hydrophobic amines containing tricyclic ring structures, such as trimipramine, alimemazine, promethazine cyamemazine and dixyrazine, are very difficult to resolve with good chromatographic performance and low retention. Normally these compounds are chromatographed at a pH around 7. However, chromatography of these compounds at pH 7 gives very high capacity factors even if the mobile phase also contains

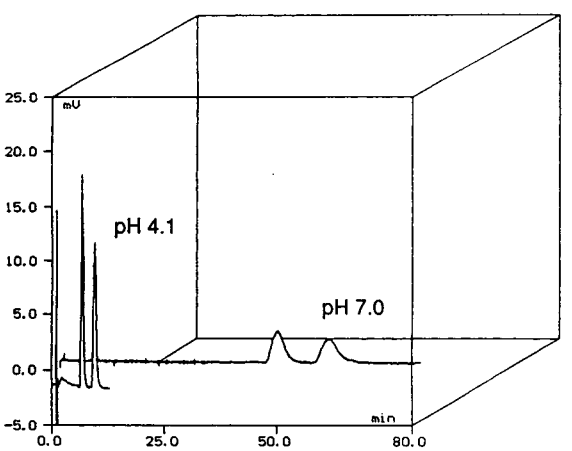


Fig. 2. Effect of pH on diperodon. Mobile phases: pH 4.1, 0.5% 2-propanol in 20 m*M* ammonium acetate buffer (total acetate concentration 96 m*M*); pH 7.0, 6% 2-propanol in 10 m*M* sodium phosphate buffer. For the preparation of mobile phases, see Experimental Column, CHIRAL-AGP (100 × 4.0 mm I.D.); flow-rate, 0.9 ml/min; detection, UV at 225 nm.

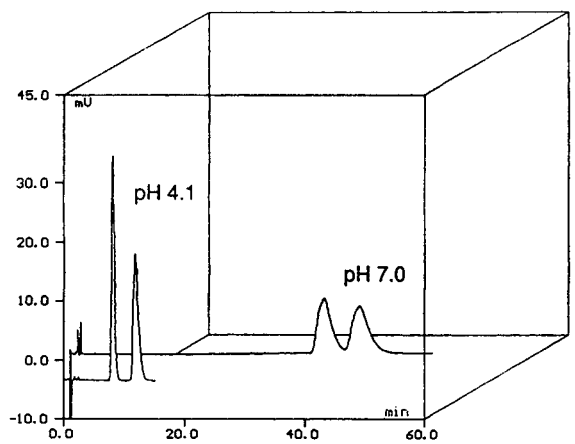


Fig. 3. Effect of pH on propranolol. Mobile phases: pH 4.1, 0.5% 2-propanol in 20 m*M* ammonium acetate buffer (total acetate concentration 96 m*M*); pH 7.0, 6% 2-propanol in 10 m*M* sodium phosphate buffer. For the preparation of mobile phases, see Experimental. Conditions, as in Fig. 2.

15% 2-propanol, as is demonstrated in Table 2. Two of the compounds, alimemazine and trimipramine, have capacity factors >60 under these conditions. The other compounds, cyamemazine, dixyrazine and promethazine, were eluted with capacity factors of the first-eluted enantiomer between 16.4 and 23.5. The enantioselectivity was also low and promethazine and dixyrazine have separation factors of 1.0 and 1.07, respectively. Cyamemazine was the only compound that could be resolved with a relatively high separation factor, 1.22, in the mobile phase with a pH of 7.0 and containing 15% 2-propanol. Decreasing the pH of the mobile phase from 7.0 to 4.0 and the content of organic modifier (acetonitrile or 2-propanol) to 1% results in drastic improvements in the enantioselectivity, as can be seen from Table 2. Separation factors between 1.31 and 1.84 were obtained. All compounds were baseline resolved with $R_s$ ranging from 1.55 to 3.03. The retention was also strongly reduced.

Tables 1 and 2 show examples of compounds where the enantioselectivity and the resolution have been strongly improved by decreasing the pH and the modifier concentration in the mobile phase. It was also observed that similar improvements can be obtained for a very large number of basic compounds that previously have been resolved at pH $\approx$ 7. Some examples of such compounds are given in Table 3, which summarizes the capacity factors, the separation factors and the resolution of the drug compounds chromatographed at optimum conditions at low pH. Nine different $\beta$-blockers were also used as model compounds to test the influence of the pH of the mobile phase on the chromatographic performance. They were chromatographed with mobile phases with pH between 4 and 7 with the purpose of finding the optimum separation conditions, i.e., as low a retention as possible with baseline resolution. From Table 4 it can be seen

Table 2
Influence of pH on the chromatographic properties of hydrophobic basic drugs

| Compound | pH 7.0 | | | | | pH 4.0 | | | | |
|---|---|---|---|---|---|---|---|---|---|---|
| | Mobile phase[a] | $k'_1$ | $k'_2$ | $\alpha$ | $R_s$ | Mobile phase[a] | $k'_1$ | $k'_2$ | $\alpha$ | $R_s$ |
| Dixyrazine | 1 | 21.3 | 22.8 | 1.07 | – | 2 | 8.29 | 12.0 | 1.45 | 1.81 |
| Trimipramine | 1 | n.e.[b] | – | – | – | 3 | 4.43 | 7.32 | 1.65 | 2.55 |
| Cyamemazine | 1 | 16.4 | 19.9 | 1.22 | 1.72 | 3 | 3.18 | 5.86 | 1.84 | 3.03 |
| Promethazine | 1 | 23.5 | 23.5 | 1 | – | 2 | 7.68 | 10.1 | 1.32 | 1.56 |
| Alimemazine | 1 | n.e.[b] | – | – | – | 2 | 10.7 | 14.0 | 1.31 | 1.55 |

[a] For the preparation of the mobile phases, see Experimental. Mobile phases: 1 = 15% 2-propanol in 10 m*M* sodium phosphate buffer (pH 7.0); 2 = 1% acetonitrile in 10 m*M* sodium acetate buffer (pH 4.0) (total acetate concentration 59 m*M*); 3 = 1% 2-propanol in 10 m*M* sodium acetate buffer (pH 4.0) (total acetate concentration 59 m*M*).
[b] Not eluted within 60 min.

Table 3
Separation of enantiomers of cationic drugs using low pH

| Compound | Mobile phase[a] | $k'_1$ | $\alpha$ | $R_s$ |
|---|---|---|---|---|
| Benfluorex | 1 | 5.72 | 1.42 | 2.80 |
| Bupropion | 2 | 1.61 | 1.40 | 1.59 |
| Clenbuterol | 10 | 2.27 | 1.55 | 2.93 |
| Cloperastine | 3 | 7.60 | 1.40 | 1.69 |
| Diperodon | 4 | 5.70 | 1.49 | 2.50 |
| Fendiline | 5 | 10.1 | 1.43 | 2.03 |
| Nefopam | 6 | 1.50 | 1.49 | 2.02 |
| Pheniramine | 7 | 4.04 | 1.46 | 2.12 |
| Procyclidine | 8 | 2.11 | 1.79 | 2.88 |
| Remoxipride | 9 | 2.03 | 1.63 | 2.50 |
| Tetrahydrozoline | 12 | 1.68 | 1.46 | 1.63 |
| Tolperisone | 10 | 2.06 | 1.40 | 1.69 |
| Trihexyphenidyl | 11 | 6.89 | 1.33 | 1.52 |

[a] For the preparation of the mobile phases, see Experimental. Mobile phases: 1 = 4% 2-propanol in 10 m*M* ammonium acetate buffer (pH 5.0) (total acetate concentration 15 m*M*); 2 = 0.5% 2-propanol in 10 m*M* ammonium acetate buffer (pH 5.0) (total acetate concentration 15 m*M*); 3 = 1% acetonitrile in sodium acetate buffer (pH 4.0) (total acetate concentration 59 m*M*); 4 = 0.5% 2-propanol in 10 m*M* ammonium acetate buffer (pH 4.1) (total acetate concentration 49 m*M*); 5 = 3% acetonitrile in 10 m*M* sodium acetate buffer (pH 4.1) (total acetate concentration 49 m*M*); 6 = 1% 2-propanol in 10 m*M* sodium acetate buffer (pH 4.5) (total acetate concentration 25 m*M*); 7 = 1% acetonitrile in 10 m*M* sodium acetate buffer (pH 5.0) (total acetate concentration 15 m*M*); 8 = 5% acetonitrile in 10 m*M* sodium acetate buffer (pH 4.1) (total acetate concentration 49 m*M*); 9 = 30 m*M* sodium acetate buffer (pH 4.0) (total acetate concentration 59 m*M*); 10 = 1% 2-propanol in 10 m*M* sodium acetate buffer (pH 5.0) (total acetate concentration 15 m*M*); 11 = 3% acetonitrile in 10 m*M* sodium acetate buffer (pH 4.1) (total acetate concentration 49 m*M*); 12 = 10 mM sodium acetate buffer (pH 5.0) (total acetate concentration 15 m*M*).

Table 4
Chromatographic properties of $\beta$-blockers

| Compound | Mobile phase[a] | $k'_1$ | $k'_2$ | $\alpha$ | $R_s$ |
|---|---|---|---|---|---|
| Carazolol | 1 | 4.34 | 5.99 | 1.38 | 1.83 |
| Propranolol | 2 | 7.04 | 10.7 | 1.52 | 2.62 |
| Bupranolol | 3 | 2.90 | 3.77 | 1.30 | 1.65 |
| Oxprenolol | 4 | 4.03 | 5.16 | 1.28 | 1.61 |
| Alprenolol | 5 | 1.34 | 2.05 | 1.53 | 1.93 |
| Tiprenolol | 6 | 11.0 | 15.1 | 1.37 | 3.13 |
| Pindolol | 7 | 7.67 | 11.1 | 1.45 | 1.61 |
| Atenolol | 8 | 3.75 | 4.62 | 1.23 | 1.46 |
| Metoprolol | 9 | 10.5 | 13.2 | 1.26 | 1.71 |

[a] For the preparation of the mobile phases, see Experimental. Mobile phases: 1 = 0.5% 2-propanol in 5 m*M* ammonium acetate buffer (pH 4.1) (total acetate concentration 25 m*M*); 2 = 0.5% 2-propanol in 20 m*M* ammonium acetate buffer (pH 4.1) (total acetate concentration 96 m*M*); 3 = 0.5% 2-propanol in 39 m*M* ammonium acetate buffer (pH 4.1) (total acetate concentration 186 m*M*); 4 = 1% 2-propanol in 10 m*M* ammonium acetate buffer (pH 4.5) (total acetate concentration 25 m*M*); 5 = 3% acetonitrile in 10 m*M* ammonium acetate buffer (pH 4.0) (total acetate concentration 59 m*M*); 6 = 3% 2-propanol in 10 m*M* sodium phosphate buffer (pH 6.0); 7 = 10% acetonitrile in 10 m*M* sodium phosphate buffer (pH 7.0); 8 = 10 m*M* sodium phosphate buffer (pH 7.0); 9 = 0.5% 2-propanol in 10 m*M* sodium phosphate buffer (pH 7.0).

that six of the nine β-blockers were best resolved at a pH lower than 7. Figs. 4 and 5 show chromatograms of clenbuterol and cyamemazine using mobile phases with a low pH and a low content of organic modifier.

### 3.3. Effect of the buffer concentration on the retention and the enantioselectivity

As has been discussed above, the pH is a very important tool in optimizing a chiral separation on the AGP column. Another way to affect the retention and the enantioselectivity is to utilize the buffer concentration. It has been demonstrated previously that the retention and the enantioselectivity of solutes of different charac-

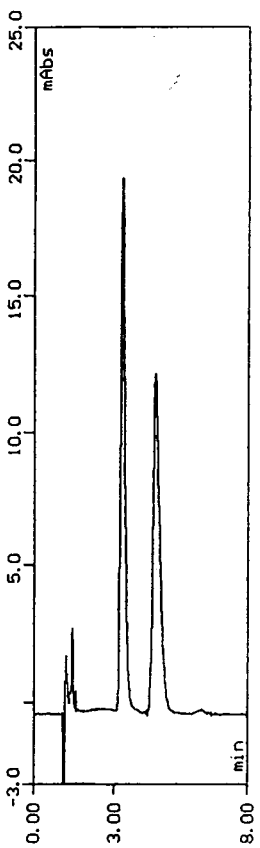


Fig. 4. Separation of the enantiomers of clenbuterol. Mobile phase: 1% 2-propanol in 10 m*M* sodium acetate buffer (pH 5.0) (total acetate concentration 15 m*M*). For preparation of mobile phase, see Experimental. Conditions, as in Fig. 2.

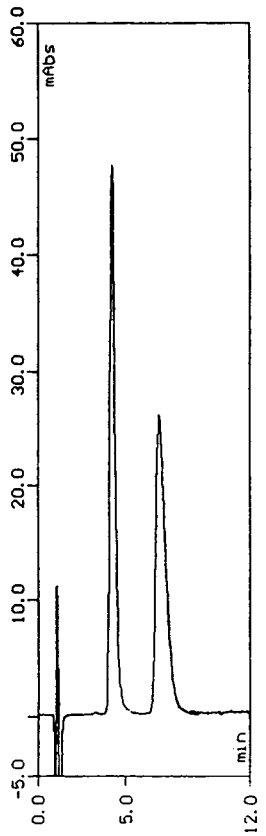


Fig. 5. Separation of the enantiomers of cyamemazine. Mobile phase: 1% 2-propanol in 10 m*M* sodium acetate buffer (pH 4.0) (total acetate concentration 59 m*M*). For preparation of mobile phase, see Experimental. Conditions, as in Fig. 2.

ter could be strongly affected by the concentration of inorganic [4] and organic [4,15,16,17] mobile phase additives. In order to establish whether the buffer ion concentration could affect the retention and the enantioselectivity of cationic solutes, a series of experiments were performed using acetate buffers with total acetate concentrations between 12 and 186 m*M* at pH 4.1. Three basic drugs were used as model compounds, i.e., bupranolol, diperodon and propranolol, with one nitrogen atom in the molecule. The results of the study are summarized in Table 5. As can be seen, the enantioselectivity increases for bupranolol and propranolol with increasing acetate concentration. The

Table 5
Influence of acetate concentration on the retention and the enantioselectivity of cationic drugs containing one or two charged nitrogen atoms.

| Acetate (mM)[a] | Bupranolol | | | Diperodon | | | Propranolol | | | Disopyramide | | |
|---|---|---|---|---|---|---|---|---|---|---|---|---|
| | $k'_1$ | $k'_2$ | $\alpha$ | $k'_1$ | $k'_2$ | $\alpha$ | $k'_1$ | $k'_2$ | $\alpha$ | $k'_1$ | $k'_2$ | $\alpha$ |
| 12 | 2.30 | 2.58 | 1.12 | 4.27 | 6.46 | 1.51 | 5.73 | 7.29 | 1.27 | 2.16 | 10.0 | 4.64 |
| 25 | 2.65 | 3.14 | 1.18 | 4.92 | 7.30 | 1.48 | 6.54 | 8.79 | 1.34 | 2.41 | 10.3 | 4.29 |
| 96 | 3.04 | 3.81 | 1.25 | 5.70 | 8.51 | 1.49 | 7.04 | 10.7 | 1.52 | 2.78 | 8.79 | 3.16 |
| 186 | 2.90 | 3.77 | 1.30 | 5.56 | 8.32 | 1.50 | 6.26 | 9.77 | 1.56 | 2.65 | 9.04 | 3.41 |

[a] Mobile phase: 0.5% 2-propanol in acetate buffers (pH 4.1) of different concentration. The mobile phases were prepared from 2.5, 4.9, 19.7 and 39.5 m*M* ammonium acetate, respectively. The pH was adjusted to 4.1 with acetic acid.

enantioselectivity for diperodon was almost constant. It is also very interesting that increasing the acetate concentration increases the retention of both enantiomers of bupranolol, diperodon and propranolol. This kind of effect has not been observed previously for cationic solutes. However, it has been reported that the retention of anionic solutes, i.e., anti-inflammatory drugs of the arylpropionic acid type, could be increased by increasing the concentration of, for example, sodium, potassium and ammonium in the mobile phase [4]. The increase in retention observed for the compounds listed in Table 5 with increasing acetate concentration, indicates that ion-pair distribution may be involved in the retention process of this kind of solute. It seems likely that this mechanism is favoured by a decrease in pH, as the net negative charge is reduced, which will suppress retention caused by ionic binding. This is supported by the fact that no increase in retention was observed on increasing the concentration of acetate at higher pH, where the protein has a higher degree of net negative charge and the ionic binding strongly affects the retention. It has also been demonstrated, for acidic drug compounds of the arylpropionic acid type, that the capacity factors increase on increasing the sodium concentration at pH 7, where the acids are negatively charged [4]. However, when performing a similar experiment at pH 2.1 where the acids are uncharged, and with no possibility of being retained as ion pairs, the result is a decrease in retention [4]. The weak acid hexobarbital, which is uncharged at pH 2.1 with no possibility of being distributed as an ion pair at this pH, demonstrated the same behaviour as the carboxylic acids on increasing the buffer concentration. These results support the assumption that ion-pair distribution might be a retention mechanism involved in the retention of both cationic and anionic solutes.

Studies with increasing buffer concentration were also performed with disopyramide, containing two charged nitrogens at pH 4.1. Most likely this kind of compound is retained according to the same mechanism as the compounds containing one charged nitrogen, by ionic binding and ion-pair adsorption. As can be seen from Table 5, chromatography of disopyramide with increasing acetate concentration at pH 4.1 results in relatively small changes in the capacity factors at total acetate concentrations >25 m*M*. This is most likely the result of a strong influence of the ion-exchange mechanism on the retention at pH 4.1. At this pH the protein has a relatively high degree of negative charge and the solute has two positively charged nitrogens. From Table 5 it can also be seen that the enantioselectivity increases on reducing the acetate concentration in the mobile phase.

In order to decrease the influence of the ion-exchange mechanism on the retention of cationic compounds the pH must be decreased to below 4. A decrease in the pH decreases the total ion-exchange binding capacity for cations, giving a larger influence of ion-pair adsorption. The nature and the concentration of the ions in the mobile phase also affect the relative influence of the two binding processes. Therefore, experiments were performed at pH 2.1 using phos-

Table 6
Influence of phosphate concentration on the retention ($k'$) of cationic drugs containing one or two charged nitrogen atoms.

| Phosphate (m$M$)[a] | Cloperastine, $k'$ | Propafenone, $k'$ | Diperodon, $k'$ | Propranolol, $k'$ | Disopyramide | |
|---|---|---|---|---|---|---|
| | | | | | $k'_1$ | $k'_2$ |
| 25.0 | 3.93 | 2.90 | 1.24 | 0.61 | 0.94 | 2.68 |
| 50.0 | 5.64 | 3.55 | 1.56 | 0.90 | 1.30 | 3.00 |
| 100.0 | 8.09 | 4.68 | 2.54 | 1.41 | 1.82 | 4.29 |

[a] For preparation, see Experimental. Mobile phase: phosphate buffer (pH 2.1) of different concentrations.

phate buffers with increasing total phosphate concentrations between 25 and 100 m$M$. As demonstrated in Table 6, the capacity factors for diperodon, propranolol, cloperastine and propafenoe, with one charged nitrogen, increase with increasing phosphate concentration, indicating that ion-pair adsorption dominates the retention process at this pH. The capacity factors increase more than 100% on increasing the total phosphate concentration from 25 to 100 m$M$. The level of the capacity factors is, however, much lower than that at pH 4.1, probably because the retention caused by ionic binding has been reduced. However, to a limited extent ionic binding is most likely still involved in the retention at pH 2.1, as carboxylic acid residues with a p$K_a$ value of 2.95 have been detected [14], which means that they are partially charged at pH 2.1. It can also be noted that the chiral selectivity is lost for these compounds.

As was mentioned above for disopyramide with two basic nitrogens, there is no increase in retention on increasing the acetate concentration at pH 4.1, indicating that ionic binding influences the retention to a high degree. However, chromatography of disopyramide at pH 2.1 means that the ionic binding of disopyramide is decreased. Increasing the phosphate concentration in the mobile phase at this pH increases the retention of disopyramide, as demonstrated in Table 6. It can also be noted that high separation factors can be obtained for disopyramide even at this very low pH. At the lowest phosphate concentration a separation factor of 2.87 was obtained for disopyramide. Increasing the phosphate concentration to 100 m$M$ decreased the separation factor to 2.31. The above findings indicate that the ionic binding of the solutes is decreased at pH 2.1 to such an extent that ion-pair adsorption, with phosphate as counter ion, strongly contributes to the retention.

## 4. Conclusions

It has been demonstrated that the cationic solutes are retained according to two mechanisms on the AGP column, ionic binding and ion-pair distribution with the anionic buffer ions acetate and phosphate as counter ions. Increasing the buffer concentration increases the retention of the enantiomers of the drugs. The relative influence of the two processes can be affected by changing the pH and the nature and concentration of the ions in the mobile phase. A decrease in the pH of the mobile phase lowers the degree of negative charge of the protein, which decreases the influence of the ionic binding. From the above it follows that the pH of the mobile phase is a very important parameter when optimizing the separation of basic drugs. The chromatographic performance of most hydrophobic basic drugs could be strongly improved by using a pH between 4 and 6 and decreasing the content of uncharged modifier in the mobile phase. The explanation of this finding is that a decrease in pH lowers the influence of ionic binding on the retention, resulting in a lower retention. A lower retention means that it is not necessary to add an uncharged modifier to the mobile phase in order to elute the enantiomers within a reasonable time. No or low modi-

fier concentrations in the mobile phase give a higher enantioselectivity, with the result that high resolution and low retention can be obtained.

## References


[1] J. Hermansson, *Trends Anal. Chem.*, 8 (1989) 251.
[2] J. Hermansson and G. Schill, in P.A. Brown and R.A. Hartwick (Editors), *High Performance Liquid Chromatography (Monographs on Analytical Chemistry Series)*, Wiley-Interscience, New York, 1988, pp. 337–374.
[3] I. Fitos, J. Visy, M. Simonyi and J. Hermansson, *J. Chromatogr.*, 609 (1992) 163.
[4] J. Hermansson and I. Hermansson, *J. Chromatogr. A*, 666 (1994) 181.
[5] U. Norinder and J. Hermansson, *Chirality*, 3 (1991) 422.
[6] M. Enquist and J. Hermansson, *J. Chromatogr.*, 519 (1990) 271.
[7] G. Schill, I.W. Wainer and S.A. Barkan, *J. Chromatogr.*, 365 (1986) 73.
[8] J.M. Evans, R.J. Smith and G. Stemp, *J. Chromatogr.*, 623 (1992) 163.
[9] J. Xaver de Vries and E. Schmitz-Kummer., *J. Chromatogr.*, 644 (1993) 315.
[10] S. Görög and B. Herenyi, *J. Pharm. Biomed. Anal.*, 8 (1990) 837.
[11] P.G. Board, I.M. Jones and A.K. Bentley, *Gene*, 44 (1986) 127.
[12] M. Enquist and J. Hermansson, *J. Chromatogr.*, 519 (1990) 285.
[13] K. Schmid, in F.W. Putnam (Editor), *The Plasma Proteins*, Academic Press, New York, 1975, p. 184.
[14] V. Karpenko and V. Kalous, *Coll. Czech. Chem. Commun.*, 42 (1977) 45.
[15] J. Hermansson and M. Eriksson, *J. Liq. Chromatogr.*, 9 (1986) 621.
[16] E. Arvidsson, S.O. Jansson and G. Schill, *J. Chromatogr.*, 506 (1990) 579.
[17] E. Arvidsson, S.O. Jansson and G. Schill, *J. Chromatogr.*, 591 (1992) 55.

ELSEVIER

Journal of Chromatography A, 694 (1995) 71–80

JOURNAL OF CHROMATOGRAPHY A

# Enantioselectivity of bovine serum albumin-bonded columns produced with isolated protein fragments

Jun Haginaka*, Naoko Kanasugi

*Faculty of Pharmaceutical Sciences, Mukogawa Women's University, 11-68, Koshien Ksuban-cho, Nishinomiya 663, Japan*

**Abstract**

The enantioselectivity of bovine serum albumin (BSA)-bonded columns produced with isolated protein fragments was investigated. The BSA fragment BSA-FG75 was isolated by size-exclusion chromatography followed by peptic digestion of BSA. The isolated BSA-FG75 was a mixture of three peptides, and was mainly an N-terminal half peptide(s) with an average molecular mass of about 35 000. The BSA and BSA-FG75 proteins were bound to aminopropylsilica gels activated by N,N′-disuccinimidyl carbonate. The amounts of the proteins bound were about 2 and 5.5 $\mu$mol/g for the BSA and BSA-FG75, respectively. Chiral recognition of 2-arylpropionic acid derivatives, benzodiazepines, warfarin and benzoin was obtained with the BSA-FG75-bonded columns, but no chiral recognition of tryptophan or kynurenine was obtained. The intact BSA column gave a higher enantioselectivity than the BSA-FG75 column for most of the compounds tested, whereas the BSA-FG75 column gave a higher enantioselectivity than the intact BSA column for lorazepam and benzoin, and had a higher capacity for benzoin. These results are due to a higher density of chiral recognition site(s) on the BSA-FG75 column. Also, the BSA-FG75 column was as stable as the intact BSA column for a continuous flow of eluent.

## 1. Introduction

Many protein-bonded stationary phases have been developed for the resolution of enantiomers [1]. These include albumins such as bovine serum albumin [2] and human serum albumin [3], glycoproteins such as $\alpha_1$-acid glycoprotein [4], ovomucoid [5], avidin [6] and cellulase [7] and enzymes such as trypsin [8], $\alpha$-chymotrypsin [9] and lysozyme [10]. Disadvantages of protein-bonded columns in general have included low capacity, lack of column ruggedness in some instances and a limited understanding of the chiral recognition mechanisms. If a chiral binding site(s) exists on a domain or fragment and if it acts independently of others, chiral columns with the domain or fragment should be able to be made, which could be of higher capacity and be more stable. Recently, it was found that the third domain of turkey ovomucoid is enantioselective to at least two classes of compounds, benzodiazepines and 2-arylpropionic acid derivatives, and the glycosylated group is not needed for chiral recognition of these compounds [11]. Also, a chiral binding site was located and the chiral recognition mechanism was elucidated by using NMR spectroscopy and computational chemistry [11].

Andersson et al. [12] isolated a bovine serum albumin (BSA) fragment, of molecular mass ca. 38 000, by enzymatic cleavage, and cross-linked the fragment into aminopropylsilica materials by

* Corresponding author.

0021-9673/95/$09.50 
*SSDI* 0021-9673(94)00692-X

glutaraldehyde or adsorbed it on silica materials. However, the BSA fragment-bonded column obtained could have less capacity and enantioselectivity, and be less stable than the intact BSA-bonded column. In this study, we modified the methods for the isolation and binding of a BSA fragment. The retention and enantioselective properties of the obtained BSA fragment column were compared with those of the intact BSA column.

## 2. Experimental

### 2.1. Reagents and materials

BSA was purchased from Nacalai Tesque (Kyoto, Japan). Pepsin from porcine stomach mucosa and N,N′-disuccinimidyl carbonate (DSC) were purchased from Sigma (St. Louis, MO, USA). 1-Propanol of HPLC grade was obtained from Wako (Osaka, Japan). Racemic benzoin was purchased from Nacalai Tesque. Other racemic drugs used were kindly donated by pharmaceutical companies. The structures of these racemates are shown in Fig. 1. Silica gels (Ultron-120, particle diameter 5 $\mu$m, pore size 120 Å, surface area 300 $m^2/g$; and Ultron-300, particle diameter 5 $\mu$m, pore size 300 Å, surface area 100 $m^2/g$) were obtained from Shinwa Chemical Industries (Kyoto, Japan). Other solvents and reagents were used without further purification.

Water purified with a Nanopure II unit (Barnstead, Boston, MA, USA) was used for the preparation of the eluent and the sample solution.

### 2.2 Isolation of BSA fragment

Half-cystinyl BSA was prepared according to the method of King [13]. Briefly, 22.4 mg of L-cystine were dissolved in 0.5 ml of 1 *M* NaOH solution and the mixture was added to 47 ml of 0.1 *M* Tris buffer (pH 7.96). A 1.04-g amount of BSA was dissolved in 34 ml of 0.1 *M* Tris buffer (pH 7.96). The two solutions were mixed and reacted at 25°C for 17 h. The reacted solution

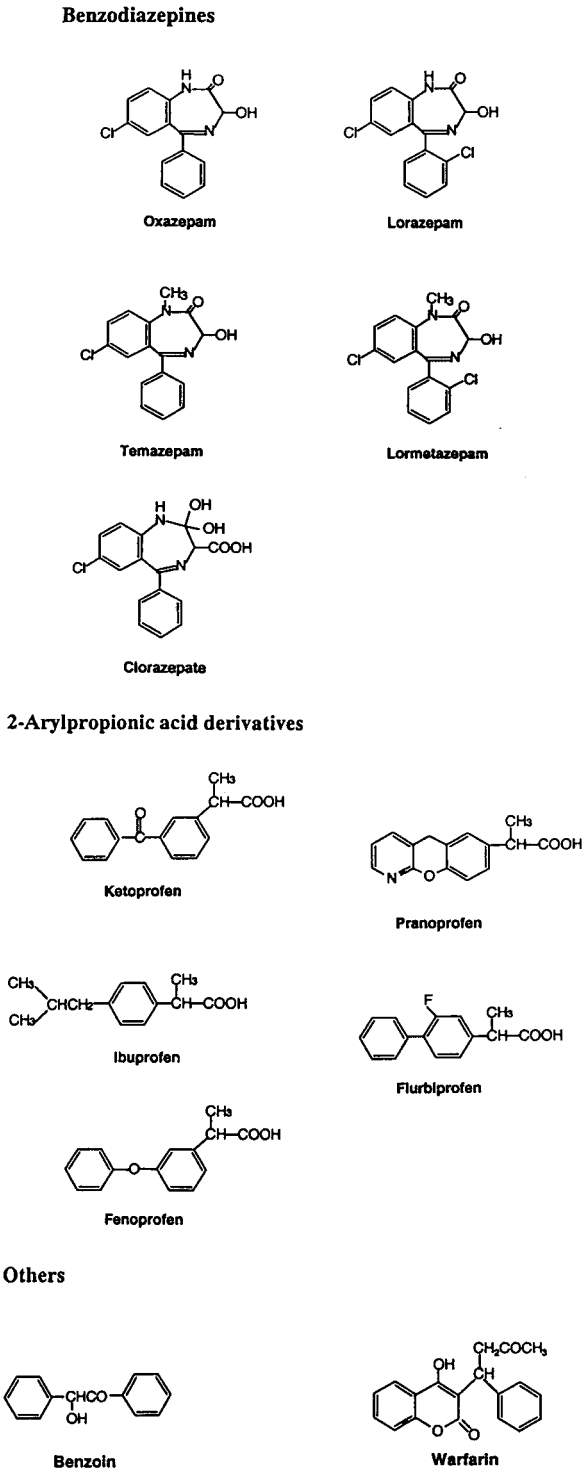


Fig. 1. Structures of the racemic solutes.

was dialysed against distilled water and lyophilized.

Peptic digestion of half-cystinyl BSA was performed according to the method of King and Spencer [14]. A 0.124-g amount of half-cystinyl BSA was dissolved in 8 ml of 0.1 *M* ammonium formate buffer (pH 3.7) containing 3.2 m*M* octanoic acid and preheated at 37°C. A 0.25-mg amount of pepsin was dissolved in the same buffer. The two solutions were mixed and reacted at 37°C for 30 min. The reaction was stopped by addition of 2 *M* Tris buffer (pH 7.9). After dialysing against 0.01 *M* Tris buffer (pH 8.0) containing 0.3 *M* NaCl, the reacted solution was applied to a Sephadex G-75 column (90 × 5 cm I.D.) that was equilibrated with 0.01 *M* Tris buffer (pH 8.0) containing 0.3 *M* NaCl at an average flow-rate of 80 ml/h. The eluate was monitored at 280 nm. The separation was performed at 4°C. The first peak was collected and lyophilized. The lyophilized sample was desalted with a Sephadex G-25 (fine) column (20 × 5 cm I.D.) using 15 m*M* $NH_4HCO_3$ as the buffer at an average flow-rate of 120 ml/h. The eluate was collected and lyophilized. The BSA fragment obtained was termed BSA-FG75.

### 2.3. Preparation of DSC-activated aminopropylsilica gels

Silica gels (5 g) were dried in vacuo over $P_2O_5$ at 150°C for 6 h and added to 120 ml of dry toluene. The mixture was heated to reflux until all the water had been removed as an azeotrope into a Dean–Stark-type trap. Next, 3-aminopropyltrimethoxysilane, corresponding to 10 $\mu$mol/m$^2$ of the specific surface area, was added and reacted for 8 h. The reaction mixture was cooled to room temperature, filtered and washed with toluene and methanol. The isolated silica gels were dried in vacuo over $P_2O_5$ at 60°C for 2 h. The aminopropylsilica gel obtained was used for the activation reaction described below.

Amounts of 5 g of the gels were slurried in 70 ml of acetonitrile and reacted with 5 g of DSC for 24 h at 30°C. The reaction mixture was filtered and washed with acetonitrile and methanol. The activated silica gels were dried in vacuo over $P_2O_5$ at 60°C for 2 h.

### 2.4. Preparation of BSA- or BSA fragment-bonded materials

BSA proteins were bound to the DSC-activated aminopropylsilica gels as follows: 0.28 g of the DSC-activated silica gels was slurried in 4 ml of 20 m*M* phosphate buffer (pH 6.6). To the mixture, 0.14 g of BSA proteins dissolved in 2 ml of the same buffer was added slowly at room temperature for 1 h and the mixture was further stirred for 20 h at 30°C. Similarly, the BSA fragment was bound to DSC-activated silica gels as follows: 0.28 g of the DSC-activated silica gels was reacted with 0.072 g of the BSA-FG75 using the same reaction conditions. Then both the reaction mixtures were filtered and washed with water and slurry solvent described below.

The BSA and BSA-FG75 materials were packed into a 100 mm × 2.1 mm I.D. stainless-steel column by the slurry packing method. The slurry solvents were 5% ethanol for the BSA materials and 50 m*M* phosphate buffer (pH 7.5)–1-propanol (60:40, v/v) for the BSA-FG75 materials. The same packing solvents were used.

### 2.5. Chromatography

For chiral resolution of racemic solutes on the BSA and BSA-FG75 columns, the HPLC system used was composed of an LC-10AD pump, an SPD-10A spectrophotometer, a Rheodyne Model 7125 injector, a C-R6A integrator and an SCL-10A system controller (all from Shimadzu, Kyoto, Japan). The flow-rate was maintained at 0.2 ml/min. Detection was performed at 220 or 254 nm. Capacity factors ($k'$), enantioseparation factors ($\alpha$), and resolutions ($R_s$) of the racemates were calculated. The asymmetry factor ($\eta$) was calculated as reported previously [15]. All separations were carried out at 25°C using a water-bath.

The eluents were prepared by using phosphoric acid–sodium dihydrogenphosphate or sodium dihydrogenphosphate–disodium hydrogenphos-

phate and organic modifier. The eluents used are specified in the figures and tables.

For reversed-phase chromatography of the BSA-FG75 protein, the same HPLC system as described above was used. The eluents used were as follows: eluent A, 0.1% trifluoroacetic acid (TFA); eluent B, water–acetonitrile (20:80, v/v) containing 0.1% of TFA; linear gradient from 25% B at 0 min to 80% B at 90 min. The column used was Cosmosil 5C18-AR (250 mm × 4.6 mm I.D.). Detection was carried out at 280 nm. The flow-rate was 1.0 ml/min. All separations were performed at ambient temperature.

### 2.6. Elemental analysis

The elemental analysis of the BSA- and BSA fragment-bonded silica materials was performed using ion chromatography combined with the oxygen flask method for sulfur.

### 2.7. N-Terminal sequencing

A 70-$\mu$g amount of the BSA fragment was reconstituted with 50 $\mu$l of water. A 5-$\mu$l portion of the solution was spotted on to a solid support for N-terminal sequencing analysis using an ABI 473A protein sequencer (Applied Biosystems Division, Perkin-Elmer Japan, Tokyo, Japan).

### 2.8. Matrix-assisted laser desorption ionization time-of-flight (MALDI-TOF) mass spectrometry

The mass spectrometer used was a Vision 2000 reflector-type TOF instrument (Finnigan MAT, Tokyo, Japan) equipped with a nitrogen laser operating at a wavelength of 337 nm with a pulse duration of 3 ns. The laser beam diameter at the sample surface was 70 $\mu$m; laser irradiances were in the low $10^6$ W/cm$^2$ range, close to the threshold for obtaining ions. The ions generated were accelerated to a potential of 5 kV in the ion source and post-accelerated to a potential of 20 kV for detection with a secondary ion multiplier. The MALDI-TOF spectra represent the accumulation of 20–25 single laser shots. They were calibrated externally by a standard sample (BSA, molecular mass of 66 430.2) that was placed on the same target. The matrix used was 2,5-dihydroxybenzoic acid, dissolved in 0.1% aqueous TFA–acetonitrile (2:1) at a concentration of 50 m$M$. Samples were dissolved in a water at a concentration of $10^{-6}$ $M$. A 0.5-$\mu$l portion of the sample solution was mixed with an equal volume of the matrix solution on the target, resulting in a sample amount used of 500 fmol. After deposition on the stainless-steel target, the sample was air-dried and introduced into the mass spectrometer.

### 2.9. Sample preparation

A known amount of a racemic solute was dissolved in methanol or water and the solution was diluted with the eluent to the desired concentration. A 5-$\mu$l aliquot of the sample solution was loaded on to the column. The amount loaded was 0.04–0.1 $\mu$g.

## 3. Results and discussion

### 3.1. Characterization of BSA fragment

Fig. 2 shows a chromatogram of half-cystinyl BSA digested by pepsin on a Sephadex G-75 size-exclusion column. The fraction of the BSA fragment BSA-FG75 was collected. It was found from reversed-phase chromatography of the BSA-FG75 that the isolated BSA-FG75 fraction was free from uncleaved BSA, and that the BSA-FG75 was a mixture of peptides. Fig. 3 shows the MALDI-TOF mass spectrum of the BSA fragment BSA-FG75. The BSA-FG75 consisted of three peptides, with molecular masses of 35 000, 32 000 and 27 000. The average molecular mass of the main digest peptide was calculated to be 35 113 ± 3, averaged from $M^{2+}$, $M^+$ and $2M^+$ ions. With regard to the N-terminal sequencing data, the first sequence of the BSA-FG75 started from Asp, which is the N-terminus of the uncleaved BSA. Also, the second and third sequences started from Phe at the 11th and 49th amino acid positions in BSA were observed, as reported by Erlandsson and Nilsson [16]. These results revealed that the isolated BSA-

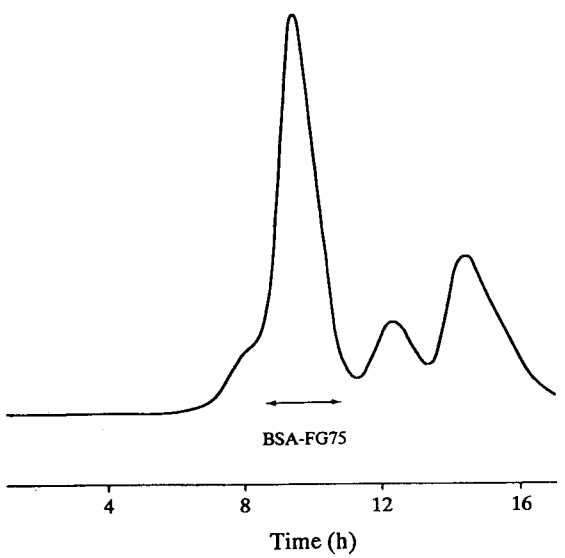


Fig. 2. Chromatogram of peptic digest of BSA on a size-exclusion column. Column, Sephadex G-75 (90 × 5 cm I.D.); eluent, 0.01 *M* Tris buffer (pH 8.0) containing 0.3 *M* NaCl; flow-rate, 80 ml/h; detection wavelength, 280 nm. The fraction of a BSA fragment, BSA-FG75, was collected.

FG75 was mainly an N-terminal half peptide(s) with an average molecular mass of about 35 000.

### *3.2. Surface coverages of BSA and BSA-FG75 proteins*

Table 1 shows the surface coverages of BSA and BSA-FG75 proteins on the protein-bonded materials. With regard to comparison of the base silica gels having 120- and 300-Å pore sizes, the former materials showed about 1.5-fold higher surface coverages of the BSA proteins. Also, the former materials gave higher enantioselectivity than the latter. Therefore, we bound the BSA-FG75 by using silica gels having a 120-Å pore size. As shown in Table 1, the BSA-FG75 materials gave about 3-fold higher surface coverages than the intact BSA materials. The higher surface coverages of the BSA-FG75 are ascribable to the fact that the BSA-FG75 proteins should be more accessible to the inner surface of the silica gels than the BSA proteins because the molecular mass of the BSA-FG75 is about half of

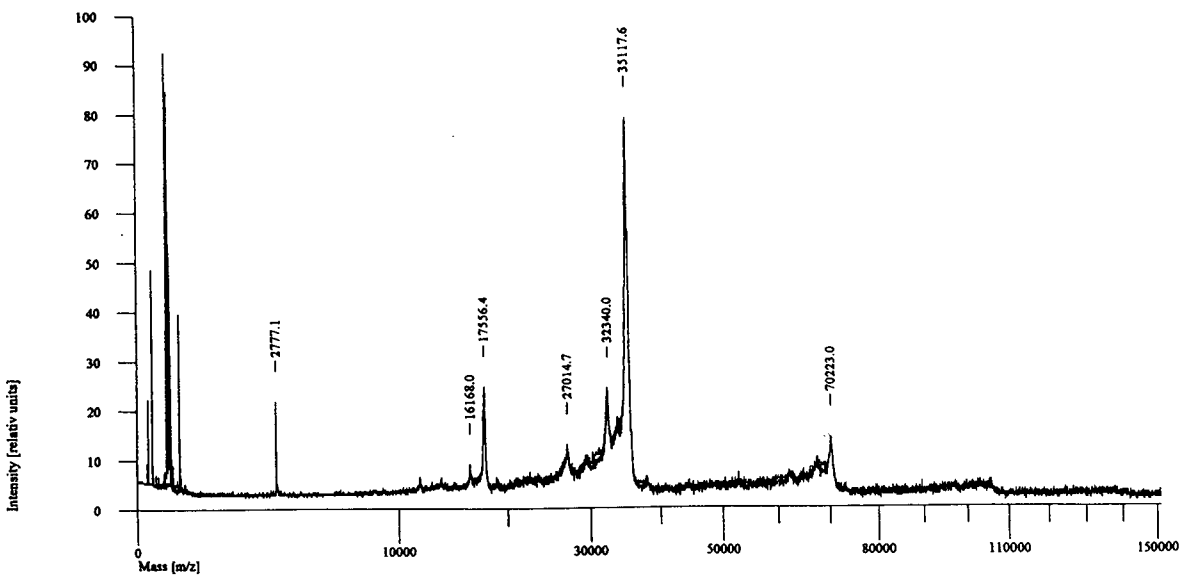


Fig. 3. MALDI-TOF mass spectrum of BSA-FG75.

Table 1
Protein coverages of BSA- and BSA fragment-bonded columns

| Packing | Pore size of base silica (Å) | Protein phase sulfur content (%)[a] | Surface coverage ($\mu$mol/g) |
|---|---|---|---|
| BSA | 120 | 0.24 | 1.9 |
| BSA | 300 | 0.16 | 1.3 |
| BSA-FG75 | 120 | 0.34 | 5.5 |

[a] Calculated from the elemental analysis data for sulfur.

that of the intact BSA. Also, the effect might be due to the shape of the BSA-FG75 being different from that of the intact BSA.

### 3.3. Comparison of retention and enantioselectivity of racemic solutes on BSA and BSA-FG75 columns

Tables 2 and 3 compare the retentions and enantioselectivities of racemic solutes on the BSA and BSA-FG75 columns. Benzodiazepine derivatives, benzoin, warfarin and 2-arylpropionic acid derivatives were resolved on the BSA-FG75 column, but tryptophan and kynurenine were not resolved (data not shown). Andersson et al. [12] reported that no chiral recognition of warfarin, tryptophan or kynurenine was obtained on a BSA fragment column. The differences between our and Andersson et al.'s methods are as follows: (1) we isolated the BSA fragment by size-exclusion chromatography, whereas Andersson et al. used anion-exchange chromatography; (2) we bound the BSA fragment to aminopropylsilica gels activated by DSC, whereas they cross-linked it into aminopropylsilica gels by glutaraldehyde or adsorbed it on silica gels; and (3) the surface coverages of the BSA fragments were 5.5 and 4 $\mu$mol/g in our and their methods, respectively. However, it is not known why warfarin was separated on our BSA fragment column but not on that of Andersson et al. [12]. Also, our BSA fragment column can resolve 2-arylpropionic acid derivatives, whose separations were not examined by Andersson et al.

With regard to the comparison of the retentions and enantioselectivities of racemates on the BSA and BSA-FG75 columns, the latter column gave longer retentions for benzoin and benzodi-

Table 2
Optical resolution of benzodiazepines, benzoin and warfarin on BSA- and BSA fragment-bonded columns

| Compound | Column | | | |
|---|---|---|---|---|
| | BSA | | BSA-FG75 | |
| | $k'_1$ | $\alpha$ | $k'_1$ | $\alpha$ |
| Oxazepam | 3.13 | 3.94 | 6.60 | 2.53 |
| Lorazepam | 5.30 | 2.01 | 13.5 | 2.34 |
| Temazepam | 2.43 | 1.83 | 4.63 | 1.05 |
| Lormetazepam | 4.98 | 1.41 | 9.96 | 1.13 |
| Clorazepate | 3.25 | 1.94 | 3.33 | 1.33 |
| Benzoin | 1.89 | 1.46 | 3.56 | 2.56 |
| Warfarin | 14.9 | 1.59 | 4.44 | 1.21 |

HPLC condition: column, 100 mm × 2.1 mm I.D.; eluent, 50 m*M* phosphate buffer (pH 7.5)–1-propanol (96:4, v/v); column temperature, 25°C; flow-rate, 0.2 ml/min; detection wavelength, 254 nm.

Table 3
Optical resolution of 2-arylpropionic acid derivatives on BSA and BSA fragment-bonded columns

| Compound | Column | | | |
|---|---|---|---|---|
| | BSA | | BSA-FG75 | |
| | $k'_1$ | $\alpha$ | $k'_1$ | $\alpha$ |
| Ketoprofen | 0.68 | 1.00 | 0.65 | 1.00 |
| Ibuprofen | 2.30 | 1.91 | 1.42 | 1.40 |
| Fenoprofen | 1.81 | 1.00 | 1.56 | 1.16 |
| Pranoprofen | 0.57 | 1.00 | 0.33 | 1.00 |
| Flurbiprofen | 4.74 | 1.30 | 2.00 | 1.16 |

HPLC conditions: column, 100 mm × 2.1 mm I.D.; eluent, 50 m*M* phosphate buffer (pH 6.9)–1-propanol (85:15, v/v) containing 4 m*M* octanoic acid; column temperature, 25°C; flow-rate, 0.2 ml/min; detection wavelength, 254 or 220 nm.

azepines, except for clorazepate, and gave higher enantioselectivities for lorazepam and benzoin, as shown in Table 2. Fig. 4A and B show chromatograms of lorazepam on BSA and BSA-FG75 columns, respectively. As shown in Table 3, fenoprofen was resolved on the BSA-FG75 column but was not resolved on the intact BSA column. These results reveal that the binding sites for tryptophan and kynurenine have been lost or otherwise affected, but that the binding site(s) for other compounds tested have been preserved throughout enzymatic cleavage or isolation. The higher enantioselectivities of lorazepam, benzoin and fenoprofen are ascribable to a higher protein density, that is, an increase in the number of chiral recognition site(s) for lorazepam, benzoin and fenoprofen.

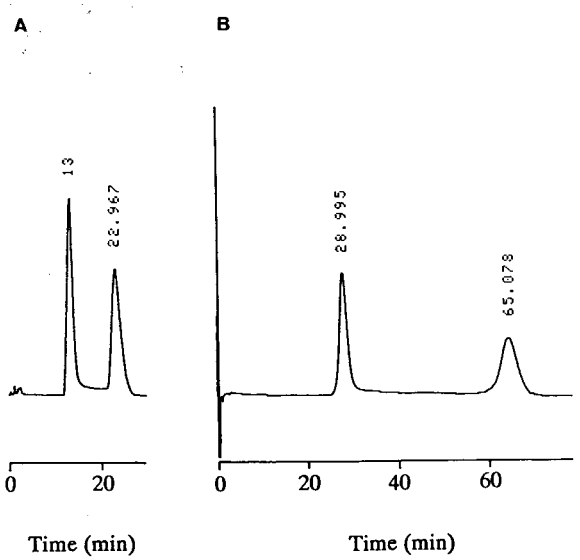


Fig. 4. Chromatograms of lorazepam on the (A) BSA and (B) BSA-FG75 columns. HPLC conditions: column, 100 mm × 2.1 mm I.D.; eluent, 50 m*M* phosphate buffer (pH 7.5)–1-propanol (96:4, v/v); column temperature, 25°C; flow-rate, 0.2 ml/min; detection wavelength, 254 nm; amount injected, 0.1 μg each.

### 3.4. Comparison of loadability of BSA and BSA-FG75 columns

Table 4 shows the influence of the amounts of benzoin loaded on the capacity factor ($k'$), peak symmetry ($\eta$), enantioselectivity ($\alpha$) and resolution ($R_s$) on the BSA and BSA-FG75 columns. Fig. 5 depicts the influence of the amounts of benzoin loaded on peak symmetry ($\eta$). The slight decrease in $\alpha$ values was observed as an increase in the amounts loaded for both the BSA and BSA fragment columns, while a marked decrease in the $R_s$ values occurred. The $\eta$ value of the second-eluted peak on the BSA column was not calculated because of overlapping with the first-eluted peak. The $\eta$ value for a 1.0-nmol injection on to the BSA column was almost the same with that for a 5.0-nmol injection on to the BSA-FG75 column. Also, the value for a 2.5-nmol injection on to the BSA column was almost the same as that for a 10-nmol injection on to the BSA-FG75 column. Fig. 6A and B show chro-

Table 4
Influence of amount of benzoin loaded on capacity factor ($k'$), peak symmetry ($\eta$), enantioselectivity ($\alpha$) and resolution ($R_s$) on BSA- and BSA fragment-bonded columns

| Amount injected (nmol) | Packing | $k'_1$ | $k'_2$ | $\eta_1$ | $\eta_2$ | $\alpha$ | $R_s$ |
|---|---|---|---|---|---|---|---|
| 0.125 | BSA | 1.91 | 2.88 | 1.03 | 1.00 | 1.51 | 2.30 |
| | BSA-FG75 | 2.90 | 6.36 | 1.03 | 0.98 | 2.19 | 5.98 |
| 0.5 | BSA | 1.90 | 2.83 | 1.06 | 1.22 | 1.49 | 1.96 |
| | BSA-FG75 | 2.90 | 6.31 | 1.15 | 1.02 | 2.18 | 5.61 |
| 1.0 | BSA | 1.89 | 2.80 | 1.57 | 1.43 | 1.48 | 1.88 |
| | BSA-FG75 | 2.88 | 6.22 | 1.25 | 1.03 | 2.16 | 5.39 |
| 2.5 | BSA | 1.87 | 2.70 | 1.60 | 1.53 | 1.44 | 1.67 |
| | BSA-FG75 | 2.83 | 5.98 | 1.42 | 1.14 | 2.11 | 4.16 |
| 5.0 | BSA | 1.83 | 2.57 | 1.71 | 1.95 | 1.41 | 1.36 |
| | BSA-FG75 | 2.74 | 5.61 | 1.55 | 1.32 | 2.05 | 3.13 |
| 10 | BSA | 1.79 | 2.39 | 2.13 | 2.00 | 1.34 | 1.05 |
| | BSA-FG75 | 2.68 | 5.25 | 1.64 | 1.66 | 1.96 | 2.35 |
| 20 | BSA | 1.73 | 2.25 | 2.17 | – | 1.30 | 0.78 |
| | BSA-FG75 | 2.58 | 4.97 | 1.66 | 1.84 | 1.93 | 1.94 |

$k'_1$ and $k'_2$ are the capacity factors of the first- and second-eluted benzoin enantiomers, respectively. $\eta_1$ and $\eta_2$ are the asymmetry factors of the first- and second-eluted benzoin enantiomers, respectively. HPLC conditions: column, 100 mm × 2.1 mm I.D.; eluent, 50 m*M* phosphate buffer (pH 7.5)–1-propanol (96:4, v/v); column temperature, 25°C; flow-rate, 0.2 ml/min; detection wavelength, 254 nm.

matograms of benzoin for 10-nmol injections on to the BSA and BSA-FG75 columns, respectively. These results reveal that the BSA-FG75 column has a higher capacity for benzoin. This is due to an increase in the number of chiral recognition site(s) for benzoin on the BSA-FG75 column compared with the intact BSA column. Andersson et al. [12] reported that the BSA fragment column showed a lower loadability for

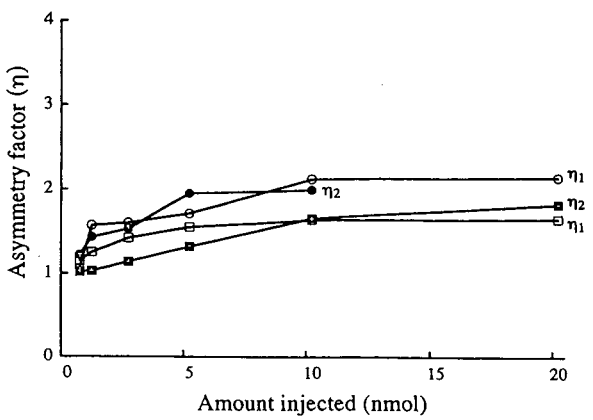


Fig. 5. Influence of the amounts of benzoin loaded on peak symmetry ($\eta$). ○ = BSA; □ = BSA-FG75. HPLC conditions as in Table 4.

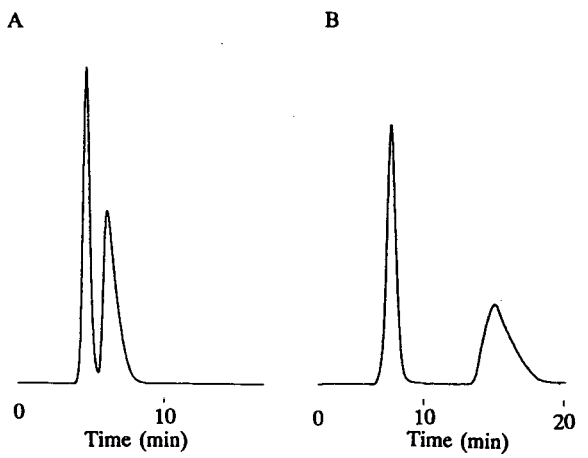


Fig. 6. Chromatograms of benzoin for 10-nmol injections on to (A) the BSA and (B) the BSA-FG75 columns. HPLC conditions as in Table 4.

Table 5
Changes in capacity factor ($k'_1$), enantioselectivity ($\alpha$) and resolution ($R_s$) of racemic solutes with continuous flow of eluent

| Solute | Parameter | BSA column | | BSA-FG75 column | |
|---|---|---|---|---|---|
| | | Before | After 200 h | Before | After 200 h |
| Lorazepam | $k'_1$ | 5.30 | 6.14 | 13.5 | 13.5 |
| | $\alpha$ | 2.01 | 1.73 | 2.34 | 2.28 |
| | $R_s$ | 3.39 | 3.07 | 7.04 | 6.76 |
| Oxazepam | $k'_1$ | 3.13 | 3.58 | 6.60 | 6.79 |
| | $\alpha$ | 3.94 | 3.22 | 2.53 | 2.37 |
| | $R_s$ | 6.69 | 5.29 | 6.73 | 6.44 |
| Clorazepate | $k'_1$ | 6.93 | 6.17 | 3.33 | 2.85 |
| | $\alpha$ | 2.85 | 2.88 | 1.33 | 1.39 |
| | $R_s$ | 4.36 | 5.46 | 1.75 | 1.72 |
| Benzoin | $k'_1$ | 1.89 | 1.99 | 3.57 | 3.52 |
| | $\alpha$ | 1.46 | 1.59 | 2.56 | 2.51 |
| | $R_s$ | 1.40 | 1.88 | 6.44 | 5.23 |

HPLC conditions: column, 100 mm × 2.1 mm I.D.; eluent, 50 m*M* phosphate buffer (pH 7.5)–1-propanol (96:4, v/v); column temperature, 25°C; flow-rate, 0.2 ml/min; detection wavelength, 254 nm.

benzoin than the intact BSA column. As described above, there are many differences between our and Andersson et al.'s methods. It is not known why the BSA-FG75 column gave a higher loadability, which is different from the result of Andersson et al. [12]. However, we can only say that the increased number of chiral recognition site(s) for benzoin was preserved on the BSA-FG75 column.

### 3.5. Stability of BSA fragment column

Table 5 shows the changes in capacity factor ($k'_1$), enantioselectivity ($\alpha$) and resolution ($R_s$) of racemic solutes with a continuous flow of eluent, where 50 m*M* phosphate buffer (pH 7.5)–1-propanol (96:4, v/v) was used. There were slight changes in the $k'_1$, $\alpha$ and $R_s$ values for both columns before and after a continuous flow of the eluent. It was found that the BSA-FG75 column is stable to the continuous flow of the eluent. Andersson et al. [12] reported that the performance of the BSA fragment column deteriorated significantly after the use of buffers with a high alkanol content. However, our results suggest that the BSA-FG75 column should be as stable as the intact BSA column.

## 4. Conclusion

A BSA fragment (BSA-FG75), isolated by size-exclusion chromatography followed by peptic digestion of BSA, had an average molecular mass of about 35 000. The intact BSA column gave higher enantioselectivities for most of the compounds tested than the BSA-FG75 column, whereas the BSA-FG75 column gave higher enantioselectivities for lorazepam and benzoin than the intact BSA column, and had a higher capacity for benzoin. These results are ascribable to the higher density of chiral recognition site(s) on the BSA-FG75 column. Also, the BSA-FG75 column was as stable as the intact BSA column for a continuous flow of eluent.

## Acknowledgements

The authors thank Dr. A. Ingendoh of Finnigan Mat (Tokyo, Japan) for the measurement of MALDI-TOF mass spectrum of the BSA fragment. This work was partly supported by a Grant-in-Aid for Scientific Research (No. 05671799 and No. 06672159) from the Ministry of Education, Science and Culture, Japan.

## References


[1] S.R. Narayanan, *J. Pharm. Biomed. Anal.*, 10 (1992) 251, and references cited therein.
[2] S. Allenmark, *J. Liq. Chromatogr.*, 9 (1986) 425.
[3] E. Domenici, C. Bertucci, P. Salvadori, G. Felix, I. Cahagne, S. Montellier and I.W. Wainer, *Chromatographia*, 29 (1990) 170.
[4] J. Hermansson, *J. Chromatogr.*, 269 (1983) 71.
[5] T. Miwa, M. Ichikawa, M. Tsuno, T. Hattori, T. Miyakawa, M. Kayano and Y. Miyake, *Chem. Pharm. Bull.*, 35 (1987) 682.
[6] T. Miwa, T. Miyakawa and T. Miyake, *J. Chromatogr.*, 457 (1988) 227.
[7] P. Erlandsson, I. Marle, L. Hansson, R. Isaksson, C. Pettersson and G. Pettersson, *J. Am. Chem. Soc.*, 112 (1990) 4573.
[8] S. Thelohan, P. Jadaud and I.W. Wainer, *Chromatographia*, 28 (1989) 551.
[9] I.W. Wainer, P. Jadaud, G.R. Schombaum, S.V. Kadodkar and M.P. Henry, *Chromatographia*, 25 (1988) 903.
[10] J. Haginaka, T. Murashima and Ch. Seyama, *J. Chromatogr. A*, 666 (1994) 203.
[11] T.C. Pinkerton and J. Haginaka, presented at the *17th International Symposium on Column Liquid Chromatography, Baltimore, June 14–19, 1992*, poster 287.
[12] S. Andersson, S. Allenmark, P. Erlandsson and S. Nilsson, *J. Chromatogr.*, 498 (1990) 81.
[13] T.P. King, *Arch. Biochem. Biophys.*, 156 (1973) 509.
[14] T.P. King and M. Spencer, *J. Biol. Chem.*, 245 (1970) 6134.
[15] L.R. Snyder and J.J. Kirkland, *An Introduction to Modern Liquid Chromatography*, Wiley-Interscience, New York, 2nd ed., 1979, p. 222.
[16] P. Erlandsson and S. Nilsson, *J. Chromatogr.*, 482 (1989) 35.

ELSEVIER

Journal of Chromatography A, 694 (1995) 81–89

JOURNAL OF CHROMATOGRAPHY A

# Study of the enantioselective binding between BOF-4272 and serum albumins by means of high-performance frontal analysis

Akimasa Shibukawa[a,*], Miki Kadohara[a], Jing-yi He[a], Masuhiro Nishimura[b], Shinsaku Naito[b], Terumichi Nakagawa[a]

[a]*Faculty of Pharmaceutical Sciences, Kyoto University, Sakyo-ku, Kyoto 606, Japan*

[b]*Laboratory of Drug Metabolism Research, Naruto Research Institute, Otsuka Pharmaceutical Factory, Inc., Naruto-shi, Tokushima 772, Japan*

**Abstract**

High-performance frontal analysis (HPFA) was incorporated in an on-line HPLC system for the study of the enantioselective binding of BOF-4272, a new xanthine oxidase inhibitor, with human, bovine and rat serum albumins. This HPLC system consists of a HPFA column (diol-silica column), an extraction column ($C_4$ column) and a chiral separation column ($\beta$-cyclodextrin immobilized silica column), which were connected in series via two column switching valves. After the direct injection of a solution of 0.5–400 $\mu M$ racemic BOF-4272 and 550 $\mu M$ serum albumin onto the HPFA column, BOF-4272 was eluted, under a mild mobile phase condition (phosphate buffer, pH 7.4, ionic strength 0.17), as a zonal peak containing a plateau region. The drug concentration in the plateau region is the same as that for the unbound drug concentration in the sample solution. A given volume of this plateau region was transferred into the extraction column, and subsequently the extracted BOF-4272 was transferred into the chiral separation column to determine the unbound concentration of each enantiomer.

The binding between BOF-4272 and the serum albumins was enantioselective and species dependent. The unbound concentration of the (+)-isomer in rat serum albumin solution was 1.04–1.14 times larger than that of the antipode, while the unbound concentration of the (−)-isomer in bovine serum albumin solution was 1.04–1.16 times larger than that of the antipode. The enantioselectivity of the binding between BOF-4272 and human serum albumin was concentration dependent. When the total concentration of racemic BOF-4272 was low (0.5 $\mu M$ or 5 $\mu M$), the unbound concentration of the (+)-isomer was 1.15 or 1.06 times larger than that of the (−)-isomer. On the contrary, the unbound concentration of the (−)-isomer was 1.05 or 1.34 times larger than the (+)-isomer in case of the higher total drug concentration (50 $\mu M$ or 400 $\mu M$). Based on the Scatchard analysis of the binding between human serum albumin and BOF-4272 enantiomers, it was found that this change is due to the enantiomeric difference in the binding constant ($K$) and the number of binding site per protein molecule ($n$); $K = 1.22 \cdot 10^5\ M^{-1}$ and $n = 2.30$ for the (+)-isomer, and $K = 2.32 \cdot 10^5\ M^{-1}$ and $n = 1.30$ for the (−)-isomer.

## 1. Introduction

Protein binding is a reversible and kinetically rapid interaction between a drug and serum proteins such as albumin or $\alpha_1$-acid glycoprotein. Protein binding plays an important role in the pharmacokinetics and pharmacodynamics of drugs [1–3]. While unbound drugs can easily transfer from blood into the target organ to exert the pharmaceutical activity or side effect, bound

* Corresponding author.

0021-9673/95/$09.50 
*SSDI* 0021-9673(94)00653-9

drugs pass hardly through the blood cell wall. Some important characteristics of drug disposition, such as hepatic metabolism, renal extraction and volume of distribution, are described as the function of the protein binding fraction (bound/total concentration ratio). Therefore, the protein binding study is important for the effective and safe use of drugs.

Since serum protein is a highly chiral compound, the protein binding of a chiral drug is potentially stereoselective [4]. In addition, serum protein of different animal species sometimes exhibit different binding characteristics, and the understanding of this difference is important for the interspecies scaling in pharmacokinetics of drugs [5]. So far, several papers have reported on the species dependent stereoselectivity of protein binding [6–13]. For example, human serum albumin (HSA) and bovine serum albumin (BSA) are very similar in primary structure [14], but sometimes exhibit different binding characteristics as in the case of the binding with warfarin; HSA binds (*S*)-warfarin more strongly, but BSA binds (*R*)-warfarin more tightly [11]. The serum protein binding of phenoprocoumon, disopyramide and MK-571 (leukotriene $D_4$ antagonist) in several mammalian species can be classified into three groups with respect to the stereospecificity; those that bind (*R*)-isomer more tightly, those that bind (*S*)-isomer bound more tightly, and those that exhibit no stereoselectivity [10,12,13].

The protein binding study of a highly bound drug often confronts an analytical problem, that is, the difficulty in the determination of low levels of unbound drug concentrations by using conventional analytical methods such as equilibrium dialysis and ultrafiltration followed by HPLC analysis. To overcome this problem, we have developed a high-performance frontal analysis (HPFA) method [15–23]. HPFA uses a special HPLC column which retains a drug of a small molecular size on the stationary phase ligand but excludes macromolecules such as proteins [24,25]. After the drug–protein solution is injected directly and continuously into HPFA column, an equilibrium zone is generated in the column. In this zone, the drug–protein binding equilibrium in the interstices of packing materials is in the same condition as that in the sample solution, and the drug concentration in the mobile phase in the micropores of the packing materials is the same as the unbound drug concentration in the sample solution. After the sample injection, the size-excluded protein is eluted first, and subsequently the drug is eluted as a trapezoidal peak having a plateau region. The concentration in the plateau region is equal to the unbound concentration in the sample solution. Therefore, the unbound drug concentration can be determined from the plateau height or by the heart-cut method of this plateau region followed by the on-line HPLC analysis. This is the principle of the HPFA method, and hence the appearance of the plateau region is essential for this method. The reliability of the HPFA method has been confirmed by comparison with conventional ultrafiltration or by Scatchard analyses using many kinds of drugs (indometacin, salicylate, acetazolamide, diclofenac, carbamazepine, warfarin, ketoprofen and fenoprofen). So far, a variety of 'restricted- access' type HPLC columns such as a Pinkerton column and a Hisep column as well as a polymer-based size-exclusion column have been used as HPFA columns. Our recent paper [23] demonstrated that a diol-silica column is useful for the HPFA of hydrophobic drugs which bind strongly with plasma protein.

BOF-4272 {sodium (±)-8-(3-methoxy-4-phenylsulfinylphenyl)- pyrazolo[1,5-*a*]-1,3,5-triazine-4-olate monohydrate} is a newly synthesized xanthine oxidase inhibitor for the treatment of hyperuricemia and gout (Fig. 1). BOF-4272 has a chiral center at its sulfur atom, and the (−)-isomer shows its pharmaceutical activity. BOF-4272 binds with plasma protein very strongly, and its low unbound concentration and severe adsorption on membranes have been hindering the accurate and precise measurement of its unbound concentration by using conventional methods.

In this paper, an on-line HPLC system which combines a HPFA column and a chiral separation column was developed for the determination of the unbound concentrations of BOF-4272 enantiomers. This system was applied for the enantioselective study on the protein binding

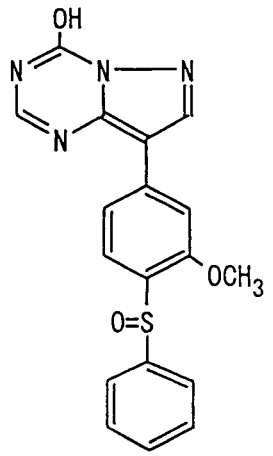


Fig. 1. Structure of BOF-4272.

between BOF-4272 and serum albumins. Interest was focused on the species difference in protein binding.

## 2. Experimental

### 2.1. Reagents and materials

Serum albumins (essentially fatty acid free) of human (Cat. No. A-3782), bovine (A-7511) and rat (A-2018) were purchased from Sigma (St.Louis, MO, USA). Racemic BOF-4272 and the enantiomers were obtained from Otsuka Pharmaceutical (Naruto, Japan).

The diol-silica column (Develosil 100Diol5, 30 cm × 8 mm I.D.) was purchased from Nomura (Seto, Japan). β-Cyclodextrin-immobilized silica column (Ultron ED-CD, 15 cm × 6 mm I.D.) was a kind gift from Shinwa (Kyoto, Japan), and the two β-cyclodextrin-immobilized silica columns were connected in tandem. $C_4$ packing material (Wakosil $5C_4$, Wako, Osaka, Japan) was packed in a stainless-steal column (1 cm × 4 mm I.D.).

### 2.2. Preparation of sample solution

The stock solutions of BOF-4272 were made up in methanol. An appropriate volume of the stock solution was put in a 10-ml screw-capped glass vial, and the solvent was evaporated by use of a nitrogen gas stream. An appropriate volume of serum albumin solution (in sodium phosphate buffer, pH 7.4, ionic strength, $I = 0.17$) was added to the vial to prepare sample solutions.

### 2.3. Determination of unbound BOF-4272 enantiomers by the on-line HPLC system

Fig. 2 shows the schematic diagram of the on-line HPLC system. HPFA column F, extraction column G and chiral separation column H were connected via a four-port switching valve I and a six-port switching valve J. Table 1 lists the HPLC conditions.

The BOF-4272–serum albumin solution was injected directly to the diol-silica column from the injector E. BOF-4272 was eluted as a zonal peak with a plateau region. A given volume of the eluent in this plateau region was then heart-cut by switching the valve I, and was transferred into the extraction column G where BOF-4272 was concentrated. The heart-cut volume (1 ml–28 ml) was selected depending on the unbound drug level. By switching the valve J, the extracted drug was desorbed and transferred into the chiral separation column H. The enantiomers were detected at UV 313 nm. The extraction column was washed with water for 1 min before and after the heart-cut procedure. The HPFA

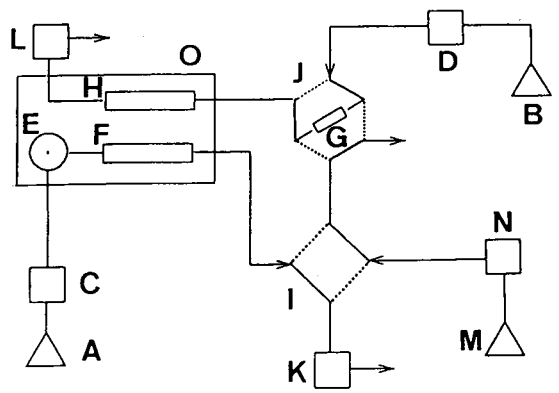


Fig. 2. Schematic diagram of the on-line HPLC system. (A) mobile phase for HPFA; (B) mobile phase for chiral separation; (C,D) pump; (E) sample injector; (F) column for HPFA; (G) column for extraction; (H) column for chiral separation; (I) four-port switching valve; (J) six-port switching valve; (K,L) UV detector; (M) distilled water to wash extraction column; (N) pump; (O) column oven.

Table 1
HPLC conditions of the HPFA–HPLC system

| Sub-system | | Condition |
|---|---|---|
| HPFA | Column | Develosil 100Diol5 (30 cm × 8 mm I.D.) |
| | Mobile phase | Sodium phosphate buffer (pH 7.4, $I = 0.17$) |
| | Flow-rate | 1.0 ml/min |
| | Detection | UV 313 nm |
| | Temperature | 37°C |
| Extraction | Column | Wakosil $5C_4$ (1 cm × 4 mm I.D.) |
| Chiral HPLC | Column | Ultron ES-CD (15 cm × 6 mm I.D.) two columns were connected in series |
| | Mobile phase | 40 m*M* $NaH_2PO_4$–MeOH (55:45, v/v), pH 5.6 |
| | Flow-rate | 1.0 ml/min |
| | Detection | UV 313 nm |
| | Temperature | 37°C |

column and the chiral separation column were kept at 37°C in a column oven.

The instruments used in this study were as follows: pumps C and D (LC-9A, Shimadzu), pump N (Model A-30-S, Eldex Lab., San Carlos, CA, USA), UV detectors K and L (SPD-6A, Shimadzu), injector E (Rheodyne Type 8125, equipped with 600 $\mu$l or 2 ml loop), integrated data analyzer (Chromatopac C-R6A, Shimadzu) and column oven (CS-300C, Chromato-Science, Osaka, Japan).

The injection procedure plays an important role in HPFA. The sample input should ideally be in a rectangular shape in order to create the same drug–protein binding equilibrium zone in the HPFA column as in the sample solution [19]. The sample solution was injected as follows. The injection loop was loaded with 600 $\mu$l of the sample solution and then connected to the mobile phase. After 20 s, the injection valve was reswitched, and the loop was detached from the mobile phase flow. Therefore, the actual injection volume was 333 $\mu$l. By this injection-reswitching technique, the diffused portion of the sample solution in the injection loop was not introduced into the column, thus preventing the perturbation of the drug–protein binding equilibrium.

Fig. 3 shows the typical time program of valve switching, where the heart-cut time is 32–37 min.

### 2.4. Calibration lines

The calibration lines were prepared as follows. The diol-silica column was removed from the line, and the injector loop volume was changed from 600 $\mu$l to 20 $\mu$l. Each 5-$\mu$l portion of racemic BOF-4272 standard solutions (5.15, 10.2, 25.3, 51.7, 113, 207 and 354 $\mu M$) made up in methanol, was injected directly into the extraction column which had been previously washed with water for 1 min. After perfusing the extraction column with water for 1 min, the adsorbed BOF-4272 was back-flashed into the chiral separation column by the column switching procedure. The calibration line of each enantiomer was prepared by plotting peak area (average of three runs) vs. the amount of each enantiomer injected. The calibration lines were: area = 5.16 × amount (pmole) − 16.2 for the (+)-isomer, and area = 5.20 × amount (pmole) − 15.8 for the (−)-isomer. Each calibration line indicated good linearity (correlation

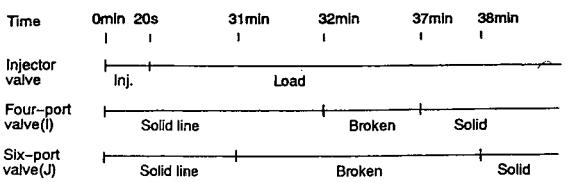


Fig. 3. Typical time program for valve switching.

coefficient, >0.99996). The unbound BOF-4272 concentration was then calculated enantioselectively from the amount of each enantiomer divided by the heart-cut volume.

### 2.5. Extraction of BOF-4272 on the extraction column

The peak areas of (+)- and (−)-BOF-4272 obtained by injecting a 5-μl portion of 51.7 μM racemic BOF-4272 methanol solution into the extraction column G were 103% and 101% of those obtained by the direct injection of the same volume of the same BOF-4272 solution into the chiral column H. This indicates the complete extraction of BOF-4272 onto the column G and the complete transfer of the extracted BOF-4272 into the chiral separation column.

## 3. Results and discussion

Fig. 4 shows the elution profile of 50 μM BOF-4272 and 550 μM human serum albumin (HSA) mixed solution. As the injection volume increased from 10 μl to 333 μl, the BOF-4272 peak height reached the maximum level, and trapezoidal drug peak having a plateau region appeared, as shown in Fig. 4C. The plateau height did not increase with the further increase in the injection volume (Fig. 4D). The sample injection volume in HPFA should be large enough to obtain the plateau region of the drug elution profile. Based on this result, the injection volume in the following analyses was 333 μl.

The unique feature of the HPFA method is that the bound drug is not separated from the unbound drug, but is converted into the unbound drug in HPFA column. The eluted amount of the drug is the same as the injected amount, but the concentration of the eluted drug is regulated by the protein binding to be the same as the unbound drug concentration. As a result of this 'regulation effect' [23], the plateau volume becomes larger than the initial injection volume. In Fig. 4C, while the injection volume was 333 μl, as much as ca. 30 ml of the plateau region was observed. As will be mentioned later, the 'regulation effect' is beneficial to detect low levels of unbound drug concentration.

Fig. 5 shows the chiral separation profiles of BOF-4272 on the β-cyclodextrin-immobilized silica column. The sample solutions used in Fig. 5 contained 5 μM racemic BOF-4272 and 550 μM bovine serum albumin (BSA) or rat serum albumin (RSA). The (+)-isomer was eluted faster than the (−)-isomer, and the baseline separation of the enantiomers was achieved within 15 min. Serum albumins did not interfere with the chiral separation, because they were completely excluded before the heart-cut time.

Table 2 lists the unbound concentrations of

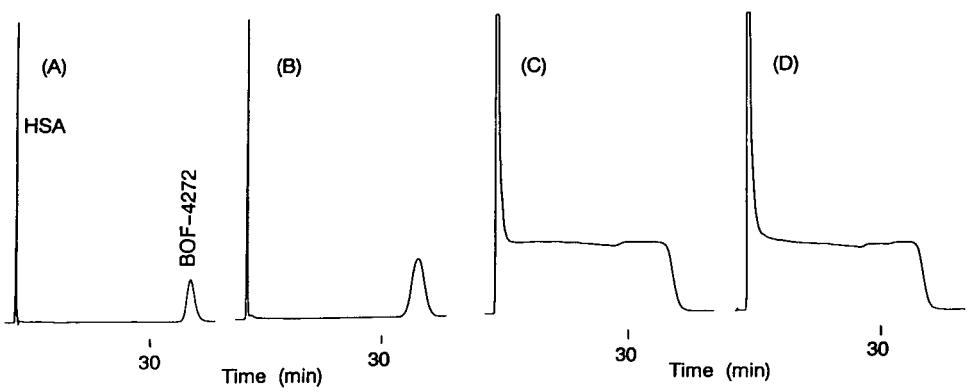


Fig. 4. Elution profile of 50 μM racemic BOF-4272 and 550 μM HSA. Injection volume; (A) 10 μl, (B) 20 μl, (C) 333 μl, (D) 667 μl. HPLC conditions; see Table 1.

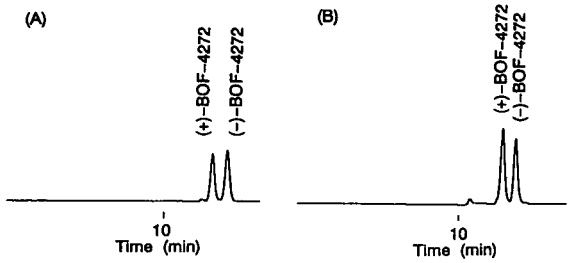


Fig. 5. Chiral separation of BOF-4272 in the heart-cut fraction. Sample solution; (A) 5 $\mu M$ BOF-4272–550 $\mu M$ BSA, (B) 5 $\mu M$ BOF-4272–550 $\mu M$ RSA. Heart-cut volume, 10 ml. HPLC conditions; see Table 1.

BOF-4272 enantiomers determined by the present on-line HPLC system. The total concentration of racemic BOF-4272 ranges from 0.5 $\mu M$ to 400 $\mu M$. The lowest concentration (0.5 $\mu M$) is within the clinical plasma concentration range of BOF-4272. The albumin concentration (550 $\mu M$) is its physiological concentration. In the analyses of the samples with the lowest drug concentration (0.5 $\mu M$), as much as 28 ml of the plateau region was heart-cut (heart-cut time was from 10 min to 38 min). As a result, low concentrations of unbound enantiomers (1.23–1.52 n$M$) could be determined by UV detection with good reproducibility (C.V. $< 3.36\%$, $n = 5$). This clearly indicates the usefulness of the 'regulation effect' of the HPFA method for the determination of low levels of unbound drug concentration.

As shown in Table 2, BOF-4272 binds strongly with serum albumins. The unbound fraction was 0.492–1.05% in HSA solutions, 0.44–0.66% in BSA solutions, and 0.532–0.744% in RSA solutions. Comparing the samples containing the same total concentration of BOF-4272 (5 or 50 $\mu M$), but different species of serum albumin, the unbound concentrations of both enantiomers were the lowest in BSA solution and were the highest in RSA solution. This means that the protein binding becomes stronger in the order RSA < HSA < BSA.

The binding of BOF-4272 with rat and bovine serum albumins exhibited slight but significant enantioselectivity, and the direction of the selectivity is opposite between these two species. The unbound concentration of the (+)-isomer was 1.04–1.14 times significantly larger ($p < 0.01$) than that of the (−)-isomer in RSA solution. On the other hand, the unbound concentration of the (−)-isomer was 1.04–1.16 times significantly larger ($p < 0.01$) than the antipode in BSA solution.

The binding between BOF-4272 and HSA was also enantioselective, and the selectivity depended on the total drug concentration. In case of the lower total drug concentration (0.5 $\mu M$ and 5 $\mu M$), the unbound concentration of the (+)-isomer was significantly larger ($p < 0.01$) than that of the (−)-isomer. On the other hand, when the total drug concentration was 50 $\mu M$,

Table 2
Unbound concentrations (mean ± S.D., $n = 2$) of BOF-4272 enantiomers

| Human | | | Bovine | | | Rat | | |
|---|---|---|---|---|---|---|---|---|
| (+) | (−) | (+)/(−) | (+) | (−) | (+)/(−) | (+) | (−) | (+)/(−) |
| 400 $\mu M$ Racemic BOV-4272 and 550 $\mu M$ albumin | | | | | | | | |
| 1.56 ± 0.091 $\mu M$ | 2.09 ± 0.182 $\mu M$ | 0.748 ± 0.021 | | | | | | |
| 50 $\mu M$ Racemic BOF-4272 and 550 $\mu M$ albumin | | | | | | | | |
| 170 ± 1.02 n$M$ | 178 ± 1.19 n$M$ | 0.960 ± 0.003 | 158 ± 1.01 n$M$ | 165 ± 1.06 n$M$ | 0.956 ± 0.001 | 186 ± 0.67 n$M$ | 180 ± 0.70 n$M$ | 1.04 ± 0.001 |
| 5 $\mu M$ Racemic BOF-4272 and 550 $\mu M$ albumin | | | | | | | | |
| 15.0 ± 0.12 n$M$ | 14.1 ± 0.13 n$M$ | 1.06 ± 0.002 | 11.0 ± 0.08 n$M$ | 12.8 ± 0.03 n$M$ | 0.861 ± 0.01 | 16.6 ± 0.05 n$M$ | 15.4 ± 0.13 n$M$ | 1.08 ± 0.01 |
| 0.5 $\mu M$ Racemic BOF-4272 and 550 $\mu M$ albumin | | | | | | | | |
| 1.42 ± 0.025 n$M$ | 1.23 ± 0.018 n$M$ | 1.15 ± 0.010 | | | | 1.52 ± 0.051 n$M$ | 1.33 ± 0.030 n$M$ | 1.14 ± 0.015 |

the unbound concentration of the (−)-isomer was significantly larger ($p < 0.01$) than the antipode. The enantiomeric difference in the unbound concentration became more prominent for the higher total drug concentration (400 $\mu M$).

To elucidate the concentration-dependent enantioselectivity observed in Table 2, Scatchard analyses of the binding between HSA and each enantiomer were performed. Two sets of sample solutions, each containing 550 $\mu M$ HSA and eight concentrations (0.25–400 $\mu M$) of (+)- or (−)-BOF-4272, were analyzed by the present on-line HPLC system, and the Scatchard plots were made as shown in Fig. 6. The correlation coefficient of the line [$r = -0.985$ and $-0.990$ for (+)-isomer and (−)-isomer, respectively] indicates the good linearity of these plots. The estimated binding parameters were listed in Table 3. The binding constant ($K$) of the (−)-isomer is almost two times larger than that of the (+)-isomer, whereas the binding site per protein molecule ($n$) of the (+)-isomer is almost two times larger than that of the (−)-isomer. By using these binding parameters, the enantiomeric unbound concentration ratio [(+)-isomer/(−)-isomer] at the same total drug concentration was calculated from Eq. (1), and was plotted against the total concentration in Fig. 7.

Table 3
Binding parameters for the interaction between HSA and BOF-4272 enantiomers

| | $K\ (M^{-1})$ | $n$ | $R$ |
|---|---|---|---|
| (+)-BOF-4272 | $1.22 \cdot 10^5$ | 2.30 | −0.985 |
| (−)-BOF-4272 | $2.32 \cdot 10^5$ | 1.30 | −0.990 |

Buffer condition: pH 7.4, $I = 0.17$, 37°C.

$$ER = \frac{K_{(-)}(\{[1 + K_{(+)}(n_{(+)}P - C_t)]^2 + 4K_{(+)}C_t\}^{1/2} - 1 - K_{(+)}(n_{(+)}P - C_t))}{K_{(+)}(\{[1 + K_{(-)}(n_{(-)}P - C_t)]^2 + 4K_{(-)}C_t\}^{1/2} - 1 - K_{(-)}(n_{(-)}P - C_t))} \quad (1)$$

where $ER$ is the enantiomeric unbound concentration ratio, $C_t$ is the total concentration of BOF-4272 enantiomer, and $P$ is the protein concentration (550 $\mu M$). The subscripts (+) and (−) imply the (+)-isomer and (−)-isomer, respectively. Fig. 7 shows the calculated concentration dependency of the enantioselective BOF-4272–HSA binding, using the enantiomeric unbound concentration ratio as the indication of the enantioselectivity. The effect of mutual enantiomeric displacement is not taken into consideration for convenience. As shown in Fig. 7, when the total drug concentration is low, the calculated (+)/(−) unbound concentration

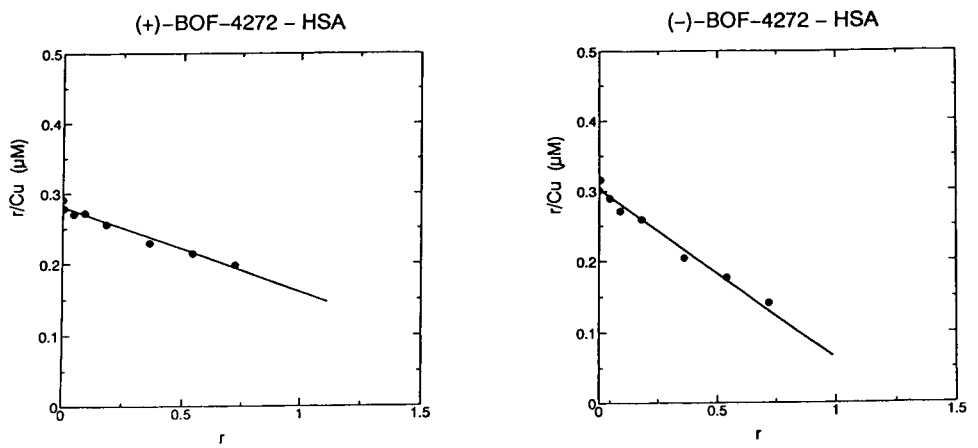


Fig. 6. Scatchard plots of the binding between HSA and BOF-4272 enantiomers. $r$ represents the moles of the bound drug per one mole of HSA. The binding constant ($K$) and the number of binding sites per protein molecule ($n$) were estimated by curve fitting using the equation $r/C_u = -Kr + Kn$, where $C_u$ is the unbound drug concentration. The solid lines were the best fitted ones.

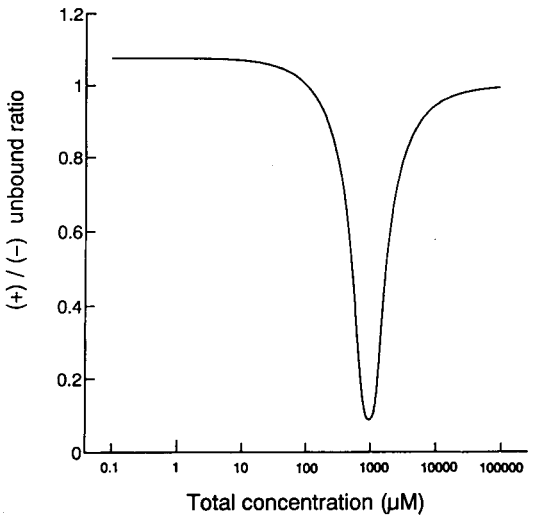


Fig. 7. The relation between the enantiomeric unbound concentration ratio [(+)-isomer/(−)-isomer] of BOF-4272 and the total drug concentration calculated from Eq. 1. The total drug concentration was logarithmically scaled on the abscissa.

ratio is larger than unity, which means that the unbound concentration of the (+)-isomer is larger than that of the antipode. However, with the increase in the total drug concentration, the ratio decreases, and the unbound concentration of the (−)-isomer becomes larger than that of the (+)-isomer. This change agrees with that observed in Table 2. With further increase in the total drug concentration, the enantiomeric unbound concentration ratio reaches the minimum value, and then increases to converge in unity. This concentration dependency can be qualitatively explained as follows. When the total drug concentration is much lower than the protein concentration, plenty of binding sites remain empty. In this condition, the enantiomeric difference in the $n$ value exhibits little effect on the enantioselectivity, and the unbound concentration of the (−)-isomer which has the larger binding constant becomes lower than that of the (+)-isomer. On the contrary, with increasing the drug concentration, the number of the occupied binding sites increases. In this condition, the difference in the $n$ value exhibits more prominent effect on the enantioselectivity than the binding constant, and consequently the unbound concentration of the (+)-isomer which has the larger $n$ value becomes lower than the (−)-isomer. With further increase in the total drug concentration, the unbound fractions of both enantiomers reach unity, and consequently the enantioselectivity diminishes.

A similar concentration dependency was observed in the stereospecific protein binding of disopyramide in cow serum [12], where the binding parameters were different between disopyramide enantiomers in the same fashion as BOF-4272 enantiomers; (*R*)-(−)- disopyramide exhibited the stronger binding constant ($K = 1.3 \cdot 10^5\ M^{-1}$) but smaller binding capacity ($n = 3.7 \cdot 10^{-5}\ M$) than (*S*)-(+)-disopyramide ($K = 0.51 \cdot 10^5\ M^{-1}$, $n = 5.4 \cdot 10^{-5}\ M$). The unbound fraction of (*R*)-(−)-disopyramide was lower than the antipode in case of lower drug concentration (less than 40 $\mu M$), and the reverse was true in case of the higher drug concentration (Fig. 2 in Ref. [12]).

For a chiral drug which binds strongly with serum protein, the stereoselectivity of the protein binding may be examined, for the convenience of detection, by using model sample solutions of much higher drug concentration than the therapeutic levels. This approach may be misleading, because the stereoselectivity in the therapeutic levels may be different as is the case for BOF-4272. HPFA serves to avoid this problem by enabling the determination of low levels of stereoselective unbound drug concentrations.

## 4. Conclusion

The present on-line HPLC system which combines a HPFA column and a chiral separation column allows the simple and easy determination of the concentration of unbound BOF-4272 enantiomers. The 'regulation effect' served to detect as low as 1 n$M$ of unbound BOF-4272 by UV detection. The binding between BOF-4272 with serum albumins was strong and enantioselective. RSA and BSA exhibited different enantioselectivity. The binding between BOF-4272 and HSA exhibited the concentration de-

pendent enantioselectivity based on the enantiomeric difference in the binding parameters.

## Acknowledgement

This study was supported by the Research Grant from the Asahi Glass Foundation, which is greatly acknowledged. The authors are also grateful to Otsuka Pharmaceutical Factory and Shinwa Chemical Industries Co. for their kind gift of BOF-4272 and chiral HPLC columns, respectively.

## References

[1] M.C. Meyer and D.E. Guttman, *J. Pharm. Sci.*, 57 (1968) 895–918.
[2] J.J. Vallner, *J. Pharm. Sci.*, 66 (1977) 447–465.
[3] T.C. Kwong, *Clin. Chim. Acta*, 151 (1985) 193–216.
[4] G.T. Tucker and M.S. Lennard, *Pharm. Ther.*, 45 (1989) 309–329.
[5] P.J. McNamara, *Drugs Pharm. Sci.*, 48 (1991) 267–300.
[6] D.T. Witiak and M.W. Whitehouse, *Biochem. Pharmacol.*, 18 (1969) 971–977.
[7] R.I. Nazareth, T.D. Sokoloski, D.T. Witiak and A.T. Hopper, *J Pharm. Sci.*, 63 (1974) 203–211.
[8] A. Yacobi and G. Levy, *J. Pharmacokinet. Biopharm.*, 5 (1977) 123–131.
[9] N.A. Brown, E. Jahnchen, W.E. Muller, W. Schmidt and U. Wollert, *Comp. Biochem. Physiol, C Comp. Pharmacol.*, 62 (1979) 101–105.
[10] W. Schmidt and E. Jahnchen, *Experientia*, 34 (1979) 1323–1325.
[11] C. Lagerorantz, T. Larsson and I. Denfors, *Comp. Biochem Physiol.*, 69C (1981) 375–378.
[12] J.J. Lima, *Drug Metab. Dispos.*, 16 (1988) 563–567.
[13] J.H. Lin, F.A. DeLuna, E.H. Ulm and D.J. Tocco, *Drug Metab. Dispos.*, 18 (1990) 484–487.
[14] U. Kragh-Hansen, *Pharmacol. Rev.*, 33 (1981) 17–53.
[15] A. Shibukawa, T. Nakagawa, N. Nishimura, M. Miyake and H. Tanaka, *Chem. Pharm. Bull.*, 37 (1989) 702–706.
[16] A. Shibukawa, N. Nishimura, K. Nomura, Y. Kuroda and T. Nakagawa, *Chem. Pharm. Bull.*, 38 (1990) 443–447.
[17] A. Shibukawa, M. Nagao, Y. Kuroda and T. Nakagawa, *Anal. Chem.*, 62 (1990) 712–716.
[18] N. Nishimura, A. Shibukawa and T. Nakagawa, *Anal. Sci.*, 6 (1990) 355–359.
[19] A. Shibukawa, A. Terakita, J. He and T. Nakagawa, *J. Pharm. Sci.*, 81 (1992) 710–715.
[20] A. Terakita, A. Shibukawa and T. Nakagawa, *Anal. Sci.*, 9 (1993) 229–232.
[21] A. Shibukawa, M. Nagao, A. Terakita, J. He and T. Nakagawa, *J. Liq. Chromatogr.*, 16 (1993) 903–914.
[22] A. Terakita, A. Shibukawa and T. Nakagawa, *Anal. Sci.*, 10 (1994) 11–15.
[23] A. Shibukawa, C. Nakao, T. Sawada, A. Terakita, N. Morokoshi and T. Nakagawa, *J. Pharm. Sci.*, 83 (1994) 868–873.
[24] T.C. Pinkerton, *J. Chromatogr.*, 544 (1991) 13–23.
[25] D.J. Anderson, *Anal. Chem.*, 65 (1993) 434R–443R.

ELSEVIER

Journal of Chromatography A, 694 (1995) 91–100

JOURNAL OF CHROMATOGRAPHY A

Review

# Development of chiral stationary phases consisting of polysaccharide derivatives

Kazuma Oguni, Hirofumi Oda, Akito Ichida*

*Daicel Chemical Industries Ltd., Research Center, Shinzaike, Aboshi-ku, Himeji, Hyogo 671-12, Japan*

**Abstract**

Various chiral stationary phases (CSPs) consisting of polysaccharide derivatives were developed by adsorbing them on silica gel on the basis of information obtained from cellulose triacetate. The chiral recognition ability increases with an increase in conformational regularity. The regularity of cellulose triacetate depends greatly on the kind of solvents used in the coating procedure. This finding seems to be applicable to other coating-type CSPs based on polysaccharide derivatives. Some interactions were considered between a CSP and an enantiomer for chiral discrimination. By using $^{13}C$ NMR spectroscopy, 1-phenylethyl alcohol was chirally recognized on cellulose tris(4-methylbenzoate).

## Contents



## 1. Introduction

The importance of the establishment of acquisition methods and analytical methods for chiral compounds has increased in various fields such as pharmaceuticals and agriculture and in asymmetric synthesis. High-performance liquid chromatographic (HPLC) resolution on chiral stationary phases (CSPs) is of interest as a simple and practical method applicable to the preparative separation and determination of optical isomers. CSPs are classified into two types according to the molecular mass of the chiral resolving agents. The first type is based on low-molecular-mass resolving agents bonded to silica gel, and the other on high-molecular-mass poly-

* Corresponding author.

*SSDI* 0021-9673(94)00789-6

mers. In the former type, the relationships between CSPs and resolved racemates has been substantially elucidated as it is possible to design CSPs based on the expected resolution mechanism. However, with high-molecular-mass CSPs, the explanation of the chiral discrimination mechanism is difficult from the structure of the constitutional monomer units. Many kinds of high-molecular-mass resolving agents are known, and various racemates from simple aliphatic carbonyl compounds to polyfunctional compounds have been resolved. In this paper, we describe our work on the development of CSPs consisting of polysaccharide derivatives.

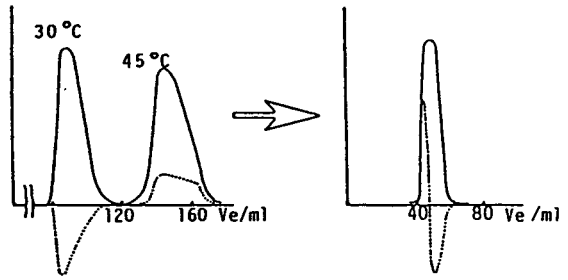


Fig. 1. Chromatograms of the separation of Tröger's base on MCTA (left) and on cellulose triacetate precipitated from acetone (right). Eluent, ethanol; column length, 16 cm; solid lines, UV detection; dotted lines, optical rotation; $V_e$, elution volume; column temperature, 30°C, increased to 45°C after the first component was eluted [3,4].

## 2. Development of CSPs

### *2.1. Factors controlling the appearance of chiral discrimination abilities of cellulose triacetates*

A high chiral discrimination ability of optically active poly(triphenylmethyl methacrylate) coated on silica gel was already known [1,2] when we began the study on CSPs. Its ability comes from the one-handed helical structure of the polymer. We therefore focused on the higher order structure of optically active polymers to attain efficient chiral discrimination. Hesse and Hagel [3,4] succeeded in the complete resolution of Tröger's base on a column packed with microcrystalline cellulose triacetate (MCTA) synthesized by acetylation of microcrystalline cellulose under heterogeneous conditions. However, the type of compounds resolved was limited and the plate number of the column was low because ground MCTA was used as a CSP. Therefore expected that these defects could be overcome if various cellulosic derivatives could be prepared and coated on silica gel as in the case of poly(triphenylmethyl methacrylate). However, Hesse and Hagel also pointed out that dissolution and consequent reprecipitation of MCTA, which was accompanied by irreversible transformation of crystalline lattice from CTA-I to CTA-II, resulted in almost complete loss of chiral discrimination ability, which even showed reversed enantioselectivity recognized by a polarimeter (Fig. 1). Hence it was widely accepted that for efficient resolution on cellulose triacetate, it is very important to keep the crystalline structure as in natural cellulose. Therefore, procedures accompanying dissolution such as homogeneous acetylation and coating on silica gel had not been applied to CSPs consisting of cellulosic derivatives.

We investigated the relationships between the chiral discrimination ability and the crystalline structure of cellulose triacetate in detail, and obtained some important results:

(i) the discrimination ability of MCTA decreased with an increase in the degree of crystallinity (Fig. 2) [5];

(ii) cellulose triacetate had chiral discrimination ability, even if it was prepared under homogeneous conditions (Fig. 3);

(iii) enantioselectivity was reversed between MCTA (CTA-1) and cellulose triacetate (CTA-II) (Fig. 4) [6,7].

(iv) high performance of the column was realized by coating on silica gel;

(v) for cellulose triacetate coated on silica gel, its chiral discrimination ability was optimized by changing the solvents used for coating (Fig. 5) [8].

The chiral discrimination ability was increased in the order of the coating solvent(s) $CH_2Cl_2$ only, $CH_2Cl_2$–$CF_3COOH$ and $CH_2Cl_2$–phenol (Fig. 5). The conformation of cellulose triacetate seems to be different in the above solutions and

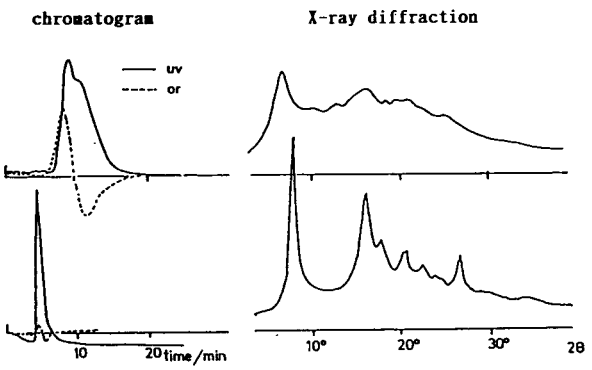


Fig. 2. Chromatograms and X-ray diffractograms of MCTA (top) and MCTA crystallized at 230°C for 1 h (bottom). Sample, mandelamide; eluent, 95% aqueous ethanol; flow-rate, 0.5 ml/min. The broken lines in the chromatograms show optical rotation curves.

the difference may be retained on the surface of silica gel after the solvents have been removed. The conformational difference was investigated by cross polarization magic angle spinning (CP/MAS)$^{13}C$ NMR spectroscopy (Fig. 6) [9]. The chemical shifts for each carbon did not change at all. However, the half-widths of the signals became sharper for the C–1 carbon of anhydroglucose in the order $CH_2Cl_2$ (315 Hz), $CH_2Cl_2$–$CF_3COOH$ (243 Hz) and $CH_2Cl_2$–phenol (218 Hz). In general, the line width of the NMR signal depends on the regularity of molecular conformation and mobility, but change in spin–lattice relaxation time ($T_1$), which reflects the latter, was not detected among the polymers recovered from the solutions. This result seems to show that the narrowing of the

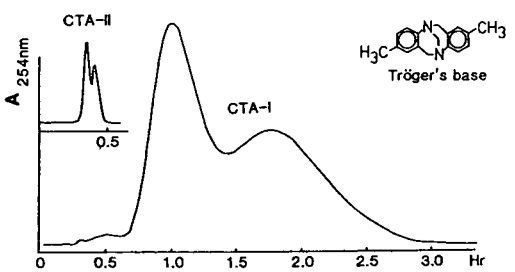


Fig. 3. Chiral discrimination of Tröger's base on CTA-II and CTA-I (MCTA). Eluent, ethanol; column, 25 cm × 0.46 cm I.D.; flow-rate, 0.2 ml/min.

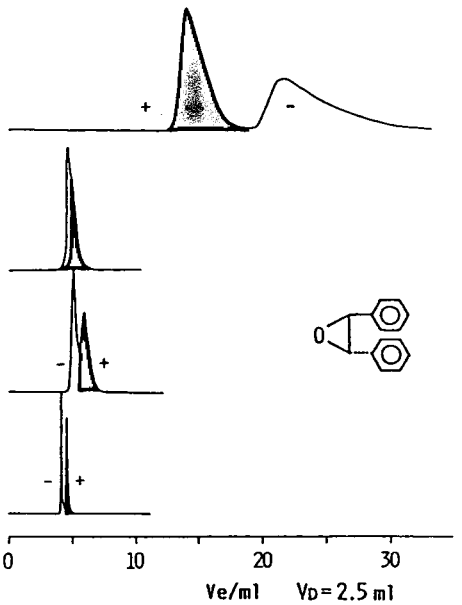


Fig. 4. Chiral discrimination of *trans*-1,2-diphenyloxirane racemate. From top to bottom: (1) on MCTA; eluent, ethanol; (2) on CTA crystallized in formamide at 180°C; eluent, ethanol; (3) on moderate crystalline CTA; eluent, ethanol; (4) on CTA coated on silica gel; eluent, *n*-hexane–2-propanol (9:1, v/v). Column, 25 cm × 0.46 cm I.D.; flow-rate, 0.5 ml/min; $V_e$, elution volume; $V_D$, dead volume.

C-1 signal is responsible for the higher regularity of the conformation of cellulose triacetate about the β-1,4-glycosidic linkage, not for enhanced molecular mobility. This phenomenon does not seem to be restricted to cellulose triacetate. For instance, cellulosic carbamate derivatives with liquid crystallinity, which relates to the regularity of the polymer conformation, have high chiral discrimination abilities [10]. From these results, it was concluded that a microcrystalline structure of cellulose triacetate was not always necessary for high chiral discrimination, and the formation of an adequate morphology of cellulose triacetate on silica gel allowed discrimination abilities to be achieved.

### 2.2. Other cellulosic derivatives

The procedure for coating cellulose triacetate on silica gel was readily applied to other derivatives of cellulose (Fig. 7). Cellulose nitrate

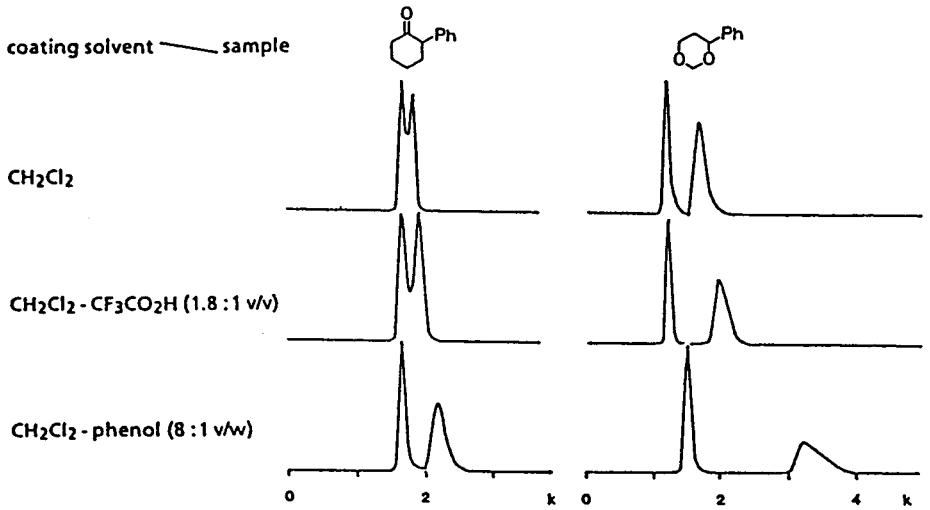


Fig. 5. Effect of coating solvents on chiral discrimination of cellulose triacetate. $k$ = Capacity factor.

[5,11], aromatic esters such as benzoate [5,12] and cinnamate [6,7] and phenylcarbamate [6,7,13] have been prepared and coated on silica gel. These CSPs have characteristic chiral discrimination abilities, which are enhanced by the introduction of substituents on the phenyl groups of the derivatives [10,12]. Commercially available cellulosic CSPs coated on silica gel are shown in Fig. 8. Various racemates can be resolved on these CSPs by using $n$-hexane–2-propanol or ethanol mixtures as the mobile phase. Among the derivatives, 3,5-dimethylphenylcarbamate and 4-methylbenzoate particularly have high chiral discrimination abilities for aryloxypropanolamines and arylpropionic acids, respectively. Although the only difference between cellulose tribenzoate and cellulose tris(4-methylbenzoate) is whether they bear a methyl on the phenyl group or not, their chiral discrimination abilities are very different (Table 1). Compounds with a larger molecular size are often better resolved on the 4-methylbenzoate, e.g., Tröger's base can be well resolved on cellulose tris(4-methylbenzoate), but cannot be resolved on the benzoate. The shape and size of the chiral adsorbing sites of the two benzoates seem dramatically different. Although the difference and the chiral discrimination mechanisms have not been clarified, such chiral sites seem to exist regularly along the polymer chain because of the ordered arrangement of ester groups.

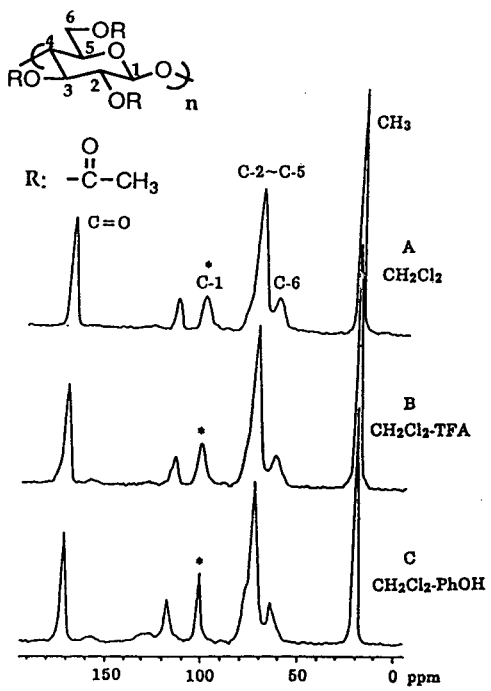


Fig. 6. 67.8 MHz CP/MAS $^{13}C$ NMR spectra of cellulose triacetates solidified from different solvents.

The CSP consisting of cellulose tris(3,5-di-

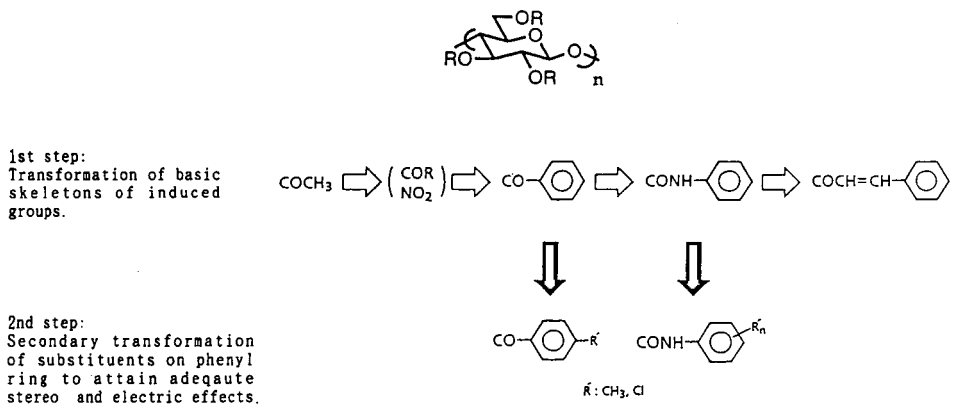


Fig. 7. Concepts of derivatization.

methylphenylcarbamate) also shows high chiral discrimination abilities when using aqueous mobile phases such as acetonitrile containing water or aqueous perchlorate buffer solution [14] (Fig. 9). Some racemates, e.g., verapamil and trimepramine, which were not resolved using *n*-hexane–2-propanol, could be resolved with acetonitrile containing water. The degree of resolution depends on the composition of the mobile phase, pH, kind of additive salt, etc. [15]. In general, the resolution of neutral compounds is not influenced by the acidity of a mobile phase and the kind of salt. In order to attain sufficient resolution of acidic compounds such as N-derivatized amino aids, a sufficient acidity of the mobile phase is necessary for the suppression of ionization of the carboxyl group. Perchloric acid and phosphoric acid are suitable for the separation of acids. For basic compounds with a primary, secondary and tertiary nitrogen such as propranolol and alimemazine, their retention and resolution depend on the kind of counter anion of the additive salt. The retention increases in the order $ClO_4^- > SCN^- > I^- > N_3^- > Br^- > Cl^- > AcO^-$. This order is in good agreement with that of chaotropicity [16] characterized by less localized electric charge, high polarizability and low degree of hydration of anions.

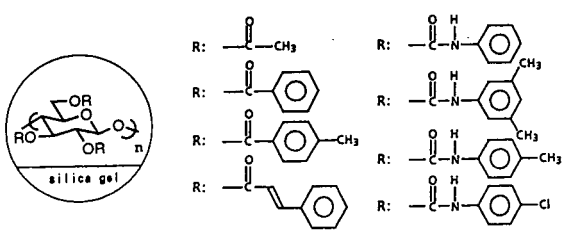


Fig. 8. Commercially available CSPs consisting of cellulose derivatives.

### 2.3. CSPs consisting of amylosic derivatives

Amylose is also a well known polysaccharide. The monomer unit of amylose is again D-glucose, which is the same as that of cellulose. However, amylose is said to have a helix structure as a higher order structure based on the $\alpha$-linkage of D-glucose units. Hence, the chiral discrimination ability of amylose derivatives [17] is very different from that of cellulose. For example, arylpropanolamines such as propranolol and pindolol are well resolved on cellulose tris(3,5-dimethylphenylcarbamate) coated on silica gel, but are not well resolved on the corresponding amylose derivative. Some other differences are shown in Table 2. The tris(3,5-dimethylphenylcarbamate) derivatives of cellulose seem to be complementary from the viewpoint of resolved compounds. A large difference in chiral discrimination ability was observed on (*S*)-methylbenzylcarbamate derivatives. With the amylose, racemates with a $\beta$-lactam skeleton were well resolved, but they could not be resolved on the corresponding cellulosic derivative.

Table 1
Difference in enantioselectivity ($\alpha$-value) between cellulose tris(4-methylbenzoate) (OJ) and cellulose tribenzoate (OB)

| | OJ | OB | | OJ | OB | | OJ | OB |
|---|---|---|---|---|---|---|---|---|
| 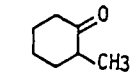 | 1.0 | 1.15 | 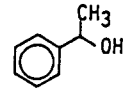 | 1.17 | 1.57 | 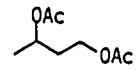 | 1.0 | 1.73 |
| 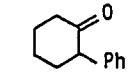 | 1.18 | 1.47 | 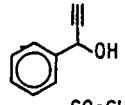 | 1.58 | 1.20 | 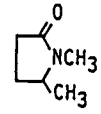 | 1.0 | 1.21 |
| 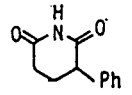 | 2.15 | 1.19 | 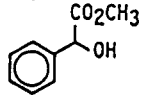 | 1.21 | 1.0 | 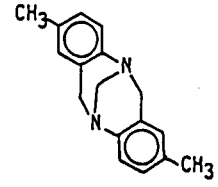 | 6.05 | ca. 1.0 |
| 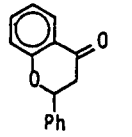 | 1.17 | 1.0 | 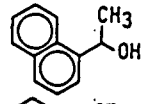 | 1.54 | 1.37 | | | |
| | | | 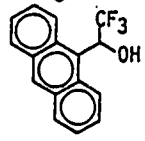 | 1.22 | 1.0 | | | |

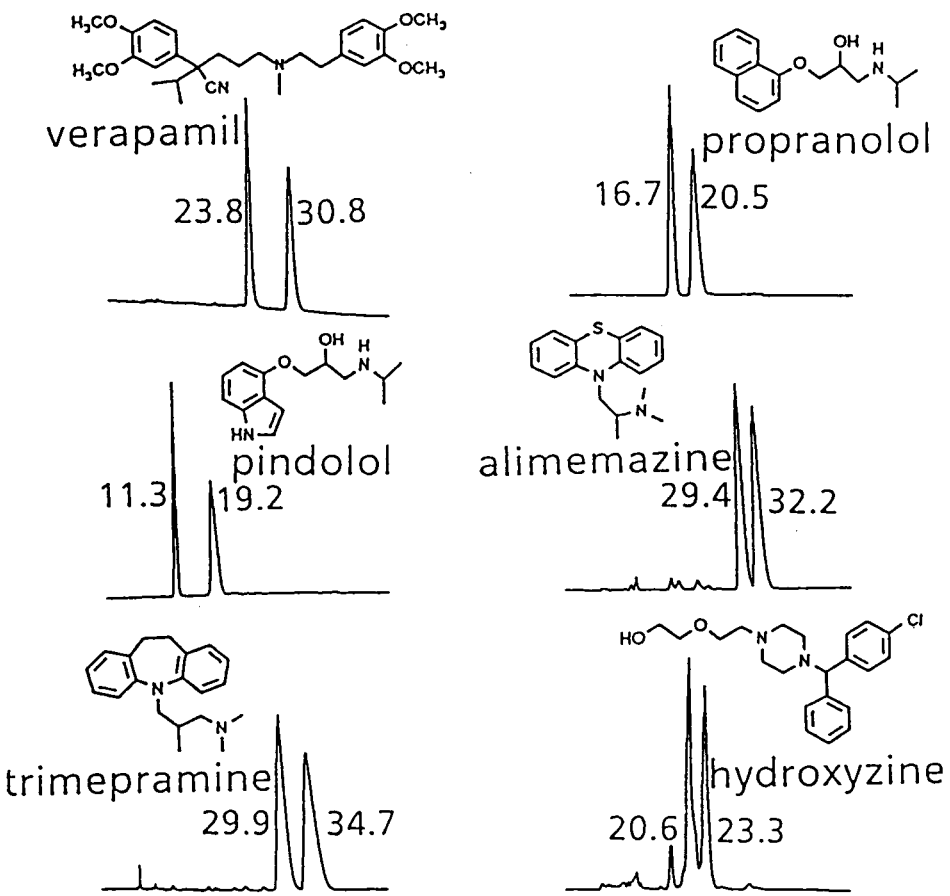


Fig. 9. Compounds resolved on cellulose tris(3,5-dimethylphenylcarbamate) (Chiralcel OD-R). The numbers on the peaks are retention times (min). Eluent, 0.1 *M* $NaPF_6$–$CH_3CN$ (6:4, v/v); flow-rate, 0.5 ml/min; detection, UV at 245 nm.

The chiral discrimination abilities of polysaccharide derivatives appear to depend on the conformation of the main chain and the structure of the substituents.

Other polysaccharide derivatives, e.g., benzoate derivatives of xylan and mannan and acetate derivatives of curdlan [10], are known. Curdlan triacetate has a considerable chiral discrimination ability. However, this ability decreases with time. Phenylcarbamate derivatives of xylan, curdlan, dextran and inuline were investigated and among these, xylan bis(3,5-dichlorophenylcarbamate) showed a high chiral discrimination ability for dihydropyridine derivatives.

### *2.4. Intermolecular interactions between CSPs and chiral molecules*

The interactions between CSPs and enantiomers have been intensively discussed. The participation of hydrogen-bonding interactions was considered for the resolution on cellulose phenylcarbamate derivatives [10]. The carbonyl and amino groups of the carbamate function are considered to be a sort of Lewis base and acid, respectively. Introduction of an electron-withdrawing atom or group on the phenyl group can enhance the acidity of the hydrogen on the amino group, which can lead to a stronger hydrogen bonding interaction with Lewis basic

Table 2
Difference in enantioselectivity between 3,5-dimethylphenylcarbamate derivatives of amylose (AD) and cellulose (OD)

| Name | Racemate | Mobile phase[a] | AD | OD |
|---|---|---|---|---|
| Verapamil | 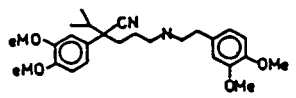 | A | $k_1 = 2.36$<br>$\alpha = 1.27$<br>$R_s = 2.19$ | $k_1 = 3.73$<br>$\alpha = 1.0$ |
| Dimethotiazine | 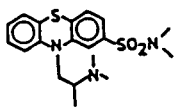 | A | $k_1 = 3.74$<br>$\alpha = 1.19$<br>$R_s = 1.67$ | $k_1 = 8.29$<br>$\alpha = 1.14$<br>$R_s = 0.65$ |
| Chlorpheniramine | 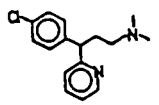 | B | $k_1 = 3.25$<br>$\alpha = 1.29$<br>$R_s = 2.11$ | $k_1 = 1.40$<br>$\alpha = 1.0$ |
| Oxyphencyclimine | 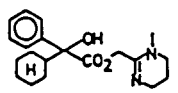 | A | $k_1 = 0.75$<br>$\alpha = 1.85$<br>$R_s = 2.83$ | $k_1 = 0.96$<br>$\alpha = 1.0$ |

[a] Mobile phases: A = *n*-hexane–2-propanol (9:1, v/v); flow-rate, 1.0 ml/min; B = *n*-hexane–2-propanol–diethylamine (98:2:0.1, v/v/v); flow-rate, 1.0 ml/min.

parts of analytes. In contrast, an electron-donating group can polarize the carbonyl group considerably, by increasing its basicity, and this can enhance the interaction with hydroxyl or amino groups of analytes. With cellulose ester derivatives, some aliphatic compounds, such as β-methylpropiolactone, 3-acetyl-4-cyclopentenone and 1,3-butanediol diacetate, without any aromatic or hydroxyl groups, could be separated. The ester groups of racemates may interact with the CSP through dipole–dipole interactions [5,11].

Recently, we found that enantiomers could be discriminated in the presence of a cellulose derivative by $^{13}C$ NMR spectroscopy in $C^2HCl_3$ [18]. In this study, cellulose tris(4-methylbenzoate) (CTMB) and 1-phenylethyl alcohol (1PE) enantiomers was chosen (Fig. 10). Both enantiomers of 1PE were well resolved by HPLC on a column packed with CTMB ($\alpha = 1.20$). The *R* and *S* enantiomers of 1PE showed different chemical shifts in the presence of CTMB (Table 3). The chemical shift difference was large at the

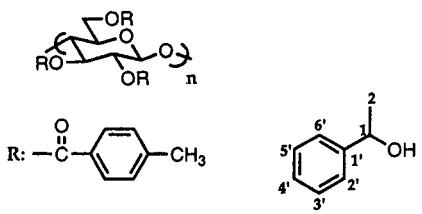


Fig. 10. Structures of compounds used for NMR study.

Table 3
Chemical shifts (ppm) of 1PE in the presence of CTMB in $C^2HCl_3$ at 35°C

| Carbon | (*R*)-1PE | (*S*)-1PE | Δδ (ppm)[a] |
|---|---|---|---|
| 1 | 70.214 | 70.224 | −0.010 |
| 2 | 25.184 | 25.178 | +0.006 |
| 1′ | 146.009 | 145.990 | +0.019 |
| 2′, 6′ | 125.436 | 125.436 | 0 |
| 3′, 5′ | 128.441 | 128.444 | −0.003 |
| 4′ | 127.337 | 127.348 | −0.011 |

[a] Chemical shift difference between the enantiomers: δ[(*R*)-1PE] − δ[(*S*)-1PE].

Table 4
Spin–lattice relaxation times, $T_1$(s), of 1PE in the presence of an equimolar amount of CTMB in $C^2HCl_3$ at 35°C

| Carbon | (*R*)-1PE | (*S*)-1PE |
|---|---|---|
| 1 | 7.12 | 7.95 |
| 2 | 3.19 | 3.30 |
| 1′ | 11.1 | 12.9 |
| 2′, 6′ | 4.88 | 5.16 |
| 3′, 5′ | 4.71 | 4.97 |
| 4′ | 3.50 | 3.68 |

aromatic *ipso* carbon (C-1′) and asymmetric carbon (C-1) with a hydroxyl group. Spin–lattice relaxation times ($T_1$) were also measured for comparison with the mobility of each enantiomer in the presence of CTMB (Table 4). The $T_1$ values for each carbon of (*R*)-1PE were smaller than those for corresponding carbons of (*S*)-1PE; the presence of CTMB restricts the mobility of (*R*)-1PE more than that of (*S*)-1PE. The $T_1$ difference was large at C-1. These results indicate that 1-PE may be chirally recognized by CTMB at the C-1 site.

These data obtained in $C^2HCl_3$ solution may not reflect the real interactions in an HPLC packed column with *n*-hexane–2-propanol as the mobile phase. We are now investigating the interaction by solid-state NMR.

### 2.5. Application of the CSPs to large-scale separations

From the beginning of the development of CSPs, the centre of our interest was the use of the CSPs for large-scale separations. As for the CSPs for preparative separations, a low cost of preparation, a high loading capacity of samples, high durability, etc., are necessary. CSPs consisting of cellulosic derivatives meet such demands. In a large-scale separation, one must obtain a large amount of an anantiomer with high optical purity in a short time. Hence, it is important to optimize the separation conditions such as the amount of sample loaded and temperature. In Fig. 11, the column performances are shown for preparative and analytical columns. Some results obtained by using a preparative column are summarized in Table 5. The efficiency of separation is very different depending on the sample. For instance, for entry 1 each enantiomer was obtained in an amount of about 160 g per day, compared with less than 0.5 g for entry 5. However, the optical purities of the enantiomers obtained were over 99%. Productivity is affected

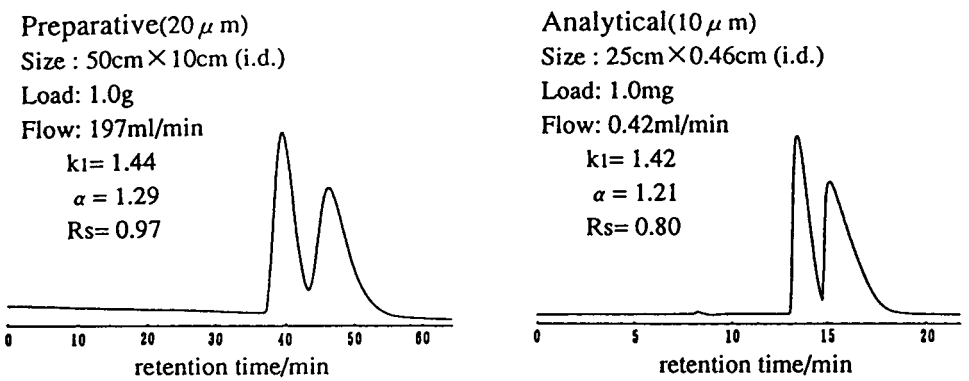


Fig. 11. Column performance of a preparative column vs. an analytical column. The values in parentheses (20 μm, 10 μm) are the silica gel particle size; sample, *trans*-1,2-diphenyloxirane racemate; $k_1$, capacity factor of first peak; $\alpha$, separation factor; $R_s$, resolution.

Table 5
Productivity of preparative chiral separation by HPLC on the 50 cm × 10 cm I.D. columns

| Entry | Parameters on analytical column | | | Elution order | Productivity | | Yield (%) | Optical purity (% e.e.)[c] |
|---|---|---|---|---|---|---|---|---|
| | | | | | g/d[a] | kg/yr[b] | | |
| | $k_1$ | $\alpha$ | $R_s$ | | | | | |
| 1 | 1.15 | 2.61 | 4.90 | 1 | 162 | 121 | 97 | >99.6 |
| | | | | 2 | 159 | 119 | 94 | 99.4 |
| 2 | 0.77 | 2.44 | 4.00 | 1 | 78 | 59 | 85 | >99.8 |
| | | | | 2 | 73 | 55 | 80 | 99.2 |
| 3 | 1.92 | 2.11 | 1.10 | 1 | 86 | 65 | 93 | >99.8 |
| | | | | 2 | 82 | 61 | 89 | 99.8 |
| 4 | 1.98 | 1.77 | 3.62 | 1 | 11 | 8.3 | 93 | >99.6 |
| | | | | 2 | 11 | 8.3 | 98 | >97.6 |
| 5 | 6.94 | 1.24 | 2.89 | 1 | 0.4 | 0.3 | 83 | >99.6 |
| | | | | 2 | 0.2 | 0.1 | 57 | >99.6 |

[a] 8 h/d.
[b] 24 h/d, 250 d/yr.
[c] e.e. = Enantiomeric excess.

by the solubility of the sample to mobile phase and the degree of separation.

## 3. Conclusions

The conformational regularity of the polysaccharide derivatives plays an important role in chiral discrimination. The regularity depends on the polysaccharides, the substituents introduced on the phenyl groups and the kind of coating solvent. The chiral recognition mechanism has not yet been clarified, but a certain "chiral field" which is constructed from a regular arrangement of ester or urethane groups of cellulosic derivatives appears to be responsible for efficient chiral recognition. A future project is to clarify the interactions between a CSP and an enantiomer at the molecular level, and NMR measurements are important in this respect.

## References

[1] Y. Okamoto, K. Suzuki, K. Ohta, K. Hatada and H. Yuki, *J. Am. Chem. Soc.*, 101 (1979) 4763.
[2] Y. Okamoto, S. Honda, I. Okamoto, H. Yuki, S. Murata, R. Noyori and H. Takaya, *J. Am. Chem. Soc.*, 103 (1981) 6971.
[3] G. Hesse and R. Hagel, *Chromatographia*, 6 (1973) 277.
[4] G. Hesse and R. Hagel, *Liebigs Ann. Chem.* (1976) 996.
[5] T. Shibata, I. Okamoto and K. Ishii, *J. Liq. Chromatogr.*, 9 (1986) 313.
[6] A. Ichida, T. Shibata, I. Okamoto, Y. Yuki, H. Namikoshi and Y. Toga, *Chromatographia*, 19 (1984) 280.
[7] Y. Okamoto, M. Kawashima, K. Yamamoto and K. Hatada, *Chem. Lett.* (1984) 739.
[8] T. Shibata, T. Sei, H. Nishimura and K. Deguchi, *Chromatographia*, 24 (1987) 552.
[9] T. Sei, H. Matsui, T. Shibata and S. Abe, *Viscoelasticity of Biomaterials*, American Chemical Society, Washington, DC, 1992, Ch. 4, pp. 53–64.
[10] Y. Okamoto, M. Kawashima and K. Hatada, *J. Chromatogr.*, 363 (1986) 173.
[11] A. Ichida and T. Shibata, in M. Zief and L.J. Crane (Editors), *Chromatographic Chiral Separations*, Marcel Dekker, New York, 1988, p. 219.
[12] Y. Okamoto, R. Aburatani and K. Hatada, *J. Chromatogr.*, 389 (1987) 95.
[13] Y. Okamoto, M. Kawashima and K. Hatada, *J. Am. Chem. Soc.*, 106 (1984) 5357.
[14] K. Ikeda, T. Hamasaki, H. Kohno, T. Ogawa, T. Matsumoto and J. Sakai, *Chem. Lett.*, (1989) 1089.
[15] A. Ishikawa and T. Shibata, *J. Liq. Chromatogr.*, 16 (1993) 859.
[16] Y. Hatehi and W.G. Hanstein, *Proc. Natl. Acad. Sci. U.S.A.*, 62 (1969) 1129.
[17] Y. Okamoto, R. Aburatani, T. Fukumoto and K. Hatada, *Chem. Lett.*, (1987) 1857.
[18] K. Oguni, A. Matsumoto and A. Isokawa, *Polym. J.*, submitted for publication.

ELSEVIER

Journal of Chromatography A, 694 (1995) 101–109

JOURNAL OF CHROMATOGRAPHY A

# Dimethyl-, dichloro- and chloromethylphenylcarbamates of amylose as chiral stationary phases for high-performance liquid chromatography

Bezhan Chankvetadze[1], Eiji Yashima, Yoshio Okamoto*

*Department of Applied Chemistry, School of Engineering, Nagoya University, Chikusa-ku, Nagoya 464-01, Japan*

**Abstract**

Twelve dimethyl-, dichloro- and chloromethylphenylcarbamate derivatives of amylose were prepared and their chiral recognition abilities were evaluated as chiral stationary phases for high-performance liquid chromatography. *ortho*-Substituted phenylcarbamate derivatives of amylose showed high chiral recognition abilities, although cellulose phenylcarbamate derivatives with *ortho* substituents on the phenyl moiety showed low chiral recognition. The superiority of 5-chloro-2-methylphenylcarbamate over the corresponding dimethyl- and dichlorophenylcarbamate derivatives of amylose was demonstrated. The roles of the NH residue of the carbamate moieties and methyl and chloro groups in chiral recognition were elucidated using IR and $^1$H NMR spectroscopic data. The tris(5-chloro-2-methylphenylcarbamate) of amylose exhibited the highest chiral recognition ability among the amylose derivatives synthesized, and can be used for the separation of some chiral drug enantiomers.

## 1. Introduction

Many derivatives (acetate, benzoates, carbamates, etc.) of polysaccharides such as cellulose [1–4], amylose [1,3,4], chitosan [1,5] and guaran [6] have been examined as chiral stationary phases (CSPs) for enantioseparation by HPLC. Among them, cellulose derivatives, especially phenylcarbamate derivatives, have been most extensively studied and many empirical correlations have been established between the physical or chemical properties and enantiomer recognition abilities of CSPs [7]. Amylose derivatives are also of potential use as CSPs, but they have not yet been studied in detail [1,3,4]. More extensive investigations will provide more practical applications of this promising chiral natural polymer for enantioseparation, and will contribute to the elucidation of the chiral recognition mechanism on polysaccharide CSPs, which still remains obscure.

The purposes of this study were to evaluate (i) the role of the nature and the position of methyl and chloro groups in the chiral recognition abilities of disubstituted phenylcarbamate derivatives of amylose; (ii) the effect of introducing both an electron-donating methyl group and an electron-withdrawing chloro group on to the phenyl moieties on the chiral recognition abilities; and (iii) the correlations between chiral

* Corresponding author.

[1] Permanent address: Department of Chemistry, Tbilisi State University, Chavchavadze ave 1, 380028 Tbilisi, Georgia.

0021-9673/95/$09.50 
*SSDI* 0021-9673(94)00729-2

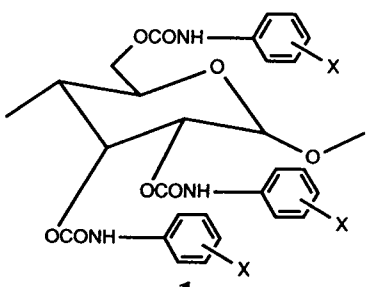


**1**

| | | | |
|---|---|---|---|
| X= | a: 3,4-$(CH_3)_2$ | e: 5-Cl-2-$CH_3$ | i: 3-Cl-2-$CH_3$ |
| | b: 2,5-$(CH_3)_2$ | f: 2-Cl-5-$CH_3$ | j: 4-Cl-2-$CH_3$ |
| | c: 3,4-$Cl_2$ | g: 4-Cl-3-$CH_3$ | k: 2-Cl-6-$CH_3$ |
| | d: 2,5-$Cl_2$ | h: 3-Cl-4-$CH_3$ | l: 2-Cl-4-$CH_3$ |

Fig. 1. Structures of CSPs.

recognition abilities and the NH frequencies in IR spectra and the chemical shifts of the NH protons in $^1H$ NMR spectra of amylose phenylcarbamate derivatives. The potential use of above amylose derivatives for the enantioseparation of some practically important drugs is also demonstrated.

In this study, twelve dimethyl-, dichloro- and chloromethylphenylcarbamate derivatives of amylose (Fig. 1) were prepared and their chiral recognition abilities as CSPs for HPLC were evaluated.

## 2. Experimental

### 2.1. Chemicals

Amlyose B ($M_r \approx 16\,000$) was purchased from Nacalai Tesque (Kyoto, Japan). (3-Aminopropyl)triethoxysilane, 2,5-dimethylaniline, 3,4-dimethylaniline, 2,5-dichlorophenyl isocyanate, 3,4-dichlorophenyl isocyanate, 3-chloro-2-methylaniline and 3-chloro-4-methylaniline were of guaranteed reagent grade from Tokyo Kasei (Tokyo, Japan). 2-Chloro-6-methylaniline was obtained from Jansen Chimica (Beerse, Belgium) and triphosgene, pyridine-$d_5$, 2-chloro-4-methylaniline, 4-chloro-2-methylaniline, 5-chloro-2-methylaniline and 2-chloro-5-methylaniline from Aldrich (Milwaukee, WI, USA). Isocyanates were prepared from the corresponding anilines by the conventional method using triphosgene. Wide-pore silica gel (Daiso gel SP-1000, pore size 100 nm, particle size 7 $\mu$m) was kindly supplied by Daiso (Osaka, Japan) and was silanized using (3-aminopropyl)triethoxysilane in benzene at 80°C before use. Hexane and 2-propanol, used as components of the eluents, were of analytical-reagent grade. Racemic compounds (**6**, **13**, **14** and **15**) were gifts from Professor Suda and Dr. Kanoh of Kanazawa University, and other compounds were commercially available or were prepared by the usual procedures [8].

### 2.2. Preparation of tris(disubstituted phenylcarbamate) derivatives of amylose

Amylose tris(disubstituted phenylcarbamate) derivatives (**1a–l**) (Fig. 1) were prepared by the reaction of amylose with an excess of the corresponding isocyanates in dry pyridine at ca. 100°C using the same procedures described previously [2] and isolated as methanol-insoluble fractions. Elemental analyses (Table 1) and IR and $^1H$ NMR spectra were used to determine the degree of conversion of the hydroxy groups of amylose into the carbamate moieties. The reactivity of amylose with the isocyanates seemed to be lower than that of cellulose. The conversion of the hydroxy groups into the carbamates was more than 90% after 24 h in most instances, but sometimes small amounts of partially or completely unreacted amylose were found in the reaction flask even after 200 h at ca. 100°C. This fraction could be easily removed by decantation or by selective dissociation of the desired carbamate derivatives in tetrahydrofuran (THF), where the unreacted amylose is insoluble.

### 2.3. Preparation of stationary phase

Column packing materials were prepared as described previously [2] using macroporous silica gel (Daiso gel SP-1000) and packed into 25 cm × 0.46 cm I.D. stainless-steel tubes by the conven-

Table 1
Elemental analyses and NH chemical shifts of **1a–l**

| Amylose derivative | C (%) | H (%) | N (%) | Cl (%) | NH proton, δ (ppm) | | |
|---|---|---|---|---|---|---|---|
| | | | | | I | II | III |
| **1a** | 61.80 | 6.02 | 6.14 | – | 9.56 | 9.28 | |
| **1b** | 57.24 | 6.04 | 4.92 | – | 8.80 | 8.35 | |
| **1c** | 43.86 | 3.32 | 4.94 | – | 10.84 | 10.12 | 10.06 |
| **1d** | 44.57 | 2.72 | 5.64 | 28.71 | 9.27 | 9.21 | 8.99 |
| **1e** | 52.66 | 4.41 | 5.75 | 14.64 | 9.55 | 8.95 | 8.21 |
| **1f** | 52.72 | 4.59 | 5.53 | 14.89 | 8.80 | 8.53 | 8.10 |
| **1g** | 51.69 | 4.66 | 5.08 | 12.63 | 10.33 | 9.71 | 9.33 |
| **1h** | 52.57 | 4.28 | 6.02 | 15.65 | 10.55 | 9.82 | |
| **1i** | 48.41 | 4.46 | 4.60 | 12.60 | 9.76 | 9.20 | 8.94 |
| **1j** | 53.67 | 4.31 | 6.17 | 14.82 | 9.26 | 8.94 | 8.42 |
| **1k** | 52.70 | 4.29 | 5.92 | 15.04 | 9.06[a] | | |
| **1l** | 53.39 | 4.46 | 5.95 | 14.98 | 9.50 | 8.92 | |

Calculated values: C 65.89, H 5.82, N 6.99% (**1a** and **b**); C 44.75, H 2.35, N 5.80, Cl 29.42% (**1c** and **d**); C 54.33, H 3.92, N 6.34, C 16.08% (**1e–l**).
[a] Very broad peak ranging from 8.2 to 10.5 ppm.

tional high-pressure slurry packing technique using a model CCP-085 Econo packer pump (Chemco, Osaka, Japan). The plate numbers of the columns were 3000–4000 for benzene with hexane–2-propanol (90:10) as the eluent at a flow-rate of 0.5 ml/min at 20°C. The dead time ($t_0$) of the columns was determined using 1,3,5-tri-*tert*.-butylbenzene as a non-retained compound.

### 2.4. Apparatus

All chromatographic experiments were performed on a Jasco Trirotar-II liquid chromatograph equipped with UV (Jasco 875-UV) and polarimetric (Jasco 181-C) detectors at ambient temperature. An injector with a 100-μl loop (Model 7125, Rheodyne, Cotati, CA, USA) was used for injection of samples. IR spectra were measured using a Jasco Fourier transform IR spectrometer with a Jasco PTL-396 data processor. UV spectra of amylose phenylcarbamate derivatives were measured in THF solutions using a Jasco Ubest-55 spectrophotometer. Circular dichroism (CD) spectra were measured in THF solutions in a 0.01-cm cell using a Jasco J-720 L spectropolarimeter. $^1$H NMR spectra were measured in pyridine-$d_5$ solutions at 80°C with a Varian VXR-500S NMR spectrometer (500 MHz). Tetramethylsilane (TMS) was used as the internal standard.

## 3. Results and discussion

The results of enantioseparation of fourteen racemic compounds (**2-15**) (Fig. 2) are given in Table 2. On the basis of separation factors ($\alpha$), the chiral recognition abilities of 2,5-dimethyl- (**1b**) and 2,5-dichlorophenylcarbamates (**1d**) of amylose were not substantially low compared

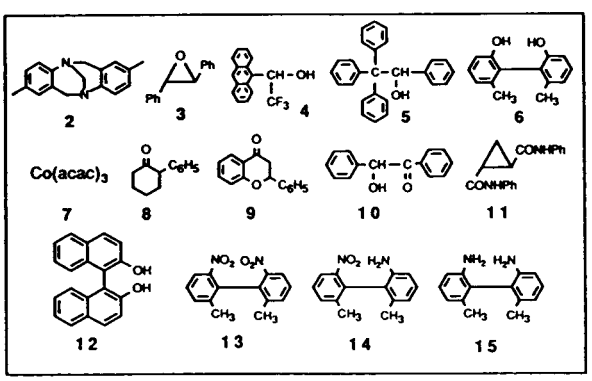


Fig. 2. Structures of racemic solutes.

Table 2
Optical resolution of racemates **2–15** on amylose derivatives **1a–l**

| Compound | **1a**: 3,4-$(CH_3)_2$ | | | **1b**: 2,5-$(CH_3)_2$ | | | **1c**: 3,4-$Cl_2$ | | | **1d**: 2,5-$Cl_2$ | | |
|---|---|---|---|---|---|---|---|---|---|---|---|---|
| | $k'_1$ | $\alpha$ | $R_s$ | $k'_1$ | $\alpha$ | $R_s$ | $k'_1$ | $\alpha$ | $R_s$ | $k'_1$ | $\alpha$ | $R_s$ |
| **2** | 1.00(+) | 1.23 | 1.4 | 0.70(−) | ca. 1 | | 0.82 | 1.22 | 0.8 | 1.33(−) | 1.38 | 0.8 |
| **3** | 0.83(+) | 1.36 | 1.8 | 0.55(+) | 1.67 | 2.2 | 0.43(+) | 1.23 | 0.6 | 1.33(+) | 1.18 | 0.7 |
| **4** | 2.10 | 1.00 | | 1.40(−) | 1.14 | 1.2 | 1.53 | 1.00 | | 1.40 | 1.00 | |
| **5** | 2.10(+) | 1.67 | 3.5 | 1.40(+) | 1.60 | 2.5 | 0.93(+) | 1.50 | 0.6 | 0.47(−) | 3.14 | 2.0 |
| **6** | 3.43(−) | 1.58 | 3.0 | 2.67(−) | 1.08 | | 1.40(−) | ca. 1 | | 2.20(+) | 1.16 | |
| **7** | 0.87(−) | 1.06 | | 0.62(+) | ca. 1 | | 1.60(−) | ca. 1 | | 1.10(+) | ca. 1 | |
| **8** | 1.33(−) | 1.06 | | 1.07(−) | 1.13 | 1.0 | 1.13(+) | ca. 1 | | 2.00(−) | 1.24 | 1.0 |
| **9** | 2.10(+) | 1.38 | 3.0 | 1.87(+) | 1.18 | 1.2 | 1.25(+) | 1.08 | | 2.37 | 1.00 | |
| **10** | 4.92(−) | 1.04 | | 3.22(+) | 1.24 | 2.0 | 3.43(−) | 1.31 | 1.3 | 0.38(+) | ca. 1 | |
| **11** | 2.70(−) | 1.11 | 0.6 | 1.67 | 1.00 | | 0.58(+) | 1.14 | | 0.83(+) | 2.04 | 1.0 |
| **12**[a] | 6.87 | 1.00 | | 7.80 | 1.10 | | 2.73 | 1.00 | | 6.67 | 1.15 | |
| **13** | 2.27(−) | ca. 1 | | 2.20(−) | ca. 1 | | 2.58(−) | 1.26 | 1.0 | 6.13(−) | ca. 1 | |
| **14** | 2.22(−) | 1.20 | 1.7 | 1.32(+) | 1.25 | 1.3 | 1.25(−) | 1.52 | 2.0 | 3.03(−) | 1.38 | 1.4 |
| **15** | 2.43(+) | 1.12 | 1.4 | 1.72(+) | 1.14 | 1.2 | 0.70(−) | 1.19 | 0.7 | 1.60(−) | ca. 1 | |
| | **1e**: 5-Cl-2-$CH_3$ | | | **1f**: 2-Cl-5-$CH_3$ | | | **1g**: 4-Cl-3-$CH_3$ | | | **1h**: 3-Cl-4-$CH_3$ | | |
| | $k'_1$ | $\alpha$ | $R_s$ | $k'_1$ | $\alpha$ | $R_s$ | $k'_1$ | $\alpha$ | $R_s$ | $k'_1$ | $\alpha$ | $R_s$ |
| **2** | 0.83(−) | 1.13 | | 0.93(−) | 1.39 | 1.1 | 0.77(+) | 1.43 | 1.0 | 0.78(+) | 1.28 | 1.4 |
| **3** | 0.67(+) | 1.70 | 2.3 | 0.77(+) | 1.43 | 0.8 | 0.60(+) | 1.66 | 2.0 | 0.57(+) | 1.29 | 1.3 |
| **4** | 0.90(−) | 1.14 | 0.6 | 2.30(−) | 1.09 | | 0.73 | 1.00 | | 0.83 | 1.00 | |
| **5** | 1.20(+) | 1.67 | 1.5 | 1.53(+) | 2.11 | 1.7 | 1.30(+) | 1.88 | 2.3 | 1.67(+) | 1.77 | 3.5 |
| **6** | 1.27(+) | 1.28 | 0.8 | 2.53(+) | 1.07 | | 2.07(−) | 1.32 | 0.8 | 1.43(−) | 1.09 | |
| **7** | 1.10(+) | 1.18 | 1.0 | 0.55 | 1.00 | | 1.07(−) | ca. 1 | | 0.68(−) | ca. 1 | |
| **8** | 1.37(−) | 1.24 | 1.0 | 0.90(−) | 1.19 | | 0.93(−) | ca. 1 | | 1.03(−) | ca. 1 | |
| **9** | 2.00(+) | 1.18 | 1.1 | 2.13 | 1.00 | | 1.13(+) | 1.11 | | 1.57(+) | 1.49 | 3.5 |
| **10** | 4.30(+) | 1.16 | 0.8 | 4.13 | 1.00 | | 2.87(−) | 1.05 | | 3.83(+) | ca. 1 | |
| **11** | 1.32(+) | 3.09 | 2.1 | 1.03(+) | 2.09 | 1.2 | 0.97(+) | 1.34 | 0.9 | 1.30(+) | 1.08 | |
| **12**[a] | 3.07(−) | 1.35 | 1.2 | 8.27 | 1.07 | | 5.73 | 1.00 | | 4.07 | 1.00 | |
| **13** | 3.67(−) | 1.13 | 1.3 | 3.80(−) | 1.10 | | 2.03(−) | 1.07 | | 2.07(−) | 1.06 | |
| **14** | 2.20(−) | 1.06 | | 2.80(−) | 1.15 | 0.7 | 1.20(−) | 1.39 | 1.3 | 1.33(−) | 2.00 | 4.4 |
| **15** | 0.43(+) | 2.38 | 1.7 | 3.80(+) | 1.10 | | 1.00(−) | ca. 1 | | 1.10(−) | 1.18 | 1.2 |
| | **1i**: 3-Cl-2-$CH_3$ | | | **1j**: 4-Cl-2-$CH_3$ | | | **1k**: 2-Cl-6-$CH_3$ | | | **1l**: 2-Cl-4-$CH_3$ | | |
| | $k'_1$ | $\alpha$ | $R_s$ | $k'_1$ | $\alpha$ | $R_s$ | $k'_1$ | $\alpha$ | $R_s$ | $k'_1$ | $\alpha$ | $R_s$ |
| **2** | 0.93(+) | 1.11 | | 1.37(+) | 1.11 | | 0.87(+) | 2.62 | 2.0 | 1.50 | 1.00 | |
| **3** | 0.50(+) | 2.00 | 2.0 | 1.05(+) | 1.54 | 2.1 | 0.60 | 1.00 | | 0.82(+) | 1.22 | 0.7 |
| **4** | 0.77 | 1.00 | | 1.28 | 1.00 | | 2.53 | 1.00 | | 2.67 | 1.00 | |
| **5** | 1.07(+) | 2.44 | 3.1 | 1.27(+) | 1.84 | 1.5 | 1.32(−) | 1.14 | | 1.67(+) | 1.36 | 1.1 |
| **6** | 1.38(−) | ca. 1 | | 2.67 | 1.00 | | 2.10 | 1.00 | | 1.93 | 1.00 | |
| **7** | 0.95(+) | ca. 1 | | 1.50(+) | ca. 1 | | 3.30(−) | 1.04 | | 0.60(+) | ca. 1 | |
| **8** | 0.52(−) | ca. 1 | | 1.73(−) | ca. 1 | | 1.70(+) | ca. 1 | | 0.87(−) | ca. 1 | |
| **9** | 1.63(+) | 1.15 | 0.5 | 2.57(+) | 1.04 | | 1.70 | 1.00 | | 2.28 | 1.00 | |
| **10** | 3.83(+) | 1.09 | 0.5 | 5.50(+) | 1.39 | 1.9 | 3.13(+) | 1.09 | | 3.70(+) | 1.07 | |
| **11** | 1.00(+) | 1.50 | 0.9 | 1.50(+) | 1.42 | 1.0 | 1.38(+) | 1.36 | 0.9 | 1.10(+) | 2.12 | 1.4 |
| **12**[a] | 3.33 | 1.00 | | 5.13 | 1.00 | | 5.20 | 1.00 | | 10.33 | 1.06 | |
| **13** | 2.90(−) | ca. 1 | | 4.83(+) | ca. 1 | | 5.67(−) | 1.03 | | 3.77 | 1.00 | |
| **14** | 1.87(+) | ca. 1 | | 3.00(−) | ca. 1 | | 3.07(+) | ca. 1 | | 2.53(−) | ca. 1 | |
| **15** | 1.20(+) | 1.06 | | 1.26(+) | ca. 1 | | 1.20(+) | ca. 1 | | 1.47(+) | ca. 1 | |

$k'_1$ = Capacity factor with optical rotation (in parentheses) of the first-eluted enantiomer. Separation factor ($\alpha$) = $k'_2/k'_1$. Resolution factor ($R_s$) = $2(t_2 - t_1)/(w_1 + w_2)$, where $t_1$ and $w_1$ are the retention time and band width of the first-eluted enantiomer and $t_2$ and $w_2$ are the retention time and band width of the second-eluted enantiomer, respectively. Eluent, hexane–2-propanol (90:10); flow-rate, 0.5 ml/min.
[a] Flow-rate, 1.0 ml/min.

with those of 3,4-dimethyl- (**1a**) and 3,4-dichlorophenylcarbamates (**1c**) of amylose, respectively, although for cellulose phenylcarbamate derivatives, *ortho* substitution with either a methyl or a chloro group lowered the chiral resolving power [2]. Differences in the chiral recognition abilities between 2,5- and 3,4-disubstituted phenylcarbamates of amylose were observed, depending on the racemic compounds. For instance, the CSP **1a** separated or at least partially separated the racemic compounds **2**, **7** and **11**, which were not separated on **1b**. Similarly, the CSP **1b** separated the racemic compounds **4** and **12**, which were not separated on **1a**. The same tendency was observed for dichlorophenylcarbamate derivatives of amylose; the racemic compounds **9**, **10** and **15** were not resolved on **1d**, but were resolved on **1c**, and the racemic compounds **6**, **8** and **12** were separated on **1d**, but not on **1c**. The differences in chiral recognition abilities of the same dimethyl- and dichlorophenylcarbamates can also be found by comparing the chiral recognition abilities of the CSPs **1a** and **1c** or **1b** and **1d**. The chiral recognition abilities of 2,5- and 3,4-disubstituted phenylcarbamate derivatives of amylose for the racemic compounds used in this study depend on the position and the type of the substituents on the phenyl moieties.

We have already demonstrated that the main chiral adsorbing sites for chiral separation on phenylcarbamate derivatives of polysaccharides are considered to be the polar carbamate residues, which can interact with a solute via hydrogen bonding with NH and C=O groups [2–4,9–11]. The importance of the carbamate residues for chiral recognition has recently been supported by a $^1$H NMR study on chiral recognition using cellulose tris(4-trimethylsilylphenylcarbamate) [12]. It has also been reported [2,4] that the introduction of either electron-donating or electron-withdrawing substituents at the *meta* or *para* position on to the phenyl moieties tends to improve the optical resolution abilities of phenylcarbamate derivatives of cellulose. For instance, cellulose tris(3,5-dimethylphenylcarbamate), having electron-donating substituents, could effectively resolve polar compounds which can interact with the carbonyl groups of the carbamate moieties, and the derivatives, for instance, cellulose tris(3,5-dichlorophenylcarbamate), having electron-withdrawing substituents could possess a higher resolving power for the compounds that can be adsorbed on the NH groups of the carbamate moieties [2]. The characteristic enantioseparation of many racemic compounds on the cellulose phenylcarbamate derivatives confirmed this explanation, but recently we have found that a better resolution of some racemic compounds was attained on some *meta*- and *para*-disubstituted chloromethylphenylcarbamates of cellulose than on the corresponding dimethyl- and dichlorophenylcarbamates [7,13]. This suggests that the above explanation needs some modification.

In order to examine the effect of the simultaneous introduction of both electron-donating and electron-withdrawing substituents on to the phenyl moieties on the chiral recognition abilities of amylose phenylcarbamate derivatives, two series of 2,5- and 3,4-substituted dimethyl-, dichloro- and chloromethylphenylcarbamate derivatives of amylose were prepared and their chiral recognition abilities were evaluated. For 3,4-disubstituted derivatives, the effect of the introduction of methyl and chloro groups was not marked and the CSPs **1a**, **1c**, **1g** and **1h** exhibited approximately the same chiral recognition abilities, whereas the chiral resolving power of 2,5-disubstituted phenylcarbamate derivatives of amylose was not similar, but was dependent on the type of the substituents. For example, the CSP **1b** could separate ten compounds among fourteen racemic compounds tested and **1d** separated eight of them, whereas **1f** separated eleven and, moreover, **1e** all fourteen racemic compounds. In some instances **1e** exhibited high separation factors ($\alpha$), shorter retention times and better resolution factors ($R_s$).

Examples of the enantioseparation of the racemic compounds **7** and **12** characterized with different functionalities are given on Figs. 3 and 4. As can be seen, racemic cobalt(III) tris(acetylacetonate) (**7**) was not resolved on either **1b** or **1d**, but was effectively resolved on **1e**. More-

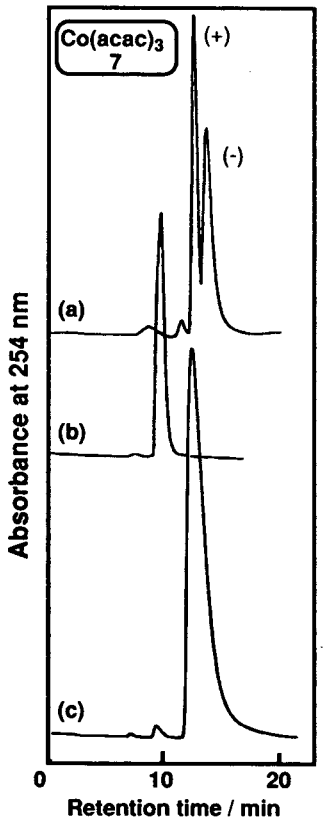


Fig. 3. Separation of enantiomers of cobalt(III) acetylacetonate (**7**) on (a) **1e**, (b) **1b** and (c) **1d**. Chromatographic conditions as in Table 2.

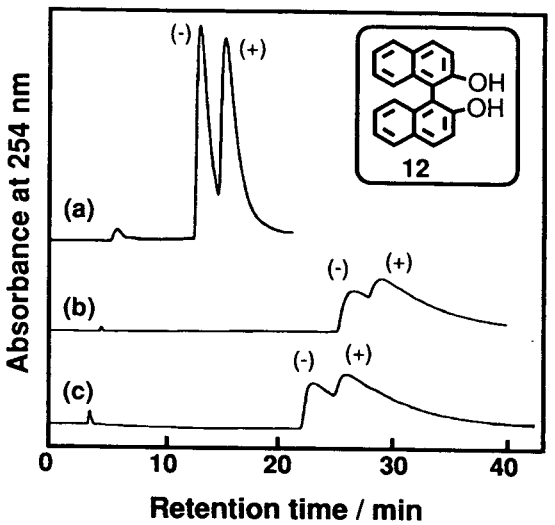


Fig. 4. Separation of enantiomers of 2,2′-dihydroxy-1,1′-binaphthyl (**12**) on (a) **1e**, (b) **1b** and (c) **1d**. Flow-rate, 1.0 ml/min.

over, racemic 2,2′-dihydroxy-1,1′-binaphthyl (**12**) was partially separated on **1b** and **1d**, whereas almost complete separation was achieved on **1e**, and the retention times are shorter and $R_s$ higher on **1e**. Another example is the racemate **13**, which was not resolved on **1b** and **1d** but was resolved on **1e** and **1f**. The chiral recognition abilities exhibited by **1e** seem higher than those of the commercially available tris(3,5-dimethylphenylcarbamate) of amylose, which shows poor chiral recognition abilities for the racemic compounds **7**, **8**, **12** and **13** [3].

The $^1$H NMR and IR spectral data for the amylose derivatives gave useful information to discuss the role of electron-donating and electron-withdrawing substituents in chiral recognition abilities of CSPs. As can be seen in the IR spectra of the amylose phenylcarbamate derivatives (Fig. 5), two peaks of the NH groups can be observed. The peak in the range 3400–3430 $cm^{-1}$ may be assigned to a free N–H bond and the band in the range 3300–3350 $cm^{-1}$ to an NH group involving intramolecular hydrogen bonding [7]. The high fraction of the latter band indirectly means a more ordered secondary structure of the CSPs. Both free NH and intramolecularly hydrogen-bonded NH groups were observed in the IR spectra of the amylose trisphenylcarbamates.

Introduction of the methyl substituents at the 2- and 5-positions increased the ratio of hydrogen-bonded NH groups, which means the formation of a more ordered rigid structure of the polysaccharide CSP, whereas the introduction of chloro substituents at the 2- and 5- positions on the phenyl moieties leads to an increase in a free NH bond, which means an increase in the number of adsorptive sites accompanied by a decrease in the regularity of the chiral polymers.

Other information on the effect of the substituents can also be obtained from the $^1$H NMR spectra. Three NH resonances in the $^1$H NMR spectra corresponding to the NH protons of carbamate groups at the 2-, 3-, and 6-positions of

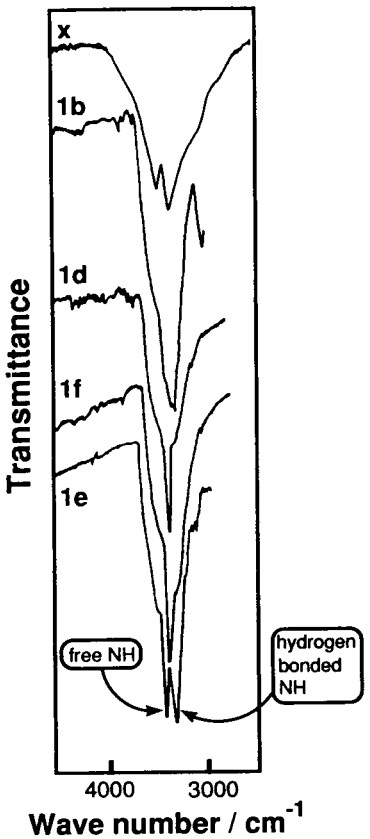


Fig. 5. IR spectra of the NH groups of 2,5-disubstituted chloromethylphenylcarbamates of amylose (**1b**, **1d**, **1e** and **1f**) and amylose trisphenylcarbamate (x).

the glucose units were observed. The resonances of the NH protons shifted upfield on introducing the methyl groups at the 2- and 5- positions, whereas the resonances of the NH protons shifted downfield on introduction of the chloro substituents at the 2- and 5-positions (Table 1). The NH chemical shifts reflect the acidity of the NH protons and the NH resonances will shift downfield with an increase in the acidity.

The effects of methyl and chloro substituents on the phenyl moieties on the properties of amylose phenylcarbamate derivatives can be summarized as follows. The introduction of the methyl groups contributes to maintaining a higher order structure of CSPs through intramolecular hydrogen bonding, but this results in decreases in the number and the acid strength of adsorptive sites, which leads to a decrease in adsorbing power to solutes capable of interacting with the NH groups of the carbamate moieties. In contrast, the introduction of the chloro groups on the phenyl moieties induces a disordered structure of CSPs, but it may cause increases in the number and the acid strength of adsorptive sites. In some instances this will lead to an increase in retention times and $\alpha$ for some racemates, but to a decrease in $R_s$ because of peak broadening. The superiority of the 2,5-disubstituted chloromethylphenylcarbamates, especially **1e**, over the corresponding dimethyl- and dichlorophenylcarbamates must be the result of the balance of the above-mentioned effects. The same changes may be induced on the C=O sites.

The CSP **1b**, in which most of the NH groups are involved in intramolecular hydrogen bonding and the acidity of the NH is low, will not exhibit universal separation abilities, but some racemic compounds could be separated on **1b** with a very high $R_s$. In contrast, the CSP **1d** with a high proportion of free NH groups, and therefore the most disordered structure, will exhibit smaller $R_s$ and large $\alpha$ for some racemates (**2**, **5**, **8**, **11** and **14**). The CSP **1f**, having a high proportion of free NH groups, also showed a small $R_s$. A balanced ratio of the free NH groups to hydrogen-bonded NH groups seems to be the reason for very high chiral recognition abilities of **1e**. The high acid strength of the NH groups of **1e** may also be important for high chiral recognition. This appears to improve both $\alpha$ and $R_s$. The high enantioselectivity of **1e** for most racemic compounds was not accompanied by an increase in retention times, indicating that the higher acidity of the NH groups is more important for intramolecular hydrogen bonding than for interaction with racemic solutes as adsorbing sites.

As can be seen from the CD spectra of these derivatives (Fig. 6), more intense peaks in the region of 210 nm (C=O region) were observed for **1e** than for **1b**, indicating that the conformation of **1e** is more regular than that of **1b**.

For 3,4-disubstituted phenylcarbamates of

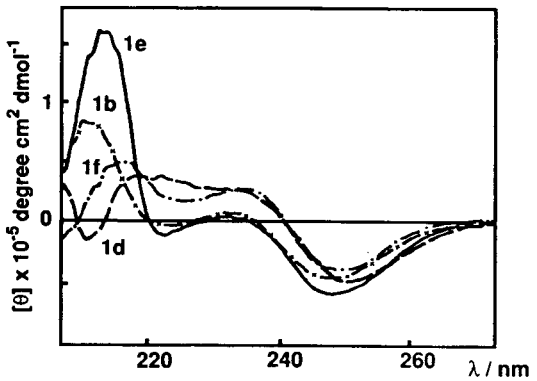


Fig. 6. CD spectra of 2,5-disubstituted chloromethylphenylcarbamates of amylose (**1b**, **1d**, **1e** and **1f**).

amylose (**1a**, **1c**, **1g** and **1h**), the ratios of free and intramolecular hydrogen-bonded NH groups were not changed substantially except for **1h**. This may be the reason for similar enantiomer resolving abilities of these derivatives. 2,4-Disubstituted derivative (**1j**) with similar NH chemical shifts to **1e** showed low chiral recognition; the geometry of the substituted phenyl group may be involved.

Besides the above-mentioned strong interactions through hydrogen bond, sometimes we must also take into account weak interactions ($\pi-\pi$, hydrophobic interactions, etc.) when discussing the mechanism of enantioseparation using polysaccharide CSPs.

Additional studies seem necessary to be able to discuss more precisely the effects of the electron-donating and electron-withdrawing substituents.

High chiral recognition abilities of amylose tris(2-methyl-5-chlorophenylcarbamate) were also shown in the separation of some other compounds (Fig. 7). These racemic drugs were completely separated on **1e**.

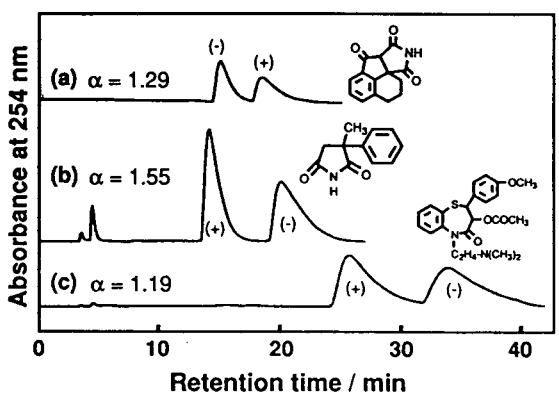


Fig. 7. Chromatographic separation of (a) 3a,4,5,6-tetrahydrosuccinimido[3,4-*b*]acenaphthen-10-one, (b) α-methyl-α-phenylsuccinimide and (c) *cis*-diltiazem on amylose tris(2-methyl-5-chlorophenylcarbamate) (**1e**). Eluent, (a) hexane–2-propanol (80:20) and (b,c) hexane–2-propanol (90:10); flow-rate, 1.0 ml/min.

## 4. Conclusions

The chiral recognition abilities of twelve dimethyl-, dichloro- and chloromethylphenylcarbamate derivatives of amylose were evaluated as CSPs for HPLC and it was established that chiral recognition ability of amylose tris(2-methyl-5-chlorophenylcarbamate) is superior to that of other 2,5-dimethyl- and 2,5-dichlorophenylcarbamates. An explanation is proposed for the role of the electron-donating and electron-withdrawing substituents on the phenyl moieties on the chiral recognition abilities of the polysaccharide phenylcarbamate derivatives.

## Acknowledgements

B.C. thanks the Japan Cultural Association for financial support during his stay at Nagoya University. This work was partially supported by Grant-in-Aids for Scientific Research Nos. 02555184 and 05559009 from the Ministry of Education, Science and Culture, Japan.

## References

[1] Y. Okamoto, M. Kawashima and K. Hatada, *J. Am. Chem. Soc.*, 106 (1984) 5357.
[2] Y. Okamoto, M. Kawashima and K. Hatada, *J. Chromatogr.*, 363 (1986) 106.
[3] Y. Okamoto, R. Aburatani, K. Hatano and K. Hatada, *J. Liq. Chromatogr.*, 11 (1988) 2147.

[4] Y. Okamoto, Y. Kaida, R. Aburatani and K. Hatada in S. Ahuja (Editor), *Chiral Separation by Liquid Chromatography* (ACS Symposium Series, No. 471), American Chemical Society, Washington, DC, 1991, Ch. 5, p. 101.
[5] K. Ohga, H. Oyama and Y. Muta, *Anal. Sci.*, 7 (1991) 653.
[6] R. Mathur, S. Bohra, C.K. Narang and N.K. Mathur, *J. Liq. Chromatogr.*, 15 (1992) 573.
[7] B. Chankvetadze, E. Yashima and Y. Okamoto, *J. Chromatogr. A*. 670 (1994) 39.
[8] Y. Kaida and Y. Okamoto, *Bull. Chem. Soc. Jpn.*, 65 (1992) 2286.
[9] Y. Okamoto, M. Kawashima, R. Aburatani, K. Hatada, T. Nishiyama and M. Masuda, *Chem. Lett.*, (1986) 1237.
[10] Y. Okamoto, Zun-Kui Cao, R. Aburatani and K. Hatada, *Bull. Chem. Soc. Jpn.*, 60 (1987) 3999.
[11] Y. Kaida and Y. Okamoto, *J. Chromatogr.*, 641 (1993) 267.
[12] E. Yashima, M. Yamada and Y. Okamoto, *Chem. Lett.*, (1994) 579.
[13] B. Chankvetadze, E. Yashima and Y. Okamoto, *Chem. Lett.*, (1993) 617.

ELSEVIER

Journal of Chromatography A, 694 (1995) 111–118

JOURNAL OF CHROMATOGRAPHY A

# Preparation and chromatographic characteristics of a chiral-recognizing perphenylated cyclodextrin column

Kazuo Nakamura[a], Hiroya Fujima[b], Hiroshi Kitagawa[b], Hiroo Wada[b,*], Keisuke Makino[a]

[a]*Department of Polymer Science and Engineering, Kyoto Institute of Technology, Matsugasaki, Sakyo-ku, Kyoto 606, Japan*
[b]*Shinwa Chemical Industries, Ltd., 50 Kagekatsu-cho, Fushimi-ku, Kyoto 612, Japan*

**Abstract**

A novel bifunctional chiral recognizing column (PhCD column) was prepared by immobilizing, on silica gel, β-cyclodextrin (CD) which was perphenylated through the reaction of phenyl isocyanate. Using several enantiomeric compounds, chiral recognition by CD was determined to be maintained in a PhCD column. The chromatographic characteristics of a PhCD column were compared with those of a column (CD column) bound with underivatized CD, and the following properties were found. For polyaromatic compounds and alkylbenzene derivatives, hydrophobic interaction is predominant, and for phenylalkyl alcohols and amines whose enantiomers are hard to recognize on a CD column, specific enantioselectivity was exhibited under the effects of the chemical structure around the chiral centre of the solutes. This added function is possibly an induced fit caused by the phenyl cluster on the CD openings. Using these properties, various enantiomeric drugs, in particular β-blockers (amino alcohols), which are hardly separated on conventional chiral separation columns, could be separated.

## 1. Introduction

In the last decade, chirality-related chemistry has become extremely important. For instance, asymmetric synthesis has increased its importance in drug preparation because one member of an enantiomeric pair frequently shows high toxicity while the other is an effective drug. To detect how such drugs with chirality are converted *in vivo*, chiral recognition analysis has also become essential. In this field, HPLC has played an important role. HPLC separation enables us to conduct pharmacokinetics studies, metabolism analysis, detection of optical impurities, etc., and is making great contributions in the life sciences.

Many chiral stationary phases have been developed. Columns carrying various chiral recognizing linkers were produced first for indirect analyses in which organic solvents are adopted. Such columns have a limited range of separable compounds. In addition to the unambiguous analytical results, therefore, users were required to stock various types of columns, from which a suitable one is chosen according to the compounds sought. Columns bonded with proteins [1–5] have been developed for aqueous phase HPLC analysis. Although a single stationary phase can separate a wide variety of compounds, such protein-bonded columns also have problems such as low loadability of samples and instability

* Corresponding author.

0021-9673/95/$09.50 
*SSDI* 0021-9673(94)00836-1

of the phases. Also, the separation mechanism still remains to be solved, preventing further improvement of the columns.

Therefore, to over these shortcomings, it is worth investigating other stationary phases that can be used in aqueous mobile phases and separate a wide range of compounds. An example is cyclodextrin (CD) immobilized on supports; CD can recognize the chirality of some samples trapped in its cavity. Columns with the stationary phases $\alpha$-, $\beta$- and $\gamma$-CDs, propylcarbamated CD and naphthylethylcarbamated CD have been developed [6–8] and are now commercially available. However, enantiomeric compounds are not always resolved satisfactorily on these CD columns and, therefore, further improvement is needed.

One idea for improvement is to modify CD stationary phases with linkers with potent hydrophilic or hydrophobic interactions so that this additional interaction can enhance the chiral recognition by CD. In this study, CD was linked with clusters of phenyl groups. The preparation was arranged so that phenyl groups are bound with all the hydroxyl groups on both the smaller and larger openings of the CD cone and the phenyl groups sticking out of the larger opening can interact with hydrophobic parts of the sample molecules in the outside of the cone. If this hydrophobic part of the solute is achiral, the hydrophobic interaction may regulate the fitness of the chiral part to the chiral recognizing centre in the cone. In this paper, we report the chromatographic characteristics of this bifunctional column.

## 2. Experimental

### 2.1. Chemicals and materials

$\beta$-Cyclodextrin ($\beta$-CD, referred to as CD hereafter) was purchased from Wako (Osaka, Japan). The silylating reagent 3-isocyanatopropyltriethoxysilane (95%) was obtained from Chisso Petrochemical (Tokyo, Japan) and was purified by distillation immediately prior to use. Phenyl isocyanate, the modifying reagent of CD, was purchased from Tokyo Kasei Kogyo (Tokyo, Japan). The silica gel used was Ultron SIL (a totally porous spherical silica gel with a mean particle diameter of 5 $\mu$m, a mean pore size of 120 Å and a specific surface area of 330 $m^2/g$), (Shinwa Chemical Industries, Kyoto, Japan). Other solvents used in the preparation of the stationary phase were of at least analytical-reagent grade and were carefully dried before use. Propranolol and its derivatives were kindly donated by Dr. J. Haginaka [9] of Mukogawa Women's University, and other samples were obtained from Wako.

### 2.2. Preparation of chiral stationary phase

Two types of CD-bonded silica stationary phases were prepared. The bonding reactions used are shown in Fig. 1. All reactions were performed under anhydrous conditions.

### 2.3. Preparation of CD column

A 5-mmol amount of CD (ca. 5.7 g), dried at 80°C under vacuum for 8 h, was dissolved in 70 ml of dry pyridine with stirring, then 5 mmol of (3-isocyanatopropyl)triethoxysilane (ca. 1.50 g) was added to the solution under a nitrogen atmosphere. The solution was allowed to stand at ca. 80°C until both the disappearance of the adsorption at 2200–2300 $cm^{-1}$ (N=C=O) and the appearance of carbonyl groups at 1700 $cm^{-1}$ were detected. This modified CD solution (solution A) was also used for the preparation of a PhCD column. To this solution, vacuum-dried silica gel (6 g, 140°C, 8 h) was added with stirring. After cooling, the CD-bonded silica was filtered, washed successively with pyridine, acetone, methanol, water, tetrahydrofuran (THF) and dichloromethane and finally dried under vacuum at 60°C for about 8 h. The amount of CD immobilized on the silica material was measured as the mass difference of the dried particles before and after functionalization, i.e., 67.8 mmol/g.

**CD-bonded Silca Gel**

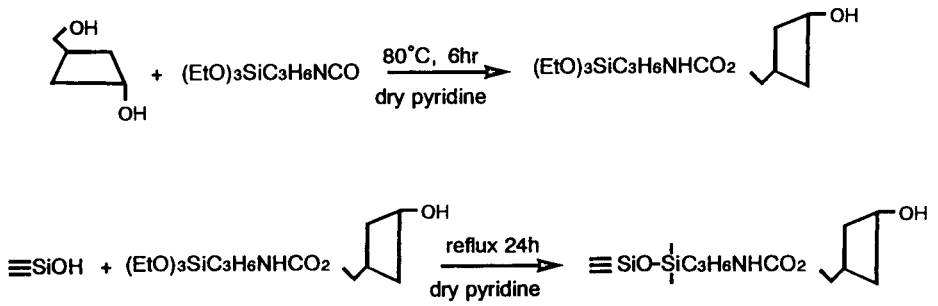


**PhCD-bonded Silica Gel**

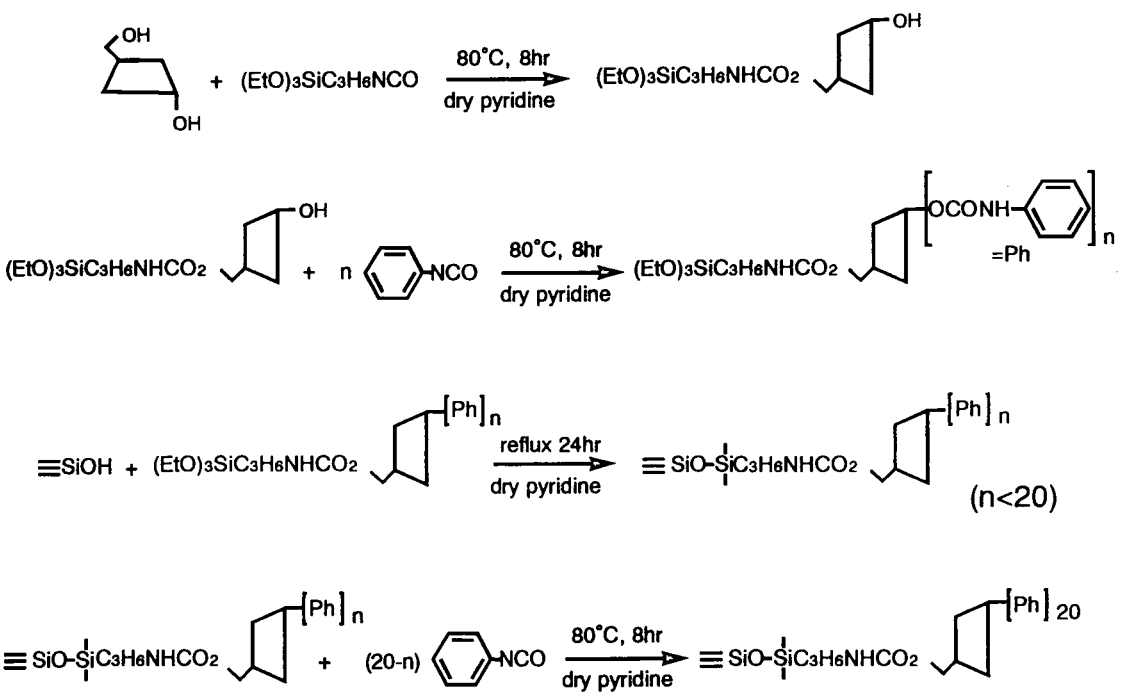


Fig. 1. Reaction schemes for the preparation of CD-bonded and PhCD-bonded silica gel.

### 2.4. Preparation of PhCD column

To solution A (see above), phenyl isocyanate (ca. 7.5 g) was added with stirring and the reaction mixture was allowed to stand at ca. 80°C for 8 h. To this solution, vacuum-dried silica gel (6 g, 140°C, 8 h) was added with stirring and the mixture was refluxed for 24 h. To this dispersion were added 7.5 g of phenyl isocyanate. The purpose of this additional reaction was to introduce phenyl isocyanate to hydroxyl groups remaining unreacted in the first reaction. The mixture was allowed to stand for 8 h at 80°C and, after cooling, the phenylcarbamoylated CD-bonded silica was filtered, washed successively with pyridine, acetone, methanol, water, THF and dichloromethane and finally dried under vacuum at 60°C for ca. 8 h. The amount of phenylisocyanated CD layer on the silica material was measured as the mass difference of the dried particles before and after functionalization, i.e., 66.8 mmol/g.

### 2.5. Measurements

The chromatographic system used consisted of an LC-6A pumping system (Shimadzu, Kyoto, Japan), an SPD-6AV UV detector (Shimadzu) and a C-R6A integrator (Shimadzu). The chromatographic conditions are given later. IR spectra were obtained on an FT/IR-5300 spectrometer (JASCO, Tokyo, Japan).

## 3. Results and discussion

As mentioned under Experimental, we prepared a perphenylated CD column (PhCD column). One of the seven primary hydroxyl groups located at the smaller opening edge of the cone was used for linking CD to the silica support. The other six groups and fourteen secondary hydroxyl groups on the larger opening edge of the cone were all subjected to reaction with phenylisocyanate. This introduction of phenyl groups was intended to introduce a hydrophobic cluster above the CD larger opening of the cone. By forming this cluster, stationary phase will be bifunctional in chiral recognition: one is chiral recognition by the CD cone and the other is hydrophobic interaction by the phenyl cluster. If phenyl cluster traps the hydrophobic part of the solute, we may be able to control the fitness of some solute to the recognition centre in the CD cone, producing the induced fit of chiral molecules.

Our major aim in preparing this column was to separate enantiomeric drugs in aqueous media, particularly $\beta$-blocking drugs such as atenolol [10]. The structure of these drugs is commonly base on amino alcohols with chiral centres. Usually such drugs are difficult to separate into individual enantiomers with aqueous mobile phases.

We first investigated the chiral recognizing ability of the PhCD column. The samples used were commercially available drugs with chirality, ibuprofen ($pK_a = 4.4$), chlorpheniramine ($pK_a = 9.2$) and hexobarbital ($pK_a = 8.2$). The eluent used was 20 m$M$ phosphate buffer containing 15% acetonitrile. Capacity factors ($k'$) and separation factors ($\alpha$) obtained at various pHs are summarized in Table 1 together with those obtained on the CD column for the same samples. At the pH values at which samples do not have charge, the chiral recognition ability [expressed as the separation factor ($\alpha$)] of the PhCD column was almost equivalent with that of the CD column, implying that chiral recognition by the CD cone was maintained in the PhCD column. It was also determined that the $k'$ values increased for the PhCD column. This is obviously due to the hydrophobic interaction by the phenyl cluster.

Polyaromatic compounds (benzene, naphthalene, anthracene and pyrene) were also tested to see the effect of the phenyl cluster. When the CD column was used, the $k'$ values increased as the number of benzene rings increased, except for anthracene, as shown in Fig. 2. This result suggests that these polyaromatic samples were retained in an aqueous acetonitrile mobile phase by hydrophobic interaction by CD and that for anthracene, some unidentified exclusive forces were combined. On the PhCD column, all four compounds had larger $k'$ values than those on

Table 1
Capacity factors ($k'$) and separation factors ($\alpha$) obtained for ibuprofen, chlorpheniramine and hexobarbital on Ultron ES-PhCD and Ultron ES-CD columns at various buffer pH values

| Column | Compound | pH 3.0 | | pH 4.0 | | pH 5.0 | | pH 6.0 | | pH 7.0 | |
|---|---|---|---|---|---|---|---|---|---|---|---|
| | | $k_1'$ | $\alpha$ | $k_1'$ | $\alpha$ | $k_1'$ | $\alpha$ | $k_1'$ | $\alpha$ | $k_1'$ | $\alpha$ |
| ES-PhCD | Ibuprofen | –[a] | – | – | – | 24.87 | 1.06 | 7.31 | 1.05 | 2.19 | 1.05 |
| (PhCD column) | Chlorpheniramine | 4.31 | 1.00 | 9.28 | 1.00 | 18.31 | 1.00 | 47.50 | 1.00 | – | – |
| | Hexobarbital | 9.99 | 1.11 | 9.97 | 1.11 | 9.95 | 1.07 | 9.87 | 1.11 | 9.13 | 1.11 |
| ES-CD | Ibuprofen | 74.08 | – | 64.78 | – | 52.14 | 1.05 | 31.93 | 1.07 | 23.47 | 1.07 |
| (CD column) | Chlorpheniramine | 2.80 | 1.09 | 4.59 | 1.09 | 6.61 | 1.09 | 11.30 | 1.08 | 28.14 | 1.06 |
| | Hexobarbital | 6.35 | 1.17 | 6.47 | 1.17 | 6.25 | 1.17 | 6.37 | 1.17 | 6.18 | 1.16 |

Eluent: 20 m*M* phosphate buffer–acetonitrile (85:15, v/v).
[a] Compound was not retained.

the CD column and the $k'$ values increased with increase in the ring number. These observations imply that on the PhCD column, hydrophobic interactions strengthened by the introduction of phenyl clusters dominate the retention of hydrophobic polyaromatic solutes. Such an enlarged retention due to the phenyl cluster was also obtained for alkylbenzenes. As represented in Fig. 3, on the PhCD column, the $k'$ values increased with increasing carbon number of the alkyl groups and were much larger than those on the CD column. Consequently, on the PhCD column, the phenyl cluster has a substantial hydrophobic interaction with hydrophobic compounds.

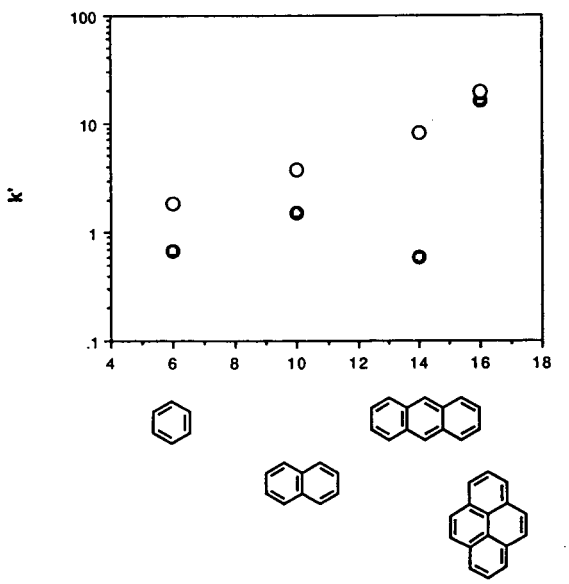


Fig. 2. Capacity factors obtained for polyaromatic compounds on (●) CD and (○) PhCD columns. HPLC conditions: columns, Ultron ES-CD (CD column, 150 × 6.0 mm I.D.) and Ultron ES-PhCD (PhCD column, 150 × 6.0 mm I.D.); eluent, water–acetonitrile (60:50, v/v); flow-rate, 1.2 ml/min; column temperature, 25°C; detection, UV at 254 nm.

For chiral compounds, CD and PhCD columns behaved differently, as shown in Fig. 4. The samples used were an amino ester, propranolol and its derivatives, which have a hydrophobic naphthalene ring and a chiral carbon several ångstroms distant from the ring. On the PhCD column, much larger $k'$ values were produced for all the compounds tested compared with those

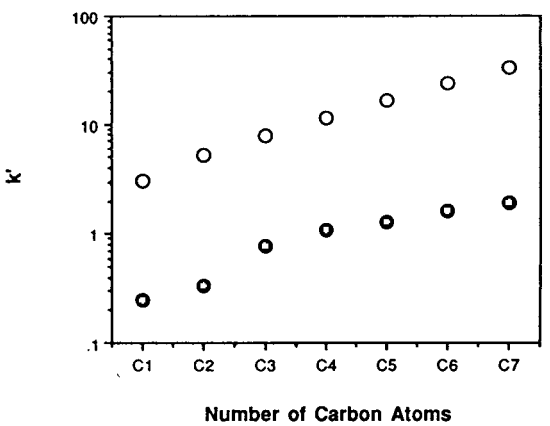


Fig. 3. Capacity factors obtained for alkylbenzenes on (●) CD and (○) PhCD columns. HPLC conditions as in Fig. 2.

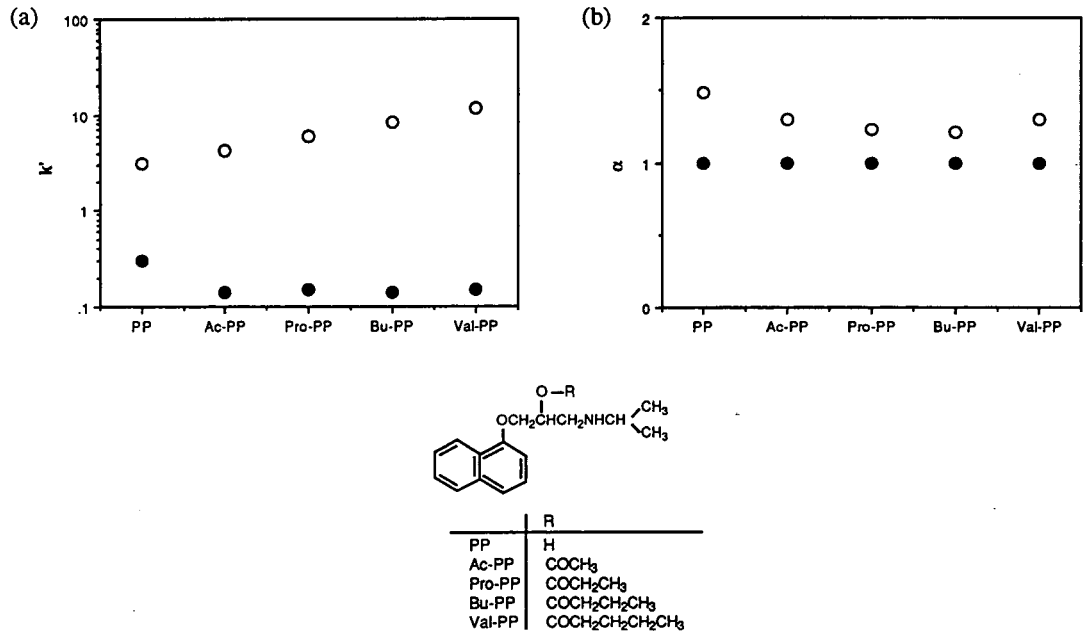


Fig. 4. Capacity factors and separation factors obtained for propranolol and its ester derivatives on (●) CD and (○) PhCD columns. HPLC conditions: columns, as in Fig. 2; eluent, 20 m*M* phosphate buffer (pH 4.6)–acetonitrile (65:35, v/v); flow-rate, 1.0 ml/min; column temperature, 25°C; detection, UV at 220 nm.

suggests that both the naphthalene ring and alkyl chain had hydrophobic interactions with the hydrophobic phenyl cluster of the PhCD column. When the length of the alkyl chain of the ester branch was increased, the $k'$ values increased on the PhCD column whereas they remained almost

Table 2
Separation of enantiometeric pairs on Ultron ES-PhCD

| Substance | $R_s$ | Substance | $R_s$ |
|---|---|---|---|
| Acetylpheneturide | 4.48 | Eperisone | 1.94 |
| Alprenolol | 2.70 | Flavanone | 3.01 |
| Arotinolol | 1.71 | Ibuprofen | 0.42 |
| Atenolol | 2.03 | Oxprenolol | 0.69 |
| Benzoin | 0.92 | Phenylethyl alcohol | 1.35 |
| 1,1'-Bi-2-naphthol | 4.50 | Phenylethylamine | 1.36 |
| Biperiden | 0.73 | Pindolol | 1.78 |
| Bunitrolol | 3.26 | Proglumide | 0.49 |
| Bupivacaine | 1.34 | Propranolol | 2.55 |
| Chlormezanone | 1.76 | *trans*-Stilbene oxide | 3.33 |
| Chlorphenesin | 2.31 | Trihexyphenidyl | 0.89 |
| DBD-APys[a] | 2.82 | DNB-MBA[b] | 2.11 |

[a] 4-(N,N-Dimethylaminosulphonyl)-7-(3-aminopyrrolidine)-2,1,3-benzoxadiazole.
[b] N-3,5-Dinitrobenzoyl-α-methylbenzylamine.

constant on the CD column. This trend also supports hydrophobic interactions. To see if this hydrophobic interaction controlled the fitting of the chiral centre of the solutes in the CD cavity, separation factors ($\alpha$) were also measured. As shown in Fig. 4b, the test samples had $\alpha$ values larger than 1 on the PhCD column whereas the values were always 1 for the separation on the CD column. The results indicate that chiral recognition by the CD cavity was enhanced by the introduction of phenyl clusters. As no recognition was observed when the CD column was used, such recognition by the PhCD column was probably produced by the cooperative action of both functions, hydrophobic interaction and inclusion.

An analogous trend was observed for phenylalkyl alcohols ($\alpha$-phenylethyl alcohol, 1-phenyl-1-propanol, 4-phenyl-2-butanol and 1-phenyl-1-pentanol). As depicted in Fig. 5a, on the PhCD column, the $k'$ values increased with increase in the chain length of alkyl groups whereas on the CD column such trend was not observed. This result also shows that phenyl clusters interact with hydrophobic parts of the solutes dominating the retention. For this series of samples, the PhCD column also produced a highly specific chiral recognition, which is represented by the $\alpha$ values. As shown in Fig. 5b, 4-phenyl-2-butanol had an extremely large $\alpha$ value compared with the others; it should be noted that on the CD column, all the samples exhibited $\alpha$ values of nearly 1, showing no specific chiral recognition. Probably on the PhCD column, a hydrophobic part (probably $-CH_2CHPh$) interacted with the phenyl cluster so that the chiral centre of this solute [$CH_3^*CH(OH)CH_2-$] was located at the chiral recognizing region of the CD cone. This induced fit is a novel characteristic of this column. It seems that in the case of the other samples, the chiral centre [$-^*CH(OH)Ph$] could not fit the recognition region because the hydrophobic interaction of the phenyl cluster and the benzene ring of the samples prevented the chiral centre entering the CD cone.

To see how effective the PhCD column is, enantiomeric drugs and chemicals were examined. Table 2 summarizes samples that showed good resolution. It is notable that $\beta$-blockers, which are hardly separated on conventional chiral columns, produced good resolution for their pairs of enantiomers on the PhCD column.

Consequently, by introducing a phenyl cluster on the large opening of CD and immobilizing this perphenylated CD on silica gel, a novel chiral recognizing column could be prepared.

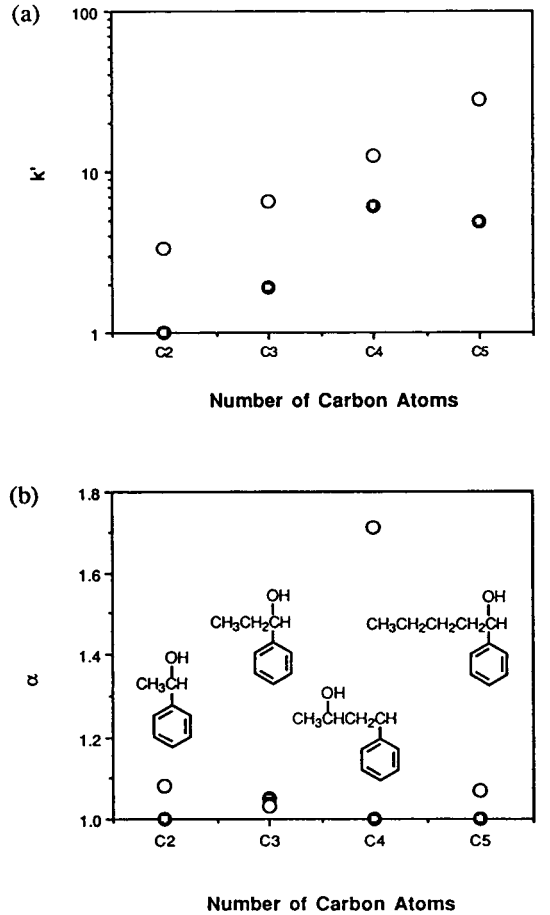


Fig. 5. Capacity factors and separation factors obtained for phenylalkyl alcohols on (●) CD and (○) PhCD columns. HPLC conditions: columns as in Fig. 2; eluent, 20 m*M* phosphate buffer (pH 4.6)–acetonitrile (80:20, v/v); flow-rate, 1.2 ml/min; column temperature, 25°C; detection, UV at 220 nm.

## References

[1] T. Miwa, M. Ichikawa, M. Kayano and Y. Miyake, *Chem. Pharm. Bull.*, 35 (1987) 682.
[2] K.M. Kirkland, K. Neilson and D.A. McCombs, *J. Chromatogr.*, 545 (1991) 43.
[3] J. Haginka, C. Seyama, H. Yasuda, H. Fujima and H. Wada, *J. Chromatogr.*, 592 (1992) 301.
[4] J. Hermansson and M. Eriksson, *J. Liq. Chromatogr.*, 9 (1983) 621.
[5] S. Allenmark and B. Bomgren, *J. Chromatogr.*, 264 (1983) 63.
[6] D.W. Armstrong and W. DeMond, *J. Chromatogr.*, 448 (1984) 411.
[7] D.W. Armstrong, C.-D. Chang and S.H. Lee, *J. Chromatogr.*, 539 (1991) 83.
[8] K. Fujimura, S. Suzuki, K. Hayashi and S. Masuda, *Anal. Chem.*, 6 (1990) 2198.
[9] J. Haginaka, J. Wakai, K. Takahashi, H. Yasuda and T. Katagi, *Chromatographica*, 29 (1990) 587.
[10] J. He, A. Shibukawa, T. Nakagawa, H. Wada, H. Fujima, E. Imai and Y. Go-oh, *Chem. Pharm. Bull.*, 41 (1993) 544.

ELSEVIER

Journal of Chromatography A, 694 (1995) 119–128

JOURNAL OF CHROMATOGRAPHY A

# Unified enantioselective capillary chromatography on a Chirasil-DEX stationary phase Advantages of column miniaturization

V. Schurig*, M. Jung, S. Mayer, M. Fluck, S. Negura, H. Jakubetz

*Institut für Organische Chemie der Universität, Auf der Morgenstelle 18, D-72076 Tübingen, Germany*

**Abstract**

Immobilized Chirasil-DEX (mono-6-O-octamethylenepermethyl-β-cyclodextrin chemically linked to dimethylpolysiloxane) can be employed as a versatile chiral stationary phase in chromatography. The chiral polymer has a long lifetime and is configurationally and thermally stable. The concept of unified enantioselective chromatography has been demonstrated for the enantiomer separation of hexobarbital by gas chromatography, supercritical fluid chromatography, liquid chromatography and capillary electrochromatography on a single open-tubular column (1 m × 50 μm I.D.) coated with Chirasil-DEX. The advantages of miniaturization in contemporary chromatographic enantiomer separation are demonstrated. Chirasil-DEX coated on porous silica is also useful for enantiomer separation in high-performance liquid chromatography.

## 1. Introduction

High-resolution enantiomer separation by chromatography has developed into an indispensable tool in contemporary chiral analysis. While the use of open-tubular columns is common in the GC and capillary electrochromatographic (CEC) modes, packed columns are used in the LC mode and both open-tubular columns and packed columns are employed in supercritical fluid chromatography (SFC). Based on both theoretical considerations and practical experiments, this paper explores the option of a unified approach, reminiscent of that pioneered in achiral separations by Ishii et al. [1], to enantioselective chromatography employing a single open-tubular column coated with a single chiral stationary phase. Attention is focused on miniaturization in modern chromatographic enantiomer analysis.

## 2. Experimental

### 2.1. Materials

Chirasil-DEX was prepared by hydrosilylation of permethylated mono-6-(oct-7-enyl)-β-cyclodextrin as described previously in detail [2]. The analytes were injected as methanolic solutions (ca. 0.1 mg/ml). HPLC-grade solvents (Merck, Darmstadt, Germany) were used. The buffers (20 m*M*), phosphate buffer (pH 7) or borate phosphate buffer (pH 7), were filtered through a

* Corresponding author.

0021-9673/95/$09.50 
*SSDI* 0021-9673(94)01075-7

0.45-μm pore-size filter (Macherey–Nagel, Düren, Germany).

### 2.2. Preparation of the open-tubular column

Fused-silica tubing (50 μm I.D., 360 μm O.D.; Chrompack International, Middleburg, The Netherlands) was heated at 260°C for 2 h at a low hydrogen flow-rate (0.1 bar inlet pressure). The column was coated without deactivation with a carefully filtered 2.0% solution of Chirasil-DEX in diethyl ether by the static method, yielding a film thickness of ca. 0.25 μm. Immobilization was carried out thermally for 20 h at 190°C in a very slow flow of hydrogen, as described previously [2]. The column was finally rinsed with dichloromethane. As before [3], immobilization was monitored by GC by measuring the retention factors ($k$) of $n$-dodecane and $n$-tridecane and the chiral separation factor ($\alpha$) of 1-phenylethanol. The column efficiency measured by GC was approximately 9000 plates/m for all three test solutes. The column length was 1 m. For UV detection, an optical window, located at a distance of 0.8 m from the injector, was prepared by burning off a section of about 3 mm of the polyimide outer coating.

### 2.3. Preparation of silica gel coated with immobilized Chirasil-DEX

A 4-g amount of porous silica (Nucleosil, 5 μm, 300 Å; Macherey–Nagel, Düren, Germany) was dried by azeotropic distillation with toluene. A slurry of this silica together with 1 g of Chirasil-DEX was prepared with 20 ml of dry dichloromethane in an ultrasonic bath. The solvent was slowly removed in a rotary evaporator, and immobilization was accomplished by heating the coated silica gel at 190°C under high vacuum (0.05 bar) for 20 h. In order to remove non-immobilized Chirasil-DEX, the product was washed with 200 ml each of methanol, dichloromethane and diethyl ether. The degree of immobilization was calculated from the C and H contents, as determined by elemental analysis before and after washing. It was found to be 70–85%, implying that this percentage of the original amount of Chirasil-DEX is deposited on the silica support.

### 2.4. Instrumentation

Carlo Erba VEGA and MEGA gas chromatographs (Fisons, Mainz, Germany), equipped with flame ionization detectors, were used. The carrier gas was hydrogen (99.999%) and the splitting ratio was 1:200. SFC was performed with a Carlo Erba SFC 3000 system as described previously [3]. The mobile phase was carbon dioxide (99.9995%) (Messer Griesheim, Düsseldorf, Germany). CEC was performed with a Kapillar-Elektrophorese System 100 (Grom, Herrenberg, Germany) and a Prince capillary electrophoresis system (Bischoff, Leonberg, Germany), both equipped with an on-column UV detector. A Shimadzu CR-6A Chromatopac integrator (Bischoff) was used for data acquisition. The sample was injected by the hydrostatic method (15 cm, 5s) or the pressure-driven method (40 mbar, 5 s) and detected at 220 nm. The coated column was conditioned with buffer for 1 h (30 kV) and was rinsed between each chromatographic run with water and methanol. Capillary LC was performed with the Prince system mentioned above. The analyte was injected by the pressure-driven method (40 mbar, 5 s) and detected at 220 nm. The operating pressure was 0.2 bar.

For HPLC a Chrompack (Middelburg, The Netherlands) instrument, equipped with a Chrompack Gras pump and a UV var detector, was used. A Rheodyne injection valve with a 20-μl sample loop was employed. Data acquisition was accomplished with a Chrompack control and integration system (PCI). HPLC columns (250 mm × 4.6 mm I.D.) were packed by the conventional slurry method. The column was first purged with methanol, methanol–water (1:1) and water, then conditioned with the operating buffer at a flow-rate of 0.5 ml/min until a stable baseline was observed.

## 3. Theoretical

The chromatographic behaviour of a solute eluted through a coated open-tubular column (Fig. 1) is governed by two principal migrations directed perpendicular to each other, i.e., (i) the

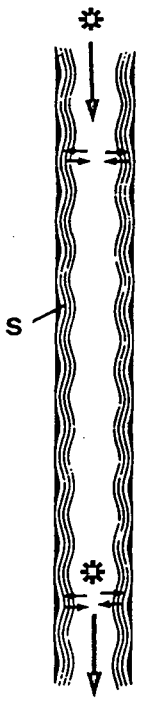


Fig. 1. Schematic view of a chromatographic process. * = Solute; S = stationary (liquid) phase; ↓ = axial migration; ⇄ = transverse migration.

axial movement carrying molecules from the column inlet to the outlet and (ii) the transversal movement necessary to distribute the molecules between the mobile and stationary phases. An important goal in open-tubular chromatography is the search for the highest efficiency as determined by the minimum height equivalent to a theoretical plate, $H_{min}$. Peak broadening caused by diffusion of the solute in the axial movement (i) can be minimized by increasing the average mobile phase velocity, $u$, and by decreasing the diffusion coefficient, $D_m$. Conversely, peak broadening caused by incomplete phase transfer in the transversal movement (ii) can be reduced by decreasing the average mobile phase velocity, $u$, and increasing the diffusion coefficient, $D_m$. Consequently, at a given $D_m$ of the solute, an optimum mobile phase velocity, $u_{opt}$, exists at which the open-tubular column performs at the highest efficiency with the minimum plate height, $H_{min}$. Thus, according to the simplified Golay equation (Eq. 1) [4], with the pressure gradient and diffusion in the stationary phase being neglected, the efficiency of an open-tubular column is governed by the opposing effects of an inverse ($\sim D_m/u$) and a linear ($\sim u/D_m$) relationship of $H$ vs. $u$ (and $1/D_m$).

$$H = \frac{B}{u} + Cu = \frac{2D_m}{u} + \frac{1 + 6k + 11k^2}{96(1+k)^2} \cdot \frac{d_c^2}{D_m} \cdot u \quad (1)$$

$$u_{opt} = \sqrt{\frac{B}{C}} = \frac{8D_m(1+k)}{d_c} \cdot \sqrt{\frac{3}{1 + 6k + 11k^2}} \quad (2)$$

$$H_{min} = 2\sqrt{BC} = \frac{d_c}{2(1+k)} \cdot \sqrt{\frac{1 + 6k + 11k^2}{3}} \quad (3)$$

The mathematical form of Eq. 1 leads to the following conclusions:

(i) if $H$ is plotted against log $u$ (at a constant retention factor $k$), symmetrical curves with nearly identical parabolic shapes result for different chromatographic methods (LC, SFC, GC) (Fig. 2) [5];

(ii) the optimum mobile phase velocity, $u_{opt}$, and the minimum plate height, $H_{min}$, are derived by differentiation of Eq. 1, i.e., $\delta H/\delta u = 0$;

(iii) the optimum mobile phase velocity, $u_{opt}$, is determined by Eq. 2 [6] and depends at a given $k$ on the diffusion coefficient $D_m$ and the column inside diameter $d_c$; consequently, speed of analysis is fast in GC, medium in SFC and slow in LC on the same coated open-tubular column operated at the respective $u_{opt}$;

(iv) the highest efficiency, expressed by the minimum plate height, $H_{min}$, is determined by eq. 3 [6] and increases with decreasing column inside diameter $d_c$, irrespective of the nature of the mobile phase; significantly, $H_{min}$ is equal for a gas, a sub- or supercritical fluid or a liquid (also containing modifiers or present as a buffer system) used as the mobile phase at a given $k$.

In electrodriven systems, i.e., capillary electrophoresis (CE), the $H$ vs. log $u$ curve (Fig. 2, dotted curve) is shifted towards higher efficiency and a favourable optimum mobile phase velocity due to the flat flow profile, as opposed to the parabolic flow profile in pressure-driven systems, e.g., LC.

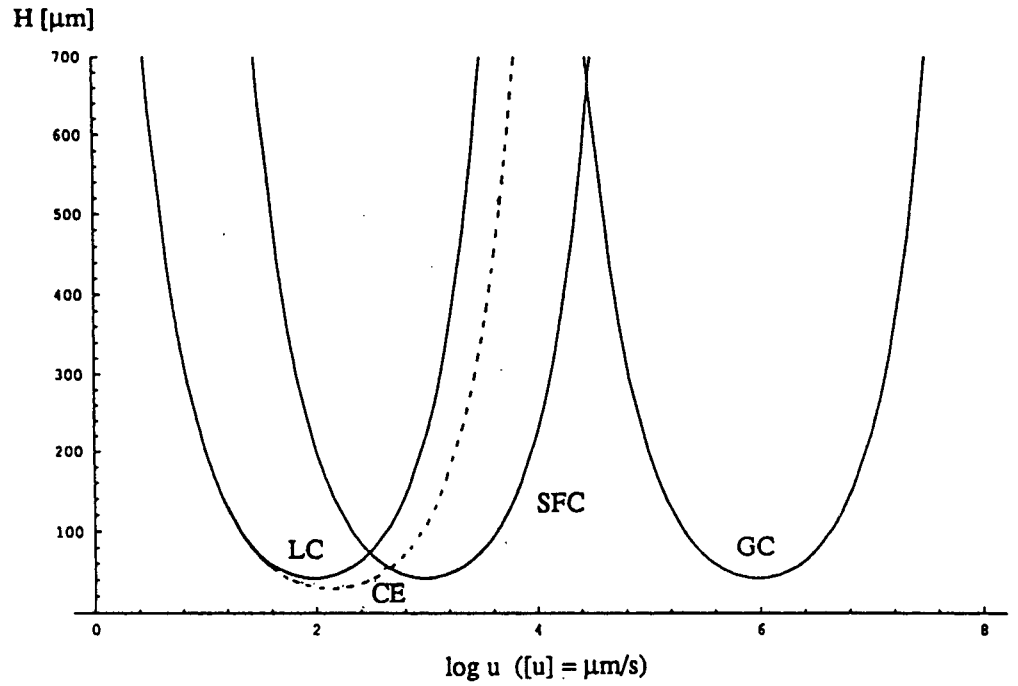


Fig. 2. Height equivalent to a theoretical plate, $H$, versus logarithm of mobile phase velocity, $u$, according to Eq. 1 for a 50 $\mu$m I.D. open-tubular column. $k = 5$; $D_m$ ($\mu m^2\ s^{-1}$) = $10^7$ (GC), $10^4$ (SFC), $10^3$ (LC, CEC); $C_{parabol} = (1 + 6k + 11k^2)/[96(1 + k)^2]$ {note that in CEC, $H_{min}$ and $u_{opt}$ are different owing to the nearly flat flow profile (dotted curve), $C_{flat} = k^2/[16(1 + k)^2]$}.

## 4. Results and discussion

### 4.1. Unified enantioselective open-tubular chromatography

A few years ago, Chirasil-DEX (mono-6-O-octamethylenepermethyl-$\beta$-cyclodextrin chemically linked to dimethylpolysiloxane; cf. Fig. 3) was synthesized and employed as an immobilizable chiral stationary phase for open-tubular GC [7,8]. Chirasil-DEX typically contains 24% (w/w) of permethylated $\beta$-cyclodextrin (i.e., 0.22 molal [2]) in polysiloxane and, thus, statistically one in sixty silicon atoms in the polymer chain carries a CD moiety. Later it was found that Chirasil-DEX is compatible with solvating mobile phases such as sub- and supercritical carbon dioxide at elevated temperature and high pressure (SFC) [3,8–10] and even with buffers over a wide pH range (CEC) [11–14]. Enantiomer separation on a chiral surface by CEC is espe-

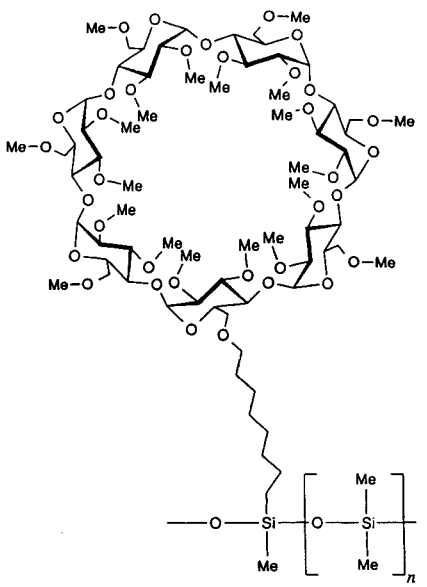


Fig. 3. Representation of Chirasil-DEX (mono-6-O-octamethylenepermethyl-$\beta$-cyclodextrin chemically linked to dimethylpolysiloxane).

cially noteworthy, while this approach was not immediately obvious [11].

Previously, the performance of open-tubular columns coated with Chirasil-DEX by SFC and CEC has always been cross-checked before and during measurements by installing the columns in a GC instrument and by monitoring the retention factors $k$ of test solutes. These investigations prompted us to generalize the principle of unified enantioselective open-tubular chromatography using one column coated with Chirasil-DEX for all important contemporary methods of enantiomer separation available, i.e., open-tubular GC, SFC, LC and CEC. The impetus of this approach arose from the prediction by Eq. 3 that the highest efficiency obtained on a given open-tubular column is independent of the nature of the mobile phase at a given $k$ (see above).

Whereas for SFC and CEC open-tubular column dimensions of 1 m × 50 μm I.D. have previously been used for practical reasons [2,3,8,12–14], larger inside diameters (250 μm) are common in GC [15] and smaller diameters (5–10 μm) are advocated in (achiral) open-tubular LC [16–21]. As a compromise, a 1 m × 50 μm I.D. fused-silica open-tubular column coated with Chirasil-DEX was used. As the result of the different diffusion coefficients $D_m$ in gases and liquids (cf. Fig. 2, caption) analysis times at optimum efficiency in open-tubular LC and CEC are slower by as much as four orders of magnitude than in GC (cf., Fig. 2), thus rendering a unified approach inpracticable in terms of analysis time because the ratio of the mobile phase velocity between GC and CEC is only about 250. However, according to Eqs. 1–3, $H_{min}$ and $u_{opt}$ depend also on the retention factor $k$. Fortunately, it has been observed that, while $k$ may be large in the GC mode [22] and intermediate in the SFC mode [2,3,8], very small values ($k < 1$) are often encountered in the CEC mode for the first-eluting peak [14]. Hence, if the retention factors $k$ observed in the various chromatographic methods involving Chirasil-DEX-coated open-tubular columns are taken into considera-

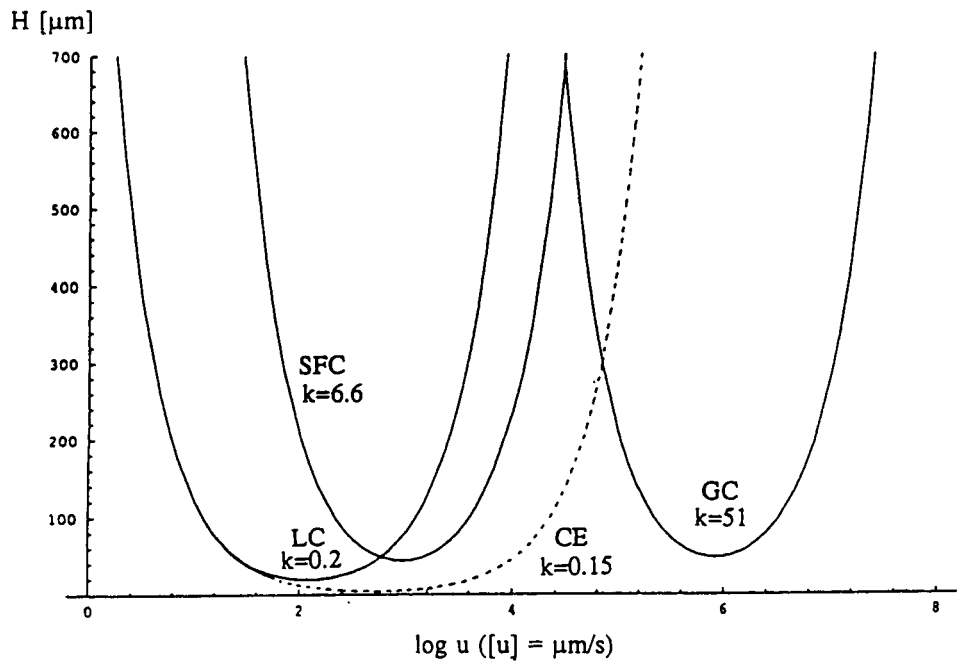


Fig. 4. Height equivalent to a theoretical plate, $H$, versus logarithm of mobile phase velocity, $u$, according to Eq. 1 for a 50 μm I.D. open-tubular column. $k$ Variable; $D_m$ ($\mu m^2\ s^{-1}$) = $10^7$ (GC), $10^4$ (SFC), $10^3$ (LC, CEC); $C_{parabol} = (1 + 6k + 11k^2)/[96(1 + k)^2]$ {note that in CEC, $H_{min}$ and $u_{opt}$ are different owing to the nearly flat flow profile (dotted curve), $C_{flat} = k^2/[16(1 + k)^2]$}.

tion, $H$ vs. log $u$ curves as shown in Fig. 4 emerge which are compatible with the unified approach envisaged. For instance, with $k = 0.15$ in the CEC mode the $H$ vs. log $u$ curve becomes very flat and the efficiency is nearly independent of the mobile phase velocity over several orders of magnitude (cf., Fig. 4). In this case, at a flow rate $u$ in the range $u_{opt,CE} < u < u_{opt,GC}$, the GC and CEC curves even intersect with an efficiency reduced by a factor of six compared with $H_{min}$ (GC) (cf., Fig. 4). These considerations led us to probe the goal of unified enantioselective open-tubular chromatography under real experimental conditions. Here we demonstrate for the first time that, e.g., for the chiral solute hexobarbital a unified enantioselective approach is indeed feasible employing the same 1 m × 50 μm I.D. open-tubular column coated with immobilized Chirasil-DEX (film thickness 250 nm) by four independent methods, i.e., open-tubular GC, SFC, CEC and LC (Fig. 5) [23].

Inspection of Fig. 5 merits a number of comments. In the CEC mode the mobile phase is driven by the electroosmotic flow. As the coating of the column wall by the polysiloxane Chirasil-DEX lowers the availability of silanol groups, electroosmosis is reduced and the dead time $t_D$ is increased, rendering the analysis time rather long (20 min). For the sake of comparison, all other separations were performed with the same analysis time (GC, SFC), except in LC (10 min), because shorter analysis times led to unacceptable peak tailing for the second-eluted enantiomer. Apart from the long analysis time, CEC is superior to GC, SFC and LC with respect to all parameters important in enantiomer separation under the practical (non-optimized) conditions applied in Fig. 5:

chiral separation factor $\alpha$: CEC ≈ LC > SFC > GC (at the given temperatures);
peak resolution $R_S$: CEC > SFC ≈ GC > LC;
efficiency $N$ (first peak): CEC > LC > GC > SFC (at the observed retention factors $k$).

The enantiomer separation of hexobarbital by CEC [13,14] on Chirasil-DEX shows interesting features. Thus, $\alpha = 4$ (Fig. 5, right) is the highest value ever observed on Chirasil-DEX. The retention factor $k$ of the first-eluted enantiomer is indeed very low, e.g., $k = 0.15$, thus resulting in further improvements in both $H_{min}$ (efficiency) and $u_{opt}$ (speed of analysis) (Fig. 4). Thus, the first-eluted enantiomer displays a much higher efficiency than the second-eluted peak lying off

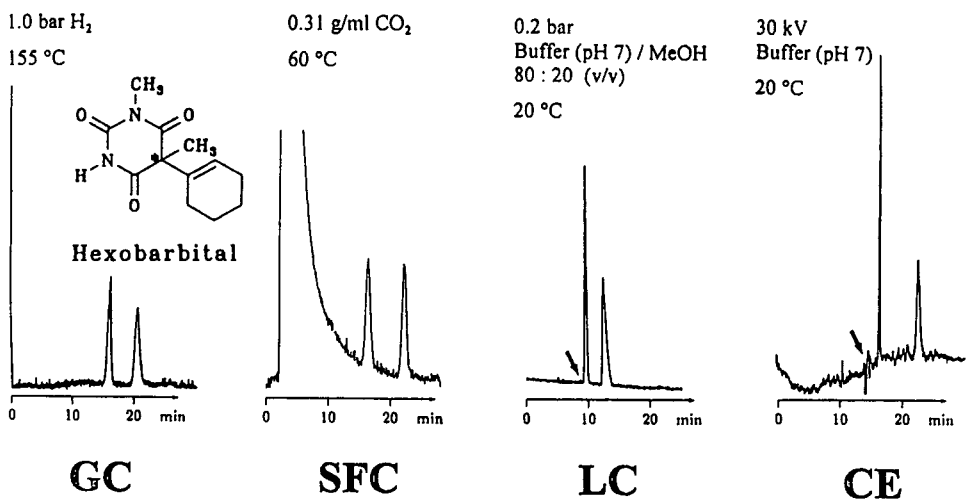


Fig. 5. Enantiomer separation of hexobarbital on a 1 m × 50 μm I.D. fused-silica column coated with Chirasil-DEX (film thickness 250 nm) by GC, SFC, LC and CEC in ca. 20 min. Effective column length in LC and CEC, 85 cm. Buffer, borate–phosphate (pH 7) (the arrow indicates the dead volume).

the $H$ vs. log $u$ optimum in both CEC and LC. When comparing GC and SFC, the gain in enantioselectivity on lowering the separation temperature in SFC is small. As is readily seen from Fig. 4, the unified approach towards enantioselective chromatography is feasible because of the favourable differences in the dead times $t_D$ and retention factors $k$ observed in the four chromatographic methods. In GC, $t_D$ is small and $k$ is large, and therefore the analyte spends most of its time in the stationary phase. In contrast in CEC and LC, $t_D$ is large and $k$ (notably for the first-eluting enantiomer) is very small, and therefore, the analyte spends most of its time in the mobile phase. Overall, these differences lead to similar retention times with acceptable efficiency characteristics. We consider the unified approach described here to be rather a unique than universal approach as it relies on a high separation factor $\alpha$ for the racemic mixture to be resolved.

Hitherto, the unified approach demonstrated here used the same open-tubular column coated with Chirasil-DEX in different chromatographic modes. In the spirit of unified chromatographic approaches advanced by Ishii et al. [1], further endeavours should be directed towards enantioselective separations also by using unified equipment. Thus, enantiomer separation by GC, subcritical-FC, SFC and LC may in principle be carried out with carbon dioxide in the same instrument with continuous transitions between the chromatographic modes by varying the temperature and pressure. CEC and LC have already been performed in this work by using a unified capillary electrophoretic equipment employing an injection system amenable to generating a voltage and pressure gradient. The expected decrease in efficiency due to the change from a flat to a parabolic flow profile when switching from CEC to LC is readily apparent by inspection of Fig. 4. Both electrically and pressure-driven methods may in principle be used in combination. The rapid evolution of instrumental design for small open-tubular column operation and on-column detection is likely to stimulate open-tubular LC investigations for both chiral and achiral separations. The use of open-

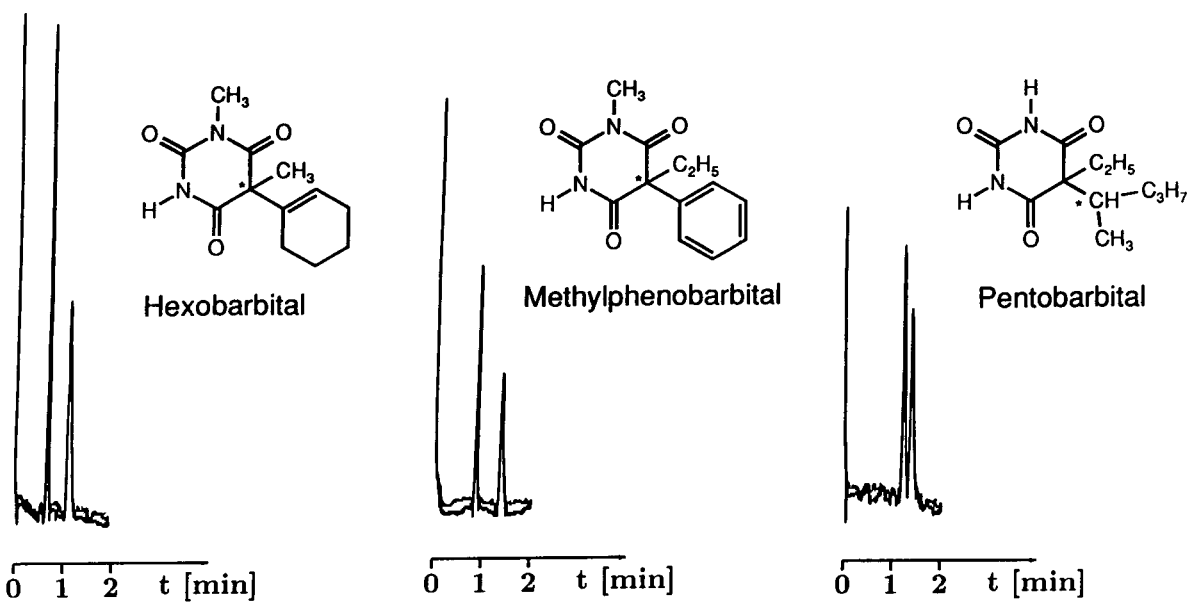


Fig. 6. Rapid enantiomer separation of barbiturates on a 35 cm × 50 μm I.D. fused-silica column coated with Chirasil-DEX (film thickness 60 nm) by GC at 130°C and 1 bar hydrogen.

tubular LC in enantiomer separation demonstrated here for the first time has the following advantages: low flow-rates facilitating coupling techniques (LC–MS); high column permeability and low pressure gradients; highly reduced amounts of chiral stationary phase and mobile phase; low heat capacity facilitating temperature programming; and increased mass sensitivity with concentration-dependent detectors [24].

Supported by theoretical considerations [25,26], it is to be expected that also enantiomer separations by CEC and LC using capillaries coated with Chirasil-DEX will strongly benefit from smaller column diameters. Further investigations are in progress.

### 4.2. Column miniaturization in enantioselective GC

The present investigations led also to the conclusion that column miniaturization is of considerable importance in enantiomer separations by GC. Traditionally, separations have been performed with long (10–25 m) and medium–bore (250 μm I.D.) open-tubular columns, although achiral separations on high-speed narrow-bore open-tubular columns were carried out as early as in 1962 by Desty et al. [27], who resolved fifteen components in few seconds on a 1.2 × 34.5 μm I.D. column. In general, a gain in analysis time [28] by a factor of nine is estimated when changing from a 320 to a 50 μm I.D. column [29]. By using short columns, high inlet pressures are not required. Surprisingly, only a few investigations have demonstrated hitherto the advantages of using short and narrow-bore open-tubular columns for fast enantiomer separations [7,30]. While the advantage of miniaturization in the GC mode is already evident in Fig. 5 (left), further decreases in column length and film thickness of Chirasil-DEX allow enantiomer separations in less than 100 s for,

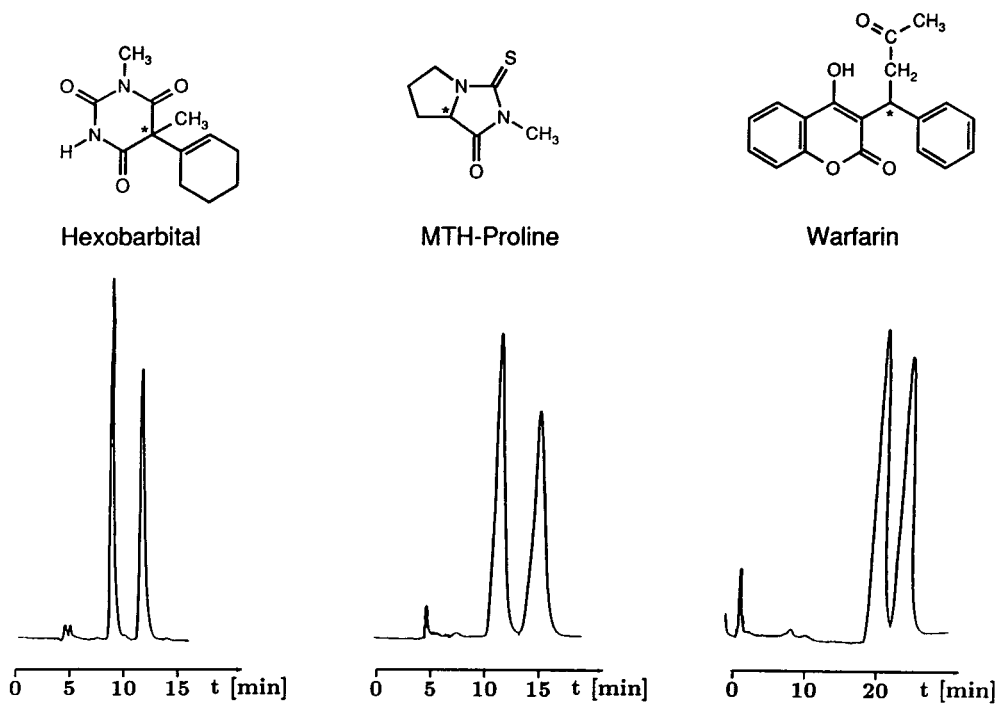


Fig. 7. Separation of enantiomers on a 250 × 4.6 mm I.D. column containing immobilized Chirasil-DEX coated on Nucleosil (300 Å, 5 μm) silica by HPLC. Left, 0.4 ml/min methanol–phosphate buffer (50:50), 240 nm; others, 1 ml/min methanol–phosphate buffer (30:70), 220 nm.

e.g., barbiturates (Fig. 6). The decrease in sample capacity (injection) is partially compensated for by a strong increase in the signal-to-noise ratio via enhanced detection sensitivity resulting from short analysis times leading to very narrow peak widths. Short, narrow-bore columns permit low elution temperatures, which in turn leads to higher separation factors $\alpha$. One disadvantage is the small sample capacity and the tendency towards overloading phenomena in narrow-bore columns [31].

### *4.3. Enantiomer separation on Chirasil-DEX-coated silica by HPLC*

In addition to its use as a versatile stationary phase for open-tubular column chromatography, we have also employed Chirasil-DEX in HPLC by coating it on porous silica. As shown in Fig. 7, this new chiral stationary phase allows the enantiomer separation of several barbiturates by reversed-phase HPLC. The coating of the surface with a non-polar film of Chirasil-DEX represents an interesting alternative to the usual method of direct chemical bonding of cyclodextrins to silica [32–34] and subsequent end-capping of the polar sites on the support. Further systematic investigations, e.g., the role of effective blocking of polar sites at the support and thus reducing mixed retention mechanisms [35] by Chirasil-DEX, are in progress.

## Acknowledgements

Support of this work by the Deutsche Forschungsgemeinschaft and the Fonds der chemischen Industrie is gratefully acknowledged.

## References

[1] D. Ishii, T. Niwa, K. Ohta and T. Takeuchi, *J. High Resolut. Chromatogr. Chromatogr. Commun.*, 11 (1988) 800.
[2] M. Jung and V. Schurig, *J. Microcol. Sep.*, 5 (1993) 11.
[3] M. Jung and V. Schurig, *J. High Resolut. Chromatogr.*, 16 (1993) 215.
[4] M.J.E. Golay, in D. H. Desty (Editor), *Gas Chromatography*, Butterworths, London, 1958, p. 36.
[5] T.L. Chester, in F.J. Yang (Editor), *Microbore Column Chromatography, a Unified Approach to Chromatography*, Marcel Dekker, New York, 1989, p. 369.
[6] G. Guiochon and C.L. Guillemin, *Quantitative Gas Chromatography (Journal of Chromatography Library*, Vol. 42), Elsevier, Amsterdam, 1988, 105.
[7] V. Schurig, D. Schmalzing, U. Mühleck, M. Jung, M. Schleimer, P. Mussche, C. Duvekot and J.C. Buyten, *J. High Resolut. Chromatogr.*, 13 (1990) 713.
[8] V. Schurig, D. Schmalzing and M. Schleimer, *Angew, Chem., Int. Ed. Engl.*, 30 (1991) 987.
[9] V. Schurig, Z. Juvancz, G.J. Nicholson and D. Schmalzing, *J. High Resolut. Chromatogr.*, 14 (1991) 58.
[10] D. Schmalzing, G.J. Nicholson, M. Jung and V. Schurig, *J. Microcol. Sep.*, 4 (1992) 23.
[11] S. Mayer and V. Schurig, *J. High Resolut. Chromatogr.*, 15 (1992) 129.
[12] S. Mayer and V. Schurig, *J. Liq. Chromatogr.*, 16 (1993) 915.
[13] S. Mayer, M. Schleimer and V. Schurig, *J. Microcol. Sep.*, 6 (1994) 43.
[14] S. Mayer and V. Schurig, *Electrophoresis*, 15 (1994) 835.
[15] V. Schurig, *J. Chromatogr. A*, 666 (1994) 111.
[16] D. Ishii et al., *J. High Resolut. Chromatogr. Chromatogr. Commun.*, 2 (1979) 371.
[17] T. Tsuda and G. Nakagawa, *J. Chromatogr.*, 268 (1983) 369.
[18] H. Engelhardt and B. Lillig, *J. High Resolut. Chromatogr. Chromatogr. Commun.*, 8 (1985) 531.
[19] O. van Berkel, H. Poppe and J.C. Kraak, *Chromatographia*, 24 (1987) 739.
[20] S. Folestad, B. Josefsson and M. Larsson, *J. Chromatogr.*, 391 (1987) 347.
[21] K. Jinno, *Chromatographia*, 25 (1988) 1004.
[22] D. Schmalzing, M. Jung, S. Mayer, J. Rickert and V. Schurig, *J. High Resolut. Chromatogr.*, 16 (1993) 215.
[23] V. Schurig, M. Jung, S. Mayer, S. Negura, H. Grosenick, M. Fluck and A. Glausch, *Analytica 94, Munich, 19–22 April 1994*, abstracts, p. 52.
[24] M. Goto, T. Takeuchi and D. Ishii, *Adv. Chromatogr.*, 30 (1989) 167.
[25] G. Guiochon and H. Colin, in P. Kucera (Editor), *Micro Column High Performance Liquid Chromatography*, Elsevier, Amsterdam, 1984.
[26] J. Vindevogel and P. Sandra, *Electrophoresis*, 15 (1994) 842.
[27] D.H. Desty, A. Goldup and W.T. Swanton, in N. Brenner, et al. (Editors), *Gas Chromatography*, Academic Press, New York, 1962, p. 105.
[28] P. Sandra, *Analusis Mag.* 20 (1992) M27.
[29] A. van Es, in W. Bertsch, H. Frank, W.G. Jennings and P. Sandra (Editors), *Chromatographic Methods*, Hüthig, Heidelberg, 1992.
[30] M. Lindström, *J. High Resolut. Chromatogr.*, 14 (1991) 765.

[31] Z. Juvancz, K. Grolimund and V. Schurig, *J. High Resolut. Chromatogr.*, 16 (1993) 140.
[32] A. Berthod, S. Chang and D.W. Armstrong, *Anal. Chem.*, 64 (1992) 395.
[33] K. Cabrera, D. Lubda and G. Jung, in V. Schurig (Editor), *3rd International Symposium on Chiral Discrimination, Tübingen, 1992*, book of abstractsf, 1992, p. 16.
[34] H. Riering, P. Wollenweber, M. Sieber and A. Neus, in W. Günther, V. Hempel and G. Wulff (Editors), *Instrumentalized Analytical Chemistry and Computer Technology, 1994*, InComBureau, Düsseldorf, 1994, p. 307.
[35] M. Schleimer and W.H. Pirkle, in V. Schurig (Editor), *3rd International Symposium on Chiral Discrimination, Tübingen, 1992*, book of abstracts, 1992, p. 73.

ELSEVIER

Journal of Chromatography A, 694 (1995) 129–134

JOURNAL OF CHROMATOGRAPHY A

# Direct enantiomer separations by high-performance liquid chromatography with chiral urea derivatives as stationary phases

Naobumi Ôi*, Hajimu Kitahara, Fumiko Aoki

*Sumika Chemical Analysis Service, Ltd., 3-1-135, Kasugade-naka, Konohana-ku, Osaka 554, Japan*

**Abstract**

The chromatographic properties of urea derivatives derived from (*S*)- and (*R*)-1-(α-naphthyl)ethylamine with (*S*)-valine, (*S*)-*tert.*-leucine, (*S*)-proline and (*S*)-indoline-2-carboxylic acid bonded to 3-aminopropylsilica gel as chiral stationary phases were examined by HPLC to investigate the effect of the structure of the amino acid moiety. The specific enantiomer separation of various racemic compounds including alcohols, esters, amines, amino alcohols, carboxylic acids and amino acids was accomplished on these phases using normal mobile phases. The effect of the stereochemical structure in these urea derivatives on chiral recognition is discussed.

## 1. Introduction

It is well known that high-performance liquid chromatography (HPLC) using chiral stationary phases (CSPs) is a powerful tool for the direct enantiomer separation [1,2]. One of the most important classes of CSPs is the "brush-type" CSP, containing various low-molecular-mass chiral selectors. Pioneering work in this area was done by Pirkle et al. [3], and many useful CSPs have subsequently been developed. It is believed that chiral recognition on this type of CSP is based on at least three simultaneous interactions, hydrogen bond formation, $\pi-\pi$ interactions and dipole–dipole stacking. We have found [4,5] that CSPs derived from (*S*)- and (*R*)-1-(α-naphthyl)-ethylamine with (*S*)-valine or (*R*)-phenylglycine chemically bonded to 3-aminopropylsilanized silica (CSPs 1, 2, 3 and 4) showed excellent enantioselectivity. Accordingly, it was expected that similar urea derivatives containing another amino acid moieties would provide characteristic enantioselectivities. Recently we have developed six CSPs (CSPs 5–10) derived from (*S*)- and (*R*)-1-(α-naphthyl)ethylamine with (*S*)-*tert.*-leucine, (*S*)-proline and (*S*)-indoline-2-carboxylic acid covalently bonded to 3-aminopropylsilanized silica. These CSPs are now commercially available, and some application data are given in brochures.

In this study, we examined their chromatographic properties as CSPs to investigate the effect of the structure of the amino acid moiety. CSPs 1 and 2 were also used to compare the enantioselectivity with these CSPs.

## 2. Experimental

### 2.1. Chiral stationary phases

The structures of the CSPs are shown in

* Corresponding author.

0021-9673/95/$09.50 
*SSDI* 0021-9673(94)00662-8

Fig. 1. CSPs 5–10 were synthesized using (*S*)-*tert.*-leucine, (*S*)-proline and (*S*)-indoline-2-carboxylic acid instead of (*S*)-valine in CSPs 1 and 2 by the procedures described previously [4]. Develosil-$NH_2$ (5 $\mu$m) (Nomura Chemical, Seto, Japan) was used as the starting material. Grafting rates were calculated according to the C and N elemental analysis for each CSP: CSP 5, 0.43; CSP 6, 0.41; CSP 7, 0.48; CSP 8, 0.49; CSP 9, 0.44; and CSP 10, 0.43 mmol/g.

### 2.2. Liquid chromatography

The experiments were carried out using a Waters Model 510 high-performance liquid chromatograph, equipped with a variable-wavelength UV detector operated at 230, 254 and 280 nm. Stainless-steel columns (250 × 4.6 mm I.D.) were slurry packed with these CSPs using a conventional technique. These columns are available from Sumika Chemical Analysis Service (Osaka, Japan), as Sumichiral OA-4000 (CSP 1), OA-4100 (CSP 2), OA-4600 (CSP 5), OA-4700 (CSP 6), OA-4400 (CSP 7), OA-4500 (CSP 8), OA-4800 (CSP 9) and OA-4900 (CSP 10). Solutes and solvents of analytical-reagent grade were purchased from Wako (Osaka, Japan). Some compounds were kindly provided by Sumitomo Chemical (Osaka, Japan). The structures of the racemic compounds used are shown in Fig. 2. The chromatographic conditions are given in Table 1.

## 3. Results and discussion

The chromatographic results are summarized in Table 1. The direct separation of a wide range of racemic compounds was accomplished on these CSPs using normal mobile phases.

The separation of racemic pyrethroid insecticide esters (**1** and **2**) was achieved on CSP 5

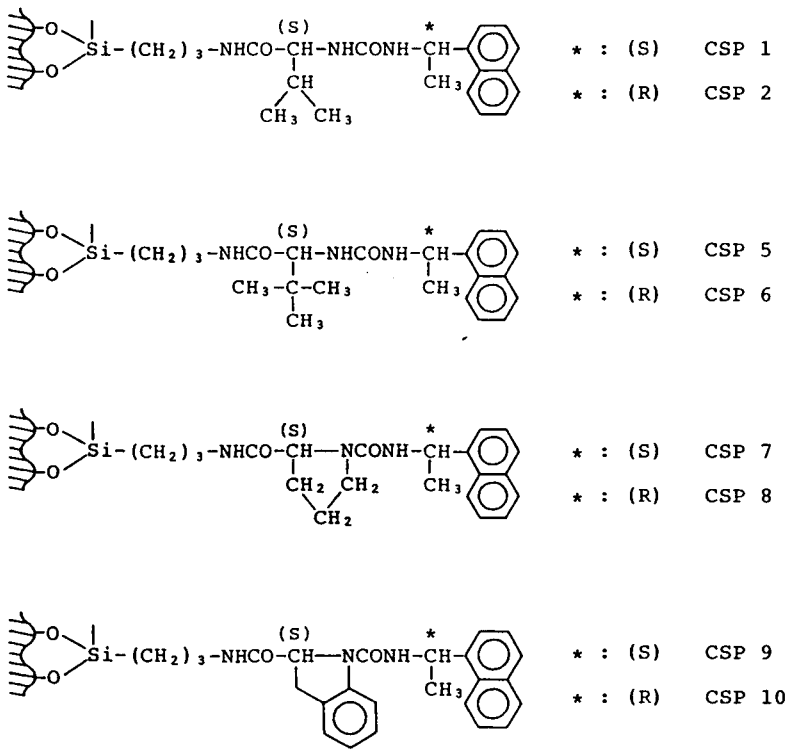


Fig. 1. Structures of the CSPs.

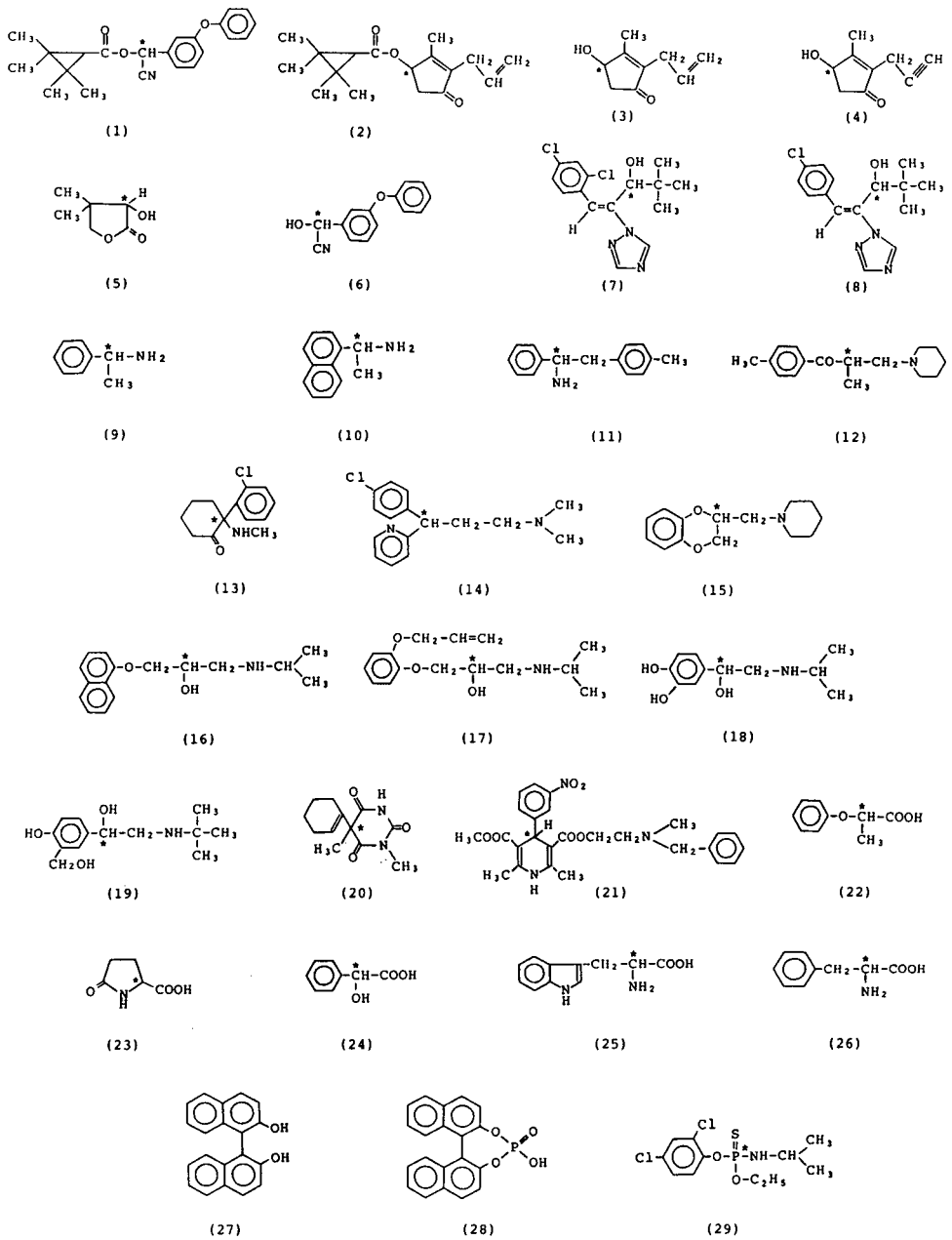

Fig. 2. Structures of racemic compounds in Table 1.

and also on CSP 1 as reported previously [6], and approximate values of the separation factors showed that the enantioselectivity was not remarkably influenced by the bulky *tert.*-butyl group in place of the isopropyl group attached to the asymmetric carbon atom in the amino acid moiety. On the other hand, various racemic alcohols, amines, amino alcohols and carboxylic acids were well resolved on CSPs 6 and 2. Typical chromatograms are shown in Figs. 3 and

Table 1
HPLC separation of enantiomers on chiral stationary phases

| No. | Compound | CSP 1 | | | CSP 2 | | | CSP 5 | | | CSP 6 | | | CSP 7 | | | CSP 8 | | | CSP 9 | | | CSP 10 | | |
|---|---|---|---|---|---|---|---|---|---|---|---|---|---|---|---|---|---|---|---|---|---|---|---|---|---|
| | | $k'_1$ | $\alpha$ | M | $k'_1$ | $\alpha$ | M | $k'_1$ | $\alpha$ | M | $k'_1$ | $\alpha$ | M | $k'_1$ | $\alpha$ | M | $k'_1$ | $\alpha$ | M | $k'_1$ | $\alpha$ | M | $k'_1$ | $\alpha$ | M |
| 1 | Fenpropathrin | 4.22 | 1.11 | A | 3.03 | 1.04 | A | 2.90 | 1.26 | A | 2.37 | 1.11 | A | 3.91 | 1.00 | A | 2.10 | 1.09 | A | 2.38 | 1.00 | A | 2.57 | 1.00 | A |
| 2 | Terallethrin | 5.32 | 1.16 | B | 3.22 | 1.00 | B | 7.48 | 1.18 | B | 3.21 | 1.02 | B | 5.57 | 1.08 | A | 2.76 | 1.03 | A | 4.66 | 1.05 | A | 6.99 | 1.00 | A |
| 3 | Allethrolone | 12.21 | 1.05 | C | 11.86 | 1.10 | C | 11.13 | 1.08 | C | 10.71 | 1.12 | C | 9.99 | 1.00 | C | 8.17 | 1.08 | C | 12.07 | 1.03 | C | 6.25 | 1.00 | C |
| 4 | Propargyllone | 15.69 | 1.04 | C | 17.19 | 1.09 | C | 14.06 | 1.06 | C | 16.78 | 1.10 | C | 17.15 | 1.00 | C | 13.46 | 1.07 | C | 21.55 | 1.04 | C | 11.09 | 1.00 | C |
| 5 | Pantolactone | 4.38 | 1.04 | D | 4.32 | 1.10 | D | 4.61 | 1.00 | D | 3.72 | 1.06 | D | 7.26 | 1.07 | C | 5.47 | 1.08 | C | 3.47 | 1.08 | C | 4.40 | 1.03 | C |
| 6 | $\alpha$-Cyano-3-phenoxybenzyl alcohol | 4.80 | 1.00 | E | 4.46 | 1.08 | E | 3.89 | 1.00 | E | 3.66 | 1.09 | E | 12.93 | 1.08 | E | 11.22 | 1.05 | E | 4.61 | 1.03 | E | 4.38 | 1.03 | E |
| 7 | Diniconazole | 3.99 | 1.22 | C | 3.32 | 1.27 | C | 2.99 | 1.32 | C | 2.53 | 1.36 | C | 3.42 | 1.00 | C | 2.99 | 1.02 | C | 4.48 | 1.05 | C | 2.70 | 1.00 | C |
| 8 | Uniconazole | 5.45 | 1.15 | C | 5.04 | 1.18 | C | 4.28 | 1.21 | C | 3.46 | 1.29 | C | 4.46 | 1.00 | C | 3.54 | 1.00 | C | 5.83 | 1.07 | C | 3.39 | 1.02 | C |
| 9 | 1-Phenylethylamine | 7.19 | 1.05 | F | 8.77 | 1.07 | F | 5.63 | 1.04 | F | 10.53 | 1.08 | F | 22.10 | 1.00 | F | 11.51 | 1.00 | F | 12.55 | 1.00 | F | 10.31 | 1.06 | F |
| 10 | 1-($\alpha$-Naphthyl)ethylamine | 7.97 | 1.04 | F | 8.61 | 1.08 | F | 8.32 | 1.03 | F | 9.08 | 1.16 | F | 24.77 | 1.03 | F | 12.93 | 1.04 | F | 13.15 | 1.08 | F | 12.03 | 1.00 | F |
| 11 | 1-Phenyl-2-($p$-tolyl)ethylamine | 5.13 | 1.00 | F | 5.47 | 1.06 | F | 4.89 | 1.04 | F | 5.63 | 1.09 | F | 15.21 | 1.09 | F | 7.77 | 1.09 | F | 10.78 | 1.09 | F | 9.39 | 1.00 | F |
| 12 | Tolperisone | 6.72 | 1.15 | F | 6.14 | 1.33 | F | 5.00 | 1.15 | F | 2.96 | 1.36 | F | 4.78 | 1.22 | F | 6.07 | 2.10 | F | 19.34 | 1.00 | F | 10.22 | 1.44 | F |
| 13 | Ketamine | 1.84 | 1.00 | G | 2.07 | 1.00 | G | 2.02 | 1.00 | G | 1.68 | 1.00 | G | 5.21 | 1.03 | G | 3.10 | 1.05 | G | 13.11 | 1.00 | G | 7.78 | 1.12 | G |
| 14 | Chlorpheniramine | 5.71 | 1.00 | H | 6.58 | 1.21 | H | 6.09 | 1.03 | H | 3.26 | 1.16 | H | 5.44 | 1.11 | H | 13.55 | 1.37 | H | 20.59 | 1.19 | H | 10.37 | 1.05 | H |
| 15 | Piperoxane | 1.50 | 1.07 | I | 2.30 | 1.11 | I | 1.75 | 1.06 | I | 1.26 | 1.00 | I | 4.80 | 1.22 | I | 2.13 | 1.07 | I | 6.72 | 1.33 | I | 6.70 | 1.00 | I |
| 16 | Propranolol | 9.50 | 1.00 | J | 9.90 | 1.08 | J | 8.09 | 1.00 | J | 9.41 | 1.10 | J | 7.71 | 1.00 | J | 11.81 | 1.00 | J | 14.83 | 1.00 | J | 10.54 | 1.13 | J |
| 17 | Oxprenolol | 5.54 | 1.00 | J | 6.04 | 1.07 | J | 5.17 | 1.00 | J | 4.97 | 1.06 | J | 5.51 | 1.00 | J | 6.41 | 1.05 | J | 10.44 | 1.00 | J | 6.25 | 1.06 | J |
| 18 | Isoproterenol | 7.97 | 1.03 | K | 5.54 | 1.09 | K | 5.59 | 1.09 | K | 6.41 | 1.10 | K | 8.84 | 1.00 | K | 12.38 | 1.03 | K | 7.15 | 1.00 | K | 8.53 | 1.17 | K |
| 19 | Salbutamol | 8.89 | 1.05 | K | 5.91 | 1.09 | K | 7.02 | 1.13 | K | 4.99 | 1.17 | K | 5.89 | 1.00 | K | 7.82 | 1.00 | K | 5.11 | 1.08 | K | 5.41 | 1.33 | K |
| 20 | Hexobarbital | 4.58 | 1.00 | L | 5.13 | 1.00 | L | 5.76 | 1.00 | L | 5.56 | 1.07 | L | 6.12 | 1.00 | L | 6.24 | 1.00 | L | 6.94 | 1.08 | L | 6.37 | 1.03 | L |
| 21 | Nicardipine | 4.51 | 1.03 | I | 4.52 | 1.00 | I | 6.76 | 1.03 | I | 3.69 | 1.00 | I | 5.67 | 1.00 | I | 8.20 | 1.06 | I | 11.03 | 1.00 | I | 9.87 | 1.00 | I |
| 22 | 2-Phenoxypropionic acid | 4.17 | 1.03 | L | 4.08 | 1.00 | L | 4.45 | 1.03 | L | 4.34 | 1.03 | L | 5.57 | 1.11 | L | 5.43 | 1.05 | L | 4.58 | 1.04 | L | 3.56 | 1.09 | M |
| 23 | Pyroglutamic acid | 6.44 | 1.07 | M | 6.91 | 1.07 | M | 6.95 | 1.08 | M | 7.04 | 1.11 | M | 8.84 | 1.09 | M | 9.46 | 1.07 | M | 8.77 | 1.00 | M | 8.45 | 1.06 | M |
| 24 | Mandelic acid | 7.32 | 1.03 | N | 7.75 | 1.03 | N | 5.80 | 1.04 | N | 4.76 | 1.04 | N | 7.82 | 1.05 | N | 10.17 | 1.06 | N | 6.59 | 1.03 | N | 7.57 | 1.04 | N |
| 25 | Tryptophan | 8.00 | 1.00 | O | 5.99 | 1.09 | O | 6.77 | 1.00 | O | 5.04 | 1.08 | O | 16.62 | 1.07 | O | 11.15 | 1.06 | O | 6.94 | 1.21 | O | 6.90 | 1.00 | O |
| 26 | Phenylalanine | 4.78 | 1.00 | O | 3.62 | 1.03 | O | 4.05 | 1.00 | O | 3.24 | 1.00 | O | 5.41 | 1.00 | O | 3.80 | 1.06 | O | 3.19 | 1.34 | O | 3.41 | 1.00 | O |
| 27 | 1,1'-Bi-2-naphthol | 1.84 | 1.34 | D | 1.87 | 1.22 | D | 1.96 | 1.35 | D | 1.90 | 1.27 | D | 12.90 | 1.10 | D | 11.16 | 1.14 | D | 2.70 | 1.10 | D | 2.63 | 1.00 | D |
| 28 | 1,1'-Binaphthyl-2,2'-diyl hydrogenphosphate | 3.70 | 1.14 | P | 4.01 | 1.13 | P | 5.04 | 1.07 | P | 3.06 | 1.21 | P | 4.22 | 1.03 | P | 1.85 | 1.00 | P | 5.08 | 1.05 | P | 6.72 | 1.09 | P |
| 29 | O-Ethyl-O-2,4-dichlorophenyl-N-isopropylphosphoramidothioate | 0.50 | 1.00 | B | 0.56 | 1.14 | B | 0.74 | 1.00 | B | 1.14 | 1.24 | B | 0.86 | 1.00 | B | 1.05 | 1.00 | B | 1.35 | 1.00 | B | 0.96 | 1.00 | B |

The separation factor of the enantiomers, $\alpha$, is the ratio of their capacity factors; $k'_1$ is the capacity factor of the initially eluted enantiomer. Mobile phase (M): A = *n*-hexane–1,2-dichloroethane–ethanol (500:10:0.05); B = *n*-hexane–1,2-dichloroethane–ethanol (500:30:0.15); C = *n*-hexane–1,2-dichloroethane–ethanol (100:20:1); D = *n*-hexane–1,2-dichloroethane–ethanol (50:10:1); E = *n*-hexane–1,2-dichloroethane–ethanol–acetic acid (500:150:5:0.6); F = *n*-hexane–ethanol–trifluoroacetic acid (240:10:1); G = *n*-hexane–ethanol–trifluoroacetic acid (200:40:0.6); H = *n*-hexane–1,2-dichloroethane–methanol–trifluoroacetic acid (250:140:10:1); I = *n*-hexane–1,2-dichloroethane–ethanol–trifluoroacetic acid (240:140:20:1); J = *n*-hexane–1,2-dichloroethane–ethanol–trifluoroacetic acid (250:140:10:1); K = *n*-hexane–1,2-dichloroethane–methanol–trifluoroacetic acid (240:140:20:1); L = *n*-hexane–ethanol–trifluoroacetic acid (500:5:0.6); M = *n*-hexane–ethanol–trifluoroacetic acid (90:10:0.2); N = *n*-hexane–1,2-dichloroethane–ethanol–trifluoroacetic acid (400:90:10:1); O = *n*-hexane–1,2-dichloroethane–methanol–trifluoroacetic acid (50:45:5:0.2), P = 0.03 *M* ammonium acetate in methanol. A flow-rate of 1.0 ml/min was used for the 250 × 4.6 mm I.D. column at room temperature.

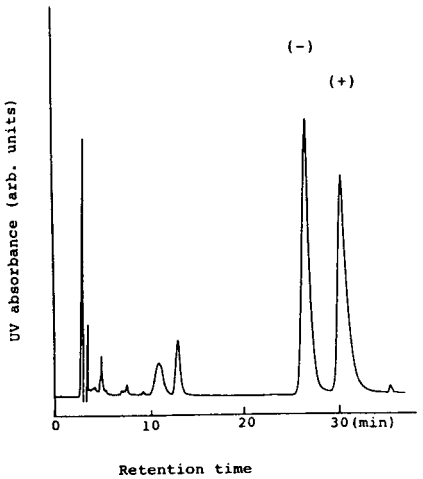


Fig. 3. Enantiomer separation of racemic 1-(α-naphthyl)-ethylamine on CSP 6. Chromatographic conditions as in Table 1.

4. Judging from the separation factors obtained on CSPs 6 and 2, the steric effect of the *tert.*-butyl group may be weak.

Racemic fenpropathrin (**1**) and terallethrin (**2**) were resolved on CSPs 5 and 1 but poorly or not resolved on CSPs 6 and 2. In contrast, racemic propranolol (**16**) and oxprenolol (**17**) were resolved on CSPs 6 and 2, but not at all on CSPs 5 and 1. Although CSPs 5 and 6 contain (*S*)-*tert.*-leucine and CSPs 1 and 2 contain (*S*)-valine, the configuration of the 1-(α-naphthyl)ethylamine moiety is reversed between CSPs 5 and 6 and between CSPs 1 and 2. The results clearly show that the combination of the configuration of two chiral centres in these urea derivatives may play an important role in chiral recognition [7].

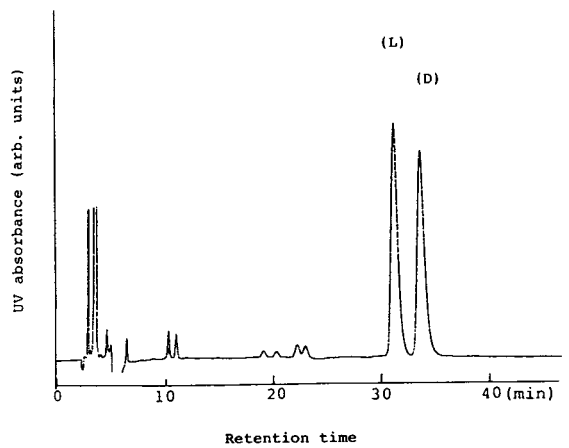


Fig. 4. Enantiomer separation of racemic pyroglutamic acid on CSP 6. Chromatographic conditions as in Table 1.

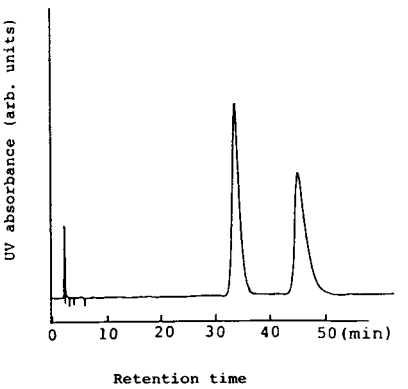


Fig. 5. Enantiomer separation of racemic chlorpheniramine on CSP 8. Chromatographic conditions as in Table 1.

A number of racemic amines, amino alcohols, carboxylic acids, amino acids and miscellaneous compounds of pharmaceutical interest were resolved specifically into their antipodes on CSPs 7, 8, 9 and 10 using normal mobile phases containing a small amount of trifluoroacetic acid. Typical examples are shown in Figs. 5–7. It should be emphasized that the enantioselectivities of CSPs 9 and 10 were different. Enantiomers of **10**, **11** and **15** were resolved on CSP 9

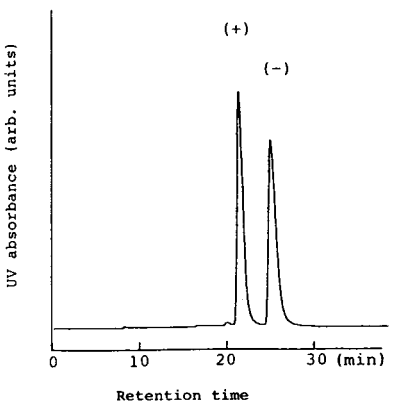


Fig. 6. Enantiomer separation of racemic isoproterenol on CSP 10. Chromatographic conditions as in Table 1.

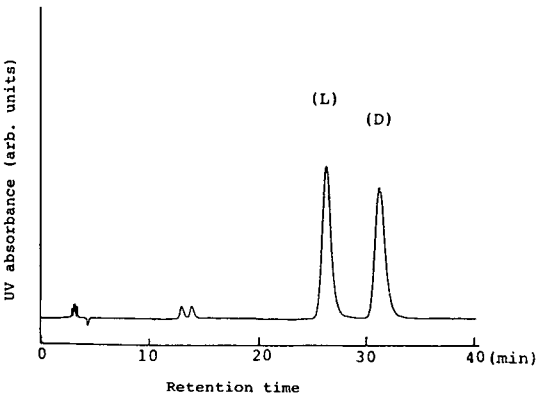


Fig. 7. Enantiomer separation of racemic tryptophan on CSP 9. Chromatographic conditions as in Table 1.

but not at all on CSP 10. In contrast, **12**, **13**, **16** and **18** enantiomers were resolved on CSP 10, but not at all on CSP 9. These results again showed that chiral recognition was controlled by the combination of configurations of the two chiral centres in the amino acid and amine moieties of these urea derivatives.

Amino acid enantiomers **25** and **26** were directly resolved on CSP 9 using normal mobile phases. Usually the direct separation of racemic amino acids can be accomplished with copper(II) complexes of chiral ligands as CSPs using aqueous mobile phases [8,9], and they are resolved in the form of derivatives such as N-acyl O-esters on brush-type CSPs using normal mobile phases [3,4].

The specific separation of various racemic compounds on these CSPs showed that the enantioselectivity of urea derivatives may depend on the structure of the amino acid moiety. However, the detailed effect of structure on chiral recognition is still unclear, and additional work is in progress.

The durability of columns packed with these CSPs was excellent; more than 300 analyses of some racemic compounds did not cause any change in their retention parameters, enantioselectivity or efficiency using the normal mobile phases described in Table 1.

## 4. Conclusions

Urea derivatives derived from (*S*)- or (*R*)-1-(α-naphthyl)ethylamine with (*S*)-valine, (*S*)-*tert.*-leucine, (*S*)-proline and (*S*)-indoline-2-carboxylic acid bonded to 3-aminopropylsilica gel are very promising as CSPs for the specific separation of various racemic compounds by HPLC. It is emphasized that the stereochemical structure of these CSPs may play an important role in the formation of interactions for chiral recognition.

## Acknowledgement

The authors thank Sumitomo Chemical for the gift of some chemicals used in this work.

## References

[1] A.M. Krstulovic (Editor), *Chiral Separations by HPLC*, Ellis Horwood, Chichester, 1989.
[2] S. Ahuja (Editor), *Chiral Separations by Liquid Chromatography* (*ACS Symposium Series*, No. 471), American Chemical Society, Washington, DC, 1991.
[3] W.H. Pirkle, D.W. House and J.M. Finn, *J. Chromatogr.*, 192 (1980) 143.
[4] N. Ôi and H. Kitahara, *J. Liq. Chromatogr.*, 9 (1986) 511.
[5] N. Ôi, H. Kitahara and R. Ôsumi, *J. Chem. Soc. Jpn.*, (1986) 997.
[6] N. Ôi, H. Kitahara and R. Kira, *J. Chromatogr.*, 515 (1990) 441.
[7] N. Ôi, H. Kitahara and R. Kira, *J. Chromatogr.*, 535 (1990) 213.
[8] N. Ôi, H. Kitahara and R. Kira, *J. Chromatogr.*, 592 (1992) 291.
[9] N. Ôi, H. Kitahara and F. Aoki, *J. Liq. Chromatogr.*, 16 (1993) 893.

ELSEVIER

Journal of Chromatography A, 694 (1995) 135–150

JOURNAL OF CHROMATOGRAPHY A

# Comparison of (*S*)-N-(3,5-dinitrobenzoyl)tyrosine derivatives as chiral selectors for high-performance liquid chromatographic enantioseparations

E. Veigl, B. Böhs, A. Mandl, D. Krametter, W. Lindner*

*Institute of Pharmaceutical Chemistry, Karl-Franzens-University of Graz, A-8010 Graz, Austria*

**Abstract**

The synthesis of a new chiral stationary phase (CSP), based on immobilized (*S*)-N-(3,5-dinitrobenzoyl)tyrosine methyl-ester, is described and its chromatographic behaviour and enantioselectivity are compared with those of a well known dinitrobenzoyltyrosine-derived stationary phase. In addition, a new "end-capping" procedure for the CSP to reduce polar but non-stereoselective selectand–selector interactions was developed and evaluated by analyzing a broad range of chiral compounds [e.g., ibuprofen-1-naphthylamide, benzoic acid 1-phenylethylamide, 1-(1-naphthyl)ethylphenylurea, sulfoxides, propranolol oxazolidin-2-one].

## 1. Introduction

Chiral stationary phases (CSPs) based on N-(3,5-dinitrobenzoyl)amino acids as chiral selectors (SOs) are widely used for the enantioseparation of compounds of pharmaceutical and biological interest (selectands, SAs). The (*S*)-N-(3,5-dinitrobenzoyl)phenylglycine phase, introduced 1980 by Pirkle and co-workers [1–3], is a resolving phase with a relatively broad range of applicability and the underlying chiral recognition mechanisms are based on hydrogen bonding and/or dipole–dipole stacking paired with charge-transfer ($\pi$–$\pi$), steric and hydrophobic interactions. Convincing SO-SA models have been drawn for certain groups of analytes [4]. Because of the broad applicability of this type of CSP, several groups have been searching for new $\pi$-acid-type CSPs owning to their different chromatographic behaviour (e.g., [5–11]). Thus many 3,5-dinitrobenzoylated (DNB) amino acid derivatives (SOs) were synthesized in the course of developing new CSPs; however, those based on DNB-tyrosine seem to have some special features [12]. There are two possibilities of immobilizing DNB-Tyr on silica gel. The first is a similar method to the usual way of binding DNB-phenylglycine (and DNB-Leu or DNB-Val, etc.) via its carboxyl function (either ionically or covalently to an amino group), but an alternative approach is via an alkyl linkage to the phenolic hydroxyl group (see Fig. 1). Tambuté et al. [13] synthesized several tyrosine-derived CSPs containing different residues including $\pi$-acids and $\pi$-bases on either the carboxyl or the amino function. Generally, all of these CSPs were immobilized via an allyl ether group obtainable by alkylation of the phenolic hydroxyl group of tyrosine followed by a radical addition reaction

* Corresponding author.

0021-9673/95/$09.50 
*SSDI* 0021-9673(94)00792-6

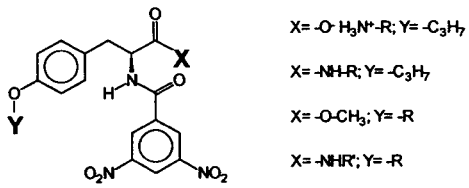


Fig. 1. DNB-Tyr derivatives as chiral selectors. The different possibilities of immobilizing DNB-Tyr on silica gel are indicated via the corresponding X and Y residues, whereas R represents various kinds of linkers between the chiral SO and the silica gel surface.

on to 3-mercaptopropylsilica gel (see CSP-Ia and CSP-Ib in Fig. 2).

In this paper we describe an alternative approach to binding DNB-Tyr covalently to silica gel, namely the formation of an allylurethane of DNB-Tyr-OMe, which was subsequently radically immobilized on 3-mercaptopropylsilica gel, resulting CSP-II (see Fig. 2). As observed by Siret et al. [14], the replacement of the methyl ester group of DNB-Tyr-OMe by a primary or secondary amide group (compare CSP-Ia and CSP-Ib in Fig. 2) causes a substantial change in the steroselectivity of the new CSPs. However, by changing the immobilization strategy of DNB-Tyr-OMe by introducing a carbamoyl group instead of an ether group (compare CSP-Ia and CSP-II), one also ends up with two amido functions but maybe less favourably positioned with respect to chiral recognition via hydrogen bonding bridges.

In order to reduce the (re)activity of the remaining mercapto groups of the starting mercaptopropylsilica material, it was "end-capped" with 1-hexene, thus reducing polar but non-stereoselective interactions of the mercapto groups and also of the silanols of the silica gel. The resulting CSP is referred to as "end-capped" CSP-IaE (see Fig. 3). The aim of this study was to compare the effects of these small structural changes to the chiral selectors on the overall

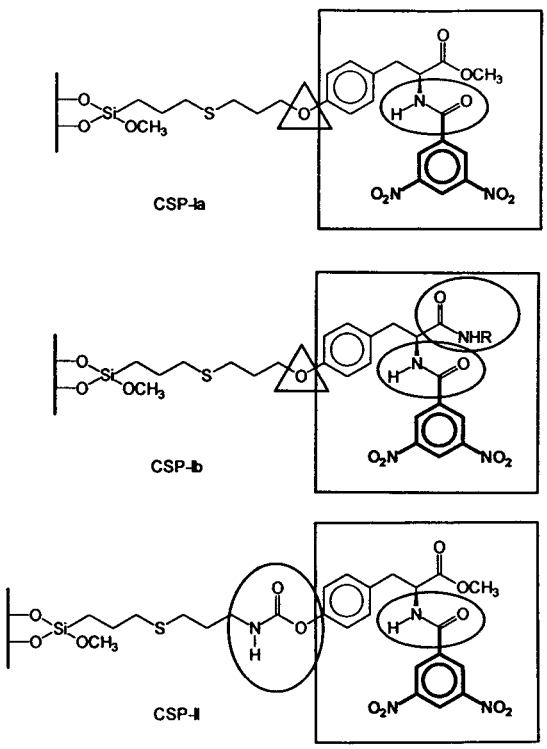


Fig. 2. Structures of CSP-Ia, CSP-Ib and CSP-II. The representation should assist the visualization of structural elements (e.g., $\pi$-acid, hydrogen donor acceptor, stereogenic centre) responsible for intermolecular interactions with suitable guest molecules. Square = identical chiral selectors; ellipse = secondary amide; triangle = ether bridge; R may contain an additional stereogenic centre and a $\pi$-basic group (see also [12]).

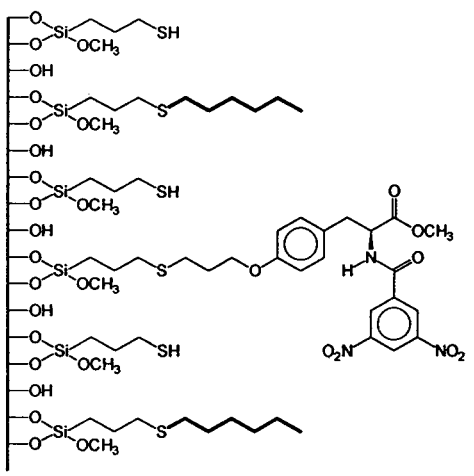

Fig. 3. Structure of CSP-IaE in the non-solvated status; the randomly selected surface structure is presented in relation to the calculated coverage of the "chiral stationary phase" to imagine the complex structure and interaction possibilities with diverse guest solutes. About 25% of the mercapto groups were reacted with the chiral SO and about 30% were alkylated with 1-hexene.

chromatographic behaviour and subsequently to draw some conclusions on chiral recognition mechanisms.

## 2. Experimental

### 2.1. Apparatus

Liquid chromatography was performed with a modular liquid chromatograph (Merck–Hitachi, Darmstadt, Germany), equipped with a Model L-6200 intelligent pump, a Model AS-2000A autosampler with a 100-$\mu$l loop, a Model L-4250 UV–Vis detector, controlled via a Model D-6000 chromatography data station software, HPLC Manager Vers. 2.09. Temperature was controlled with a column thermostat (B.O. Electronics, Austria). Standard operating conditions were detection at 254 nm and a column temperature of 20°C. A guard column (LiChroCART 4-4, LiChrosorb Si 60, 5 $\mu$M; Merck, Darmstadt, Germany) was used throughout.

### 2.2. Chemicals

(*S*)-Tyrosine methyl ester hydrochloride was obtained from Bachem (Switzerland) and 3,5-dinitrobenzoyl chloride, propene oxide, dibutyltin (IV) acid dilaurate, azobisisobutyronitrile (AIBN) and allyl isocyanate from Aldrich (Germany). Other solvents and reagents were of analytical-reagent grade from Merck.

3-Mercaptopropylsilicagel for CSP-Ia and CSP-IaE was prepared from Kromasil-100-A spherical silica (5 $\mu$m) (EKA Nobel, Nobel Industries, Sweden) and 3-mercaptopropyltrimethoxysilane (Aldrich) in the same manner. Elemental analysis indicated 788 $\mu$mol of bonded 3-mercaptopropyl residues per gram of modified silica gel (based on C analysis; found, 4.73% C).

3-Mercaptopropylsilicagel for CSP-II was prepared from LiChrosorb Si-100 (5 $\mu$m) using 3-mercaptopropyltrimethoxysilane (Aldrich) as described previously [15]. Elemental analysis indicated 784 $\mu$mol of bonded 3-mercaptopropyl residues per gram of modified silica gel (based on C analysis: found, 4.83% C; starting material 0.12% C, a value which should be zero according to the materials specification).

The specific surface areas of the two starting silica gels were 360 and 380 $m^2$ according to the provided information by the suppliers.

Mobile phases were prepared from *n*-heptane of HPLC grade and 2-propanol and diethylamine of analytical-reagent grade from Merck.

The racemic and optically pure test compounds were available from previous studies.

### 2.3. Chiral stationary phases

*CSP-Ia*

The starting material [(S)-N-(3,5-dinitrobenzoyl)tyrosine-O-(2-propen-1-yl)methylester] was kindly provided by A. Tambuté (Centre d'Études du Bouchet, Vert-le-Petit, France). CSP-Ia was prepared by refluxing 6 g of 3-mercaptopropylsilica gel with 3.15 mmol (1.35 g) of CS-Ia and 100 mg of AIBN in 200 ml of azeotropically dried chloroform for 40 h. The modified silica gel was successively washed with chloroform, methanol, acetonitrile, methanol and diethyl ether and air dried at 40°C. After sieving (25 $\mu$m), 6.2 g of modified silica gel were obtained. Elemental analysis afforded C 9.40, H 1.54, N 0.81%. The calculated coverage was 192 $\mu$mol of chiral selector bonded per gram (based on N analysis) and 194 $\mu$mol of chiral selector per gram (based on C analysis), respectively.

The final CSP-Ia material was packed into a 150 × 4.0 mm I.D. stainless-steel column using $CHCl_3$–MeOH (9:1) as slurry and heptane as packing solvent.

*CSP-IaE*

CSP-Ia (4 g), 20 mmol (1.96 g) of 1-hexene and 0.66 g of AIBN were refluxed in azeotropically dried chloroform for 35 h. The modified silica was washed with chloroform, methanol, diethyl ether and light petroleum and dried in air at 40°C. After sieving (25 $\mu$m), 3.2 g of slightly yellow silica gel were obtained. Elemental analysis afforded C 11.17, H 1.80, N 0.93%. An additional coverage of 246 $\mu$mol of hexyl groups per gram (based on C analysis) was calculated.

The microanalytical data for CSP-Ia and CSP-IaE show differences in C, H and surprisingly

also in N values. The unexpected higher content of nitrogen may be due to the usual deviations of C, N analysis of modified silica gels or may be caused by remaining residues from AIBN and/or its degradation products; therefore, the calculated additional coverage with hexyl residues is an approximate value and the effectiveness of the "end-capping" procedure should preferably be evaluated from chromatographic results.

The final CSP-IaE material was slurry packed in the same manner as CSP-Ia into a 150 × 4.0 mm I.D. stainless-steel column.

*CSP-II*

The preparation of CSP-II is outlined and briefly described in Fig. 4.

Elemental analysis of CSP-II afforded C 10.28, H 1.58, N 1.42%. A coverage of 253 μmol of chiral selector bonded per gram (based on N analysis) and 216 μmol of chiral selector per gram (based on C analysis), respectively, was calculated (note again the difference depending whether the C or the N analysis data are taken as a basis).

The final CSP-II material was slurry packed in the same manner as CSP-Ia into a 250 × 4.6 mm I.D. stainless-steel column.

## 3. Results and discussion

As mentioned above, small structural changes in a chiral selector may have a pronounced influence on the overall enantioselectivity of so-called "Pirkle-type" CSPs, in particular when the position of the amido function is shifted within an SO molecule. To focus on such phenomena, two slightly different CSPs based on differently immobilized L-Tyr-OMe (see CSP-Ia and CSP-II) were compared.

Futhermore, we investigated the effect of "end-capping" (comparison of CSP-Ia and CSP-IaE; see also Figs. 2 and 3) on the overall chromatographic behaviour of two CSPs based on identical chiral SO molecules. When evaluating chromatographic results one must bear in mind that the observed retention and resolution data are due to the sum of stereoselective and non-stereoselective interactions of the solutes with the chiral selector (SO) moiety and the additional anchor and spacer groups and/or surface-modifying molecule increments, as was discussed by Däppen *et al.* [16] and Pirkle and Readnour [17]. This touches to some extent on the question of the input of "end-capping" on non-stereoselective retention characteristics.

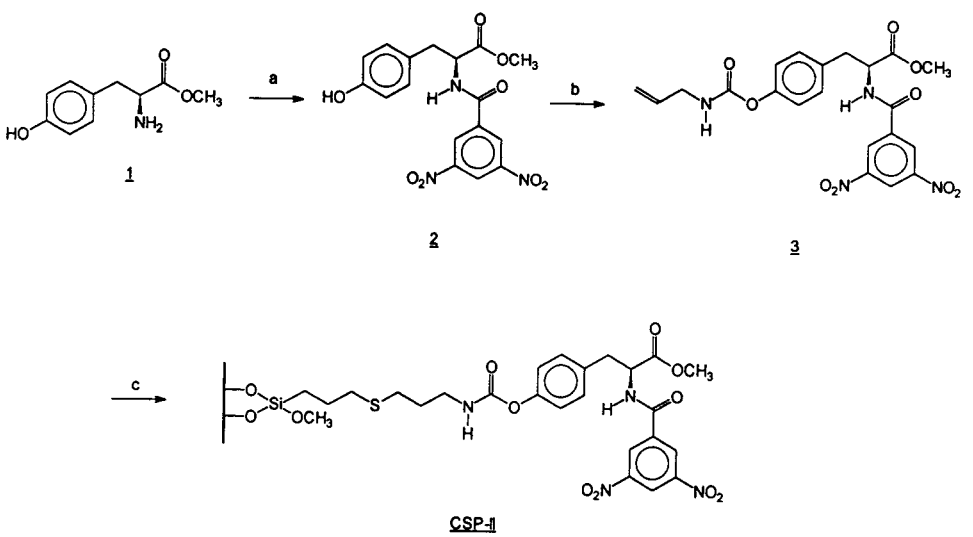


Fig. 4. Reaction scheme for preparing CSP-II. (a) 3,5-Dinitrobenzoyl chloride (1.1 equiv.), propene oxide (6 equiv.), dioxane, 2.5 h at 40°C. (b) Allyl isocyanate (1.1 equiv.), dibutyltin (IV) acid dilaurate (catalytic amount), dioxane, 2 h reflux. (c) 1.5 g of **3**, 2 g of 3-mercaptopropylsilica gel, 100 mg of AIBN, $CHCl_3$, 40 h reflux.

As can be seen in Fig. 2 (compare CSP-Ia and CSP-II), the structure of the chiral SO molecules is similar in many respects (as indicated by the square), but with one exception. For CSP-Ia the derivatized (*S*)-Tyr-OMe is immobilized on silica gel via an ether bond (indicated by a triangle in Fig. 2), whereas in CSP-II this ether bond is replaced by a carbamate bridge (ellipse in Fig. 2). In terms of possible intermolecular SO–SA interactions, the inert ether group (triangle in Fig. 2) has been replaced by a polar and hydrogen bonding amide group (or carbamoyl function) (ellipse in Fig. 2). As a consequence, the two CSPs may have different enantioselectivities. Despite the variation of the selector molecule and the locating of a binding group far away from the stereogenic centre, the observed overall enantioselectivity of a CSP is a result of all interactions of the chiral solutes with the chiral selector, both stereoselective and non-stereoselective; by varying only one intermolecular binding element we thought we could recognize some specific stereoselective SO–SA interaction domains by synthesizing CSP-Ia, CSP-IaE and CSP-II.

CSP-Ia is known to resolve a broad range of analytes [12], e.g., DNB-amino acids (derivatized to esters or amides), alkyl N-arylsulfinamoyl esters, phosphine oxides, ibuprofen derivatives and lactams. For this study, we selected a representative collection of chiral acids, amines, alcohols (derivatized to amides, ureas and carbamates, respectively) as analytes; they had already been used in previous studies with (*S*,*S*)diphenylethylethanediamine derivatives as chiral model compounds [5,6,18]. The chromatographic results obtained with CSP-Ia, CSP-IaE and CSP-II are summarized in Tables 1–3 and are discussed below.

### 3.1. Using equal mobile phase conditions

First we compared the behaviours of CSP-Ia, CSP-IaE and CSP-II using identical mobile phase conditions in order to elucidate increments responsible for non-stereoselective and stereoselective retention characteristics. As can be clearly seen, the enantioselectivities were, with exceptions, relatively similar, although the absolute retention varied and in particular was lower for the "end-capped" CSP-IaE. For simply structured analytes such as amides or ureas, the 3,5-dinitrobenzamide function seems to be the most important binding domain and the additional amido (carbamoyl) group of CSP-II has little influence on the total enantioselectivity, whereas for more complex analytes such as oxazepam and indapamide this carbamate group seems to take part. The additional amido group of CSP-II, being fairly distant from the stereogenic centre, seems to compete for binding sites of the analytes. Oxazepam and indapamide were resolvable to a small extent on CSP-Ia, whereas CSP-II showed no enantioselectivity, despite the fact that both drugs show higher retention times on CSP-II than on CSP-Ia.

Interestingly, the ibuprofen naphthylamide and anilide enantiomers were resolvable on both CSPs Ia and II, but ibuprofen naphthylmethylamide was only resolved on CSP-Ia. Changing the naphthyl or phenyl group to the more flexible naphthlymethyl, group which should be accompanied by a lower steric hindrance of the chiral solutes, resulted in a general diminishment of chiral recognition on CSP-II. In contrast, there were also solutes resolvable on CSP-II and not on CSP-Ia, namely 2-phenylpropionic acid anilide and 2-naphthoic acid 1-phenylethylamide.

Another interesting phenomenon is the opposite elution order of chiral acids as amides (*S* before *R*) and chiral amines as amides (*R* before *S*). Changing the chiral centre from the carboxyl to the amine function caused a reversal of the elution order, indicating a chiral recognition mechanism based on a combination of charge-transfer interaction, hydrogen bonding and dipole–dipole stacking.

For 1-phenylethylamine and 1-(1-naphthyl) ethylamine (derivatized to the corresponding amides with 1-naphthoic acid), an unusual retention behaviour was observed. The former optical antipodes showed higher retention on CSP-Ia, whereas the latter enantiomers were more strongly retained on CSP-II. Similar differences were observed for the $\beta$-blocking agents

Table 1
Enantioseparation of representative analytes on CSP-Ia, CSP-IaE and CSP-II

| Compound | Derivatizing reagent | CSP-Ia | | | CSP-IaE | | | CSP-II | | |
|---|---|---|---|---|---|---|---|---|---|---|
| | | $k_1'$ [a] | $\alpha$ [b] | $R_s$ [c] | $k_1'$ | $\alpha$ | $R_s$ | $k_1'$ | $\alpha$ | $R_s$ |
| Acids as amides | | | | | | | | | | |
| 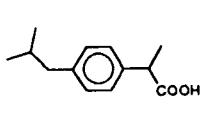 | 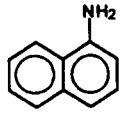 | 3.16 | 1.15 | 1.66 | 1.96 | 1.17 | 1.53 | 2.87 (*S*) | 1.15 | 2.24 |
| | 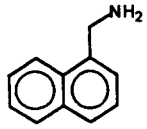 | 2.63 | 1.04 | <0.7 | 1.70 | 1.00 | – | 2.68 | 1.00 | – |
| | 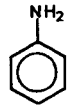 | 0.62 | 1.15 | <0.7 | 0.42 | 1.14 | <0.7 | 0.85 (*S*) | 1.11 | 0.97 |
| | 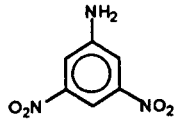 | 0.99 | 1.00 | – | 0.79 | 1.00 | – | 1.16 | 1.00 | – |
| 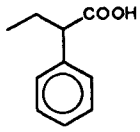 | 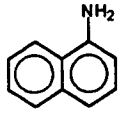 | 3.70 | 1.11 | 0.73 | 2.49 | 1.09 | 0.75 | 3.75 | 1.07 | <0.7 |
| | 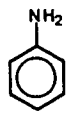 | 0.87 | 1.00 | – | 0.61 | 1.00 | – | 1.09 | 1.00 | – |
| 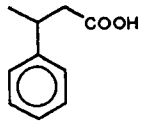 | 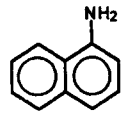 | 3.82 | 1.00 | – | 2.47 | 1.00 | – | 3.94 | 1.00 | – |

| | | | | | | | | | | |
|---|---|---|---|---|---|---|---|---|---|---|
| | 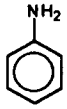 | 0.78 | 1.10 | <0.7 | 0.62 | 1.02 | <0.7 | 1.02 | 1.07 | <0.7 |
| 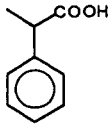 | 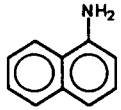 | 4.51 | 1.09 | 1.08 | 2.95 | 1.12 | 1.11 | 4.52 (*S*) | 1.08 | 1.15 |
| | 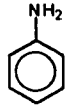 | 0.98 | 1.00 | – | 0.76 | 1.01 | <0.7 | 1.19 (*S*) | 1.05 | 0.49 |
| Amines as amides | | | | | | | | | | |
| 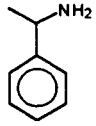 | 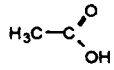 | 0.83 (*R*) | 1.21 | 1.09 | 0.50 | 1.28 | 0.83 | 1.05 (*R*) | 1.12 | 1.05 |
| | 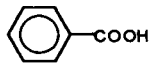 | 1.62 (*R*) | 1.14 | 1.23 | 1.13 | 1.16 | 1.15 | 1.89 (*R*) | 1.12 | 1.38 |
| | 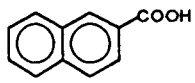 | 6.75 | 1.00 | – | 4.34 | 1.00 | – | 4.14 (*R*) | 1.04 | <0.7 |
| 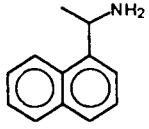 | 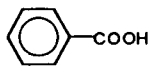 | 4.00 | 1.41 | 4.1 | 2.66 | 1.46 | 4.09 | 4.11 (*R*) | 1.41 | 5.23 |
| | 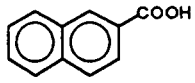 | 9.64 | 1.15 | 2.03 | 6.03 | 1.22 | 2.36 | 14.88 (*R*) | 1.10 | 1.18 |
| Alcohols as carbamates | | | | | | | | | | |
| 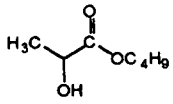 | 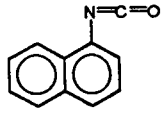 | 1.00 | 1.15 | 0.84 | 0.75 | 1.18 | < 0.7 | 1.23 | 1.08 | <0.7 |

(Continued on p. 142)

Table 1 (*continued*)
Enantioseparation of representative analytes on CSP-Ia, CSP-IaE and CSP-II

| Compound | Derivatizing reagent | CSP-Ia | | | CSP-IaE | | | CSP-II | | |
|---|---|---|---|---|---|---|---|---|---|---|
| | | $k_1'$ [a] | $\alpha$ [b] | $R_s$ [c] | $k_1'$ | $\alpha$ | $R_s$ | $k_1'$ | $\alpha$ | $R_s$ |
| Amines as ureas | | | | | | | | | | |
| 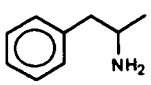 | 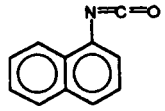 | | | | | | | 3.54 | 1.07 | 0.91 |
| 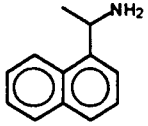 | 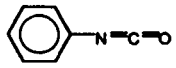 | 3.26 | 1.39 | 3.11 | 2.32 | 1.50 | 2.82 | 2.94 (*R*) | 1.41 | 3.54 |
| | 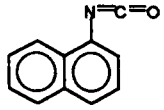 | 9.15 | 1.34 | 3.24 | 6.54 | 1.42 | 3.58 | 9.47 | 1.36 | 3.48 |
| Sulfoxides | | | | | | | | | | |
| 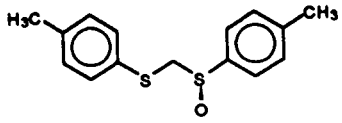 | | 1.46 | 1.07 | <0.7 | 1.01 | 1.09 | <0.7 | 1.56 | 1.06 | <0.7 |
| 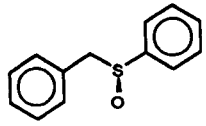 | | 1.37 | 1.00 | – | 0.96 | 1.00 | – | 1.44 | 1.00 | – |
| $\beta$-Blockers as oxazolidin-2-ones | | | | | | | | | | |
| 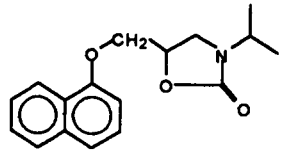 | | 5.79 | 1.12 | 1.52 | 4.29 | 1.12 | 1.07 | 7.61 (*S*) | 1.15 | 1.53 |
| 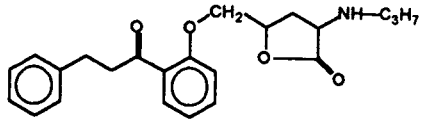 | | 6.01 | 1.00 | – | 4.35 | 1.00 | – | 7.22 | 1.00 | |

| | | | | | | | | | |
|---|---|---|---|---|---|---|---|---|---|
| Miscellaneous<br>Oxazepam<br> 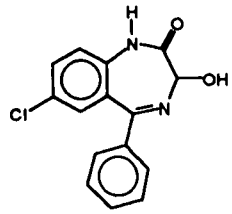 | 2.34 | 1.06 | <0.7 | 1.82 | 1.00 | – | 3.04 | 1.00 | – |
| Indapamid<br> 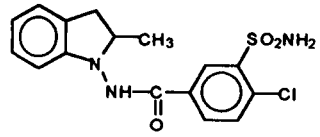 | 5.89 | 1.05 | <0.7 | 4.56 | 1.00 | – | 8.84 | 1.00 | – |
| Benzoin<br> 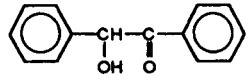 | | | | 0.40 | 1.48 | 1.13 | 1.01 | 1.00 | – |

Mobile phase: *n*-heptane–2-propanol–diethylamine (DEA) (70:30:0.1, v/v/v).

[a] Capacity factor: $k' = (t_r - t_0)/t_0$.

[b] Selectivity: $\alpha = k'_2/k'_1$.

[c] Resolution: $R_s = 1.18\ (t_{r_2} - t_{r_1})/(w_{1/2_1} + w_{1/2_2})$.

Table 2
Enantioseparation of representative analytes on CSP-Ia and CSP-II under isoeluotropic conditions

| Compound | Derivatizing reagent | CSP-Ia | | | | CSP-II | | | |
|---|---|---|---|---|---|---|---|---|---|
| | | $k_1'$ [a] | $k_2'$ | $\alpha$ [b] | $R_s$ [c] | $k_1'$ | $k_2'$ | $\alpha$ | $R_s$ |
| Acids as amides | | | | | | | | | |
| 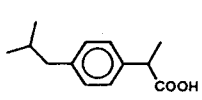 | 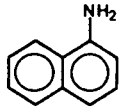 | 3.16 | 3.36 | 1.15 | 1.66 | 2.87 (*S*) | 3.30 | 1.15 | 2.24 |
| 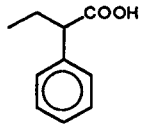 | 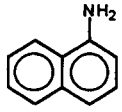 | 3.70 | 4.11 | 1.11 | 0.73 | 3.75 | 4.01 | 1.07 | <0.7 |
| 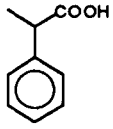 | 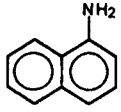 | 4.51 | 4.92 | 1.09 | 1.08 | 4.52 (*S*) | 4.88 | 1.08 | 1.15 |
| Amines as amides | | | | | | | | | |
| 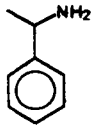 | 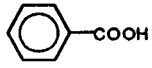 | 1.62 (*R*) | 1.85 | 1.14 | 1.23 | 1.70 (*R*) | 1.86 | 1.09 | 0.95 |
| 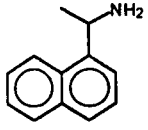 | 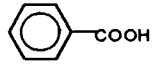 | 4.00 | 5.64 | 1.41 | 4.41 | 4.11 (*R*) | 5.80 | 1.41 | 5.23 |

Alcohols as carbamates

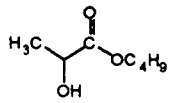

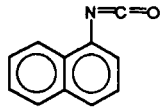

| | | | | | | | |
|---|---|---|---|---|---|---|---|
| 1.00 | 1.15 | 1.15 | 0.84 | 1.05 | 1.13 | 1.08 | <0.7 |

Amines as ureas

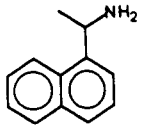

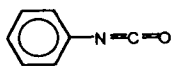

| | | | | | | | |
|---|---|---|---|---|---|---|---|
| 3.26 | 4.53 | 1.39 | 3.11 | 3.32 (*R*) | 4.56 | 1.37 | 2.91 |

$\beta$-Blockers as oxazolidin-2-ones

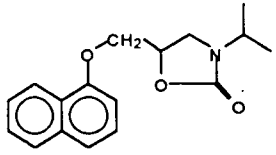

| | | | | | | | |
|---|---|---|---|---|---|---|---|
| 5.79 | 6.49 | 1.12 | 1.52 | 5.88 (*S*) | 6.59 | 1.12 | 1.18 |

Mobile phases: CSP-Ia, *n*-heptane–2-propanol–diethylamine (DEA) (70:30:0.1), v/v/v); CSP-II, *n*-heptane–2-propanol–diethylamine (DEA) (between 65:35:0.1 and 72:28:0.1, v/v/v).

[a–c] See Table 1.

Table 3
Enantioseparation of representative analytes on CSP-Ia and CSP-IaE under isoeluotropic conditions

| Compound | Derivatizing reagent | CSP-Ia | | | | CSP-IaE | | | |
|---|---|---|---|---|---|---|---|---|---|
| | | $k_1'$ [a] | $k_2'$ | $\alpha$ [b] | $R_s$ [c] | $k_1'$ | $k_2'$ | $\alpha$ | $R_s$ |
| Acids as amides | | | | | | | | | |
| 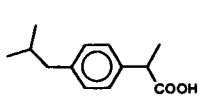 | 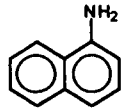 | 3.16 | 3.36 | 1.15 | 1.66 | 2.83 | 3.32 | 1.17 | 2.14 |
| 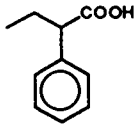 | 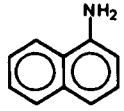 | 3.70 | 4.11 | 1.11 | 0.73 | 3.72 | 4.04 | 1.09 | 1.04 |
| 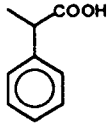 | 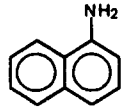 | 4.51 | 4.92 | 1.09 | 1.08 | 4.54 | 5.00 | 1.10 | 1.02 |
| Amines as amides | | | | | | | | | |
| 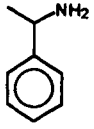 | 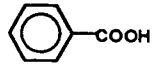 | 1.62 (*R*) | 1.85 | 1.14 | 1.23 | 1.60 | 1.84 | 1.15 | 1.48 |
| 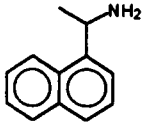 | 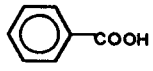 | 4.00 | 5.64 | 1.41 | 4.41 | 3.97 | 5.77 | 1.45 | 5.06 |

Alcohols as carbamates

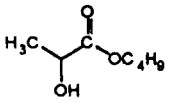

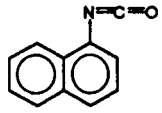

| | | | | | | | |
|---|---|---|---|---|---|---|---|
| 1.00 | 1.15 | 1.15 | 0.84 | 1.04 | 1.18 | 1.14 | 0.90 |

Amines as ureas

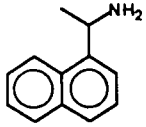

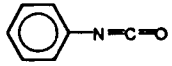

| | | | | | | | |
|---|---|---|---|---|---|---|---|
| 3.26 | 4.53 | 1.39 | 3.11 | 3.01 | 4.44 | 1.47 | 2.15 |

$\beta$-Blockers as oxazolidin-2-ones

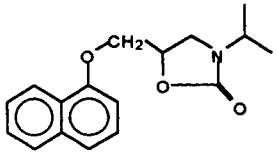

| | | | | | | | |
|---|---|---|---|---|---|---|---|
| 5.79 | 6.49 | 1.12 | 1.52 | 5.94 | 6.65 | 1.12 | 1.50 |

Mobile phases: CSP-Ia, *n*-heptane–2-propanol–diethylamine (DEA) (70:30:0.1, v/v/v); CSP-IaE, *n*-heptane–2-propanol–diethylamine (DEA) (between 78:22:0.1 and 73:27:0.1, v/v/v).

[a–c] See Table 1.

propranolol and propafenone (as their oxazolidinones) and the antihypertonic acting drug indapamide, which were more strongly retained on CSP-II, probably owing to additional interactions with the second amido group of CSP-II.

To obtain further information about the chromatographic properties of CSP-Ia and CSP-II, we focused on the retention behaviour caused by $\pi-\pi$ interactions. In general, and as also observed by others, the naphthyl derivatives were more retained than their phenyl analogues. Within the ibuprofen derivatives both CSPs showed decreasing capacity factors on going from the naphthyl- to 1-naphthylmethylamide and to the anilide, caused by weaker $\pi-\pi$ interactions with the DNB residue of the stationary phase within this series. Interestingly, the 3,5-dinitroanilide, a $\pi$-acid compound, showed higher $k'$ values than the anilide. This behaviour may be explained by interaction of the $\pi$-acid solute with the weak $\pi$-basic phenyl ring of the stationary phases. As was mentioned above, this phenyl ring has different electron densities in CSP-Ia and CSP-II owing to the stronger electron-withdrawing effect of the carbamate function compared with the ether function enhancing the electron density within the aromatic ring.

### *3.2. Using isoeluotropic mobile phase conditions and judging the "end-capping"*

As already pointed out, the capacity factors for many compounds are similar on CSP-Ia and CSP-II, although these two CSPs have a slightly different loadings of the SO on a molecular basis (N values 192 $\mu$mol of SO per gram of CSP-Ia and 253 $\mu$mol of SO per gam of CSP-II, corresponding to C values of 194 and 216 $\mu$mol, respectively). Therefore, the chiral SO of CSP-Ia seems to cause stronger retention of the analytes than the chiral SO of CSP-II. However, retention of analytes may also be caused by interactions with remaining silanol and other polar groups stemming from the silica gel and its degree of premodification. However, stereoselective retention can only be generated by SO–SA interactions, and the question remains of how strong the influence of the SO density on the surface is on the observed enantioselectivity. "End-capping" reduces the polar interaction sites on the CSP and should result in reduced retention under normal-phase conditions. When comparing two CSPs (e.g., CSP-Ia and CSP-IaE), it should be possible to extract the increment responsible only for chiral recognition within the chromatographic process by normalizing the retention of the second eluting peak of resolved pairs of enantiomers by adjusting the mobile phase and measuring the resulting $\alpha$ values.

For such isoeluotropic conditions, the data are summarized in Tables 2 and 3 and we found that the stereoselectivity did not change significantly whether we compare CSP-Ia with CSP-II or CSP-Ia with CSP-IaE. The observed differences in the enantioselectivity of CSP-Ia and CSP-II seems to be mainly due to their different selector molecules and not to their different grafting rates. Hence, the usual arguments that one can only compare CSPs and their stereoselectivities for a set of chiral analytes when the CSPs are based on the same silica or silica gel modification and with the same selector density per square metre of surface area seem doubtful. However, by examining also the resolution values of the resolved pairs, one might obtain additional information on unwanted polar interactions and/or packing characteristics of the columns.

As was indicated previously, an additional "end-capping" procedure was developed and the CSPs were evaluated by comparison of CSP-Ia and CSP-IaE. The remaining mercapto and silanol groups represent polar residues able to influence the overall selectivity of the chromatographic system. About 40% (judged by C analysis data) of the remaining free mercapto groups of CSP-Ia reacted with 1-hexene to give the corresponding 1-hexane thioether (see Fig. 3), resulting in the reduction of polar but non-stereoselective interactions of the solutes with the remaining polar groups, as was described in a previous paper [15]. In general, the capacity factors of almost all analytes were smaller on CSP-IaE than on the comparable CSP-Ia, but at

the same time the $\alpha$ values did not change significantly and the resolution was inconsistently slightly increased or decreased. In the present case, the interaction of the analytes with the chemically modified silica surface to which the chiral selector groups are bound does not play a significant role in the course of chiral recognition.

Concerning the comparison of CSP-Ia and CSP-IaE under isoeluotropic conditions, these stationary phases showed almost identical $\alpha$-values, indicating that the "end-capping" procedure does not influence the stereoselective intermolecular interactions of the chiral SO and SA moiety, in contrast to the non-stereoselective interactions.

Increased retention will cause higher enantioselectivity but only if the main retention mechanism is enantioselective, as was stressed by Boehm *et al.* [19]. The enhanced retention of the analytes on CSP-Ia in contrast to retention on CSP-IaE seems to be due to polar, non-stereoselective interactions of the solutes with the stationary phase.

The column efficiency of CSP-Ia and CSP-IaE was calculated either for pure aromatic compounds without functional groups (e.g., benzene) and pure heptane as eluent or for the above-mentioned mobile phase and test solutes containing a $\pi$-basic site and additional polar functional groups. For benzene, the reduced plate heights were 4.8 for CSP-Ia and 4.5 for CSP-IaE, as is more or less usual for this type of CSP. Calculating the reduced plate heights for ibuprofen-1-naphthylamide the values were 20.2 and 24.3, respectively. As can be extracted from these data, solutes containing polar functional groups interacting with polar groups of the total CSP (see Fig. 3) showed slow mass transfer and/or pronounced adsorption phenomena. However, the calculated reduced plate heights are similar for both CSPs and from this point of view the "end-capping" procedure did not lead to better results. The symmetry factor for the more strongly retained ibuprofen-1-naphthylamide enantiomer were calculated as 0.96 for CSP-Ia and 1.2 for the "end-capped" CSP; however, for a clear interpretation of this behaviour the number of data is not sufficient. These discouraging data show the discrepancies between theoretical calculations and virtual effects of retention mechanisms on chiral supports that have to be taken into account when working with CSPs. However, and as additional assumption, it seems possible to obtain the same enantioselectivity and almost the same resolution but within a shorter analysis time by using "end-capped" CSPs and non-aqueous mobile phases.

## 4. Conclusions

The two chiral selectors derived from L-tyrosine presented in this paper proved to be enantioselective for a broad range of chiral analytes. The synthesis of CSP-Ia and CSP-II is comparable with regard to costs and time consumption. They do show comparable enantioselectivity and resolution and the substitution of the ether group with a carbamate group does not influence the chromatographic behaviour to a great extent. Working with similar chiral selectors, a carbamate linkage sufficiently distant from the dominating interaction groups or/and the stereogenic centers may be chosen if there are any problems by conveniently synthesizing an ether bond. The "end-capping" method presented offers a simple route to enhance the applicability of the CSPs due to a shortening of the analysis time but maintaining the enantioselectivity and resolution.

## Acknowledgements

The authors express their grateful thanks to Dr. A. Tambuté (Centre d'Études du Bouchet, Vert-le-Petit, France) for the gift of the chiral selector [(*S*)-N-(3,5-dinitrobenzoyl)tyrosine-O-(2-propen-1-yl)methyl ester]. Acknowledgement is made to the Austrian Fonds zur Förderung der wissenschaftlichen Forschung, project number P-8898-CHE, for the support of this project.

## References


[1] W.H. Pirkle, D.W. House and J.M. Finn, *J. Chromatogr.*, 192 (1980) 143.

[2] W.H. Pirkle and J.M. Finn, *J. Org. Chem.*, 46 (1981) 2935.

[3] W. Pirkle, C. Welch and M. Hyun, *J. Org. Chem.*, 48 (1983) 5022.

[4] W. Pirkle and T. Pochapsky, *Chem. Rev.*, 89 (1989) 347.

[5] G. Uray and W. Lindner, *Chromatographia*, 30 (1990) 323.

[6] W. Lindner, G. Uray and U. Steiner, *J. Chromatogr.*, 553 (1991) 373.

[7] G. Gargaro, F. Gasparrini, D. Misiti, G. Palmieri, M. Pierini and C. Villani, *Chromatographia*, 24 (1987) 505.

[8] F. Gasparrini, D. Misiti, C. Villani and F. La Torre, *J. Chromatogr.*, 539 (1991) 25.

[9] N. Oi, M. Nagase, Y. Inda and T. Doi, *J. Chromatogr.*, 265 (1983) 111.

[10] J. Kip, van Haperen and J.C. Kraak, *J. Chromatogr.*, 356 (1986) 423.

[11] L. Oliveros, C. Minguillon and T. González, presented at the *17th International Symposium on Column Liquid Chromatography, 9–14 May, 1993, Hamburg*, poster.

[12] M. Caude, A. Tambuté and L. Siret, *J. Chromatogr.*, 550 (1991) 357.

[13] A. Tambute, A. Begos, M. Lienne, P. Macaudiere, M. Caude and R. Rosset, *New J. Chem.*, 13 (1989) 625.

[14] L. Siret, A. Tambute, M. Caude and R. Rosset, *J. Chromatogr.*, 540 (1991) 129.

[15] E. Veigl and W. Lindner, *J. Chromatogr. A*, 660 (1994) 255.

[16] R. Däppen, V.R. Meyer and H. Arm, *J. Chromatogr.*, 464 (1989) 39.

[17] W.H. Pirkle and R.S. Readnour, *Chromatographia*, 31 (1991) 129.

[18] G. Uray, N. Maier and W. Lindner, *J. Chromatogr. A*, 666 (1994) 41.

[19] R.E. Boehm, D.E. Martire and D.W. Armstrong, *Anal. Chem.*, 60 (1988) 522.

ELSEVIER

Journal of Chromatography A, 694 (1995) 151–161

JOURNAL OF CHROMATOGRAPHY A

# Evaluation of silica gel-based brush type chiral cation exchangers with (*S*)-N-(3,5-dinitrobenzoyl)tyrosine as chiral selector: attempt to interpret the discouraging results

E. Veigl, B. Böhs, A. Mandl, D. Krametter, W. Lindner*

*Institute of Pharmaceutical Chemistry, Karl-Franzens-University of Graz, A-8010 Graz, Austria*

**Abstract**

The synthesis and evaluation of new chiral stationary phases (CSPs) immobilized on silica gel and based on N-3,5-dinitrobenzoyl-(*S*)-tyrosine [DNB-(*S*)-TyrOH] as chiral selector and to be used in HPLC with buffered aqueous mobile phases are described. The CSPs differ in the linkage of DNB-(*S*)-TyrOH to the silica gel and their end-capping treatment. The applicability of the acidic and $\pi$-acidic CSPs to resolve partially enantiomers of basic drugs such as bupivacaine involving a chiral cation-exchange mechanism is demonstrated. Possible limitations of this concept are discussed.

## 1. Introduction

Ion-exchange chromatography is a well established chromatographic method for the separation of ionic compounds according to their $pK_a$ values and to isolate ionizable from non-ionizable molecules. All applications have in common the use of aqueous and buffered mobile phases, thus regulating the retention of the analytes. Many applications have been described, for example nucleotide and amino acid analysis and the determination of organic acids in wine and fruit juices and of alkaloids in plant extracts [1,2]. A special analytical challenge remains the separation of enantiomers of ionic species, although to date numerous papers have been published in the field of liquid chromatographic enantioseparation (Refs. [3 and 4] and references cited therein). The enantioseparation of biologically active agents is important as it is known that stereoisomers sometimes have different pharmacological profiles, side-effects, efficacy, toxicology, metabolism and excretion rates. Despite the fact that there is a huge number of polar, basic and acidic chiral compounds, only a few papers have dealt with chiral ion-exchange chromatography. Particularily alkaloids such as quinine and brucine or amino acid derivatives have been used as chiral and ionic selectors (SOs) immobilized on different support materials as chiral stationary phases (CSPs) [5–11].

Recently, protein-type CSPs, e.g., $\alpha_1$-AGP or OVM, have also become popular with respect to enantioseparation, mainly owing to their broad applicability for ionic and also for non-ionic and/or polar analytes [12–14]. The pH of the aqueous mobile phase influences significantly the overall retention of the analytes and the enantioselectivity mainly by changing the tertiary structure of the protein-type selector, but also its and

* Corresponding author.

0021-9673/95/$09.50 
*SSDI* 0021-9673(94)00793-4

the analytes' degree of ionization. Hence it becomes evident that electrostatic interactions between the SO and charged analytes (selectands, SAs) can be one of the main SO–SA binding principles. The above-mentioned glycosylated proteins $\alpha_1$-AGP and OVM have acidic isoelectric points, and therefore they are particularly attractive to basic components, with a similar behaviour to cation exchangers. To generalize chiral recognition in such chromatographic systems one have to consider additional intermolecular interactions coming into action; their description by simple models is complicated because of the great variety of binding sites within the protein molecule and its tertiary structure, leading to diverse "chiral cavities, niches, bays or clefts" formed by the unique sequence of (glycosylated) polypeptide chains and their conformations.

However, for simple-structured but ionizable selector molecules it should be easier to elucidate the chiral recognition mechanism more rationally. Recently, Lindner and co-workers [15,16] developed CSPs based on dihydroquinine and dihydroquinidine carbamates covalently immobilized on a silica gel surface and to be used under aqueous mobile phase conditions; these CSPs and selector molecules separate chiral acidic solutes (e.g., 3,5-dinitrobenzoylated and FMOC amino acids) via an anion exchange mechanism in conjunction with additional intermolecular SO–SA interactions.

The aim of this work was to develop new silica-type CSPs based on small amino acid derivatives, in particular DNB-(*S*)-TyrOH, and combining the binding principles of so-called "Pirkle-type" CSPs (involving charge-transfer interactions, hydrogen bonding, dipole–dipole stacking and steric interactions) with cation-exchange mechanisms (similar to those with protein-type CSPs). Thus, the new CSPs (see Fig. 1) should contain free carboxylic acid functionalities and should be operated under buffered aqueous mobile phase conditions. However, similar structured CSPs were presented in 1989 by Moriguchi and Pirkle [17] and were reviewed recently [18]. Despite the poor enantioselectivity of these CSPs, judging the retention and resolution properties of such "simple"-structured CSPs and comparing the results with previous data evaluated for the above-mentioned anion-exchange type CSPs might be a possibility to obtain a clearer insight into the retention and chiral recognition processes taking place.

## 2. Experimental

### 2.1. Apparatus

Liquid chromatography was performed with a modular liquid chromatograph (Merck–Hitachi, Darmstadt, Germany), equipped with an L-6200 intelligent pump, a Model AS-2000A autosampler with a 100-$\mu$l loop, an L-4250 UV–Vis detector, controlled via D-6000 chromatography data station software, HPLC Manager Vers. 2.09. Temperature was controlled with a column thermostat (B.O. Electronics, Austria). Standard operating conditions were detection at 254 nm and a column temperature of 20°C. A guard column (LiChroCART 4-4, LiChrospher 100, RP-18, 5 $\mu$m, from Merck was used in all instances.

Infrared spectra in the diffuse reflection mode were recorded on a Perkin-Elmer (Beaconsfield, UK) 1720-x Fourier transform infrared spectrometer.

### 2.2. Chemicals

Acetonitrile was of gradient grade. Other chemicals were of analytical-reagent quality, purchased from Merck. Water used for HPLC was obtained from a Milli-Q system (Millipore). pH was adjusted with either glacial acetic acid or aqueous ammonia. Mobile phases were filtered and degassed in an ultrasonic bath before use.

Racemic and optically pure drugs were obtained from different pharmaceutical companies.

### 2.3. Chiral stationary phases

*CSP-III*

CSP III (see Fig. 1) was prepared from the corresponding ester phase CSP-II. The reaction

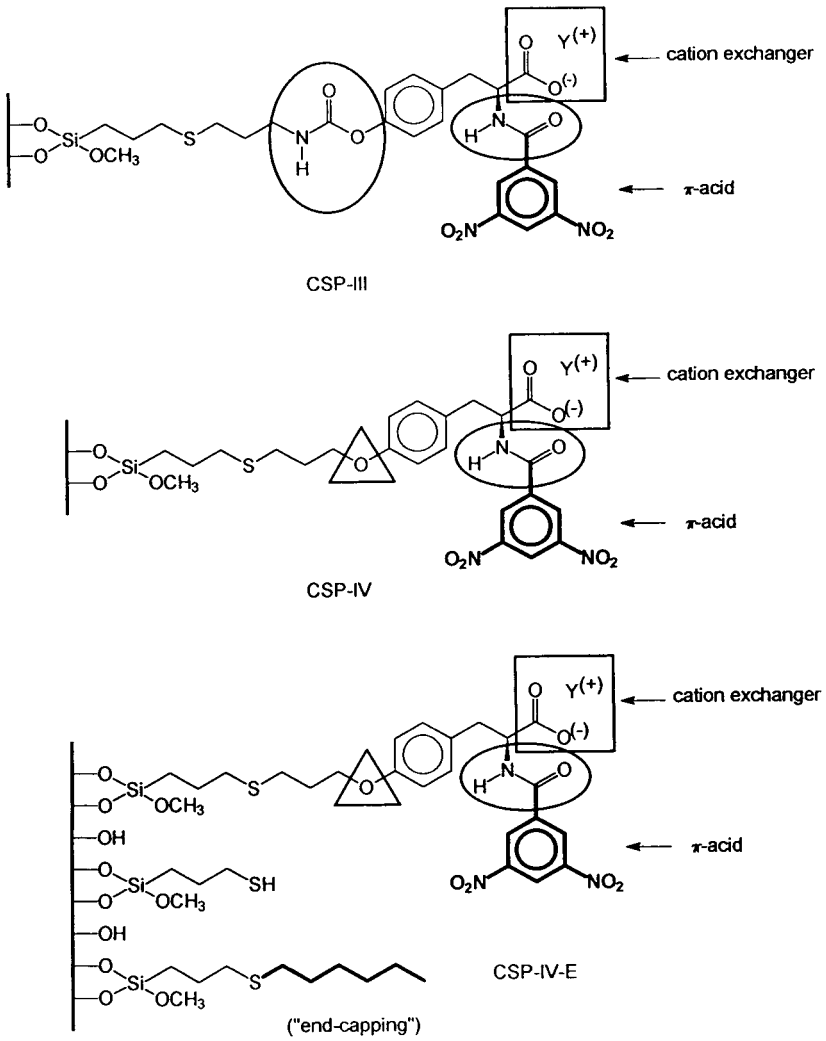


Fig. 1. Structures of CSP-III, CSP-IV and CSP-IV-E. To focus on potential binding sites, the charge-transfer interaction possibilities by the π-acid DNB residue are drawn with bold lines, the cation-exchange functionality is indicated by the square box and the amido groups, offering hydrogen bonding and dipole–dipole stacking properties, are emphasized by the ellipses. The triangle indicates the structural difference between CSP-IV and CSP-IV-E.

scheme for CSP-II, as described previously [19], is based on the following steps: (*S*)-TyrOMe and 3,5-dinitrobenzoylchloride (1.1 equiv.) were reacted in propene oxide (6 equiv.) and dioxane for 2.5 h at 40°C. The N-3,5-dinitrobenzoyl-(*S*)-tyrosine methyl ester [DNB-(*S*)-TyrOMe] formed was refluxed with allyl isocyanate (1.1 equiv.) and dibutyltin(IV) acid dilaurate (catalytic amount) in dioxane for 2 h. A 1.5-g amount of the resulting chiral selector and 2 g of 3-mercaptopropylsilica gel were refluxed with 100 mg of azobisisobutyronitrile (AIBN) in azeotropically dried chloroform for 40 h, resulting in a modified silica with a calculated coverage of the dry material of 216 μmol chiral SO/g silica gel based on C analysis. The final CSP material was obtained by stirring 6 g of modified silica gel CSP-II in 200 ml of methanol with aqueous $KHCO_3$–$K_2CO_3$ (10% w/v, pH 9) for 24 h at room temperature, followed by adjusting the pH

to 2.5 with hydrochloric acid (1 *M*). This modified silica gel (CSP) was sedimented and washed with methanol, methanol–water, methanol, acetone and finally light petroleum. After drying in air at 40°C, the slightly yellow silica was sieved (0.0315 mm) and slurry packed into a stainless-steel column (150 × 4.6 mm I.D.).

*CSP-IV and CSP-IV-E*

CSP-IV and CSP-IV-E (see Fig. 1) were similarly prepared from the previously described [19] corresponding ester phases CSP-Ia and CSP-IaE. In brief, CSP-Ia was synthesized by refluxing 6 g of 3-mercaptopropylsilica gel with 3,15 mmol (1.35 g) of N-(3,5-dinitrobenzoyl)-(*S*)-tyrosine-O-(2-propen-1-yl) methyl ester and 100 mg of AIBN in 200 ml of azeotropically dried chloroform for 40 h, resulting in a calculated coverage of the final dry material of 194 μmol chiral SO/g silica gel based on C analysis. Similarly, CSP-IaE (the "end-capped" version of CSP-Ia) was prepared by refluxing 4 g of CSP-Ia with 20 mmol (1.96 g) of 1-hexene and 0.66 g of AIBN in azeotropically dried chloroform for 35 h, resulting in a calculated coverage of 246 μmol hexyl residues/g silica gel based on C analysis. The methyl ester cleavage of the CSPs was performed by flushing the packed "ester" columns with 0.1 *M* $KHCO_3$–$K_2CO_3$ aqueous solution (pH 8.9) for 12 h at 20°C and at a flow-rate of 0.5 ml (see also Fig. 2).

The cleavage of the ester bond was monitored off-line by DRIFT spectroscopy. Further proof of the successful cleavage was the chromatographic behaviour and the strong dependence of the *k'* values on the ionic strength of the mobile

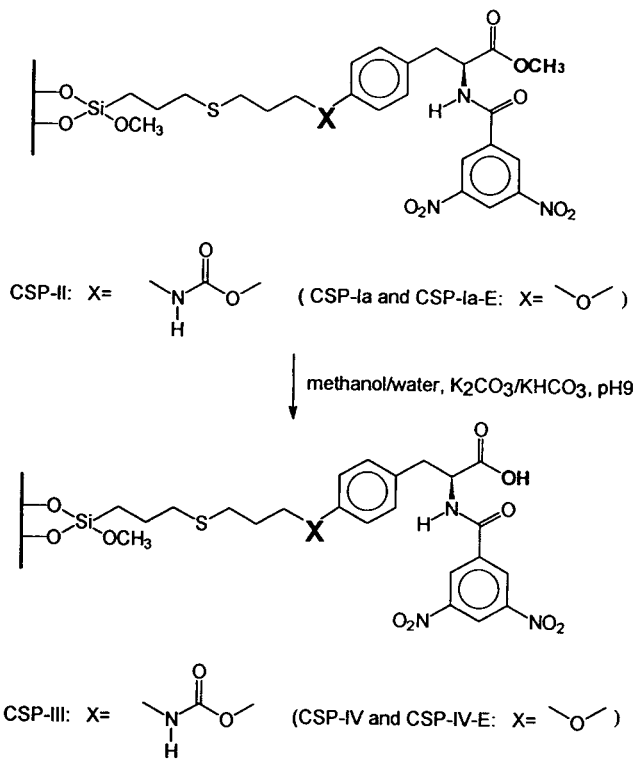


Fig. 2. Reaction scheme for preparing CSP-III, CSP-IV and CSP-IV-E from previously described CSP-II, CSP-I-a and CSP-I-aE [19].

phase, indicating an ion-exchange mechanism; the existence of free carboxylate functions on the final CSP material could safely be postulated.

## 3. Results and discussion

As mentioned above, the concept of chiral anion exchangers based on immobilized dihydroquinine and dihydroquinidine carbamate derivatives (having a tertiary amine group), developed by Lindner and co-workers [15,16], proved its usefulness in resolving very efficiently, for instance, the enantiomers of 3,5-dinitrobenzoylamino acids, with $\alpha$-values between 1.5 and 5 and $R_s$ values between 1.5 and 15. As indicated in Fig. 3, the chiral recognition mechanism of these cinchona alkaloid-type CSPs seems to be based mainly on interactions of charge-transfer character (the $\pi$-basic group, the quinoline ring, is indicated by bold lines, similar to the $\pi$-acid group, the DNB residue in the selector molecule), dipole–dipole binding and/or hydrogen bonding (indicated by ellipses) and ionic interaction of the basic centre of the SO (tertiary or quaternary amine, indicated by the arrow) with the acid function of the SA (carboxylic acid, indicated by the arrow) [15]. The mobile phase conditions were aqueous and pH controlled.

Adopting the principle of reciprocity and thus using chiral DNB-amino acid derivatives as CSPs, they should now express some stereoselectivity for basic analytes (amines) containing $\pi$-basic or electron-rich ring systems, and additional amide structure elements. Many drugs such as antidepressants, antihistaminics, anaesthetics and analgesics should, to a certain extent, meet such criteria. Pirkle et al. [20] introduced the concept of reciprocity first by immobilizing DNB-amino acids as chiral SOs on silica gel to resolve electron-rich compounds, but under normal-phase conditions and without involving ion-exchange interactions. To continue our work on the development of cation-exchange type CSPs, we immobilized 3,5-DNB-(*S*)-TyrOH having a free carboxylic function (see Fig. 1) to be access-

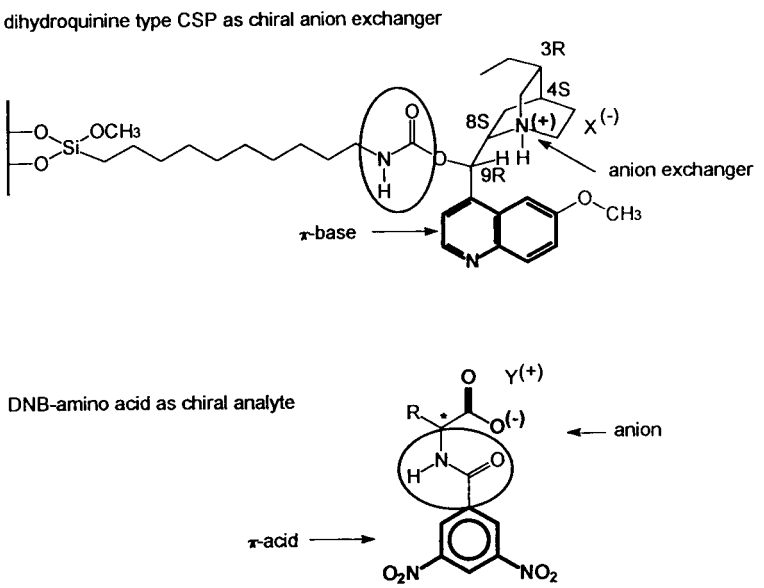


Fig. 3. Chiral anion exchanger based on dihydroquinine derivative [15,16]. The $\pi$-basic and basic centres of the stationary phase are emphasized with bold lines and arrows, whereas the amido group, offering hydrogen bonding and dipole–dipole stacking properties, is emphasized by the ellipse. DNB-$\alpha$-amino acids, containing an $\pi$-acid, acidic and amido functional groups (indicated by bold lines, arrows and ellipses, respectively), were very well resolved on such stationary phases.

ible for electrostatic interactions with amines under aqueous buffered mobile phase conditions. A representative set of chiral analytes containing an amino function and $\pi$-basic aromatic ring systems was chosen (for structures see Fig. 4).

As indicated in Fig. 1, the chiral selectors of CSP-III, CSP-IV and CSP-IV-E consist of one or two amido groups (ellipses), accessible for hydrogen bonding and/or dipole–dipole interaction, a $\pi$-acid group and a free carboxylate function with ionic interaction possibilities. As deduced from previous experiments [15], for these SOs ideal reciprocal selectands (SAs) should be

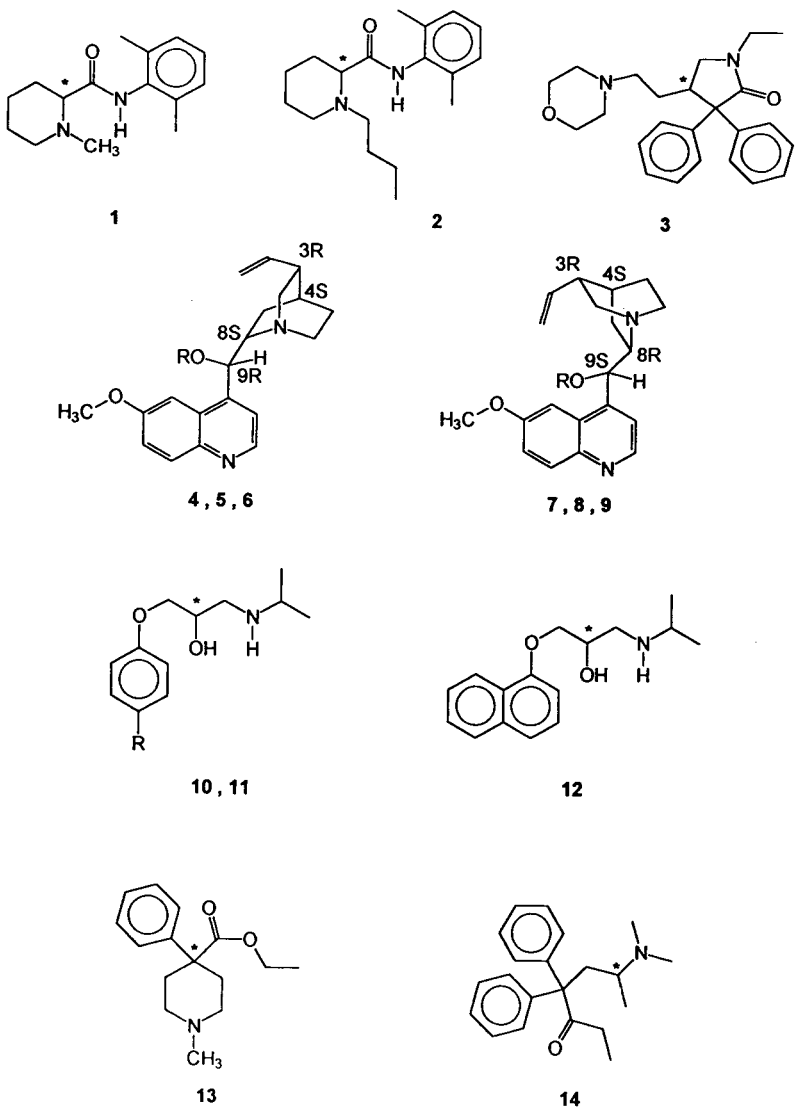


Fig. 4. Structures of some chiral drugs tested for evaluating the retention and enantioselectivity of CSP-III, CSP-IV and CSP-IV-E. **1** = Mepivacaine; **2** = bupivacaine; **3** = doxapram; **4** = quinine; **5** = 10,11-dihydroquinine; **6** = dihydroquinine allylcarbamate (R = $CH_2$=CH–); **7** = quinidine; **8** = 10,11-dihydroquinidine; **9** = dihydroquinidine allylcarbamate (R = $CH_2$=CH–); **10** = atenolol (R = $H_2NCOCH_2$–); **11** = metoprolol (R = $H_3COCH_2CH_2$–); **12** = propranolol; **13** = pethidine; **14** = methadone.

quinine or quinidine but as carbamate derivatives (e.g., allyl carbamates as listed in Table 2, similar to those depicted in Fig. 3).

The retention and ion-exchange properties of CSP-III were evaluated with different aqueous mobile phases. Because of the strong retention of the analytes when using methanol as organic modifier in the mobile phase (data not shown), throughout this work only acetonitrile was used as organic solvent owing to its stronger elution power; acetonitrile decreased considerably the overall retention, which is an indicator not only for a strong hydrophobic but also for strong $\pi-\pi$ type SO–SA interactions. With a mobile phase consisting of acetonitrile–40 m*M* ammonium acetate (60:40, v/v) and a pH of 7, the $k'$ values for the test compounds were between 1.4 and 5 (see data summarized in Table 1). Under these conditions only a few analytes (quinine/quinidine and their dihydro derivatives, chloroquine and thioridazine) still showed very high capacity factors.

### 3.1. *Influence of buffer concentration*

As is well known in ion-exchange chromatography, the retention times of the solutes are strongly influenced by the buffer concentration and ionic strength and the pH of the mobile phase. This behaviour was observed also with CSP-III and CSP-IV, indicating that a real cation-exchange mechanism may take place as depicted in Fig. 5 for bupivacaine as a test solute (for chromatographic data see also Table 1). As can be seen from Fig. 6, the capacity factors were enhanced to about 140% on decreasing the buffer concentration from 80 to 40 m*M* whilst maintaining the acetonitrile content (60%, v/v) and the pH of the mobile phase (7) constant. A further decrease in the ionic strength to 8 m*M* (10% of the starting ionic strength) had an even greater effect on the $k'$ values.

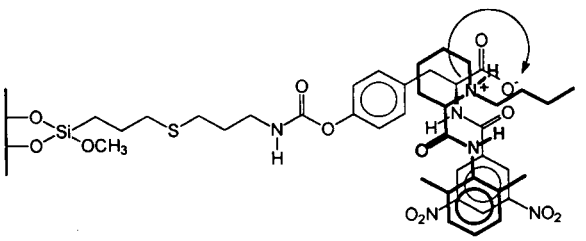

Fig. 5. Theoretical model of chiral recognition mechanism of bupivacaine on CSP-III. As can be seen from the superimposed SO and SA, a simultaneous interaction of the SO carboxylate and the SA ammonium ions (Coulombic attraction), the two amido groups (hydrogen bonding and/or dipole–dipole stacking) and the SO $\pi$-acid DNB residue and the SA $\pi$-basic dimethylphenyl residue (charge transfer) may take place, thus forming diastereomeric molecular associates with different free energy values.

Table 1
Capacity factors ($k'_1$) of representative chiral analytes on CSP-III

| Analyte | Mobile phase A | | | Mobile phase B | | |
|---|---|---|---|---|---|---|
| | 80 m*M* | 40 m*M* | 8 m*M* | pH 6 | pH 7 | pH 7.9 |
| (*R*,*S*)-Mepivacaine (**1**) | 1.66 | 2.81 | – | 5.90 | 5.40 | 2.62 |
| (*R*,*S*)-Bupivacaine (**2**) | 2.27 | 3.01 | 10.16 | 6.30 | 5.99 | 2.82 |
| (*R*,*S*)-Doxapram (**3**) | – | 1.60 | 4.01 | 5.07 | 2.82 | 1.22 |
| Quinine (**4**)/quinidine (**7**) | – | 13.22 | – | 12.88 | 30.10 | – |
| Dihydroquinine (**5**)/dihydroquinidine (**8**) | – | 14.59 | – | 13.93 | 26.38 | – |
| (*R*,*S*)-Atenolol (**10**) | 0.82 | 1.39 | 5.18 | 4.13 | 5.87 | 6.31 |
| (*R*,*S*)-Metoprolol (**11**) | 1.46 | 2.24 | 8.47 | 4.92 | 7.21 | 8.33 |
| (*R*,*S*)-Propranolol (**12**) | 3.84 | 5.57 | 22.61 | – | – | – |
| (*R*,*S*)-Pethidine (**13**) | 2.20 | 3.15 | 11.21 | 6.18 | 8.64 | 7.70 |
| (*R*,*S*)-Methadone (**14**) | 3.44 | 4.45 | 17.23 | 7.13 | 10.14 | 10.57 |

Mobile phase: A = acetonitrile–ammonium acetate buffer (60:40, v/v), pH 7; B = acetonitrile–ammonium acetate buffer (75:25, v/v), 8 m*M*; flow-rate, 0.9 ml/min; temperature, 30°C; detection, UV at 230 nm. Capacity factor $k' = (t_{r_1} - t_0)/t_0$.

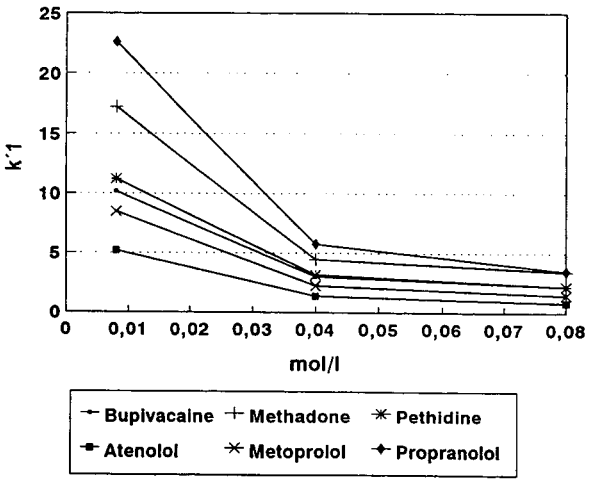


Fig. 6. $k'_1$-Values as a function of ionic strength. Stationary phase, CSP-III; mobile phase, acetonitrile–ammonium acetate (60:40, v/v), pH 7; flow-rate, 0.9 ml/min; detection, UV at 230 nm; temperature, 30°C.

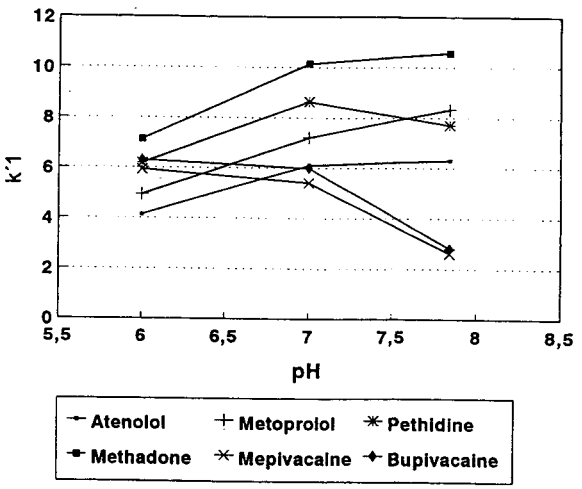


Fig. 7. $k'_1$-Values as function of pH. Stationary phase CSP-III; mobile phase, acetonitrile–ammonium acetate (75:25, v/v), 8 m*M*; flow-rate, 0.9 ml/min; detection, UV at 230 nm; temperature, 30°C.

### 3.2. *Influence of pH*

The variation of the mobile phase pH will influence the dissociation of the immobilized acidic chiral SO and the basic analytes according to their dissociation constants. The $pK_a$ value of the carboxyl group of the chiral SO DNB-(*S*)-TyrOH was measured titrimetrically and found to be surprisingly high, namely between 6.5 and 7, depending on the composition of the aqueous–organic (methanol) titration medium (similar to mobile phase medium); therefore, these CSPs should be weak ion exchangers which are not fully dissociated within the pH range 5.5–7.5. To enhance the ionic interactions of the acidic SO with the basic SAs, a fairly high mobile phase pH should be appropriate, but at this point one must also consider that relatively weak basic solutes will not be fully protonated at high pH values. To summarize , the ionic interactions expressed as retention data are the result of the degrees of dissociation of the SO and the SAs and the applicable pH window of the mobile phase is rather limited in the present instance. Additional SO–SA interactions may become dominant. Subsequently, the influence of mobile phase pH on the capacity factors of the solutes was found to be inconsistent, as is shown in Fig. 7. For the enantiomers of mepivacaine and bupivacaine, possessing $pK_a$ values of 7.7 and 8.1, respectively, the $k'$-value decreased on increasing the pH from 6 to 7.8; for pethidine ($pK_a = 8.7$) the $k'$ value showed a maximum at pH 7 and for atenolol ($pK_a = 9.6$), metoprolol ($pK_a = 9.7$) and methadone ($pK_a = 8.3$) the $k'$ values increased considerably. Comparing the dissociation constants of the analytes and their retention behaviour it becomes obvious that on increasing the pH the dissociation of mepivacaine and bupivacaine was decreased, resulting in weaker ionic interactions with the CSP and subsequently reduced retention times. Relatively strong bases such as atenolol and metoprolol remain protonated at higher pH values, and therefore they showed higher capacity factors owing to enhanced ionic interactions with the carboxylate function of the CSP. However, the retention behaviour of methadone (also a strong base) cannot be fully explained.

### 3.3. *Chiral recognition*

The overall enantioselectivity of the DNB-(*S*)-TyrOH-based CSP-III, CSP-IV and CSP-IV-E

Table 2
Enantioselectivity of CSP-III, CSP-IV and CSP-IV-E

| Solute | CSP-III | | CSP-IV | | CSP-IV-E | |
|---|---|---|---|---|---|---|
| | $k'_1$ | $\alpha$ | $k'_1$ | $\alpha$ | $k'_1$ | $\alpha$ |
| Mepivacaine (**1**) | 5.93 | 1.01 | 6.07[+] | 1.00[+] | 4.02[+] | 1.00[+] |
| Bupivacaine (**2**) | 6.30 | 1.03 | 5.40 | 1.03 | 3.29 | 1.00 |
| Doxapram (**3**) | 5.07 | 1.04 | 3.38 | 1.04 | 2.27 | 1.01 |
| Dihydroquinine (**5**)/dihydroquinidine (**8**) | 11.50[a] | 1.12[a] | 20.07[b] | 1.03[b] | 10.38 | 1.02 |
| **5**/**8** as their allylcarbamates (**6**/**9**) | | | 5.99[b] | 1.26[b] | | |

Mobile phase: acetonitrile–ammonium acetate (75:2, v/v), 8 m*M*, pH 6; flow-rate, 0.9 ml/min; temperature, 30°C; detection, UV at 230 nm. Capacity factor $k' = (t_{r_1} - t_0)/t_0$; selectivity $\alpha = k'_2/k'_1$.
[a] Mobile phase: acetonitrile–ammonium acetate (40:60, v/v), 120 m*M*, pH 7.
[b] Mobile phase: acetonitrile–ammonium acetate (75:25, v/v), 4 m*M*, pH 6.

was small (see Table 2). Of the various solutes tested, only the pseudo-enantiomeric analytes such as quinine/quinidine and dihydroquinine/dihydroquinidine, in addition to bupivacaine, mepivacaine and doxapram, could be partially resolved into their enantiomers. This is in great contrast to the dihydroquinine and dihydroquinidine carbamate-based CSPs, offering $\alpha$-values up to 5 for DNB-$\alpha$-amino acids. The quinine/quinidine and dihydroquinine/dihydroquinidine pseudo-enantiomers were resolved on the DNB-(*S*)-TyrOH-derived CSPs with $\alpha$-values of only 1.03, whereas the respective carbamates, offering an additional amide function for intermolecular interaction, showed higher enantioselectivity ($\alpha = 1.26$, $R_s = 2.56$; see also Table 2). This observation is in accordance with previous statements [15,16].

Mepivacaine (**1**), bupivacaine (**2**) and doxapram (**3**) possess similar structural elements, as can be seen in Fig. 4. The basic nitrogen and the chiral centre are sterically fixed in a ring system, and additionally a carbonyl function of an amide is in close vicinity to the stereogenic centre. However, the analgesic drug pethidine, with a similar structure, was not resolvable. By comparing bupivacaine and mepivacaine, the influence of the substituent of the basic nitrogen can be clearly pointed out: the butyl residue caused higher enantioselectivity than the methyl group. Whether this behaviour is based on the steric hindrance of the residue or the enhanced basicity of the nitrogen due to the stronger inductive effect of the butyl residue is not clear.

For bupivacaine, a simplified chiral recognition model based on Coulombic attraction in combination with hydrogen bonding and/or dipole–dipole stacking and/or $\pi$–$\pi$ interactions is proposed (see Fig. 5). However, the chromatographic experiments showed poor enantioseparations and therefore this chiral recognition mechanism may not be the dominant one. Charge-transfer interactions seem mainly responsible for retention of the solutes (high capacity factors for solutes containing $\pi$-basic ring systems), but concerning the chiral recognition they seem to be too dominant in comparison with the additional interactions necessary for pronounced enantioselectivity. This could also be supported by the poor resolution of quinine and quinidine lacking the dipole–dipole-type interaction possibilities, as is the case for the respective allyl carbamates.

Two types of chemical linking of the chiral SO to the silica surface, thus introducing sensitive or non-sensitive groups with respect to the overall enantioselectivity and retention characteristics, were studied (see also Fig. 1). In previous work with the corresponding methyl ester phases CSP-II and CSP-Ia applying normal-phase conditions [19], only a very small effect of the amido versus the ether linkage was noticed. Under aqueous mobile phase conditions CSP-III and CSP-IV, as presented in this paper, showed similar behaviour, despite the greater differences in the over-

all capacity factors. Assuming comparable surface coverages of CSP-III and CSP-IV, the stronger retention characteristic of CSP-III is probably based on the additional "strong" interactions of the amido group (see Fig. 1) with the solutes containing several functional groups. However, these additional dipole–dipole and/or hydrogen-bonding interactions are unspecific in terms of chiral recognition, mainly owing to the large distance to the centre of chirality.

In contrast to the earlier described DNB-(*S*)-TyrOMe phases [19], the end-capping procedure did not influence the applicability of the DNB-(*S*)-TyrOH phases in a positive way. Similarly to the other phases, end-capping reduces the overall retention of the analytes on the stationary phase, but also the enantioselectivity (see Table 2). The remaining acidic silanol groups of the support material seem to have an attractive and orientating influence for the chiral amine-type solutes (SAs) and participate in the retention and chiral recognition mechanism of basic analytes, resulting in enhanced enantioselectivity. Because of the weak acidic group of the chiral SO, the acidic silanols may enhance the overall enantioselectivity in this special case, but in general a stronger acidic chiral selector and reduced interactions of the solutes with the remaining acidic groups of the silica gel should give better results and should be easier to interpret. The close $pK_a$ values of silanols and the chiral SO result in competing attractive forces for basic guest molecules and therefore hardly explainable chromatographic data may result.

Based on the experimental data, the following assumptions concerning retention and enantioselectivity may be drawn:

(i) The retention of the basic analytes was strongly influenced by the mobile phase pH and ionic strength, and therefore ion-exchange mechanisms are clearly involved. Owing to the unexpected high $pK_a$ value of the acidic DNB-amino acid-type SO, ionic interactions with weak bases are relatively low.

(ii) Competing attractive forces of the acidic silanols and the carboxylate function of the SO to the amine-type SA may on the one hand enhance the resolution of enantiomers, but on the other hand may also destroy significantly the spatial arrangement of the SO and SAs. Unspecific silanol interactions generally lead to broad peaks of basic compounds at higher pH of the mobile phase.

(iii) In contrast to the earlier mentioned chiral anion exchangers based on dihydroquinine and dihydroquinidine carbamate-type CSPs, of which the SOs consist of several chiral centres close to the binding domain, including the chiral nitrogen atom, and which are responsible for a relatively rigid conformation of the SO moiety, the new, simply structured DNB-(*S*)-TyrOH-type cation exchanger seems conformationally less rigid and offers less binding features. The SO and SA interactions are not as stereoselective as expected and the reciprocity concept failed to some extent.

(iv) $\pi-\pi$ Interactions seem mainly responsible for retention, but their portion in spatial arrangements seems to be poor.

## 4. Conclusions

Two new chiral cation-exchange stationary phases based on DNB-(*S*)-TyrOH have been synthesized and their applicability using buffered aqueous mobile phases and chiral amines as analytes was investigated. Based on the strong influence of the mobile phase pH and ionic strength, a cation-exchange mechanism could be established but competing non-stereoselective silanol effects seem to play a significant role. The CSPs described showed some enantioselectivity towards chiral drugs with a basic nitrogen atom, an amido structural element and additional $\pi$-basic ring systems. The applicability of these new chiral cation-exchange phases was also limited, however, owing to an unexpected high dissociation constant of the chiral selector DNB-(*S*)-TyrOH and problems with the inherent silanol amine binding. It could therefore be concluded that better designed chiral selector molecules combined with a more effective shielding and end-capping of silanol groups may have some

potential also in the field of cation-exchange type CSPs based on modified silica gel.

## Acknowledgements

The authors express their grateful thanks to Dr. A. Tambuté (Centre d'Études du Bouchet, Vert-le-Petit, France) for the gift of the chiral selector [N-(3,5-dinitrobenzoyl)-(*S*)-tyrosine-O-(2-propen-1-yl) methyl ester]. Acknowledge ment is made to the Austrian Fonds zur Förderung der wissenschaftlichen Forschung, Project Number P-8898-CHE, for support of this project.

## References

[1] H.F. Walton and R.D. Rocklin, *Ion Exchange in Analytical Chemistry*, CRC Press, Boca Raton, FL, 1990.
[2] H.F. Walton, in E. Heftmann (Editor), *Chromatography, Part A: Fundamentals and Techniques (Journal of Chromatography Library*, Vol. 41A), Elsevier, Amsterdam, 5th ed., Ch. 5, p. A227.
[3] S.G. Allenmark, *Chromatographic Enantioseparation: Methods and Applications*, Ellis Horwood, Chichester, 1988.
[4] W. Lindner and C. Pettersson, in J.W. Wainer (Editor), *LC in Pharmaceutical Development*, Aster, Springfield, VA, 1985, p. 63.
[5] W. Rieman, III, and H.F. Walton, *Ion Exchange in Analytical Chemistry*, Pergamon Press, New York, 1970, p. 254.
[6] N. Grubhofer and L. Schlieth, *Z. Physiol. Chem.*, 296 (1954) 262.
[7] R.J. Baczuk, G.K. Landram, R.J. Dubois and H.C. Dehm, *J. Chromatogr.*, 60 (1971) 351.
[8] C. Bertucci, C. Rosini, D. Pini and P. Savadori, *J. Pharm. Biomed. Anal.*, 5 (1987) 171.
[9] C. Pettersson and C. Gioeli, *J. Chromatogr.*, 398 (1987) 247.
[10] C. Pettersson and C. Gioeli, *J. Chromatogr.*, 435 (1988) 225.
[11] C. Rosini, P. Altemura, D. Pini, C. Bertucci, G. Zullino and P. Salvadori, *J. Chromatogr.*, 348 (1985) 79.
[12] J. Hermansson, *Trends Anal. Chem.*, 8 (1989) 251.
[13] W. Lindner, *Chromatographia*, 24 (1987) 97.
[14] G. Gübitz, *Chromatographia*, 30 (1990) 555.
[15] F. Reiter, A. Fragner and W. Lindner, presented at the *13th International Symposium on Column Liquid Chromatography, Stockholm, June 1989.*
[16] M. Lämmerhofer, S. Peyer, F. Reiter and W. Lindner, *Chromatographia*, submitted for publication.
[17] K. Moriguchi and W.H. Pirkle, presented at the *13th International Symposium on Column Liquid Chromatography, Stockholm, 1989.*
[18] C.J. Welch, *J. Chromatogr. A*, 666 (1994) 3.
[19] E. Veigl, B. Böhs, A. Mandl, D. Krametter and W. Lindner, *J. Chromatogr. A*, 694 (1995) 135.
[20] W.H. Pirkle, D.W. House and J.M. Finn, *J. Chromatogr.*, 192 (1980) 143.

ELSEVIER

Journal of Chromatography A, 694 (1995) 163–167

JOURNAL OF CHROMATOGRAPHY A

# Behaviour of allyl aryl sulfoxides in high-performance liquid chromatography on a chiral stationary phase

F. Gasparrini*, D. Misiti, C. Villani

*Dipartimento di Studi di Chimica e Tecnologia delle Sostanze Biologicamente Attive, Università "La Sapienza", P. le A. Moro 5, 00185 Rome, Italy*

**Abstract**

Several racemic allyl aryl sulfoxides were resolved by HPLC on a brush-type chiral stationary phase based on the 3,5-dinitrobenzoyl derivative of (*R*,*R*)-1,2-diaminocyclohexane. Peak deformations due to exchange phenomena (on-column enantiomerization) were observed at high column temperatures and low eluent flow-rates; under these conditions the extent of interconversion during chromatography was dependent on the kind of substitution of the aromatic ring of the analytes. Kinetic data for the racemization process in solution were also obtained after preparative HPLC separation of the individual enantiomers.

## 1. Introduction

Thermal racemization of allylic sulfoxides was extensively investigated by Mislow and co-workers [1,2], who showed that the $R \rightleftharpoons S$ interconversion is due to a [2,3]-sigmatropic process involving an achiral sulfenate ester as intermediate (Fig. 1); polar solvents and electron-releasing groups on the aromatic ring of allyl aryl sulfoxides were found to decrease the racemization rates and the amount of sulfenate present at equilibrium.

The values of the activation parameters (e.g., $\Delta H^{\#} = 22.5$ kcal/mol and $\Delta S^{\#} = -6.2$ cal/mol · K for allyl phenyl sulfoxide in benzene) [2] indicate that the interconversion can be conveniently investigated by HPLC on a chiral stationary phase under conditions of slow exchange (room temperature) and fast exchange ($T >$ 70°C).

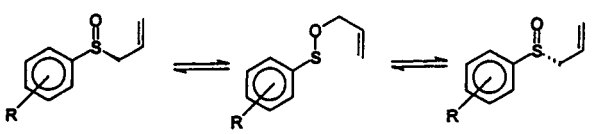

Fig. 1. $R \rightleftharpoons S$ interconversion of allylic sulfoxides.

A totally synthetic chiral sorbent [(*R*,*R*)-DACH-DNB chiral stationary phase (CSP)] [3] containing the 3,5-dinitrobenzoyl derivative of (*R*,*R*)-1,2-diaminocyclohexane has been successfully used [4,5] for the resolution of a broad range of alkyl aryl sulfoxides on the analytical and preparative scales and for the low-temperature investigation of hindered naphthyl sulfoxides undergoing fast *E*–*Z* isomerization [6]. In this work, the application range of the above CSP was extended to the analysis of interconverting allyl sulfoxides (Fig. 2).

## 2. Experimental

The synthesis of the CSP and the HPLC

* Corresponding author.

0021-9673/95/$09.50 
*SSDI* 0021-9673(94)01076-5

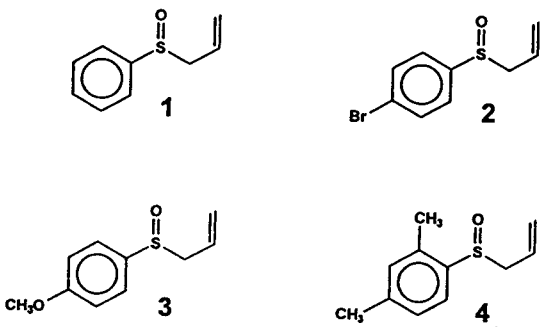


Fig. 2. Structures of the allyl sulfoxides studied.

apparatus have been described elsewhere [3]. Allyl phenyl sulfoxide (**1**) is commercially available (Fluka, Buchs, Switzerland); sulfoxides **2–4** were obtained by alkylation of the appropriate thiophenol with allyl bromide under phase-transfer conditions followed by 3-chloroperbenzoic acid oxidation in $CHCl_3$ at −20°C and column chromatography on silica gel ($CHCl_3$–AcOEt); satisfactory analytical values for C, H and S and spectral data (IR and $^1H$ NMR) were obtained.

The individual enantiomers of compounds **1–4** were obtained by semi-preparative HPLC on (*R*,*R*)-DACH-DNB CSP (column dimensions 250 × 10 mm I.D.) on a 10–20-mg scale using the same eluents listed in Table 1 at a flow-rate of 7.0 ml/min; in all instances the enantiomeric excess of the collected fractions was >98% with recoveries of 95% and 80% for the first- and second-eluted enantiomers, respectively.

Out-of-column racemization kinetics were conducted on 1–2 mg of enantiomerically pure sulfoxides dissolved in 1 ml of solvent at three temperatures (50, 60 and 70°C); the enantiomeric excess was monitored as a function of time by HPLC on the analytical chiral column kept at 15°C.

## 3. Results and discussion

Chromatographic data collected under standard conditions are given in Table 1; dioxane–methanol proved to be the best combination of polar modifiers in terms of selectivity and peak shapes, permitting fast and complete separations of all the analytes. As expected on the basis of previous investigations on closely related compounds, both retention and selectivity are raised by electron-donating substituents on the aromatic moiety of the analytes as a result of increased interaction with the π-acidic aromatic groups of the CSP [4,5]. The elution order of the enantiomers (established by a combination of polarimetric and circular dichroism measurements and comparison with literature data [1,2]) is also consistent with previous findings [5], the sulfoxides with *R* configuration being the first eluted on the (*R*,*R*)-CSP. Under standard chromatographic conditions no detectable interconversion occurs during the analysis as judged by the absence of any reaction zone (plateau) between the resolved peaks (Fig. 3); this result was expected on the basis of the known barriers of activation for the racemization of **1** and **3**: at room temperature the overall chromatographic process occurs at a higher rate relative to the interconversion process. The two rates become

Table 1
Chromatographic data

| Compound | $k'_1$ | α |
|---|---|---|
| **1** | 8.11 | 1.36 |
| **2** | 4.19 | 1.24 |
| **3** | 14.86 | 1.47 |
| **4** | 10.54 | 1.65 |

CSP, (*R*,*R*)-DACH-DNB-LiChrosorb Si100, 5-μm (250 × 4 mm I.D.); eluent, *n*-hexane–dioxane–methanol (70 : 30 : 1); flow-rate, 2.0 ml/min; temperature, 25°C; UV detection at 254 nm. $k'_1$ = Retention factor; α = separation factor.

Table 2
Chromatographic data with different eluents

| Compound | Eluent | $k'_1$ | α |
|---|---|---|---|
| **1** | A | 4.64 | 1.21 |
| **2** | A | 3.02 | 1.14 |
| **3** | B | 3.03 | 1.14 |
| **4** | B | 2.09 | 1.26 |

Eluent A, *n*-hexane–dioxane–methanol (70 : 30 : 1); eluent B, *n*-hexane–dioxane–methanol (60 : 20 : 5); flow-rate, 0.5 ml/min; temperature, 85°C; other conditions as in Table 1. $k'_1$ = Retention factor; α = separation factor.

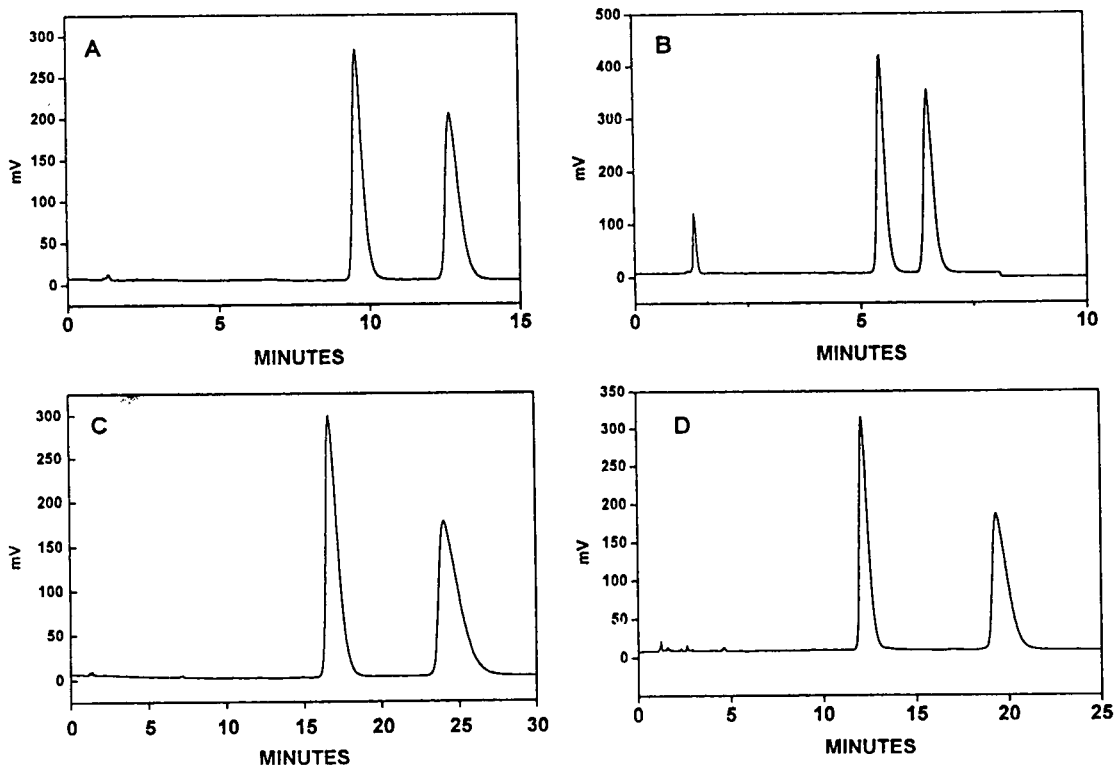


Fig. 3. Resolution of racemic allylic sulfoxides on (*R*,*R*)-DACH-DNB CSP. Chromatograms A, B, C and D for compounds **1**, **2**, **3** and **4**, respectively. Chromatographic conditions as in Table 1.

Table 3
Kinetic data for the out-of-column racemization of compounds **1–4**

| *R*-Enantiomer of compound | T(°C) | $K_{rac} \times 10^4$ ($s^{-1}$) | Solvent | $\Delta G^{\#}$ (kcal/mol) | $\Delta H^{\#}$ (kcal/mol) | $\Delta S^{\#}$ (cal/mol · K) |
|---|---|---|---|---|---|---|
| **1** | 50 | 1.74 | A | 24.08 | | |
| | 60 | 5.59 | A | 24.07 | 21.77 | −7.1 |
| | 70 | 13.3 | A | 24.22 | | |
| **2** | 50 | 3.31 | A | 23.67 | | |
| | 60 | 8.69 | A | 23.78 | 20.69 | −9.2 |
| | 70 | 23.0 | A | 23.85 | | |
| **3** | 50 | 0.73 | B | 24.64 | | |
| | 60 | 2.30 | B | 24.66 | 22.80 | −5.7 |
| | 70 | 6.10 | B | 24.75 | | |
| **4** | 50 | 3.84 | B | 23.57 | | |
| | 60 | 11.0 | B | 23.62 | 22.57 | −3.1 |
| | 70 | 31.7 | B | 24.63 | | |

Solvent A, *n*-heptane–dioxane–methanol (70 : 30 : 1); solvent B, *n*-heptane–dioxane–methanol (60 : 20 : 5). 1 cal = 4.184 J.

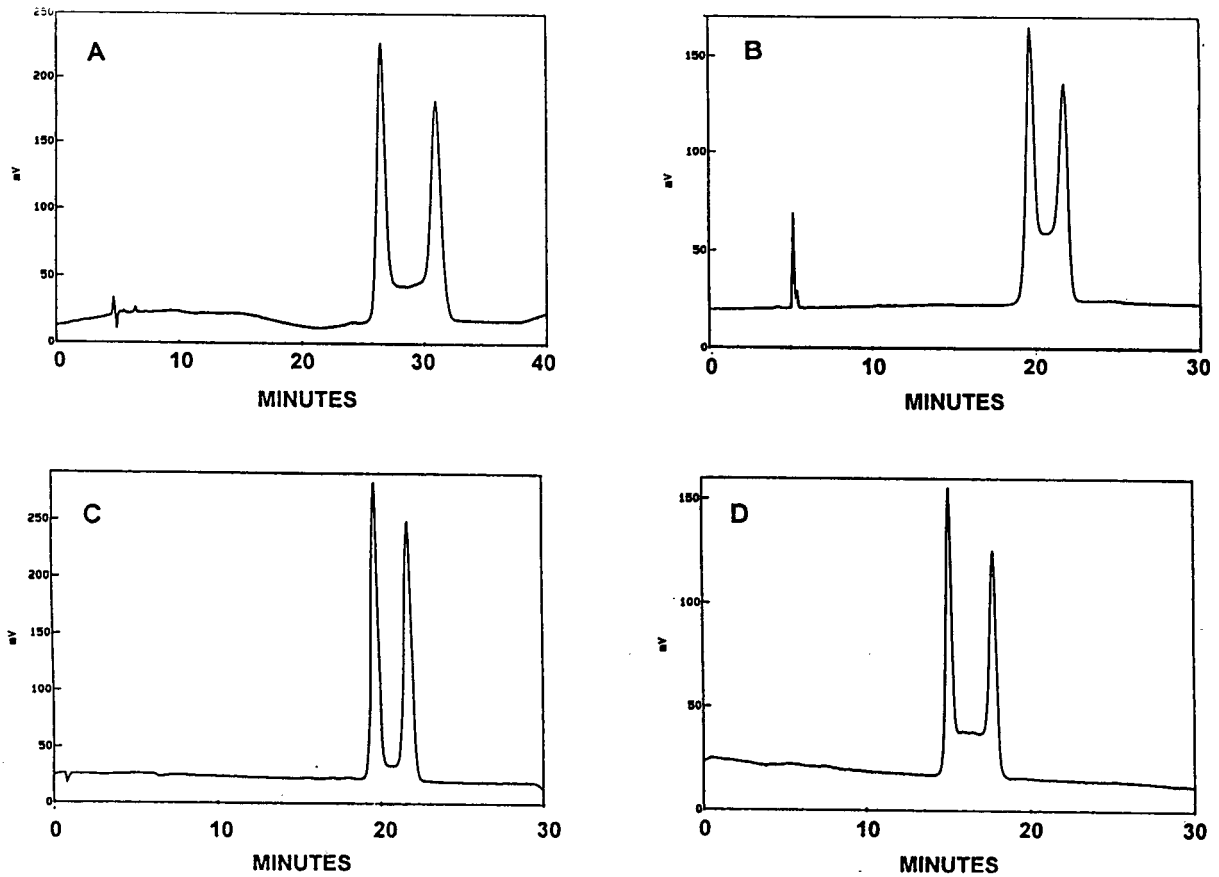


Fig. 4. On-column enantiomerization of racemic allylic sulfoxides on (*R*,*R*)-DACH-DNB CSP. Chromatograms A, B, C and D for compounds **1**, **2**, **3** and **4**, respectively. Chromatographic conditions as in Table 2.

commensurable as the column temperature is raised to 85°C (increase in the interconversion rate) and the eluent flow-rate is lowered to 0.5 ml/min (decrease in the separation rate) and the typical dynamic patterns due to on-column exchange phenomena are clearly observed in Fig. 4.

At 85°C the enantioselectivity of the CSP is still large enough to permit almost complete resolution of the analytes (Table 2); two different mobile phases were used for these resolutions in order to obtain reasonable analysis times for the more strongly retained sulfoxides **3** and **4**. The extent of interconversion between two enantiomeric species during their passage through the chiral column is, to a first approximation, related to the area of the "reaction zone" observed between the two peaks: it is clear that on-column interconversion is less pronounced for sulfoxide **3**, which shows a small plateau region (Fig. 4C) in comparison with the remaining compounds.

Inspection of the data obtained for the out-of-column racemization processes (Table 3) reveals qualitative agreement with the high-temperature chromatographic analysis: again, sulfoxide **3** is found to have the highest barrier to racemization under our experimental conditions. Although two different solvents were used for compounds **1–2** and **3–4**, the solvent effect on the reaction rate is not expected to obscure their relative stereochemical stabilities; larger solvent effects have been observed on passing from non-polar

solvents (e.g., methylcyclohexane or benzene) to polar solvents (ethanol, 2,2,3,3-tetrafluoro-1-propanol) [1,2].

Extrapolation of the data of Table 3 to 85°C reveals that the interconversion is very fast at this temperature, the complete loss of optical activity occurring in a few minutes in solution (i.e., in the absence of the chiral solid support).

On the other hand, interconversion during chromatography takes place both in solution and on the silica surface, and the two rate constants may in principle be different [7,8]; in the present case, a retarding effect of the chiral stationary phase on the interconversion process is observed, the two enantiomeric peaks being still recognizable even after long residence times in the chiral column.

## 4. Conclusions

The application range of DACH-DNB CSP has been extended to the investigation of interconverting enantiomeric species featuring relatively high activation barriers. The above CSP is particularly suited for the study of on-column isomerizations even at unusually high temperatures in view of its thermal stability, and may be a valid alternative to polarimetric measurements for the investigation of the same processes in solution.

## References

[1] P. Bickart, F.W. Carson, J. Jacobus, E.G. Miller and K. Mislow, *J. Am. Chem. Soc.*, 90 (1968) 4869.
[2] R. Tang and K. Mislow, *J. Am. Chem. Soc.*, 92 (1970) 2100.
[3] F. Gasparrini, D. Misiti and C. Villani, *Chirality*, 4 (1992) 447, and references cited therein.
[4] G. Gargaro, F. Gasparrini, D. Misiti, G. Palmieri, M. Pierini and C. Villani, *Chromatographia*, 24 (1987) 505.
[5] C. Altomare, A. Carotti, S. Cellamare, F. Fanelli, F. Gasparrini, C. Villani, P.-A. Carrupt and B. Testa, *Chirality*, 5 (1993) 527.
[6] D. Casarini, E. Foresti, F. Gasparrini, L. Lunazzi, D. Misiti, D. Macciantelli and C. Villani, *J. Org. Chem.*, 58 (1993) 5674.
[7] J. Veciana and M.I. Crespo, *Angew. Chem., Int. Ed. Engl.*, 30 (1991) 74.
[8] A. Mannschreck, H. Zinner and N. Pustet, *Chimia*, 58 (1989) 165.

ELSEVIER

Journal of Chromatography A, 694 (1995) 169–179

JOURNAL OF CHROMATOGRAPHY A

# Using chirality as a unique probe of pharmacological properties

Irving W. Wainer*, Julie Ducharme, Camille P. Granvil, Heli Parenteau, Sami Abdullah

*Department of Oncology, McGill University, Montreal, Quebec, Canada*

**Abstract**

The development of enantioselective chromatographic techniques has made it feasible to routinely follow the metabolism and disposition of the separate enantiomers of a chiral drug. These studies are a source of data about in vivo pharmacological processes. The key question is recognition of the fundamental information contained within the results and the application of this data to the development of a deeper understanding of the clinical consequences of stereochemistry. This manuscript presents two examples of how chirality can be used as a unique probe of basic pharmacological properties.

## 1. Introduction

*"The difficulty in science is often not so much how to make the discovery but to know that one has made it. In all experiments there are a number of effects, produced by all kinds of extraneous causes, which are not in the least significant, and it requires a certain degree of intelligence or intuition to see which of them really means anything"* (J.D. Bernal [1]).

The pharmacological importance of stereoisomerism has been established by numerous in vitro studies involving ligand-biopolymer and substrate–enzyme interactions. At the same time, the in vivo fate of chiral compounds has not received the same attention. This has been primarily due to the lack of adequate analytical methodology.

In the past few years this situation has dramatically changed with the rapid increase in commercially available chromatographic chiral stationary phases (CSPs) for both HPLC and GC. These phases have formed the backbone of many enantioselective bioanalytical methods which have been used in pharmacokinetic and metabolic studies of chiral drugs.

These technological advances have resulted in an increased interest in the in vivo disposition of the enantiomers of chiral substances; particularly from the drug regulatory agencies. This, in turn, has produced a steady rise in enantioselective pharmacokinetic and metabolic studies which are now standard procedures in the development and testing of new chiral drugs, for both racemic and single isomer formulations.

The routine determination of enantioselective pharmacokinetics represents a positive scientific advance and the realization that pharmacology is a complex three-dimensional phenomenon. However, as this pharmacokinetic approach be-

* Corresponding author. Address for correspondence: Montreal General Hospital, Room B7113, 1650 Cedar Avenue, Montreal, Quebec H3G 1A4, Canada.

0021-9673/95/$09.50 
*SSDI* 0021-9673(94)00749-7

comes routine, the possibility arises that the innovative and extraordinary data provided by enantioselective analysis will be lost in the day-to-day activities. Indeed, pharmacokinetic and metabolic studies of a chiral compound contain an abundance of unique information. For example, since the physicochemical properties of enantiomers are the same, an enantioselective difference in distribution can be used to probe for specific ligand–biopolymer binding interactions or a distinct enantiomer-related metabolic pattern may lead to the identification of multiple enzyme systems. These possibilities will be illustrated by recent studies with the drugs hydroxychloroquine (HCQ) and ifosfamide (IFF).

In the first example, the results from pharmacokinetic studies of HCQ enantiomers in the human and in the rabbit suggested that the observed differences might be due to an enantioselective sequestration. This led to a further study of the enantioselective ocular distribution of HCQ in the rabbit which confirmed that enantioselective accumulation occurs in ocular tissues. The data also indicated that the observed enantioselectivity is a result of binding to an as of yet unidentified biopolymer.

In a similar manner, the relative enantiomeric metabolite patterns of the anticancer agent IFF were determined during a clinical pharmacokinetic study. Addressing metabolite stereoselectivity becomes critical if the metabolite is pharmacologically active, either contributing to the parent drug's activity or to its toxicity. Through a comparison of the different urinary excretion patterns from patients, it was concluded that at least two microsomal isoenzymes are responsible for the metabolism of this drug. These results suggest that treatment-limiting neurotoxicity may be linked to a particular metabolic phenotype which reflects an overexpression of one or both of these enzymes.

Neither of these conclusions could have been drawn from the experimental data without using chirality "to see which of them (i.e. results) really means anything". These studies are presented below.

## 2. Distribution of the enantiomers of hydroxychloroquine in ocular tissues: observing a new ligand–biopolymer interaction

HCQ is an aminoquinolone used in the treatment of malaria, extraintestinal amebiasis, rheumatoid arthritis, discoid and systemic lupus erythematosus. Ocular toxicity, in particular pigmentary retinopathy, has been associated with the clinical use of HCQ [2,3]. The mechanism producing retinal damage is unknown.

HCQ is an enantiomeric compound which is administered as a racemic mixture. HCQ undergoes hepatic metabolism and after chronic oral administration, the plasma and whole blood contain significant levels of HCQ and of three metabolites, desethylchloroquine (DCQ), desethylhydroxychloroquine (DHCQ) and bisdesethylchloroquine (BDCQ). Since DCQ, DHCQ and BDCQ are also enantiomeric, the plasma and whole blood can contain up to eight distinct chemical entities.

### *2.1. Pharmacokinetics and metabolism of HCQ enantiomers*

The clinical pharmacokinetics and metabolism of HCQ enantiomers, *R*-HCQ and *S*-HCQ, have been studied after multiple [4–6] and single [7] doses of the racemate, *rac*-HCQ. These studies have demonstrated that the distribution, elimination and metabolism of HCQ is enantioselective. After administration of *rac*-HCQ, the systemic exposure, calculated from the plasma and whole blood concentration–time plots as area-under-the-curve (AUC), was greater for *R*-HCQ than for *S*-HCQ. Conversely, for the metabolites, the levels of the *S*-enantiomers were always higher. In addition, *S*-HCQ renal clearance was also higher than that of *R*-HCQ.

The enantioselective pharmacokinetics of *R*- and *S*-HCQ in the rabbit has also been investigated [8]. Both albino (New Zealand White, NZW) and pigmented rabbits were used in the study which involved oral dosing of *rac*-HCQ and the separate enantiomers. Following the administration of *rac*-HCQ, the whole blood

levels of *R*-HCQ always surpassed those of *S*-HCQ, while the opposite situation was found in plasma. In whole blood, *R*/*S* ratios varied from 1.3 to 3 [8], similar to the 1.6–2.9 range found in human blood [6]. No significant difference was observed between the HCQ whole blood or plasma levels in the NZW and the pigmented rabbits. In addition, no stereochemical interconversion was detected after separate administrations of *R*-HCQ and *S*-HCQ [8].

### 2.2. Determination of ocular concentrations of HCQ enantiomers

The results from the rabbit studies indicated that this species could be a useful model for the investigation of the distribution of the enantiomers of HCQ and its metabolites in ocular tissues. This study was undertaken and the results have been recently reported [9]. In this study, both NZW and pigmented animals were used and single and multiple daily oral doses of *rac*-HCQ or the separate enantiomers were administered. In addition, NZW and pigmented animals were dosed with *rac*-HCQ for 8 days and washed out for an additional 7 days. At the end of the study periods, plasma and whole blood samples were collected and the rabbits were sacrificed. The eyes were collected, the aqueous humor removed and the eyes separated into the cornea, lens, vitreous body, iris, retina/choroid, sclera and conjunctiva. The concentrations of *R*-HCQ, *S*-HCQ and their respective metabolites were determined using a validated enantioselective liquid chromatographic assay [10] (Fig. 1).

The mean HCQ levels in the cornea, sclera, iris, retina/choroid and conjunctiva determined at the time of sacrifice for the NZW rabbits dosed daily for 8 days are presented in Table 1. The plasma levels of HCQ were significantly lower than those found in the ocular tissues indicating that the drug had accumulated in these tissues. The mean concentrations of HCQ in the cornea, sclera, iris, retina/choroid and conjunctiva after daily oral dosing with *rac*-HCQ for 8 days followed by a 7-day washout are also presented in Table 1. The results from the washout study indicate that the accumulations of HCQ in these ocular tissues were reversible. After the 7-day washout period, the levels of HCQ in these tissues decreased by an average of 74%. The average *R*-HCQ:*S*-HCQ ratio fell from approximately 60:40 to 52:48 at the end of the 7-day washout, indicating that there was no preferential sequestration of one enantiomer.

The mean HCQ levels in the cornea, sclera, iris, retina/choroid and conjunctiva determined at the time of sacrifice for the pigmented rabbits dosed daily for 8 days are presented in Table 1. The plasma levels of HCQ were significantly lower than those found in the ocular tissues indicating that the drug had accumulated in these tissues. The mean concentrations of HCQ in the cornea, sclera, iris, retina/choroid and conjunctiva after daily oral dosing with *rac*-HCQ for 8 days followed by a 7-day washout are also presented in Table 1. Unlike the NZW rabbits, the HCQ levels either remained unchanged during the washout period, cornea and conjunctiva, or increased; the HCQ concentrations in the sclera and iris doubled and the levels in the retina/choroid increased by 78%. The data suggest that melanin, found in the iris and retina/choroid, continues to concentrate HCQ and acts as a intraocular source of the drug for the non-pigmented tissues, cornea, sclera and conjunctiva. The observed enantioselectivity of the non-melanin containing tissues, 55:45 *R*-HCQ:*S*-HCQ, versus the 50:50 *R*-HCQ:*S*-HCQ ratios determined in the iris and retina/choroid indicates that HCQ-melanin binding is not enantioselective.

### 2.3. Summary and conclusions: the identification of a HCQ-binding biopolymer

The data from this study indicates that after systemic administration of *rac*-HCQ, *R*-HCQ and *S*-HCQ accumulate in the ocular tissues of the rabbit. Comparison of the enantioselectivities of the accumulations in albino and pigmented rabbits demonstrates that HCQ binds to two biopolymers —melanin which is found in the

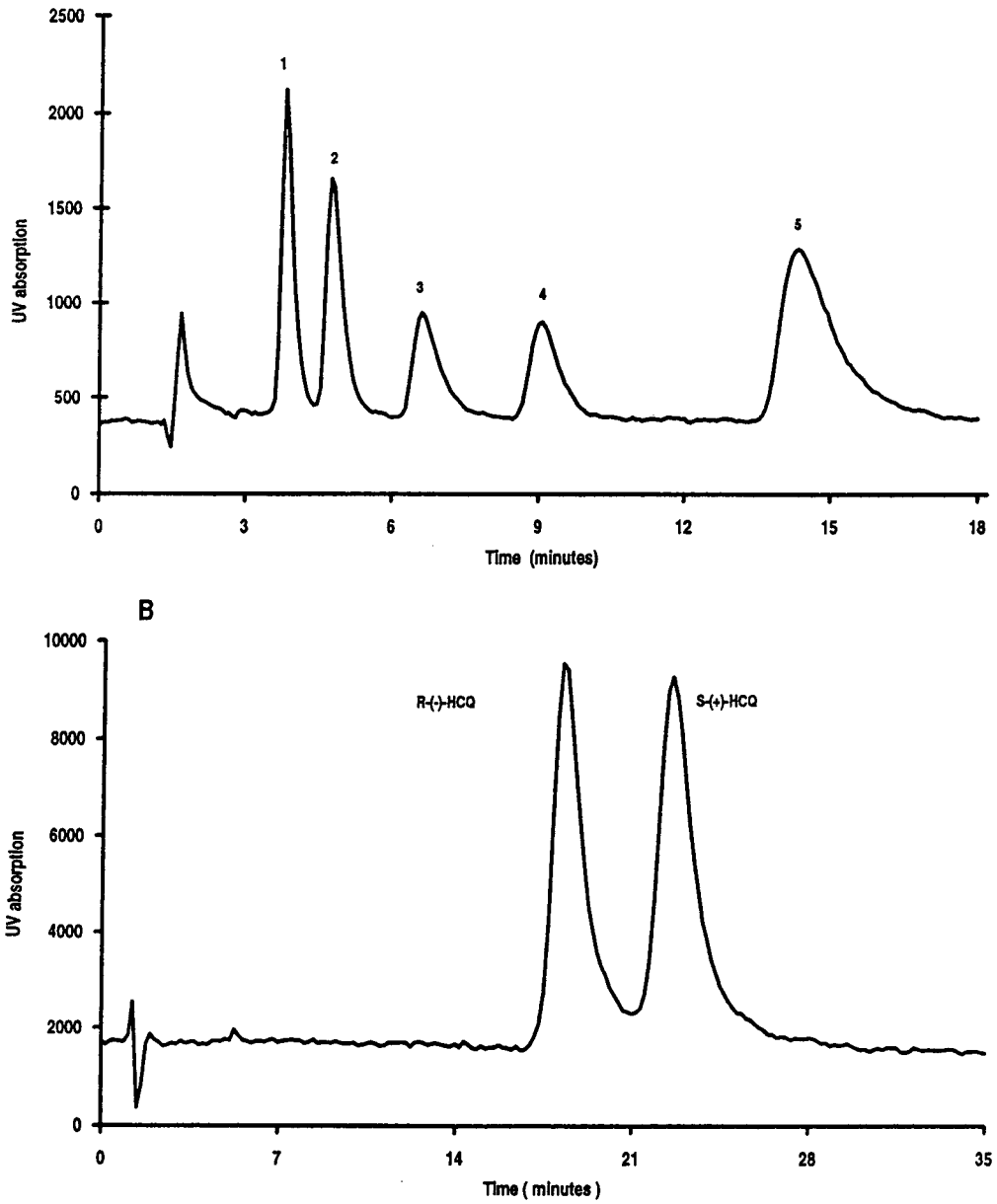


Fig. 1. (A) The chromatographic analysis of a urine sample spiked with 100 ng/ml each of HCQ and its major metabolites, where 1 = BDCQ, 2 = DHCQ, 3 = DCQ, 4 = HCQ and 5 = chloroquine (internal standard). (B) The chromatographic separation of a racemic (50:50 mixture) of the enantiomers of HCQ; (−)-HCQ and (+)-HCQ. See Ref. [10] for experimental conditions.

pigmented iris and retina/choroid and a currently unidentified biopolymer (BP-X) which is present in the cornea, sclera, iris, retina/choroid and conjunctiva. These conclusions are based upon the following observations:

(1) The accumulation of HCQ in non-melanin containing ocular tissues is enantioselective: in the non-pigmented ocular tissues, the mean *R*-HCQ:*S*-HCQ ratio was 60:40. The observed enantioselectivity mirrored the relative distribu-

Table 1
Ocular tissue concentrations of hydroxychloroquine in the rabbit presented as ng/g tissue after daily oral dosing of *rac*-HCQ, 20 mg/kg

| Tissue | Pigmented dosing schedule | | | Albino dosing schedule | | |
|---|---|---|---|---|---|---|
| | 8 days | 22 days | 8 days + 7-day washout | 8 days | 15 days | 8 days + 7-day washout |
| Cornea | 644 ± 716 | 165 ± 80 | 436 ± 91 | 6 361 ± 4 416 | 1 211 ± 665 | 1 364 ± 1 177 |
| Sclera | 2 960 ± 1 905 | 1 342 ± 1 494 | 6 735 ± 1 578 | 3 028 ± 462 | 1 298 ± 253 | 593 ± 64 |
| Iris | 154 029 ± 13 555 | 80 923 ± 15 415 | 314 154 ± 386 326 | 8 362 ± 4 244 | 679 ± 145 | 2 239 ± 335 |
| Retina/choroid | 51 911 ± 33 161 | 45 455 ± 13 537 | 92 191 ± 17 501 | 5 225 ± 630 | 544 ± 143 | 884 ± 95 |
| Conjunctiva | 1 678 ± 1 274 | 621 ± 35 | 1 490 ± 21 | 1 204 ± 311 | 0 | 977 ± 178 |

tion of *R*-HCQ and *S*-HCQ in whole blood where the average *R*-HCQ:*S*-HCQ ratio was also 60:40 (range 54:46 to 67:33). The opposite result was observed for the total plasma concentration of HCQ where the average *R*-HCQ:*S*-HCQ ratio is 40:60 (range 47:53 to 39:61).

(2) *R*- and *S*-HCQ do not compete for transport or binding: when the albino animals were dosed with the separate enantiomers of HCQ, the resulting average tissue concentrations were similar to those attained after dosing with the racemate. This indicates that *R*-HCQ and *S*-HCQ do not compete with each other for transport into the ocular tissues and in binding to BP-X. These results were also similar to the relative whole blood concentrations achieved after dosing with the separate enantiomers; after 5 days of dosing with either *R*-HCQ or *S*-HCQ, the whole blood concentrations of *R*-HCQ were two-fold higher than the corresponding concentrations of *S*-HCQ. HCQ was stereochemically stable in the rabbit and an enantioselective interconversion between *R*-HCQ and *S*-HCQ was not observed [8].

(3) The enantioselective ocular accumulation is not primarily due to plasma protein binding: the in vitro human plasma protein binding of *R*-HCQ and *S*-HCQ has been studied and found to be enantioselective; the binding of *S*-HCQ was almost two-fold higher than *R*-HCQ, 64 and 37%, respectively [11]. Since only the free fraction of a drug can pass through biological membranes and distribute into tissues, *R*-HCQ, with a 63% unbound fraction, would be expected to accumulate to higher levels in ocular tissues. Thus, the observed enantioselectivity may only be a reflection of the enantioselectivity of the protein binding.

However, the low proportion of protein binding and the of loss of enantioselectivity in the melanin binding suggests that the difference between the free fractions of *R*-HCQ and *S*-HCQ in the plasma is probably not the determinant influence on the ocular distribution of these enantiomers. The principal determinant appears to be enantioselective binding to BP-X and the importance of this interaction will only be ascertained when the biopolymer is isolated, identified and its binding properties elucidated.

(4) The binding of HCQ to melanin is not enantioselective: When melanin is present in the iris and retina/choroid, the enantioselective accumulations observed in these tissues in the albino rabbits is lost. The presence of melanin in the iris and retina/choroid of the pigmented rabbits resulted in an 18-fold increase in the HCQ concentration in the iris and a 13-fold increase in the retina/choroid; the average concentration in the iris of pigmented rabbits was 154.029 ng/g tissue which was more than 50-fold higher than the mean of the concentrations found in the non-pigmented tissues. The increases in HCQ concentrations in the iris and retina/choroid were accompanied by a loss of enantioselectivity as the *R*-HCQ:*S*-HCQ ratio fell from 65:35 (albino rabbits) to 50:50 (pigmented rabbits).

These results indicate that melanin has a relatively higher affinity for HCQ than BP-X. However, confirmation of this supposition also

awaits the isolation and identification of BP-X and elucidation of its binding properties.

(5) The distribution of HCQ metabolites into ocular tissues: the distribution of the enantiomers of DCQ and DHCQ into the ocular tissues studied in this program follows the same patterns as HCQ. The accumulations are reversible and enantioselective. The presence of melanin in the retina/choroid and iris results in a significant increase in the quantity of metabolite accumulated in the tissue relative to the non-pigmented tissues. The affinity of DCQ and DHCQ binding to BP-X and the enantioselectivity of this process remain to be described.

## 3. Enantioselective N-dechloroethylation of ifosfamide: uncovering a multiple-enzyme metabolic pathway

IFF is an alkylating agent which has demonstrated activity against a wide range of tumor types [12] including Ewings sarcoma, osteosarcoma and rhabdomyosarcoma. IFF is a chiral molecule which contains an asymmetrically substituted phosphorous atom and exists in two enantiomeric forms, *R*-IFF and *S*-IFF. In clinical practice, IFF is administered as a racemic (50:50) mixture of the two enantiomers and the majority of reported pharmacological studies have been carried out without consideration of the metabolic and pharmacokinetic fate of *R*- and *S*-IFF.

In its original form, IFF is not an active antitumor agent. The compound must be metabolically transformed into the cytotoxic agent, isophosphoramide mustard (IPM, Fig. 2). IPM is an active alkylating agent responsible for the cross-linking of DNA produced by IFF [13,14]. The initial metabolic step in the transformation of IFF to IPM is the oxidation of the 4-carbon of the oxazaphosphorine ring by hepatic microsomal enzymes to form 4-hydroxy-IFF, efficacious pathway (Fig. 2). Oxidation also occurs (up to 48% of the dose) at one of the two β-chloroethyl side chains, toxic pathway (Fig. 2). This pathway produces the N-dechloroethylated metabolites, 2-dechloroethyl-IFF (2-DCE-IFF) and 3-dechloroethyl-IFF (3-DCE-IFF) which are not active antitumor agents, and chloroacetaldehyde, a central nervous system (CNS) toxin [13,14].

### *3.1. Quantitation of the enantiomeric composition of IFF, 2-DCE-IFF and 3-DCE-IFF*

In order to follow the in vivo and in vitro metabolism and distribution of IFF, an enantioselective GC–MS method was developed for the quantitation of the enantiomers of IFF and 2-DCE-IFF and 3-DCE-IFF in biological matrices [15]. IFF and the two dechloroethylated metabolites were extracted into chloroform, enantioselectively resolved on a GC CSP based upon heptakis(2,6-di-O-methyl-3-O-pentyl)-β-cyclodextrin and quantitated using mass selective detection with selective ion monitoring (Fig. 3). The limits of quantitation for the enantiomers of IFF, 2-DCE-IFF and 3-DCE-IFF in plasma were 250 and 500 ng/ml, respectively. In urine, the limits of quantitation for the enantiomers of IFF, 2-DCE-IFF and 3-DCE-IFF were 500 ng/ml. The method is able to detect concentrations as low as 250 ng/ml of each enantiomer of 2-and 3-DCE-IFF in plasma and urine. The intra- and inter-day relative standard deviations for this method were with one exception less than 8%. The assay was validated for enantioselective pharmacokinetic studies in humans and rats and was the first reported enantioselective assay for the measurement of the enantiomers of 2- and 3-DCE-IFF in plasma.

### *3.2. Enantioselective metabolism and distribution of IFF*

Initial studies by Misiura et al. [16] indicated that there were stereochemical differences in the human metabolism of IFF. Urine samples contained more *R*-IFF than *S*-IFF and the production of 2-DCE-IFF from *S*-IFF was 2.7- to 6.7-fold higher than from the corresponding *R*-isomer. Boss et al. [17] and Wainer et al. [18] have confirmed these results.

The plasma concentration vs. time profiles

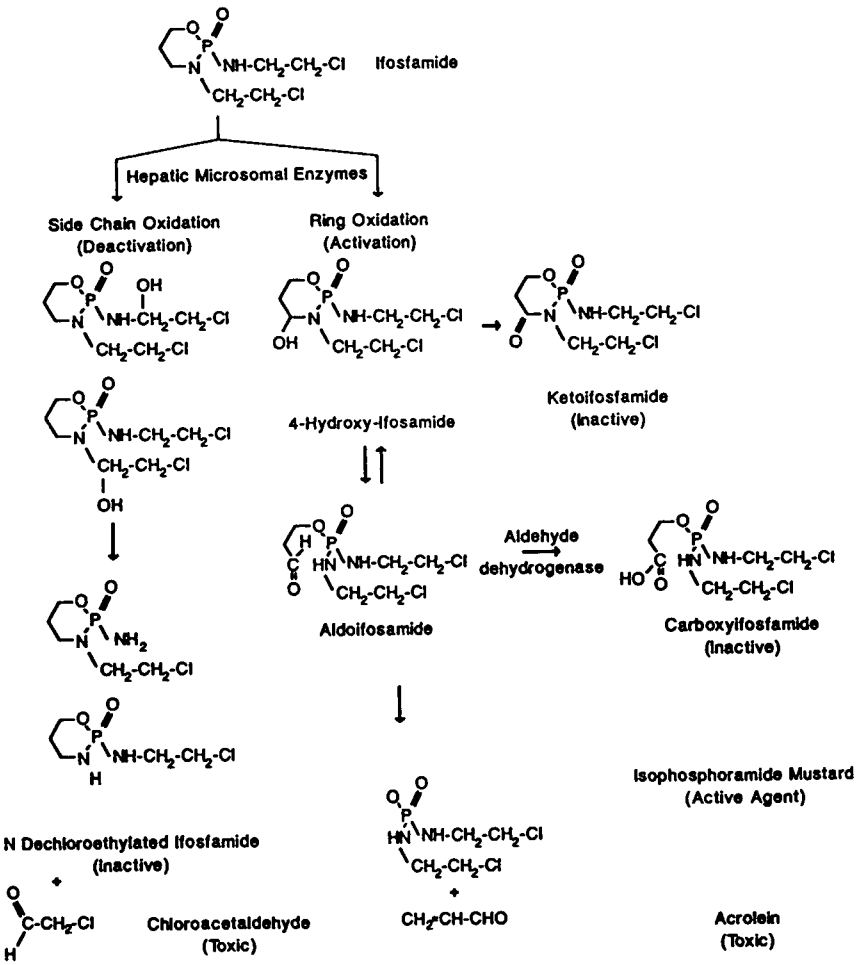


Fig. 2. The metabolic pathways of ifosfamide.

(AUCs) of *R*- and *S*-IFF and their metabolites have been recently measured in women receiving IFF for treatment of pelvic carcinomas [19] and the data are presented in Table 2. The plasma AUC for *R*-IFF was significantly greater than the AUC of *S*-IFF while the AUCs for the metabolites arising from *S*-IFF were greater than those of the metabolites produced from *R*-IFF. It is important to note that *S*-IFF gives rise to *S*-2-DCE-IFF and *R*-3-DCE-IFF while *R*-2-DCE-IFF and *S*-3-DCE-IFF are produced from *R*-IFF; the apparent change in stereochemical configuration is a result of the Cahn–Ingold–Prelog nomenclature system. The results indicate that enantioselective dechloroethylation occurs and favors *S*-IFF.

### 3.3. Neurotoxic side-effects associated with IFF

Neurotoxic side-effects such as cerebellar dysfunction, seizures and changes in mental status have been reported in up to 30% of patients on high-dose IFF [20] and as a dose-limiting toxicity with oral IFF in up to 50% of

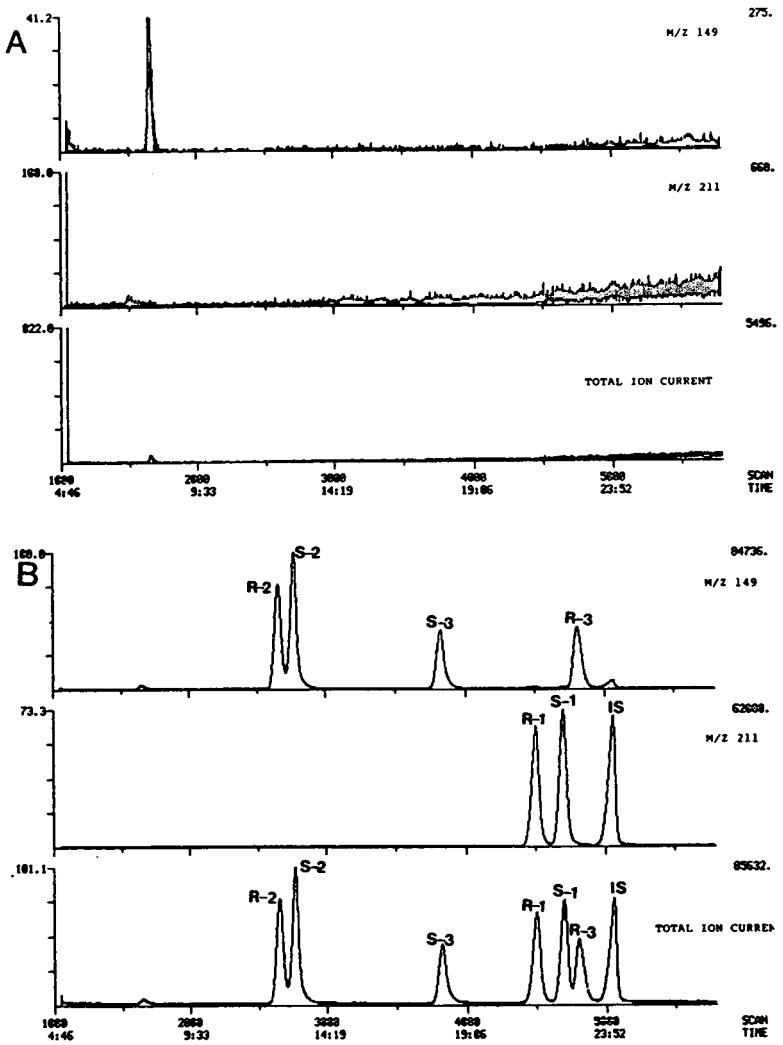


Fig. 3. Typical selected ion chromatograms and total ion current of *rac*-IFF and its metabolites. (A) Blank samples (urine or plasma). (B) Samples (urine or plasma) spiked with 20 $\mu$g/ml IFF and its metabolites. R-2 = *R*-2-DCE-IFF; S-2 = *S*-2-DCE-IFF; S-3 = *S*-3-DCE-IFF; R-1 = *R*-IFF; S-1 = *S*-IFF; R-3 = *R*-3-DCE-IFF; IS = cyclophosphamide (CP). See Ref. [17] for experimental conditions.

the patients [21]. This neurotoxicity has been attributed to the chloroacetaldehyde produced by the metabolic pathway involving side chain oxidation, toxic pathway (Fig. 2). Studies in patients undergoing treatment with IFF have associated CNS toxicity with high blood levels of chloroacetaldehyde [21].

Work in this laboratory has described for the first time a relationship between CNS toxicity and urinary excretion of the dechloroethylated metabolites of IFF [22]. In the study of gynecological cancer described above, the patient with the highest levels of *R*-3-DCE-IFF in urine (28% dose) experienced severe neuro-

Table 2
Plasma area-under-the-curves (AUCs) for *R*- and *S*-ifosfamide (IFF) and their 2- and 3-N-dechloroethylated metabolites (2-DCE-IFF, 3-DCE-IFF) after a 3-h infusion of *rac*-IFF (3 g/m$^2$)

| Compound | AUC (mg/l · h) |
|---|---|
| *R*-IFF | 688 ± 244 |
| *S*-IFF | 515 ± 158 |
| *R*-2-DEC-IFF | 24 ± 8 |
| *S*-2-DCE-IFF | 61 ± 62 |
| *R*-3-DCE-IFF | 121 ± 63 |
| *S*-3-DCE-IFF | 63 ± 46 |

Data obtained fron Ref. [19].

toxicity, precluding any further IFF administration (Table 3, patient 5). When *R*-2-DCE-IFF was elevated, so was *R*-3-DCE-IFF (e.g. patient 5). The same trend was observed for *S*-2-DCE-IFF and *S*-3-DCE-IFF (e.g. patient 4).

### *3.4. Identification of multiple metabolic pathways for IFF*

The results from the patient study indicate that at least two microsomal enzymes, i.e. cytochrome P450 isoenzymes (CYP), are responsible for the N-dechloroethylation of IFF. One CYP catalyzes the transformation of *S*-IFF and *R*-IFF to *S*-2-DEC-IFF and *S*-3-DCE-IFF, respectively, while the other is responsible for the production of *R*-3-DCE-IFF from *S*-IFF and *R*-2-DCE-IFF from *R*-IFF. The existence of at least two CYPs could not have been determined without a careful examination of the enantioselectivity of the N-dechloroethylation process.

The results from the patient studies are consistent with in vivo and in vitro studies in the rat of the effect of phenobarbital induction on the microsomal N-dechloroethylation of IFF. In the in vivo studies [23], the rats were treated with phenobarbital for one-week and then administered a single i.v. dose of IFF. Phenobarbital pretreatment induced the N-dechloroethylation of IFF in an enantioselective manner relative to the controls; in particular, there was a statistically significant increase in the formation of *S*-2-DCE-IFF from *S*-IFF at the apparent expense of the other metabolite of IFF, *R*-3-DCE-IFF. These results suggest that the phenobarbital inducible CYPs are responsible for the observed increases in *S*-2-DCE-IFF and *S*-3-DCE-IFF, but had no effect on *R*-2-DCE-IFF and *R*-3-DCE-IFF.

In order to determine the source of the in vivo effects on IFF metabolism observed after phenobarbital induction an in vitro study was conducted utilizing microsomes prepared from a series of rats pretreated with known inducers of cytochrome P450 isoenzymes [24]. The inducers were: clofibric acid, 2,4-dichlorophenoxyacetic acid and perfluorodecanoic acid (which induce the CYP4A family); phenobarbital (which in-

Table 3
Total 24-h urinary excretion of the enantiomers of 2- and 3-N-dechloroethylated ifosfamide (2-DCE-IFF, 3-DCE-IFF) as per cent of administered dose (% dose)

| Patients and observed CNS toxicity | *S*-2-DCE (% dose) | *R*-2-DCE (% dose) | *S*-3-DCE (% dose) | *R*-3-DCE (% dose) |
|---|---|---|---|---|
| Mean of 8 patients | 6 | 4 | 5 | 13 |
| Patient 5 | 7 | 8 | 6 | 28 |
| Patient 4 | 11 | 4 | 10 | 6 |

duces mainly CYP2Bs but also CYP2Cs and CYP3As); β-naphthoflavone (which inhibits the CYP1A family); and dexamethasone (which induces the CYP3A family). Liver microsomes were prepared using standard techniques from experimental and control animals and the production of DCE-IFF metabolites was monitored by enantioselective GC–MS.

The results from these initial experiments are presented in Fig. 4. From these data it appears that pretreatment with perfluorodecanoic acid (PFDA), clofibric acid (CLOF), 2,4-dichlorophenoxyacetic acid (2,4D) and dexamethasone (DEX) had no significant effect on the dechloroethylation of IFF. However, phenobarbital (PB) induction increased the production of *S*-2-DCE-IFF and *S*-3-DCE-IFF relative to control while having no significant effect on the metabolism of *S*-IFF to *R*-3-DCE-IFF and *R*-IFF to *R*-2-DCE-IFF. These results are consistent with the observations from the in vivo studies with phenobarbital induced rats and indicate that one isoenzyme, PB-inducible (CYPs 2B, 2C or 3A), is responsible for the production of *S*-2-DCE-IFF and *S*-3-DCE-IFF while a second isoenzyme, BF-inhibited (CYP1A), controls the metabolism of IFF to *R*-3-DCE-IFF and *R*-2-DCE-IFF. In humans, CYP3As appear to be implicated [25], but a second CYP has not been identified.

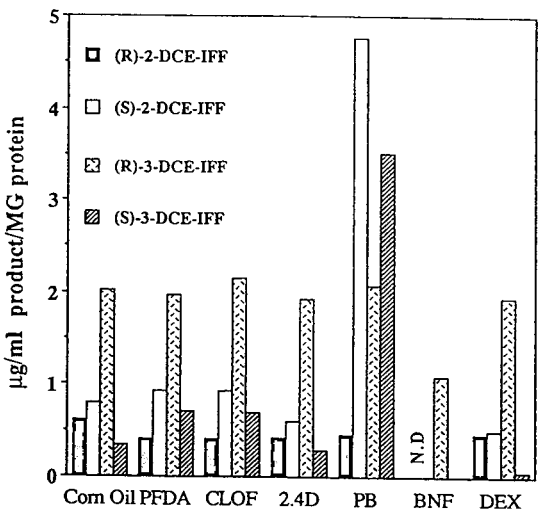


Fig. 4. Effect of microsomal inducers on the in vitro N-dechloroethylation of ifosfamide enantiomers. See Ref. [24] for experimental details. N.D. = Not detected.

## 4. Conclusions

The existence of stereoisomeric forms of a chemical has been a recognized fact for almost 150 years. However, the clinical consequences of symmetry and asymmetry are only just beginning to be considered. The next few years should see a growth in the realization that within the three-dimensional structures of the human body lie tremendous potentials for differential drug actions and, perhaps, new keys to the treatment of cancer and other diseases. The challenge will be to know when we have found these keys.

## References

[1] J.D. Bernal, in *Science in History*, Vol. 2, M.I.T. Press, Cambridge, MA, 1971, p. 608.
[2] H. Hobbs and C. Calnan, *Lancet*, i (1958) 1207.
[3] M. Easterbrook, *Semin Arthritis Rheum.*, 23 (Suppl 2) (1993) 62.
[4] A.J. McLachlan, S.E. Tett and D.J. Cutler, *J. Chromatogr.*, 570 (1991) 119.
[5] S.E. Tett, A.J. McLachlan, R.O. Day and D.J. Cutler, *Agents Actions Suppl.*, 44 (1993) 145.
[6] A.J. McLachlan, S.E. Tett, D.J. Cutler and R.O. Day, *Br. J. Clin. Pharmacol.*, 36 (1993) 78.
[7] J. Ducharme, I.W. Wainer, H. Fieger and S.K.W. Khalil, *Br. J. Clin. Pharmacol.*, in press.
[8] J. Ducharme I.W. Wainer, H.I. Parenteau and J.H. Rodman, *Chirality*, 6 (1994) 337.
[9] I.W. Wainer, J.C. Chen, H. Parenteau, S. Abdullah, J. Ducharme, H. Fieger and J. Iredale, *Chirality*, 6 (1994) 347.
[10] J. Iredale and I.W. Wainer, *J. Chromatogr.*, 573 (1992) 253.
[11] A.J. McLachlan, D.J. Cutler and S.E. Tett, *Eur. J. Clin. Pharmacol.*, 44 (1993) 401.
[12] H. Jurgens, J. Treuner, K. Winkler and U. Gobel, *Seminars Oncol.*, 16 (Suppl. 3) (1989) 46.
[13] L.M. Allen and P.J. Craven, *Cancer Chemother. Rep.*, 56 (1972) 603.
[14] M. Colvin, *Seminars Oncol.*, 9 (Suppl. 1) (1982) 2.
[15] C.P. Granvil, B. Gehrcke, W.A. Konig and I.W. Wainer, *J. Chromatogr.*, 622 (1993) 21.

[16] K. Misiura, A. Okruszek, K. Pankiewick, W.K. Stec, Z. Czownicki, and B. Utracka, *J. Med. Chem.*, 26 (1983) 674.
[17] J. Boss, U. Welslau, J. Ritter, G. Blaschke, and G. Schellong, *Cancer Chemother. Pharmacol.*, 28 (1991) 455.
[18] I.W. Wainer, C.F. Stewart, C.L. Young, D. Measurel, and H. Frank, *Proc. Am. Soc. Clin. Oncol.*, 7 (1988) 72.
[19] J. Ducharme, C.P. Granvil, B. Leyland-Jones, M. Trudeau and I.W. Wainer, *Proc. Am. Assoc. Cancer Res.*, 35 (1994) 423.
[20] L.D. Lewis and C.A. Meanwell, *Lancet*, 335 (1990) 175.
[21] M.J. Lind, H.L. Roberts, N. Thatcher and J.R. Idle, *Cancer Chemother. Pharmacol.*, 26 (1990) 105.
[22] I.W. Wainer, J. Ducharme, C.P. Granvil, B. Leyland-Jones and M. Trudeau, *Lancet*, 343 (1994) 982.
[23] C.P. Granvil, T. Wang, G. Batist and I.W. Wainer, *Drug Metab. Dispos.*, 22 (1994) 165.
[24] I.W. Wainer, J. Ducharme, C.P. Granvil, U. Sanzgiri and A. Parkinson, *Proc. Am. Assoc. Cancer. Res.*, 35 (1994) 423.
[25] D. Walker, J.P. Flinois, S.C. Monkman, C. Beloc, A.V. Boddy, S. Cholerton, A.K. Daly, M.J. Lind, A.D.J. Pearson, P.H. Beaune and J.R. Idle, *Biochem. Pharmacol.*, 47 (1994) 1157.

ELSEVIER

Journal of Chromatography A, 694 (1995) 181–193

JOURNAL OF CHROMATOGRAPHY A

Review

# Stereoselective pharmacokinetics of dihydropyridine calcium antagonists

Yoji Tokuma*, Hideyo Noguchi

*Pharmaceutical and Pharmacokinetic Research Laboratories, Fujisawa Pharmaceutical Co. Ltd., 1-6, 2-Chome, Kashima, Yodogawa-ku, Osaka 532, Japan*

**Abstract**

Many dihydropyridine calcium antagonists are widely used for the treatment of angina and hypertension, and many more are under development. Most of these drugs have one or more chiral centre, and the pharmacological activity between the enantiomers for these drugs is known to be markedly different. First, the stereospecific assay methods for these drugs in plasma or serum are reviewed with emphasis on chiral stationary phase high-performance liquid chromatography for their determination. Next, the stereoselective pharmacokinetics of these drugs (nilvadipine, nitrendipine, felodipine, nimodipine, manidipine, benidipine and nisoldipine) in animals, healthy subjects and patients with hepatic disease is reviewed. Enantiomer–enantiomer interaction, enantiomeric inversion and the stereochemical aspects of pharmacokinetic drug interactions in these drugs are also described.

## Contents



* Corresponding author.

*SSDI* 0021-9673(94)00832-9

## 1. Introduction

Calcium antagonists are currently one of the major classes of cardiovascular drugs, and are valuable and widely used in the treatment of essential hypertension and angina. The development of calcium antagonists has been somewhat unusual, as the three agents that are now in extensive clinical use, verapamil (phenylalkyl amine derivative), diltiazem (benzodiazepine derivative) and nifedipine [1,4-dihydropyridine (DHP) derivative], are chemically unrelated, sharing only the property of blocking calcium slow channels, while otherwise producing disparate pharmacological effects [1,2]. Most of the research on new calcium antagonists during the last decade has principally concerned various derivatives based of the DHP structure; much less has been directed towards the discovery and development of new phenlyalklylamine and benzodiazepine derivatives. Many DHP calcium antagonists have been designed to modify both physico-chemical (photochemical stability, water solubility) and pharmacokinetic properties of the DHP structure while retaining the capacity to block selectively the potential-operated calcium channel. Except for nifedipine, the carbon in position 4 of the DHP ring of all these drugs exhibits chirality due to asymmetric ester moieties. Most of these drugs are used as a racemic mixture, and the pharmacological effects of the enantiomers of these drugs can be different. In nilvadipine, for example, the (*S*)-(+)-enantiomer is about 100 times more potent in relaxing potassium-induced contractions of isolated dog coronary arteries than the (R)-(−)-enantiomer. In the dihydropyridine derivative 202-719 [3,4], furthermore, the (+)-enantiomer is a pure inhibitor of calcium entry, whereas the (−)-enantiomer enhances calcium entry into cells. Thus its enantiomers show opposite actions.

The active processes which are receptor, enzyme or binding dependent, such as renal and biliary secretion, protein binding or drug metabolism, could all be expected to show stereoselectivity. In fact, stereoselectivity in the pharmacokinetics of many drugs has been reported and reviewed [5–12]. Likewise, the pharmacokinetics of racemic DHP calcium antagonists in animals and man have been extensively described and reviewed [13–15]. The common characteristics of these drugs with the exception of amlodipine include extensive first-pass hepatic extraction after oral administration, high clearance and extensive binding to plasma proteins, but stereoselective pharmacokinetic data were not available for these drugs.

In 1987, Tokuma et al. [16] first reported the stereoselective pharmacokinetics in man of a DHP calcium antagonist, nilvadipine. It was shown that the plasma concentrations of the pharmacological more potent (*S*)-enantiomer were about three times higher than those of the (*R*)-enantiomer. Thereafter, the stereochemical aspects of the pharmacokinetics of nilvadipine and other DHP calcium antagonists were extensively studied. This review attempts to bring up to date the information on the stereospecific assay methods for the plasma or serum and the stereoselective pharmacokinetics in animals and man of these drugs. The structures of the selected DHP calcium antagonists covered in this review are shown in Fig. 1. The criteria for inclusion is that data on stereoselective pharmacokinetics in man are available.

## 2. Analytical methods

### *2.1. Chiral stationary phase high-performance liquid chromatography*

Chiral resolution of enantiomers by high-performance liquid chromatography (HPLC) is generally approached in three ways [17,18]: (1) derivatization to corresponding diastereomers using a chiral reagent, followed by achiral (conventional) stationary phase chromatography; (2) addition of chiral reagent to the mobile phase, followed by achiral stationary phase chromatography; (3) separation of the enantiomers on a chiral stationary phase (CSP). Many kinds of CSP columns are now commercially available and they have rapidly become major tools in the analysis of enantiomers [18–20]. It is now possible to separate the anantiomers of DHP cal-

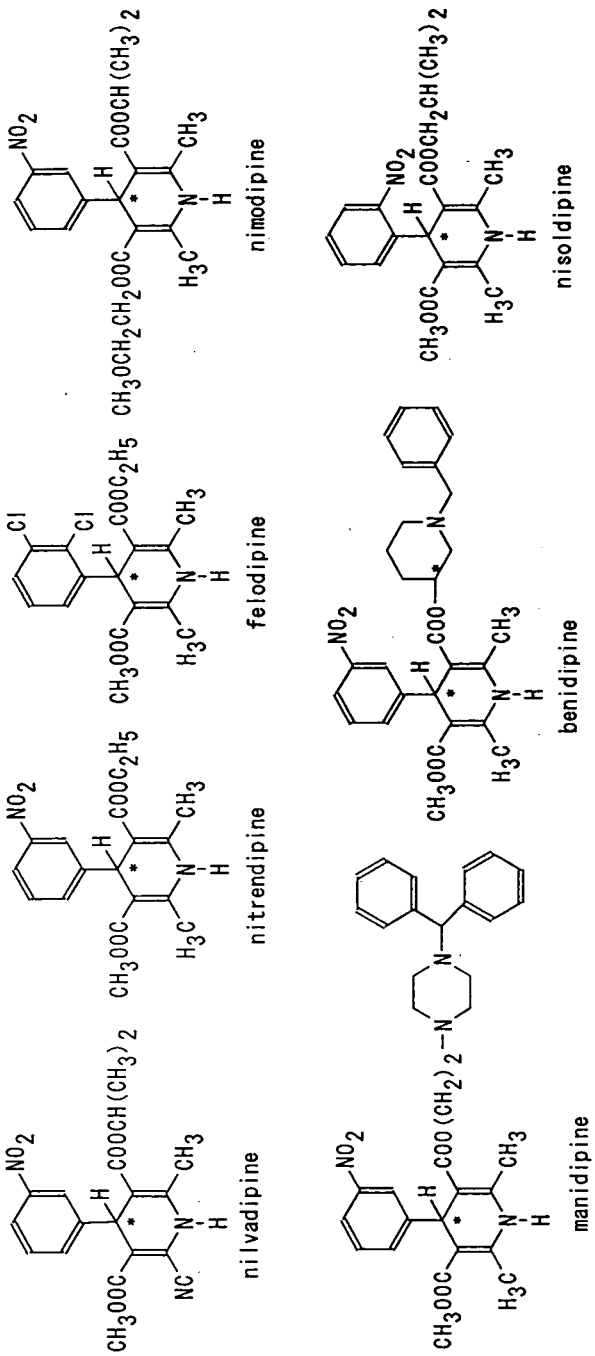


Fig. 1. Structures of dihydropyridine calcium antagonists. The position of the chiral centre is indicated by an asterisk.

cium antagonists with acid glycoprotein [21], polysaccharide phenylcarbamates [22–24] and Pirkle-type [25] CSP-HPLC. Nakagawa et al. [26] used a CSP column for the stereospecific determination of nilvadipine in dog plasma, with a limit of determination of 1 ng/ml (Table 1). However, the limit of quantification was insufficient to assess the kinetic parameters in man, because the concentrations of DHP calcium antagonists in man would be low in relation to the dose applied (2–40 mg), its rapid presystemic elimination and its high apparent volume of distribution [13–15]. Gas chromatography–mass spectrometry (GC–MS) with detection in the electron-capture negative-ion chemical ionization (NICI) mode and gas chromatography–electron capture detection (GC–ECD) using a capillary column have the sensitivity required to obtain the values necessary for human pharmacokinetic studies because concentrations as low as 0.01–0.4 ng/ml can be measured with DHP compounds that possess a phenyl group with a high electron affinity substituent ($NO_2$, Cl, etc.), as in nilvadipine [27,28], nitrendipine [29], felodipine [30], nimodipine [31,32] and nicardipine [33].

Tokuma et al. [16] were the first to report the off-line measurement of a DHP calcium antagonist, nilvadipine, which was separated into enatiomers with a CSP-HPLC system and subsequently quantified by GC–NICI-MS. A HPLC stationary phase that consisted of a chiral poly(triphenylmethyl methacrylate)polymer [Chiralpak OT(+)] was used. This method has also been applied to the sensitive stereospecific determination of nimodipine [34] (Table 1). Soons et al. [35] applied CSP-HPLC combined with GC–ECD to the stereospecific determination of DHP calcium antagonists. A variety of racemic drugs such as nitrendipine and felodipine could be separated and the method applied to serum. This method has also been applied to the stereospecific determination of benidipine [36]. Another successful application of CSP-HPLC combined with sensitive column-switching HPLC [37,38] to the stereospecific determination of manidipine in human serum was reported by Yamaguchi et al. [39]. These methods using CSP-HPLC would be very useful in the study of the pharmacokinetics, metabolism and relationships between kinetics and effects of the enatiomers, as there is no need to synthesize and administer a racemate in which one enantiomer is labelled with a stable isotope (so-called pseudo-racemate) or pure enatiomers.

Table 1
Stereospecific determination for dihydropyridine calcium antagonists in plasma or serum

| Drug | Method | Sensitivity (ng/ml) | Ref. |
|---|---|---|---|
| Nilvadipine | Chiral HPLC and off-line GC–NICI–MS | 0.025 | 16 |
| | Chiral HPLC | 1 | 26 |
| Nitrendipine | Chiral HPLC and off-line GC–ECD | 0.2 | 57 |
| | Pseudo-racemate and GC–NICI-MS | 0.3 | 40 |
| Felodipine | Chiral HPLC and off-line GC–ECD | 0.1 | 36 |
| | Pseudo-racemate and GC–NICI-MS | 0.3 | 41 |
| Nimodipine | Chiral HPLC and off-line GC–NICI-MS | 0.1 | 34 |
| Manidipine | Chiral HPLC and off-line HPLC | 0.2 | 39 |
| Benidipine | Chiral HPLC and off-line GC–ECD | –[a] | 36 |
| Nisoldipine | Pseudo-racemate and GC–NICI-MS | –[a] | 42 |

[a]Data not reported.

### 2.2. Stable isotope technique

The use of individual enantiomers in the study of the pharmacokinetics and metabolism of the enantiomers has limitations. Because of both pharmacodynamic and pharmacokinetic enantiomer–enantiomer interactions, the disposition may be different after administration of the individual enantiomers and racemate [8,9,11]. However, by using a pseudo-racemate in combination with GC–MS, an unequivocal allocation of the respective enantiomers and metabolites formed from the respective enantiomers is possible. This technique relies on the detection of the mass difference between the isotope-labelled and unlabelled drug by MS. This method has been used in the stereospecific determination of nitrendipine [40], felodipine [41] and nisoldipine [42] in plasma or serum (Table 1).

The use of drugs labelled with stable isotopes in combination with GC–MS measurement has been proved to be a powerful tool for simultaneously assessing the disposition and bioavailability of a drug that is administered at same time either by different routes [intravenous (i.v.) versus oral] or two different preparations using the same route of administration (tablet versus solution). This method has been successfully used in both absolute and relative bioavailability studies [43]. Fischer et al. [44] investigated whether a stable labelled drug together with an internal standard labelled differently could be used to combine the two techniques CSP-HPLC and GC–MS, and allow the simultaneous administration of racemic labelled drug i.v. and the racemic unlabelled drug orally. This combination allowed the simultaneous assessment of the absolute bioavailability of the enantiomers. The authors have performed studies with the two DHP calcium antagonists nimodipine and nitrendipine.

## 3. Species differences in stereoselective pharmacokinetics

Tokuma et al. [16,45] examined the pharmacokinetics of nilvadipine enantiomers in healthy subjects, dogs and male and female rats after an oral administration of racemic nilvadipine (Table 2), and showed that $AUC$ and $C_{max}$ were higher

Table 2
Pharmacokinetic parameters of (*S*)- and (*R*)-nilvadipine after oral administration of racemic nilvadipine

| Species | Dose | | $C_{max}$ (ng/ml) | $t_{max}$ (h) | $AUC$ (ng h/ml) | $CL_o$ (ml/min · kg) | $t_{1/2}$ (h) |
|---|---|---|---|---|---|---|---|
| Man | 6 mg | (*S*)-Nilvadipine | 4.11 ± 1.41 | 1.0 ± 0.0 | 11.8 ± 2.3 | 75.5 ± 12.2 | 4.21 ± 0.53 |
| | | (*R*)-Nilvadipine | 1.52 ± 0.53 | 1.0 ± 0.0 | 3.95 ± 0.87 | 229 ± 36 | 3.58 ± 0.21 |
| | | *S*/*R* ratio | 2.78 ± 0.28 | 1.0 ± 0.0 | 3.07 ± 0.30 | 0.34 ± 0.04 | 1.16 ± 0.09 |
| Dog | 1 mg/kg | (*S*)-Nilvadipine | 102 ± 23 | 0.5 ± 0.0 | 392 ± 50 | 22.1 ± 2.3 | 6.46 ± 1.01 |
| | | (*R*)-Nilvadipine | 34.6 ± 9.1 | 0.5 ± 0.0 | 105 ± 16 | 84.8 ± 12.1 | 7.44 ± 0.87 |
| | | *S*/*R* ratio | 3.13 ± 0.32 | 1.0 ± 0.0 | 3.83 ± 0.35 | 0.27 ± 0.03 | 0.85 ± 0.05 |
| Male rat | 10 mg/kg | (*S*)-Nilvadipine | 14.1 | 0.5 | 24.8 | 3360 | –[a] |
| | | (*R*)-Nilvadipine | 23.6 | 0.25 | 41.8 | 1990 | –[a] |
| | | *S*/*R* ratio | 0.60 | 2.0 | 0.59 | 1.69 | |
| Female rat | 10 mg/kg | (*S*)-Nilvadipine | 144 | 0.25 | 264 | 316 | 2.78 |
| | | (*R*)-Nilvadipine | 159 | 0.25 | 276 | 302 | 2.87 |
| | | *S*/*R* ratio | 0.91 | 1.0 | 0.96 | 1.05 | 0.97 |

Values are means ± S.E. ($n = 4$).
[a]Could not be determined.

for more potent (*S*)-(+)-nilvadipine in man and dogs, were lower for the (*S*)-enantiomer in male rats and were almost equal for the (*S*)- and (*R*)-enantiomers in female rats. The *S*/*R* ratios of the apparent oral clearance ($CL_o$) were 0.34, 0.27, 1.69 and 1.05 in man, dogs, male rats and female rats, respectively. The values of $t_{1/2}$ in all species were similar for the (*S*)- and (*R*)-enantiomers. Thus, the stereoselective disposition of nilvadipine was species-dependent and sex-related in rats.

Assuming complete absorption and only liver elimination in the case of nilvadipine [46,47], $CL_o$ based on plasma concentration is represented by the product of free fraction of plasma protein binding ($f_p$) and intrinsic hepatic clearance of free drug [48]. In other words, stereoselectivity of the $CL_o$ is ascribed to the stereoselective differences in plasma protein binding and/or liver metabolism, and therefore stereoselectivity for the plasma protein binding and pyridine formation in the liver microsomes of nilvadipine have been examined [49,50]. The aromatization of nilvadipine and other DHP calcium antagonists to the correspond pyridine has been consistently reported as a primary metabolic step [14,47,51]. In dogs, because the $f_p$ of (*S*)-nilvadipine was only about half that of the (*R*)-enantiomer, the stereoselectivity in plasma protein binding would seem to contribute at least partially to the stereoselective difference in the $CL_o$. However, the *S*/*R* ratios of the $f_p$ values in man and male and female rats were close to unity. Kinetic parameters for oxidation reaction of (*S*)- and (*R*)-nilvadipine to the pyridine analogue by liver microsomes are shown in Table 3. When the substrate concentration is far below $K_m$, intrinsic hepatic clearance is proportional to $V_{max}/K_m$ [52,53]. The *S*/*R* ratios of $V_{max}/K_m$ in man, dogs, male rats and female rats were 0.49, 0.69, 1.59 and 1.23, respectively. The *S*/*R* ratios of the product of $f_p$ and $V_{max}/K_m$ were 0.54, 0.35, 1.81 and 1.21, respectively; these ratios were similar to those of $CL_o$ in vivo. From these results, it is speculated that the differences between (*S*)- and (*R*)-nilvadipine in $CL_o$ for man and male rats are mainly due to the differences in the pyridine formation in the liver microsomes, whereas the difference in dogs is due both to the difference in pyridine formation in the liver microsomes and plasma protein binding. Eriksson et al. [54] have also shown that the oxidative metabolism of felodipine is stereoselective in rats, dogs and human liver microsomes. This difference is expected to give a higher bioavailability of the more potent (*S*)-enantiomer in man, whereas the opposite is expected for rats and dogs. This prediction agreed with in vivo observations in dogs [41] and man [55]. These findings for nilvadipine and felodipine

Table 3
Kinetic parameters for oxidation reaction of (*S*)- and (*R*)-nilvadipine to its pyridine analogue by liver microsomes

| Species | | $V_{max}$ (nmol/mg protein · min) | $K_m$ ($\mu M$) | $V_{max}/K_m$ (ml/mg protein · min) | *S*/*R* ratio for $V_{max}/K_m$ |
|---|---|---|---|---|---|
| Man (A,B,C) | (*S*)-Nilvadipine | 0.927,0.423, 4.71 | 19.6,40.6, 32.7 | 0.0473,0.0104, 0.144 | 0.49 ± 0.03 |
| | (*R*)-Nilvadipine | 0.996,0.392, 4.46 | 10.5,16.1, 16.8 | 0.0949,0.0243, 0.265 | (0.50,0.43,0.54) |
| Dog | (*S*)-Nilvadipine | 3.02 ± 0.15 | 21.9 ± 1.3 | 0.139 ± 0.012 | 0.69 ± 0.2 |
| | (*R*)-Nilvadipine | 2.45 ± 0.15 | 12.2 ± 0.1 | 0.201 ± 0.012 | |
| Male rat | (*S*)-Nilvadipine | 7.48 ± 0.29 | 11.2 ± 0.2 | 0.668 ± 0.021 | 1.59 ± 0.12 |
| | (*R*)-Nilvadipine | 3.37 ± 0.04 | 8.06 ± 0.72 | 0.426 ± 0.041 | |
| Female rat | (*S*)-Nilvadipine | 0.392 ± 0.017 | 2.99 ± 0.16 | 0.131 ± 0.003 | 1.23 ± 0.10 |
| | (*R*)-Nilvadipine | 0.222 ± 0.020 | 2.10 ± 0.28 | 0.108 ± 0.009 | |

Values are individual values for man or means ± S.E. for dogs and rats ($n = 3$).

illustrate that in vitro data are useful for predictions or explanations of in vivo observations.

## 4. Stereoselectivity in human pharmacokinetics

The pharmacokinetics of nilvadipine enantiomers after oral administration of 6 mg of racemic nilvadipine to four healthy subjects have been studied (Fig. 2) [16]. The plasma levels of (*S*)- and (*R*)-nilvadipine in four subjects peaked at 1 h, and the $C_{max}$ and *AUC* of the more potent (*S*)-enantiomer were 2.0–3.2 and 2.4–3.6 times, respectively, higher than those of its optical antipode. The $t_{1/2}$ values were mostly similar. Similar $t_{1/2}$s of the enantiomers regardless of the differential $CL_o$ values have been reported with most DHP antagonists [34,36,42,55–57].

Soons and Breimer [57] examined the pharmacokinetics of nitrendipine enantiomers after 40 μg/kg i.v. and 20 mg oral administration of racemic nitrendipine to healthy subjects. Upon oral administration the bioavailability (*F*) of the more potent (*S*)-enantiomer (13%) was 75% higher than that of the (*R*)-enantiomer (7.9%). The *AUC* and $C_{max}$ for the (*S*)-enantiomer were 90% and 77% higher, respectively, than those for the (*R*)-enantiomer. After i.v. administration, the *AUC* was slightly (7%) higher than that of the (*R*)-enantiomer, but $t_{1/2}$ and $V_{dss}$ were similar. Thus, the stereoselective disposition of nitrendipine in man was dosing route dependent, as reported with high clearance and all hepatically eliminated drugs such as verapamil [58] and propranolol [59]. This is in line with theories on the hepatic elimination of high-clearance drugs [60,61]. A difference in stereoselective pharmacokinetics according to dosing route has also been reported with nisoldipine in man [42] and nilvadipine in dogs [45].

For DHPs of which the stereoselective pharmacokinetics in man and absolute configuration have been reported, the stereoselectivity of plasma concentrations after oral administration of racemate and pharmacological activity are summarized in Table 4. For DHPs (nilvadipine, nitrendipine, felodipine, manidipine and benidipine) which have a methyl ester moiety (Fig. 1), the (*S*)-enantiomers were pharmacologically more potent than the (*R*)-enantiomers and the plasma or serum concentrations of the (*S*)-enantiomers were higher than those of the (*R*)-enantiomers. Although nisoldipine has a methyl ester moiety and the *AUC* of the more potent (+)-enantiomer is reported to be 6.3 times higher than that of (−)-enantiomer [42], data on its absolute configuration are not available. For nimodipine, which has no methyl ester moiety, the (*S*)-enantiomer was pharmacologically more potent but its concentrations were lower. The similarity for stereoselective pharmacokinetics in man of DHP calcium antagonists except for nimodipine suggests that there are identical or closely related rate-limiting steps in the metabolism. The similarity can be explained by the rate-limiting of a single cytochrome P-450 en-

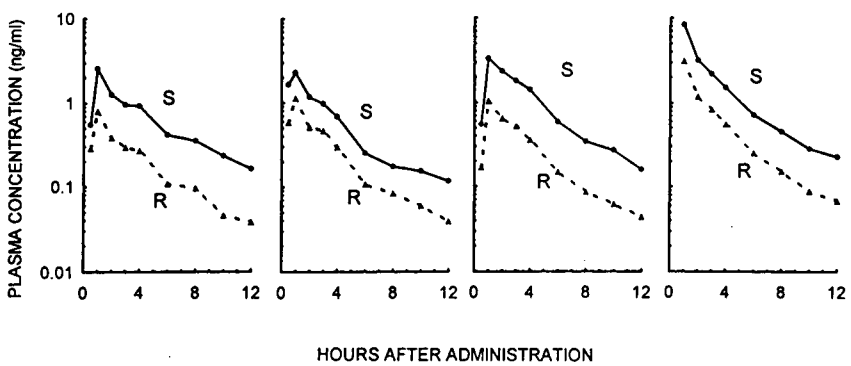


Fig. 2. Plasma concentrations of (*S*)- and (*R*)-nilvadipine in healthy subjects after oral administration of 6 mg of racemic nilvadipine.

Table 4
S/R ratios for plasma or serum enantiomer concentrations in man after oral administration of racemate and pharmacological activity in dihydropyridine calcium antagonists

| Drug | Plasma or serum concentration | Pharmacological activity | Ref. |
|---|---|---|---|
| Nilvadipine | 3.1 (*AUC*) | 100 | 16 |
| Nitrendipine | 1.9,2.2 (*AUC*) | 8,30 | 55,57,62,63 |
| Felodipine | 2.4 (*AUC*) | 3–5,12–13 | 41,55,63 |
| Nimodipine | 0.15 (*AUC*) | 5 | 34,64,81 |
| Manidipine | 2 (concentration) | 30–80 | 56,65 |
| Benidipine | 1.9 ($C_{max}$) | 30–100 | 36 |

zyme in vivo and similar stereoselectivity of the enzyme for these structurally related drugs. Experiments in vitro confirm the presence of a single human cytochrome P-450 enzyme (P-450 IIIA4) which has by far the highest activity towards most if not all DHP calcium antagonists [66–68].

## 5. Inter-individual variability in stereoselective pharmacokinetics

Most clinically used DHP calcium antagonists exhibit wide inter-individual variability in pharmacokinetics after oral administration [69–72], which is caused by extensive and variable presystemic elimination in the liver [73,74]. Wide inter-individual variability in the ratio between plasma levels of the enantiomers has been reported in alprenolol [75] and mephenytoin [76]. For mephenytoin, stereoselective disposition kinetics have been reported to be related to the oxidation phenotype. The subjects in this study were phenotyped as extensive metabolizers (EM) or poor metabolizers (PM) of mephenytoin. In the EM group, the $CL_o$ of (*S*)-mephenytoin was about 170 times that of (*R*)-mephenytoin, whereas in the PM group the $CL_o$ of the enantiomers were apparently similar. Tokuma et al. [77] examined the plasma levels of the enantiomers 1 h (at or near $C_{max}$) after oral administration of 4 mg of racemic nilvadipine to sixteen healthy subjects. The variability in the *S*/*R* ratios [relative standard deviation (R.S.D.) = 21%] of enantiomer concentrations was much less than in the plasma concentration of the enantiomers [R.S.D. = 61% and 66% for the (*S*)- and (*R*)-enantiomers respectively]. Soons et al. [55] investigated the stereoselective pharmacokinetics of the administration of 20 mg each of felodipine and nitrendipine in a randomized cross-over study in twelve healthy subjects. The variability in the *S*/*R* ratio for plasma concentrations of felodipine enantiomers (R.S.D. = 12%) and nitrendipine enantiomers (R.S.D. = 30%) was much less than the variability in the *AUC* of felodipine enantiomers [R.S.D. = 45% for the (*S*)- and (*R*)-enantiomers] and nitrendipine enantiomers (R.S.D. = 80% and 65%). For these DHP calcium antagonists, the variability in stereoselectivity therefore represents only a minor contribution to the observed variability in the pharmacokinetics of racemates, and is only a minor contributor to the variability in the plasma concentrations of the active enantiomers.

## 6. Enantiomer–enantiomer interaction

Nakagawa et al. [26] studied the pharmacokinetics of (*S*)- and (*R*)-nilvadipine in six beagle dogs following oral administration of 0.5 mg/kg of (*S*)-, 0.5 mg/kg of (*R*)- and 1 mg/kg of racemic nilvadipine (Fig. 3). After administration of each enantiomer, a pronounced difference in *AUC*s (*S*, 270; *R*, 70.7 ng h/ml) was observed between the (*S*)- and (*R*)-enantiomers. When the racemate was given, the *AUC*s (*S*, 234; *R*, 78.0 ng h/ml) of the (*S*)- and (*R*)-

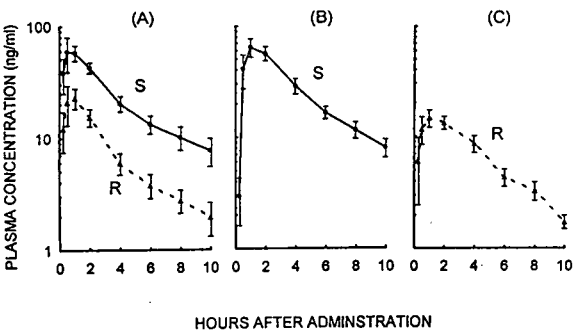


Fig. 3. Plasma concentrations of (*S*)- and (*R*)-nilvadipine in dogs after oral administration of (A) 1.0 mg/kg of racemic, (B) 0.5 mg/kg of (*S*)- and (C) 0.5 mg/kg of (*R*)-nilvadipine. Values are means ± S.E.

enantiomers were not different from the values after administration of either enantiomer, suggesting that there is no enantiomer–enantiomer interaction for the pharmacokinetics of nilvadipine enantiomers in dogs. The $t_{1/2}$ and $t_{max}$ values were not different between the enantiomers, nor were the values different after administration of each enantiomer or racemate. The antipode was not detected in plasma after oral administration of each enantiomer, which indicates that enantiomeric inversion does not occur. Experiments involving the administration of separate enantiomers of nitrendipine to man [40] and of manidipine to dogs [39] also did not reveal any sign of their inter-conversion.

Mast et al. [40] have reported the pharmacokinetics of (*S*)- and (*R*)-nitrendipine in six healthy subjects following random oral administration of 20 mg each of (*S*)-, (*R*)- and racemic nitrendipine {pseudo-racemic mixture of 10 mg of unlabelled (*S*)- and 10 mg of [$^{13}C_4$]-(*R*)-enantiomer}. After administration of each enantiomer, pronounced differences in the *AUC* (*S*, 123.8; *R*, 29.9 ng h/ml), *F* (*S*, 44.6; *R*, 10.7%) and $C_{max}$ (*S*, 72.5; *R*, 14.4 ng/ml) were observed between the (*S*)- and (*R*)-enantiomers. When the racemate was given, the *F* and dose-normalized *AUC* and $C_{max}$ values for the (*S*)-enantiomer were not different from the values after administration of the (*S*)-enantiomer. In contrast, the *F* (*R*, 10.7%; racemate, 22.1%) and dose-normalized *AUC* (*R*, 15.0; racemate, 29.5 ng h/ml) and $C_{max}$ (*R*, 7.2; racemate, 16.8 ng/ml) of the (*R*)-enantiomer were doubled following administration of the racemate as compared with the (*R*)-enantiomer. The $t_{1/2}$ and $t_{max}$ values were not different between the enantiomers, nor were the values different after administration of each enantiomer or racemate. The *F* and dose-normalized *AUC* of (*R*)-nitrendipine doubled after administration of the racemate as compared with (*R*)-nitrendipine, suggesting a metabolic enantiomer–enantiomer interaction with the (*S*)-enantiomer acting as an inhibitor of (*R*)-nitrendipine metabolism.

## 7. Stereoselective pharmacokinetics in hepatic disease

The DHP calcium antagonists are high-clearance drugs and metabolized almost entirely by the liver [13–15,47,78,79]. Hepatic cirrhosis, with its decreases of functional liver mass and reduction of hepatic blood flow, would be expected to be associated with changes in the pharmacokinetics of these drugs. As first-pass metabolism is a major characteristic of the DHP calcium antagonists, a decrease in this factor in hepatic disease would be expected to alter their oral bioavailability, and result in higher plasma concentrations and lower $CL_o$. Various studies have confirmed that chronic cirrhosis can influence the elimination of racemic DHP calcium antagonists, although other chronic or acute liver diseases are associated with no or only slight effects on pharmacokinetics [15,80].

Two studies of the stereoselective pharmacokinetics of DHP calcium antagonists in patients with liver cirrhosis have been reported. Fisher et al. [81] studied the absolute bioavailability of racemic nimodipine in eight patients with liver cirrhosis (2 mg of the stable isotope-labelled racemic analogue simultaneously administered i.v. with 30 mg orally), and found that F was 3.6% for the (*S*)-enantiomer and 20.3% for the (*R*)-enantiomer in healthy subjects and 42.1% for the (*S*)-enantiomer and 67.3% for the (*R*)-enantiomer in the patients. These results revealed a dramatic increase in *F*

in patients with liver cirrhosis. The $CL_o$ values of the enantiomers were significantly reduced and consequently the *AUC*s were significantly greater when compared with the healthy subjects in the control group. The stereoselectivity of $CL_o$ in these patients was reduced to an *S/R* ratio of 1.8 compared with 6.9 in healthy subjects; the $t_{1/2}$ values were increased about 1.5-fold. In the other study, Mettang et al. [82] investigated the stereoselective disposition of nitrendipine in six patients with liver cirrhosis and six age-matched healthy subjects who received 20-mg of racemic nitrendipine. $CL_o$ was 3.6 l/min for the (*S*)-enantiomer and 9.6 l/min for the (*R*)-enantiomer in the healthy subjects, and 0.72 l/min for the (*S*)-enantiomer and 1.33 l/min for the (*R*)-enantiomer in the patients. The stereoselectivity of $CL_o$ in the patients was reduced to an *R/S* ratio of 1.8 compared with 2.7; the $t_{1/2}$ values were increased about twofold. Thus, liver cirrhosis had a profound impact on the pharamacokinetics and stereoselectivity of nimodipine and nitrendipine. In the case of racemic drugs with extensive stereoselective first-pass metabolism such as DHP calcium antagonists, the aspect of altered stereoselective disposition has to be considered.

## 8. Stereochemical aspects of pharmacokinetic drug interaction

Cimetidine is a well known inhibitor of the microsomal cytochrome P-450 mixed-function oxidase system [83], whereas certain flavonoids present in grapefruit juice have also been shown to inhibit cytochrome P-450 IIIA4 activity [84]. P-450 IIIA4 catalyzes the oxidation of DHP ring to form the corresponding pyridine metabolite [66–68]. This oxidation is a predominant metabolic step that determines the extent of first-pass extraction of DHPs [14,47,51]. The interaction with cimetidine has been reported for most racemic DHP calcium antagonists such as nilvadipine, nitrendipine, felodipine, nifedipine, nimodipine and nisoldipine [13–15,85–87]. The interaction with grapefruit juice has also been reported for racemic nitrendipine, felodipine, nifedipine and nisoldipine [88–91]. A few studies with cimetidine have been published in which the stereochemical aspects of pharmacokinetic interactions with verapamil, metoprolol, warfarin and flurbiprofen were evaluated [92–95]. Soons et al. [96] investigated the effects of grapefruit juice (150 ml at −15, −10, −1/4, +5 and +10 h) and cimetidine (200 mg at the same times) on the stereoselective pharmacokinetics of oral administration of 20 mg of racemic nitrendipine in a placebo-controlled crossover study in nine healthy subjects. In all subjects the *AUC* of racemic nitrendipine was increased by grapefruit juice (by 106%) and cimetidine treatment (by 154%). Comparable results were obtained for the $C_{max}$ of the racemic drug and for the *AUC* and $C_{max}$ of (*S*)- and (*R*)-nitrendipine. There was a highly significant difference in the *AUC* and $C_{max}$ between the enantiomers within all treatments: grapefruit juice had no effect on this stereoselectivity, but cimetidine increased the *S/R* ratio of the *AUC* (2.25) by 20% compared with placebo treatment (1.89). The $t_{1/2}$ and $t_{max}$ values were not different within and between treatments. Cimetidine treatment resulted in a small but significant increase in the *S/R* ratio of *AUC*, indicating a more pronounced inhibition of presystemic metabolism of the (*S*)-enantiomer. Grapefruit juice did not show this effect.

## 9. Conclusions

The stereoselective pharmacokinetics of DHP calcium antagonists (nilvadipine, nitrendipine, felodipine, nimodipine, benidipine and nisoldipine) in animals and man have been extensively reported, and is reviewed. The stereoselective pharmacokinetics of nilvadipine have been studied by giving its racemate to man, dogs and male and female rats. After oral administration to man and dogs, the *AUC*s of the pharmacologically more potent (*S*)-enantiomer were 3–4 times those of the (*R*)-enantiomer, whereas in male and female rats the *AUC*s of the (*S*)-enantiomer were 0.59 and 0.96 times those of the (*R*)-enantiomer, respectively. Thus the stereoselective pharmacokinetics of nilvadipine

was species-dependent and sex-related in rats. The stereoselectivity of in vivo kinetics was explained by the stereoselectivity of the aromatization of nilvadipine to the corresponding pyridine in the liver microsomes and plasma protein binding. For DHPs (nilvadipine, nitrendipine, felodipine, manidipine and benidipine), which have a methyl ester moiety, these (*S*)-enantiomers were pharmacologically more potent than the (*R*)-enantiomers and the plasma or serum concentrations of the (*S*)-enantiomers after oral administration to man were higher than those of the (*R*)-enantiomers. Similarity of the stereoselectivity of pharmacokinetics in man and the pharmacological activity of DHP calcium antagonists was observed. Most clinically used DHP calcium antagonists exhibit wide inter-individual variability in pharmacokinetics after oral administration of racemates. The variability in the *S*/*R* for plasma enantiomer concentrations in man of nilvadipine, nitrendipine and felodipine was much less than the variability in the plasma concentration of the enantiomers. After oral administration of racemic nitrendipine to man, the plasma concentrations of the (*S*)-enantiomer were not different from those after administration of the (*S*)-enantiomer alone. In contrast, the plasma concentrations of the (*R*)-enantiomer were doubled following administration of the racemate as compared with the (*R*)-enantiomer alone. This suggests a metabolic enantiomer–enantiomer interaction with the (*S*)-enantiomer acting as an inhibitor of (*R*)-nitrendipine metabolism. Liver cirrhosis had a profound impact on the pharmacokinetics and stereoselectivity of nimodipine and nitrendipine. In the case of racemic drugs with extensive stereoselective first-pass metabolism such as DHP calcium antagonists, the aspect of altered stereoselective disposition has to be considered.

## Acknowledgements

Our thanks are due to the collaboration of Dr. Toshirou Niwa, Mr. Tomoichi Fujiwara, Ms. Tomoko Hashimoto and Ms. Kikuko Nakagawa.

## Symbols and abbreviations

| | |
|---|---|
| $AUC$ | Area under the plasma or serum concentration–time curve |
| $CL_o$ | Apparent oral clearance |
| $CL$ | Total body clearance |
| $C_{max}$ | Maximum plasma or serum concentration |
| CSP | Chiral stationary phase |
| DHP | Dihydropyridine |
| ECD | Electron-capture detection |
| EM | Extensive metabolizer |
| $F$ | Extent of bioavailability |
| $f_p$ | Free fraction of plasma protein binding |
| GC | Gas chromatography |
| HPLC | High-performance liquid chromatography |
| i.v. | Intravenous or intravenously |
| $K_m$ | Michaelis–Menten constant |
| MS | Mass spectrometry |
| NICI | Negative-ion chemical ionization |
| R.S.D. | Relative standard deviation |
| S.D. | Standard deviation |
| S.E. | Standard error |
| $t_{max}$ | Time to reach maximum concentration |
| $t_{1/2}$ | Terminal half-life |
| $V_{dss}$ | Volume of distribution at steady state |
| $V_{max}$ | Maximum rate of metabolism |

## References

[1] W.G. Nayler and J.D. Horowitz, *Pharmacol. Ther.*, 20 (1983) 203.
[2] S.H. Snyder and I.J. Reynolds, *N. Engl. J. Med.*, 313 (1985) 995.
[3] R.P. Hof, U.T. Rüegg, A.Hof and A. Vogel, *J. Cardiovasc. Pharmacol.*, 7 (1985) 689.
[4] S. Kongsamut, T.J. Kamp, R.J. Miller and M.C. Sanguinetti, *Biochem. Biophys. Res. Commun.*, 130 (1985) 141.
[5] E.J. Ariëns, *Eur. J. Clin. Pharmacol.*, 26 (1984) 663.
[6] K. Williams and E. Lee, *Drugs*, 30 (1985) 333.
[7] D.E. Drayer, *Clin. Pharmacol. Ther.*, 40 (1986) 125.
[8] B. Testa, *Trends Pharmacol. Sci.*, 7 (1986) 60.
[9] J. Caldwell, S.M. Winter and A.J. Hutt, *Xenobiotica*, 18 (1988) 59.
[10] F. Jamali, R. Mehvar and F.M. Pasutto, *J. Pharm. Sci.*, 78 (1989) 695.

[11] G.T. Tucker and M.S. Lennard, *Pharmacol. Ther.*, 45 (1990) 309.
[12] D.B. Campbell, *Eur. J. Drug Metab. Pharmacokinet.*, 15 (1990) 109.
[13] D.R. Abernethy and J.B. Schwartz, *Clin. Pharmacokinet.*, 15 (1988) 1.
[14] C.G. Regårdh, C. Bäärnhielm, B. Edgar and K.-J. Hoffmann, in C.G. Gibson (Editor), *Progress in Drug Metabolism*, Vol. 12, Taylor & Francis, London, 1990, Ch. 2, p. 41.
[15] J.G. Kelly and K. O'Malley, *Clin. Pharmacokinet.*, 22 (1992) 416.
[16] Y. Tokuma, T. Fujiwara and H. Noguchi, *J. Pharm. Sci.*, 76 (1987) 310.
[17] B. Testa, *Xenobiotica*, 16 (1986) 265.
[18] H.T. Karnes and M.A. Sarkar, *Pharm. Res.*, 4 (1987) 285.
[19] I.W. Wainer and T.D. Doyle, *J. Chromatogr.*, 284 (1984) 117.
[20] W.H. Pirkle and A. Tsipouras, *J. Chromatogr.*, 291 (1984) 291.
[21] E. Delee, I. Jullien and L. Le Garrec, *J. Chromatogr.*, 450 (1988) 191.
[22] Y. Okamoto, R. Aburatani, K. Hatano and K. Hatada, *J. Liq. Chromatogr.*, 11 (1988) 2147.
[23] Y. Okamoto, K. Hatano, R. Aburatani and K. Hatada, *Chem. Lett.*, (1989) 715.
[24] Y. Okamoto, R. Aburatani, K. Hatada, M. Honda, N. Inotsume and M. Nakano, *J. Chromatogr.*, 513 (1990) 375.
[25] T. Ohkubo, T. Uno and K. Sugawara, *J. Chromatogr., A*, 659 (1994) 467.
[26] K. Nakagawa, T. Niwa, T. Hashimoto, Z. Tozuka, Y. Tokuma and H. Noguchi, *Xenobiot. Metab. Dispos.*, 3 (1988) 594.
[27] Y. Tokuma, T. Fujiwara and H. Noguchi, *Biomed. Environ. Mass Spectrom.*, 13 (1986) 251.
[28] Y. Tokuma, T. Fujiwara, M. Sekiguchi and H. Noguchi, *J. Chromatogr.*, 415 (1987) 156.
[29] C. Fischer, B. Heuer, K. Heuck and M. Eichelbaum, *Biomed. Environ. Mass Spectrom.*, 13 (1986) 645.
[30] M. Ahnoff, *J. Pharm. Biomed. Anal.*, 2 (1984) 519.
[31] G.J. Krol, A.J. Noe and S.C. Yeh, *J. Chromatogr.*, 305 (1984) 105.
[32] P. Jakobsen, E.O. Mikkelsen, J. Laursen and F. Jensen, *J. Chromatogr.*, 374 (1986) 383.
[33] A.T. Wu, I.J. Massey and S. Kushinsky, *J. Chromatogr.*, 415 (1987) 65.
[34] K. Sprockmann and M. Eichelbaum, *Arch. Pharmacol.*, 343 (Suppl.) (1991) R124.
[35] P.A. Soons, M.C.M. Roosemalen and D.D. Breimer, *J. Chromatogr.*, 528 (1990) 343.
[36] H. Kobayashi, H. Magara, S. Okumura and S. Kobayashi, presented at the *5th Japanese–American Conference on Pharmacokinetics and Biopharmaceutics, Tokyo, July 1990*, abstracts, p. 78.
[37] K. Yamashita, M. Motohashi and T. Yashiki, *J. Chromatogr.*, 487 (1989) 357.
[38] T. Miyabayashi, K. Yamashita, I. Aoki, M. Motohashi, T. Yashiki and K. Yatani, *J. Chromatogr.*, 494 (1989) 209.
[39] M. Yamaguchi, K. Yamashita, I. Aoki, T. Tabata, S. Hirai and T. Yashiki, *J. Chromatogr.*, 575 (1992) 123.
[40] V. Mast, C. Fischer, G. Mikus and M. Eichelbuam, *Br. J. Clin. Pharmacol.*, 33 (1992) 51.
[41] U.G. Eriksson, K.-J. Hoffmann, R. Simonsson and C.G. Regårdh, *Xenobiotica*, 21 (1991) 75.
[42] N. Frost, G. Ahr, H. Weber, W. Wingender and J. Kuhlmann, in J. Kuhlmann and W. Wingender (Editors), *Dose–Response Relationship of Drugs*, W. Zuckschwerdt, Munich, 1990, p. 87.
[43] M. Eichelbaum, G.E. von Unruh and A. Somogyi, *Clin. Pharmacokinet.*, 7 (1982) 490.
[44] C. Fischer, F. Schönberger, W. Mück, K. Heuck and M. Eichelbaum, *J. Pharm. Sci.*, 82 (1993) 244.
[45] Y. Tokuma, T. Fujiwara, T. Niwa, T. Hashimoto and H. Noguchi, *Res. Commun. Chem. Pathol. Pharmacol.*, 63 (1989) 249.
[46] Y. Tokuma, T. Fujiwara and H. Noguchi, *Xenobiotica*, 17 (1987) 1341.
[47] T. Niwa, Y. Tokuma and H. Noguchi, *Xenobiotica*, 18 (1988) 217.
[48] M. Gibaldi and D. Perrier, *Pharmacokinetics*, Marcel Dekker, New York, 2nd ed., 1982.
[49] T. Niwa, Y. Tokuma, K. Nakagawa, H. Noguchi, Y. Yamazoe and R. Kato, *Res. Commun. Chem. Pathol. Pharmacol.*, 60 (1988) 161.
[50] T. Niwa, Y. Tokuma, K. Nakagawa and H. Noguchi, *Drug Metab. Dispos.*, 17 (1989) 64.
[51] C. Bäärnhielm, I. Skånberg and K.O. Borg, *Xenobiotica*, 14 (1984) 719.
[52] A. Rane, G.R. Wilkinson and D.G. Shand, *J. Pharmacol. Exp. Ther.*, 200 (1977) 420.
[53] A. Rane, J. Säwe, B. Lindberg, J.-O. Svensson, M. Garle, R. Erwald and H. Jorulf, *J. Pharmacol. Exp. Ther.*, 229 (1984) 571.
[54] U.G. Eriksson, J. Lundahl, C. Bäärnhielm and C.G. Regårdh, *Drug Metab. Dispos.*, 19 (1991) 889.
[55] P.A. Soons, T.M.T. Mulders, E. Uchida, H.C. Schoemaker, A.F. Cohen and D.D. Breimer, *Eur. J. Clin. Pharmacol.*, 44 (1993) 163.
[56] M. Yamaguchi, T. Miyabayashi, I. Aoki and T. Yashiki, *Xenobiot. Metab. Dispos.*, 4 (1989) 252.
[57] P.A. Soons and D.D. Breimer, *Br. J. Clin. Pharmacol.*, 32 (1991) 11.
[58] B. Vogelgesang, H. Echizen, E. Schmidt and M. Eichelbaum, *Br. J. Clin. Pharmacol.*, 18 (1984) 733.
[59] C. von Bahr, J. Hermansson and K. Tawara, *Br. J. Clin. Pharmcol.*, 14 (1982) 79.
[60] G.R. Wilkinson and D.G. Shand, *Clin. Pharmacol. Ther.*, 18 (1975) 377.
[61] T. Walle and U.K. Walle, *Trends Pharmacol. Sci.*, 7 (1986) 155.
[62] H. Meyer, F. Bossert, E. Wehinger, R. Towart and P. Bellemann, *Hypertension*, 5 (Suppl. II) (1983) II-2.

[63] M. Eltze, R. Boer, K.H. Sanders, H. Boss, W.-R. Ulrich and D. Flockerzi, *Chirality*, 2 (1990) 233.
[64] R. Towart, E. Wehinger, H. Meyer and S. Kazda, *Arzneim.-Forsch.*, 32 (1982) 338.
[65] M. Kajino, Y. Wada, Y. Nagai, A. Nagaoka and K. Meguro, *Chem. Pharm. Bull.*, 37 (1989) 2225.
[66] R.H. Böcker and F.P. Guengerich, *J. Med. Chem.*, 29 (1986) 1596.
[67] F.P. Guengerich and R.H. Böcker, *J. Biol. Chem.*, 263 (1988) 8168.
[68] F.P. Guengerich, W.R. Brian, M. Iwasaki, M.-A. Sari, C. Bäärnhielm and P. Berntsson, *J. Med. Chem.*, 34 (1991) 1838.
[69] E. Blychert, B. Edgar, D. Elmfeldt and T. Hedner, *Br. J. Clin. Pharmacol.*, 31 (1991) 15.
[70] B. Edgar, P. Lundborg and C.G. Regårdh, *Drugs*, 34 (Suppl. 3) (1987) 16.
[71] C.H. Kleinbloesem, P. van Brummelen, H. Farber, M. Danhof, N.P.E. Vermeulen and D.D. Breimer, *Biochem. Pharmacol.*, 33 (1984) 3721.
[72] P.A. Soons, A.G. De Boer, P. van Brummelen and D.D. Breimer, *Br. J. Clin. Pharmacol.*, 27 (1989) 179.
[73] F.P. Guengerich, M.V. Martin, P.H. Beaune, P. Kremers, T. Wolff and D.J. Waxman, *J. Biol. Chem.*, 261 (1986) 5051.
[74] V.F. Challenor, D.G. Waller, A.G. Renwick, B.S. Gruchy and C.F. George, *Br. J. Clin. Pharmacol.*, 24 (1987) 473.
[75] J. Hermansson and C. von Bahr, *J. Chromatogr.*, 227 (1982) 113.
[76] P.J. Wedlund, W.S. Aslanian, E. Jacqz, C.B. McAllister, R.A. Branch and G.R. Wilkinson, *J. Pharmacol. Exp. Ther.*, 234 (1985) 662.
[77] Y. Tokuma, T. Fujiwara and H. Noguchi, *Res. Commun. Chem. Pathol. Pharmacol.*, 57 (1987) 229.
[78] M. Terakawa, Y. Tokuma, A. Shishido and H. Noguchi, *J. Clin. Pharmacol.*, 27 (1987) 111.
[79] Y. Tokuma, M. Sekiguchi, T. Niwa and H. Noguchi, *Xenobiotica*, 18 (1988) 21.
[80] A. von Nieciecki, H.J. Huber and F. Stanislaus, *J. Cardiovasc. Pharmacol.*, 20 (Suppl. 6) (1992) S22.
[81] C. Fischer, K. Sporckmann, W. Mück and K. Heuck, *Arch. Pharmacol.*, 345 (Suppl. 1) (1992) R7.
[82] T. Mettang, C. Fischer and M. Eichelbaum, *Arch. Pharmacol.*, 347 (Suppl.) (1993) R37.
[83] A. Somogyi and M. Muirhead, *Clin. Pharmacokinet.*, 12 (1987) 321.
[84] A. Miniscalco, J. Lundahl, C.G. Regårdh, B. Edgar and U.G. Eriksson, *J. Pharmacol. Exp. Ther.*, 261 (1992) 1195.
[85] W. Kirch, C.H. Kleinbloesem and C.G. Belz, *Pharmcol. Ther.*, 45 (1990) 109.
[86] K.D. Schlanz, S.A. Myre and M.B. Bottorff, *Clin. Pharmacokinet.*, 21 (1991) 344.
[87] K.D. Schlanz, S.A. Myre and M.B. Bottorff, *Clin. Pharmacokinet.*, 21 (1991) 448.
[88] D.G. Bailey, C. Munoz, J.M.O. Arnold, H.A. Strong and J.D. Spence, *Clin. Pharmacol. Ther.*, 51 (1992) 156.
[89] D.G. Bailey, J.D. Spence, C. Munoz, J.M.O. Arnold, *Lancet*, 337 (1991) 268.
[90] D.G. Bailey, J.M.O. Arnold, C. Munoz and J.D. Spence, *Clin. Pharmacol. Ther.*, 53 (1993) 637.
[91] D.G. Bailey, J. Malcolm, O. Arnold, H.A. Strong, C. Munoz and J.D. Spence, *Clin. Pharmacol. Ther.*, 54 (1993) 589.
[92] G. Mikus, M. Eichelbaum, C. Fischer, S. Gumulka, U. Klotz and H.K. Kroemer, *J. Pharmcol. Exp. Ther.*, 253 (1990) 1042.
[93] S. Toon, E.M. Davidson, F.M. Garstang, H. Batra, R.J. Bowes and M. Rowland, *Clin. Pharmacol. Ther.*, 43 (1988) 283.
[94] S. Toon, K.J. Hopkins, F.M. Garstang and M. Rowland, *Eur. J. Clin. Pharmacol.*, 32 (1987) 165.
[95] R.E. Small, S.R. Cox and W.J. Adams, *J. Clin. Pharmacol.*, 30 (1990) 660.
[96] P.A. Soons, B.A.P.M. Vogels, M.C.M. Roosemalen, H.C. Schoemaker, E. Uchida, B. Edgar, J. Lundahl, A.F. Cohen and D.D. Breimer, *Clin. Pharmacol. Ther.*, 50 (1991) 394.

ELSEVIER

Journal of Chromatography A, 694 (1995) 195–208

JOURNAL OF CHROMATOGRAPHY A

Review

# Diastereomeric β-lactam antibiotics Analytical methods, isomerization and stereoselective pharmacokinetics

Tomoo Itoh, Hideo Yamada*

*Department of Pharmacokinetics and Biopharmaceutics, School of Pharmaceutical Sciences, Kitasato University, 5-9-1 Shirokane, Minato-ku, Tokyo 108, Japan*

**Abstract**

Stereospecific HPLC methods for the determination of various diastereomeric β-lactam antibiotics are reviewed. Stereoselectivity in the absorption, distribution and excretion of several diastereomeric β-lactams is summarized. The isomerization of β-lactam isomers and its influence on the pharmacokinetics and pharmacodynamics are discussed.

## Contents



* Corresponding author.

0021-9673/95/$09.50 
*SSDI* 0021-9673(94)00932-5

## 1. Introduction

Pencillins and cephalosporins are prepared by reaction of the appropriate acylating agent with 6-aminopenicillanic acid or 7-aminocephalosporanic acid. If the acylating agent is a mixture of optical isomers, the penicillin or cephalosporin obtained is a mixture of two diastereomers with a racemic side-chain. It is known that the antimicrobial activities of the diastereomers thus obtained are not identical [1–4]. As the D-epimers of ampicillin, amoxicillin, azidocillin, cephalexin and cephaloglycin are considerably more potent than their corresponding L-epimers, only the more active epimer is prepared as a commercial form. The antimicrobial activities are also different between the epimers of phenethicillin, propicillin, clometocillin. However, as the differences in antimicrobial activities are small, the use of pure epimers may not be necessary for these penicillins. On the other hand, the biological activities of carbenicillin epimers have been reported to be equivalent, probably owing to rapid epimerization during biological assay procedures.

However, the information appears to be limited with regard to the stereospecific analytical methods and the differences in pharmacokinetics for diastereomeric $\beta$-lactam antibiotics. In this review, methods for the determination of various diastereomeric $\beta$-lactam antibiotics are summarized. The discussions are extended to the isomerization of the diastereomers, its influence on the pharmacokinetics and the differences between diastereomers in the processes of absorption, distribution and disposition.

## 2. Analytical methods

Proton nuclear magnetic resonance ($^1$H NMR) has been successfully utilized to determine the configuration at C-10 for the penicillins which possess an aromatic group attached to C-10 [4,5]. The differences in chemical shifts between the epimers were attributed to the shielding effect of the aromatic ring in the side-chain, which was caused by the folded conformation. Although the ratios of sulbenicillin epimers in various preparations were quantitatively determined by $^1$H NMR spectroscopy, high-performance liquid chromatography (HPLC) appears to be most convenient for the determination of diastereomeric $\beta$-lactam antibiotics. Therefore, stereospecific HPLC methods reported for various diastereomeric $\beta$-lactams (Fig. 1) are summarized in this section.

### 2.1. Carbenicillin

Carbenicillin epimers (**1**) were determined by reversed-phase HPLC using a $\mu$Bondapak $C_{18}$ column (300 × 4.0 mm I.D.) [6]. The mobile phase was methanol–0.01 *M* tetrabutylammonium bromide (4:7, v/v) at a flow-rate of 3.0 ml/min. Carbenicillin was detected at 254 nm. Two epimers were incompletely resolved under these conditions. When the mobile phase changed to methanol–0.05% acetic acid, the resolution was even poorer. On the other hand, the D-(−)-epimer content in the commercial preparation was 55% as determined by $^1$H NMR.

Carbenicillin epimers were also determined by Gupta and Stewart [7]. The analytical column used was $\mu$Bondapak phenyl (300 × 4 mm I.D.) with 0.01 *M* ammonium acetate as the mobile phase. The flow-rate was 1.6 ml/min and the epimers were detected at 245 nm. The two epimers were resolved close to the baseline, but the absolute configurations of the eluted peaks were not determined.

An HPLC method for the determination of carbenicillin epimers was also reported by Twomey [8]. Carbenicillin epimers were determined with a Spherisorb ODS column (150 × 4.6 mm I.D.) using methanol–0.05 *M* $KH_2PO_4$ (37:63, v/v) as the mobile phase. Tetrabutylammonium bromide (0.1%, w/v) was added as the ion-pair reagent, and the pH was adjusted with 10% $H_3PO_4$. The flow-rate was 1.2 ml/min and the epimers were detected at 220 nm. Carbenicillin epimers could be either resolved or eluted as a single peak, depending on the mobile phase pH. The resolution was very poor at pH 3.00 and 3.70, and the epimers eluted as a single peak at

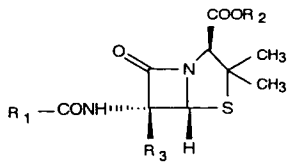


| | $R_1$ | $R_2$ | $R_3$ |
|---|---|---|---|
| 1 | 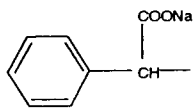 | Na | H |
| 2 | 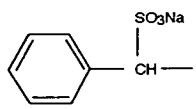 | Na | H |
| 3 | 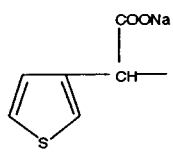 | Na | $OCH_3$ |
| 4 | 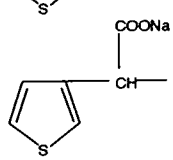 | Na | H |
| 5 | 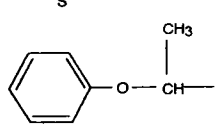 | K | H |
| 6 | 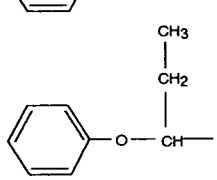 | K | H |
| 7 | 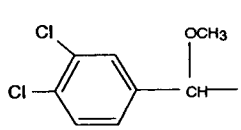 | H | H |
| 8 | 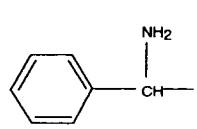 | H | H |
| 9 | 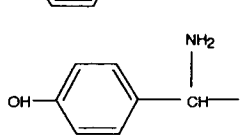 | H | H |
| 10 | 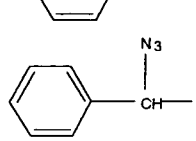 | K | H |

Fig. 1. (*Continued on p. 198.*)

11

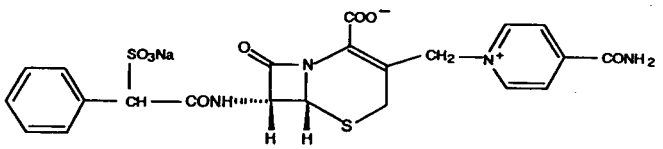


12

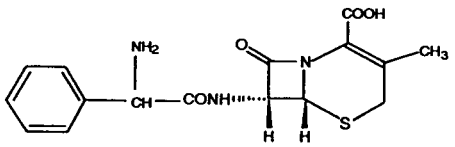


13

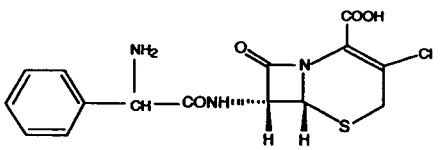


14

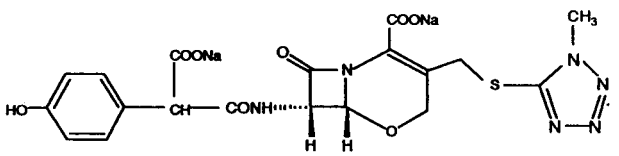


15

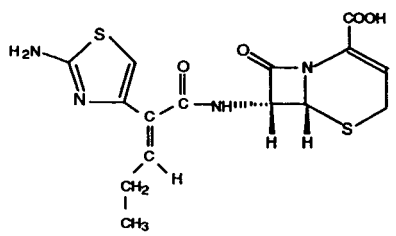


Fig. 1. Structures of diastereomeric β-lactam antibiotics.

pH 3.35. Although carbenicillin epimers were fairly well resolved at pH 4.35, baseline resolution was not achieved. Absolute configurations of the eluting epimers were not determined.

An HPLC method developed by Hoogmartens et al. [4] employed a Zorbax $C_8$ column (250 × 4.6 mm I.D.) with a mobile consisting of methanol–water–5% 0.2 *M* phosphate buffer (pH 7.0). The flow-rate was 1.0 ml/min and carbenicillin epimers were detected at 254 nm. With 5% methanol in the mobile phase, the two epimers were resolved close to the baseline. As the absolute configurations of the eluting epimers were not determined, it was not known which epimer eluted faster under their HPLC conditions. However, it is most likely that the D- (or *R*-) epimer eluted faster according to the results obtained by Aso et al. [9]. They also found that the content of the first-eluting epimer was ca. 54% in commercial preparations, which suggested that the commercial preparations did not contain equal amounts of each epimer.

Hashimoto et al. [10] also reported an HPLC method for epimerization studies in aqueous solutions. A Nucleosil $5C_{18}$ column (150 × 4.6 mm I.D.) with a mobile phase consisting of 0.05 *M* ammonium acetate–methanol (17:1) was used for the determination of carbenicillin epimers. Also, a glass column (86 × 3 cm I.D.) packed with porous polystyrene was used to isolate each carbenicillin epimer in their study.

For epimerization studies in aqueous solutions, Aso et al. [9] developed an HPLC method for carbenicillin epimers. A TSKgel ODS-80TM column (150 × 4.6 mm I.D.) with a mobile phase consisting of 0.05 *M* phosphate (pH 7.0)–methanol (4:1) was used and carbenicillin epimers were detected at 220 nm. The D- (or *R*-) epimer eluted faster than the L- (or *S*-) epimer with retention times of ca. 5 and 6 min for D- and L-carbenicillin, respectively. The two epimers were baseline separated.

Ishida et al. [11] reported an HPLC method for the determination of carbenicillin epimers in biological fluids. Plasma and urine samples were prepared for HPLC by solid-phase extraction using SAX-Bond Elut. Analytical column used was Cosmosil $5C_{18}$-AR (250 × 4.6 mm I.D.) with a mobile phase consisting of 0.05 *M* ammonium acetate–methanol (9:1, v/v). The flow-rate was 1.2 ml/min and carbenicillin epimers were detected at 254 nm. The method was applicable to plasma and urine samples from humans, rats and rabbits. The epimers were resolved to the baseline with no interfering peaks (Fig. 2). The *R*-epimer eluted faster than the *S*-epimer with retention times of ca. 18 and 23 min for the *R*- and *S*-epimers, respectively. In their studies, carbenicillin epimers were resolved and isolated using a glass column (100 × 3 cm I.D.) packed with porous polystyrene (250–800-μm particle size), and the absolute configurations of the epimers were assigned using $^1$H NMR. The *R*- to *S*-epimer ratio (*R*/*S* ratio) was ca. 1.1 for carbenicillin disodium salt purchased from Sigma.

### 2.2. Cefsulodin

An HPLC method for the determination of cefsulodin epimers (**11**) was reported by Fujita and Koshiro [12] using a μBondapak $C_{18}$ column (300 × 3.9 mm I.D.). They used two kinds of mobile phase compositions; mobile A consisted of 0.0168 *M* dibasic ammonium phosphate–acetic acid–methanol (100:1.68:5.98) containing 5 m*M* triethylamine, and mobile phase B consisted of an aqueous solution (containing 0.0388 *M* ammonium acetate, 0.292 m*M* dibasic ammonium phosphate and 9.363 μ*M* triethylamine) – acetonitrile – methanol – dimethylformamide

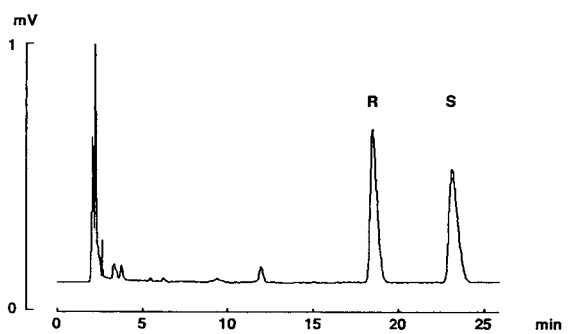


Fig. 2. Chromatogram of human plasma spiked with carbenicillin. R = *R*-epimer and S = *S*-epimer.

–acetic acid (1000:7.6:1.05:1.31:0.30). For both mobile phase compositions, the flow-rate was 1.2 ml/min and cefsulodin epimers were detected at 260 nm. Phthalic acid and tegafur were used as internal standards for mobile phase A and B, respectively. For both mobile phase compositions L-(+)-cefsulodin eluted faster than D-(−)-cefsulodin, and the two epimers were separated to the baseline. Commercial preparations contain only the D-(−)-epimer, which is the more active isomer.

### 2.3. Ceftibuten

Ceftibuten (**15**) is an oral cephem antibiotic which possesses a double bond in the side-chain. Although commercially available formulations contain only the *cis* isomer, HPLC methods for the determination of both *cis* and *trans* isomers were developed because the isomerization from the *cis* to *trans* isomer was observed in vivo. Matsuura et al. [13] developed an automated HPLC method for the determination of ceftibuten isomers in plasma and urine using a column-switching technique. Nucleosil $5C_{18}$ (150 × 4.6 mm I.D.) was used as an analytical column. The mobile phase for plasma assay was [10 m*M* tetra-*n*-butylammonium bromide–2 m*M* monobasic ammonium phosphate (pH 5.0)]–acetonitrile–methanol (25:6:3, v/v/v), and that for urine assay was an aqueous mixture of three salts (5 m*M* tetra-*n*-butylammonium bromide, 5 m*M* tetra-*n*-amylammonium bromide and 8 m*M* monobasic ammonium phosphate)–acetonitrile–methanol (65:25:10, v/v/v). The flow-rate was 1.5 ml/min and the isomers were detected at 256 nm in both plasma and urine assays. In the plasma assay, the *trans* isomer eluted faster than the *cis* isomer with retention times of 20.8 and 22.9 min, respectively. The *trans* isomer also eluted faster than the *cis* isomer in the urine assay with the retention times of 18.6 and 20.0 min, respectively.

An HPLC method for ceftibuten isomers was also reported by Shimada et al. [14]. A Nucleosil $10C_{18}$ column (150 × 4 mm I.D.) was used with a mobile phase consisting of tetrabutylammonium phosphate–acetonitrile–methanol (50:6:3, v/v/v). The flow-rate was 1.2 ml/min and the isomers were detected at 256 nm. The retention times of the *cis* and *trans* isomers were 10.7 and 12.3 min, respectively. Although the HPLC conditions were similar to those reported by Matsuura et al., the elution order was different.

### 2.4. Cephalexin

Cephalexin epimers (**12**) were determined by Salto [3] with a μBondapak $C_{18}$ column (300 × 4 mm I.D.) The mobile phase was 0.1 *M* phosphate buffer (pH 3.5) containing 5% methanol at a flow-rate of 1.5 ml/min and the epimers were detected at 254 nm. The two epimers were separated to the baseline with retention times of ca. 10 and 20 min for the L- and D-epimers, respectively.

Cephalexin epimers in rat serum and urine were separated by Tamai et al. [15] using TSKgel ODS-80TM (150 × 4.6 mm I.D.) as an analytical column. The mobile phase compositions were methanol–10 m*M* ammonium acetate (20:80) for the determination of the D-epimer and methanol–10 m*M* phosphate buffer (pH 3.0) containing 10 m*M* ammonium acetate and 10 m*M* pentanesulphonic acid (10:90) for the L-epimer. The flow-rate was 1.0 ml/min and the epimers were detected at 260 nm. No information on the resolution was given.

HPLC methods for cephalexin have also been reported by Hendrix et al. [16] using various ODS columns under the conditions prescribed in the European Pharmacopoeia and the US Pharmacopeia. The mobile phase composition was methanol–acetonitrile–1.36% (w/v) aqueous $KH_2PO_4$–water (2:5:10:85, v/v) or water–acetonitrile–methanol–triethylamine–sodium 1-pentanesulphonate (850:100:50:15:1, v/v/v/v/w). The flow-rate was 1.5 ml/min and cephalexin epimers were detected at 254 nm. Resolution of the epimers appeared to be good as judged by the differences in capacity factors.

Cephalexin epimers were also separated using poly(styrene–divinylbenzene) as the stationary phase [16,17]. The mobile phase was acetonitrile–0.02 *M* sodium 1-octanesulphonate–0.2 *M* phosphoric acid–water (15.5:10:5:69.5,

v/v) at a flow-rate of 1.0 ml/min. Cephalexin epimers were detected at 254 nm. Baseline separation of the two epimers was observed under the HPLC conditions.

### 2.5. Moxalactam

There have been several reports on HPLC method for the determination of moxalactam epimers (**14**). Konaka et al. [18] used Nucleosil $10C_{18}$ (300 × 4 mm I.D.) as an analytical column. The mobile phases used were as follows: methanol–0.05 *M* monobasic potassium phosphate (5:95) adjusted to pH 6.5 at a flow-rate of 2.0 ml/min for raw material analysis, and methanol–0.005 *M* tetra-*n*-butylammonium phosphate (25:75) adjusted to pH 6.0 at a flow-rate of 1.0 ml/min for the urine analysis. Moxalactam epimers were detected at 254 nm. Urine samples were prepared for HPLC by solid-phase extraction using a Sep-Pak cartridge. The *R*-epimer eluted faster than the *S*-epimer under both HPLC conditions. The *R*/*S* ratios in the raw materials were 1.05–1.11.

Determination of moxalactam epimers in plasma and urine was also reported by Miner et al. [19]. Plasma samples were deproteinized with ice-cold methanol and the epimers were separated with a Chromegabond $C_{18}$ column (30 × 4.6 mm I.D.) using 0.1 *M* ammonium acetate–acetonitrile (95:5) adjusted to pH 6.5 as the mobile phase. The flow-rate was 1.5 ml/min, and moxalactam epimers were detected at 270 nm. Urine samples were analysed with a Zorbax TMS column (250 × 4.6 mm I.D.) using 5 m*M* *n*-heptylamine in 11% methanol–distilled water (pH adjusted to 6.0). The flow rate was 1.4 ml/min, and the epimers were detected at 280 nm. The *R*-epimer eluted faster than the *S*-epimer under their HPLC conditions. After oral administration of moxalactam, the plasma concentrations were determined with both HPLC and biological assays, with a good correlation between the two methods.

The HPLC method developed by Aravind et al. [20] employed a Perkin-Elmer $C_{18}$-ODS-HC-SIL-X column (250 × 4.6 mm I.D.). The mobile phase was methanol–10 m*M* ammonium acetate (pH 6.5) (4:96). The flow-rate was 1.0 ml/min and moxalactam epimers were detected at 230 nm. The retention times of moxalactam epimers were 2.16 and 2.63 min, but the absolute configurations of the eluting epimers were not determined. In the commercial preparation, the ratio of the first to second peak was 54:46, suggesting that the content of one epimer was greater than that of the other. Serum, cerebrospinal fluid and urine samples were also analysed with the same HPLC method after deproteinization with ice-cold methanol. 8-Chlorotheophylline was used as an internal standard.

Ziemniak et al. [21] reported an HPLC method for moxalactam using a μBondapak $C_{18}$ column. The mobile phase was acetonitrile–0.05 *M* ammonium acetate (3:97) with a flow-rate of 1.5 ml/min. Moxalactam epimers were detected at 275 nm. Plasma and urine samples were acidified with hydrochloric acid and were extracted with ethyl acetate. The organic layer was then back-extracted into tromethamine buffer (pH 8.0), which was subjected to HPLC analysis. Allopurinol was used as an internal standard. The D-epimer eluted faster than the L-epimer, with retentions times of 7.8 and 10.5 min, respectively. The two epimers were separated to the baseline with no interfering peaks on the chromatogram.

Moxalactam epimers in serum and myometrial tissue were separated by Bawdon et al. [22] using a μBondapak $C_{18}$ column. The mobile phase was 0.1 *M* sodium phosphate–methanol (84:16) at pH 3.2. The flow-rate was 2.0 ml/min and the epimers were detected 254 nm. The *R*-epimer eluted faster than the *S*-epimer under their HPLC conditions. They observed a good correlation between the HPLC and microbiological assay methods.

### 2.6. Sulbenicillin

The contents of D-(−)- and L-(+)-epimers of sulbenicillin (**2**) were determined by Nomura et al. [2] using $^1H$ NMR spectroscopy. Owing to folded conformations, the shielding effects of the side-chain aromatic ring were different between

the two epimers, resulting in differences in the chemical shifts assigned to the 3-$CH_3$ groups. Good correlation was observed between the bioactivity and the D-(−)-epimer content, which was consistent with the fact that the D-(−)-epimer is far more potent than the L-(+)-epimer. The antimicrobial activity of the L- (or *S*-) epimer was only 2.7% of that of the D- (or *R*-) epimer.

For the determination of sulbenicillin epimers, Yamaoka et al. [6] applied the same HPLC method as described above for carbenicillin, which resulted in no resolution of the sulbencillin epimers. However, the D-(−)-epimer content in the commercial preparation was ca. 77% as determined by $^1$H NMR.

We also separated sulbenicillin epimers by HPLC with methods similar to those reported by Ishida et al. [11] for carbenicillin, and obtained a baseline separation of sulbenicillin epimers (unpublished results). The *R*/*S* (or D/L) ratio was approximately 3 in the commercial preparation as determined by HPLC. Therefore, the more potent isomer appears to be the dominant isomer in the commercial preparation.

### 2.7. Temocillin

Temocillin epimers (**3**) were determined by Bird et al. [23] using two kinds of reversed-phase HPLC conditions. For the first HPLC system, a μBondapak $C_{18}$ column (300 × 3.9 mm I.D.) was used with a mobile phase consisting of methanol–0.1 *M* phosphate buffer (pH 7.0) (1:9, v/v) at a flow-rate of 2.0 ml/min. Temocillin epimers were detected at 230 nm. The retention times were 6.0 and 7.5 min for the *R*- and *S*-epimer, respectively, with baseline separation. For the second system, Zorbax $C_8$ (250 × 4.6 mm I.D.) was used as an analytical column with a mobile phase consisting of methanol–0.1 *M* phosphate buffer (pH 7.0) (16:84, v/v). The flow-rate was 1.5 ml/min and temocillin epimers were detected at 230 nm. The retention times were 8.0 and 9.5 min for the *R*- and *S*-epimer, respectively. The second system gave a better resolution of the epimers. In their studies, the *R*-epimer was separated by crystallization of the dibenzylethylenediamine salt and the *S*-epimer by preparative HPLC. Absolute configurations of both epimers were assigned from the $^1$H NMR spectra in comparison with those of ticarcillin.

### 2.8. Ticarcillin

Gupta and Stewart [7] reported the determination of ticacillin epimers (**4**) in an aqueous solution with the same HPLC method as described above for carbenicillin [7]. The two epimers were resolved, but not to the baseline.

Hoogmartens et al. [4] used the same HPLC method as described above for carbenicillin for the determination of ticarcillin epimers. Two epimers were resolved, but the absolute configurations of the eluting epimers were not determined. They found that the amount of the first-eluting epimer was approximately 56% in the commercial preparations, suggesting that the commercial preparations were not 1:1 mixtures of the epimers.

An HPLC method was also reported by Watson [24] for the determination of ticarcillin epimers in serum and urine samples from patients. Serum and diluted urine samples were acidified with hydrochloric acid, and ticarcillin epimers were extracted with dimethyl ether. A Hypersil ODS column (100 × 5 mm I.D.) was used with a mobile phase consisting of methanol–0.05 *M* phosphoric acid (25:75 for serum and 30:70 for urine). The flow-rate was 2.0 ml/min and ticarcillin epimers were detected at 214 nm. Thienylbutyric acid was used as an internal standard. For the serum sample the two epimers appeared to be separated to the baseline, although an interfering peak partially overlapped one of the epimers. For the urine sample no interfering peaks were observed with a baseline separation of the epimers. Ticarcillin sodium salt in the commercial preparation was a 45:55 mixture of the two epimers (according to the peak ratio on the chromatogram). As absolute configurations were not assigned to the eluting peaks, it was not known which epimer content was greater.

### 2.9. Other β-lactams

Hoogmartens et al. [4] developed HPLC methods for the determination of the epimers of

phenethicillin (**5**), propicillin (**6**) and clometocillin (**7**). Zorbax $C_8$ (250 × 4.6 mm I.D.) was used as an analytical column with a mobile phase composed of methanol–water–5% 0.2 *M* phosphate buffer (pH 7.0). The flow-rate was 1.0 ml/min and the epimers were detected at 254 nm. The methanol contents in the mobile phase were 37.5, 45 and 50% for phenethicillin, propicillin and clometocillin, respectively. The epimers were resolved close to the baseline, and the D-epimer eluted faster than the L-epimer for all three penicillins. It was found that the commercial preparations were not 1:1 mixtures of the epimers and that the epimer ratio in the preparation varied from one manufacturer to another. The D-epimer contents of phenethicillin, propicillin and clometocillin varied from 33 to 46%, 24 to 49% and 56 to 59%, respectively.

They used the same HPLC method for the determination of ampicillin, amoxicillin and azidocillin (**10**), except that the methanol content was varied between 10 and 40%. The L-epimer eluted faster for ampicillin, whereas the D-epimer eluted faster for amoxicillin and azidocillin. The less active epimers were not detected in the commercial preparations of these penicillins.

For the determination of carfecillin, they applied the same HPLC method with various methanol contents and pH. All the HPLC conditions resulted in only one peak, although the presence of two diastereomers was confirmed by $^1$H NMR.

HPLC methods were reported by Salto [3] for the determination of ampicillin and α-phenoxyethylpenicillin using a μBondapak $C_{18}$ column. The mobile phases were mixtures of methanol and 0.1 *M* phosphate buffer in various proportions. The mobile phase pH was also varied. Under the HPLC conditions studied, the L-epimer eluted faster than the D-epimer for ampicillin, whereas the D-epimer eluted faster for α-phenoxyethylpenicillin. The epimers seemed to be well resolved for both penicillins.

Epimers of 7-ureidoacetamido cephalosporins were determined by Young [25] using a μBondapak $C_{18}$ column. The mobile phase was 0.01 *M* diammonium hydrogenphosphate containing 5–20% methanol. For the series of cephalosporins studied, the L-epimers eluted faster than D-epimers. The epimers were well resolved under the HPLC conditions.

Ampicillin prodrugs, such as bacampicillin and talampicillin, are commercially available as mixtures of two epimers due to the chirality of the prodrug moiety. However, no information is available on the stereoselective analytical method or the stereoselectivity in the pharmacokinetics of the ampicillin prodrugs, as the prodrugs are rapidly hydrolysed to release ampicillin once they are absorbed in the body.

## 3. Isomerization

Hoogmartens et al. [4] studied the epimerization of carbenicillin in aqueous solution at pH 7.0. The epimerization rate from the second-eluting epimer in their HPLC method (probably the *S*-epimer as mentioned above) to the first-eluting epimer was faster than that from the first- to the second-eluting epimer. The results suggest that owing to epimerization it may be impossible to determine the activity of isolated epimers by the usual microbiological methods [1]. The same held true for ticarcillin, i.e. the epimerization rate from the second-eluting epimer to the first-eluting epimer was faster than that from the first- to the second-eluting epimer. When the results obtained in our laboratory are compared with those obtained by Hoogmartens et al. [4] and Aso et al. [9], the *R*-epimer is likely to elute faster than the *S*-epimer under their HPLC conditions. It is also probably true that owing to the epimerization the activity of isolated ticarcillin epimers may not be determined by the conventional microbiological methods, as stated by Hoogmartens et al.

Epimerization of carbenicillin in aqueous solutions was studied by Hashimoto et al. [10]. It was found that the epimerization rate was greater at pH 11 than at pH 9, which was catalysed by hydroxide ion. Epimerization of carbenicillin was also studied by Aso et al. [9] at pH 7.4 in the absence and presence of human serum albumin (HSA). The epimerization rate constant increased and reached a plateau value as the HSA concentration increased. It was revealed that the

epimerization was catalysed by HSA and that the Michaelis–Menten-type complex was formed between carbenicillin and HSA.

Epimerization of cefsulodin in aqueous solutions was studied by Fujita and Koshiro [12]. D-(−)-Cefsulodin was stable to epimerization below neutral pH but was sensitive to epimerization in alkaline solution, suggesting that the epimerization was catalysed by hydroxide ion. The epimerization constant increased as the temperature increased, with an activation energy of ca. 27 kcal/mol. Moreover, the concentration of the D-(−)-epimer was slightly greater than that of the L-(+)-epimer at equilibrium, which suggested that the conformation of the D-(−)-epimer was more stable than the L-(+)-epimer.

Isomerization of *cis*-ceftibuten to the *trans* isomer in serum was measured by Shimada et al. [14]. The isomerization rate constants of both isomers correlated well with their binding percentages in serum, suggesting that the binding to serum protein exerted a catalytic effect on the isomerization. When the isomerization rate was compared between serum and albumin-deficient serum, it was found that the isomerization was accelerated in the presence of HSA and that the catalytic effect was inhibited by warfarin. However, since the inhibitory effect of warfarin was observed only at higher warfarin to HSA molar ratios, the isomerization may be catalysed not only by the warfarin site but also by other binding sites. On the other hand, the presence of $\alpha_1$-acid glycoprotein did not affect the isomerization.

Epimerization of temocillin in aqueous solutions was studied by Bird et al. [23], who observed significant effects of pH and temperature on the epimerization rate. The equilibration half-life ($t_{1/2}$) increased as the pH increased, the $t_{1/2}$ values at 25°C being 0.22 and 5.0 h at pH 5.0 and 7.0, respectively. On the other hand, $t_{1/2}$ decreased as the temperature increased; the $t_{1/2}$ values at pH 7.0 were 5.0 and 2.0 h at 25 and 37°C, respectively. The equilibration rate was also affected by the phosphate concentration with the half-life at pH 7.0 decreasing at higher phosphate concentrations, suggesting a catalytic effect of phosphate on epimerization. Moreover, the percentage of the *R*-epimer at equilibrium was dependent on the temperature; the percentage of the *R*-epimer at equilibrium was 70.5, 65.0 and 62.5% at 0, 25 and 37°C, respectively. However, the pH did not affect the *R*-epimer percentage at equilibrium.

Hashimoto and co-workers [10,26] studied the epimerization of moxalactam epimers in aqueous solutions at various pH. The epimerization rate constants for both epimers were smallest around pH 7.0 and were greater in both acidic and basic solutions. It was found that the epimerization was water catalysed in acidic solutions and that the epimerization in basic solutions was catalysed by hydroxide ion.

Epimerization of moxalactam was also studied in frozen aqueous solutions [27]. Although the epimerization rate constant decreased as the temperature decreased, the epimerization did not stop until the temperature fell below the collapse temperature of the moxalactam aqueous solution (−19°C). Also, the *R*/*S* ratio at equilibrium increased as the temperature decreased, which could be ascribed to the difference in the activation energy of epimerization between the epimers.

Epimerization of moxalactam was further studied by Hashimoto et al. [28] in frozen urine and plasma samples during long-term storage. The *R*/*S* ratio at equilibrium in plasma was found to differ from that in aqueous solutions, owing to the difference in plasma protein binding between the epimers. Urine components also affected the *R*/*S* ratio at equilibrium. These observations suggested that the *R*/*S* ratio may change during storage depending on the components in samples. It was recommended that biological samples should be stored at or below −70°C to prevent epimerization.

## 4. Stereoselectivity in absorption

The stereospecific absorption and degradation of cephalexin have been reported by Tamai et al. [15]. After oral administration to rats the D-epimer was detected in serum and urine, whereas the L-epimer was not detected in either serum or urine. However, the L-epimer competitively inhibited the uptake of the D-epimer by the

everted intestine in vitro, suggesting that both epimers can be absorbed from the intestine. Moreover, the affinity to the transporter, probably the dipeptide transporter, was found to be greater for the L-epimer than the D-epimer. On the other hand, the L-epimer rapidly degraded in the intestinal tissue homogenate, serum and urine, whereas no appreciable degradation was observed for the D-epimer. It was concluded that both cephalexin epimers may be absorbed from the intestine but that only the D-epimer can be detected in the body owing to immediate hydrolysis of the L-epimer after absorption.

Kramer et al. [29] measured the uptake of cephalexin epimers into rabbit small intestinal brush border membrane vesicles. The D-epimer was taken up by the vesicles, whereas the L-epimer was not taken up to a significant extent. After reconstitution of brush border membrane proteins into proteoliposomes, only liposomes containing the $M_r$ 127 000 binding protein showed a significant uptake of the D-epimer, whereas the L-epimer was not transported by the proteoliposomes. However, the L-epimer was slightly more effective than the D-epimer in preventing the photolabelling of the $M_r$ 127 000 protein, suggesting that the affinity to the intestinal dipeptide transport system may be greater for the L-epimer than for the D-epimer. This observation appeared to be consistent with that reported by Tamai et al. as described above.

Uptake of cefaclor (**13**) was studied by Dantzig et al. [30] using human CaCo-2 cell line. It was found that cefaclor was transported by a dipeptide carrier and that the uptake was inhibited to a greater extent by the presence of the L-isomer than the D-isomer of the dipeptide, Gly–Phe. The concentration required for 50% inhibition was ten times greater for Gly–D-Phe than for Gly–L-Phe, suggesting that the carrier may have a preference for the L-isomer.

The transport of ceftibuten and its *trans* isomer into rat intestinal brush border membrane vesicles was studied by Yoshikawa et al. [31] and Muranushi et al. [32]. *cis*-Ceftibuten was transported via the oligopeptide transport system, and its uptake into the vesicles was stimulated in the presence of an $H^+$ gradient. In contrast, the uptake of the *trans* isomer was very small, and was not stimulated by the $H^+$ gradient. As the lipophilicity was similar between the *cis* and *trans* isomers, it was concluded that the uptake of ceftibuten and its *trans* isomer was stereoselective.

## 5. Stereoselectivity in distribution and disposition

Plasma protein binding of carbenicillin epimers was measured in vitro in humans [11,33]. The binding was stereoselective with the unbound fraction of the *R*-epimer being greater than that of the *S*-epimer (Fig. 3). It was revealed that the stereoselectivity in human plasma resulted from that in the binding to albumin (HSA) [34]. There were at least three binding sites on HSA for both epimers, and only one of the binding sites showed stereoselectivity; the affinity of the *S*-epimer to the stereoselective site was about four times greater than that of the *R*-epimer. The affinities to other binding sites were similar between the epimers. Moreover, the epimers seemed to compete at all the binding sites.

Carbenicillin was intravenously administered to human volunteers and the plasma concentrations and urinary excretion were measured [33]. Renal clearance was greater for the *R*-epimer than for the *S*-epimer, indicating the stereoselectivity in renal excretion. Renal clearance of unbound drug was greater than the

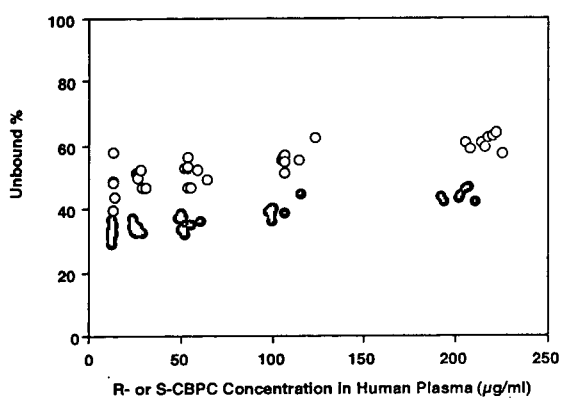


Fig. 3. Unbound fraction of (○) *R*- and (●) *S*-epimers of carbenicillin (CBPC) in human plasma.

glomerular filtration rate (GFR) for both epimers, suggesting that both epimers are actively secreted. Moreover, when probenecid was coadministered, the renal clearances decreased, and the renal clearances for unbound drug were almost equal to the GFR for both epimers. These results indicate that both epimers are secreted by the organic anion transport system in the renal proximal tubules. The secretion rate calculated was greater for the *S*-epimer than for the *R*-epimer, suggesting that the organic anion transport system may distinguish carbenicillin epimers. However, in the glomerular filtration process the *R*-epimer is cleared faster than the *S*-epimer owing to the greater unbound fraction of the *R*-epimer in plasma. Therefore, in the overall renal excretion process, the faster glomerular filtration of the *R*-epimer overrides the faster renal tubular secretion of the *S*-epimer, which results in greater renal clearance of the *R*-epimer.

In rabbits, the stereoselectivity in plasma protein binding was opposite to that in humans, i.e., the unbound fraction was greater for the *S*-epimer than for the *R*-epimer (Fig. 4) [11]. This suggests that the stereoselectivity in binding may differ from one species to another, which will make it difficult to predict the stereoselectivity in humans from animal data.

Binding of *cis*-ceftibuten and its *trans* isomer in human serum was also stereoselective; the binding was more extensive for the *cis* than for the *trans* isomer [14]. The major binding protein appeared to be HSA, and both isomers were mainly bound to the warfarin binding site. Therefore, it was most likely that the warfarin site exhibited the stereoselectivity in the binding of ceftibuten and its *trans* isomer.

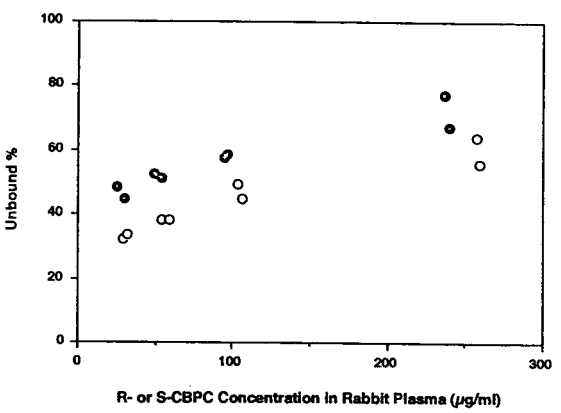


Fig. 4. Unbound fraction of (○) *R*- and (●) *S*-epimers of carbenicillin (CBPC) in rabbit plasma.

The effect of isomerization on the pharmacokinetics of ceftibuten was studied in humans [14]. Plasma concentrations and urinary excretion of both *cis* and *trans* isomers following oral administration of *cis*-ceftibuten were simulated using a physiological model. The model incorporated the isomerization of ceftibuten in plasma and interstitial fluid. The urinary excretion of the *trans* isomer was fairly well predicted, which confirmed that the isomerization of ceftibuten to its *trans* isomer actually occurs in the body.

The isomerization of ceftibuten to its *trans* isomer in the body was also suggested by Matsuura et al. [13]. In their studies, after oral adminstration of ceftibuten to humans, approximately 9% of the dose was recovered in urine as the *trans* isomer, whereas the urinary recovery of ceftibuten was ca. 70%.

Binding of moxalactam in human plasma was measured in vitro using an ultrafiltration method [35]. The binding was stereoselective with the unbound fraction of the *R*-epimer being greater than the *S*-epimer (47% and 33%, respectively). After intravenous administration of moxalactam to humans, more than 90% of the dose was recovered unchanged in urine, indicating that the urinary excretion is the major elimination route for both epimers. Although renal clearance was greater for the *R*-epimer than for the *S*-epimer, the renal clearances for the unbound drug were similar between the epimers. Moreover, the renal clearance values for the unbound epimers were very close to the GFR. These observations suggested that the contribution of renal secretion was insignificant in the renal excretion of moxalactam epimers and that the difference in the renal clearances between the epimers reflected that in the plasma protein binding.

Binding of moxalactam epimers in dog plasma was also stereoselective, with the unbound fraction of the *R*-epimer being greater than that of the *S*-epimer (76% and 55%, respectively) [36].

Urinary excretion was the major elimination route, and the glomerular filtration was dominant with almost no contribution from tubular secretion. The difference in the renal clearances between the epimers could be accounted for by the difference in plasma protein binding. Therefore, the pharmacokinetics of moxalactam epimers in dogs appeared to be similar to those in humans.

Pharmacokinetics of moxalactam epimers were also studied in rats [37]. The plasma protein binding was not stereoselective (unbound fraction of ca. 50% for both epimers), nor was the renal clearance. The results indicated that the stereoselectivity may differ among animal species and that it may be difficult to predict the stereoselectivity unless a suitable model animal is chosen.

## 6. Conclusions

β-Lactam antibiotics have been used clinically for a number of years. Most of the β-lactams, e.g., ampicillin, are used as a single isomer owing to the significant difference in activity between isomers. However, some β-lactams are used as mixtures of diastereomers in spite of the fact that the activities of the isomers are not equal. For sulbenicillin commercial preparations, the content of the more potent epimer is greater than that of the less active epimer, and the epimer/epimer ratio appears to be somewhat controlled. For other β-lactams, the commercial preparations are ca. 1:1 mixtures of isomers, but the content of the more active isomers seem to vary from one manufacturer to another, the clinical importance of which is yet to be clarified.

There have been numerous studies to determine antimicrobial activity, pharmacokinetics and pharmacodynamics of the diastereomeric β-lactam antibiotics. However, most studies employed conventional microbiological methods which failed to distinguish diastereomers. Also, many HPLC methods failed to resolve diastereomers, which again failed to give information on the differences between isomers with regard to activity, stability, pharmacokinetics and pharmacodynamics.

Stereoselectivity appears to exist for diastereomeric β-lactams in various processes in the body, such as absorption, distribution and excretion. If the drug is transported by the carrier system, diastereomers may be distinguished by the system, e.g., cephalexin, cefaclor and ceftibuten in the absorption process and carbenicillin in the secretion process. As it is well known that many β-lactams are absorbed from the intestine by the dipeptide carrier system and are secreted in the renal proximal tubule by the organic anion transport system, it is very likely that these processes are stereoselective for many β-lactam isomers.

Stereoselectivity may also exist in distribution. Plasma protein binding has been shown to be stereoselective for carbenicillin and moxalactam. The binding of the geometric isomer ceftibuten is also stereoselective. Moreover, epimer–epimer interaction has been observed in the binding of carbenicillin epimers to HSA. It has to be clarified if the differences in binding and the existence of isomer–isomer interactions are clinically important. The isomer–isomer interaction may also occur in the processes of absorption and secretion, the possibility of which has not been studied.

As the L-epimer of cephalexin is so susceptible to degradation, the significant difference in activity between cephalexin isomers may be due to the difference in stability, not to the difference in intrinsic activity. In contrast, isomerization during microbiological assay procedures may result in a lack of difference in the activity between the isomers of some β-lactam antibiotics, as has been suggested by Butler et al. [1] and also by Hoogmartens et al. [4]. The difference in stability between isomers and also the isomerization have to be taken into account when the activities between isomers are compared.

Isomerization may occur not only in solutions but also in the body, as has been shown for ceftibuten. Further, isomerization in the body may occur for many diastereomeric β-lactams. Indeed, epimerization in serum has been observed for carbenicillin, moxalactam and sul-

benicillin. Isomerization is one of the critical factors in evaluating chiral drugs as to whether the drug should be used as a single isomer or can be used as a mixture of isomers. Even if the single isomer is isolated and administered, the efficacy of the single isomer may be equal to that of the isomeric mixture owing to isomerization. Therefore, isomerization of diastereomeric β-lactams and the differences in activity and stability should be thoroughly studied in order to justify the clinical use of diastereomeric mixtures. Moreover, as the isomerization may occur both in frozen biological samples and in solutions, the storage conditions for diastereomeric β-lactams should be studied beforehand.

Despite the long history of clinical use of diastereomeric β-lactam antibiotics, the differences between isomers are not very well understood with respect to activity, stability, pharmacokinetics and pharmacodynamics. A better understanding of the differences between β-lactam isomes will contribute to the better clinical use of conventional diastereomeric β-lactam antibiotics and the development of novel chiral drugs.

## References


[1] K. Butler, A.R. English, V.A. Ray and A.E. Timreck, *J. Infect. Dis.*, 122 (1970) S1–S8.

[2] H. Nomura, K. Kawamura, M. Shinohara, Y. Masuda, Y. Okada and S. Fujii, *J. Takeda Res. Lab.*, 31 (1972) 442–452.

[3] F. Salto, *J. Chromatogr.*, 161 (1978) 379–385.

[4] J. Hoogmartens, E. Roets, G. Janssen and H. Vanderhaeghe, *J. Chromatogr.*, 244 (1982) 299–309.

[5] A.E. Bird and B.R. Steele, *J. Chem. Soc., Perkin Trans. 1* (1982) 563–569.

[6] K. Yamaoka, S. Narita, T. Nakagawa and T. Uno, *J. Chromatogr.*, 168 (1979) 187–193.

[7] V.D. Gupta and K.R. Stewart, *J. Pharm. Sci.*, 69 (1980) 1264–1267.

[8] P.A. Twomey, *J. Pharm. Sci.*, 70 (1981) 824–826.

[9] Y. Aso, S. Yoshioka and Y. Takeda, *Chem. Pharm. Bull.*, 38 (1990) 180–184.

[10] N. Hashimoto and H. Tanaka, *J. Pharm. Sci.*, 74 (1985) 68–71.

[11] M. Ishida, Y. Tsuda, Y. Onuki, T. Itoh, H. Shimada and H. Yamada, *J. Chromatogr. B*, 652 (1994) 43–49.

[12] T. Fujita and A. Koshiro, *Chem. Pharm. Bull.*, 32 (1984) 3651–3661.

[13] A. Matsuura, T. Nagayama and T. Kitagawa, *J. Chromatogr.*, 494 (1989) 231–245.

[14] J. Shimada, S. Hori, T. Oguma, T. Yoshikawa, S. Yamamoto, T. Nishikawa and H. Yamada, *J. Pharm. Sci.*, 82 (1993) 461–465.

[15] I. Tamai, H. Ling, S. Timbul, J. Nishikido and A. Tsuji, *J. Pharm. Pharmacol.*, 40 (1988) 320–324.

[16] C. Hendrix, Z. Yongxin, C. Van houtven, J. Thomas, E. Roets and J. Hoogmartens, *Int. J. Pharm.*, 100 (1993) 213–218.

[17] C. Hendrix, J. Thomas, L.-M. Yun, E. Roets and J. Hoogmartens, *J. Liq. Chromatogr.*, 16 (1993) 421–445.

[18] R. Konaka, K. Kuruma, R. Nishimura, Y. Kimura and T. Yoshida, *J. Chromatogr.*, 225 (1981) 169–178.

[19] D.J. Miner, D.L. Coleman, A.M.M. Shepherd and T.C. Hardin, *Antimicrob. Agents Chemother.*, 20 (1981) 252–257.

[20] M.K. Aravind, J.H. Miceli and R.E. Kauffman, *J. Chromatogr.*, 228 (1982) 418–422.

[21] J.A. Ziemniak, D.A. Chiarmonte, D.J. Miner and J.J. Schentag, *J. Pharm. Sci.*, 71 (1982) 399–402.

[22] R.E. Bawdon, F.G. Cunningham, J.G. Quirk and M.L. Roark, *Am. J. Obstet. Gynecol.*, 144 (1982) 546–550.

[23] A.E. Bird, C. Charsley, K.R. Jennings and C. Marshall, *Analyst*, 109 (1984) 1209–1212.

[24] I.D. Watson, *J. Chromatogr.*, 337 (1985) 301–309.

[25] M.G. Young, *J. Chromatogr.*, 150 (1978) 221–224.

[26] N. Hashimoto, T. Tasaki and H. Tanaka, *J. Pharm. Sci.*, 73 (1984) 369–373.

[27] H. Hashimoto, T. Ichihashi, E. Yamamoto, K. Hirano, M. Inoue, H. Tanaka and H. Yamada, *Pharm. Res.*, 5 (1988) 266–271.

[28] N. Hashimoto, T. Ichihashi, K. Hirano and H. Yamada, *Pharm. Res.*, 7 (1990) 364–369.

[29] W. Kramer, F. Girbig, U. Gutjahr, S. Kowalewski, F. Adam and W. Schiebler, *Eur. J. Biochem.*, 204 (1992) 923–930.

[30] A.H. Dantzig, L.B. Tabas and L. Bergin, *Biochim. Biophys. Acta*, 1112 (1992) 167–173.

[31] T. Yoshikawa, N. Muranushi, M. Yoshida, T. Oguma, K. Hirano and H. Yamada, *Pharm. Res.*, 6 (1989) 302–307.

[32] N. Muranushi, T. Yoshikawa, M. Yoshida, T. Oguma, K. Hirano and H. Yamada, *Pharm. Res.*, 6 (1989) 308–312.

[33] T. Itoh, M. Ishida, Y. Onuki, Y. Tsuda, H. Shimada and H. Yamada, *Antimicrob. Agents Chemother.*, 37 (1993) 2327–2332.

[34] T. Itoh, K. Nakashima, Y. Tsuda and H. Yamada, presented at the *International Symposium on Molecular Chirality (Kyoto, 1994)*, Abstracts, pp. 291–294.

[35] H. Yamada, T. Ichihashi, K. Hirano and H. Kinoshita, *J. Pharm. Sci.*, 70 (1981) 112.

[36] M. Nakamura, K. Sugeno, R. Konaka, H. Yamada and T. Yoshida, *J. Pharm. Sci.*, 71 (1982) 1188–1189.

[37] H. Yamada, T. Ichihashi, K. Hirano and H. Kinoshita, *J. Pharm. Sci.*, 70 (1981) 113.

ELSEVIER

Journal of Chromatography A, 694 (1995) 209–218

JOURNAL OF CHROMATOGRAPHY A

# Direct determination of E2020 enantiomers in plasma by liquid chromatography–mass spectrometry and column-switching techniques

Kenji Matsui[a,*], Yoshiya Oda[b], Hiroshi Ohe[b], Shigeru Tanaka[a], Naoki Asakawa[b]

[a]*Department of Drug Metabolism and Pharmacokinetics, Tsukuba Research Laboratories, Eisai Co., Ltd., 1–3 Tokodai 5-chome, Tsukuba-shi, Ibaraki 300-26, Japan*

[b]*Department of Physical and Analytical Chemistry, Tsukuba Research Laboratories, Eisai Co., Ltd., 1–3 Tokodai 5-chome, Tsukuba-shi, Ibaraki 300-26, Japan*

**Abstract**

High-performance liquid chromatography with column switching and mass spectrometry (MS) was applied to the on-line determination and resolution of the enantiomers of E2020 (acetylcholinesterase inhibitor) in plasma. This system employs two avidin columns and fast atom bombardment (FAB)-MS. A plasma sample was injected directly into an avidin trapping column (10 mm × 4.0 mm I.D.). The plasma protein was washed out from the trapping column immediately while E2020 was retained. After the column-switching procedure, E2020 was separated enantioselectivity in an avidin analytical column. The separated E2020 enantiomers were specifically detected by FAB-MS without interference from metabolites of E2020 and plasma constituents. The limit of quantification for each enantiomer of E2020 in plasma was 1.0 ng/ml and the intra- and inter-assay relative standard deviations for the method were less than 5.2%. The assay was validated for enantioselective pharmacokinetic studies in the dog.

## 1. Introduction

E2020 is a novel inhibitor of acetylcholinesterase being developed for the treatment of the symptoms of Alzheimer's disease [1]. E2020, the hydrochloride salt of (*R*,*S*)-1-benzyl-4-[(5,6-dimethoxy-1-indanon)-2-yl]methylpiperidine, is a racemic mixture due to the presence of an asymmetric carbon atom. The enantiomer ratio (*R*:*S*) is 1:1.

It is necessary to clarify the pharmacokinetic profiles of the individual isomers in a drug development programme [2]. Because E2020 enantiomers interconvert in aqueous solutions and plasma via a ketoenol intermediate, the rates of racemization for both the (*R*)- and (*S*)-E2020 were the same and the half-life of racemization was about 77.7 h at 37°C, the determination of each enantiomer by LC with a clean-up procedure is very difficult. A rapid and accurate quantitative method without any clean-up procedure such as deproteination, was developed using column-switching techniques [3–7]. The plasma samples were injected directly into the trapping column, which was an avidin column of 10 mm × 4.0 mm I.D. [8,9], without any pretreatment. Plasma proteins and other hydrophilic constituents were washed out, the valve was then switched and E2020, which was retained on the trapping column, was transferred to an analytical

* Corresponding author.

0021-9673/95/$09.50 
*SSDI* 0021-9673(94)01005-6

avidin column (150 mm × 1.5 mm I.D.), where E2020 enantiomers were optically resolved. Further, owing to the detection of E2020 enantiomers using fast atom bombardment mass spectrometry (FAB-MS) [10], which is suitable for the ionization of polar, non-volatile and thermally labile compounds, E2020 could be detected specifically without interference from metabolites of E2020 and plasma constituents. Moreover, the use of a deuterium-labelled internal standard (E2020-$d_7$) markedly improved the reproducibility for the quantification and the wide linear range of the assay is useful for the monitoring of E2020 enantiomers in plasma. When this LC–MS system is used, the sample work-up can be minimized and the risk of artificial interconversion of E2020 enantiomers is reduced.

This method was applied to the simultaneous determination of the enantiomers of E2020 in dog plasma. There was no difference in the pharmacokinetic profiles of the individual isomers and the *in vivo* interconversion of E2020 enantiomers was slow.

## 2. Experimental

### 2.1. Chemicals

E2020, which is a racemic mixture and a hydrochloride salt, was synthesized at Eisai. Each enantiomer [(*R*)- and (*S*)-E2020] was isolated from racemic E2020 by HPLC as the free base. Its plausible metabolites and E2020-$d_7$, were synthesized at Eisai. Structures are shown in Fig. 1. Other reagents and solvents were of analytical-reagent or LC grade (Wako, Osaka, Japan).

### 2.2. Apparatus

The LC system consisted of an SCL-10A system controller, an LC10AD pump, an SIL-10A autosampler and an FCV-12AH switching valve (Simadzu, Kyoto, Japan). In this system, a 5-$\mu$m Bioptick AV-1 column of 10 mm × 4.0 mm I.D. (GL Sciences, Tokyo, Japan) as a trapping column was eluted with 50 m*M* ammonium

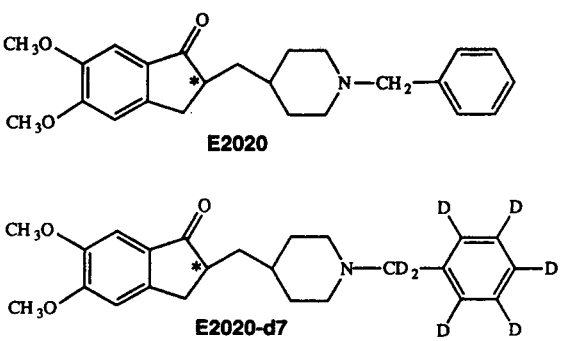


Fig. 1. Structures of E2020 and the internal standard (E2020-$d_7$). The asterisk indicates an asymmetric carbon.

acetate (pH 7.8) at a flow-rate of 1 ml/min, and a 5-$\mu$m Bioptick AV-1 column of 150 mm × 1.5 mm I.D. (GL Sciences) as an analytical column was eluted with 50 m*M* ammonium acetate (pH 5.3) containing 24% methanol and 1.5% glycerol at a flow-rate of 0.1 ml/min. There was no effect of glycerol in the mobile phase on the separation of the enantiomers except for the retention time of each enantiomer.

The MS analyses was performed with a JMS-SX102A instrument (JEOL, Tokyo, Japan) with a frit-FAB interface. MS ionization in the FAB positive-ion mode was performed with a xenon atom beam from a saddle field gun operated at 6 kV and 5 mA. The acceleration voltage, MS resolution and emission current were 10 kV, 1000 and 5 mA, respectively. The mass spectrometer was a DA700 system (Hewlett-Packard, Avondale, PA, USA) operating in the selected-ion monitoring (SIM) mode, where the target ions were at $m/z$ 380 and 387 at a switching rate of 1000 ms per scan. The introduction to the frit-FAB-MS system was performed by using a pneumatic splitter [11] (Model MS-PNS; JEOL) in order to lower the flow-rate from 100 to 5 $\mu$l/min.

### 2.3. Column-switching procedure

As shown in Fig. 2, the system consisted of two LC instruments, which were run independently. In the first stage, the plasma samples were injected directly into the trapping column,

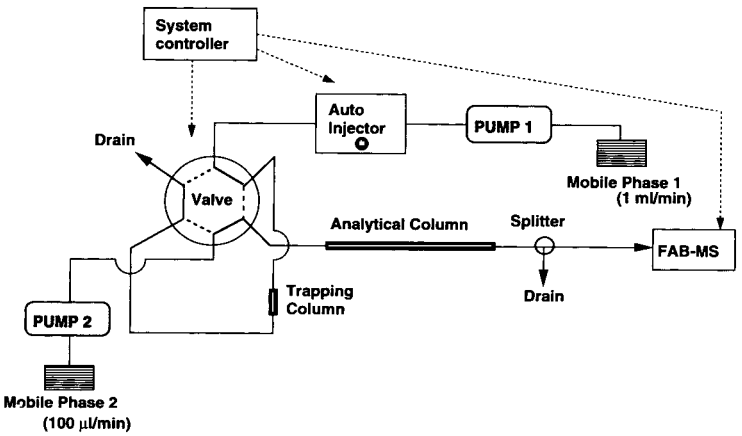


Fig. 2. Schematic diagram of the automated column-switching system for LC–MS.

plasma proteins and other hydrophilic constituents were then washed out and E2020 and E2020-$d_7$ were retained. In second stage, the valve was switched and E2020 and E2020-$d_7$ were transferred to the analytical column, where the enantiomers were optically resolved. Further, the flow from the analytical column was split and about 5% of the total flow was transferred to the frit-FAB interface, because the introduction of mobile phase into the MS ion source was restricted. After the completion of these two stages, the procedure was repeated with another sample.

### 2.4. Preparation of standard solutions

A racemic mixture of E2020 was used as standards for each enantiomer of E2020. A stock standard solution of racemic E2020 was prepared by dissolution in 0.0001 *M* hydrochloric acid at a concentration of 10 $\mu$g/ml and dilution to make calibration standards. A stock standard solution of E2020-$d_7$ (racemic mixture) was prepared by dissolution in 0.0001 *M* hydrochloric acid at a concentration of 500 ng/ml. These solutions were stored at 4°C.

### 2.5. Quality control sample preparation

Quality control samples were prepared by adding an E2020 enantiomer to a pool of dog blank plasma. The plasma pool was divided into 0.5-ml aliquots and stored frozen at −20°C.

### 2.6. Sample preparation

To 0.5 ml of the plasma sample were added 100 $\mu$l of the E2020-$d_7$ solution (500 ng/ml). The resulting mixture was vortex mixed for 1 min and centrifuged and the supernatant was transferred into a disposable syringe and filtered with a Millex-GV filter (Millipore, Tokyo, Japan), in order to remove solid particles. Then 500 $\mu$l of the filtered fluid were injected into the LC–MS system.

### 2.7. Calculation of concentration

Peak areas of E2020 enantiomer and E2020-$d_7$ enantiomer on the selected-ion chromatograms were read by the DA700 system. Peak-area ratios ($Q_T$) of the E2020 enantiomer to E2020-$d_7$ enantiomer were calculated, then the results for calibration standards were fitted to the following equation:

$$Q_T = AC_p + B$$

where $C_p$ is the added concentration. The values of $A$ and $B$ were determined by non-linear least-

squares regression analysis, using a weighting factor of $1/Y^2$. This fitting was performed using the Multi program [12].

Measured concentrations were expressed as ng/ml of E2020 as hydrochloride (1 ng of this salt form is equivalent to 0.912 ng of free base).

### 2.8. Validation studies

The intra-assay variability was determined for five replicates of spiked samples at each calibration concentration, which were assayed against a single calibration graph.

The inter-assay variation was determined by analysis of spiked plasma samples (QC samples) on separate occasions, relative to calibration samples which were freshly prepared each time.

### 2.9. Animal samples

Male beagle dogs, obtained from CSK Research Park (Gifu, Japan), weighing about 10 kg and aged 8 months, were used. The animals were fasted from 5.00 pm on the day before dosing, with access to water ad libitum. E2020 enantiomer was administered according to a cross-over design with 1 week of a wash-out period between each administration.

The E2020 enantiomer dissolved in ethanol was intravenously administered (in about 10 s), via the cephalic vein using a disposable syringe at a dose of 1.0 mg/kg. Blood samples of 1.5 ml were drawn into heparin-treated disposable syringes, from the cephalic vein immediately before and at 5, 15 and 30 min and 1, 2, 4, 6, 8, 10, 12 and 24 h after intravenous administration of E2020. Blood was separated by centrifugation at 4°C at 3000 rpm (KL20000T centrifuge; Kubota, Tokyo, Japan) for 10 min, and 0.5 ml of plasma was then taken and stored at −20°C until analysis.

## 3. Results and discussion

### 3.1. Clean-up and chromatographic conditions

A typical chromatogram of filtered plasma sample, which was injected directly into the avidin column (150 mm × 4.6 mm I.D.), is presented in Fig. 3. Although the enantiomeric resolution is best in the mobile phase at pH 5.3, enantiomers were eluted at pH 7 in this chromatogram because plasma proteins were retained on the column and were not eluted at pH 4–5 [4]. Plasma proteins and other hydrophilic components were not absorbed and were excluded from the avidin column within 5 min. On the other hand, E2020 enantiomers were retained on the avidin column and these enantiomers were separated.

The plausible metabolic pathways of E2020 are shown in Fig. 4. For E2020, demethylation followed by O-glucronide conjugation, N-dealkylation, N-oxidation or aromatic hydroxylation and then sulfate conjugation were the main metabolic pathways. The chromatograms of E2020 and its six metabolites (M1–M6) are shown in Fig. 5. The avidin column separates all

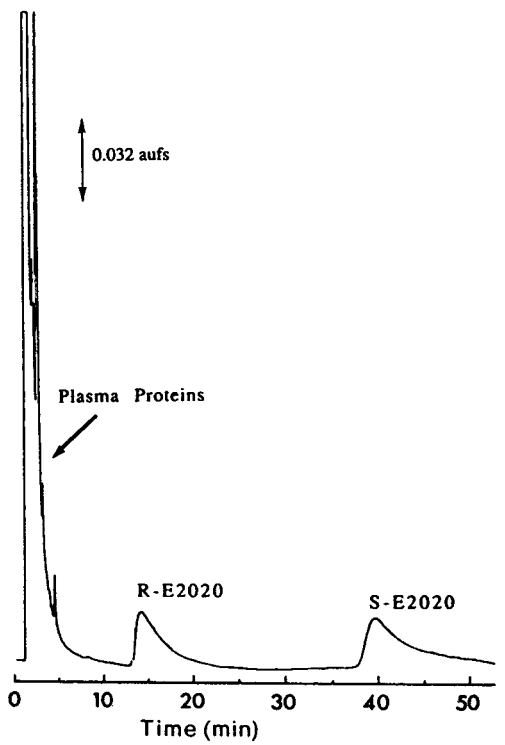


Fig. 3. Chromatogram of racemic E2020 (2 μg) in plasma after direct injection. Mobile phase, 7.5% acetonitrile in 0.1 *M* phosphate buffer (pH 7); flow-rate, 1.0 ml/min; detection, UV at 270 nm.

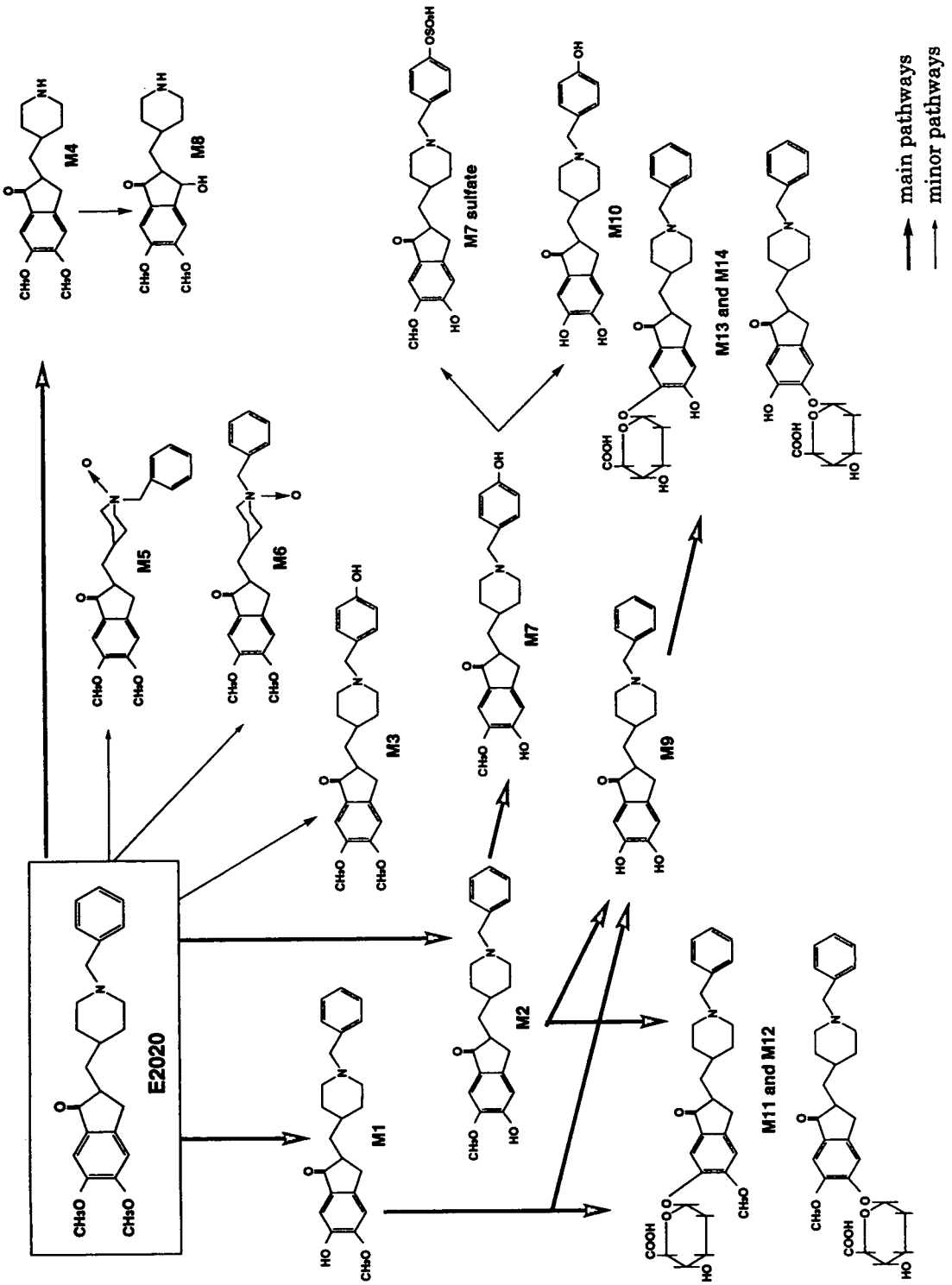


Fig. 4. Plausible metabolic pathways of E2020.

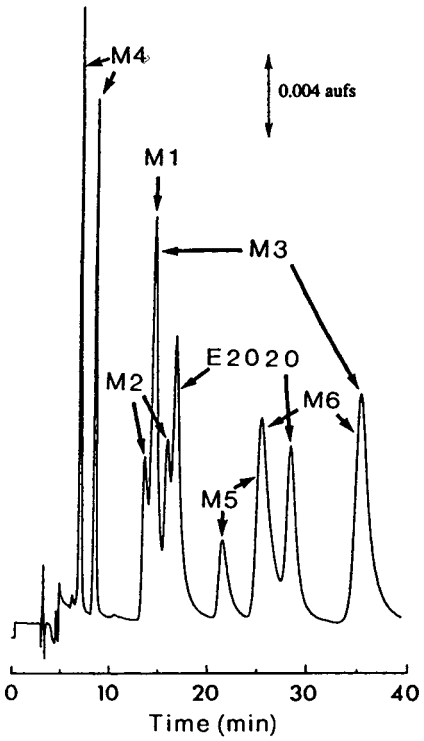


Fig. 5. Chromatogram of E2020 and its six metabolites in plasma after the column-switching procedure. Mobile phase for trapping E2020 and metabolites, 0.2 *M* ammonium acetate buffer (pH 5); mobile phase for enantioselective separation, 5% acetonitrile in 0.1 *M* phosphate buffer (pH 5); detection, UV at 271 nm.

their enantiomers except M1, so ten peaks on the chromatogram were detected. It seems to be difficult to find the optimum condition to separate E2020 enantiomers from all the metabolites. Therefore, we investigated the use of MS to detect E2020 enantiomers specifically without interference from metabolites and plasma constituents. As the introduction of the mobile phase from LC is restricted, the eluent from conventional LC columns must be split and only a small fraction of the mobile phase flow passes into the MS ion source. However, the flow from microbore columns is very low so that the use of a microbore avidin column not only gives high mass sensitivity but also improves the splitting ratio at the interface [13]. In this study, the column-switching technique was employed using a microbore avidin column (150 mm × 1.5 mm I.D.) as analytical column. This column-switching technique has the advantages that it allows the on-line measurement of enantiomers without any clean-up procedure, high sensitivity can be achieved as the result of concentration of sample on the trapping column and enantiomers are separated effectively in the mobile phase at pH 5.3.

An internal standard method was employed to compensate for run-to-run variability in the efficiency of the frit-FAB ionization process. E2020-$d_7$ was used as the internal standard.

### 3.2. Mass spectrometric conditions

The FAB mass spectrum of E2020 is shown in Fig. 6. The major ion was the protonated molecular ions as the base peaks (*m/z* 380) and only a few fragment ions were observed. The ion at *m/z* 380 for E2020 was not detected in the mass spectra of E2020-$d_7$, M1, M2, M3, M4, M5, M6, M1-glucuronide and M2-glucuronide (data not shown). Therefore, the ions at *m/z* 380 and 387 were monitored by SIM as the target ions. Fig. 7 shows typical SIM chromatograms for blank and spiked plasma samples.

### 3.3. Limit of detection

Detection by MS and UV in this method were compared. The detection limit with MS (50 pg) was 100 times lower than that with a conventional UV detector (5 ng) (data not shown).

### 3.4. Linearity of calibration graph

Visual examination indicated that the responses of (*R*)- and (*S*)-E2020 were linear with respect to the concentration of E2020 enantiomers added. This was confirmed by the determination of the intra-assay variability (Tables 1 and 2).

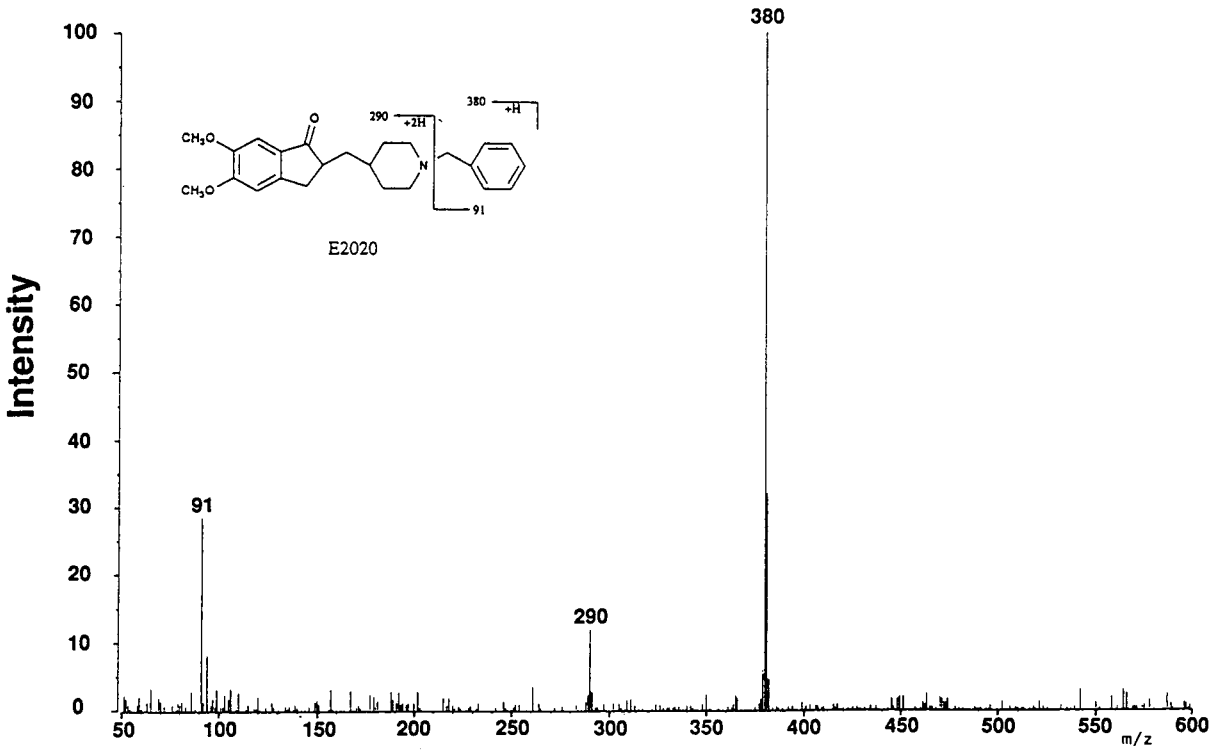


Fig. 6. Positive product ion mass spectra (background subtracted) of the protonated molecular ions of E2020; 20 ng of substance analyzed by LC–MS.

### 3.5. Assay validation

The intra- and inter-assay precision of the analysis were examined with samples of dog plasma spiked with E2020 enantiomers.

As shown in Tables 1 and 2, the intra-assay variability was determined for five replicates of spiked samples at each calibration concentration, which were assayed against a single calibration graph. The intra-assay relative standard deviations (R.S.D.s) in the range 1.00–502 ng/ml of each enantiomer were within 5.2% and the accuracy was from −7.4 to +7.6%, indicating that this method is reliable within that range.

As shown in Tables 3 and 4, the inter-assay variation was determined by analysis of the spiked plasma samples (QC samples) on three separate occasions, relative to calibration samples that were freshly prepared each time. The inter-assay R.S.D.s in the range 1.00–502 ng/ml of each enantiomer were within 4.5% and the accuracy was from −4.8 to +4.0%, indicating that this method is reliable within that range.

These results indicate that the use of an internal standard, i.e., a stable isotope of E2020, is very effective for reproducibility of determination by LC–MS.

### 3.6. Limit of quantification

Based on the results of the assay validation, the limit of quantification was set at 1.00 ng/ml.

### 3.7. Plasma samples

The method was applied to the simultaneous determination of the enantiomers of E2020 in

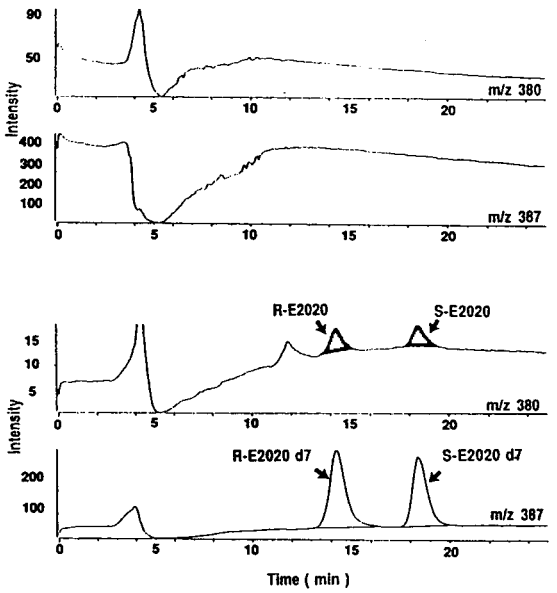


Fig. 7. Typical selected-ion chromatograms of the enantioselective separation of the enantiomers of E2020 and E2020-$d_7$. (Top) blank plasma; (bottom) plasma sample spiked with 0.5 ng of E2020 and 50 ng of E2020-$d_7$.

dog plasma undergoing treatment with (*R*)- or (*S*)-E2020.

The mean plasma levels of (*R*)-E2020 at 5 min after intravenous administration of (*R*)-E2020 (optical purity 99.43%), the first time point of sampling, was 290 ng/ml. This was followed by a biphasic exponential decline, with an apparent $t_{1/2}$ for the terminal phase of 3.05 ± 0.71 h. Similarly, the mean plasma levels of (*S*)-E2020 at 5 min after intravenous adminstration of (*S*)-E2020 (optical purity 98.25%) was 400 ng/ml and then showed biphasic exponential decline, with an apparent $t_{1/2}$ for the terminal phase of 2.87 ± 0.27 h. These results indicated that there is no difference in the pharmacokinetic profiles of (*R*)- and (*S*)-E2020 in dogs.

Moreover, the concentration of (*S*)-E2020 5 min after intravenous adminstration of (*R*)-E2020 and of (*R*)-E2020 5 min after intravenous administration of (*S*)-E2020 corresponded to the concentration of optical impurity in the dosing solution, and the mean plasma levels of (*S*)-E2020 after intravenous administration of (*R*)-E2020 showed a biphasic exponential decline with an apparent $t_{1/2}$ for the terminal phase of 2.73 ± 0.52 h, which is very similar to the $t_{1/2}$ of (*R*)-E2020 after administration of (*R*)-E2020. These results indicate that, even if E2020 enantiomers interconvert in plasma, the interconversion is very slow after intravenous administration to dogs.

## 4. Conclusions

The LC–MS method using column-switching techniques described in this paper is sensitive, reproducible, precise and stable. The method was found to be applicable to the study of the

Table 1
Intra-assay validation for (*R*)-E2020 in plasma ($n = 5$)

| Parameter | Theoretical concentration (ng/ml) | | | | | | | | |
|---|---|---|---|---|---|---|---|---|---|
| | 1.00 | 2.51 | 5.02 | 10.0 | 25.1 | 50.2 | 100 | 251 | 502 |
| Measured concentration (ng/ml) | 1.02 | 2.40 | 4.62 | 9.72 | 24.9 | 49.0 | 102 | 270 | 512 |
| | 1.03 | 2.35 | 4.61 | 9.67 | 25.5 | 50.6 | 103 | 268 | 517 |
| | 0.97 | 2.33 | 4.28 | 9.93 | 25.7 | 49.9 | 102 | 271 | 510 |
| | 0.94 | 2.43 | 4.81 | 9.71 | 26.0 | 50.0 | 109 | 266 | 512 |
| | 0.97 | 2.32 | 4.92 | 9.72 | 25.1 | 51.1 | 103 | 275 | 513 |
| Mean | 0.99 | 2.37 | 4.65 | 9.75 | 25.4 | 50.1 | 104 | 270 | 513 |
| S.D. | 0.04 | 0.05 | 0.24 | 0.1 | 0.44 | 0.79 | 2.95 | 3.39 | 2.59 |
| R.S.D. (%) | 4.0 | 2.1 | 5.2 | 1.0 | 1.7 | 1.6 | 2.8 | 1.3 | 0.5 |
| Accuracy (%) | −1.0 | −5.6 | −7.4 | −2.5 | 1.2 | −0.2 | 4.0 | 7.6 | 2.2 |

Table 2
Intra-assay validation for (*S*)-E2020 in plasma ($n = 5$)

| Parameter | Theoretical concentration (ng/ml) | | | | | | | | |
|---|---|---|---|---|---|---|---|---|---|
| | 1.00 | 2.51 | 5.02 | 10.0 | 25.1 | 50.2 | 100 | 251 | 502 |
| Measured concentration (ng/ml) | 1.06 | 2.37 | 4.82 | 9.84 | 26.4 | 48.9 | 104 | 267 | 499 |
| | 1.03 | 2.55 | 5.05 | 9.54 | 26.1 | 49.8 | 104 | 258 | 499 |
| | 1.04 | 2.42 | 4.69 | 9.21 | 25.9 | 50.4 | 102 | 256 | 520 |
| | 1.02 | 2.43 | 4.62 | 9.75 | 26.9 | 48.0 | 100 | 263 | 506 |
| | 0.98 | 2.42 | 4.61 | 9.40 | 25.6 | 50.4 | 102 | 256 | 524 |
| Mean | 1.03 | 2.44 | 4.76 | 9.55 | 26.2 | 49.5 | 102 | 260 | 510 |
| S.D. | 0.03 | 0.07 | 0.18 | 0.26 | 0.5 | 1.04 | 1.67 | 4.85 | 11.76 |
| R.S.D. (%) | 2.9 | 2.9 | 3.8 | 2.7 | 1.9 | 2.1 | 1.6 | 1.9 | 2.3 |
| Accuracy (%) | 3.0 | −2.8 | −5.2 | −4.5 | 4.4 | −1.4 | 2.0 | 3.6 | 1.6 |

Table 3
Intra-assay validation for (*R*)-E2020 in plasma ($n = 3$)

| Parameter | Theoretical concentration (ng/ml) | | | | | | | | |
|---|---|---|---|---|---|---|---|---|---|
| | 1.00 | 2.51 | 5.02 | 10.0 | 25.1 | 50.2 | 100 | 251 | 502 |
| Measured concentration (ng/ml) | 0.97 | 2.44 | 4.90 | 9.83 | 25.1 | 49.5 | 97.7 | 242 | 483 |
| | 1.03 | 2.49 | 5.11 | 10.6 | 25.3 | 51.0 | 101 | 251 | 510 |
| | 0.95 | 2.56 | 4.70 | 9.82 | 24.3 | 48.0 | 98.1 | 255 | 508 |
| Mean | 0.98 | 2.50 | 4.90 | 10.1 | 24.9 | 49.5 | 98.9 | 249 | 500 |
| S.D. | 0.04 | 0.06 | 0.21 | 0.45 | 0.53 | 1.50 | 1.80 | 6.66 | 15.04 |
| R.S.D. (%) | 4.1 | 2.4 | 4.3 | 4.5 | 2.1 | 3.0 | 1.8 | 2.7 | 3.0 |
| Accuracy (%) | −2.0 | −0.4 | −2.4 | 1.0 | −0.8 | −1.4 | −1.1 | −0.8 | −0.4 |

Table 4
Intra-assay validation for (*S*)-E2020 in plasma ($n = 3$)

| Parameter | Theoretical concentration (ng/ml) | | | | | | | | |
|---|---|---|---|---|---|---|---|---|---|
| | 1.00 | 2.51 | 5.02 | 10.0 | 25.1 | 50.2 | 100 | 251 | 502 |
| Measured concentration (ng/ml) | 1.00 | 2.37 | 4.92 | 10.4 | 25.5 | 50.0 | 99.0 | 251 | 501 |
| | 0.98 | 2.41 | 4.88 | 10.0 | 25.1 | 51.8 | 105 | 255 | 499 |
| | 1.00 | 2.39 | 4.98 | 10.0 | 25.5 | 50.3 | 108 | 257 | 507 |
| Mean | 0.99 | 2.39 | 4.93 | 10.1 | 25.5 | 50.3 | 104.0 | 254 | 502 |
| S.D. | 0.01 | 0.02 | 0.05 | 0.23 | 0.4 | 1.42 | 4.58 | 3.06 | 4.16 |
| R.S.D. (%) | 1.0 | 0.8 | 1.0 | 2.3 | 1.6 | 2.8 | 4.4 | 1.2 | 0.8 |
| Accuracy (%) | −1.0 | −4.8 | −1.8 | 1.0 | 1.6 | 0.2 | 4.0 | 1.2 | 0.0 |

pharmacokinetics of E2020 in biological samples and is the first reported assay capable of measuring the enantiomeric concentration of E2020 in plasma.

## References

[1] Y. Yamanishi, *Basic, Clinical, and Therapeutic Aspect of Alzheimer's and Parkinson's Diseases*, Vol. 2, Plenum Press, New York, 1990, p. 409.
[2] E.J. Ariens, *Eur. J. Clin. Parmacol.*, 26 (1934) 663.
[3] J. van der Grief, W.M.A. Niessen and U.R. Tjaden, *J. Chromatogr.*, 474 (1989) 5.
[4] P. Kokkonen, W.M.A. Niessen, U.R. Tjaden and J. van der Grief, *J. Chromatogr.*, 474 (1989) 59.
[5] A. Walhagen, L.E. Edholm, C.E.M. Heeremans, R.A.M. van der Hoeven, W.M.A. Niessen, U.R. Tjaden and J. van der Grief, *J. Chromatogr.*, 474 (1989) 257.
[6] W. Luiten, G. Damien and J. Capart, *J. Chromatogr.*, 474 (1989) 265.
[7] E.R. Verheij, H.J.E.M. Reeuwijk, W.M.A. Niessen, U.R. Tjaden, J. van der Grief and G.F. LaVos, *Biomed. Environ. Mass Spectrom.*, 16 (1989) 393.
[8] Y. Oda, N. Asakawa, S. Abe, Y. Yoshida and T. Sato, *J. Chromatogr.*, 572 (1991) 133.
[9] Y. Oda, H. Ohe, N. Asakawa, Y. Yoshida, T. Sato, and T. Nakagawa, *J. Liq. Chromatogr.*, 15 (1992) 2997.
[10] N. Asakawa, H. Ohe, M. Tsuno, Y. Yoshida and T. Sato, *J. Chromatogr.*, 541 (1991) 231.
[11] T. Kobayashi, presented at the *36th ASMS Conference on Mass Spectrometry and Allied Topics, 5–10 June, 1988, San Francisco, CA.*
[12] K. Yamaoka, *J. Pharmacobio-Dyn*, 4 (1981) 879.
[13] Y. Oda, N. Asakawa, Y. Yoshida and T. Sato, *J. Pharm. Biomed. Anal.*, in press.

ELSEVIER

Journal of Chromatography A, 694 (1995) 219–225

JOURNAL OF CHROMATOGRAPHY A

# Investigation of the stereoselective metabolism of the chiral $H_1$-antihistaminic drug terfenadine by high-performance liquid chromatography ☆

A. Terhechte, G. Blaschke*

*Institute of Pharmaceutical Chemistry, University of Münster, Hittorfstrasse 58–62, D-48149 Münster, Germany*

**Abstract**

The enantiomers of the racemic $H_1$-antihistaminic drug terfenadine (**1**) have been resolved by fractional crystallization of the diastereomeric salts with optically active 2-chlorotartranilic acid. The enantiomeric excess of both terfenadine enantiomers was determined using an achiral and a chiral HPLC system after formation of diastereomers with *S*-(+)-naphthylethylisocyanate. To investigate the metabolism of terfenadine after oral administration, an achiral HPLC system, equipped with a conventional reversed-phase column, was used to quantify the main metabolite MDL 16.455 (**2**) in human serum and urine. The determination of the enantiomeric composition of **2** was achieved using an Ultron ES-OVM® column as chiral stationary phase. Metabolite **2**, extracted from human blood plasma, was found to be enriched in the *R*-enantiomer, but was excreted in urine as racemate. The results of a study including six volunteers are presented.

## 1. Introduction

Terfenadine, Teldane®, α-[4-(1,1-dimethylethyl)phenyl] - 4 - (hydroxydiphenylmethyl) - 1 - piperidinebutanol, structure **1** in Fig. 1 is a $H_1$-antihistaminic drug. It is successfully used in the therapy of allergic diseases as allergic rhinitis and chronic urticaria [1]. The most important advantage over the $H_1$-antihistamic drugs of the first generation is its lack of effects on the central nervous system.

Terfenadine, a chiral drug, is used in therapy as the racemate. After oral application terfenadine is almost completely absorbed, undergoing a strong first-pass-metabolism [2], in which ca. 99% of the drug is metabolized to its carboxylic acid analogue MDL 16.455 (**2**) (Fig. 1), resulting in extremely low plasma concentrations and almost non-detectable urinary levels of the

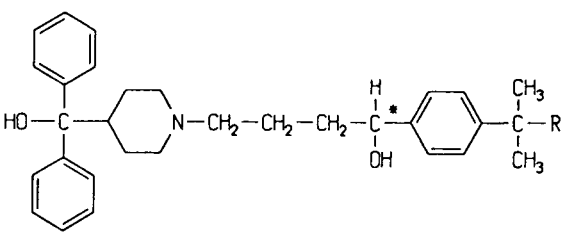


1: R = $CH_3$ Terfenadine
2: R = COOH MDL 16.455

Fig. 1. Structures of terfenadine (**1**) and its major acid metabolite MDL 16.455 (**2**).

* Corresponding author.

☆ Dedicated to Professor Dr. H.J. Roth on the occasion of his 65th birthday.

0021-9673/95/$09.50 
*SSDI* 0021-9673(94)01086-2

unmetabolized drug. The carboxylic acid metabolite **2** possesses about 30% of the $H_1$-antihistaminic activity of terfenadine and it was stated that this metabolite is exclusively responsible for the pharmacological effects of the drug [3].

Many chiral drugs show an enantioselective metabolism. However, in case of terfenadine it is reported [4] that metabolite **2** is excreted in human urine as a racemate indicating no enantioselectivity in the formation of **2**. In contrast an animal metabolic study with rats after oral administration of a high dose of terfenadine showed [5] that the *S*-enantiomer of terfenadine and the *R*-enantiomer of metabolite **2** was enriched in blood plasma. The absolute configuration of terfenadine had been determined previously by synthesis [6] and for terfenadine and its metabolite 2 by circular dichroism (CD) spectra [5]: the laevorotatory enantiomers are *S*-, the dextrorotatary enantiomers *R*-configurated.

This paper describes an economic method for the preparative separation of both enantiomers of terfenadine via diastereomeric salt formation with optically active 2-chlorotartranilic acid. The enantiomeric excess of both terfenadine enantiomers was determined using an achiral HPLC method after derivatisation of terfenadine (**1**) with *S*-(+)-naphthylethylisocyanate [*S*-(+)-NEIC] as well as by chiral HPLC columns. Furthermore, a chiral HPLC assay was used to determine the enantiomeric ratios of metabolite **2** in human serum and urine after oral application of the racemic drug.

## 2. Experimental

### 2.1. Chemicals

Terfenadine and the metabolite MDL 16.455 (**2**) were gifts from Marion Merrell Dow (Rüsselsheim, Germany). *n*-Hexane, 2-propanol, ethyl acetate and acetonitrile were Lichrosolv reagents (Merck, Darmstadt, Germany). The other chemicals were of analytical grade. Buffer solutions were prepared in double-distilled, deionized water and filtered (0.22 μm).

### 2.2. Apparatus

The HPLC system consisted of a Merck-Hitachi L 6200 pump (Darmstadt, Germany), a Merck-Hitachi variable-wavelength UV monitor 655A or a fluorescence detector Merck-Hitachi F-1250 and a Merck-Hitachi D-2500 chromato-intergrator.

### 2.3. Preparative separation

A mixture of racemic terfenadine (5.0 g, 10.6 mmol) and either (+)- or (−)-2-chlorotartranilic acid [7] (1.38 g, 5.32 mmol) were dissolved in 125 ml of hot ethanol (96%) and allowed to crystallize for 24 h at room temperature. Five recrystallization steps afforded the pure diastereomeric salts. After decomposition of the salts with 1 *M* NaOH and extraction with dichloromethane, the optically pure enantiomers [determination by HPLC on an achiral column after derivatization with *S*-(+)-NEIC and thereafter directly determined on chiral stationary phases] of terfenadine were obtained with a yield of >50%, m.p. 144–145°C.

The enantiomers were characterized by mass spectrometry, NMR and elemental analysis.

### 2.4. Achiral chromatography

The separation of the main metabolite MDL 16.455 (**2**) and the internal standard diphenylpyraline was achieved on a RP-Select B column (Merck, 125 × 4.6 mm I.D., particle size 5 μm) and a LiChrosorb $NH_2$ guard column. The mobile phase was a mixture of 0.01 *M* phosphate buffer pH 2.5–methanol–acetonitrile (52:48:1.5, v/v/v) with a flow-rate of 1.0 ml/min.

### 2.5. Indirect chromatographic resolution of terfenadine enantiomers

The enantiomeric purity of the enantiomers of terfenadine was determined by HPLC resolution on a RP-Select B column (Merck, 250 × 4.6 mm I.D., particle size 5 μm) after formation of the diastereomers with *S*-(+)-NEIC. The mobile

phase was methanol–0.1 *M* ammonium acetate–acetonitrile (75:25:1, v/v/v) and the flow-rate 0.5 ml/min. To form the diastereomers 12 mg of terfenadine were dissolved in 2 ml of dichloromethane and were allowed to react at room temperature for 20 h after addition of 40 μl *S*-( + )-NEIC (Sigma).

### 2.6. Chiral chromatography

Direct chromatographic resolution of terfenadine enantiomers was achieved by HPLC on a Ultron ES-OVM column (Grom, Germany, 150 × 4.6 mm, I.D., particle size 5 μm). The same column was used for the separation of the enantiomers of the metabolite MDL 16.455 (**2**). The use of a 0.01 *M* phosphate buffer pH 4.0–7.0 in combination with 2-propanol as organic modifier yields enantioseparations of **2**. The flow-rate was 0.5 ml/min and a fluorescence detector was used ($\lambda_{ex}$ = 230 nm and $\lambda_{em}$ = 280 nm).

Starting with a 0.01 *M* phosphate buffer pH 5.5–2-propanol (96:4, v/v) the simultaneous enantioseparation of **1** and **2** was achieved on a Ultron ES-OVM column. For the elution of terfenadine the concentration of the organic modifier 2-propanol was gradually increased up to 12% (Fig. 2).

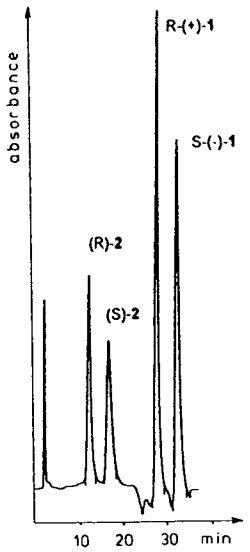


Fig. 2. Simultaneous resolution of terfenadine (**1**) and MDL 16.455 (**2**) on a Ultron ES-OVM column using a gradient HPLC system. Mobile phase composition: 0–19 min: 0.1 *M* phosphate buffer pH 5.5–2-propanol (94:4); 20–21 min: 4% 2-propanol up to 12%; 21–40 min: 0.1 *M* phosphate buffer pH 5.5–2-propanol (88:12); flow-rate, 1.0 ml/min; detection UV at 224 nm.

### 2.7. Quantification of MDL 16.455 in serum and urine (achiral assay)

For the quantification of **2** 1.0 ml of serum or 100 μl of urine, both adjusted with 1 ml 0.1 *M* sodium acetate buffer to pH 4.0, were extracted using Bakerbond octadecyl extraction columns 7020-3. After conditioning of the columns with 2 × 3 ml methanol, followed by 1 ml of double-distilled water and 2 ml 0.1 *M* sodium acetate buffer (pH 4.0), the sample was applied and soaked through the column by vacuum. The columns were washed with 2 ml double-distilled water, twice with 1 ml acetonitrile:water (1:2, v/v) and once with 0.7 ml acetonitrile. After drying the column for 10 min by suction the adsorbent was extracted with 1.5 ml of a 0.1 *M* solution of triethylamine in methanol. To quantify **2** in serum and urine on an achiral RP-Select B column the first aliquot was taken up in 50 μl of the mobile phase containing the internal standard diphenylpyraline. The second aliquot was used to determine the enantiomeric ratios of **2** in serum and urine.

### 2.8. Determination of the enantiomeric ratio of MDL 16.455 (2) in serum and urine by chiral chromatography (chiral assay)

After oral administration of racemic terfenadine the enantiomeric ratios of **2** were determined in the serum and urine samples by dissolving the second aliquot (see above) in 60 μl of the mobile phase without internal standard and HPLC analysis on an Ultron ES-OVM column. For these determinations a fluorescence detector ($\lambda_{ex}$ = 230 nm, $\lambda_{em}$ = 280 nm) was used.

### 2.9. In vivo study

Six healthy volunteers received once 120 mg terfenadine (Teldane forte, Merrell Dow) p.o. on an empty stomach. Blood was collected before and 0.5, 1.5, 2.5, 5, 8, 12, and 24 h after application. Serum was obtained by centrifugation at 1000 *g* for 25 min and stored frozen (−20°C) until analysis. Additionally the urine samples of three volunteers were collected after 2, 4, 6, 8, 10, 12 and 24 h, and were stored accordingly.

## 3. Results and discussion

### 3.1. Preparative separation and determination of the enantiomeric excess

Both enantiomers of terfenadine were obtained on a preparative scale by fractional crystallisation of the salts of (+)- and (−)-2-chlorotartranilic acid, respectively. They were used in this study as reference substances to determine the elution order of terfenadine enantiomers. To determine the enantiomeric excess (ee) of terfenadine in the beginning of our work an achiral HPLC system was used after derivatisation with *S*-(+)-NEIC. Later the enantiomeric purity of **1** was determined directly on a commercially available Ultron ES-OVM column. In both cases the enantiomeric excess (ee) was found to be higher than 99%.

With several chiral stationary phases (CSPs) such as Chiracel OD and Chiralpak AD we obtained good enantioseparations for **1** and **2** with an Ultron ES-OVM in a wide pH range of 5–7. During these experiments similar resolutions on the same column were published [5]. The enantioseparation of the main metabolite MDL 16.455 (**2**) was previously achieved on a Resolvosil BSA-7 protein column using a phosphate buffer pH 8.0 and 2-propanol as organic modifier [4]. Due to the high enantioselectivity of the Ultron ES-OVM column a simultaneous separation of **1** and **2** (Fig. 2) was achieved. However, because of the extensive first-pass effect of terfenadine it was not possible to analyze the very low serum and urine concentrations of terfenadine (**1**) using the Ultron column.

### 3.2. Quantitative determination of metabolite 2 in serum and urine (achiral assay)

Precision and accuracy of the assay were determined in blank serum samples spiked with known amounts of **2** in the range of 17.8–284.8 ng/ml (Table 1). Each concentration was analyzed three times. A linear correlation was found ($y = 0.0055x + 0.04004$, $r = 0.9876$). Recovery values were evaluated by comparing the peak areas from serum samples spiked with different amounts of **2**, and those of unextracted standard solutions. The recovery (± S.D.) of **2** was 80.2 ± 4.8% (Table 2). Fig. 3 shows typical chromatograms of (a) blank serum and (b) a serum sample 2.5 h after oral administration of 120 mg racemic terfenadine. Unmetabolized terfenadine was not detected in the serum samples.

Precision, accuracy and recovery of the assay in urine were determined accordingly in a concentration range of 71.2–569.7 ng/ml. A linear correlation was found ($y = 0.00479x + 0.00479$, $r = 0.9798$). The recovery (± S.D.) of **2** was

Table 1
Reproducibility (intra-day) and accuracy after extraction of MDL 16.455 (**2**) from serum and urine

| | Concentration (ng/ml) | Average peak area **2**/I.S. | S.E.M. |
|---|---|---|---|
| Serum: | 17.8 | 0.1223 | 0.0038 |
| | 35.6 | 0.2280 | 0.0151 |
| | 71.2 | 0.4626 | 0.0059 |
| | 142.4 | 0.8190 | 0.0558 |
| | 284.8 | 1.6020 | 0.1181 |
| Urine: | 71.2 | 0.3432 | 0.0437 |
| | 142.4 | 0.6797 | 0.1335 |
| | 284.8 | 1.3186 | 0.1317 |
| | 569.7 | 2.6748 | 0.3293 |

$n = 3$. Column: RP Select B, 125 × 4.0 mm I.D. (5 μm). Fluorimetric detection, $\lambda_{ex} = 230$ nm, $\lambda_{em} = 280$ nm.

Table 2
Recovery of **2** after extraction from serum and urine

| | Concentration (ng/ml) | Average recovery (%) | S.E.M. |
|---|---|---|---|
| Serum: | 17.8 | 81.5 | 0.993 |
| | 35.6 | 83.7 | 5.964 |
| | 71.2 | 84.5 | 2.991 |
| | 142.4 | 76.6 | 5.483 |
| | 284.8 | 74.9 | 5.621 |
| Urine: | 71.2 | 72.2 | 6.886 |
| | 142.4 | 89.0 | 6.084 |
| | 284.8 | 70.8 | 6.660 |
| | 569.7 | 76.0 | 5.531 |

77.0 ± 10.7%. During 24 h intervals about 4.5–8.5% of the applicated dose were eliminated as the carboxylic metabolite MDL 16.455. Also in urine unmetabolized terfenadine was not found during this study. Typical chromatograms of (a) blank urine and (b) a urine sample interval 2–4 h after oral administration of 120 mg racemic terfenadine are presented in Fig. 4.

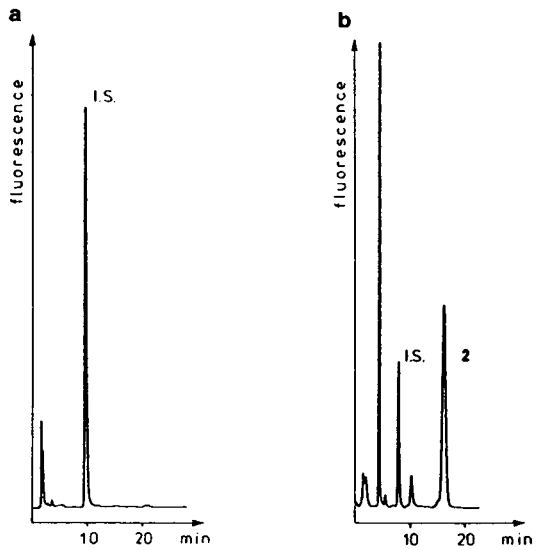


Fig. 4. Typical chromatograms of (a) blank urine containing the I.S. and (b) a urine sample interval 2–4 h after oral administration of 120 mg racemic terfenadine using an achiral HPLC system with a RP Select B column.

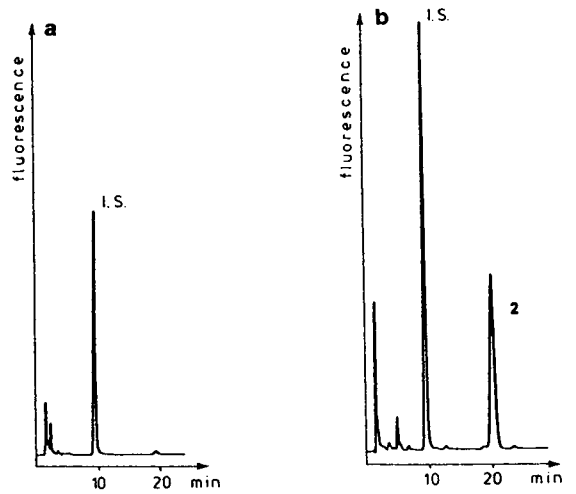


Fig. 3. Chromatograms of a blank serum spiked with the internal standard (I.S.) diphenylpyralin (a) and a serum sample 2.5 h after oral administration of 120 mg racemic terfenadine (b). Conditions: RP Select B column; 0.01 *M* phosphate buffer pH 2.5–methanol–acetonitrile (52:48:1.5); flow-rate, 1.0 ml/min; fluorimetric detection.

### *3.3. Determination of the enantiomeric ratio of MDL 16.455 (2) in serum and urine (chiral assay)*

To exclude a discrimination one of the enantiomers during the extraction procedure the percentage of (*R*)-**2** was determined after extraction of racemic terfenadine from spiked serum and urine samples. Using a HPLC system with an Ultron ES-OVM column as a CSP the composition of the enantiomers after extraction was found to be 49.6–50.1% in both cases. Therefore, a correction of the determined enantiomeric ratios of **2** was not necessary.

In urine a non-stereoselective excretion of **2** was found (Table 3). Representative chromatograms of serum samples are given in Fig. 5. The elution order of the enantiomers of **2** was determined by incubation of terfenadine enantiomers with rat liver microsomes and analysing the extracts by HPLC on the Ultron ES-OVM col-

Table 3
Cumulative excretion (ng) and enantiomeric ration (*R*/*S*) of MDL 16.455 (**2**) in urine of three volunteers after oral application of 120 mg of terfenadine

| Collection interval (h) | Volunteer | | | | | |
|---|---|---|---|---|---|---|
| | 1 | | 2 | | 3 | |
| | mg | *R*/*S* | mg | *R*/*S* | mg | *R*/*S* |
| 0–2 | 0.88 | 1.11 | 0.74 | 1.35 | 2.60 | 1.27 |
| 2–4 | 2.36 | 1.02 | 1.79 | 1.11 | 3.87 | 1.00 |
| 4–6 | 3.80 | 1.03 | 3.05 | 1.11 | 4.96 | 1.11 |
| 6–8 | 4.72 | 1.03 | 4.04 | 1.09 | 7.45 | 1.07 |
| 8–10 | 5.03 | 0.90 | 4.74 | 1.00 | 8.15 | 0.96 |
| 10–12 | 5.40 | 0.79 | 5.06 | 1.09 | 8.46 | 0.86 |
| 12–24 | n.d. | n.d. | 6.66 | 0.85 | 10.2 | 0.78 |

n.d. = Not determined.

umn. The percentage of (*R*)-MDL 16.455 in serum was found to be significantly higher in the samples of all six volunteers over 24 h (Table 4).

## 4. Conclusion

The HPLC assays described are suitable methods for the quantification of MDL 16.455 in serum and urine as well as for the determination of the enantiomeric composition of the investigated samples. In serum samples the metabolite (*R*)-**2** predominates. However, the excretion of **2** in urine was found to be non-stereoselective.

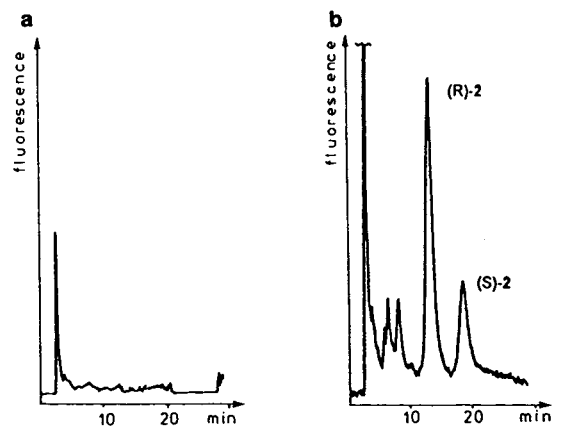


Fig. 5. Determination of the enantiomeric composition in serum using an Ultron ES-OVM column. Typical chromatograms of (a) blank serum and (b) a serum sample 0.5 h after oral administration of 120 mg racemic terfenadine.

Table 4
Averages of serum concentrations (ng/ml) and enantiomeric ratios (*R*/*S*) of MDL 16.455 (**2**) after oral application of 120 mg of terfenadine to six human volunteers

| Time after application (h) | ng/ml | S.E.M. | *R*/*S* | S.E.M. |
|---|---|---|---|---|
| 0.5 | 69 | 19 | 2.59 | 0.50 |
| 1.5 | 253 | 53 | 2.44 | 0.16 |
| 2.5 | 203 | 55 | 2.31 | 0.19 |
| 5.0 | 104 | 16 | 2.20 | 0.21 |
| 8.0 | 82 | 11 | 2.36 | 0.40 |
| 12.0 | 38 | 9.3 | 2.14 | 0.35 |
| 24.0 | 20 | 5.2 | 2.40 | 0.68 |

## Acknowledgements

The authors thank Dr. E. Ernst (Marion Merrell Dow, Rüsselsheim, Germany) for his interest, support and helpful discussions, the Deutsche Forschungsgemeinschaft and the Fonds der Chemischen Industrie for financial support. Also gratefully acknowledged are the volunteers G.B., M.H., B.K., B.S., A.T. and E.W. for their cooperation.

## References

[1] D. McTavish, K.L. Goa and M. Ferril, *Drugs*, 39 (1990) 552.
[2] R.A. Okerholm, D.L. Weiner, R.H. Hook, B.J. Walker, G.A. Leeson, S.A. Biedenbach, M.J. Cawein, T.D. Dusebout and G.J. Wright, *Biopharm. Drug Disp.*, 2 (1981) 185.
[3] D.A. Garteiz, R.H. Hook, B.J. Walker and R.A. Okerholm, *Arzneim.-Forsch./Drug Res.*, 32(II) (1982) 1185.
[4] K.Y. Chan, R.C. George, T.M. Chen and R.A. Okerholm, *J. Chromatogr.*, 571 (1991) 291.
[5] K. Zamani, D.P. Conner, H.B. Weems, S.K. Yang and L.R. Cantilena, *Chirality*, 3 (1991) 467.
[6] M.Q. Zang, A.M. ter Laak and H. Timmerman, *Bioorg. Med. Chem. Lett.*, (1991) 387.
[7] T.H. Montzka, T.L. Pindell and J.D. Matiskella, *J. Org. Chem.*, 33 (1968) 3993.

ELSEVIER

Journal of Chromatography A, 694 (1995) 227–236

JOURNAL OF CHROMATOGRAPHY A

# Gas chromatographic separation of enantiomeric amino acids and amines with α-methoxy-α-trifluoromethylpropionic acid as a chiral derivatizing agent

Fujiko Yasuhara[a], Shozo Yamaguchi[b], Masayuki Takeda[c], Yoshiro Ochiai[c], Sotaro Miyano[c,*]

[a]*Sendai National College of Technology, Kami-ayashi, Aoba-ku, Sendai 989-31, Japan*
[b]*Faculty of Liberal Arts, Tohoku Gakuin University, Ichinasaka, Izumi-ku, Sendai 981-31, Japan*
[c]*Department of Biochemistry and Engineering, Faculty of Engineering, Tohoku University, Aramaki-Aoba, Aoba-ku, Sendai 980-77, Japan*

**Abstract**

Enantiopure α-methoxy-α-trifluoromethylpropionic acid was prepared from 1,1,1-trifluoroacetone for the chiral separation of amino acids and amines by gas chromatography. Separation of the diastereomeric amide analytes was carried out on a capillary column coated with polyethylene glycol and showed good selectivity for these amino compounds at low column temperatures. A regularity was observed in the elution order, namely that a heterochiral diastereomer, *i.e.*, the *S,R*-isomer, eluted faster than the homochiral *S,S* counterpart.

## 1. Introduction

Although the direct separation of enantiomers by gas chromatography (GC) and high-performance liquid chromatography (HPLC) on chiral stationary phases has progressed greatly in the last decade [1–3], indirect separation *via* conversion into a pair of diastereomers by use of a chiral derivatizing agent (CDA) still remains a widely used and reliable method for the determination of enantiomeric purity and the assignment of absolute configuration by NMR and HPLC and less frequently by GC [4–7].

Among the variety of proposed CDAs [8–12], α-methoxy-α-trifluoromethylphenylacetic acid (MTPA) has been the most widely used for the derivatization of secondary alcohols and amines to the diastereomeric esters and amides [13,14]. However, CDAs that afford readily volatile diastereomers, amides in particular, suitable for GC analysis are limited, in spite of the fact that GC on an achiral column is operationally more advantageous than LC or NMR for the rapid analysis of many samples [15]. Ishikawa and co-workers developed two CDAs, perfluoro-2-propoxypropionic acid (PPPA) [16,17] and perfluoro-2-isopropoxypropionic acid (PIPA) [15], for the GC separation of 1-arylalkylamines and α-amino acids. Herein, we report that α-methoxy-α-trifluoromethylpropionic acid (MTPr), which can readily be prepared in an enantiopure form in substantial amounts, is an improved addition to these reagents for the separation of optically active amino acids and

* Corresponding author.

0021-9673/95/$09.50 
*SSDI* 0021-9673(94)00833-7

amines by achiral capillary GC at low operating temperatures [18].

## 2. Experimental

### 2.1. Apparatus

Gas chromatography was peformed using a Shimadzu GC-7AG instrument on the following fused-silica capillary columns: (A) CBJ17-W30-100 (30 m × 0.53 mm I.D. column coated with OV-17-type phenylmethylsilicone; Shimadzu); (B) Stabilwax (30 m × 0.25 mm I.D. column coated with Crossbonded Carbowax PEG; Restek) and (C) CBP20-W25-100 (25 m × 0.53 mm I.D. column coated with PEG-20M-type polyethylene glycol; Shimadzu). The instrument was equipped with a flame ionization detector and data collection was carried out on a Shimadzu C-R3A data processor. The splitting ratio was *ca.* 1:100 with the use of a Shimadzu-9 apparatus and the carrier gas was helium at 0.5 kg/cm$^2$. Liquid chromatography was performed using a Shimadzu LC-6A apparatus equipped with a Shimadzu SPD-6A ultraviolet detector (254 nm) on a 250 mm × 4.6 mm I.D. stainless-steel column packed with silica gel (Hitachi Gel 3056).

IR spectra were recorded on a Shimadzu IR-460 grating spectrophotometer. Optical rotations were measured on a Perkin-Elmer Model 241 polarimeter in a 10- or 1-cm thermostated microcell. $^1$H NMR spectra were recorded on a Hitachi R-90H or JEOL JNM-FX 60 instrument with tetramethylsilane as internal standard. Melting points were measured on a Yamato MP-21 apparatus and are uncorrected.

### 2.2. Materials

1,1,1-Trifluoroacetone (Aldrich) was distilled before use. Enantiomeric amino acids, amines and alcohols used for derivatization were of commercial origin unless stated otherwise. (*S*)-2-Amino-4-phenylbutyric acid {$[\alpha]_D^{29} + 49.6°$ (*c* 1.27, 1 *M* HCl), 95% enantiomeric excess (ee)} [19] and (*S*)-2-amino-5-phenylvaleric acid {$[\alpha]_D^{26} + 19.4°$ (*c* 0.36, 1 *M* HCl)} [20] were prepared by the literature procedures. Amino acid methyl esters were prepared according to the conventional method by reaction with methanol–HCl or –thionyl chloride [21]. Tetrahydrofuran (THF) and benzene were distilled from sodium diphenylketyl. Carbon tetrachloride ($CCl_4$) and pyridine were distilled from $CaH_2$. Solvents used for HPLC were distilled before use. Column chromatography was performed using Nacalai Tesque silica gel 60.

### 2.3. Preparation of racemic MTPr (*3*)

*1,1,1-Trifluoroacetone cyanohydrin*

According to the method reported by Darrall *et al.* [22], 1,1,1-trifluoroacetone (**1**) (98.2 g, 877 mmol) was treated with sodium cyanide (44.3 g, 903 mmol). After the usual work-up, distillation gave 1,1,1-trifluoroacetone cyanohydrin (90.8 g, 75% yield) as a clear liquid, b.p. 53–58°C/27 mmHg (1 mm Hg = 133.322 Pa); IR (liquid film), 3400, 1920, 1620 cm$^{-1}$; $^1$H NMR ($CDCl_3$), $\delta$ (ppm) 1.77 (3H, s, $CH_3$), 4.24 (1H, br, OH). The IR spectrum was devoid of the cyano group absorption, presumably owing to the strong electron-withdrawing effect of the $CF_3$ moiety.

*α-Hydroxy-α-trifluoromethylpropionic acid (2)*

The cyanohydrin (85.0 g, 612 mmol) was cautiously dissolved in concentrated $H_2SO_4$ (60 ml) at 70–80°C and the mixture was gradually heated to *ca.* 120°C, after which water was added (550 ml). After the mixture had been heated at reflux for 9 h, it was extracted with diethyl ether (× 5) and dried over $MgSO_4$. Removal of the solvent by distillation and crystallization from $CHCl_3$ gave α-hydroxy-α-trifluoromethylpropionic acid (**2**) as colourless crystals (66.8 g, 69.8% yield); m.p. 87–88°C (lit. [22] m.p., 88°C); IR (KBr), 3405, 3025, 1745, 1289, 1253, 1183, 1111 cm$^{-1}$; $^1$H NMR (acetone-$d_6$), $\delta$ (ppm) 1.60 (3H, s, $CH_3$), 5.85 (2H, s, br, OH and COOH). The methyl signal was slightly split by a long-range coupling with the $CF_3$ group.

*α-Methoxy-α-trifluoromethylpropionic acid (MTPr, 3)*

Under nitrogen, to a stirred suspension of sodium hydride (38.2 g, 1.60 mol) in THF (240 ml) were added methyl iodide (74.4 ml, 1.22

mol) and then a solution of hydroxy acid **2** (60.0 g, 382 mmol) in THF (240 ml). After the mixture had been stirred overnight at room temperature, the bulk of the volatiles was removed by distillation. The residue was dissolved in water and washed with diethyl ether. The aqueous alkaline solution was made acidic by addition of concentrated HCl and extracted with portions of diethyl ether. The combined ether extracts were dried over $MgSO_4$ and distillation gave **3** as a clear liquid (55.7 g, 84.8% yield), b.p. 100.5°C/25 mmHg; IR (liquid film), 3208, 3016, 2984, 1742, 1188 $cm^{-1}$; $^1H$ NMR ($CDCl_3$), $\delta$ (ppm) 1.68 (3H, s, $CH_3$), 3.50 (3H, s, $OCH_3$), 5.74 (1H, s, COOH). The methyl and methoxy signals were slightly split by long-range coupling with the $CF_3$ group.

### 2.4. Optical resolution of racemic MTPr (3) via (S)-1-phenylethylamides

#### Preparation of the diastereomeric amides by reaction with (S)-1-phenylethylamine

Racemic acid **3** (55.7 g, 318 mmol) was boiled with thionyl chloride (50 ml) for 24 h. Distillation of the reaction mixture under atmospheric pressure afforded the acid chloride of **3** (38.1 g, 62% yield) as a pale-yellow liquid, b.p. 115–117°C; IR (liquid film), 2960, 1796, 1462, 1302, 1188, 1112, 958, 790, 690 $cm^{-1}$; $^1H$ NMR ($CDCl_3$), $\delta$ (ppm) 1.67 (3H, s, $CH_3$), 3.52 (3H, s, $OCH_3$).

The acid chloride was used for reaction with (*S*)-1-phenylethylamine (29.0 g, 240 mmol) in $CCl_4$ (250 ml) and pyridine (40 ml) in the presence of 4-dimethylaminopyridine (DMAP) (1.27 g, 10.4 mmol). After the reaction mixture had been stirred for several hours at room temperature, it was diluted with diethyl ether and washed successively with portions of 2 *M* HCl, saturated $NaHCO_3$ and saturated brine and then dried over $MgSO_4$. Removal of the solvent gave 1-phenylethylamides **4** as a colourless solid (46.8 g, 85%).

#### Separation of amides into components

The mixture of the diastereomeric amides was recrytallized twice from hexane to afford the *R*, *S*-diastereomer as needles of essentially 100% diastereomeric excess (de), as evidenced by GC on column C, 11.9 g (51% yield based on the enantiomeric **3**); m.p. 99.4–100°C; $[\alpha]_D^{20}$ −88.9° ($CHCl_3$, *c* 0.97); IR (KBr), 3315, 1661, 1528 $cm^{-1}$; $^1H$ NMR ($CDCl_3$), $\delta$ (ppm) 1.51 (3H, d, $J = 6.82$ Hz, $CH_3$), 1.59 (3H, s, $CH_3$), 3.38 (3H, s, $OCH_3$), 5.61 (1H, m, C–H), 7.02 (1H, br, N–H), 7.32 (5H, s, $C_6H_5$). The absolute stereochemistry of the amide as *R*, *S* was determined by X-ray crystallographic analysis, the details of which will be reported elsewhere [23].

The mother liquors from the above crystallizations were combined and the solvents were distilled off. The residue (34.5 g) was chromatographed on a silica gel column (1 kg) with ethyl acetate–hexane (3:10) as the eluent to give the following fractions after distillation of the solvent: (1) 6.10 g (*R*, *S*-isomer of 99.4% de); (2) 5.09 g (*R*, *S*, 90.6% de); (3) 2.85 g (*S*,*S*, 97.0% de); (4) 18.43 g (*S*,*S*, 100% de). The last diastereomerically pure (*S*,*S*)-**4** fraction had the following physical data: m.p. 40.4–41°C; $[\alpha]_D^{20}$ −43.8° ($CHCl_3$, *c* 1.04); IR (KBr), 3310, 3315, 1663, 1533, 1309, 1180, 1144, 1100, 1043, 767, 698 $cm^{-1}$; $^1H$ NMR ($CDCl_3$), $\delta$ (ppm) 1.52 (3H, d, $J = 6.82$ Hz, $CH_3$), 1.64 (3H, s, $CH_3$), 3.45 (3H, s, $OCH_3$), 5.11 (1H, m, C–H), 7.22 (1H, br, N–H), 7.30 (5H, s, $C_6H_5$).

#### Hydrolysis of (S,S)-4 to enantiopure (S)-(+)-MTPr

Diastereopure (*S*,*S*)-**4** (18.4 g, 66.8 mmol) was dissolved in concentrated $H_2SO_4$ (185 ml) and stirred for 3 h at room temperature. This was slowly poured into ice–water (1.1 l) and extracted with portions of diethyl ether. After drying over $MgSO_4$, the solvent was distilled off to leave a solid (13.0 g), which was boiled in a solution of KOH (37.5 g) in methanol (150 ml) and water (12.5 ml) for 7 h. The mixture was diluted with water and washed with several portions of diethyl ether. The aqueous layer was made acidic by addition of concentrated $H_2SO_4$ and extracted with diethyl ether. After drying over $MgSO_4$, the solvent was distilled off. Distillation of the residue under reduced pressure afforded (*S*)-(+)-**3** as a colourless liquid (8.58 g,

75% yield), b.p. 93.1°C/18 mmHg; $d_4^{18}$ 1.32; $[\alpha]_D^{20}$ + 4.29°, $[\alpha]_{365}^{20}$ + 13.9° (neat); $[\alpha]_D^{20}$ + 4.88° ($CH_3OH$, *c* 3.63); IR (liquid film), 3216, 3012, 2980, 1736, 1464, 1312, 1166, 1045, 684 $cm^{-1}$; $^1H$ NMR ($CDCl_3$), $\delta$ (ppm) 1.67 (3H, s, $CH_3$), 3.53 (3H, s, $OCH_3$), 7.49 (1H, br, COOH).

The acid chloride of (*S*)-**3** [(*S*)-MTPr-Cl] was prepared as above by treatment with thionyl chloride and distillation, and divided into small glass ampoules for storage. A sample of (*S*)-MTPr-Cl was treated with 3,5-dinitroaniline in THF and triethylamine in the presence of DMAP to give the 3,5-dinitroanilide according to the method described previously [24]. HPLC of the anilide on a chiral stationary phase prepared in this laboratory by bonding (*S*)-1,1′-binaphthyl-2,2′-dicarboxylic acid to 3-aminopropylsilanized silica showed that the enantiomeric purity of the sample should be more than 99.5% ee [24]. The relevant chromatographic data for the anilide from partially active **3** were as follows: eluent, 2-propanol–hexane (15:85); flow-rate, 1 ml/min; capacity factor (*k′*) of (*R*)-**3** anilide = 4.32; *k′* of *S*-isomer = 3.78.

*Hydrolysis of (R,S)-4 to enantiopure (R)-(−)-MTPr*

Diastereomer (*R,S*)-**4** (2.65 g, 9.63 mmol) was treated as above to give (*R*)-**3** (1.06 g, 64%) after distillation, b.p. 95°C/24 mmHg; $[\alpha]_D^{20}$ −4.31°, $[\alpha]_{578}^{20}$ − 4.48°, $[\alpha]_{546}^{20}$ − 5.11°, $[\alpha]_{436}^{20}$ − 8.69°, $[\alpha]_{365}^{20}$ − 14.0° (neat).

### 2.5. Preparation of diastereomeric MTPr amide analytes

In a vial blown with dry nitrogen were placed a partially active amine (or an amino acid methyl ester) adjusted to 20–25% ee (30–50 mg), THF (1.5 ml), triethylamine (0.5 ml), DAMP (10 mg) and then (*S*)-MTPr-Cl (1.5 equiv.). After the mixture had been stirred overnight at room temperature, it was diluted with diethyl ether and successively washed with 2 *M* HCl, 5% aqueous $NH_3$ and brine and dried over $MgSO_4$. The solvents were removed under reduced pressure to give a sample of the MTPr amide analyte. When only one enantiomeric amino compound was available, derivatization was carried out by using partially active (*S*)-MTPr-Cl (*ca.* 25% ee). These data were also presented as if derivatization had been carried out by using partially active amino compounds and enantiopure (*S*)-MTPr-Cl for the sake of clarity [25].

*Test of kinetic resolution during derivatization*

DL-Glutamic acid dimethyl ester was derivatized as above; the flame ionization detection (FID) response of the diastereomers on column C was 50.39:49.61 (see Fig. 2). The analyte prepared from (*R*)-1-phenylethylamine of 25.0% ee showed two peaks with FID intensities of 62.78:37.22, respectively (see Table 3).

## 3. Results and discussion

### 3.1. Preparation of enantiopure (S)-(+)-MTPr

Treatment of 1,1,1-trifluoroacetone (**1**) with sodium cyanide according to the method of Darrall *et al.* [22] readily afforded the corresponding cyanohydrin, acid hydrolysis of which gave α-hydroxy-α-trifluoromethylpropionic acid (**2**) as colourless crystals (Fig. 1). Darrall *et al.* [22] resolved **2** into the enantiomers by fractional crystallization of the brucine salt, but attempts to resolve **2** by use of several chiral amines including brucine turned out to be very ineffective and another route to optically pure MTPr was desired for practical synthesis.

Selective methylation of the hydroxyl function of acid **2** by treatment with methyl iodide and sodium hydride in THF afforded (±)-MTPr (**3**) in good yield. Optical resolution of **3** could be accomplished according to essentially the same method as used for the resolution of PPPA [17]. After conversion of **3** into the diastereomeric amides **4** with (*S*)-1-phenylethylamine, they were separated into the diastereomers (*R,S*)-**4** and (*S,S*)-**4** by crystallization from hexane and silica gel column chromatography. The absolute stereochemistry of the acid part of the (*R,S*)-amide was determined by reference to the *S* configuration of the 1-phenylethylamine based

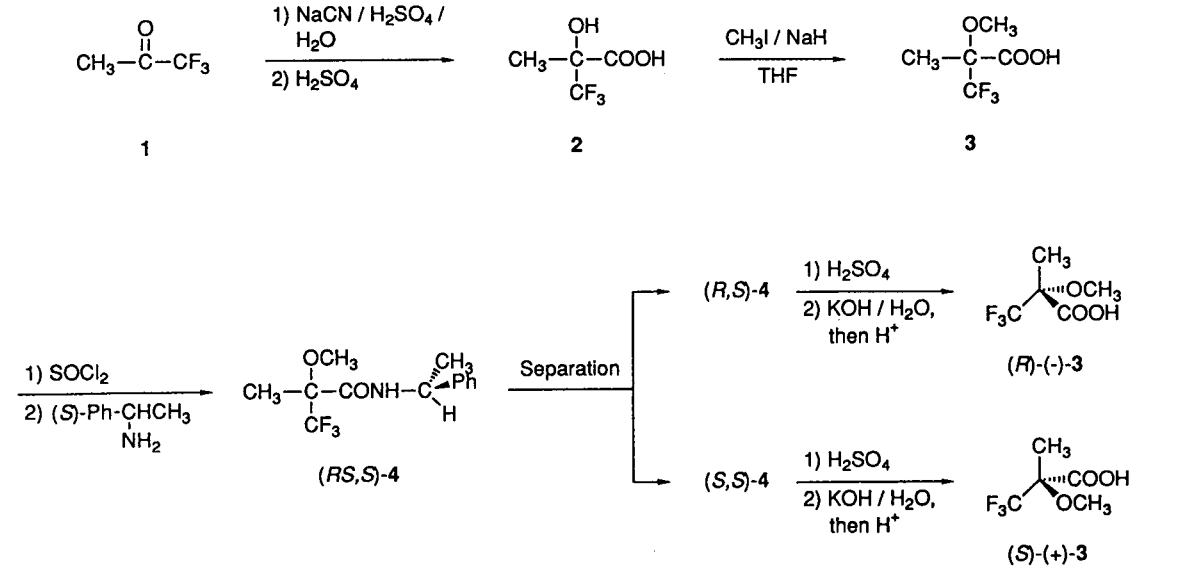


Fig. 1. Scheme of synthesis.

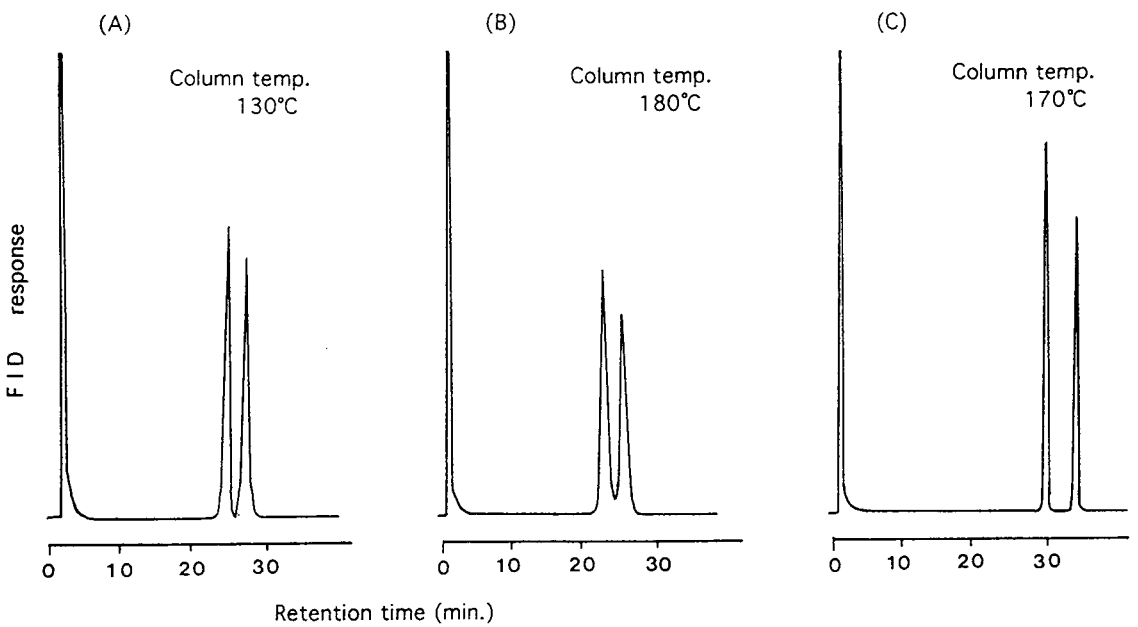


Fig. 2. GC separation of MTPr amides derived from racemic dimethyl glutamate on fused-silica capillary columns coated with (A) phenylmethylsilicone (CBJ17-W30-100), (B) Carbowax (Stabilwax) and (C) polyethylene glycol (CBP20-W25-100) (see Experimental for details). Carrier gas, He at 0.5 kg/cm$^2$.

on X-ray crystallographic structure analysis, and the relevant experimental details will be reported elsewhere [23].

Treatment of (*S*,*S*)-**4** with concentrated sulfuric acid followed by alkaline hydrolysis and distillation afforded enantiopure (*S*)-(+)-MTPr as a clear liquid for the first time. Boiling (*S*)-MTPr with thionyl chloride followed by distillation gave the acid chloride [(*S*)-MTPr-Cl] as a pale-yellow liquid, which was divided into small glass ampoules for storage. Enantiomeric homogeneity of the acid chloride (>99.5% ee) was confirmed by HPLC analysis on an axially chiral binaphthalene-based stationary phase after conversion into the 3,5-dinitroanilide [24]. Similar treatment of (*R*,*S*)-**4** gave enantiopure (*R*)-(−)-MTPr.

Although the optical resolution of MTPr required the formation of the diastereomeric 1-phenylethylamides and removal of the amine auxiliary, this in turn permitted a ready improvement in the optical purity of the MTPr as desired. It should be recalled that commercially available, but expensive, MTPA is an oil of 97.9–99.7% ee, which imposes an inevitable chiral discrimination limit [26].

### *3.2. GC separation of enantiomeric amino acids and amines as the MTPr amides*

At first, the inherent possibility of fractionation accompanying chiral derivatization was checked with the use of MTPr. A sample of racemic dimethyl glutamate was *N*-acylated with an excess of (*S*)-MTPr-Cl in THF and triethylamine in the presence of DMAP by stirring overnight at room temperature in a capped vial. The derivatized glutamide sample was obtained after the usual work-up and subjected to GC analysis. Fig. 2 shows the chromatograms for the separation of the glutamide diastereomers on three different capillary columns coated with a silicone oil (column A), carbowax (column B) and polyethylene glycol (column C). Although

Table 1
GC separation of diastereomeric MTPr amides derived from enantiomeric amino acid methyl esters

| Run No. | Amino acid | Column temperature (°C) | $k'$ | | $\alpha$ | $R_s$ |
|---|---|---|---|---|---|---|
| | | | (*S*,*S*) | (*R*,*S*) | | |
| 1 | Alanine | 140 | 9.67 | 7.56 | 1.27 | 4.70 |
| 2 | Valine | 140 | 10.59 | 8.63 | 1.23 | 5.00 |
| 3 | Leucine | 140 | 16.13 | 12.58 | 1.28 | 6.84 |
| 4 | Isoleucine | 140 | 15.06 | 12.21 | 1.23 | 4.29 |
| 5 | Norleucine | 140 | 20.94 | 16.85 | 1.24 | 8.43 |
| 6 | Aspartic acid[a] | 170 | 20.66 | 18.21 | 1.13 | 2.94 |
| 7 | Glutamic acid[a] | 170 | 37.86 | 32.97 | 1.15 | 4.28 |
| 8 | Phenylglycine | 170 | 13.51 | 9.87 | 1.37 | –[b] |
| 9 | Phenylalanine | 200 | 13.85 | 12.58 | 1.10 | 2.76 |
| 10 | $EtCH(NH_2)COOH$ | 140 | 11.09 | 8.85 | 1.25 | 5.48 |
| 11 | $Ph(CH_2)_2CH(NH_2)COOH$ | 200 | 25.16 | 21.90 | 1.15 | 5.00 |
| 12 | $Ph(CH_2)_3CH(NH_2)COOH$ | 200 | 32.46 | 29.05 | 1.12 | 4.00 |

Column, CBP20-W25-100; carrier gas, helium at 0.5 kg/cm$^2$; $k'$ = capacity factor; $\alpha$ = separation factor, $R_s$ = resolution.
[a] Dimethyl ester.
[b] Epimerization occurred; see text.

all of these columns separated the diastereomers, column C seemed the best considering the column performance, which included separability and column temperature required. The difference in the FID response between the diastereomeric pair of the glutamides was 0.78% on this column, which may be regarded as within the experimental error of integration. Another separation of the diastereomeric MTPr amides prepared from 1-phenylethylamine of 25.0% ee showed the difference in FID response to be less than 0.60%. These results suggest that the standard precautions will substantially reduce the kinetic resolution problem.

Twelve partially active amino acid methyl esters were acylated with (*S*)-MTPr-Cl as above and the results of the GC separation of these analytes are summarized in Table 1. Complete baseline separation was attained with all amide pairs tested except derivatized phenylglycine (run 8) (see below). It is noted that a resolution ($R_s$) larger than 8 was attained for norleucine (run 5). As an $\alpha$ value (separation factor) of 1.02 or greater is considered to be of practical application in chiral discrimination by capillary GC, hence it can be said that MTPr is an excellent CDA for discrimination of these amino acids. To demonstrate the selectivity obtainable with MTPr, a simultaneous separation of a mixture composed of seven diastereomeric pairs of MTPr amides prepared from the corresponding $\alpha$-amino acid methyl esters is shown in Fig. 3. Under the conditions employed, all the diastereomeric pairs could be separated in a single temperature-programmed run within a short period, although partial overlap of the peaks of L-leucine and D-norleucine occurred.

The data in Table 1 reveal that in all instances heterochiral diastereomers, i.e., *R,S* pairs, elute faster than the *S,S* counterparts. At present we cannot deduce any mechanisms concerning the regularity of the elution orders, while it may still be of use in assigning the absolute configurations of amino acids. Fig. 4 compares the chiral discrimination ability of MTPr with that of the perfluoro analogue, PPPA. It is seen that the MTPr amides derived from phenylalanine methyl ester separate well but the PPPA amides not at

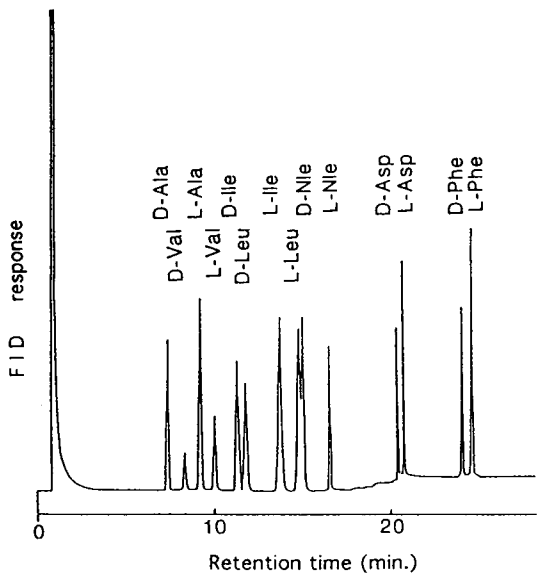


Fig. 3. GC separation of a mixture composed of seven diastereomeric pairs of MTPr amides prepared from the corresponding $\alpha$-amino acid methyl esters. Conditions: column, CBP20-W25-100; carrier gas, He at 0.5 kg/cm$^2$; column temperature, programmed from 140 to 220°C, 16°C/min starting 14 min after the injection.

all on column C, although the latter elutes at a lower column temperature than the former.

Fig. 5A shows the elution behaviour of the MTPr amides derived from partially active phenylglycine methyl ester. The chromatogram shows a plateau with a small peak between the

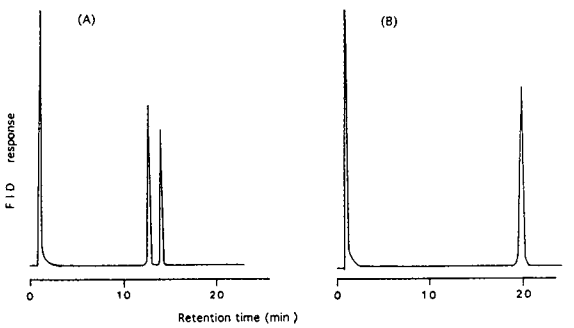


Fig. 4. Comparison of the separation of MTPr amides and PPPA amides derived from enantiomeric phenylalanine methyl ester. Conditions: column, CBP20-W25-100; carrier gas, He at 0.5 kg/cm$^2$; column temperature, (A) 200 and (B) 120°C.

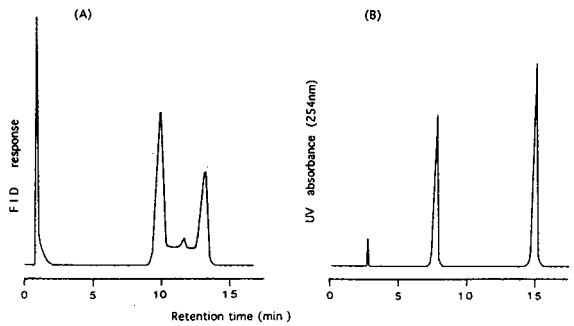


Fig. 5. GC and HPLC separation of MTPr amides derived from phenyglycine methyl ester. (A) GC separation on column CBP20-W25-100; carrier gas, He at 0.5 kg/cm$^2$; column temperature, 170°C. (B) HPLC separation on silica gel column; eluent, 2-propanol–hexane (1:99) at 1 ml/min; detection, UV at 254 nm.

two diastereomeric peaks, indicating the occurrence of epimerization of the diastereomers during the elution [27]. This may be ascribed to the presence of a labile hydrogen on the chiral carbon atom of the amino acid residue activated by the co-existing phenyl substituent. In such a case, however, HPLC separation is an alternative resort, as Fig. 5B and Table 2 indicate, by using a phenyl nucleus as the UV-responsive moiety. Good selectivity as shown by the $\alpha$ and $R_s$ values is noticeable and, interestingly, *S,S*-diastereomers eluted faster than the *R,S* counterparts, indicating that the mechanism of chiral discrimination of these MTPr amides by normal-phase HPLC is different from that by capillary column GC.

Table 3 summarizes the results of the GC separation of eleven partially active amines and four alcohols. For all the amines examined, chiral separation was attained, better selectivity being obtained with alkylarylamines than with simple alkylamines. It should be noted that there seems to be no report on the application of the Ishikawa and co-workers' PPPA and PIPA to GC separation of such simple alkylamines. As can be seen in Table 3, the separability of the diastereomeric esters is inferior to that of the amides. Hence, MTPr may be used more advantageously for the GC separation of amino compounds than that of alcohols [7]. With respect to the elution order of these amides and esters, here again the *R,S*-diastereomers always eluted before the *S,S* counterparts.

## 4. Conclusions

A practical method has been developed for the preparation of enantiopure MTPr, which in turn has been demonstrated to be an efficient CDA

Table 2
HPLC separation of diastereomeric MTPr amides derived from amino acids methyl esters bearing a phenyl group

| Run No. | Amino acid | $k'$ | | $\alpha$ | $R_s$ |
|---|---|---|---|---|---|
| | | (*S, S*) | (*R, S*) | | |
| 1 | Phenylglycine | 1.38 | 3.52 | 2.55 | 7.23 |
| 2 | Phenylalanine | 2.27 | 3.86 | 1.70 | 5.67 |
| 3 | $Ph(CH_2)_2CHCOOH$ <br> $\vert$ <br> $NH_2$ | 2.34 | 4.11 | 1.76 | 10.00 |
| 4 | $Ph(CH_2)_3CHCOOH$ <br> $\vert$ <br> $NH_2$ | 1.87 | 3.55 | 1.90 | 11.27 |

Conditions: mobile phase, 2-propanol–hexane (1:99); flow-rate 1 ml/min; column, silica gel (250 mm × 4.6 mm I.D.); detection, UV at 254 nm.

Table 3
GC separation of diastereomeric MTPr amides derived from enantiomeric amines and alcohols

| Run No. | Amine or alcohol | Column temperature (°C) | $k'$ | | $\alpha$ | $R_s$ |
|---|---|---|---|---|---|---|
| | | | (*S*,*S*) | (*R*,*S*) | | |
| 1 | $PhCH(NH_2)CH_3$ | 160 | 14.67 | 12.45 | 1.18 | 5.71 |
| 2 | $(1\text{-Naph})CH(NH_2)CH_3$ | 210 | 23.84 | 19.42 | 1.23 | 6.19 |
| 3 | $(2\text{-Naph})CH(NH_2)CH_3$ | 210 | 25.15 | 24.14 | 1.04 | 4.92 |
| 4 | $C_2H_5CH(NH_2)CH_3$ | 100 | 8.38 | 7.99 | 1.05 | 0.70 |
| 5 | *c*-$HexylCH(NH_2)CH_3$ | 110 | 38.60 | 36.77 | 1.05 | 1.89 |
| 6 | *n*-$C_5H_{11}CH(NH_2)CH_3$ | 120 | 12.26 | 11.27 | 1.09 | 0.89 |
| 7 | 3-(Aminomethyl)pinane | 150 | 41.46 | 39.26 | 1.05 | 1.17 |
| 8 | Menthylamine | 160 | 7.84 | 7.04 | 1.11 | 2.00 |
| 9 | Bornylamine | 160 | 8.87 | 7.98 | 1.11 | 2.94 |
| 10 | Isobornylamine | 160 | 10.16 | 9.31 | 1.09 | 2.00 |
| 11 | $Ph(CH_2)_2CH(NH_2)CH_3$ | 220 | 15.74 | 14.94 | 1.05 | 1.35 |
| 12 | *n*-$C_6H_{13}CH(OH)CH_3$ | 80 | 26.33 | 25.36 | 1.04 | 0.57 |
| 13 | Menthol | 100 | 25.15 | 24.24 | 1.04 | 0.90 |
| 14 | Borneol | 100 | 28.56 | 28.56 | 1.00 | 0 |
| 15 | $PhCH(OH)CH_3$ | 110 | 30.96 | 29.41 | 1.05 | 1.30 |

See Table 1 for GC conditions.

for the GC discrimination of enantiomeric amino acids and amines. It should be noted that MTPr is a low-boiling variant of MTPA in which a methyl substituent replaces the phenyl residue, and hence it is a potential CDA for the chiral discrimination of enantiomeric amino compounds by not only GC but also by $^1H$ and $^{19}F$ NMR [23]. It should also be noted that MTPr does not bear an $\alpha$-hydrogen or $\alpha$-fluorine on the carbon atom adjacent to the carboxylic function, which may cause racemization during the derivatization or high toxicity [4].

## References

[1] V. Schurig and H.-P. Nowtny, *Angew. Chem., Int. Ed. Engl.*, 29 (1990) 939.
[2] W.H. Pirkle and T.C. Pochapsky, *Chem. Rev.*, 89 (1989) 347.

[3] S.G. Allenmark, *Chromatographic Enantioseparation, Methods and Applications*, Ellis Horwood, Chichester, 1988.
[4] D. Parker, *Chem. Rev.*, 91 (1991) 1441.
[5] S. Yamaguchi, in J.D. Morrison (Editor), *Asymmetric Synthesis*, Vol. 1, Academic Press, New York, 1983, Ch. 7.
[6] W.H. Pirkle, M.R. Robertson and M.H. Hyun, *J. Org. Chem.*, 49 (1984) 2433.
[7] R.E. Doolittle and R.R. Heath, *J. Org. Chem.*, 49 (1984) 5041.
[8] M. Koos and H.S. Mosher, *Tetrahedron*, 49 (1993) 1541.
[9] Y. Nishida, M. Abe, H. Ohrui and H. Meguro, *Tetrahedron: Asymmetry*, 4 (1993) 1431.
[10] Y. Takeuchi, N. Itoh, T. Satoh, T. Koizumi and K. Yamaguchi, *J. Org. Chem.*, 58 (1993) 1812.
[11] A. Heumann and R. Faure, *J. Org. Chem.*, 58 (1993) 1276.
[12] Y. Adegawa, T. Kashima and K. Saigo, *Tetrahedron: Asymmetry*, 4 (1993) 1421.
[13] J.A. Dale, D.L. Dull and H.S. Mosher, *J. Org. Chem.*, 34 (1969) 2543.
[14] I. Ohtani, T. Kusumi, Y. Kashman and H. Kakisawa, *J. Am. Chem. Soc.*, 113 (1991) 4092.
[15] H. Kawa, F. Yamaguchi and N. Ishikawa, *Chem. Lett.*, (1982) 745.
[16] H. Kawa, F. Yamaguchi and N. Ishikawa, *J. Fluorine Chem.*, 20 (1982) 475.
[17] H. Kawa and N. Ishikawa, *Chem. Lett.*, (1980) 843.
[18] F. Yasuhara, M. Takeda, Y. Ochiai, S. Miyano and S. Yamaguchi, *Chem. Lett.*, (1992) 251.
[19] A. Tanaka and N. Izumiya, *Bull. Chem. Soc. Jpn.*, 31 (1958) 529.
[20] Y. Shimohigashi, S. Lee and N. Izumiya, *Bull. Chem. Soc. Jpn.*, 49 (1976) 3280.
[21] R.A. Boissonnas, S. Guttmann, P.A. Jaquenoud and J.P. Waller, *Helv. Chim. Acta*, 38 (1955) 1491.
[22] R.A. Darrall, F. Smith, M. Stacey and J.C. Tatlow, *J. Chem. Soc.*, (1951) 2329.
[23] F. Yasuhara, M. Takeda, C. Kabuto, Y. Ochiai, S. Yamaguchi and S. Miyano, to be published.
[24] S. Oi, M. Shijo, H. Tanaka, S. Miyano and J. Yamashita, *J. Chromatogr.*, 645 (1993) 17.
[25] F. Yasuhara, K. Kabuto and S. Yamaguchi, *Tetrahedron Lett.*, (1987) 4289.
[26] W.A. Konig, K.-S. Nippe and P. Mischnik, *Tetrahedron Lett.*, 31 (1990) 6867.
[27] W. Brürkle, H. Karfunkel and V. Schurig, *J. Chromatogr.*, 288 (1984) 1.

ELSEVIER

Journal of Chromatography A, 694 (1995) 237–243

JOURNAL OF CHROMATOGRAPHY A

# Gas chromatographic enantiomer separation of pharmaceuticals on capillary columns coated with novel chiral polysiloxanes

Iwao Abe[a,*], Takako Nishiyama[a], Taketoshi Nakahara[a], Hartmut Frank[b]

[a]*Department of Applied Chemistry, College of Engineering, University of Osaka Prefecture, 1-1 Gakuen-Cho, Sakai, Osaka 593, Japan*

[b]*Institute for Toxicology, University of Tübingen, Wilhelmstrasse 56, D-72074 Tübingen, Germany*

**Abstract**

Six chiral polysiloxanes were prepared by block condensation of 3-(dichloromethylsilyl)-2-methylpropionic acid 2′,2′,2′-trifluoroethyl ester with disodium tetramethyldisiloxane1-,3-diolate and subsequent nucleophilic displacement with chiral amines. The polysiloxanes were coated on to capillaries and the capillary columns were used for the gas chromatographic separation of pharmaceutical enantiomers. The columns showed sufficient enantioselectivity and thermal stability to separate various pharmaceuticals into enantiomeric pairs within a reasonable time. (*S*)-Valine-(*R*)-1-(α-naphthylethyl)amide-modified polysiloxane showed better enantioselectivity, and (*S*)-valine-(*d*)-menthylamide-modified polysiloxane gave a higher coating efficiency than the other phases.

## 1. Introduction

Chiral stationary phases in gas chromatography (GC) afford enantiomer separations with a mechanism due to solute–solvent enantioselective hydrogen bonding interactions; they are still indispensable for the separation of amino acid and amine enantiomers. Since the first successful report of this type of phase by Gil-Av et al. [1], significant developments in increasing the thermal stability and enantioselectivity of the phases have made [2–6]. In 1977, Chirasil-Val, a chiral polysiloxane with (*S*)-valine-*tert.*-butylamide anchored to carboxypropyl-modified dimethylpolysiloxane was reported [7]. Since then, polysiloxanes have received increasing attention as suitable liquid matrices for anchoring and dispersing chiral moieties [8–11]. The Chirasil-Val capillary column can be obtained commercially. Polysiloxanes with different chiral moieties have also been reported [12–14].

In previous papers [15,16], we described a novel method for the synthesis of functionalized polysiloxanes by block condensation followed by nucleophilic displacement of active ester groups for chiral amines such as (*S*)-valine-*tert.*-butylamide or (*S*)-α-naphthylethylamine in the presence of imidazole. The method was found to yield chiral polysiloxanes with high thermal stability and enantioselectivity.

In this paper, we report on the synthesis of various types of chiral polysiloxanes by nucleophilic displacement introduction of chiral amines to functionalized polysiloxanes prepared by block condensation, and their application to the enantiomer separation of pharmaceuticals.

* Corresponding author.

0021-9673/95/$09.50 
*SSDI* 0021-9673(94)00835-3

The GC enantiomer separation of pharmaceuticals on a conventional-type Chirasil-Val capillary column has been described [17]. For pharmaceuticals, one enantiomer is usually more effective than the other. In a few instances the less effective enantiomer even has toxic properties. Therefore, we tried to develop a fast and inexpensive analytical method for the separation of pharmaceutical enantiomers by capillary GC with chiral polysiloxane stationary phases prepared by rigorously regulated processes.

## 2. Experimental

### 2.1. Materials

(*S*)-α-Naphthylethylamine, (*R*)-α-naphthylethylamine, N-*tert.*-butoxycarbonyl (BOC)-(*S*)-valine, dicyclohexylcarbodiimide (DCC) and imidazole were obtained from Wako (Osaka, Japan), *l*-menthol, *d*-menthol and pentafluoropropionic anhydride (PFPA) from Tokyo Kasei Organic Chemicals (Tokyo, Japan) and pharmaceuticals from Aldrich (Milwaukee, WI, USA). All solvents were obtained from Wako and were distilled once before use.

### 2.2. Synthesis

*Trifluoroethyl ester-functionalized polysiloxane*

The polysiloxane was prepared according to the literature [16] by block condensation of 3-(dichloromethylsilyl)-2-methylpropionic acid 2′,2′,2′-trifluoroethyl ester with disodium tetramethyldisiloxane-1,3-diolate by use of dichlorodimethylsilane as a diluent to adjust the ratio of functionalized ester to unsubstituted dimethylsiloxane units to at least 1:2, with an average of 1:4.

*d- and l-menthylamine*

As *d*- and *l*-menthylamine were not available commercially, we prepared them for the corresponding menthols. First, 1.5 *M* $H_2SO_4$ (600 ml) was placed in a round-bottomed flask and $K_2Cr_2O_7$ (11.8 g, 0.4 mol) was added with stirring at room temperature. Menthol was slowly added to the solution in three or four portions. The solution was heated at 60°C for 1 h and then cooled. The oxidized product of menthone was extracted with 600 ml of diethyl ether. The ether layer was washed three times with 200 ml of 5% NaOH and three times with 200 ml of water, successively, followed by drying over anhydrous $Na_2SO_4$. After filtration from $Na_2SO_4$, the ethereal solution was condensed to about 100 ml on a Rotavapor and then distilled under reduced pressure to yield 72 g (0.47 mol) of menthone (b.p. 88–92°C/17 mmHg; yield 80%).

Menthone (30 g, 0.19 mol) and hydroxylamine hydrochloride (21 g, 0.3 mol) were dissolved in 84 ml of ethanol–water (5:1, v/v) and cooled in an ice-bath with stirring. After addition of ground NaOH (38 g), the solution was refluxed for about 1 h. The solution was cooled to room temperature and poured into 1.8 *M*- HCl (800 ml). A white precipitate formed, which was filtered off. The solution was evaporated almost to dryness on a Rotavapor and the residue was recrystallized from methanol. After drying the crystal over $P_2O_5$ under vacuum, 24 g of menthoneoxime were obtained (yield 75%).

Next, 200 ml of freshly distilled ethanol and menthone oxime (15 g) were placed in a round-bottomed flask equipped with a reflux condenser. The ethanol solution was heated until it began to boil, the heating was stopped instantaneously, and 25 g of sodium (1.1 mol) were added immediately. Soon after completion of the reaction of the sodium, the solution was cooled to room temperature, 250 ml of water were added and the mixture was distilled. The distillates were poured into 600 ml of 6 *M* HCl. After the reaction mixture had almost distilled off, about 150 m of water were added and the distillation was continued for complete azeotropic distillation of the required compound. The distillate of HCl solution was evaporated on a Rotavapor to remove HCl, water, alcohol and unchanged menthone oxime. A white precipitate of menthylamine hydrochloride salt was obtained, which was transferred into a round-bottomed flask (100-ml volume) fitted with a reflux condenser. KOH (40%) (50 ml) was added and the mixture was refluxed for about 1 h to isolate

free *d*- or *l*-menthylamine. At room temperature, the solution was transferred into a separating funnel, 100 ml of diethyl ether were added to extract menthylamine and the lower aqueous layer was discarded. About 50 ml of saturated KOH were added to the ethereal solution and the lower aqueous layer was discarded. After repeating this procedure three times, anhydrous $Na_2SO_4$ was added to dry the ethereal solution. The $Na_2SO_4$ was removed by filtration and the solution was distilled twice (b.p. 94–94.5°C) to yield 12 g of menthylamine (yield 77%). $^1H$ NMR (270 MHz, $CHCl_3$); $\delta$ (ppm) = 2.45–2.53 (m, 1H), 2.04–2.12 (m, 1H), 0.86–0.92 (q, 6H), 0.74–0.77 (d, 3H).

*(S)-Valine-tert.-butylamide, (S)-valine-(S)-1-(α-naphthylethyl)amide, (S)-valine-(R)-1-(α-naphthylethyl)amide, (S)-valine-(l)-menthylamide and (S)-valine-(d)-menthylamide*

(*S*)-Valine-*tert.*-butylamide was prepared as described previously [16]. The other (*S*)-valineamides were prepared in a similar manner.

*Chiral polysiloxanes*

Chiral polysiloxanes were synthesized almost according to the previously published procedure [16]. The polysiloxanes were prepared by nucleophilic displacement of trifluoroethyl ester-functionalized polysiloxane for chiral amines in the presence of imidazole. Imidazole works as an accelerating catalyst of the reaction rate. For example, trifluoroethyl ester-functionalized polysiloxane (200 mg), (*S*)-valine-*d*-menthylamide (120 mg, 0.47 mmol) and imidazole (30 mg, 0.44 mmol) were dissolved in 50 μl of freshly distilled dioxane and placed in a Pyrex test-tube (100 × 13 mm) equipped with a Teflon-lined screw-cap and small magnetic stirrer. Dry argon was slowly bubbled through the solution for 10 min at room temperature to remove dissolved oxygen. The tube was capped tightly and heated at 120°C for 24 h with continuous stirring. The tube was cooled and 3 ml of dichloromethane were added. The solution was washed with 1 *M* HCl and three times with water and dried over anhydrous $Na_2SO_4$. After removal of the $Na_2SO_4$ by centrifugation, the solvent was evaporated on a Rotavapor and the residue was redissolved in a 5 ml of *n*-hexane. The solution was cooled in ice and centrifuged again to remove undissolved material. The supernatent was brought to dryness under high vacuum (below 2 mmHg) on a water-bath at 90°C for 1 h. A colourless, transparent, viscous, oily liquid was obtained in a yield of 245 mg (95%).

A schematic diagram of the synthesis of the chiral polysiloxane is shown in Fig. 1. A representative Fourier transform (FT) IR spectrum of the chiral polysiloxane prepared from (*S*)-valine-(*R*)-1-(α-naphthylethyl)amide is shown in Fig. 2.

### 2.3. Column preparation

Pyrex glass capillaries (0.25 mm I.D.) were leached with 6 *M*- HCl, dehydrated at 300°C under vacuum and silylated with diphenyltetramethyldisilazane at 420°C [18]. The capillaries were coated with 0.25% solutions of the chiral polysiloxane stationary phases in *n*-pentane–dichloromethane (2:1, v/v) by means of a static method.

### 2.4. Apparatus

Measurements were performed on a Shimadzu (Kyoto, Japan) Model 9AM gas chromatograph with flame ionization detection in the split mode. A Shimadzu C-R7A data processor was used for the determination of retention times, separation factors and resolution. The carrier gas was helium. The columns were first conditioned by programming from 60 to 230°C at 4°C/min and holding at 230°C for 3 h, after which they were ready for use.

### 2.5. Sample derivatization

The pharmaceuticals used were synephrine, penicillamine, octopamine, metanephrine, isoproterenol, norepinephrine, β-3,4-dihydroxyphenylalanine (DOPA) and propranolol. These samples were acylated with PFPA prior to GC injection, except penicillamine and DOPA, which were esterified with 2-propanol before acylation.

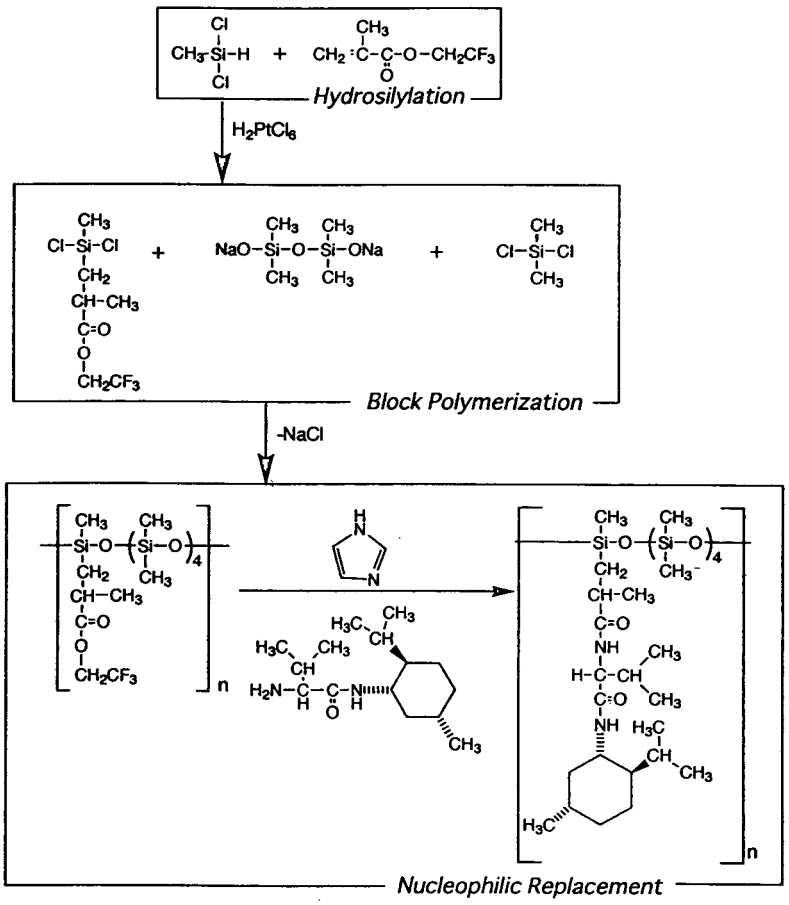


Fig. 1. Scheme of the synthesis of (*S*)-valine-*d*-menthylamide-linked polysiloxane.

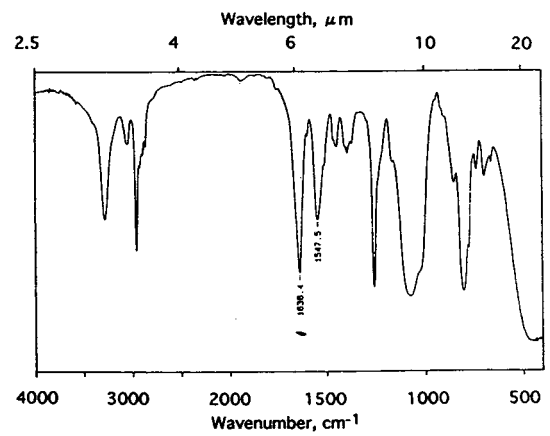


Fig. 2. FT-IR spectrum of (*S*)-valine-(*R*)-1-(α-naphthylethyl)amide-linked polysiloxane.

## 3. Results and discussion

Nucleophilic displacement of trifluoroethyl ester groups with chiral compounds was found to be efficient for the introduction of various types of chiral amines. The trifluoroethyl group linked to the polysiloxane chain is completely displaced with chiral amines with a molar ratio of only 10–20% excess of amines, as shown in Fig. 2; this is particularly important when precious chiral amines are employed. The chiral polysiloxanes are stable for use at least up to 210°C with continuous operation. The enantioselectivities of the six chiral stationary phases were characteristic and it was possible to separate the pharmaceutical enantiomers.

Table 1
GC separation factors and resolutions for N,O,S-pentafluoropropionyl derivatives of pharmaceutical enantiomers on chiral polysiloxanes with various selectors coated on 20 m × 0.25 mm I.D. glass capillaries

| Selector | Pharmaceutical | | | | | | |
|---|---|---|---|---|---|---|---|
| | Synephrine (140°C)[a] | Penicillamine[b] (160°C)[a] | Octopamine (160°C)[a] | Metanephrine (160°C)[a] | Isoproterenol (160°C)[a] | Norepinephrine (180°C)[a] | DOPA[b] (180°C)[a] |
| *(S)-Val-amides* | | | | | | | |
| *-tert.*-Butyl | 1.011(0.60) | 1.000 | 1.043(2.51) | 1.025(1.34) | *1.024(1.32)*[c] | 1.024(1.32) | 1.079(3.78) |
| -(*S*)-1-(α-Naphthylethyl) | 1.000 | 1.139(6.27) | 1.026(1.28) | 1.000 | 1.000 | 1.000 | *1.114*(5.06) |
| -(*R*)-1-(α-Naphthylethyl) | *1.053(2.72)* | *1.337(9.76)*[c] | *1.200(9.15)* | 1.016(0.81) | 1.000 | *1.097(4.58)* | 1.050(2.47) |
| -*l*-Menthyl | 1.016(1.03) | 1.172(8.20)[c] | 1.082(5.00) | 1.000 | 1.000 | 1.049(2.89) | 1.036(2.09) |
| -*d*-Menthyl | 1.000 | 1.195(9.02) | 1.034(2.08) | *1.026(1.52)* | 1.000 | 1.000 | 1.113(*6.10*) |
| *Monoamide* | | | | | | | |
| (*S*)-1-(α-Naphthylethyl) | 1.000 | 1.089(2.94) | 1.035(1.73) | 1.014(0.68) | 1.000 | 1.000 | 1.031(1.41) |

The highest separation factor and resolution of each compound are in italics. For each enantiomeric pair, the *d*-enantiomer eluted faster. Data in parentheses are resolutions, calculated with the equation [19] $R = 1.18(t_{R_2} - t_{R_1})/(W_{1/2,1} + W_{1/2,2})$, where $R$ = resolution, $t_{R_1}$ = retention time of the first-eluted enantiomer, $t_{R_2}$ = retention time of the second-eluted enantiomer, $W_{1/2,1}$ = peak width at half-height of the first-eluted enantiomer and $W_{1/2,2}$ = peak width at half-height of the second-eluted enantiomer.
[a] Column temperature.
[b] Isopropyl ester.
[c] Reversal of elution order of enantiomers.

Chromatographic data obtained for seven pharmaceutical enantiomers are given in Table 1. The highest separation factors and resolution obtained with six chiral polysiloxane stationary phases are given in italics. DOPA enantiomers could be separated completely on all chiral polysiloxanes. Similarly, penicillamine showed complete separation on all phases except (*S*)-

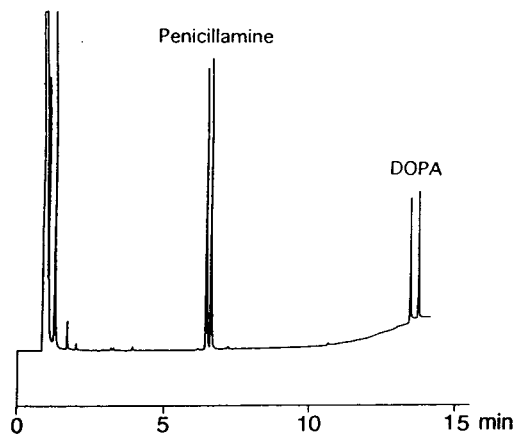


Fig. 3. GC enantiomer separation of pharmaceuticals. Column, glass capillary (20 m × 0.25 mm I.D.) coated with (*S*)-valine-*tert.*-butylamide-functionalized polysiloxane (Chirasil-Val); column temperature, 120°C for 2 min, then increased at 3°C/min to 130°C, 5°C/min to 150°C and 10°C/min to 170°C. For more details, see text.

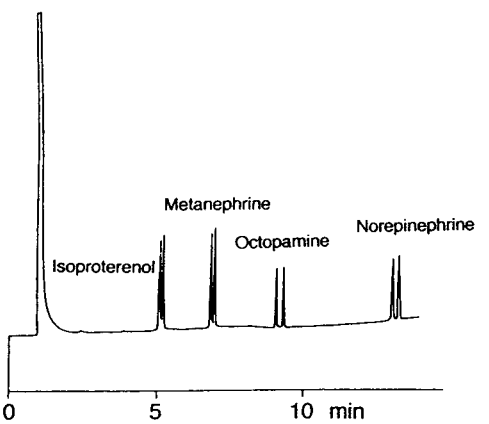


Fig. 4. GC enantiomer separation of pharmaceuticals. Column, Chirasil-Val; column temperature, 150°C for 2 min, then increased at 2°C/min to 170°C and 4°C/min to 200°C. For other conditions, see Fig. 3 and text.

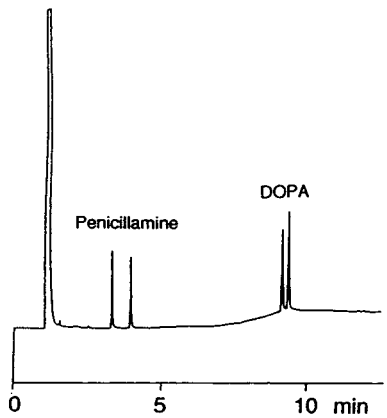


Fig. 5. GC enantiomer separation of pharmaceuticals. Column, glass capillary (20 m × 0.25 mm I.D.) coated with (*S*)-valine-(*R*)-1-(α-naphthylethyl)amide-linked polysiloxane; column temperature, 160°C for 2 min, then increased at 3°C/min to 170°C and 6°C/min to 190°C.

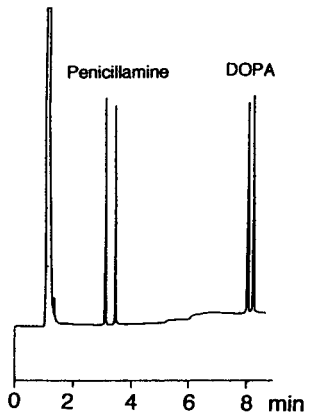


Fig. 6. GC enantiomer separation of pharmaceuticals. Column, glass capillary (20 m × 0.25 mm I.D.) coated with (*S*)-valine-*l*-menthylamide-linked polysiloxane; column temperature, 160°C for 2 min, then increased at 3°C/min to 180°C.

valine-*tert.*-butylamide-anchored polysiloxane (Chirasil-Val). However, Chirasil-Val could separate penicillamine enantiomers completely at a lower column temperature, as shown in Fig. 3. The enantioselectivity of Chirasil-Val was not very high towards these pharmaceuticals, but all of them could be separated into enantiomeric pairs (Fig. 4) Overall, (*S*)-valine-(*R*)-1-(α-naphthylethyl)amide-linked polysiloxane offered the highest separation factors. Figs. 5 and 6 show typical chromatograms.

The enantioselectivities of the polysiloxanes functionalized with (*S*)-valine-*l*-menthylamide and (*S*)-valine-*d*-menthylamide were unexpectedly low. However, the capillary columns coated with these chiral polysiloxanes showed fairly high column efficiencies, which may be due to their low polarities. The highest separation factors coincide with the highest resolutions, except for DOPA, which showed the highest resolution on (*S*)-valine-*d*-menthylamide-linked polysiloxane.

Table 2 represents the coating efficiencies of the capillary columns with different types of chiral polysiloxanes. The efficiencies obtained from the capillaries coated with (*S*)-valine-*d*-

Table 2
Efficiencies of the capillary columns coated with polysiloxanes with different selector groups

| Selector | Capillary I.D. (mm) | Film thickness (μm) | HETP for methyl *n*-decanoate at 80°C (mm) | Coating efficiency (%) |
|---|---|---|---|---|
| (*S*)-Valine-*tert.*-butylamide | 0.25 | 0.14 | 0.30 | 74 |
| (*S*)-Valine-(*S*)-1-(α-naphthylethyl)amide | 0.25 | 0.14 | 0.37 | 60 |
| (*S*)-α-Naphthylethylamine | 0.25 | 0.14 | 0.43 | 52 |
| (*S*)-Valine-*d*-menthylamide | 0.25 | 0.14 | 0.25 | 89 |
| (*S*)-Valine-*d*-menthylamide | 0.15 | 0.11 | 0.14 | 94 |

The capillaries were all made of Pyrex glass and deactivated as described in the text. Carrier gas, helium; linear gas velocity, 32 cm/s.

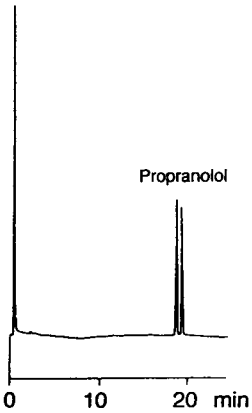


Fig. 7. GC enantiomer separation of propranolol. Column, glass capillary (10 m × 0.15 mm I.D.) coated with (*S*)-valine-*d*-menthylamide-linked polysiloxane; column temperature, 180°C isothermal.

menthylamide-functionalized polysiloxane were found to be the highest. This phase is particularly useful for the separation of the less volatile propranolol enantiomers (Fig. 7).

## 4. Conclusions

Chiral polysiloxane stationary phases for capillary GC prepared by block condensation and nucleophilic displacement are applicable to the preparation of chiral polysiloxanes with a wide variety of selectors. The phases were found to be efficient for the separation of pharmaceutical enantiomers of the amino acid and amino alcohol types. This method for the preparation of functional polysiloxanes is considered to be useful in other areas of research.

## Acknowledgement

This work was supported partially by the Ministry of Education of Japan, Culture and Science: Project No. 05835009.

## References

[1] E. Gil-Av, B. Feibush and R. Charles-Sigler, *Tetrahedron Lett.*, (1966) 1009.
[2] U. Beitler and B. Feibush, *J. Chromatogr.*, 123 (1976) 149.
[3] W.A. Konig, W. Parr, H.A. Lichtenstein, E. Bayer and J. Oro, *J. Chromatogr. Sci.*, 8 (1970) 183.
[4] B. Feibush, *Chem. Commun.*, (1971) 544.
[5] R. Charles, U. Beitler, B. Feibush and E. Gil-Av, *J. Chromatogr.*, 112 (1975) 121.
[6] R. Charles and E. Gil-Av, *J. Chromatogr.*, 195 (1980) 317.
[7] H. Frank, G.J. Nicholson and E. Bayer, *J. Chromatogr. Sci.*, 15 (1977) 174.
[8] H. Frank, G.J. Nicholson and E. Bayer, *Angew. Chem.*, 90 (1978) 396.
[9] T. Saeed, P. Sandra and M. Verzele, *J. Chromatogr.*, 186 (1979) 61.
[10] T. Saeed, P. Sandra and M. Verzele, *J. High Resolut. Chromatogr.*, 3 (1980) 35.
[11] W.A. Konig and I. Benecke, *J. Chromatogr.*, 209 (1981) 91.
[12] M. Schleimer and V. Schurig, *J. Chromatogr.*, 638 (1993) 85.
[13] M. Jung and V. Schurig, *J. Microcol. Sep.*, 5 (1993) 11.
[14] C.Y. Wu, J.S. Cheng and Z.R. Zeng, *Chromatographia*, 35 (1993) 33.
[15] H. Frank, I. Abe and G. Fabian, *J. High Resolut. Chromatogr.*, 15 (1992) 444.
[16] I. Abe, T. Nishiyama and H. Frank, *J. High Resolut. Chromatogr.*, 17 (1994) 9.
[17] H. Frank, G.J. Nicholson and E. Bayer, *J. Chromatogr.*, 146 (1978) 197.
[18] K. Grob, *Making and Manipulating Capillary Columns for Gas Chromatography*, Hüthig, Heidelberg, 1986.
[19] L.R. Snyder, *J. Chromatogr. Sci.*, 10 (1972) 200.

ELSEVIER

Journal of Chromatography A, 694 (1995) 245–276

JOURNAL OF CHROMATOGRAPHY A

Review

# Optical resolution of drugs by capillary electrophoretic techniques

Hiroyuki Nishi*[,a], Shigeru Terabe[b]

[a]*Analytical Chemistry Research Laboratory, Tanabe Seiyaku Co., Ltd., 16-89, Kashima 3-chome, Yodogawa-ku, Osaka 532, Japan*

[b]*Faculty of Science, Himeji Institute of Technology, Kamigori, Hyogo 678-12, Japan*

**Abstract**

This review surveys the optical resolution of drugs by capillary electrophoretic (CE) techniques. The CE techniques involve capillary zone electrophoresis, electrokinetic chromatography, capillary gel electrophoresis, capillary isotachophoresis and electrochromatography. Each section is arranged according to species of chiral selectors used in CE from the viewpoint of practical use. Optical resolution of enantiomers by CE techniques is mainly achieved through the modification of the separation solution with chiral additives such as cyclodextrins or proteins. A brief separation theory or separation procedure for each CE technique and some typical applications are also described for practical guidelines.

## Contents



* Corresponding author.

0021-9673/95/$09.50 
*SSDI* 0021-9673(94)00682-2

## 1. Introduction

Capillary electrophoresis (CE) has become a powerful and a popular separation technique because of the rapid separation and high resolution achieved [1–3] and fully automated instrumentation. Several different separation modes, from capillary gel electrophoresis (CGE) to micellar electrokinetic chromatography (MEKC) [4,5], have been developed and consequently a wide variety of substances such as ions, drugs and biopolymers can be analysed by CE, according to the physico-chemical properties of the analyte. In particular, for small molecules such as pharmaceuticals, CE offers adequate separation, detection, simplicity, etc., for a method of quality control. CE is now recognized as an important option among separation methods in pharmaceutical analysis, because its separation principle differs from those of other separation methods such as high-performance liquid chromatography (HPLC). Some monographs [6–12] and reviews [13–16] that provide overviews of CE techniques are available. Some review papers that have focused on the qualitative aspects of CE techniques have been published [17–23].

Concerning the separation of enantiomers, CE techniques can take advantage of an ultra-high separation efficiency, easy exchanges of separation media, extremely small volumes of the sample and the media, etc., in comparison with HPLC. This means that, in the development of a CE chiral separation method, one can easily alter the separation solution to find the optimum separation medium and can also use an expensive chiral selector. This is a great advantage of CE as a quality control method from an economic viewpoint. Some papers reviewing chiral separations by CE have recently become available [24–27].

In CE chiral separations, much work has been reported on the direct resolution of enantiomers by capillary zone electrophoresis (CZE) employing cyclodextrins (CDs) (CD-CZE) [28–73]. Differential inclusion-complex formations of CD with the solute provide differential solute migrations and chiral recognition. CDs have also been successfully used in the chiral separation by CGE [74,75], MEKC (CD-MEKC) [76–87] or capillary isotachophoresis (ITP) [88–94]. Chiral separation by CE using a CD immobilized capillary tube [commercially available as chiral stationary phases for gas chromatography (GC)] has been also reported [95–98]. CD derivatives having a charge have been used in CE (CD-EKC) to separate enantiomers [69–73,97,99].

Other than CDs, proteins have been vigorously investigated as chiral selectors in CE chiral separations [100–109]. In the addition of proteins, the separation mode can be classified as one of EKC, i.e., affinity EKC. These chiral selectors have already been successfully applied to HPLC and been demonstrated to be effective in chiral separations [110]. The chiral selector used in HPLC such as polysaccharides should be applicable in CE apart from CDs or proteins. Further investigations of adopting chiral selectors known from HPLC or GC in CE will be made to extend the application range.

In this paper, chiral separations of drugs by CE techniques are described mainly on the basis of practical use, with the structures of the drugs that are enantioresolved by the method. Various CE techniques for optical resolution are also overviewed briefly. A detailed separation theory of each CE chiral separation has been described previously [27].

## 2. Capillary electrophoretic techniques and approach to chiral separation

CE or high-performance capillary electrophoresis, which was first introduced by Mikker et al. [1], Jorgenson and Lukacs [2] and Hjerten [3], has been demonstrated to be highly efficient. Several modes, which are used routinely in conventional electrophoretic methods, have been exploited in capillary systems to obtain a highly efficient separation. The most successful and popular operational mode is zone electrophoresis. In zone electrophoresis, background electrolytes or gels are filled in the capillary to maintain a constant electric field along the tube. The former is CZE and the latter method is

called CGE. The results obtained are recorded as electropherograms, which are similar to chromatograms in HPLC, and can be easily handled with a data processor as used in HPLC. ITP separation has been performed in the capillary system. Capillary isoelectric focusing (IEF) has also been reported with some detection systems, specially developed for IEF.

Although CE has a high resolving power, it can separate only ionic or charged compounds, because its separation principle is based on the difference in electrophoretic mobilities. To overcome this problem, Terabe and co-workers [4,5,99] combined CE and chromatographic separation principles. This method is called electrokinetic chromatography (EKC). EKC can be considered as a branch of CE and performed with the same apparatus as CZE based on chromatographic principles. A homogeneous solution that contains an ionic pseudo-stationary phase is used to separate electrically neutral solutes. Various compounds are available as pseudo-stationary phases for EKC. Among many modes of EKC, micellar EKC (MEKC), which uses micellar solutions of ionic surfactants such as sodium dodecyl sulphate (SDS), has become the most popular method. Besides MEKC, CD-EKC, in which charged CD derivatives are employed as a carrier, can be applied to the chiral separation.

Other than CZE, CGE, ITP, IEF and EKC, electrochromatography (EC) can be also classified as a branch of CE, although the separation principle is identical with that of conventional liquid chromatography. EC uses electroosmosis for mobile phase delivery instead of a high-pressure pump as in HPLC. Many wall-coated or packed capillary columns can be used in the EC mode. The operational formats in the CE separations mentioned above are summarized in Table 1. The detailed separation principle of each CE mode has been described in other reviews and monographs [6–16] and is not given here.

In CE chiral separations, the same strategies as have been exploited in chiral separations in HPLC can be used. There are two possible techniques to resolve enantiomers in CE: (1) direct chiral separation and (2) separation of enantiomers derivatized to diastereomers with chiral reagents. Direct enantiomeric separation by CE can be achieved through modification of the buffer solutions with chiral additives to form a diastereomeric pair. The difference in the stability of diastereomeric complexes leads to a successful enantioseparation. CDs or CD derivatives [29–99], proteins [100–109], crown ethers [25,62,111,112] and polysaccharides [113,114] can be applied in CE as chiral selectors. The addition of chiral ligands and metals can be

Table 1
Modes of capillary electrophoretic techniques and applicability to chiral separation

| Mode | Applicability[a] | Chiral selector |
|---|---|---|
| Capillary zone electrophoresis (CZE) | VG | CD, crown ether |
| Cyclodextrin-modified CZE (CD-CZE) | | |
| Capillary gel electrophoresis (CGE) | G | CD |
| Isoelectric focusing (IEP) | × | |
| Capillary isotachophoresis (ITP) | NVG | CD |
| Electrokinetic chromatography (EKC) | VG | |
| Micellar EKC (MEKC) using chiral surfactants | | Chiral surfactant |
| Cyclodextrin-modified MEKC (CD-MEKC) | | CD |
| EKC with charged cyclodextrins (CD-EKC) | | Charged CD |
| Affinity EKC | | Protein, polysaccharide |
| Electrochromatography (EC) | G | Chiral column (for GC) |

[a] VG, very good; G, good; NVG, not very good; ×, out of adaptability.

effective for the enantiomeric separation of amino acids [115,116]. These chiral additives have been successfully demonstrated to be effective for chiral separations in HPLC [110]. In MEKC, besides the addition of chiral compounds mentioned above, direct chiral separation can be obtained with the use of chiral surfactants [117–130]. The basic theory of each CE mode as a chiral separation method has been described previously [27] and in this review recent applications of CE chiral separations are reported according to the chiral selector. Most chiral compounds developed are pharmaceuticals, pesticides, herbicides, etc., and these are all small molecular compounds. Therefore, the CZE or EKC mode is the most successful and easy to adopt as a chiral separation method among the many CE modes. IEF is not suitable for enantiomeric separation.

## 3. Chiral separation by host–guest interaction

### 3.1. Use of cyclodextrins (CDs)

#### 3.1.1. Addition of neutral CDs

CDs are cyclic oligosaccharides consisting of six, seven or eight glucopyranose units corresponding to the particular names, α-, β- or γ-CD. The structure of CDs is that of a truncated cone with a hydrophobic cavity, whose size differs significantly among the CDs. Some properties of CDs and a schematic structure are given in Table 2. CDs tend to include compounds that fit their cavities by hydrophobic interaction. The host–guest complexation constants depend on the suitability between the guest molecule and the CD, where the cavity diameter and the geometry of the CD are important factors. Successful enantioresolution results from the

Table 2
Physico-chemical properties and structure of α-, β- and γ-cyclodextrin [110]

| Parameter | Type of CD | | |
|---|---|---|---|
| | α- | β- | γ- |
| Number of glucose units | 6 | 7 | 8 |
| Molecular mass | 972 | 1135 | 1297 |
| Inner diameter of cavity (Å) | 5.7 | 7.8 | 9.5 |
| Outer diameter of cavity (Å) | 13.7 | 15.3 | 16.9 |
| Cavity volume ($Å^3$) | 174 | 262 | 427 |
| Solubility in water (25°C) (%, w/v) | 14.5 | 1.8 | 23.2 |

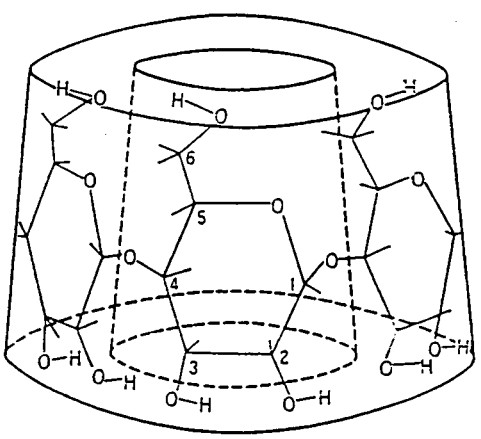

differences in the inclusion-complex formation constants. Other than natural α-, β- and γ-CDs, many CD derivatives have been developed for increased solubility in water or to modify the cavity shape or to add a special function. Table 3 summarizes enantiomeric separations by CZE through the addition of neutral CDs (CD-CZE). For some drugs, unmodified β- and γ-CD were successful, but for many enantiomeric drugs derivatized CDs such as heptakis-(2,6-di-O-methyl)-β-CD (DM-β-CD) or hydroxypropyl-β-CD (HP-β-CD) were effective. CD-CZE is the most successful technique for enantiomeric separation by CE and a variety of applications have been reported [28–73]. As shown in Table 3, typically acidic buffer solutions are employed in CD-CZE, because suppressed electroosmosis yields a higher enantiomeric resolution.

Optical resolution by CZE with CD as the chiral selector (CD-CZE) was first introduced by Fanali's group [28]. They successfully separated enantiomers of ephedrine alkaloids [28,29], isoproterenol [28], terbutaline [30], propranolol [30], tryptophan derivatives [29,31], ketamine [32], octopamine [32] and folinic acids [33] by CZE employing CDs. Wren and Rowe [34–37] described a separation model in CD-CZE and derived an equation describing the differential mobility between an enantiomeric pair (1 and 2), $\Delta\mu$, as follows:

$$\Delta\mu = \frac{[C](\mu_f - \mu_c)(K_1 - K_2)}{1 + [C](K_1 + K_2) + K_1K_2[C]^2} \quad (1)$$

where $\mu_f$ is the electrophoretic mobility of the enantiomers in free solution, $\mu_c$ is the electrophoretic mobility of the CD-complexed enantiomers, $K_1$ and $K_2$ are the formation constants of inclusion complexes of the two enantiomers and [C] is the concentration of the CD. The mobility of each complex, $\mu_c$, is assumed to be equal to the mobility of the chiral selector. Eq. 1 shows the dependence of $\Delta\mu$ on the difference in the mobilities between the free and the CD-complexed enantiomer, $\mu_f - \mu_c$, the formation constants, $K_1$ and $K_2$, and the concentration of CD. It is obvious that the larger difference $\mu_f - \mu_c$ the greater is the $\Delta\mu$ value. It was also reported that there is an optimum concentration of CD giving the maximum enantioselectivity. Successful applications of this model to the enantiomeric separation of propranolol [34,35], oxprenolol, metoprolol, atenolol [36], practolol and ephedrine [37] were reported by Wren and Rowe. Rawjee and co-workers [38–40] also described a more complex model of CD-CZE and applied it to the enantiomeric separation of fenoprofen, ibuprofen [38], naproxen [39] and homatropine [40].

Snopek et al. [41] used hydroxyalkylcelluloses such as methylhydroxyethylcellulose (MHEC) and hydroxyethylcellulose (HEC) in CD-CZE with uncoated capillaries under acidic conditions to suppress the electroosmotic flow (EOF). The addition of HEC or MHEC was found to be effective in improving the resolution of enantiomers of chloramphenicol, thioridazine and ketotifen. They also investigated the ITP chiral separation of the same solutes employing CDs. Soini et al. [42] used cationic surfactants such as cetyltrimethylammonium bromide (CTAB) and cetylpyridinium chloride (CPC) together with MHEC in CD-CZE with uncoated or polyacrylamide-coated capillaries at pH 2.7–3.0. The presence of CTAB or CPC at around their critical micelle concentration improved the reproducibility of the migration times and peak shapes of basic solutes such as verapamil and fluoxetine with uncoated capillaries. They also determined verapamil and bupivacaine extracted from serum and reported that the CE chiral separation was better than HPLC or GC chiral separations because of the easy development and optimization of the method. Belder and Schomburg [43] added poly(vinyl alcohols) and HEC to the buffers in CD-CZE with uncoated capillaries. Besides the effects of the reduction of the EOF, i.e., increase in the migration times, both the peak symmetry and peak width were considerably improved and good enantiomeric separations were achieved for four tocainide compounds. This can be ascribed to the suppression of the solute adsorption to the wall through the dynamic coating with the additives. Quang and Khaledi [44,45] employed tetraalkylammonium

Table 3
Chiral separation by capillary zone electrophoresis with neutral CDs (CD-CZE)

| Compound[a] | CD | pH | Additive | Ref. |
|---|---|---|---|---|
| *Amino acids (AAs)* | | | | |
| Ala-β-naphthylamide | β, γ, diacetyl-β | 2.0 | | 60 |
| DNS-AAs (Asp, Glu, Leu, Nle, Nva, Phe, Val, Met, Ser, Thr, Trp, α-amino-*n*-butyric acid) | α, β, γ<br>DM-α, DM-β<br>TM-α, TM-β | 9.0 | | 59,61 |
| DNS-AAs (Leu, Thr, Met) | γ | 9.0 | | 25 |
| DNS-AAs (Trp) | α | 2.2 | | 25 |
| DNS-AAs (Phe) | HP-β | 9.0, 6.0 | | 57,69 |
| Phe, Tyr, Trp | α | 2.5 | | 29,62 |
| Trp derivatives | α | 2.5 | | 31 |
| *Antidepressants* | | | | |
| Fluoxetine[1] | TM-β | 2.7 | MHEC, CTAB | 42 |
| Mianserin[2] | HP-β | 3.3 | | 53 |
| Nefopam[3] | HP-β | 3.3 | | 53 |
| Nomifensine[4] | HP-β | 3.3 | | 53 |
| *Antipsychotics* | | | | |
| Promethazine[5] | γ | 3.0 | | 66 |
| Thioridazine[6] | γ | 2.5 | | 41 |
| *Hypnotics* | | | | |
| Metomidate[7] | HP-β | 3.3 | | 53 |
| Zopiclone[8] | HP-β | 3.3 | | 53 |
| *Barbiturates* | | | | |
| Hexobarbital[9] | DM-β, α, β | 9.0 | | 59 |
| | DM-β, β, HP-β | 8.3 | EDTA | 69 |
| Pentobarbital[10] | TM-α, TM-β | 9.0 | | 59 |
| Secobarbital[11] | TM-α, α | 9.0 | | 59 |
| *Anaesthetics* | | | | |
| Bupivacaine[12] | DM-β | 2.9 | MHEC, CTAB | 42 |
| Ketamine[13] | DM-β | 2.5 | | 32 |
| | β | 3.3 | | 53 |
| Mepivacaine[14] | DM-β | 2.9 | MHEC, CTAB | 42 |
| *Adrenergic drugs* | | | | |
| Epinephrine[15] | DM-β | 2.4, 2.5 | | 20,28,29,32,46,65 |
| | β | 2.5 | TMA | 44 |
| Norepinephrine | DM-β | 2.4, 2.5 | | 28,32 |
| | β | 2.5 | TMA | 44 |
| Ephedrine (*SR*, *RS*)[16] | DM-β | 2.4, 2.5, 3.3 | | 28,37,53,56 |
| | β | 2.5 | TBA | 44 |
| | DM-β | 2.5 | MeOH | 58 |
| | DM-β | 2.5 | HPC, TBA | 73 |
| Norephedrine | DM-β | 2.4, 2.5, 3.3 | | 28,53,56 |
| | DM-β | 2.5 | HPC, TBA | 73 |
| Pseudoephedrine (*SS*, *RR*) | β | 2.5 | TBA | 44 |
| N-Methylephedrine | DM-β | 2.5, 3.3 | | 53,56 |
| | DM-β | 2.5 | HPC, TBA | 73 |
| N-Methylpseudoephedrine | DM-β | 2.5 | HPC, TBA | 73 |
| Etilefrine[17] | HP-β | 3.3 | | 53 |
| | DM-β | 3.0 | | 66 |
| Norfenefrine[18] | HP-β | 3.3 | | 53 |
| Octopamine[19] | DM-β | 2.5 | | 32 |
| | HP-β | 3.3 | | 53 |
| Pholedrine[20] | HP-β | 3.3 | | 53 |
| Synephrine[21] | DM-β | 3.3 | | 53 |
| *Cardiotonic* | | | | |
| Denopamine[22] | DM-β | 2.2 | Urea | 52 |
| *Dopamine agonist* | | | | |
| Quinagolide[23] | β | 2.5 | | 62 |

Table 3 *(continued)*

| Compound[a] | CD | pH | Additive | Ref. |
|---|---|---|---|---|
| *Bronchodilators* | | | | |
| Clenbuterol[24] | HP-β | 2.2, 3.3 | | 47,53 |
| | β | 4.0 | | 49 |
| Isoproterenol[25] | DM-β | 2.4, 2.5, 3.3 | | 28,32,53 |
| | β | 2.5 | TBA, TMA | 44 |
| | DM-β | 2.5 | TMA | 45 |
| Picumeterol[26] | DM-β | 2.,2, 2.3 | | 23, 50 |
| | β | 4.0 | | 49 |
| Salbutamol[27] | DM-β | 3.3 | | 53 |
| Terbutaline[28] | DM-β, β | 2.5 | | 30 |
| Trimetoquinol[29] | DM-β, β | 2.2–2.5 | | 66 |
| Trimetoquinol, analogues | β-CD polymer | 2.7, 6.5 | | 51 |
| *β-Blockers* | | | | |
| Alprenolol[30] | HP-β | 2.5 | TMA | 45 |
| Atenolol[31] | DM-β | 3.0, 2.5, 2.4 | | 36,37,65 |
| | DM-β | 2.5 | TMA | 45 |
| Carvedilol[32] | DM-β | 2.9 | MHEC, CTAB | 42 |
| | β | 3.3 | | 53 |
| Labetalol[33] | HP-β | 2.5 | TMA | 45 |
| Metoprolol[34] | DM-β | 3.0 | | 36 |
| Nadolol[35] | HP-β | 2.5 | TMA | 45 |
| Oxprenolol[36] | DM-β | 3.0 | | 36 |
| | DM-β | 2.5 | TMA | 45 |
| Pindolol[37] | DM-β | 2.5 | TMA | 45 |
| | DM-β | 3.0 | MHEC, CTAB | 42 |
| Practolol[38] | DM-β | 2.5 | | 37 |
| Propranolol[39] | DM-β, β | 3.1, 2.5 | MeOH, urea | 30,34 |
| | DM-β | 3.0 | MeOH, ACN | 35,36 |
| | DM-β, TM-β, β | 2.5 | TBA, TMA | 44,45 |
| | HE-β, HP-β | 2.4 | | 65 |
| *Ca-channel blocker* | | | | |
| Verapamil[40] | TM-β | 2.7 | MHEC, CTAB | 42 |
| *Antihypertensive* | | | | |
| Lofexidine[41] | HP-β | 3.3 | | 53 |
| *Antiarrhythmics* | | | | |
| Sotalol[42] | HP-β | 3.3 | | 53 |
| Tocainide,[43], analogues | γ | 3.0 | HEC | 43 |
| *Anticholinergics* | | | | |
| Ambucetamide[44] | HP-β | 3.3 | | 53 |
| Benzetimide[45] | HP-β | 4.0 | | 19 |
| Homatropine[46] | β | 6.25 | HEC | 40 |
| Timepidium[47] | γ | 2.7 | Urea | 52 |
| *Antihistaminics* | | | | |
| Carbinoxamine[48] | β | 2.5 | Urea | 20 |
| Chlorpheniramine[49] | β | 2.5 | MeOH, urea | 64 |
| Dimethindene[50], metabolites | β, HP-β, HE-β | 3.3 | | 53 |
| Doxylamine[51] | β | 2.5 | (CTAB) | 44 |
| *Antiasthmatics* | | | | |
| Ketotifen[52] | β, γ | 3.5, 3.75 | MHEC | 41 |
| Ketotifen intermediate, analogue | γ | 3.75, 3.5 | | 41 |
| Ketotifen, N-oxide form | β | 2.5 | | 41 |
| *Anti-inflammatories* | | | | |
| Fenoprofen[53] | β, HP-β | 4.50, 4.41 | HEC | 38,39 |
| Ibuprofen[54] | β | 4.50 | HEC | 38 |
| Naproxen[55] | HP-β | 4.86 | HEC | 39 |
| *Anticoagulant* | | | | |
| Warfarin[56] | DM-β-MA | 9.2 | | 54 |
| *Antifungal* | | | | |
| Tioconazole[57] | HP-β | 4.3 | MeOH | 63 |

*(Continued on p. 252)*

Table 3 *(continued)*

| Compound[a] | CD | pH | Additive | Ref. |
|---|---|---|---|---|
| *Antibacterial* | | | | |
| Chloramphenicol[58] | DM-β | 3.5 | MHEC | 41 |
| *Antimalarials* | | | | |
| Mefloquine[59] | HP-β | 3.3 | | 53 |
| Primaquine[60] | γ | 3.0 | | 66 |
| *Anticancer agents* | | | | |
| Leucovorin[61] (6*S*, 6*R*) | DM-β | 6.0 | | 33 |
| Leucovorin, metabolite (6*S*, 6*R*) | γ | 7.0 | Urea | 67 |
| *Aldose reductase inhibitor* | | | | |
| AL03152[62], AL03363 | β, DM-β, HE-β, HP-β | 11 | | 65 |
| *Aromatase inhibitors* | | | | |
| Aminoglutethimide[63] | α, β, γ | 2.5 | | 68 |
| Aminoglutethimide analogues | β, DM-β | 2.5 | | 68 |
| Fadrozole[64] | β, DM-β | 2.5 | | 68 |
| *Others* | | | | |
| Benzoin[65] | γ | 3.0 | Urea | 66 |
| 1,1′-Binaphthyl-2,2′-diyl hydrogenphosphate[66] | β, glycosylated α | 9.0 | | 57 |
| 1,1′-Binaphthyl-2,2′-dicarboxylic acid[67] | α, glycosylated α | 9.0 | | 57 |
| Fluparoxan[68], analogues | β | 2.5, 2.7 | IPA, urea | 48,71 |
| Phenoxy acid herbicides[69] | α, DM-β | 4.8 | | 55 |
| Troger's base | β | 2.5 | | 25 |
| Mandelic acid | HP-β | 6.0 | | 72 |
| *m*-Hydroxymandelic acid | HP-β | 6.0 | | 72 |
| *p*-Hydroxymandelic acid | HP-β | 6.0 | | 72 |
| 3,4-Dihydromandelic acid | HP-β | 6.0 | | 72 |
| 2-Phenyllactic acid | β, HP-β | 5.0, 6.0 | | 72 |
| 3-Phenyllactic acid | β, HP-β | 5.0, 6.0 | | 72 |
| Precursor of drug ENX 792 | β | 2.5 | | 62 |
| CNS-active compounds | α, β, DM-β | 2.5 | | 56 |
| Imafen | HP-β | 3.3 | | 53 |

[a] Superscript numbers refer to structures of the solutes shown in Fig. 13.

(TAA) cations in CD-CZE with uncoated capillaries for the enantiomeric separation of basic compounds such as ephedrine alkaloids, doxylamine, isoproterenol, metaphrine [44] and some β-blockers [45]. TAA cations added to the buffer covered the capillary wall, leading to the suppression of solute adsorption and the reduction of the EOF.

Peterson and Trowbridge [46] applied the CE technique for the determination of *d*-epinephrine in a pharmaceutical formulation containing *l*-epinephrine. The enantiomers of epinephrine were resolved by CD-CZE employing DM-β-CD at pH 2.4. Quantification using an internal standard method showed good reproducibility and small amounts of *l*-epinephrine (around 1%) could be determined. Altria et al. [47] examined inter-company cross-validation on CE chiral separations of clenbuterol racemates to check the repeatability of the CE method. Three different CE instruments were employed among seven pharmaceutical companies for this exercise. The good repeatability obtained from the seven companies showed that a CE method is transferable between different companies. Altria and coworkers also successfully employed a CE chiral separation method for the enantiomeric purity testing of fluparoxan [48] and picumeterol [23,49,50]. They reported that the detection limits of the undesired enantiomers of fluparoxan and picumeterol were 0.3% and 0.1%, respectively. In CE chiral analysis, peak area normalization is performed because the later migrating enantiomer migrates more slowly through the detector and gives an overestimated peak area [23].

Recently, Nishi and co-workers [51,52] used β-CD polymer as a chiral selector in CD-CZE. The structure of the β-CD polymer, which is synthesized by condensation of β-CD molecules with epichlorohydrin, is shown in Fig. 1. The enantiomers of trimetoquinol and related compounds except for laudanosine were successfully resolved by CD-CZE with β-CD polymer. An electropherogram of five racemates is shown in Fig. 2, where one of the enantiomers of norlaudanosoline was co-eluted with one of the enantiomers of laudanosoline. They also applied the method to the optical purity testing of the drug and reported that about 0.1% of the minor enantiomer was detectable by the method. A typical electropherogram for ca. 0.2% of the *R*-form (inactive) added to the standard trimetoquinol (*S*-form) is shown in Fig. 3 [52]. β-CD polymer will be more favourable than the usual CDs because the high molecular mass of the polymer cause a reduced mobility, leading to a larger difference in $\Delta\mu$ in Eq. 1.

Heuermann and Blaschke [53] reported the enantiomeric separation of 23 basic drugs by CD-CZE. Many of them were successfully enantioresolved by employing HP-β-CD. An example is shown in Fig. 4, where six chiral drugs with different structures were separated in a single run. Gareil et al. [54] reported the chiral separation of warfarin by CZE with DM-β-CD.

As in CD-CZE, introduction of CD in the MEKC mode (CD-MEKC) is also successful for enantiomeric separations [76–87] because CD has chirality. Apparent distribution coefficients of the solutes between the micelle and the nonmicellar phase are changed through the addition of CD, hence the CD-MEKC mode has been also effective for the separation of highly hydrophobic solutes, which are almost totally incorporated in the micelle and cannot be separated in simple MEKC [131–133]. Miyashita and Terabe [76,77] employed CD-MEKC for the separation of dansylated (DNS) DL-amino acids (DL-AAs) using γ-CD and SDS. A more successful separation of eleven DNS-DL-AAs was achieved by using a mixture of β-CD and γ-CD with SDS [78].

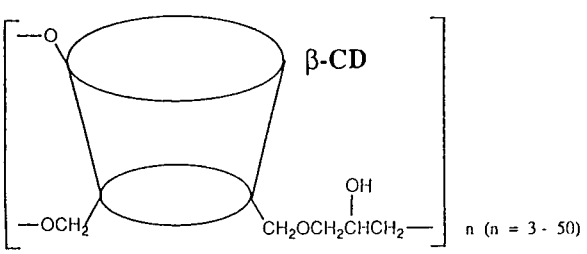


Fig. 1. Structure of β-CD polymer.

Nishi et al. [79] examined the enantiomeric separation of various compounds by CD-MEKC with four CDs. Enantiomers of binaphthyl compounds, thiopental, pentobarbital, etc., were successfully resolved with γ-CD and SDS. They also reported that some other chiral additives such as *l*-menthoxyacetic acid (*l*-MEN) or *d*-camphor-10-sulphonate (*d*-CAM) to a solution of SDS and γ-CD considerably improved the enantioresolution of pentobarbital and thiopental. Ueda and co-workers [80,81] applied CD-MEKC to the separation of naphthalene-2,3-dicarboxaldehyde (CBI)-labelled DL-AAs using β-CD or γ-CD with SDS. CBI-DL-AAs were more effectively enantioresolved using γ-CD and SDS. Generally, γ-CD showed a higher enantioselectivity than β-CD in CD-MEKC chiral separations with SDS as mentioned above. In the MEKC system, a surfactant monomer exists in the aqueous phase and can be included by the CD. The presence of a surfactant monomer will be related to the above-observed results. Prunonosa and co-workers [82,83] successfully resolved the enantiomers of cicletanine by using CD-MEKC with β- or γ-CD. They also applied this CD-MEKC method to the determination of cicletanine in human plasma and reported a detection limit of 10 ng/ml for each enantiomer [83]. Recently enantiomers of diniconazol and uniconazol were successfully resolved by MEKC using SDS and γ-CD [84].

In chiral separations by CD-CZE, the most effective parameter for the enantioselectivity, other than the cavity size and the concentration of CD, is the buffer pH. This is also the case for CD-MEKC. However, selectivity manipulation and separation optimization for solutes in a more complex matrix seem to be more easily achieved using CD-MEKC than CD-CZE, because

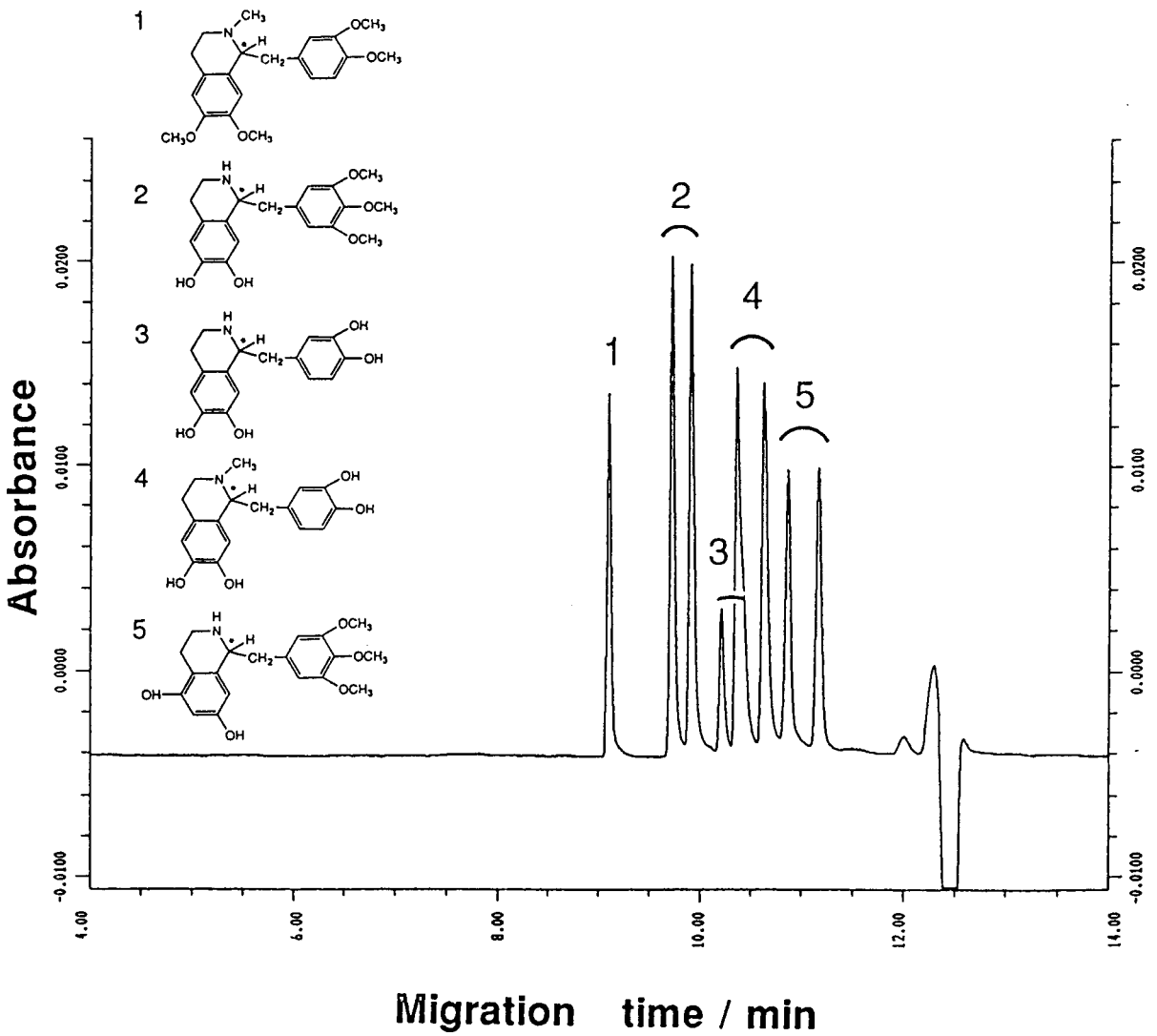


Fig. 2. Separation of enantiomers of trimetoquinol and related compounds by CD-CZE using β-CD polymer. Solutes: 1 = laudanosine; 2 = trimetoquinol; 3 = norlaudanosoline; 4 = laudanosoline; 5 = trimetoquinol isomer. Buffer, 7% β-CD polymer in 25 m*M* phosphate buffer of pH 6.5. Separation tube, fused-silica capillary, 57 cm (effective length 50 cm) × 75 μm I.D.; 15 kV; 214 nm; 23°C.

another interaction mechanism such as solubilization is operational in CD-MEKC. This is one of great advantages of CD-MEKC as in simple MEKC.

Other than CD-MEKC with SDS, Okafo et al. [85] used a mixture of sodium taurodeoxycholate (STDC) with β-CD for the separation of enantiomers of DNS-DL-AAs, methenytoin and fenoldopam. As discussed below, MEKC with STDC is effective for the enantiomeric separation of DNS-DL-AAs, diltiazem, trimetoquinol, etc. The resolution of DNS-DL-AAs in a mixture of STDC and β-CD was considerably improved compared with those obtained with either of the two chiral additives. Good enantiomeric separation of methenytoin and its principle

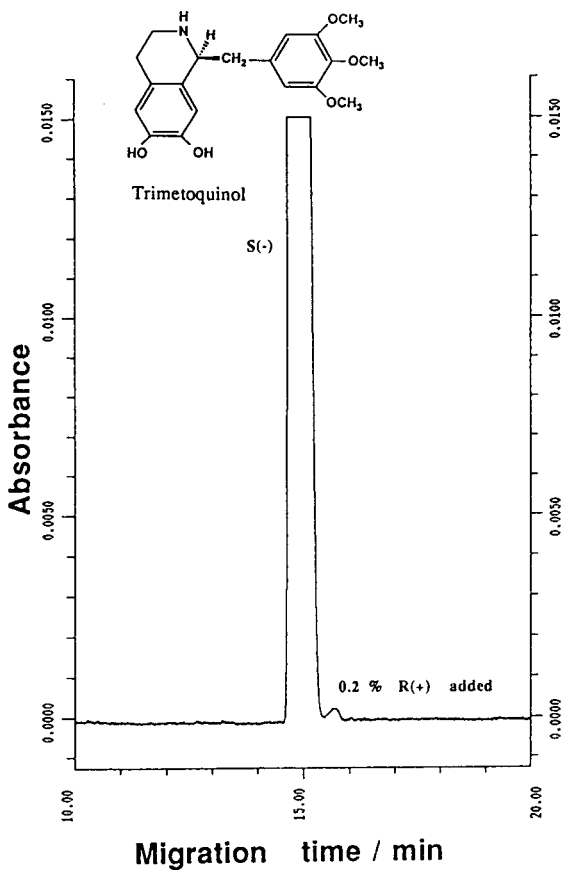


Fig. 3. Optical purity testing of trimetoquinol hydrochloride by CD-CZE with β-CD polymer. Buffer, 5% β-CD polymer in 25 m*M* phosphate buffer of pH 2.7. Other conditions as in Fig. 2 (from Ref. [52]).

metabolite 4-hydroxymethenytoin was only achieved in a mixture of STDC and β-CD.

Okafo and Camilleri [86] also applied CD-MEKC with STDC with β-CD to separate CBI-DL-AAs, CBI derivatives of baclofen and CBI derivatives of three aminophosphates. CBI derivatives of glutamic acid and histidine, which were not resolved by CD-MEKC using SDS and β-CD or γ-CD [80], were successfully resolved by using STDC and β-CD. They used this method for the determination of the chirality of amino acids, which are obtained by hydrolysis of D-Phe$^7$-bradykinin. Lin et al. [87] reported the separation of some DNS-DL-AAs by MEKC with STDC and β-CD. Chiral separation using a CD–bile salt system showed great enantioselectivity and can be recommended for one of starting conditions in CE chiral separations. Successful chiral separations by CD-MEKC are summarized in Table 4.

CDs have also been successfully used in ITP for the separation of enantiomers. Snopek and co-workers [24,88–94] extensively studied the separation of enantiomers by ITP and have reviewed the field [24].

### 3.1.2. Use of charged CDs (CD-EKC)

Other than neutral CDs or CD derivatives mentioned above, charged CDs have also been applied to CE as chiral selectors based on the concept of EKC [69–73,97,99]. Charged CDs used in CE enantiomeric separations are summarized in Table 5. This type of CD was first used by Terabe et al. for the separation of positional isomers of aromatic compounds [134] and the enantiomeric separation of DNS-AAs [99]. In CD-CZE or CD-MEKC, CDs added to the buffer solution are electrically neutral and move under the described conditions with the velocity of the EOF. In case of the charged CDs, they migrate with their own electrophoretic mobilities according to the polarity, and consequently this mode can be classified as one branch of EKC (CD-EKC). In CD-EKC, neutral compounds can be enantioresolved as well as ionic compounds. The migration order between the enantiomer (i.e., D or L) also can be manipulated by selecting natural CDs or charged CDs as described below. These are great advantages of CD-EKC as a quality control method for optical purity testing.

Terabe and co-workers prepared two β-CD derivatives to be used in EKC: mono(6-β-aminoethylamino-6-deoxy)-β-CD (CDen) [99] and 2-O-carboxymethyl-β-CD [134]. Enantiomeric separation of six DNS-AAs was successfully achieved by CD-EKC using a 25 m*M* CDen solution at pH 3.0. Hydroxypropylcellulose (HPC) (0.1%) was added to the buffer to suppress the EOF. Under these conditions CDen migrates to the negative electrode, and therefore solutes strongly included by the CDen have short

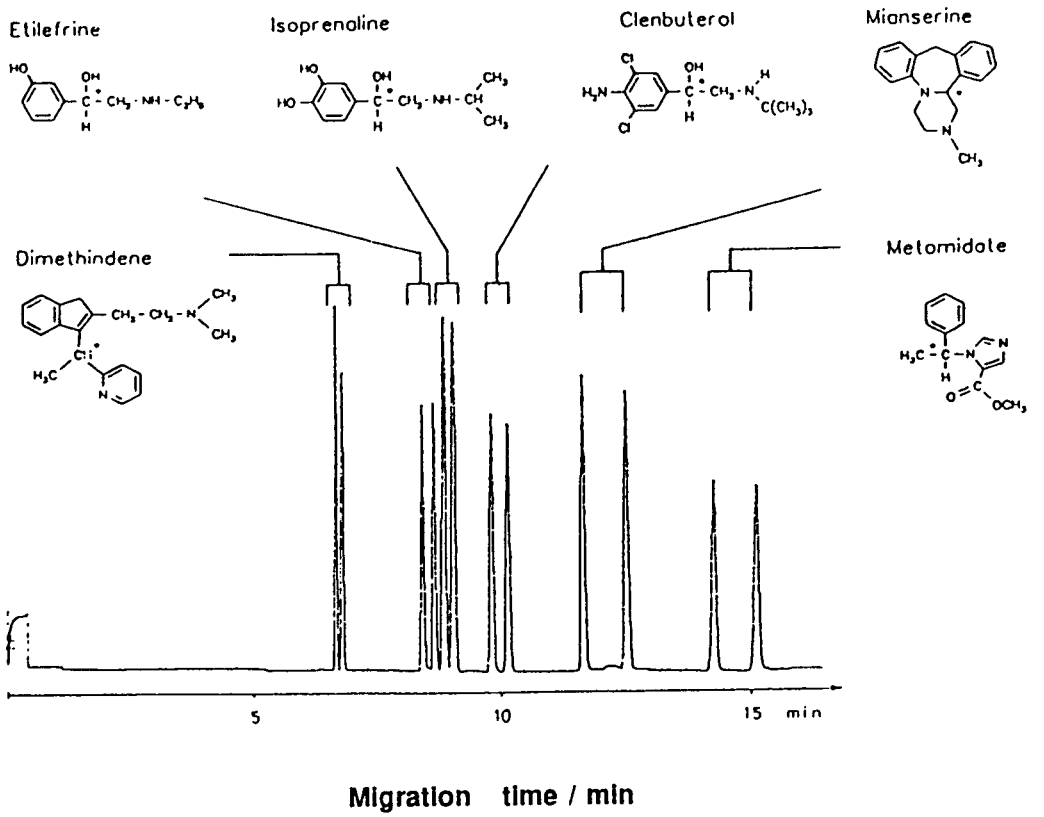


Fig. 4. Separation of enantiomers of some basic drugs by CD-CZE with HP-β-CD. Buffer, 0.3% HP-β-CD in 50 m*M* phosphate buffer of pH 3.3. Separation tube, fused-silica capillary, 40 cm effective length × 50 μm I.D.; 400 V/cm; 200–205 nm; 21°C (from Ref. [53]).

migration times and the weakly included solutes have long migration times.

Schmitt and Engelhardt employed carboxymethylated β-CD [69,70], carboxyethylated β-CD [70] and succinylated β-CD [70], which all have carboxyl groups, for the separation of enantiomers of oxazolidine, doxylamine, ephedrine, dimetinden and propranolol at pH 5.5–6.0. At pH < 4 all carboxylic functions on the CD are protonated, and hence it behaves like an uncharged CD (CD-CZE mode).At high pH (>5), deprotonation of the carboxyl groups leads to mobility of the negatively charged chiral selector as a micelle-like system (CD-EKC mode). Under such conditions (pH > 5), enantiomers of electrically neutral solutes such as hexobarbital, binaphthyl and oxazolidinone were successfully resolved as well as charged solutes. These solutes were also resolved under acidic conditions, i.e., with uncharged CDs. Smith [71] used a carboxymethylethyl β-CD for the CE chiral separation of a neutral drug GR57888X (under development) at pH 12.4.

To determine the enantiomeric excess of an enantiomeric drug, it is advantageous to determine an enantiomer migrating faster than the main component. In order to change the migration order of enantiomers in HPLC, another column with the complementary chiral selector must be used. However, this can be obtained by the reversal of the EOF with the same chiral selector in CE. Reversal of EOF is usually achieved by coating the capillary wall with a cationic surfactant, etc. Other than this, by employing these modified CDs, which can be used in the charged or uncharged mode under

Table 4
Chiral separation by cyclodextrin-modified MEKC (CD-MEKC)

| Compound[a] | CD | Surfactant | pH | Additive | Ref. |
|---|---|---|---|---|---|
| *Amino acids (AAs)* | | | | | |
| DNS-AAs | γ, β | SDS | 8.3, 8.6 | MeOH | 76,77,78 |
| | β | STDC | 7.2, 7.8 | | 85,87 |
| CBI-AAs | γ, β | SDS | 9.0 | | 80,81 |
| | β | STDC | 7.0 | | 86 |
| *Antiepileptic* | | | | | |
| Mephenytoin[70], metabolite | β | STDC | 7.2 | | 85 |
| *Hypnotic* | | | | | |
| Glutethimide[71] | β | SDS | 7.0 | Urea, MeOH | 68 |
| *Barbiturates* | | | | | |
| Hexobarbital[9] | β, DM-β | SDS | 7.0 | Urea, MeOH | 68 |
| Mephobarbital[72] | β | SDS | 7.0 | Urea, MeOH | 68 |
| Pentobarbital[10] | γ | SDS | 9.0 | *l*-MEN, *d*-CAM | 79 |
| Secobarbital[11] | γ | SDS | 7.0 | Urea, MeOH | 68 |
| Thiopental[73] | γ | SDS | 9.0 | *l*-MEN, *d*-CAM | 79 |
| *Antihypertensives* | | | | | |
| Cicletanine[74] | β, γ | SDS | 8.6 | | 82,83 |
| Fenoldopam[75], analogue | β | STDC | 7.2 | | 85 |
| *Aromatase inhibitors* | | | | | |
| Aminoglutethimide analogue | DM-β | SDS | 7.0 | Urea, MeOH | 68 |
| Fadrozole[63] | β, DM-β | SDS | 9.0 | Urea, MeOH | 68 |
| *Muscle relaxant* | | | | | |
| Baclofen[76] (CBI derivative) | β | STDC | 7.0 | | 86 |
| *Antifungals* | | | | | |
| Diniconazole[77] | γ | SDS | 9.0 | Urea | 84 |
| Uniconazole[78] | γ | SDS | 9.0 | Urea | 84 |
| *Others* | | | | | |
| Aminophosphates (CBI derivative) | β | STDC | 7.0 | | 86 |
| 1,1′-Binaphthyl-2,2′-diyl hydrogenphosphate[66] | β, DM-β TM-β, γ | SDS | 9.0 | *l*-MEN, *d*-CAM | 79 |
| 2,2′-Dihydroxy-1,1′-dinaphthyl[79] | TM-β, γ | SDS | 9.0 | *l*-MEN, *d*-CAM | 79 |
| 2,2,2-Trifluoro-1-(9-anthryl)ethanol[80] | β, γ | SDS | 9.0 | *l*-MEN, *d*-CAM | 79 |

[a] Superscript numbers refer to structures of the solutes shown in Fig. 13.

the low EOF conditions, reversal of the migration order of the enantiomers was achieved for the enantiomeric separation of ephedrine [70].

Nardi et al. [72] employed $6^A$-methylamino and $6^A$,$6^D$-dimethylamino-β-CD for the enantiomeric separation of some 2-hydroxy acids including mandelic acid. These CD derivatives having positive charges were effective for the optical resolution of these acidic solutes. Dette et al. [73] used tetrakis [6-O-(4-sulphobutyl)]-β-CD ($Na^+$ salt) as an anionic carrier in CD-EKC for the separation of enantiomers of four ephedrine alkaloids. This CD has the benefit of a wide range of basic pH available for the optical resolution to manipulate selectivity for both enantiomeric separation and different solutes.

### 3.1.3. Immobilization of CDs (EC and CGE)

CDs have been used in CE enantiomeric separations through immobilization other than addition. Mayer and co-workers [95–98] reported the application to CE of CD derivative-

Table 5
Charged cyclodextrins used in chiral separations by capillary electrophoresis (CD-EKC)

| Charged cyclodextrin | Solute[d] | pH | Ref. |
|---|---|---|---|
| *Cationic CD derivatives* | | | |
| Mono-(6-β-aminoethylamino-6-deoxy)-β-CD[a] | DNS-AAs | 3.0 | 99 |
| $6^{A}$-Methylamino-β-CD | Mandelic Acid | 5.0 | 72 |
| $6^{A}$,$6^{D}$-Dimethylamino-β-CD | *m*-Hydroxymandelic acid | | |
| | *p*-Hydroxymandelic acid | | |
| | 3,4-Dihydroxymandelic acid | | |
| | 2-Phenllactic acid | | |
| | 3-Phenllactic acid | | |
| *Anionic CD derivatives* | | | |
| 2-O-Carboxymethyl-β-CD[b] | (Aromatic isomers) | | 134 |
| Carboxymethylated β-CD (3.6 per CD ring) | Doxylamine[51] | 2.5 | 70 |
| Carboxyethylated β-CD (ca. 6 per CD ring) | Ephedrine[16] | 5.8 (charged) | |
| Carboxysuccinated β-CD (3.5 per CD ring) | Dimenthinden[50] | | |
| | 2,2-Dihydroxy-1,1′-dinaphthyl[79] | | |
| | Hexobarbital[9] | | |
| | Oxazolidine[81] | | |
| | Propranolol[39] | | |
| Carboxymethylated β-CD (3.6 per CD ring) | Ephedrine[16] | 2.5 | 69 |
| | Dimenthinden[50] | 6.0 (charged) | |
| | Doxylamine[51] | | |
| Carboxymethylated β-CD (3.6 per CD ring) | GR57888X[82] | 12.4 | 71 |
| Tetrakis[6-O-(4-sulphobutyl)]-β-CD ($Na^+$ salt)[c] | Ephedrine[16] | 10.0 | 73 |
| | Norephedrine | | |
| | Pseudoephedrine | | |
| | Methylephedrine | | |
| | Methylpseudoephedrine | | |
| 6-O-Trimethylenesulphonic acid β-CD ($Na^+$ salt) (mixture of mono-, bis- and tri-) | 1,1′-Binaphthyl-2,2′-diyl hydrogenphosphate[66] | | 97 |

a b c

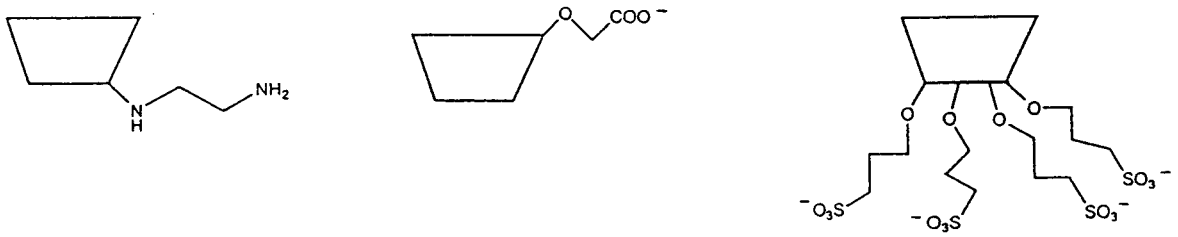


[d] Superscript numbers refer to structures of the solutes shown in Fig. 13.

coated capillary tubes, which are commercially available as a chiral capillary column for GC (Chiralsil-Dex). This mode can be classified as electrochromatography (EC), in which the mobile phase is driven by the EOF instead of a high-pressure pump as used in HPLC.

Chiralsil-Dex with permethylated β-CD has been found to be effective for the enantiomeric separation of 1,1′-dinaphthyl-2,2′-diyl hydrogenphosphate, 1-phenylethanol [95], ibuprofen, flurbiprofen, cicloprofen [96] and hexobarbital [97], and also has numerous applications in GC and supercritical fluid chromatography (SFC). The optical resolution of etodolac, which was not enantioresolved by the β-CD-type Chiralsil-Dex, was also achieved by employing Chiralsil-Dex

with permethylated γ-CD [96]. These highly hydrophobic and polar compounds, which cannot be analysed with Chiralsil-Dex in the GC mode, were successfully analysed and enantioresolved by using the CE technique. In the enantiomeric separation of 1,1′-dinaphthyl-2,2′-diyl hydrogenphosphate by Chiralsil-Dex, reversal of the elution order was obtained through the addition of sulphonated β-CD to the buffer solution [97]. This is explained by the opposite enantioselectivity of the CD selectors employed in the mobile and stationary phases. Armstrong et al. [98] synthesized another type CD derivative, permethylated allyl-substituted β-CD, and used a capillary coated with this derivatized CD and organosilane copolyer in CE analysis and also in GC and SFC. Racemic mephobarbitol was baseline resolved with a 50 m*M* phosphate buffer of pH 7.8.

Besides the wall coating method, CDs have been immobilized by using a gel. A capillary filled with a gel containing CD was employed for the enantiomeric separation of DNS-AAs by Guttman et al. [74]. The mode of separation is CGE. They prepared a cross-linked polyacrylamide gel incorporating a CD by simply adding the CD to the solution prior to polymerization. They reported that β-CD was the most effective and the addition of methanol (MeOH) (10%) enhanced the enantioselectivity. Cruzado and Vigh [75] synthesized allyl carbamoylated β-CD, and prepared both cross-linked (solid-type) and linear (liquid-type) gels after copolymerization with acrylamide for use in CGE to separate enantiomers. The cross-linked gel was not stable enough to operate for a long time because of bubble formation, etc., although good enantioselectivity of DNS-DL-Phe was obtained. In contrast, the liquid gel showed much better stability and reproducibility although the enantioselectivity was slightly lower than with the solid gel. Nine DNS-AAs and homatropine were successfully enantioresolved using the liquid gel-filled capillary.

### 3.2. Use of crown ethers

Crown ethers are known to form stable complexes with alkali metals, alkaline earth metals and primary amine ions. Recently the use of a crown ether as a chiral selector in CE has been reported by Kuhn and co-workers [25,62,111]. Only one crown ether, 18-crown-6-tetracarboxylic acid (18C6) (see Fig. 5), is known to have been successfully used for the separation of enantiomers of primary amines. A separation of three DL-AAs by CZE with 18C6 is shown in Fig. 6 [25]. To form host–guest complexes, the amino groups must be protonated, and therefore acidic conditions are essential. They reported the separation of the enantiomers of 22 different amines such as some AAs, dopa, noradrenaline, norephedrine and naphthylethylamine by using 10 m*M* Tris–citrate buffer solution of pH 2.2. In that case, the ionization of carboxyl groups is suppressed, and the solutes migrate to the negative electrode owing to the positive charge on the ammonium group. That means solutes separated by CZE. When the chiral centre of the guest molecule is adjacent to the amine functionality, the best enantioresolutions are achieved. Hohne

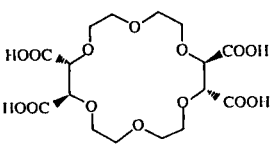


Fig. 5. Structure of 18-crown-6-tetracarboxylic acid (18C6).

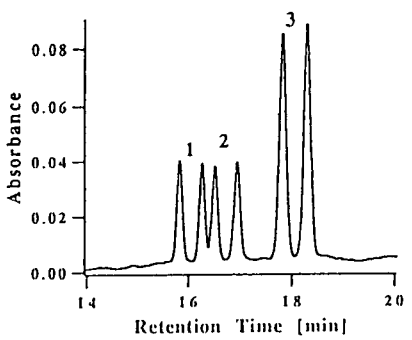


Fig. 6. Separation of three DL-amino acids by CZE with 18C6. Solutes: 1 = DL-Trp, 2 = DL-Phe, 3 = DL-Dopa. Buffer, 10 m*M* 18C6 in 10 m*M* Tris–citric acid buffer of pH 2.2. Separation tube, fused-silica capillary, 50 cm effective length × 75 μm I.D.; 260 V/cm; 214 nm (from Ref. [25]).

et al. [112] also applied the same crown ether to CE enantiomeric separations at pH 2.07 and reported the successful enantiomeric separation of six amines such as octopamine, methoxamine and norephedrine. The synergistic effect of CDs and crown ethers on the enantiomeric separation has also been reported [25]. By using 10 m*M* 18C6 and 20 m*M* α-CD, the resolution of DL-Trp improved to 7.37, compared with those obtained from either used alone (1.29 and 5.67, respectively).

## 4. Chiral separation by affinity interaction

### 4.1. Use of proteins (affinity EKC)

To separate enantiomers, the idea of using proteins as the chiral selector is natural from their great success in HPLC. Some of protein-coated stationary phases [ovomucoid (OVM), avidin, $\alpha_1$-acid glycoprotein (AGP) and bovine serum albumin (BSA)] are commercially available and have been demonstrated to be effective for a wide variety of enantiomers. A protein has charge and migrates according to its electrophoretic mobility in CE. Therefore, the separation mode can be classified as a branch of EKC (affinity EKC). The solutes, both ionic and neutral, form diastereomeric complexes with the protein in dynamic equilibrium. The difference in the formation constant between the diastereomeric pair causes the difference in effective electrophoretic mobilities between the enantiomers. Assuming a similar model to that reported by Wren and Rowe for CD-CZE, the difference in apparent mobilities, $\Delta\mu_{app}$, between the enantiomers can be described as follows [106]:

$$\Delta\mu_{app} = \frac{(\mu_s - \mu_p)(K_2 - K_1)[P]}{(1 + K_1[P])(1 + K_2[P])} \quad (2)$$

where P is a protein employed as a pseudo-stationary phase, $K_1$ and $K_2$ are binding constants of the enantiomeric pair 1 and 2 and $\mu_s$ and $\mu_p$ are the electrophoretic mobilities of the free analyte and of the protein, respectively. The mobility of each complex is assumed to be equal to $\mu_p$. It is obvious in Eq. 2 that $K_1$ and $K_2$, and also $\mu_s$ and $\mu_p$, must be different. It is clear that the larger the difference between $\mu_s$ and $\mu_p$, the greater is the resolution (the larger is $\Delta\mu_{app}$). Therefore, the optimization of the pH will be important to improving the enantiomeric separation.

Various proteins have been employed for the separation of enantiomers in affinity EKC: BSA [100–102], AGP [102], OVM [102,103], fungal cellulase [102], human serum albumin (HSA) [104], cellulase [cellobiohydrolase I (CBH I)] [105] and avidin [106]. Some characteristics of the protein used in affinity EKC are summarized in Table 6 [135]. In the practical use of proteins as chiral selectors, some problems such as protein adsorption on the capillary wall, absorption of UV light in the shorter wavelength region and relatively low purity of the proteins occur. These effects cause irreproducible separations and band broadening. However, affinity EKC with proteins is an attractive mode, particularly for investigating the interaction of drugs with specific proteins. Wall-coated capillaries and some additives such as organic modifiers or surfactants have been used to prevent adsorption or to improve the peak shape.

Barker et al. [100] used BSA (0.1% solution) to separate 6*S*- and 6*R*-stereoisomers of leucovorin with a bare capillary at pH 7.0 or a PEG-coated capillary at pH 7.2. It was found that the 6*R*-isomer has a greater affinity for BSA. The migration orders are reversed between the two capillaries because of the difference in the EOF velocities. The detection wavelength was 280 nm, where the difference between leucovorin absorption and BSA absorption is large. They also used BSA in addition to dextran for the optical resolution of leucovorin and some drugs in a linear polyacrylamide-coated capillary [101].

Busch et al. [102] applied four proteins, AGP, OVM, fungal cellulase and BSA, to affinity EKC using an untreated fused-silica capillary under neutral conditions (pH 6.8 or pH 7.4). These problems have been demonstrated to be effective in chiral HPLC. Detection was carried out at 280 or 260 nm. BSA was effective for the enantio-

Table 6
Some characteristics of proteins used in CE as a chiral selectors and their application

| Property | BSA | OVM | AGP | HSA | Fungal cellulase | CBH I | Avidin |
|---|---|---|---|---|---|---|---|
| Molecular mass | 67 000 | 28 000 | 44 000 | 68 000 | 60 000–70 000 | 60 000–70 000 | 70 000 |
| Isoelectric point | 4.7 | 4.5 | 2.7 | 4.7 | 3.9 | 3.9 | 10 |
| Sialic acid residues | – | 0.3 | 14 | – | – | – | – |
| Disulphide bridges | 17 | 8 | 2 | – | 12 | – | – |
| Carbohydrate (%) | – | 30 | 45 | – | 6 | 6 | 20.5 |
| CE mode [ref.] | EKC [100–102]<br>CGE [107,108] | EKC [103] | EKC [102]<br>EC [109] | EKC [104] | EKC [102] | EKC [105] | EKC [106] |
| Separated solutes[a] | Benzoin[65]<br>DNS-Nva, DNS-Leu<br>Ibuprofen[54]<br>Leucovorin[61]<br>Promethazine[5]<br>Trp<br>Warfarin[56] | Benzoin<br>Chlorpheniramine[49]<br>Eperisone[83]<br>Tolperisone[84] | Alprenolol[30]<br>Benzoin<br>Cyclophosphamide[85]<br>Disopyramide[86]<br>Hexobarbital[9]<br>Metoprolol[34]<br>Oxprenolol[36]<br>Pentobarbital[10]<br>Promethazine | 2,3-Dibenzoyl tartaric acid<br>N-2,4-Dinitrophenyl glutamic acid<br>3-Indolelactic acid<br>Kynurenine[87]<br>Trp | Pindolol[37] | Alprenolol[30]<br>Labetolol[33]<br>Metoprolol[34]<br>Pindolol<br>Propranolol[39] | Flurbiprofen[88]<br>Ibuprofen[54]<br>Ketoprofen[89]<br>Leucovorin[61]<br>Vanilmandelic acid<br>Warfarin[56] |

[a] Superscript numbers refer to structures of the solutes shown in Fig. 13.

meric separation of Trp, benzoin and warfarin. The addition of 1-propanol (3–6%) improved the enantioselectivity through the improvement of peak shapes. The enantiomers of promethazine, which were not resolved with BSA alone, were successfully resolved by addition of 3% 1-propanol to 0.33% BSA solution. However, too large an addition (found 10%) of 1-propanol reduced the enantiomeric resolution, contrary to expectation. AGP (ca. 0.1% solution) recognized enantiomers of promethazine, and fungal cellulase (ca. 0.1% solution) was effective for the separation of enantiomers of pindolol. OVM was unsuccessful with the test analytes. However, Ishihama et al. [103] recently employed OVM in affinity EKC and a successful enantioseparation of benzoin, tolperisone, eperisone and chlorpheniramine was obtained.

Vespalec et al. [104] used 1% HSA in 10 m*M* acetic acid–Tris buffer solution of pH 9.6 with a bare capillary and pH 8 for a linear polyacrylamide-coated capillary to separate enantiomers of Trp, kynurenine and some other compounds. They heated alkaline HSA solutions mildly to achieve stabilization of the enantioselectivity of HSA. Valtcheva et al. [105] employed CBH I (0.4%) to separate enantiomers of five β-blockers: (*R*,*S*)-propranolol, (*R*,*S*)-pindolol, (*R*,*S*)-metoprolol, (*SS*,*RR*)- and (*RS*,*SR*)-labetolol and (*R*,*S*)-alprenolol, with non-cross-linked polyacrylamide-coated capillaries at pH 5.1. They also introduced a 2–3 mm long agarose plug at one end of the capillary to prevent any hydrodynamic flow. By using a high concentration (25–30%) of 2-propanol (IPA), a satisfactory peak shape was obtained, leading to good enantioresolution.

Tanaka et al. [106] employed avidin, which is a basic protein having p*I* ≈ 10, to separate enantiomers of acidic compounds such as ibuprofen, ketoprofen, flurbioprofen and leucovorin. Avidin is positively charged under neutral or acidic conditions, hence a wall-coated capillary was used to prevent the adsorption of avidin. Peak shapes were improved through the addition of alcohols such as ethanol, 1-propanol and (IPA). The enantiomeric separation of racemic ibuprofen and ketoprofen by affinity EKC with avidin is shown in Fig. 7, where 10% IPA was added to the protein solution [106].

Immobilized proteins have been also successfully used in CE as chiral selectors other than by addition. Birnbaum and Nilsson [107] prepared a capillary filled with gels consisting of BSA (ca. 1.7%) cross-linked with glutaraldehyde for the separation of DL-Trp. Sun et al. [108] immobilized BSA on dextran by using cyanogen bromide. The linear polyacrylamide-coated capillary was filled with the BSA–dextran polymer and used for the separation of diastereomers of leucovorin. Li and Lloyd [109] investigated the applicability of capillaries packed with an im-

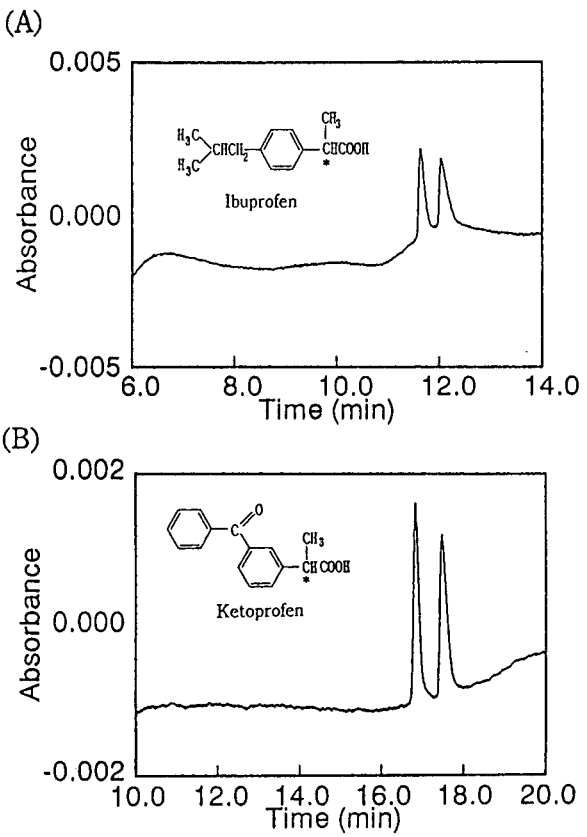


Fig. 7. Enantiomeric separation of racemic (A) ibuprofen and (B) ketoprofen by affinity EKC with avidin. Buffer, 25 μ*M* avidin in 50 m*M* phosphate buffer of pH 6.0 containing 10% IPA. Separation tube, coated capillary tube cartridge, 31.5 cm effective length × 50 μm I.D. (Bio-Rad); −12 kV; (A) 230 nm, (B) 270 nm; 25°C (from Ref. [106]).

mobilized AGP stationary phase to direct chiral separations. The separation mode can be classified as EC. The AGP stationary phase has been found to be effective for chiral separations in HPLC [110]. Ten compounds including hexobarbital, pentobarbital, benzoin, ifosfamide, cyclophosphamide and β-blockers were successfully optically resolved by EC with a capillary packed with AGP stationary phase. A variety of applications using proteins as chiral selectors in CE are also summarized in Table 6. Most proteins are considered to recognize chirality, and therefore enantiomer separations by CE using proteins will increase.

### 4.2. Use of polysaccharides

Besides proteins, various natural products can be applied to separate enantiomers for CE. Polysaccharides such as cellulose and amylose are the most readily available from successful enatioseparations in HPLC. Many cellulose derivatives have already been found to be effective in HPLC chiral separations and most of them are now commercially available [110].

Concerning enantiomeric separation, only two papers have reported the addition of saccharides as a chiral selector in CE. D'Hulst and Verbeke [113] used maltodextrins and corn syrups as chiral additives in CZE. The former are mixtures of linear α-(1,4)-linked D-glucose polymers and the latter are maltooligosaccharide mixtures. The enantiomers of non-steroidal anti-inflammatory drugs such as flurbiprofen and ibuprofen, and warfarin and some other drugs, were successfully optically resolved with 10 m*M* phosphate buffer solution of pH 7.0–7.5 through the addition of saccharides. The separation mechanism is not clear; however, some affinity interaction may cause the chiral recognition.

Nishi et al. [114] used dextran sulphate as a chiral selector in CE for the enantiomeric separation of trimetoquinol and clentiazem. Dextran sulphate ($Na^+$ salt), which is a mixture of linear α-(1,6)-linked D-glucose polymers having a sulphate group in the molecule, has three sulphate groups per D-glucose unit, as shown in Fig. 8.

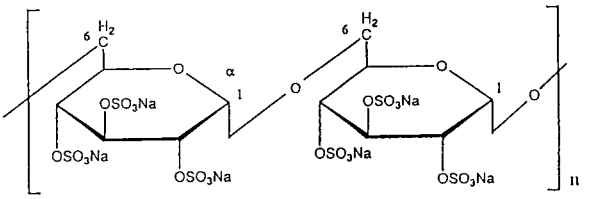


Fig. 8. Unit structure of dextran sulphate ($Na^+$ salt).

Therefore, it can be used as a chiral pseudo-stationary phase in affinity EKC like proteins. As expected from affinity EKC with proteins, pH values in addition to the concentration of the chiral selector are most critical for the enantioselectivity. A chromatogram of racemates of trimetoquinol and its hydroxy positional isomer obtained by affinity EKC with dextran sulphate is shown in Fig. 9. With both maltodextrin and dextran sulphate, trials to improve the enantioselectivity by combination with another additive

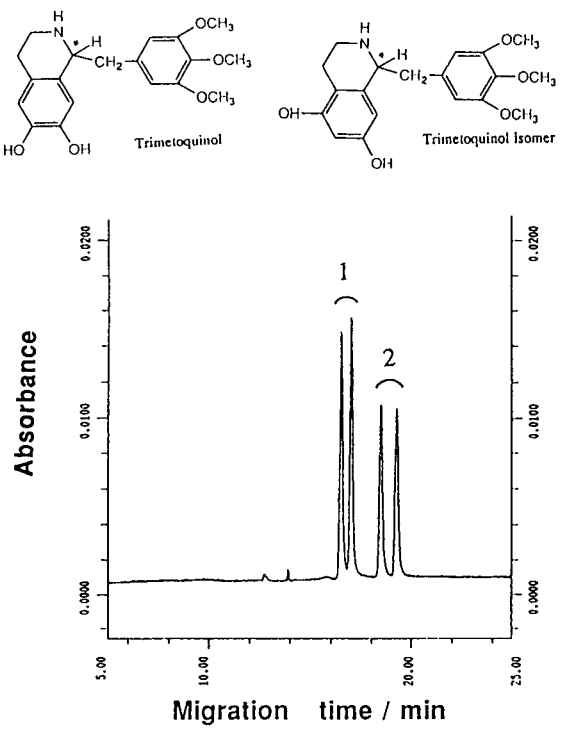


Fig. 9. Separation of enantiomers of trimetoquinol and its isomer by affinity EKC with dextran sulphate. Buffer, 3% sulphate in 25 m*M* phosphate buffer of pH 5.5. Other conditions as in Fig. 2 (from Ref. [114]).

such as an organic modifier or a surfactant were not successful.

Besides the addition of saccharides as chiral selectors, Sun et al. [101] used dextran as an additive to improve the resolution of enantiomers in affinity EKC with protein. By adding dextran (ca. 5%) to a 10 m*M* phosphate buffer solution of pH 7.12 containing 0.1% BSA, enantiomers of ibuprofen, leucovorin, DNS-DL-Leu, DNS-DL-Nva and mandelic acid, which are all difficult to separate using BSA alone as the chiral selector in CE, were successfully resolved. They reported that the effect is ascribable to the decrease in migration velocity of BAS, leading to an enhancement of enantioselectivity. Large species such as proteins have a much larger effect on the mobility in comparison with small species (i.e., samples) with the polymer network of dextran. It is reasonable to expect that dextran will also influence the enantioselectivity of the solute.

## 5. Chiral separation by solubilization

### 5.1. Use of chiral micelles (micellar EKC)

In MEKC, enantiomeric separations have been successfully achieved by employing chiral surfactants [26,84–86,117–130]. The chiral surfactants used in CE chiral separations are summarized in Table 7. Although CZE is only applicable to ionic compounds, MEKC can separate both ionic and non-ionic enantiomers, as in CD-EKC mentioned above. In MEKC chiral separations, a chiral surfactant solution or a mixed micelle solution of a chiral and an achiral surfactant can be employed. Two classes of chiral surfactants have been successfully employed for enantiomeric separations by MEKC: optically active amino acid-derived synthetic surfactants [117–122] and natural surfactants such as bile salts [123,125–129], digitonin [119], glycyrrhizic acid and β-escin [130]. Non-ionic

Table 7
Chiral surfactants used in MEKC chiral separations

| Surfactant | Solute[a] | Additive | Ref |
|---|---|---|---|
| *Amino acid derivatives* | | | |
| SDVal, SDAla | Amino acid derivatives<br>N-(3,5-Dinitrobenzoyl)-O-isopropyl<br>N-(4-Ditrobenzoyl)-O-isopropyl<br>N-Benzoyl-O-isopropyl | MeOH | 117,118 |
| SDVal | PTH-AAs | MeOH, urea | 119–121 |
| | Benzoin[65] | MeOH, urea | 120 |
| | Warfarin[56] | MeOH, urea | 120 |
| SDGlu | PTH-AAs | MeOH, urea | 122 |
| | Benzoin | MeOH, urea | 122 |
| *Bile salts analogues* | | | |
| SC, STC, SDC, STDC | DNS-AAs | SDS | 123 |
| | Carboline derivatives[90] | | 125 |
| | 2,2′-Dihydroxy-1,1′-dinaphthyl[79] | | 125,128,129 |
| | Diltiazem[91], analogues | | 125,126 |
| | 1-Naphthylethylamine | | 125 |
| | Trimetoquinol[29], analogues | | 125–127 |
| | 1,1′-Binaphthyl-2,2′-diyl hydrogenphosphate[66] | | 128 |
| | 1,1′-Binaphthyl-2,2′-dicarboxylic acid[67] | | 128 |
| Digitonin | PTH-AAs | SDS | 119 |
| Glycyrrhizic acid | PTH-AAs, DNS-AAs | SDS | 130 |
| β-Escin | PTH-AAs, DNS-AAs | SDS | 130 |

[a] Superscript numbers refer to structures of the solutes shown in Fig. 13.

surfactants such as digitonin must be used together with an ionic surfactant such as SDS to form a mixed micelle having electrophoretic mobility. Most analytes are adsorbed on the surface of the micelle and interact with the polar groups of the surfactants, and therefore surfactants having chiral polar groups will be effective.

The first chiral separation by MEKC was reported by Cohen et al. [136]. They used N,N-didecyl-L-alanine as a chelating surfactant together with SDS and metal ions ($Cu^{2+}$) to form mixed micelles having a chiral ligand. The difference in the formation constants led to the successful chiral separation of DNS-DL-AAs.

Dobashi et al. [117,118] used sodium N-dodecanoyl-L-valinate (SDVal) and sodium N-dodecanoyl-L-alaninate to separate N-(3,5-dinitrobenzoyl) derivatives of DL-AAs, etc. Otsuka and Terabe [119–121] also used SDVal for the separation of phenylthiohydantoin (PTH)-DL-AAs. They reported that the addition of MeOH and urea improved peak shapes, hence improving the resolution [120,121]. Beozoin and warfarin were also enantioresolved under the same conditions. Addition of SDS or a high concentration of urea was effective for the enhancement of the selectivity. Recently, Otsuka et al. [122] employed N-dodecanoyl-L-glutamate (SDGlu) for the MEKC enantiomeric separation of PTH-DL-AAs. Through the addition of MeOH and urea, three PTH-DL-AAs, Nva, Val and Trp, were successfully separated. By using mixed micelles of SDGlu and SDS, five PTH-DL-AAs were enantioseparated.

Terabe et al. [123] first used bile salts for the separation of enantiomers by MEKC. By using sodium taurocholate (STC) or sodium taurodeoxycholate (STDC) under acidic conditions, some DNS-DL-AAs were enantioresolved, although a long separation time was required. Various bile salts are well known as natural anionic surfactants. The structures of some bile salts are shown in Fig. 10. Bile salts are assumed to form helical-structured micelles with a reversed micelle conformation [124], leading to unique characteristics compared with long-chain alkyl-type surfactants. Although not many applications have been published on enantiomeric

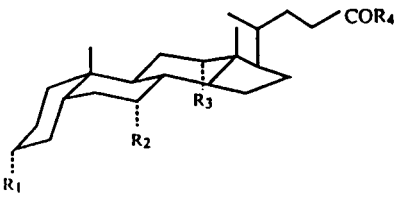


| Bile salt | $R_1$ | $R_2$ | $R_3$ | $R_4$ |
|---|---|---|---|---|
| Sodium cholate | OH | OH | OH | Onn |
| Sodium taurocholate | OH | OH | OH | $NHCH_2CH_2SO_3Na$ |
| Sodium deoxycholate | OH | H | OH | $ON_a$ |
| Sodium taurodeoxycholate | OH | H | OH | $NHCH_2CH_2SO_3Na$ |

Fig. 10. Structures of some bile salts.

separations with bile salts, the enantioselectivity of bile salt micelles seems to be greater for relatively flat and rigid compounds, expected from its micelle structure.

Nishi et al. [125–127] successfully used four bile salts for the separation of enantiomers of diltiazem, trimetoquinol and some other drugs under neutral conditions. Enantiomers of carboline derivatives and 2,2′-dihydroxy-1,1′-dinaphthyl were well separated with four bile salts [125]. However, enantiomers of diltiazem and trimetoquinol were separated with only STDC at pH 7.0 [126,127]. Enantiomers of diltiazem, which were not enantioresolved by CD-CZE or CD-MEKC, were only resolved by MEKC with STDC. A chromatogram of racemic diltiazem and related compounds is shown in Fig. 11, where 50 m*M* STDC was added to the 20 m*M* phosphate–borate buffer solution of pH 7.0. Cole and co-workers [128,129] also separated enantiomers of three binaphthyl derivatives by MEKC with bile salts. They reported that the addition of MeOH improved the resolution owing to the expansion of elution range. Okafo and co-workers [85,86] and Lin et al. [87] used STDC with or without $\beta$-CD for the separation of DNS-DL-AAs.

Otsuka and Terabe [119] used a non-ionic surfactant, digitonin, which is a natural product, the glycoside of digitogenin, for the optical separation of PTH-DL-AAs. To form a charged micelle, SDS was added to the digitonin solutions. Six PTH-DL-AAs were optically separated

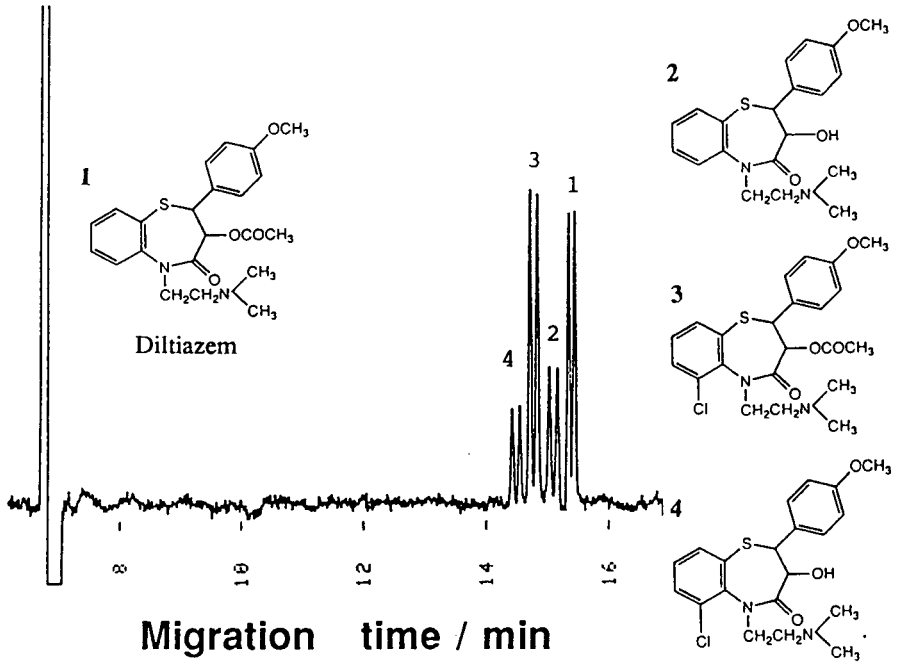


Fig. 11. Separation of enantiomers of diltiazem and related compounds by MEKC with bile salt. Solutes: 1 = diltiazem; 2 = desacetyldiltiazem; 3 = 6-chlorodiltiazem; 4 = desacetyl-6-chlorodiltiazem. Buffer, 50 mM STDC in 20 m*M* phosphate–borate buffer of pH 7.0. Separation tube, fused-silica capillary, 65 cm (effective length 50 cm) × 50 μm I.D.; 20 kV; 210 nm; ambient temperature (from Ref. [126]).

under acidic conditions, although a long analysis time was required. No enantiomeric separation was achieved under neutral conditions. Two other natural surfactants, glycyrrhizic acid and β-escin, were employed by Ishihama and Terabe [130] in MEKC for the optical resolution of DNS-DL-AAs and PTH-DL-AAs. Single micelles of these surfactants were not effective for enantiorecognition. Glycyrrhizic acid was then used with octyl-β-glucoside and SDS at pH 7.0. In this instance, fluorescence detector should be used because of the strong UV absorption of glycyrrhizic acid due to the carbonyl group conjugated to a carbon–carbon double bond. Some DNS-DL-AAs were successfully resolved under neutral conditions with a long analysis time. As for β-escin, nine PTH-DL-amino acids were optically resolved by adding SDS under acidic conditions.

Besides the applicability of MEKC to the optical resolution of neutral compounds, another advantage of MEKC is the easy manipulation of selectivity [137]. The selectivity can be changed by changing surfactants or adding various additives. The MEKC mode is suitable for separating solutes in complicated matrices, as in the case of CD-MEKC. It is desirable that many other chiral surfactants become available as separation carriers for enatiomeric separations by MEKC.

### *5.2. Use of microemulsions (microemulsion EKC)*

Microemulsion EKC uses a microemulsion, which is prepared by mixing oil, water, a surfactant and a cosurfactant such as a medium alkyl-chain alcohol, as a pseudo-stationary phase instead of a micelle as in MEKC [138,139]. A microemulsion works similarly to ionic micelles for the separation of neutral compounds. Solutes are incorporated into the microemulsion according to their hydrophobicity. In chiral separations by microemulsion EKC, a lipophilic chiral selector must be used. Aiken and Huie [140] used a microemulsion consisting (2*R*,3*R*)-di-*n*-butyl tar-

trate–SDS–butanol–buffer (pH 8.1) (0.5:0.6:1.2:97.7) for the chiral separation of ephedrine. A selectivity value of 2.6 was obtained.

## 6. Chiral separation by ligand-exchange complexation

CE optical resolution by ligand exchange was first reported by Gassman et al. [115] in 1985. They employed a Cu(II)–histidine complex as an additive to buffer solutions for the optical resolution of DNS-DL-AAs. DNS-DL-AAs will form ternary complexes, which consist of Cu(II), L-histidine and DNS-L-AA or DNS-D-AA. These diastereomeric complexes are electrically identical and probably have close electrophoretic mobilities; however, the formation (or stability) constants of the complexes are different and hence enantiomeric separation can be achieved. They also used an Cu(II)–aspartame complex system for the separation of the same class of compounds [116]. Fourteen of eighteen DNS-DL-AAs were successfully optical resolved by employing aspartame. This can be ascribed to the instability of the six-membered chelate rings of Cu(II)–aspartame compared with the five-membered ring of Cu(II)–histidine. Fanali et al. [141] separated enantiomers and diastereomers of Co(III) complexes with ethylenediamine, *o*-phenanthroline, etc., by using sodium L-(+)-tartrate at pH 5.25. Cohen et al. [136] used ligand-exchange complexation with N,N-didecyl-L-alanine in MEKC as mentioned above.

## 7. Chiral separation by derivatization to diastereomers

When a direct chiral separation by CE is not successful, chiral derivatization techniques can be adopted, as in HPLC. Schutzner et al. [142] derivatized DL-Trp with (+)-diacetyl-L-tartaric anhydride to diastereomeric pairs and separated these diastereomers by CZE with a polyacrylamide-coated capillary at pH 6.35. They added polyvinylpyrrolidone to the CZE buffer as a polymer network additive. The diastereomers, which have identical electrophoretic mobilities at 0% polyvinylpyrrolidone and pH 6.35, were separated through the addition of the polymer. An increase in the concentration of the polymer to 6% improved the optical resolution. Some kind of interaction as in a reversed-phase HPLC system probably caused the separation. It was essential to add the polymer to CZE buffer for the diastereomeric separation of the solutes.

As already mentioned, the separation of diastereomers by a simple CZE system is usually difficult, and therefore an EKC system such as MEKC must be employed for this purpose. Nishi et al. [143] derivatized DL-AAs with 2,3,4,6-tetra-O-acetyl-β-D-glucopyranosyl isothiocyanate (GITC) and separated the GITC-derivatized DL-AAs by MEKC using SDS at pH 7.0 or 9.0 with high efficiency. An example is shown in Fig. 12. Lurie [144] also used GITC to derivatize six phenethylamines including amphetamine, ephedrine and norephedrine and separated the GITC derivatives by MEKC with SDS and MeOH at pH 9.0.

Tran et al. [145] used 1-fluoro-2,4-dinitrophenyl-5-D- (or -L-)alaninamide (Marfey reagent) to derivatize DL-AAs and some peptides. The separation of the derivatized compounds was carried out by MEKC with SDS at pH 8.5. The migration order between D- and L-AAs was reversed by changing the reagent chirality (D- or L-Marfey reagent). These results show that the separation of diastereomers by MEKC is far superior to that by CZE with respect to high efficiency and easy manipulation of selectivity.

Kang and Buck [146] separated OPA-derivatized DL-AAs by MEKC with SDS and MeOH at pH 9.5. They used both N-acetyl-L-cysteine and N-*tert*.-butyloxycarbonyl-L-cysteine as a chiral reagent together with OPA. Some diastereomers were separated by a simple CZE with some additives such as TAA salts. However, MEKC gave a better resolution than CZE.

## 8. Conclusions

Most of the separation principles are the same as those applied in HPLC. Naturally, most

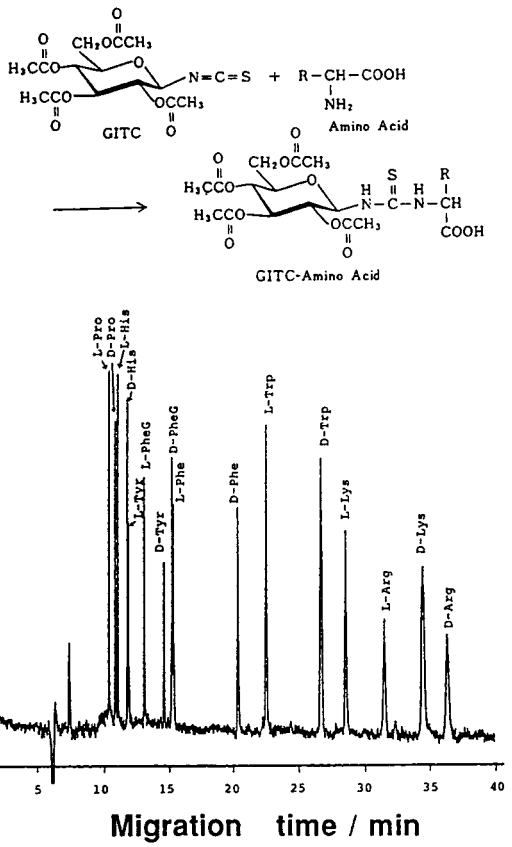


Fig. 12. Separation of eight GITC-derivatized DL-amino acids by MEKC with SDS. Buffer, 0.2 *M* SDS in 20 m*M* phosphate–borate buffer of pH 9.0. Other conditions as in Fig. 11 (from Ref. [143]).

additives or chiral selectors used in CE are borrowed from that used in HPLC, except for the chiral surfactants in MEKC. However, CE chiral separation has many advantages over HPLC chiral separation, such as its high separation efficiency and easy manipulation of selectivity. As discussed in CD-EKC, the migration order between D- and L-forms in CE also can be selected without changing the column and chiral selector, which is often required in HPLC chiral analysis, to obtain a favourable migration order. Another is related to economic aspects. To find the optimum separation media, one can simply alter the separation solution, which has an extremely small volume. This means that the use of several kinds of chiral columns, which are relatively expensive, and an organic solvent is not necessary in CE chiral separations. Extremely small volumes of media also allow the use of expensive chiral additives in CE. Although the relative standard deviation (R.S.D.) in the migration times and peak areas in CE analysis are inferior to those given by fully automated modern HPLC instruments, in which usually R.S.D. values not more than 0.5% are obtained without difficulty, CE chiral separations are suitable as a quality control method of optical purity testing, where R.S.D. values of around 1% and the sensitivity of UV detection are satisfactory for the purpose. Other than CDs or proteins, some specially designed chiral selectors will become

Table 8
Recommended starting conditions for a first attempt at CE chiral separation

| Solute | Chiral additive | Buffer |
|---|---|---|
| Cationic solutes | i 20 m*M* DM-β-CD | Phosphate buffer of pH 2.5 |
| | ii 20 m*M* HP-β-CD | Phosphate buffer of pH 2.5 |
| | iii 5% β-CD polymer | Phosphate buffer of pH 2.5 |
| | iv 20 m*M* γ-CD | Phosphate buffer of pH 2.5 |
| Anionic solutes | i 20 m*M* DM-β-CD | Phosphate buffer of pH 7.0 |
| | ii 20 m*M* HP-β-CD | Phosphate buffer of pH 7.0 |
| | iii 5% β-CD polymer | Phosphate buffer of pH 7.0 |
| | iv 20 m*M* γ-CD | Phosphate buffer of pH 7.0 |
| | v (i, ii, iii, or iv)–100 m*M* STDC | Phosphate buffer of pH 7.0 |
| Neutral solutes | i 50 m*M* STDC | Phosphate buffer of pH 9.0 |
| | ii 20 m*M* β-CD–50 m*M* STDC | Phosphate buffer of pH 9.0 |
| Primary amine | 10 m*M* 118C6 | Tris–citrate buffer of pH 2.2 |

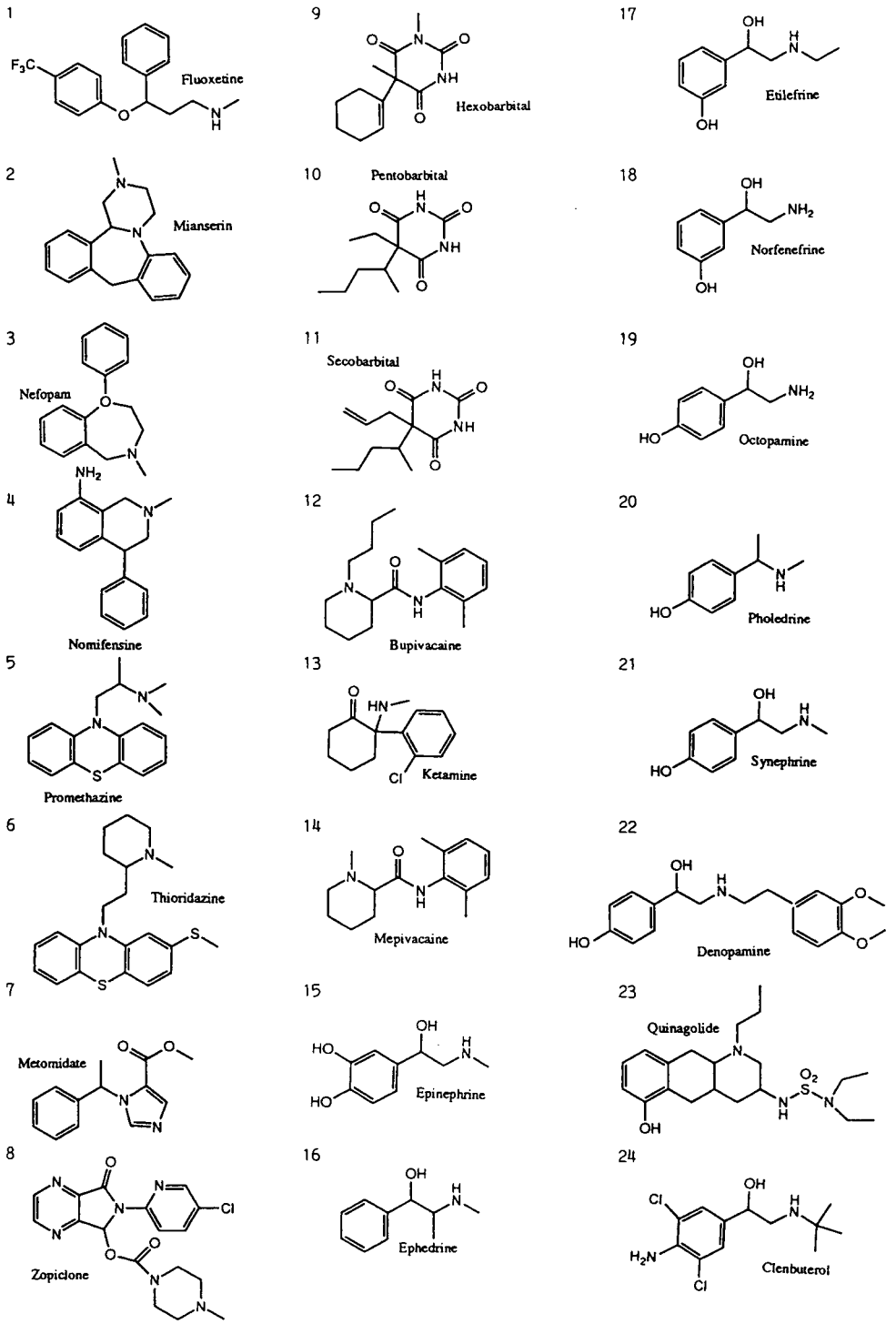


Fig. 13. (*Continued on p. 270*)

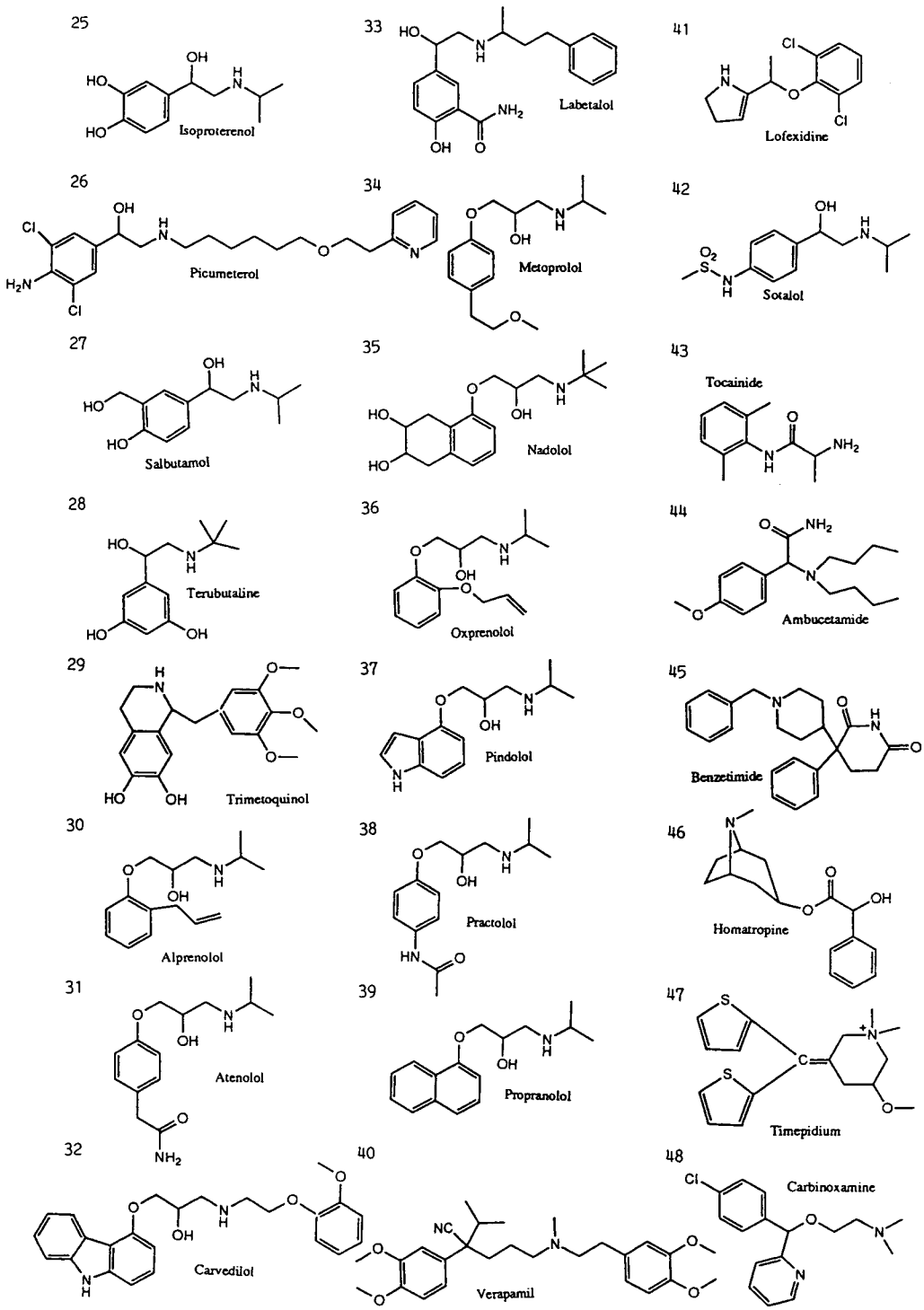
25
Isoproterenol
26
Picumeterol
27
Salbutamol
28
Terubutaline
29
Trimetoquinol
30
Alprenolol
31
Atenolol
32
Carvedilol
33
Labetalol
34
Metoprolol
35
Nadolol
36
Oxprenolol
37
Pindolol
38
Practolol
39
Propranolol
40
Verapamil
41
Lofexidine
42
Sotalol
43
Tocainide
44
Ambucetamide
45
Benzetimide
46
Homatropine
47
Timepidium
48
Carbinoxamine

Fig. 13.

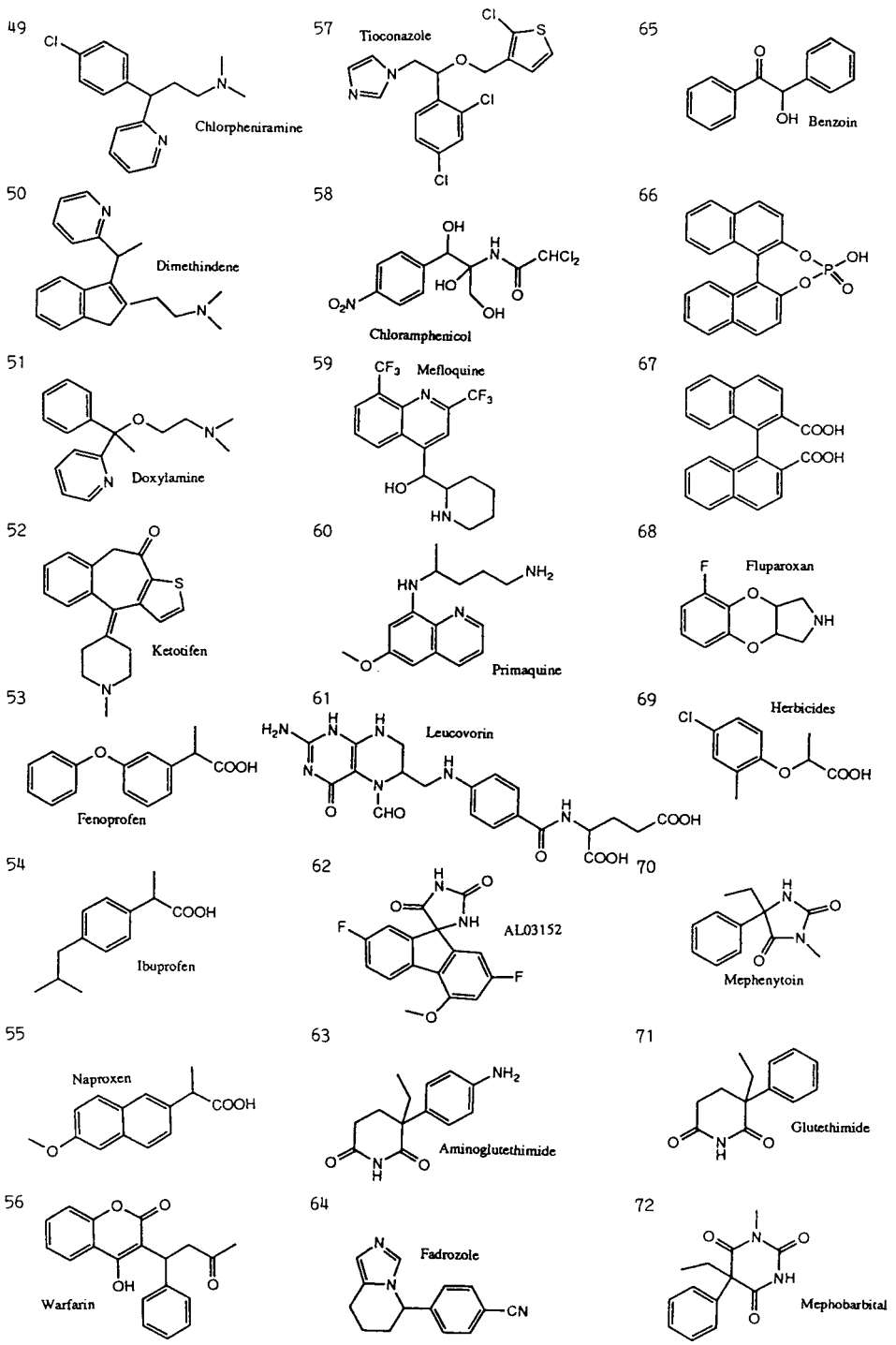


Fig. 13. (*Continued on p. 272*)

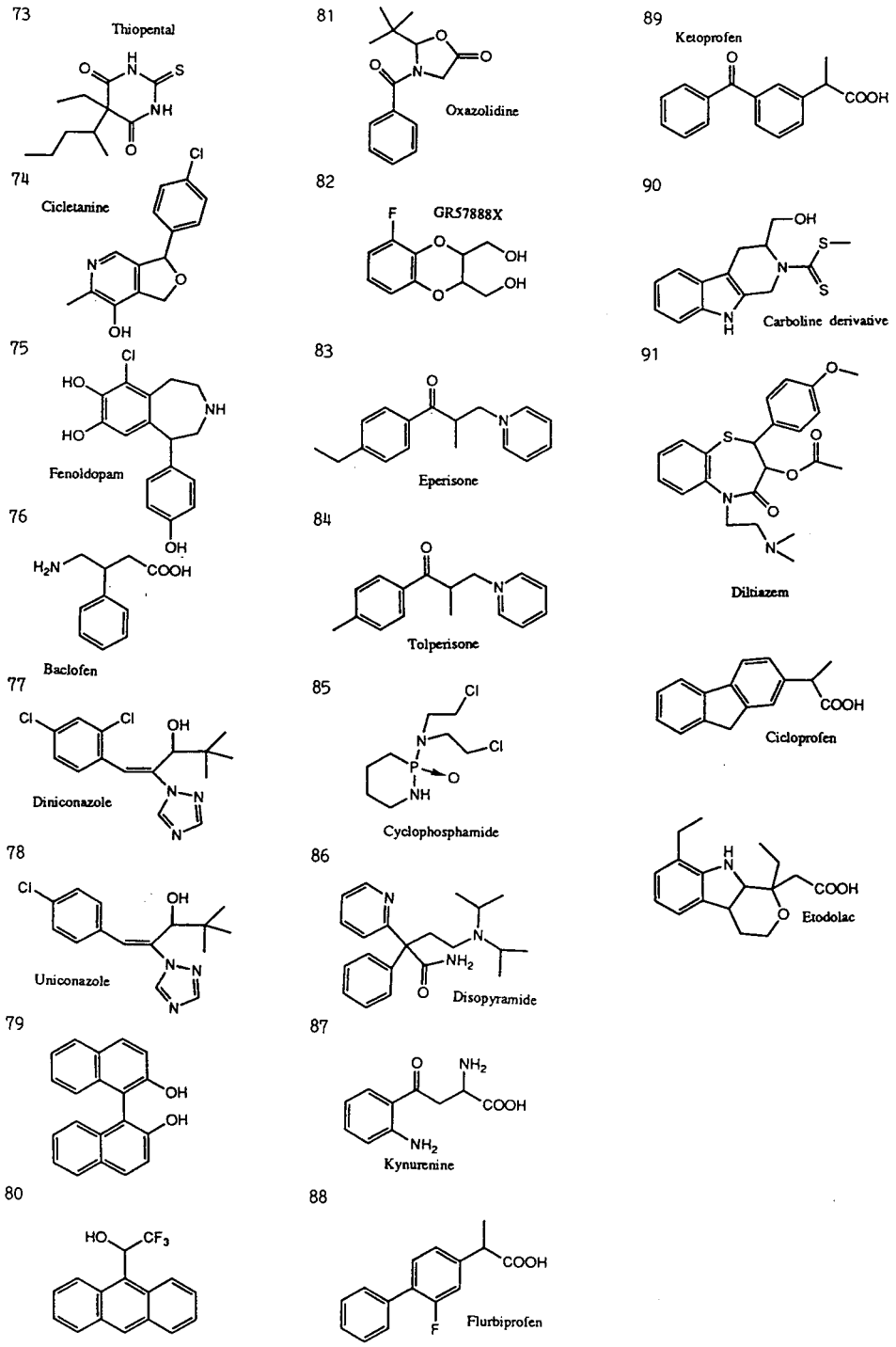


Fig. 13. Structures of the solutes.

available for CE chiral separations. Recently a chiral method development kit, which consists of several buffer solutions containing some chiral additives, was made commercially available. According to the brochure, the kit consists of four CDs. From the results summarized in Tables 3 and 4, and the wide enantioselectivity of DM-β-CD or HP-β-CD in CD-CZE, some starting buffer conditions to be attempted can be described in Table 8. Affinity EKC with proteins is also included in Table 8. The structure of the drugs summarized in Tables 3–7 with identification numbers and some other compounds described in the text are shown in Fig. 13.

## Abbreviations

| | |
|---|---|
| AAs | Amino acids |
| ACN | Acetonitrile |
| AGP | Orosomucoid ($\alpha_1$-acid glycoprotein) |
| BSA | Bovine serum albumin |
| 18C6 | 18-Crown-6-tetracarboxylic acid |
| *d*-CAM | Sodium *d*-camphor-10-sulphonate |
| CBH I | Cellobiohydrolase I |
| CBI | Naphthalene-2,3-dicarboxaldehyde |
| CD-CZE | Cyclodextrin-modified capillary zone electrophoresis |
| CD-EKC | Cyclodextrin-modified electrokinetic chromatography |
| CD-MEKC | Cyclodextrin-modified micellar electrokinetic chromatography |
| CDen | Mono-(6-β-aminoethylamino-6-deoxy)-β-cyclodextrin |
| CD(s) | Cyclodextrin(s) |
| CE | Capillary electrophoresis |
| CGE | Capillary gel electrophoresis |
| CPC | Cetylpyridinium chloride |
| CTAB | Cetyltrimethylammonium chloride |
| CZE | Capillary zone electrophoresis |
| DM-β-CD | Heptakis(2,6-di-O-methyl)-β-cyclodextrin |
| DM-β-MA | Dimethylcyclomaltoheptaose |
| DNS | Dansyl |
| EC | Electrochromatography |
| EDTA | Ethylenediaminetetraacetic acid |
| EKC | Electrokinetic chromatography |
| EOF | Electroosmotic flow |
| GC | Gas chromatography |
| GITC | 2,3,4,6-tetra-O-acetyl-β-D-glucopyranosyl isothiocyanate |
| HEC | Hydroxyethylcellulose |
| HPC | Hydroxypropylcellulose |
| HP-β-CD | Hydroxypropyl-β-cyclodextrin |
| HPLC | High-performance liquid chromatography |
| HSA | Human serum albumin |
| IEF | Isoelectric focusing |
| IPA | 2-Propanol |
| ITP | Isotachophoresis |
| MEKC | Micellar electrokinetic chromatography |
| *l*-MEN | *l*-Menthoxyacetic acid |
| MeOH | Methanol |
| MHEC | Methylhydroxyethylcellulose |
| OVM | Ovomucoid |
| PTH | Phenylthiohydantoin |
| R.S.D. | Relative standard deviation |
| SC | Sodium cholate |
| SDC | Sodium deoxycholate |
| SDS | Sodium dodecyl sulphate |
| SDAla | Sodium N-dodecanoyl-L-alaninate |
| SDGlu | Sodium N-dodecanoyl-L-glutamate |
| SDVal | Sodium N-dodecanoyl-L-valinate |
| SFC | Supercritical fluid chromatography |
| STC | Sodium taurochlote |
| STDC | Sodium taurodeoxycholate |
| TAA | Tetraalkylammonium |
| TBA | Tetrabutylammonium |
| TMA | Tetramethylammonium |
| TM-β-CD | Heptakis(2,3,6-tri-O-methyl)-β-cyclodextrin |

## References

[1] F.E.P. Mikker, F.M. Everaerts and Th.P.E.M. Verheggen, *J. Chromatogr.*, 169 (1979) 11–20.
[2] J.W. Jorgenson and K.D. Lukacs, *Anal. Chem.*, 53 (1981) 1298–1302.
[3] S. Hjerten, *J. Chromatogr.*, 270 (1983) 1–6.
[4] S. Terabe, K. Otsuka, K. Ichikawa, A. Tsuchiya and T. Ando, *Anal. Chem.*, 56 (1984) 111–113.
[5] S. Terabe, K. Otsuka and T. Ando, *Anal. Chem.*, 57 (1985) 834–841.

[6] J. Vindevogel, P. Sandra, *Introduction to Micellar Electrokinetic Chromatography*, Hüthig, Heidelberg, 1992.
[7] S.F.Y. Li, *Capillary Electrophoresis: Principle, Practice and Applications*, Elsevier, Amsterdam, 1992.
[8] P.D. Grossmann and J.C. Colburn (Editors), *Capillary Electrophoresis: Theory and Practice*, Academic Press, San Diego, 1992.
[9] R. Kuhn and S. Hoffstetter-Kuhn, *Capillary Electrophoresis: Principles and Practice*, Springer, Berlin, 1993.
[10] N.A. Guzman (Editor), *Capillary Electrophoresis Technology*, Marcel Dekker, New York, 1993.
[11] R. Weinberger, *Practical Capillary Electrophoresis*, Academic Press, San Diego, 1993.
[12] P. Jandik and G. Bonn, *Capillary Electrophoresis of Small Molecules and Ions*, VHC, Weinheim, 1993.
[13] B.L. Karger, A.S. Cohen and A. Guttman, *J. Chromatogr.*, 492 (1989) 585–614.
[14] Z. Deyl and R. Struzinsky, *J. Chromatogr.*, 569 (1991) 63–122.
[15] W.G. Kuhn, *Anal. Chem.*, 62 (1990) 403R–414R.
[16] W.G. Kuhn and C.A. Monnig, *Anal. Chem.*, 64 (1992) 389R–407R.
[17] H. Nishi and S. Terabe, *Electrophoresis*, 11 (1990) 691–701.
[18] D.M. Goodall, S.J. Willams and D.K. Lloyd, *Trends Anal. Chem.*, 10 (1991) 272–279.
[19] A. Pluym, W. Van Ael and M. De Smet, *Trends Anal. Chem.*, 11 (1992) 27–32.
[20] G.M. McLaughlin, J.A. Nolan, J.L. Lindahl, R.H. Palmieri, K.W. Anderson, S.C. Morris, J.A. Morrison and T.J. Bronzert, *J. Liq. Chromatogr.*, 15 (1992) 961–1021.
[21] D. Perrete and G. Ross, *Trends Anal. Chem.*, 11 (1992) 156–163.
[22] N. Nishi and S. Terabe, *J. Pharm. Biomed. Anal.*, 11 (1993) 1277–1287.
[23] K.D. Altria, *J. Chromatogr.*, 646 (1993) 245–257.
[24] J. Snopek, I. Jelinek and E. Smolkova-Keulemansova, *J. Chromatogr.*, 609 (1992) 1–17.
[25] R. Kuhn and S. Hoffstetter-Kuhn, *Chromatographia*, 34 (1992) 505–512.
[26] K. Otsuka and S. Terabe, *Trends Anal. Chem.*, 12 (1993) 125–130.
[27] S. Terabe, K. Otsuka and N. Nishi, *J. Chromatogr. A*, 666 (1994) 295–319.
[28] S. Fanali, *J. Chromatogr.*, 474 (1989) 441–446.
[29] S. Fanali and P. Bocek, *Electrophoresis*, 11 (1990) 757–760.
[30] S. Fanali, *J. Chromatogr.*, 545 (1991) 437–444.
[31] A. Nardi, L. Ossicini and S. Fanali, *Chirality*, 4 (1992) 56–61.
[32] W. Schutzner and S. Fanali, *Electrophoresis*, 13 (1992) 687–690.
[33] L. Cellai, C. Desiderio, R. Filippetti and S. Fanali, *Electrophoresis*, 14 (1993) 823–825.
[34] S.A.C. Wren and R.C. Rowe, *J. Chromatogr.*, 603 (1992) 235–241.
[35] S.A.C. Wren and R.C. Rowe, *J. Chromatogr.*, 609 (1992) 363–367.
[36] S.A.C. Wren and R.C. Rowe, *J. Chromatogr.*, 635 (1993) 113–118.
[37] S.A.C. Wren, *J. Chromatogr.*, 636 (1993) 57–62.
[38] Y.Y. Rawjee, D.U. Staerk and G. Vigh, *J. Chromatogr.*, 635 (1993) 291–306.
[39] Y.Y. Rawjee and G. Vigh, *Anal. Chem.*, 66 (1994) 619–627.
[40] Y.Y. Rawjee, R.L. Williams and G. Vigh, *J. Chromatogr. A*, 652 (1993) 233–245.
[41] J. Snopek, H. Soini, M. Novotony, E. Smolkova-keulemansova and I. Jelinek, *J. Chromatogr.*, 559 (1991) 215–222.
[42] H. Soini, Marja-Liisa Reikkola and M.V. Novotny, *J. Chromatogr.*, 608 (1992) 265–274.
[43] D. Belder and G. Schomburg, *J. High Resolut. Chromatogr.*, 15 (1992) 686–693.
[44] C. Quang and G. Khaledi, *Anal. Chem.*, 65 (1993) 3354–3358.
[45] C. Quang and G. Khaledi, *J. High Resolut. Chromatogr.*, 17 (1994) 99–101.
[46] T.E. Peterson and T. Trowbridge, *J. Chromatogr.*, 603 (1992) 298–301.
[47] K.D. Altria, R.C. Harden, M. Hart, J. Hevizi, P.A. Hailey, J.V. Makwana and M.J. Portsmouth, *J. Chromatogr.*, 641 (1993) 147–153.
[48] K.D. Altria, A.R. Walsh and N.W. Smith, *J. Chromatogr.*, 645 (1993) 193–196.
[49] K.D. Altria, D.M. Goodall, M.M. Rogan, *Chromatographia*, 34 (1992) 19–24.
[50] K.D. Altria, *Chromatographia*, 35 (1993) 177–182.
[51] H. Nishi, K. Nakamura, H. Nakai and T. Sato, *J. Chromatogr. A*, 678 (1994) 333–342.
[52] H. Nishi, K. Nakamura, H. Nakai, T. Sato and S. Terabe, *J. Chromatogr.*, submitted for publication.
[53] M. Heuermann and G. Blaschke, *J. Chromatogr.*, 648 (1993) 267–274.
[54] P. Gareil, J.P. Gramond and F. Guyon, *J. Chromatogr.*, 615 (1993) 317–325.
[55] M.W.F. Nielen, *J. Chromatogr.*, 637 (1993) 81–90.
[56] M.W.F. Nielen, *Anal. Chem.*, 65 (1993) 885–893.
[57] M.J. Sepaniak, R.O. Cole and B.K. Clark, *J. Liq. Chromatogr.*, 15 (1992) 1023–1040.
[58] M.E. Swartz, *J. Liq. Chromatogr.*, 14 (1991) 923–938.
[59] M. Tanaka, S. Asano, M. Yoshinago, Y. Kawaguchi, T. Tetsumi and T. Shono, *Fresenius' J. Anal. Chem.*, 339 (1991) 63–64.
[60] Y. Yamashoji, T. Ariga, S. Asano and M. Tanaka, *Anal. Chim. Acta*, 268 (1992) 39–47.
[61] M. Tanaka, M. Yoshinaga, S. Asano, Y. Yamashoji and Y. Kawaguchi, *Fresenius' J. Anal. Chem.*, 343 (1992) 896–900.
[62] R. Kuhn, F. Stoecklin and F. Enri, *Chromatographia*, 33 (1992) 32–36.

[63] S.G. Penn, D.M. Goodall and J.S. Loran, *J. Chromatogr.*, 636 (1993) 149–152.
[64] K. Otsuka and S. Terabe, *J. Liq. Chromatogr.*, 16 (1993) 945–953.
[65] T.E. Peterson, *J. Chromatogr.*, 630 (1993) 353–361.
[66] N. Nishi, Y. Kokusenya, T. Miyamoto and T. Sato, *J. Chromatogr. A*, 659 (1994) 449–457.
[67] A. Shibukawa, D.K. Lloyd and I.W. Wainer, *Chromatographia*, 35 (1993) 419–429.
[68] E. Francotte, S. Cherkaoui and M. Faupel, *Chirality*, 5 (1993) 516–526.
[69] T. Schmitt and H. Engelhardt, *J. High Resolut. Chromatogr.*, 16 (1993) 525–529.
[70] T. Schmitt and H. Engelhardt, *Chromatographia*, 37 (1993) 475–481.
[71] N.W. Smith, *J. Chromatogr. A*, 652 (1993) 259–262.
[72] A. Nardi, A. Eliseev, P. Bocek and S. Fanali, *J. Chromatogr.*, 638 (1993) 247–253.
[73] C. Dette, S. Ebel and S. Terabe, *Electrophoresis*, in press.
[74] A. Guttman, A. Paulus, A.S. Cohen, N. Grinberg and B.L. Karger, *J. Chromatogr.*, 448 (1988) 41–53.
[75] I.D. Cruzado and G. Vigh, *J. Chromatogr.*, 608 (1992) 421–425.
[76] Y. Miyashita and S. Terabe, *Chromatogram*, 11, No. 2 (1990) 6–7.
[77] Y. Miyashita and S. Terabe, *Application Data DS-767*, Beckman, Fullerton, CA, 1990.
[78] S. Terabe, Y. Miyashita, Y. Ishihama and O. Shibata, *J. Chromatogr.*, 636 (1993) 47–55.
[79] H. Nishi, T. Fukuyama and S. Terabe, *J. Chromatogr.*, 553 (1991) 503–516.
[80] T. Ueda, F. Kitamura, R. Mitchell, T. Metcalf, T. Kuwana and A. Nakamoto, *Anal. Chem.*, 63 (1991) 2979–2981.
[81] T. Ueda, R. Mitchell, F. Kitamura, T. Metcalf, T. Kuwana and A. Nakamoto, *J. Chromatogr.*, 593 (1992) 265–274.
[82] J. Prunonosa, A.D. Gascon and L. Gouesclou, *Application Data DS-767*, Beckman, Fullerton, CA, 1991.
[83] J. Prunonosa, R. Obach, A. Diez-Cascon and L. Gouesclou, *J. Chromatogr.*, 574 (1992) 127–133.
[84] R. Furuta and T. Doi, *J. Chromatogr. A*, 676 (1994) 431–436.
[85] G.N. Okafo, C. Bintz, S.E. Clarke and P. Camilleri, *J. Chem. Soc., Chem. Commun.*, (1992) 1189–1192.
[86] G.N. Okafo and P. Camilleri, *J. Microcol. Sep.*, 5 (1993) 149–153.
[87] M. Lin, N. Wu, G.E. Barker, P. Sun, C.W. Huie and R.A. Hartwick, *J. Liq. Chromatogr.*, 16 (1993) 3667–3674.
[88] J. Snopek, I. Jelinek and E. Smolkova-Keulemansova, *J. Chromatogr.*, 438 (1988) 211–218.
[89] I. Jelinek, J. Snopek and E. Smolkova-Keulemansova, *J. Chromatogr.*, 439 (1988) 386–392.
[90] I. Jelinek, J. Dohnal, J. Snopek and E. Smolkova-Keulemansova, *J. Chromatogr.*, 464 (1989) 139–147.
[91] I. Jelinek, J. Snopek, J. Dian and E. Smolkova-Keulemansova, *J. Chromatogr.*, 470 (1989) 113–121.
[92] J. Snopek, I. Jelinek and E. Smolkova-Keulemansova, *J. Chromatogr.*, 472 (1989) 308–313.
[93] I. Jelinek, J. Snopek and E. Smolkova-Keulemansova, *J. Chromatogr.*, 557 (1991) 215–226.
[94] E. Dubrovcakova, B. Gas, J. Vacik and E. Smolkova-Keulemansova, *J. Chromatogr.*, 623 (1992) 337–344.
[95] S. Mayer and V. Schurig, *J. High Resolut. Chromatogr.*, 15 (1992) 129–131.
[96] S. Mayer and V. Schurig, *J. Liq. Chromatogr.*, 16 (1993) 915–931.
[97] S. Mayer, M. Schleimer and V. Schurig, *J. Microcol. Sep.*, 6 (1994) 43–48.
[98] D.W. Armstrong, Y. Tang, T. Ward and M. Nichols, *Anal. Chem.*, 65 (1993) 1114–1117.
[99] S. Terabe, *Trends Anal. Chem.*, 8 (1989) 129–134.
[100] G.E. Barker, P. Russo and R.A. Hartwick, *Anal. Chem.*, 64 (1992) 3024–3028.
[101] P. Sun, N. Wu, G.E. Barker and R.A. Hartwick, *J. Chromatogr.*, 648 (1993) 475–480.
[102] S. Busch, J.C. Kraak and H. Poppe, *J. Chromatogr.*, 635 (1993) 119–126.
[103] Y. Ishihama, Y. Oda, N. Asakawa, Y. Yoshida and T. Sato, *J. Chromatogr. A*, 666 (1994) 193–201.
[104] R. Vespalec, V. Sustacek and P. Bocek, *J. Chromatogr.*, 638 (1993) 255–261.
[105] L. Valtcheva, J. Mohammad, G. Pettersson and S. Hjerten, *J. Chromatogr.*, 638 (1993) 263–267.
[106] Y. Tanaka, N. Matsubara and S. Terabe, *Electrophoresis*, in press.
[107] S. Birnbaum and S. Nilsson, *Anal. Chem.*, 64 (1992) 2872–2874.
[108] P. Sum, N. Wu, G.E. Barker, R.A. Hartwick, N. Grinberg and R. Kaliszan, *J. Chromatogr. A*, 652 (1993) 247–252.
[109] S. Li and D.K. Lloyd, *Anal. Chem.*, 65 (1993) 3684–3690.
[110] A.M. Krstulvic (Editor), *Chiral Separation by HPLC*, Ellis Horwood, Chichester, 1989.
[111] R. Kuhn, F. Enri, T. Bereuter and J. Hansler, *Anal. Chem.*, 64 (1992) 2815–2820.
[112] E. Hohne, G.J. Krauss and G. Gubitz, *J. High Resolut. Chromatogr.*, 15 (1992) 698–700.
[113] A. D'Hulst and N. Verbeke, *J. Chromatogr.*, 608 (1992) 275–287.
[114] H. Nishi, K. Nakamura, H. Nakai, T. Sato and S. Terabe, *Electrophoresis*, in press.
[115] E. Gassman, J.E. Kuo and R.N. Zare, *Science*, 230 (1985) 813–814.
[116] P. Gozel, E. Gassmann, H. Michelsen and R.N. Zare, *Anal. Chem.*, 59 (1987) 44–49.
[117] A. Dobashi, T. Ono, S. Hara and J. Yamaguchi, *Anal. Chem.*, 61 (1989) 1984–1986.
[118] A. Dobashi, T. Ono, S. Hara and J. Yamaguchi, *J. Chromatogr.*, 480 (1989) 413–420.
[119] K. Otsuka and S. Terabe, *J. Chromatogr.*, 515 (1990) 221–226.

[120] K. Otsuka and S. Terabe, *J. Chromatogr.*, 559 (1991) 209–214.
[121] K. Otsuka and S. Terabe, *Electrophoresis*, 11 (1990) 982–984.
[122] K. Otsuka, M. Kashihara, Y. Kawaguchi, R. Koike, T. Hisamitsu and S. Terabe, *J. Chromatogr. A*, 652 (1993) 253–257.
[123] S. Terabe, M. Shibata and Y. Miyashita, *J. Chromatogr.*, 480 (1989) 403–411.
[124] A.R. Campanelli, S.C. De Sanctis, E. Chiessi, M. D'Alagni, E. Giglio and L. Scaramuzza, *J. Phys. Chem.*, 93 (1989) 1536–1542.
[125] H. Nishi, T. Fukuyama, M. Matsuo and S. Terabe, *J. Microcol. Sep.*, 1 (1989) 234–241.
[126] H. Nishi, T. Fukuyama, M. Matsuo and S. Terabe, *J. Chromatogr.*, 515 (1990) 233–243.
[127] H. Nishi, T. Fukuyama, M. Matsuo and S. Terabe, *Anal. Chim. Acta.*, 236 (1990) 281–286.
[128] R.O. Cole, M.J. Sepaniak and W.L. Hinze, *J. High Resolut. Chromatogr.*, 13 (1990) 579–582.
[129] R.O. Cole and M.J. Sepaniak, *LC·GC*, 10 (1992) 380–385.
[130] Y. Ishihama and S. Terabe, *J. Liq. Chromatogr.*, 16 (1993) 933–944.
[131] S. Terabe, Y. Miyashita, O. Shibata, E.R. Barnhart, L.R. Alexander, D.J. Patterson, B.L. Karger, K. Hosoya and N. Tanaka, *J. Chromatogr.*, 516 (1990) 23–31.
[132] H. Nishi and M. Matsuo, *J. Liq. Chromatogr.*, 14 (1991) 973–986.
[133] T. Imasaka, K. Nishitani and N. Ishibashi, *Anal. Chim. Acta*, 256 (1992) 3–7.
[134] S. Terabe, H. Ozaki, K. Otsuka and T. Ando, *J. Chromatogr.*, 332 (1985) 211–217.
[135] S. Allenmark and S. Andersson, *Molecular Interaction in Bioseparation*, Plenum Press, New York, 1993, pp. 179–187.
[136] A.S. Cohen, A. Paulus and B.L. Karger, *Chromatographia*, 24 (1987) 15–24.
[137] S. Terabe, *J. Pharm. Biomed. Anal.*, 10 (1992) 705–715.
[138] H. Watarai, *Chem. Lett.*, (1991) 391–394.
[139] S. Terabe, N. Matsubara, Y. Ishihama and Y. Okada, *J. Chromatogr.*, 608 (1992) 23–29.
[140] J.H. Aiken and C.W. Huie, *Chromatographia*, 35 (1993) 448–450.
[141] S. Fanali, L. Ossicini, F. Forest and P. Bocek, *J. Microcol. Sep.*, 1 (1989) 190–194.
[142] W. Schutzner, S. Fanali, A. Rizzi and E. Kenndler, *J. Chromatogr.*, 639 (1993) 375–378.
[143] H. Nishi, T. Fukuyama and M. Matsuo, *J. Microcol. Sep.*, 2 (1990) 234–240.
[144] I.S. Lurie, *J. Chromatogr.*, 605 (1992) 269–275.
[145] A.D. Tran, T. Blanc, E.J. Leopold, *J. Chromatogr.*, 516 (1990) 241–249.
[146] L. Kang and R.H. Buck, *Amino Acids*, 2 (1992) 103–109.

ELSEVIER

Journal of Chromatography A, 694 (1995) 277–284

JOURNAL OF CHROMATOGRAPHY A

# Partial separation zone technique for the separation of enantiomers by affinity electrokinetic chromatography with proteins as chiral pseudo-stationary phases

Yoshihide Tanaka[a,*], Shigeru Terabe[b]

[a]*Department of Analytical Chemistry, Nippon Boehringer Ingelheim Co. Ltd., 3-10-1, Yato, Kawanishi, Hyogo 666-01, Japan*
[b]*Faculty of Science, Himeji Institute of Technology, Kamigori, Hyogo 678-12, Japan*

**Abstract**

A previously reported technique which employed a discontinuous separation zone built in a part of a capillary was applied to the separation of enantiomers by affinity electrokinetic chromatography using proteins as chiral pseudo-stationary phases to avoid a detection problem caused by the presence of UV-absorbing materials in the separation solution. The technique was named "partial separation zone technique", where the capillary was partially filled with a solution containing a protein and the protein was not in the detector cell when analytes reached that cell. It was shown that the technique was successfully performed automatically using a commercial capillary electrophoresis instrument. The migration velocity of the protein was practically reduced to zero by using a coated capillary. The protein concentration could be increased in this technique to enhance resolution without the deterioration of the detector sensitivity. The detection sensitivity was remarkably improved using short-wavelength light in comparison with the conventional technique where the protein was added to the whole separation solution. The reproducibilities of the migration time and the peak area were evaluated, giving results comparable to those with the conventional method. Successful separations of basic racemates were achieved by the technique using bovine serum albumin, $\alpha_1$-acid glycoprotein, ovomucoid and conalbumin.

## 1. Introduction

The separation of enantiomers is critical in the development of new medicines, because enantiomers have not only different pharmacological activities but also different pharmacokinetic and pharmacodynamic effects. High-performance liquid chromatography (HPLC) is the most popular tool for the separation of enantiomers at present. Various kinds of chiral stationary phases have been developed and are commercially available for the separation of various racemic compounds. In particular, stationary phases with bonded proteins such as bovine serum albumin (BSA), $\alpha_1$-acid glycoprotein ($\alpha_1$-AGP) and ovomucoid have been widely accepted in the pharmaceutical field because of an extremely wide range of applications under reversed-phase conditions [1–4]. The drawbacks of these stationary phases are that: (1) the columns are relatively expensive; (2) many different types of columns are required for successful separations; (3) lifetimes of the columns are short; and that (4) the efficiency of the columns is rather low.

Affinity electrokinetic chromatography (EKC), where a charged biopolymer such as a

* Corresponding author.

0021-9673/95/$09.50 
*SSDI* 0021-9673(94)00790-X

protein or polysaccharide is employed as a pseudo-stationary phase, is a new separation technique having high resolving power, short separation time, simple operating procedure, and minimal sample and solvent requirements similarly to the capillary electrophoretic (CE) techniques for enantiomer separation [5–8]. Many papers have been published on successful separations of enantiomers using BSA [9–11], human serum albumin [12], $\alpha_1$-AGP [11], ovomucoid [13] and avidin [14] as chiral selectors. A major drawback of affinity EKC with the protein as a pseudo-stationary phase is in low detection sensitivity caused by the UV absorption by the proteins in the shorter-wavelength region, in addition to an inherent weak point of low concentration sensitivity of CE detectors. In order to overcome this drawback, Valtcheva et al. [15] developed an approach in which the protein did not pass through the detection cell and did not interfere with the detection of analytes. However, in the technique, a 2–3 mm long agarose gel must be plugged at the injection end of the capillary prior to each run in order to prevent hydrodynamic flow. We modified the technique to run automatically using a commercial CE instrument. The technique is named "partial separation zone technique", which keeps the same advantage in detection sensitivity as the original method mentioned above. In this paper, the operating principle and the procedure of the technique are described, and the method validations for a quantitative analysis are discussed. Separations of various basic racemic drugs by this method using BSA, $\alpha_1$-AGP, ovomucoid and conalbumin as chiral selectors are presented.

## 2. Experimental

### 2.1. Apparatus

Affinity EKC was performed with a BioFocus 3000 automated CE system (Bio-Rad, Hercules, CA, USA). A 50 $\mu$m I.D. fused-silica capillary (Polymicro Technologies, Phoenix, AZ, USA) was coated with linear polyacrylamide by the method reported by Nakatani et al. [16]. A coated capillary of 36 cm in total length (31.5 cm to the detector) was incorporated into a user-assembled capillary cartridge. The instrument control and data collections were performed with a Bravo LC 4/33 personal computer (AST Research, Irvine, CA, USA).

### 2.2. Reagents

Ovomucoid and conalbumin were gifts from Eisai (Tokyo, Japan). BSA as fraction V powder and bovine $\alpha_1$-AGP as Cohn fraction VI were purchased from Sigma (St. Louis, MO, USA). These proteins were used as received. Bunitrolol and epinastine were pharmaceutical products of Nippon Boehringer Ingelheim (Hyogo, Japan). Tolperisone and clorprenaline were obtained from Eisai. Chlorpheniramine was purchased from Tokyo Kasei Kogyo (Tokyo, Japan), oxyphencyclimine was from Sigma, and pindolol was from Wako (Osaka, Japan). Primaquine, propranolol, trimebutine and trimetoquinol were donated by Tanabe Seiyaku (Osaka, Japan). Homochlorcyclizine, arotinolol and verapamil were obtained from Shinwa Chemical (Kyoto, Japan). All other reagents were of analytical grade. Water was purified with a Milli-Q Labo system (Nihon Millipore, Yonezawa, Japan)

### 2.3. Procedure

Electrophoretic buffer (running buffer) solutions used in this study were 50 m*M* phosphate buffers containing appropriate amounts of an organic solvent or an amphoteric surfactant, when necessary. The running buffer solution was placed in multiple buffer vials and the running buffer was exchanged before every run in order to obtain reproducible results. Separation solutions were freshly prepared by dissolving a protein as a chiral selector in the running buffer, and filtered through a 0.45-$\mu$m syringe-type membrane filter prior to use. Stock solutions of samples (ca. 500 $\mu$g/ml) were prepared in water or methanol. Sample solutions for injection were prepared by tenfold dilution of the stock solution with water.

The capillary was thermostated at 25°C with a liquid coolant. The temperature of vial holders for the separation solution, running buffer solu-

tion and sample solutions were maintained at 15°C. The capillary was rinsed with water followed by the running buffer for 30 s each prior to the run, and was partially filled with the separation solution at 1 p.s.i. (6.9 kPa) for 190 s. The sample solution was injected at 1 p.s.i. for 2 s. Both ends of the capillary were dipped into the running buffer, and a constant voltage of 12.0 kV was applied for the separation. Migrating analytes were detected by on-column measurement of UV absorption at 210 or 220 nm.

## 3. Results and discussion

### 3.1. Principle of the partial separation zone technique

The operating principle of the technique is illustrated schematically in Fig. 1. The capillary is rinsed with water and the running buffer at 100 p.s.i. for 30 s each. The capillary is then partially filled with the separation solution containing a protein as a chiral selector at 1 p.s.i. for 190 s (Fig. 1a). The separation zone thus built in the capillary is about 27 cm in length. Because the distance from the injection end of the capillary to the detector cell is 31.5 cm, the separation zone does not reach the detection cell. A sample solution is introduced at the end of the capillary filled with the separation solution (Fig. 1b), and the injection end is dipped into the running buffer followed by the application of a high voltage. Basic analytes which are positively charged in the running buffer (pH 4.0–7.0) migrate toward the cathode. On the other hand, $\alpha_1$-AGP (p*I* 2.9–3.2), ovomucoid (p*I* 3.9–4.3), BSA (p*I* 4.7–4.9) and conalbumin (p*I* 6.1–6.6) are slightly negatively charged in the running buffers (pH 4.0 for $\alpha_1$-AGP, pH 5.0 for ovo-

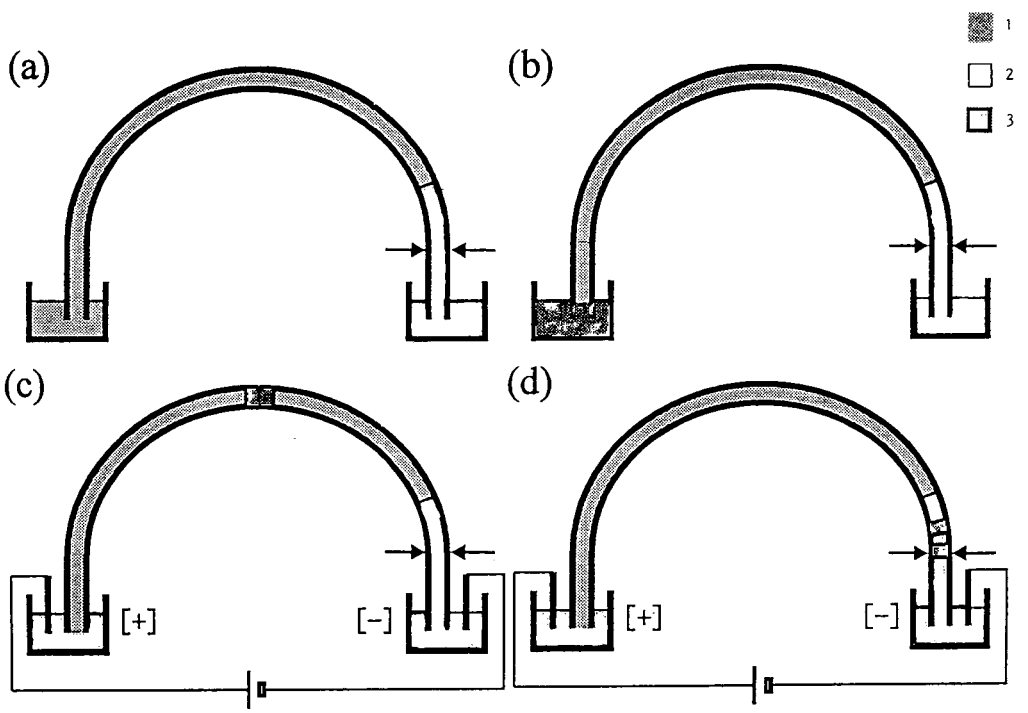


Fig. 1. Schematic illustration of the partial separation zone technique: 1 = separation zone; 2 = running buffer; 3 = sample solution; arrows indicate detection window. (a) The separation zone is introduced from the injection end to a point short of the detector cell after the rinse of the capillary with water followed by the running buffer; (b) the sample solution is introduced into the capillary; (c) a high voltage is applied between both ends of the capillary after both ends are dipped into the running buffer and the analytes migrate toward the detector; (d) a separated zone reaches the detector cell but the separation zone does not reach this cell.

mucoid, pH 6.0 for BSA and pH 7.0 for conalbumin) and migrate in the opposite direction. However, the electrophoretic velocities of these proteins are very low. In this study, a linear polyacrylamide-coated capillary was used to suppress the electroosmotic flow as well as to reduce the protein adsorption on the capillary wall. Therefore, the separation zone or the protein did not migrate significantly during the run. The separation of enantiomers is achieved only while the solute is migrating in the separation zone (Fig. 1c). The enantiomers migrate at identical velocities outside the separation zone, reaching the detection cell. The protein is absent in the detector cell when the enantiomers pass through that cell (Fig. 1d). In this method, the detection sensitivity can be remarkably improved by measuring absorption at a shorter wavelength. Although the separation solution must be replaced before each run, the consumption of the separation solution is only about 0.5 $\mu$l for each run. Therefore, the total volume of the separation solution required for a series of analysis is less than that required for the conventional method, where the protein must be dissolved into the whole running solution. The whole running solution containing the protein must often be replaced in the conventional method to obtain good reproducibility, whereas the total protein solution can be used for the separation in the partial separation zone technique. For only one or two runs, the technique may not be advantageous, but for several runs with a protein, the advantage is clear.

In a previous paper [14], we proposed a simple model based on the model developed for cyclodextrin-modified capillary zone electrophoresis [17] for the separation of enantiomers by affinity EKC using a protein as a chiral selector. If we assume that the analyte interacts with a single site of the protein, the apparent mobility of the analyte in the separation zone, $\mu_{app,s}$, is written as

$$\mu_{app,s} = \mu_{eo} + \frac{1}{1 + K[P]} \cdot \mu_a + \frac{K[P]}{1 + K[P]} \cdot \mu_p \quad (1)$$

where $\mu_{eo}$ is the electroosmotic mobility, $\mu_a$ the electrophoretic mobility of the free analyte, $\mu_p$ the electrophoretic mobility of the protein, which is assumed to be equal to the mobility of the protein–analyte complex, $K$ the binding constant and [P] the protein concentration. Since $\mu_{eo}$ and $\mu_p$ are negligible in this technique as described above, Eq. 1 is simplified to

$$\mu_{app,s} = \frac{1}{1 + K[P]} \cdot \mu_a \quad (2)$$

Actually, $\mu_{eo}$ and $\mu_p$ could not be measured because the velocities were too low and the estimated values were less than $1.1 \cdot 10^{-4}$ mm$^2$ s$^{-1}$ V$^{-1}$ for $\mu_{eo}$ and less than $4.2 \cdot 10^{-4}$ mm$^2$ s$^{-1}$ V$^{-1}$ for $(\mu_{eo} + \mu_p)$. Enantiomers 1 and 2 have different binding constants, $K_1$ and $K_2$, and therefore apparent mobilities of the enantiomers are different. However, when the analytes migrate in the buffer zone out of the separation zone, $K_1$ and $K_2$ become zero and both enantiomers have the same mobility, $\mu_{app,b}$,

$$\mu_{app,b} = \mu_{eo} + \mu_a \approx \mu_a \quad (3)$$

Therefore, only the separation zone is effective for the separation of enantiomers and the rest of the zone to the detector, which does not contain the protein, serves to transport the separated zones to the detector. Band broadening outside the separation zone can be expected to be minimum, because the same running buffer is employed in both separation and transportation zones. A representative electropherogram observed at 210 nm is shown in Fig. 2 for the separation of epinastine racemates with 750 $\mu M$ BSA at pH 6.0. Baseline drift was not observed in spite of the short-wavelength detection at 210 nm in Fig. 2.

### 3.2. Concentration of chiral selector

For the separation of enantiomers, the difference in apparent mobilities, $\Delta\mu_{app}(= \mu_{app,1} - \mu_{app,2})$, between the two enantiomers must be maximized. The difference in mobilities in affinity EKC with a protein is given as a function of the concentration of the protein as [14],

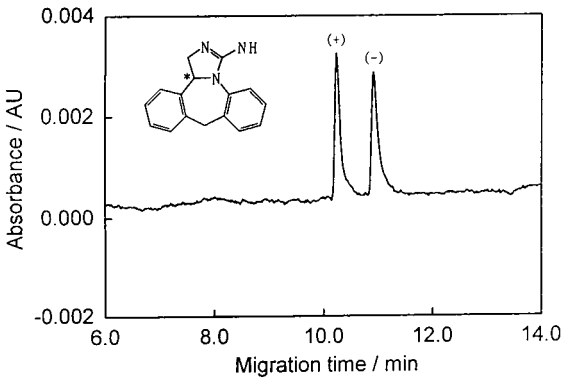


Fig. 2. A representative electropherogram obtained by the partial separation zone technique for the separation of (±)-epinastine with BSA as the chiral selector. Conditions: capillary, 36 cm (31.5 cm to the detector) × 50 μm I.D.; separation zone length, 27 cm; separation solution, 750 μ*M* BSA in the running buffer; running buffer, 50 m*M* phosphate buffer (pH 6.0); applied voltage, 12.0 kV; detection wavelength, 210 nm.

$$\Delta\mu_{app} = \frac{(\mu_s - \mu_p)(K_2 - K_1)[P]}{(1 + K_1[P])(1 + K_2[P])} \quad (4)$$

where subscripts 1 and 2 refer to enantiomers 1 and 2. The optimum concentration of the protein, which gives the maximum resolution, can be calculated as [14],

$$[P]_{opt} = (K_1 K_2)^{-1/2} \quad (5)$$

Although the binding constants of most racemates are not known, if we assume the binding constants are in the order of from $1 \cdot 10^3$ to $1 \cdot 10^5$ $M^{-1}$, $[P]_{opt}$ will be in the range 10–1000 μ*M*. Thus, the optimum concentration of the protein can be very high. Actually, the concentrations of the proteins used for the separation of enantiomers were in the range of 20–100 μ*M* [9–13], except for two cases: ca. 600 μ*M* cellulase [15] and 250 μ*M* ovomucoid [13]. The use of a high concentration of cellulase was allowed by a similar technique [15], whereas 250 μ*M* ovomucoid caused noisy and unstable baselines [13]. We observed that increasing the protein (avidin) concentration higher than 50 μ*M* caused a serious baseline drift even with detection at 240 nm, although the resolution was improved for most enantiomers [14]. Therefore, the maximum avidin concentration in the running solution was usually limited lower than 50 μ*M* in the conventional method when the analytes were to be detected at a wavelength below 240 nm. On the other hand, the partial separation zone technique permits the use of a high protein concentration without the detection problems in order to enhance resolution.

The relationship between the migration time, $t_a$, and [P] can be given by assuming Eq. 2,

$$t_a = \frac{l_s}{\mu_{app,s}E} + \frac{l_b}{\mu_{app,b}E} = \frac{l_s(1 + K[P])}{\mu_a E} + \frac{l_b}{\mu_a E} \quad (6)$$

where $l_s$ is the length of the separation zone, $l_b$ the rest of the effective length filled with the running buffer and $E$ the electric field strength. To obtain reproducible results, it is essential to build separation zones of identical length in the capillary. The length of the separation zone can be determined experimentally from the time the separation solution is delivered into the capillary at a constant pressure and the time required for the separation solution to reach the detector cell at the same pressure. In this experiments, the separation solution was introduced at 1 p.s.i. The effect of the protein concentration on the length of the separation zone built during a constant time at a constant pressure was examined by measuring the filling time required for the separation solution to reach the detector cell (31.5 cm) when it was introduced into the capillary at 1 p.s.i. The results are given in Table 1, from which data the times to fill a constant length of the capillary (27 cm) with BSA solutions of different concentrations can be easily calculated. When the BSA concentration was higher than 1 m*M*, significant increases in viscosity were observed, as shown in Table 1.

The effect of the protein concentration on the migration time was examined for the separation of epinastine racemate with BSA as a chiral selector. The complete resolution was achieved with the concentration higher than 750 μ*M* BSA. The resolution increased with an increase

Table 1
Effect of BSA concentration on the time required to fill the capillary with the BSA solution by pressurization at a constant pressure

| Concentration of BSA/$\mu M$ | Detection time[a] of BSA/s |
|---|---|
| 100 | 220 |
| 250 | 225 |
| 500 | 225 |
| 750 | 225 |
| 1000 | 230 |
| 1500 | 240 |
| 2000 | 268 |

Conditions: capillary, 36 cm (31.5 cm to the detector) × 50 $\mu$m I.D.; BSA solution, BSA in 50 m$M$ phosphate buffer (pH 6.0); pressure, 1 p.s.i.
[a] The time required to observe a stepwise change of the baseline.

in the protein concentration as shown in Fig. 3. As expected from Eq. 6, the migration times of epinastine enantiomers increased almost linearly with increasing BSA concentration. Above 1 m$M$ BSA the plots slightly deviated from linearity because of the significant increase in viscosity, as given in Table 1. The linear plots below 1 m$M$ BSA given in Fig. 3 permitted the calculation of the binding constants of epinastine enantiomers with BSA, giving 830 $M^{-1}$ for (+)-epinastine and 910 $M^{-1}$ for the (−)-enantiomer. It should be mentioned that the binding constants obtained here are rough estimates, because [P] in Eq. 2 is the concentration of the non-binding protein but the total protein concentration is used instead here. However, it is not the purpose of this paper to discuss the binding constant and therefore, the detailed discussion will be given elsewhere.

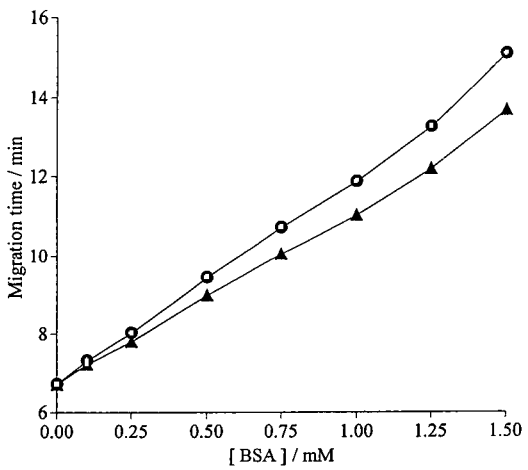


Fig. 3. Dependence of the migration times of (+)- and (−)-epinastine on the BSA concentration. Conditions as in Fig. 2 except for the BSA concentration.

### 3.3. Assay validation

Reproducibilities of migration times and peak areas were measured for the separation of enantiomers of epinastine with BSA as the pseudo-stationary phase by the partial separation zone technique. The results in Table 2 are comparable to those obtained with conventional capillary zone electrophoresis and suggest that if the automated CE instrument is employed, high reproducibility can be obtained even for the partial separation zone technique.

A calibration curve was prepared for each enantiomer of epinastine separated with 750 $\mu M$ BSA in the range 10–500 $\mu$g ml$^{-1}$ of epinastine racemate hydrochloride. The peak areas divided by the migration times were plotted against the concentration of each enantiomer. The calibration curve was linear below 100 $\mu$g ml$^{-1}$ for each enantiomer [$r = 0.9997$ for (+)- and 0.9996 for (−)-enantiomer], but above 100 to 200 $\mu$g the plotted line for (+)-epinastine, which migrated faster than the (−)-enantiomer, slightly deviated from linearity, probably due to the incomplete resolution of enantiomers at the high concentrations.

### 3.4. Separations of some enantiomers by the partial separation zone technique

The partial separation zone technique was applied to the separation of various basic drug racemates using BSA, $\alpha_1$-AGP, ovomucoid and conalbumin as chiral selectors, and the results are summarized in Table 3. In the case of ovomucoid, most analytes were not detected using 500 $\mu M$ ovomucoid in 50 m$M$ phosphate buffer (pH 5.0) without any additives to the

Table 2
Repeatability of migration time and peak area by the partial separation zone technique ($n = 5$)

| | Migration time | | Peak area | |
|---|---|---|---|---|
| | Average (min) | R.S.D. (%)[a] | Average (arbitrary units) | R.S.D. (%)[a] |
| (+)-Epinastine | 10.20 | 0.19 | 123 784 | 2.95 |
| (−)-Epinastine | 10.86 | 0.21 | 121 707 | 3.12 |

Conditions as in Fig. 2.
[a] Relative standard deviation.

separation solution. The additives were often required not only for ovomucoid [13] but also for the other proteins [12,14]. In most cases, organic solvents or amphoteric surfactants were used as effective additives. In this study, an alcohol or an amphoteric surfactant was added both in the separation solution and the running buffer solution at an identical concentration. A combination of a high concentration (500 $\mu M$) of ovomucoid and a relatively higher concentration of alcohol that reduce the interaction between the analyte and protein seemed unreasonable, because the choice of a low concentration of ovomucoid without additive could be natural judging from the separation mechanism. The additive was essential even for the use of a low concentration of ovomucoid [13,18] and the use of the high concentration of ovomucoid with the

Table 3
Separation of basic racemates with proteins by affinity electrokinetic chromatography employing the partial separation zone technique

| Protein | Concentration ($\mu M$) | pH | Additive | Compound | Migration times/min | $R_s$ |
|---|---|---|---|---|---|---|
| BSA | 500 | 6.0 | None | Homochlorcyclizine | 12.29, 13.42 | 1.8 |
| | | | | Oxyphencyclimine | 8.93, 9.22 | 1.1 |
| | | | | Propranolol | 11.44, 12.04 | 1.7 |
| | | | | Trimebutine | 13.04, 13.48 | 0.8 |
| | 750 | 6.0 | None | Epinastine | 10.23, 10.91 | 3.1 |
| OVM | 500 | 5.0 | CHAPS (10 m$M$) | Bunitrolol | 8.98, 9.15 | 0.9 |
| | | | Ethanol (8%) | Pindolol | 10.93, 11.36 | 1.5 |
| | | | 2-Propanol (6%) | Arotinolol | 12.97, 13.42 | 1.3 |
| | | | 2-Propanol (8%) | Oxyphencyclimine | 12.64, 12.97 | 1.1 |
| | | | 2-Propanol (10%) | Tolperisone | 11.51, 12.00 | 2.0 |
| | | | 2-Propanol (10%) | Verapamil | 17.65, 18.02 | 0.9 |
| | | | 1-Propanol (8%) | Chlorpheniramine | 11.49, 11.83 | 1.5 |
| | | | 1-Propanol (8%) | Primaquine | 11.83, 12.24 | 1.5 |
| | | | 1-Propanol (8%) | Trimebutine | 13.92, 14.35 | 1.6 |
| $\alpha_1$-AGP | 500 | 4.0 | None | Clorprenaline | 9.58, 9.92 | 1.3 |
| Conalbumin | 500 | 7.0 | None | Trimetoquinol | 12.40, 13.17 | 1.5 |

BSA = Bovine serum albumin; OVM = ovomucoid; $\alpha_1$-AGP = $\alpha_1$-acid glycoprotein; CHAPS = 3-[(3-cholamidopropyl)-dimethylammonio]-1-propanesulfonate.

additive gave better resolution than the use of the low concentration, although the reason is not clear. The other proteins, BSA, $\alpha_1$-AGP and conalbumin, did not require the additive. With these proteins relatively high concentrations were necessary to achieve successful enantiomer separations, and the partial separation zone technique was extremely effective especially for these conditions.

## 4. Conclusions

For the separation of enantiomers by affinity EKC, we described the partial separation zone technique previously developed by Valtcheva et al. [15] in which UV absorption by a protein used as a chiral selector did not disturb the detection. The resolution of enantiomers was enhanced by increasing the protein concentration without losing the detection sensitivity. The technique could be performed automatically using commercial CE instruments. Separations of some basic drug racemates were successful by this method employing relatively high concentrations of BSA, $\alpha_1$-AGP, ovomucoid and conalbumin as pseudo-stationary phases. An additional advantage of the technique is a low consumption of the protein solution in comparison with the conventional method. The method validations in terms of the linearity of the calibration curve, reproducibility of peak areas, and that of the migration times make it clear that the technique can be used for quantitative analysis.

In conclusion, the partial separation zone technique is very powerful for the separation of enantiomers by affinity EKC using high concentrations of proteins. Furthermore, it is remarkably useful for a routine analysis with commercial instruments because of the automated procedures and good reproducibilities. We are convinced that many other enantiomeric separations can be achieved by the technique. Furthermore, the technique can be easily extended to the use of other UV-absorbing pseudo-stationary phases or additives in capillary zone electrophoresis. However, when the pseudo-stationary phase migrates in the same direction as the analytes, this method cannot be used because of migration of the pseudo-stationary phase through the detection cell.

## Acknowledgement

The authors are grateful to Mr. Y. Ishihama and Eisai Co. for kindly providing ovomucoid, conalbumin and some racemic compounds, Dr. H. Nishi and Tanabe Seiyaku Co., and also Dr. H. Wada and Shinwa Chemical Co. for the gift of some valuable samples.

## References

[1] K.M. Kirkland, K.L. Neilson and D.A. McCombs, *J. Chromatogr.*, 545 (1991) 43–58.
[2] S.R. Narayanan, *J. Pharm. Biomed. Anal.*, 10 (1992) 251–262.
[3] L. Siret, N.B. Leyder, A. Tambuté and M. Caude, *Analusis*, 20 (1992) 427–435.
[4] Y. Oda, N. Mano, N. Asakawa, Y. Yoshida, T. Sato and T. Nakagawa, *Anal. Sci.*, 9 (1993) 221–228.
[5] S. Terabe, K. Otsuka and H. Nishi, *J. Chromatogr.*, 666 (1994) 295–319.
[6] M.M. Rogan, K.D. Altria and D.M. Goodall, *Chirality*, 6 (1994) 25–40.
[7] T.J. Ward, *Anal. Chem.*, 66 (1994) 632A–640A.
[8] M. Novotny, H. Soini and M. Stefansson, *Anal. Chem.*, 66 (1994) 646A–655A.
[9] G.E. Barker, P. Russo and R.A. Hartwick, *Anal. Chem.*, 64 (1992) 3024–3028.
[10] P. Sun, N. Wu, G. Barker and R.A. Hartwick, *J. Chromatogr.*, 648 (1993) 475–480.
[11] S. Busch, J.C. Kraak and H. Poppe, *J. Chromatogr.*, 635 (1993) 119–126.
[12] R. Vespalec, V. Šustáček and P. Boček, *J. Chromatogr.*, 638 (1993) 255–261.
[13] Y. Ishihama, Y. Oda, N. Asakawa, Y. Yoshida and T. Sato, *J. Chromatogr. A*, 666 (1994) 193–201.
[14] Y. Tanaka, N. Matsubara and S. Terabe, *Electrophoresis*, 15 (1994) 848–853.
[15] L. Valtcheva, J. Mohammad, G. Petterson and S. Hjertén, *J. Chromatogr.*, 638 (1993) 263–267.
[16] M. Nakatani, A. Shibukawa and T. Nakagawa, *Biol. Pharm. Bull.*, 16 (1993) 1185–1188.
[17] S.A.C. Wren and R.C. Rowe, *J. Chromatogr.*, 603 (1992) 235–241.
[18] S. Terabe, H. Ozaki and Y. Tanaka, *J. Chin. Chem. Soc.*, 41 (1994) 251–257.

ELSEVIER

Journal of Chromatography A, 694 (1995) 285–296

JOURNAL OF CHROMATOGRAPHY A

# Protein chiral selectors in free-solution capillary electrophoresis and packed-capillary electrochromatography

David K. Lloyd*, Song Li, Patricia Ryan

*Department of Oncology, Pharmacokinetics Division, McGill University, McIntyre Medical Building, Room 717, 3655 Drummond, Montreal, Quebec H3G 1Y6, Canada*

**Abstract**

The use of proteins as chiral selectors in CE is reviewed. The performance of packed-capillary electrochromatography with protein phases is compared with free-solution systems. The use of free-solution CE with protein additives for the determination of protein–ligand binding and ligand–ligand interactions is discussed. Some new results are presented using capillaries packed with immobilized human serum albumin. The measurement by free-solution CE of binding of three cationic phenothiazine derivatives to human serum albumin is also shown, and the potential and pitfalls of this method are discussed. Finally some data on the use of dextran to modify protein mobility are shown, and effects of the dextran co-additive on the binding of some ligands to human serum albumin are shown.

## 1. Introduction

Proteins may display considerable stereoselectivity in their binding of xenobiotics [1]. This stereoselectivity may usefully be exploited in HPLC to perform chiral separations by immobilizing the protein on a suitable support [2,3]. An attractive feature of protein-based chiral stationary phases (CSPs) is that they often display stereoselectivity for a wider range of solutes than do other CSPs. Furthermore, in many cases the native properties of the free biopolymer are retained, and so HPLC with immobilized proteins can be used to probe pharmacologically important interactions [4].

Over the last few years it has been shown that many of the chiral selectors which have been successfully used in HPLC can also be applied in CE [5,6], although the majority of published work has focused on the use of cyclodextrins as chiral selectors. As with HPLC, CE with protein chiral selectors may be used as an analytical technique for chiral separations, or as a method for determining physico-chemical properties such as binding constants.

In this article the use of proteins as chiral selectors in CE will be reviewed. Some new results will also be presented on the use of immobilized human serum albumin (HSA) in packed-capillary electrochromatography (CEC), and the behaviour of this column is compared with our previous work using capillaries packed with $\alpha_1$-acid glycoprotein (AGP). The use of HSA as a buffer additive will also be discussed. Addition of viscosifiers such as dextran to alter the mobility of the protein and thus extend its range of application will be considered. It is shown that some caution must be used with this

* Corresponding author.

0021-9673/95/$09.50 
*SSDI* 0021-9673(94)00695-4

approach, since the viscosifier may affect the binding properties of the protein.

## 2. Capillary electrochromatography

Proteins are not ideal for use as buffer additives in CE because their presence at the detection window elicits a strong detector response. Thus it is necessary for analytical purposes to explore ways of using proteins other than simply adding them to the buffer solution. One option is to use CEC [7] with protein stationary phases. An electrically driven flow of liquid through the chromatographic column can give higher separation efficiencies than a similar flow produced by pressure drive [7], and impressive reversed-phase separations with small-diameter packings and high efficiencies have been reported [8]. We have performed initial studies using both AGP [9] and HSA (work described herein) in CEC with commercially available protein CSPs, as well as a comparison between β-cyclodextrin (β-CD) as an additive and as an immobilized chiral selector in CE [10]. The capillary packing process is described in detail in Ref. [9].

In CEC, electroosmosis replaces the pressure-driven flow of HPLC. Thus, a strong electroosmotic flow is vital to give reasonably short separation times. Because of this, our initial studies with protein-based stationary phases have focused on the electroosmotic flow characteristics of these capillaries. Relatively large packing particles have been used (5 μm for AGP and 7 μm for HSA) because they are readily available and are quite suitable for the investigation of electroosmotic flow properties. However, the ultimate chromatographic performance of CEC systems will only be realized with smaller packings.

Electroosmotic flow is weaker in packed capillaries than in open tubes, and a number of reasons for this including non-alignment of the flow channels with the electric field and the packing porosity are discussed by Knox and Grant [7]. A further effect is the alteration of the ζ potential at the packing particle surface, due to the presence of the immobilized chiral selector (although the coverage of the surface silanol groups by the bonded phase is never complete). The effect of the bonded phase on the electroosmotic flow depends on its charge. In packed capillaries with the neutral bonded phase β-CD, the electroosmotic flow was between 25 and 33% of the measured electroosmosis in an open tubular fused-silica capillary over the pH range 4–7.5 using a sodium phosphate background electrolyte [10]. Using AGP-derivatized silica packings, the electroosmotic flow velocity was 37–38% of the open-capillary flow over the pH range 4.5–7.5 when 1-propanol (2%, v/v) was used as an organic modifier in a 2 m*M* sodium phosphate background electrolyte. However, when the 1-propanol was replaced by 2-propanol in the same system the electroosmosis fell to just 12% of the open tubular value at pH 4.5, increasing to 39% of the open tubular value at pH 7.5 [9]. Clearly the effect of the bonded phase on electroosmotic flow in CEC can be quite significant, and in particular protein phases may display quite major changes in electroosmotic flow after relatively minor alterations in the mobile phase composition. Data on the electroosmotic flow in HSA-packed capillaries are presented in this article.

One limitation of CEC is that ionic analytes will migrate either with or against the electroosmotic flow depending on the sign of their charge, and those migrating against the electroosmosis may have such a low velocity that elution will be impossible within a reasonable time period. With some CSPs it is possible to control the direction of electroosmosis by using the appropriate buffer ions or additives, as we have shown with the β-CD phase [10]; manipulation of electroosmosis is more difficult with protein phases because of the ability of the biopolymers to strongly bind so many different ligands, and the significant effects that additives could have on the binding of analytes. Many cationic and neutral compounds separated by HPLC with the AGP CSP were also separated by CEC, although we had limited success with anions for the reasons mentioned above. The behaviour of the phase in terms of the resolutions achieved and the effect of operating

parameters such as organic modifier type and concentration, mobile phase pH and ionic strength indicate that the electric field in CEC has minimal effect on the immobilized biopolymer. Use of smaller packing materials, and perhaps pressurized systems to avoid bubble formation [8], should allow the full potential of CEC for chiral separations to be realized.

## 3. Chiral separations using HSA in solution or immobilized in gels

Proteins have been used in CE as buffer additives in solution to separate stereoisomers [11–17], including: bovine serum albumin (BSA) for the separation of leucovorin stereoisomers [11], for tryptophan, benzoin and warfarin [13] and for some amino acids [17]; HSA for benzoin and various phenothiazine derivatives [12], and for kynurinine, tryptophan, 3-indolelactic acid, 2,3-dibenzoyl tartrate and N-2,4-dinitrophenyl glutamate [14]; a cellulase (cellobiohydrolase I) for some β-blockers [15]; AGP for promethazine [13]; a fungal cellulase for pindolol [15]; avidin for leucovorin, warfarin, some profens and other compounds [16]; ovomucoid for chlorpheniramine and epinastine [16].

To achieve chiral separations, the mobilities of the free and protein-bound ligand must be significantly different (this is discussed at length in the following section on ligand–protein binding). Thus the separation at neutral pH of an anionic ligand such as ibuprofen with a protein such as HSA can be problematic. An approach which offers a solution to this problem has been pursued by Sun et al. [18] using BSA with dextran as a co-additive. By doing this the protein mobility is considerably reduced, while the mobility of small molecules is affected to a much smaller degree. This is advantageous in separations where the protein and analyte would otherwise have too-similar mobilities. In this way a separation of ibuprofen enantiomers was achieved, as well as chiral resolution of dansyl-leucine, dansyl-norvaline and mandelic acid. A refinement of this method was to covalently link BSA to a high-molecular-mass dextran [19], and then pump this BSA–dextran network into the capillary with a syringe. Electroosmotic flow was minimized in the capillaries used by coating them with linear polyacrylamide. This resulted in a system where the protein was practically immobile in the gel which was stable within the capillary because of the elimination of electroosmosis. Thus only analysis of charged species is possible.

As previously mentioned, the potential use of protein additives has been limited as an analytical technique because of the large detector response due to the protein. A solution to this problem has been suggested by Vlatcheva et al. [15]. They filled only part of the capillary with protein, and arranged the experiment so that the protein migrated away from the detector window, while the analyte migrated through the protein, and then went past the detection point. The pH of the background electrolyte was chosen such that the migration of the protein and the analyte were in opposite directions. This was facilitated by the use of a coated capillary to suppress electroosmosis. In principle it might be possible to have both analyte and protein move in the same direction with significantly different mobilities, although this would most likely result in lengthy analysis times. The electrochromatographic approach described above is one alternative possibility for the analytical use of proteins as chiral selectors in CE. Another option with proteins, termed capillary affinity gel electrophoresis (cAGE) was developed by Birnbaum and Nilsson [20]. They used BSA cross-linked with glutaraldehyde in situ in the capillary. The reaction mixture was pumped into the capillary until just before the detection window and then allowed to set, thus detection was not hampered by the presence of the protein. Separation efficiencies of up to 280 000 plates $m^{-1}$ were observed in the analysis of the enantiomers of tryptophan. The use of immobilized proteins in gels allows improved detection, unlike replaceable gels [19], but the potentially limited life of the immobilized gel system may be of concern.

Although the use of CEC with protein phases, proteins immobilized in gels or proteins made to migrate away from the detection window are all

interesting possibilities for the development of analytical separation methods, one must consider whether or not protein chiral selectors are the optimum choice for most chiral separations by CE. In HPLC, protein CSPs are attractive because of their broad range of application and, as Wainer [21] noted, AGP has perhaps the broadest utility of any of the current range of CSPs. In CE the situation is somewhat different. Because of the high separation efficiency typical of CE, baseline resolution can be achieved with certain chiral selectors for compounds which our HPLC experience and intuition would say are not amenable for analysis by that type of chiral selector. An example is the enantiomeric resolution of (6*R*)- and (6*S*)-5-methyl-tetrahydrofolate by CE using $\alpha$, $\beta$- or $\gamma$-CDs [22]. It is difficult to imagine that the mechanism of inclusion complexation which is almost mandatory for HPLC enantioseparations with CD CSPs can be operating here since the analyte is too large to include into $\alpha$-CD. Derivatization of cyclodextrins further increases their applicability [5,6], and so it is becoming clear that protein chiral selectors will have a more limited role in CE analysis than they do in HPLC. However, CE with protein additives may become an important tool for the determination of ligand–protein binding, and ligand–ligand interactions, as is described below.

## 4. Ligand–protein binding and ligand–ligand interactions studied by CE

In any electrokinetic capillary chromatography method the mobility of a solute, $\mu$, is related to its own intrinsic mobility in the background electrolyte, $\mu_S$, and to the strength with which it binds to a buffer additive (for example, a chiral selector) and the mobility of the analyte–additive complex, $\mu_{CS}$, thus [22,23]

$$\mu = ([S]/[S] + [CS])\mu_S + ([CS]/[S] + [CS])\mu_{CS} \quad (1)$$

Where [S] and [CS] the concentrations of the free and bound solute, respectively. For a simple one-to-one liaison the binding constant, $K$, is

$$K = [CS]/[S][C] \quad (2)$$

where [C] is the free chiral selector concentration, and thus

$$\mu = (\mu_S + \mu_{CS}K[C])/(1 + K[C]) \quad (3)$$

There are several examples of the use of CE for the determination of the binding of chiral compounds to CDs [22–24]. Typically the chiral selector concentration is varied over a wide range, and a non-linear least-squares curve fitting procedure is used to model the data to Eq. 3. Some important points have been emphasized: correction of mobilities for viscosity changes in the solution on addition of chiral selector is vital, and the use of total rather than free concentration of chiral selector in Eq. 3 is only a reasonable approximation at very high selector to analyte concentration ratios. In protein-based separations binding constants are frequently quite high ($>10^4$), and so the optimum protein concentration for maximum resolution is typically $<100$ $\mu M$. Because of the high background, and the limited sensitivity of commonly used absorbance detectors, the solute concentration may have to be similar to the selector concentration. Using this technique, Lloyd et al. [12] investigated the binding of benzoin enantiomers to HSA; in this article, the use and limitations of this approach to determine the binding to HSA of three phenothiazine derivatives, promethazine, propiomazine and thioridazine, is discussed.

To achieve a chiral separation the enantiomers of the analytes must have different binding affinities for the protein, and the bound and free forms of the analyte must have significantly different mobilities (Eq. 1). If the protein is immobilized the second criteria is easy to meet. However, this may not be so simple if the desired separation is of an acidic compound with an acidic protein. As previously indicated, using a simple system with HSA as an additive in a pH 7 phosphate buffer and ibuprofen as the analyte, we found that separation of the enantiomers was

difficult to achieve despite the fact that there is considerable stereoselectivity in this interaction as is known from numerous studies, including HPLC measurements with immobilized HSA [25]. In this case the problem arises because both analyte and selector have similar mobilities. Of course, it should generally be possible to find a pH at which the protein and analyte mobilities are different, but whether this is worth doing depends on what information one wants to obtain from the separation. Moving away from pseudo-physiological conditions removes many of the advantages of using CE to measure binding interactions —although a separation at low pH might be possible, it would be difficult to claim that any measurements made had relevance in vivo.

If co-additives are used along with the protein in the separation buffer then any effect they have on the binding of the ligand to the protein will be directly reflected by an alteration in the mobility of the ligand. The co-additive may take the form of a simple organic modifier such as 2-propanol which generally causes a non-specific reduction in hydrophobic interactions between the ligand and protein. Alternatively, the co-additive may be a ligand which binds to a specific site on the protein, and in this way the CE experiment may be used as a probe of ligand–ligand interactions. For example, the use of co-additives to determine the binding site(s) for benzoin and phenothiazine derivatives has been investigated [12]. Co-additives used included octanoic acid, and enantiomers of oxazepam hemisuccinate and of warfarin.

The use of CE with proteins in solution is particularly attractive for the study of protein–ligand interactions for a number of reasons. Perhaps the foremost advantage is that, unlike chromatographic or conventional affinity electrophoretic methods, in many cases neither the protein nor ligand need be immobilized. Therefore the issue of whether or not the immobilization process has altered the binding never arises. Other useful characteristics are the very small amounts of protein and ligand which are necessary, and for chiral compounds, the fact that enantioselectivity in the binding is revealed as an enantioselective separation, so that pure single enantiomers are not needed. There are limitations to the method, because of the range of mobilities of the analyte/protein combination which may usefully be studied. Although immobilization of the protein or use a co-additive such as dextran which serves the function of entrapment offer useful approaches to achieve separations, some caution should be used if one wishes to apply such systems for binding studies. In such cases, a question which one must ask is how the binding of ligands to the protein might be affected. Results which indicate a change in the binding of some drugs to HSA when using a dextran co-additive will be reported below.

## 5. Experimental

CE separations were carried out using Applied Biosystems 270-A or 270A-HT (ABI, Foster City, CA, USA) integrated CE systems. Fused-silica capillaries of 375 $\mu$m O.D. $\times$ 50 $\mu$m I.D. were obtained from Polymicro Technologies (Phoenix, AZ, USA) and cut to length. Open-tubular separations were performed in 72-cm capillaries, while packed-capillaries were of 42 cm overall length. The polyamide coating on the capillary was removed 22 cm from one end to provide a detection window. The capillary oven temperature was set at 30°C. Injections were made by applying a vacuum (17 kPa) to the anodic end of the capillary (open-tubular), or electrokinetically (5 kV for 1 s) in packed systems. Detection was by on-capillary UV absorbance. Data were analysed using a Spectra-Physics (San Jose, CA, USA) Datajet integrator, and stored on a personal computer running Spectra-Physics Winner System software. Relative viscosity measurements were made by measuring the elution time for a marker compound to pass through the capillary using the 17 kPa vacuum on the ABI instrument (the accuracy of this method has previously been validated [22]).

Packed capillaries were prepared according to the method described in Ref. [9]. Phosphate buffer was prepared by mixing solutions (usually

4 m*M*) of analytical grade disodium hydrogenphosphate and sodium dihydrogenphosphate (BDH, Toronto, Canada) to give the desired pH. Deionized water for all solutions was obtained from a Milli-Q$^{50}$ system (Millipore, Montreal, Canada). Organic modifiers (Accusolve-grade acetonitrile, 1-propanol, 2-propanol; Anachemia, Montreal, Canada) were added to give the desired volume percentage. A separation potential of 10 kV was generally used for the HSA-packed capillaries. The electroosmotic flow point was measured from the baseline disturbance caused by the sample solvent.

For open-tubular separations, HSA (fatty acid free, fraction V) and dextran (average $M_r$ 267 000) were obtained from Sigma (St. Louis, MO, USA). Phosphate buffer (pH 7) was prepared by mixing solutions of 50 m*M* sodium dihydrogenphosphate and disodium hydrogenphosphate. HSA was added to this buffer to give the required concentration, typically in the range 10–75 $\mu M$. A separation potential of 25 kV resulted in a current of ca. 60 $\mu$A without dextran.

Test compounds were obtained from Sigma except for hexobarbital and pentobarbital (U.S.P.C., Rockville, MD, USA) and benzoin (Aldrich, Milwaukee, WI, USA). Solutions were made in water or water–methanol (depending on the solubility of the compound), at a concentration of ca. 1 mg ml$^{-1}$ unless otherwise stated.

## 6. Results and discussion

### 6.1. Capillary electrochromatography with a HSA stationary Phase

A HSA CSP which retains many of the ligand-binding properties of the native protein has been developed for HPLC [3,4]. Here, some preliminary CEC results with a capillary packed with this HSA CSP are presented. Packing material (HSA immobilized on 7 $\mu$m silica particles) was a gift from Shandon Scientific (Runcorn, UK). A number of chiral solutes could be fully or partially resolved by CEC, including benzoin and some benzodiazepines. Separations of benzoin and temazepam are shown in Fig. 1. In electrokinetic chromatography, the capacity factor, $k'$ can be calculated using the relationship [26]

$$k' = (\mu - \mu_0)/(\mu_p - \mu) \quad (4)$$

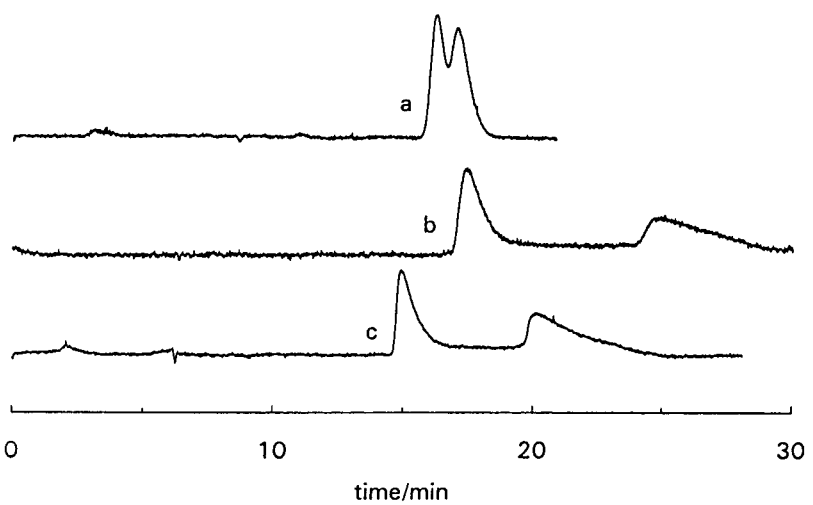


Fig. 1. Chiral separations of benzoin and temazepam by packed-capillary electrochromatography with a HSA CSP. a = Benzoin, modifier 6% 2-propanol; b = temazepam, modifier 5% 2-propanol; c = temazepam, modifier 7.5% 2-propanol. Buffer, 4 m*M* phosphate, pH 7; separation potential, 10 kV. Capillary, 42 cm overall length (20 cm to the detector) with 17 cm packed with the HSA CSP.

Table 1
Effect of type of organic modifier and of 2-propanol concentration on $k'$ and $\alpha$ for oxazepam and temazepam using a HSA-packed capillary (42 cm overall length, 20 cm to the detector, 15 cm packed with HSA)

| Modifier | Oxazepam: $k'_1$, $k'_2$ ($\alpha$) | Temazepam: $k'_1$, $k'_2$ ($\alpha$) |
|---|---|---|
| 2% 2-Propanol | 2.7, 4.2 (1.6) | 2.2, 5.3 (2.4) |
| 5% 2-Propanol | 2.1, 2.6 (1.3) | 1.7, 2.8 (1.7) |
| 7.5% 2-Propanol | 1.6, 2.0 (1.3) | 1.4, 2.2 (1.6) |
| 6% 1-Propanol[a] | 1.6, 1.7 (1.1) | 1.2, 1.5 (1.3) |
| 3% Acetonitrile | 2.9, 3.9 (1.4) | 2.7, 4.7 (1.8) |

Applied potential, 10 kV; buffer, 4 m*M* pH 7 phosphate, except where indicated otherwise.
[a] 5 m*M* phosphate.

where $\mu$ is the analyte mobility, $\mu_p$ is the mobility of the pseudostationary phase and $\mu_0$ is the mobility of the analyte under non-chromatographic conditions. Using this expression, $k'$ may also be calculated for neutral solutes in CEC ($\mu_p = 0$ and $\mu_0$ = electroosmotic flow mobility), but for charged analytes it is impossible to accurately measure $\mu_0$ [9].

With the HSA CSP, 1- and 2-propanol and acetonitrile were used as organic modifiers, with the best enantioselectivity being seen with 2-propanol or acetonitrile (Table 1). Chosson et al. [27] also noted that poorer enantioselectivity was achieved for benzodiazepines using 1-propanol (e.g., $\alpha = 1.3$ for oxazepam) when compared with acetonitrile ($\alpha = 4.5$ for oxazepam) in HPLC with the HSA CSP. This similarity of behaviour between the pressure-driven and electrically driven systems suggests that, as with AGP [9], the electric field (238 V cm$^{-1}$) has only a small effect if any on the immobilized protein. The applied field was limited such that the current in all CEC separations was $< 4$ $\mu$A, so there were no difficulties due to bubble formation in the capillary.

Electroosmotic flow in the HSA-packed capillary is quite weak, similar to that measured with AGP. A comparison of the electroosmotic flow in both capillaries is shown in Table 2. In both cases electroosmosis reduces with increasing organic modifier concentration, and a somewhat lower electroosmotic flow is observed with 2-propanol than with acetonitrile. The variation in electroosmosis as a function of organic modifier concentration is consistent with the alteration of the dielectric constant and viscosity of the background electrolyte [28], and need not be ascribed to any specific interaction of the modifier with the immobilized protein.

Separation efficiencies are, by CE standards, low, with $N \approx 15\,000$ plates m$^{-1}$ for benzoin and $N \approx 7000$ plates m$^{-1}$ for temazepam (Fig. 1), very similar to the efficiency of HPLC columns made with this packing (e.g. see separation of temazepam in Ref. [27], $N \approx 5500$ plates m$^{-1}$ for first eluted enantiomer). Overloading was found not to be a major factor in the performance of the AGP phase under the conditions which we used [9], and so it is assumed that this is also the case with the HSA capillaries. Electrically driven capillaries with AGP immobilized on 5-$\mu$m par-

Table 2
Electroosmotic flow in AGP- and HSA-packed capillaries

| | EOF mobility in AGP capillary ($10^{-4}$ cm$^2$ V$^{-1}$ s$^{-1}$) | | EOF mobility in HSA capillary ($10^{-4}$ cm$^2$ V$^{-1}$ s$^{-1}$) | |
|---|---|---|---|---|
| | Modifier: 2-propanol | Modifier: acetonitrile | Modifier: 2-propanol | Modifier: acetonitrile |
| 2% | 3.18 | 3.42 | 2.54 | 2.9 (3%) |
| 7% | 2.51 | 3.06 | 2.3 (7.5%) | |

All mobilities in $10^{-4}$ cm$^2$ V$^{-1}$ s$^{-1}$. Buffer, 4 m*M* phosphate, pH 6.8 (AGP), pH 7 (HSA). HSA-Packed capillary, 42 cm long, 20 cm to detector, 15 cm packed; applied potential, 10 kV. AGP-Packed capillary, 42 cm long, 20 cm to detector, 17 cm packed with AGP); applied potential, 18 kV (for other details of AGP-packed capillaries, see Ref. [9]). EOF = Electroosmotic flow.

ticles were also found to have efficiencies comparable with the pressure-driven columns [9], and for both HSA and AGP the separation efficiencies are much lower than for CEC with an β-CD phase [10].

### 6.2. Determination of the binding of the enantiomers of promethazine to HSA, using the protein as a run buffer additive

We have previously shown that CE with a HSA buffer additive could be used to measure the binding of the enantiomers of an uncharged analyte (benzoin), as well as being a useful method to screen for drug–drug interactions [12]. We have now also attempted to use the same method for determination of the binding of the cationic ligands promethazine, propiomazine and thioridazine to HSA (structures of the analytes used in this and the following section are shown in Fig. 2). Fig. 3 illustrates the variation of electrophoretic mobility of the enantiomers of promethazine, propiomazine and thioridazine as a function of the concentration of HSA added to the background electrolyte. Chiral separations are achieved for each compound, indicating stereoselectivity in their binding to HSA. If the protein concentration were further increased the measured mobility would eventually reach that of the protein–analyte complex when the analyte was 100% bound. However, the practical range of protein concentrations is limited because of the background signal and problems with capillary blockages at higher protein concentrations. The mobility difference between the enantiomers can be seen to be function of the protein concentration; for the more strongly bound thioridazine and propiomazine the mobility difference reaches a maximum with ca. 50–100 μM HSA.

For an uncharged analyte such as benzoin it is reasonable to expect that the mobility of the protein–ligand complex is very similar to that of the free protein, and so using the free protein mobility in Eq. 3 will result in a negligible error [12] (the effective mobility of the free HSA was measured to be $-1.82 \cdot 10^{-4}$ $cm^2$ $V^{-1}$ $s^{-1}$). However, binding of a charged ligand will lead

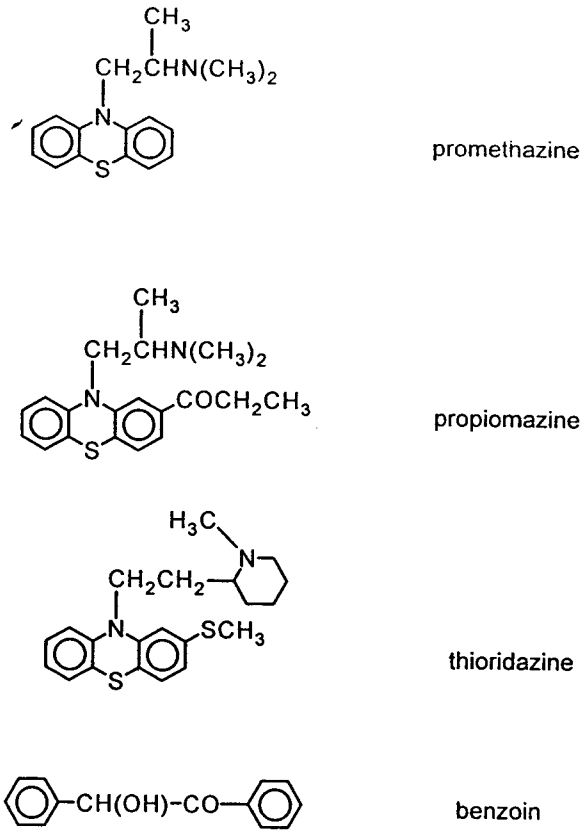


Fig. 2. Structures of the solutes used with HSA as a buffer additive.

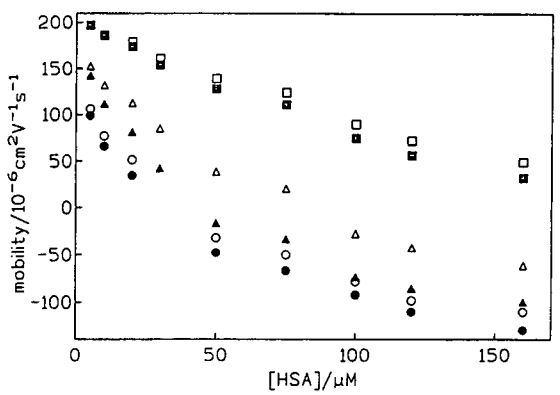


Fig. 3. Variation of analyte effective mobility as a function of the concentration of HSA added to the run buffer. □, ■ = Promethazine; △, ▲ = propiomazine; ○, ● = thioridazine. Open symbols, first detected enantiomer, filled symbols, second detected enantiomer.

to a significant alteration in the protein mobility, and so the effective mobility of the protein–ligand complex must be measured. It is not practical to increase the protein concentration until the analyte enantiomers are so completely bound that their overall mobility approaches that of the analyte–protein complex. However, the mobility can be found by performing a complementary experiment (similar to measurements performed by Avila et al. [29]), using the protein as a sample and adding ligand to the separation buffer. The mobility of a HSA sample (22 $\mu M$) was measured in a 50 m$M$, pH 7 phosphate buffer; the monovalent cationic ligand thioridazine was then added to the buffer at concentrations of 22 and 110 $\mu M$, and the protein mobility was measured again. The effective mobility of the HSA–thioridazine complex was found to be 82% of that of the free HSA, with no measurable difference found between the two buffers containing thioridazine. This particular ligand was chosen because it has the strongest binding for HSA, and so it could be used at a relatively low concentration in the buffer (thus there was relatively little interference with detection).

Using a non-linear regression program (Minsq; MicroMath Scientific Software, Salt Lake City, UT, USA), the data shown in Fig. 3 for promethazine were fitted to Eq. 3. Binding to protein adsorbed on the capillary surface also leads to retention of the analyte; measurement of the solute mobility in a new capillary, and in a capillary washed with a HSA-containing solution reveals a difference in mobility, due to chromatographic interactions with the protein adsorbed on the capillary surface [12]. In the case of promethazine this resulted in a reduction of $\mu$ by $4 \cdot 10^{-6}$ cm$^2$ V$^{-1}$ s$^{-1}$, and this value was added to the measured mobilities to give a value for $\mu$ to be used in the modelling. This is an approximation, since of course two competing equilibria are occurring with analyte binding both to free and surface-adsorbed HSA, but it is a minor effect except at very low dissolved HSA concentrations. The free HSA concentration, [C], was calculated from Eq. 1 (note that in Fig. 3 the total concentration of HSA additive is shown on the $x$-axis, while the free protein concentration is used in the curve-fitting). The concentration of racemic promethazine was 143 $\mu M$. The measured data (after correction for surface interactions) and the fitted data are shown in Table 3. The binding constants were estimated to be $K_1 = 6300 \pm 140$ $M^{-1}$ ($r^2 = 0.9994$) and $K_2 = 7800 \pm 170$ $M^{-1}$ ($r^2 = 0.9993$). The data for the more strongly bound propiomazine and thioridazine were also modelled, but without success. The difficulty in these cases was accounting for the interactions with protein bound at the capillary surface. As we have previously reported, the average $k'$ for surface interactions (Eq. 4) was only 0.01 for promethazine and propiomazine and 0.17 for thioridazine [12]. However, there was considerable error in some of these measurements, with variations between different capillaries. Uncertainty in the contribution from the surface binding leads to considerable errors in the calculation of the free HSA concentration at low protein additive concentrations and thus makes estimates of the binding constants very unreliable. This seems to be particularly a problem for solutes which are more highly bound. Clearly in these cases there is considerable advantage to be had in using coated capillaries where protein adsorption is minimized.

### 6.3. Effect of a dextran co-additive on binding to HSA

Use of proteins with a co-additive such as dextran has already been mentioned [18,19]. If one is interested in studying protein–ligand interactions rather than simply making separations then the effect of the co-additive must be determined. We have studied the effect of addition of dextran (average $M_r$ 267 000) in concentrations up to 10% on the separation of benzoin, promethazine, propiomazine and thioridazine, with 50 $\mu M$ HSA as chiral selector. In Table 4 the relative change in current, electroosmotic flow mobility, viscosity and effective mobility of HSA and the three phenothiazine derivatives is shown as a function of dextran concentration. These data reveal that it is somewhat difficult to

Table 3
Free protein concentration and measured and estimated effective mobilities (and the difference between these two values) for promethazine

| [C] ($\mu M$) | Measured $\mu$ ($10^{-4}$ cm$^2$ V$^{-1}$ s$^{-1}$) | Calculated $\mu$ ($10^{-4}$ cm$^2$ V$^{-1}$ s$^{-1}$) | Deviation ($10^{-4}$ cm$^2$ V$^{-1}$ s$^{-1}$) |
|---|---|---|---|
| *First eluted enantiomer* | | | |
| 3.09 | 2.03 | 2.06 | 0.03 |
| 6.05 | 1.93 | 2.00 | 0.07 |
| 14.2 | 1.84 | 1.83 | −0.01 |
| 20.6 | 1.66 | 1.72 | 0.06 |
| 36.2 | 1.44 | 1.46 | 0.02 |
| 56.9 | 1.22 | 1.18 | −0.04 |
| 76.9 | 0.97 | 0.95 | −0.02 |
| 92.9 | 0.77 | 0.80 | 0.03 |
| 128.0 | 0.54 | 0.52 | −0.02 |
| *Second eluted enantiomer* | | | |
| 3.09 | 2.03 | 2.04 | 0.01 |
| 5.78 | 1.92 | 1.97 | 0.05 |
| 13.2 | 1.79 | 1.79 | 0.00 |
| 19.2 | 1.59 | 1.66 | 0.07 |
| 34.1 | 1.33 | 1.37 | 0.04 |
| 54.5 | 1.10 | 1.05 | −0.05 |
| 73.8 | 0.81 | 0.80 | −0.01 |
| 89.8 | 0.61 | 0.63 | 0.02 |
| 125.0 | 0.37 | 0.34 | −0.03 |

adequately correct for the effects of the dextran; the proportional changes in HSA mobility, viscosity and current are all different, although the electroosmotic flow and analyte mobilities reduce by similar amounts. To compensate for viscosity effects on addition of the chiral selector measurement of the current [23] or the mobility of a non-bound marker compound [22] have been proposed. When protein additives are used alone the concentrations are so low that viscosity effects are generally negligible [12]. Therefore, in this case it seems most appropriate to measure the analyte mobility in dextran-containing buffers with and without protein, to determine the mobility change due to protein binding.

The effective mobilities of benzoin, promethazine, propiomazine and thioridazine were determined in buffers containing 0, 1, 5 and 10%

Table 4
Variation in electroosmotic flow mobility, analyte mobility, HSA mobility, electric current and solution viscosity as a function of % dextran, all values taken relative to 0% dextran

| | 1% Dextran | 5% Dextran | 10% Dextran |
|---|---|---|---|
| $\mu_{EOF}$ ($10^{-4}$ cm$^2$ V$^{-1}$ s$^{-1}$) | 0.91 | 0.75 | 0.51 |
| $\mu_{promethazine}$ ($10^{-4}$ cm$^2$ V$^{-1}$ s$^{-1}$) | 0.94 | 0.77 | 0.56 |
| $\mu_{propiomazine}$ ($10^{-4}$ cm$^2$ V$^{-1}$ s$^{-1}$) | 0.94 | 0.77 | 0.54 |
| $\mu_{thioridizine}$ ($10^{-4}$ cm$^2$ V$^{-1}$ s$^{-1}$) | 0.93 | 0.69 | 0.49 |
| $\mu_{HSA}$ ($10^{-4}$ cm$^2$ V$^{-1}$ s$^{-1}$) | 0.93 | 0.62 | 0.41 |
| Current ($\mu$A) | 1 | 0.86 | 0.70 |
| Viscosity (cP) | 1.7 | 5.0 | 12 |

Table 5
Variation of $k'$ as a function of dextran concentration for the first ($k'_1$) and second ($k'_2$) eluted enantiomers of benzoin, promethazine, propiomazine and thioridazine

| Dextran (%) | Benzoin | | Promethazine | | Propiomazine | | Thioridazine | |
|---|---|---|---|---|---|---|---|---|
| | $k'_1$ | $k'_2$ | $k'_1$ | $k'_2$ | $k'_1$ | $k'_2$ | $k'_1$ | $k'_2$ |
| 0 | 0.25 | 0.36 | 0.26 | 0.33 | 0.81 | – | 1.79 | 2.27 |
| 1 | 0.25 | 0.36 | 0.28 | 0.32 | 0.73 | – | 1.77 | 2.22 |
| 5 | 0.26 | 0.39 | 0.28 | 0.34 | 0.75 | – | 1.73 | 2.07 |
| 10 | 0.20 | 0.40 | 0.07 | 0.12 | 0.28 | 0.82 | 1.75 | 2.14 |

Only one value of $k'_2$ is shown for propiomazine since this peak eluted close to the electroosmotic flow point at the other dextran concentrations, making accurate determination of its migration time impossible.

dextran, with and without 50 $\mu M$ HSA. $k'$ as a function of dextran concentration is shown for these solutes in Table 5. $k'$ for the enantiomers of the solutes were then calculated using the Eq. 4, where $\mu_0$ is the mobility of the analyte without chiral selector and $\mu_p$ is the mobility of the solute–selector complex; $\mu_p$ was taken as being a constant fraction of the protein mobility as determined above for the three phenothiazine derivatives, or equal to the protein mobility for the uncharged benzoin. The $k'$ values are shown in Table 5. For promethazine and propiomazine there is a considerable decrease in $k'$ at 10% dextran. Benzoin and thioridazine are practically unaffected even with 10% dextran. Since all four compounds do not behave similarly, it seems that these effects are not due to a general decrease in non-specific binding, but rather that they are due to a specific alteration or blocking of one binding site on HSA. We have previously shown that the binding of promethazine and propiomazine share many common properties, and that they probably bind to the same region, which is distinct from the binding areas for thioridazine and benzoin [12]. This lends support to the suggestion that the dextran is in this case affecting specific binding, since two ligands which share the same site are similarly affected.

## 7. Conclusions

CEC can produce high-efficiency chiral separations [10], but with protein phases the efficiency seen so far is rather disappointing ([9], and work reported therein). Optimum performance will only be realized with smaller packings, but it is difficult to foresee CEC with protein phases rivalling the efficiency of other chiral selectors used in CE in solution. Nevertheless, the wide applicability of protein chiral selectors, and the difficulty in their use as additives in CE make their use in CEC an area worthy of further investigation.

A number of reports have dealt with the use of proteins as chiral buffer additives or in gels. In only a couple of these articles has the problem of detection been addressed [15,20], and for a variety of reasons the applicability of these solutions to the detection problem may be somewhat limited. Although analytical applications appear to be somewhat limited, the use of proteins in free-solution CE has a bright future as a method for the determination of protein–ligand binding, and as a method to screen for ligand–ligand interactions. Although not limited to chiral ligands, the utility seems greatest for these compounds since, if the experiment is devised correctly, enantioselectivity in the binding is revealed as a chiral separation. Thus individual enantiomers are not needed. One further attractive feature of this method is that the binding properties of the free protein are measured —when making binding measurements using immobilized proteins the question of whether the binding is affected by the immobilization needs to be answered. Certainly there are instances where the properties of solution or

bound proteins seem different [15]. However, as we have described in this article, co-additives in free solution may also have a significant effect on the protein's binding properties and thus must be used with some degree of caution. A further question to be answered is what would be the ideal medium in which to perform such measurements, after all a pH 7, 50 m*M* phosphate buffer bears only a limited resemblance to the protein's milieu in vivo. Avila et al. [29] have investigated the protein-binding of some non-chiral ligands by free solution CE with organic buffers, and it has been suggested that organic buffers may offer a more realistic environment for the protein than inorganic buffer ions such as the phosphate used here. Whether or not this is really the case requires further study.

## Acknowledgements

This work was funded in part by the Natural Sciences and Engineering Research Council of Canada. D.K.L. would also like to thank the Fonds de Recherche en Santé du Québec for a Chercheur–Boursier scholarship.

## References

[1] T.A.G. Noctor, in I.W. Wainer (Editor), *Drug Stereochemistry*, Marcel Dekker, New York, 2nd ed., 1993, Ch. 12, pp. 337—364.
[2] J. Hermansson, *J. Chromatogr.*, 269 (1983) 71.
[3] E. Domenici, C. Bertucci, P. Salvadori, G. Felix, I. Cahagne, S. Motellier and I.W. Wainer, *Chromatographia*, 29 (1990) 170.
[4] E. Dominici, C. Bertucci, P. Salvadori, S. Motellier and I.W. Wainer, *Chirality*, 2 (1990) 263.
[5] R. Kuhn and S. Hoffstetter-Kuhn, *Chromatographia*, 34 (1992) 505.
[6] M.M. Rogan, K.D. Altria and D.M. Goodall, *Chirality*, 6 (1994) 25.
[7] J.H. Knox and I.H. Grant, *Chromatographia*, 32 (1991) 317.
[8] N.W. Smith and M.B. Evans, *Chromatographia*, 38 (1994) 649.
[9] S. Li and D.K. Lloyd, *Anal. Chem.*, 65 (1993) 3684.
[10] S. Li and D.K. Lloyd, *J. Chromatogr. A*, 666 (1994) 321.
[11] G.E. Barker, P. Russo and R.A. Hartwick, *Anal. Chem.*, 64 (1992) 3024.
[12] D.K. Lloyd, S. Li and P. Ryan, *Chirality*, 6 (1994) 230.
[13] S. Busch, J.C. Kraak and H. Poppe, *J. Chromatogr.*, 635 (1993) 119.
[14] R. Vespalec, V. Šustáček and P. Boček, *J. Chromatogr.*, 638 (1993) 255.
[15] L. Vlatcheva, J. Mohammed, G. Pettersson and S. Hjertén, *J. Chromatogr.*, 638 (1993) 263.
[16] S. Terabe, Y. Tanaka and K. Hirota, presented at the *6th International Symposium on High Performance Capillary Electrophoresis, San Diego, CA, February 1994*, abstract 015.
[17] A. Werner, E. Spiesser, P. Kiechle, F. Erni and A. Roth, presented at the *4th International Symposium on Chiral Discrimination, Montreal, September 1993*, abstract 166.
[18] P. Sun, N. Wu, G. Barker and R.A. Hartwick, *J. Chromatogr.*, 648 (1993) 475.
[19] P. Sun, G.E. Barker, R.A. Hartwick, N. Grinberg and R. Kaliszan, *J. Chromatogr. A*, 652 (1993) 247.
[20] S. Birnbaum and S. Nilsson, *Anal. Chem.*, 64 (1992) 2872.
[21] I.W. Wainer, in I.W. Wainer (Editor), *Drug Stereochemistry*, Marcel Dekker, New York, 2nd ed., 1993, Ch. 6, pp. 139–182.
[22] A. Shibukawa, D.K. Lloyd and I.W. Wainer, *Chromatographia*, 35 (1993) 419.
[23] S.A.C. Wren and R.C. Rowe, *J. Chromatogr.*, 603 (1992) 235.
[24] S.G. Penn, D.M. Goodall and J.S. Loran, *J. Chromatogr.*, 636 (1993) 149.
[25] T.A.G. Noctor, G. Felix and I.W. Wainer, *Chromatographia*, 31 (1991) 55.
[26] M.G. Khaledi, S.C. Smith and J.K. Strasters, *Anal. Chem.* 63 (1991) 1820.
[27] E. Chosson, S. Uzan, F. Gimenez, I.W. Wainer and R. Farinotti, *Chirality*, 5 (1994) 71.
[28] C. Schwer and E. Kenndler, *Anal. Chem.*, 63 (1991) 1801.
[29] L.Z. Avila, Y.-H. Chu, E.C. Blossey and G.M. Whitesides, *J. Med. Chem.*, 36 (1993) 126.

ELSEVIER

Journal of Chromatography A, 694 (1995) 297–305

JOURNAL OF CHROMATOGRAPHY A

# Use of cyclodextrins in capillary electrophoresis for the chiral resolution of some 2-arylpropionic acid non-steroidal anti-inflammatory drugs

Salvatore Fanali*, Zeineb Aturki

*Istituto di Cromatografia del CNR, Area della Ricerca di Roma, P.O. Box 10, 00016 Monterotondo Scalo (Rome), Italy*

**Abstract**

The enantiomeric separation of racemic compounds of some 2-arylpropionic acid non-steroidal anti-inflammatory drugs (profens), namely fenoprofen, ibuprofen, flurbiprofen, suprofen, ketoprofen and indoprofen, was performed by capillary zone electrophoresis. The separation was obtained by supporting the background electrolyte with derivatized β-cyclodextrins. The type and concentration of cyclodextrin used and the background electrolyte composition (pH and amount of methanol) influenced the complexation and the chiral resolution. All the modified β-cyclodextrins used (heptakis-2,6-di-O-methyl-β-, heptakis-2,3,6-tri-O-methyl- and $6^{A}$-methylamino-β-cyclodextrin) showed good complexing effects with the profens tested. Tri-O-methyl-β-cyclodextrin proved to be the best stereoselective additive because it allowed the enantiomeric resolution of all the profens studied whereas the dimethylated and methylamino-β-cyclodextrin were able to separate only some of them.

## 1. Introduction

In the last decade, the resolution of racemic compounds has attracted great interest in analytical chemistry, especially in pharmaceutical analysis. Several drugs are administered as racemates, but very often one of the two enantiomers can be pharmacologically more active than its antipode, which might be even toxic. For example, (−)-epinephrine and (−)-terbutaline are ten and four times more potent than their optical antipodes, respectively [1]. The anti-inflammatory activity of flurbiprofen and ibuprofen is mainly ascribed to the (*S*)-(+)-isomer [2] whereas the (*S*)-(−)-thalidomide has teratogenic effects [3]. The aim in the pharmaceutical industry, therefore, is the production and marketing of drugs containing only the active enantiomers. Furthermore, rapid, sensitive and selective analytical methods are required to control the chiral purity of the products.

The separation of a wide variety of enantiomers has been performed predominantly by high performance-liquid chromatography (HPLC), thin-layer chromatography (TLC) and gas chromatography (GC) [4–7]. Recently, capillary electrophoresis (CE) has been used for chiral separations, applying different kinds of resolution mechanisms. The methods include micellar electrokinetic chromatography (MEKC) with chiral additives [8,9], ligand exchange with metal and chiral compound complexes [10,11], affinity electrophoresis with proteins [12,13] and inclu-

* Corresponding author.

0021-9673/95/$09.50 
*SSDI* 0021-9673(94)00945-7

sion–complexation with cyclodextrins or its derivatives and crown ether derivatives [14–18].

Commercially available cyclodextrins (CDs) have been widely employed in CE for the separation of enantiomers, including compounds of pharmaceutical interest. Despite its low solubility [19], β-CD has been used several times in derivatized (methylated, carboxymethylated, hydroxypropylated, soluble β-CD polymer, etc.) forms having higher solubility, different cavity dimensions and different substituent groups on the rim of the molecule as compared with the parent compound [20].

The 2-arylpropionic acid non-steroidal antiinflammatory drugs (2APAs), also known as profens, are used for the treatment of several inflammatory diseases and are often administered as racemic mixtures. The need for the stereoselective methods for the determination of 2-APAs has been demonstrated. Brune et al. [21] used HPLC for a study of pharmacodynamic effects of pure enantiomers of flurbiprofen and of the inversion of (*R*)- to (*S*)-enantiomers of flurbiprofen, ibuprofen and ketoprofen in different species (man, rat, dog, etc.) [21]. The resolution of 2-APA enantiomers can be achieved either after derivatization using a chiral reagent or with a chiral stationary phase using HPLC [22–26] or GC [27]. The enantiomeric separation of fenoprofen, ibuprofen and naproxen by capillary electrophoresis utilizing β-cyclodextrin or hydroxypropyl-β-cyclodextrin [28,29] or maltodextrins [30] added to the background electrolyte (BGE) has been reported.

In this work, we studied the effect of different β-cyclodextrin derivatives, added to the BGE, on the resolution of several 2-APAs with the aim of optimizing the electrophoretic separation and describing the parameters that influence the chiral resolution.

## 2. Experimental

Heptakis-2,6-di-O-methyl-β-cyclodextrin (di-OMe-β-CD) and heptakis-2,3,6-tri-O-methyl-β-cyclodextrin (tri-OMe-β-CD) were purchased from Cyclolab (Budapest, Hungary). Morpholinoethanesulfonic acid (MES), racemic fenoprofen (Fen), ibuprofen (Ibu), ketoprofen (Ket), flurbiprofen (Flu), indoprofen (Ind), suprofen (Sup) and (*S*)-(+)-ibuprofen were obtained from Sigma (St. Louis, MO, USA). $6^A$-Methylamino-β-CD (Me-NH-β-CD) was prepared as described previously [16]. (−)- and (+)-suprofen and (−)- and (+)-flurbiprofen were kindly supplied by Dr. Cecilia Bartolucci (Istituto di Strutturistica Chimica, Consiglio Nazionale delle Ricerche, Montelibretti, Rome, Italy). The optical purity of (−)- and (+)-suprofen was about 98% and that of flurbiprofen was about 99%, as measured by CE (peak-area ratio) using as the BGE 0.1 *M* MES at pH 5 containing 30 m*M* tri-OMe-β-CD.

Electrophoretic experiments were carried out using a Biofocus 3000 apparatus (Bio-Rad Labs., Hercules, CA, USA). The injection of the samples was done by pressure (10 p.s.i. s; 1 p.s.i. = 6894.76 Pa). The separations were performed in a fused-silica capillary of 35 cm (effective length 31.5 cm) × 0.050 mm I.D. (Polymicro Technologies, Phoenix, AZ, USA) coated with polyacrylamide according to the method described by Hjertén [31]. The polyimide coating was removed using hot $H_2SO_4$ in order to prepare a detector window of about 0.5 cm. The capillary assembled in a cartridge (Bio-Rad) was thermostated by circulating liquid at 25°C. Detection was performed with a UV–visible detector at 206 nm. The carousel temperature was kept at 25°C. The high-voltage power supply was operated in the constant-voltage mode, applying 20 kV, and the substances migrated towards the positive pole.

The BGE in the electrophoretic experiments was 0.1 *M* MES (pH adjusted with sodium hydroxide to the desired value between 4 and 7). The appropriate amount of cyclodextrin was dissolved in the BGE before the electrophoretic experiments to yield concentrations in the range 0–30 m*M* (tri-OMe-β-CD) and 0–20 m*M* (di-OMe-β-CD and Me-NH-β-CD). The concentrations of methanol used for the electrophoretic experiments in organic/aqueous BGE were 10, 20, 30 and 40% (v/v).

Stock standard solutions ($10^{-3}$ *M*) of standard racemic 2-APAs and their enantiomers were

prepared in methanol and diluted at the desired concentration with 5 m*M* MES at pH 5.

Two different 2-APA formulations, namely Moment and Orudis, containing ibuprofen (200 mg per tablet) and ketoprofen (50 mg per tablet), respectively, were weighted and triturated separately and methanol was added and stirred at room temperature for 10 min. The mixture was filtered and the volume adjusted in order to obtain two solutions containing about $10^{-3}$ *M* of ibuprofen and ketoprofen. The stock standard solutions were diluted tenfold with 5 m*M* MES at pH 5 and injected for electrophoresis analysis.

The resolution, $R$, was calculated using the following equation:

$$R = \frac{t_2 - t_1}{w_2 - w_1} \cdot 2 \quad (1)$$

where $t_2$, $t_1$ and $w_2$, $w_1$ are the migration times and the widths of the peaks, respectively, measured at the baseline in seconds for the two enantiomers (1 and 2) of the same compound.

## 3. Results and discussion

The enantiomers of several 2-APAs (Fig. 1) were studied in the pH range 4–7 by free solution capillary electrophoresis in the absence or presence of derivatized cyclodextrins. In this pH range the carboxylic group of all 2-APAs is dissociated and thus the analytes migrate as anions [28,29].

In the absence of cyclodextrins no resolution of enantiomers was obtained, which is in accordance with the fact that the enantiomers of the same compound possess similar physico-chemical properties and similar electrophoretic mobilities. The direct resolution method [32], introducing stereoselective interactions, was used for the enantiomeric separation of the six 2-APAs, using several modified β-CDs, such as heptakis-2,6-di-O-methyl-β-CD, heptakis-2,3,6-tri-O-methyl-β-CD and $6^A$-methylamino-β-CD.

β-CD and hydroxypropyl-β-CD in the presence of hydroxypropylcellulose were used by Rawjee and Vigh [29] for the separation of the enantiomers of naproxen and fenoprofen.

Modified β-CDs can give several advantages over the native compounds for enantiomeric separations by CE, e.g., higher solubility in the BGE, different depth of the cavity and different stereoselective interactions due to the presence of different substituents on the rim of the CD (di-OMe-β-CD and tri-OMe-β-CD). The utility of chargeable groups on the CD structure (MeNH-β-CD) when CE separation is per-

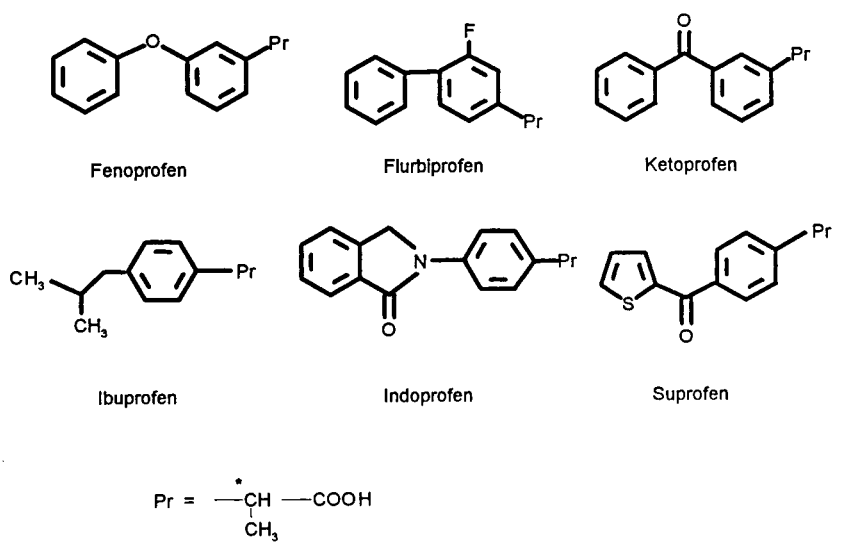


Fig. 1. Structures of the non-steroidal anti-inflammatory drugs studied.

formed should be noted. In fact, the CD can move in the opposite direction to the analytes (in coated capillaries) and can show capability as an ion-pairing agent and thus enhance the resolution of the enantiomers.

Fig. 2a and b show the effect of tri-O-methyl-β-cyclodextrin concentration on the migration times of 2-APAs at pH 5. Higher concentrations of the modified CD caused a decrease in the effective mobilities (increased migration times) of all the 2-APAs investigated except ketoprofen. This increase in migration time was due to the complex formation between CD and the analytes with a probable complexation order Ibu > Indo ≈ Flu > Fen > Sup > Ket.

The migration order of the separated enantiomers was verified for ibuprofen, flurbiprofen and suprofen by spiking the racemic samples with the pure optical isomers. In all instances the (*R*)-(−)-isomer moved with a lower velocity than the (*S*)-(+)-isomer, indicating that the (*R*)-(−)-isomers form more stable inclusion complexes than their optical antipodes with tri-OMe-β-CD.

In order to explain the different stabilities of the diastereomers formed during the electrophoretic runs, we may consider the data on the crystal structures of the flurbiprofen enantiomers complexed with tri-OMe-β-CD [33]. In this case, the fluorobiphenyl groups of the (*R*)-(−) and (*S*)-(+)-isomers are included similarly in the cavity of the modified CD stabilized by hydrophobic interactions, but the carboxyl group of the (*S*)-(+)-isomer forms a hydrogen bond with the oxygen at position 2 of the CD molecule, whereas the (*R*)-(−)-isomer is linked to the adjacent tri-OMe-β-CD by the –COOH–water–O(6) hydrogen-bond bridge. As a result of such complexation, two diastereomers with different mass-to-charge ratios are formed, which are then separable by CE.

The higher complexation of ibuprofen and indoprofen compared with the other compounds analysed is probably due to the *para* position of the substituent (containing the chiral centre) on the aromatic ring. Earlier data have already shown that *para*-substituted aromatic rings can fit properly into the CD cavity [34,35]. The relatively low complexation of the modified CD with ketoprofen is, therefore, easily understandable if we consider that the analyte can be oriented in an unfavourable way in the CD cavity owing to its substituent in the *meta* position.

Fig. 3a and b show the resolution (*R*) of the enantiomeric pairs of the 2-APAs as a function of the tri-O-methyl-β-CD concentration at pH 5. The resolution increased with increasing amount of CD. Baseline separation ($R \geq 1$) of the enantiomers was obtained at different tri-OMe-β-

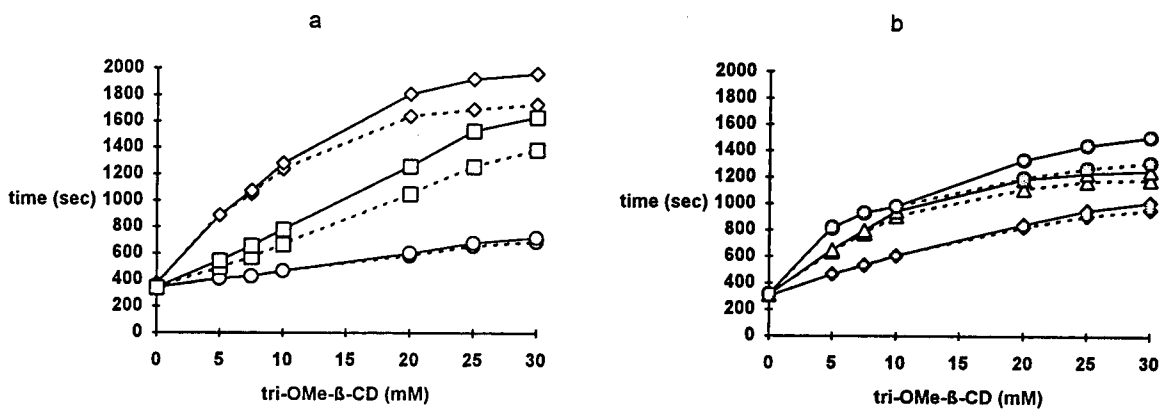


Fig. 2. Effect of the heptakis-tri-O-methyl-β-cyclodextrin (tri-OMe-β-CD) concentration on the migration time of the profens studied. Capillary 35 (31.5) cm × 0.050 mm I.D., coated; background electrolyte, 100 m*M* MES at pH 5 with the appropriate amount of CD; applied voltage, 20 kV, 6.6 μA; pressure injection, 10 psi s; sample concentration, $5 \times 10^{-5}$ *M* fenoprofen, flurbiprofen and ketoprofen, $10^{-4}$ *M* suprofen, ibuprofen and indoprofen. □ = Indoprofen; ○ = ketoprofen; ◇ = ibuprofen; △ = fenoprofen; ● = flurbiprofen; ◆ = suprofen.

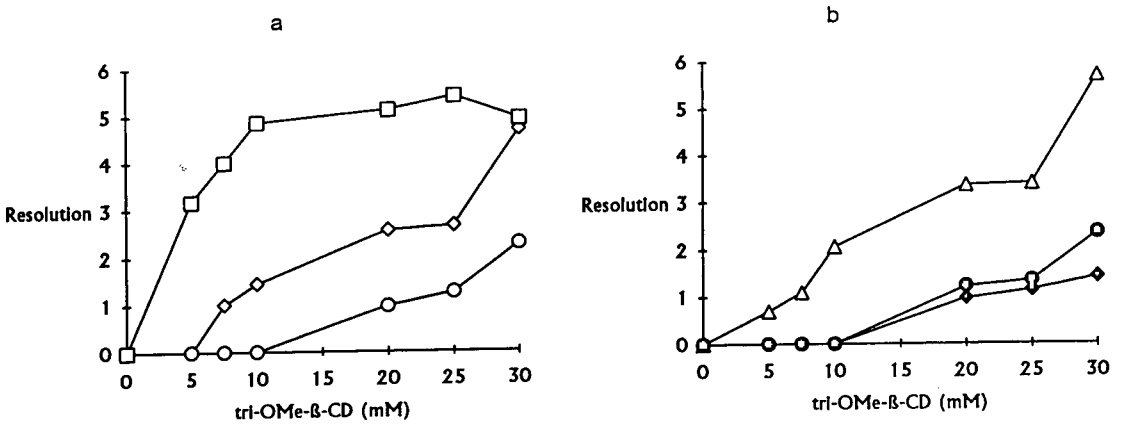


Fig. 3. Effect of the amount of 2,3,6-heptakis-tri-O-methyl-β-cyclodextrin on the enantiomeric resolution of 2-APAs. Experimental conditions and symbols as in Fig. 2.

CD concentrations: indoprofen (<5 m*M*), fenoprofen and ibuprofen (7.5 m*M*) and suprofen, flurbiprofen and ketoprofen (20 m*M*).

### 3.1. Effect of the pH of the background electrolyte on the resolution

Experiments performed using the BGE at different pH values in the range 4–7, in the absence of a chiral additive, showed a general decrease in the migration time for all the compounds analysed with increase in pH owing to the increased dissociation of the carboxylic group on the analytes. In order to verify the effect of pH on the resolution of the enantiomers of the 2-APAs studied, the same amount of tri-OMe-β-CD (25 m*M*) was added to the BGE at pH 4, 5, 6 and 7.

Fig. 4a and b show the effect of pH on the chiral resolution of fenoprofen, flurbiprofen, suprofen, ibuprofen, ketoprofen and indoprofen. At pH 4 it was possible to record the chiral separation of suprofen and indoprofen only because the other racemic compounds were moving too slowly owing to the strong complexation with the chiral selector. These findings were confirmed using a smaller amount of tri-OMe-β-CD (0.5–2.5 m*M*) that allowed the detection of the analyte compounds and the resolution of flurbiprofen, indoprofen and ketoprofen (at 2.5 m*M* of CD, $R = 1.77$, 1.74 and 0.5, respectively) (results not shown).

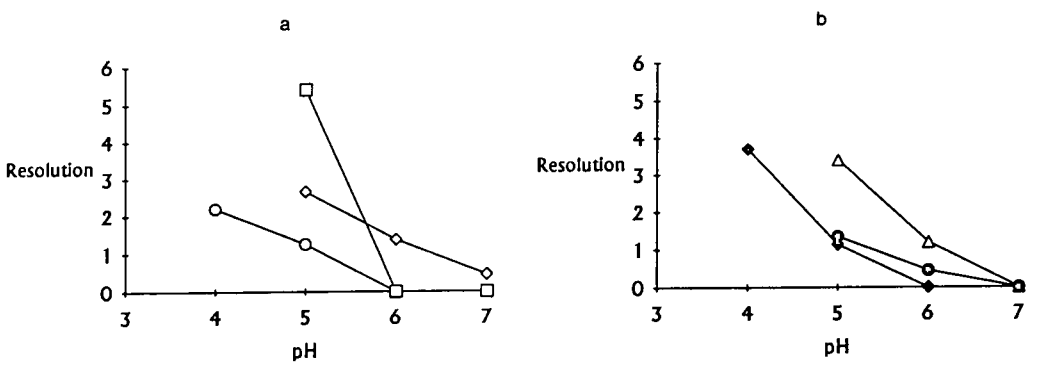


Fig. 4. Effect of the pH of the background electrolyte of the resolution of the compounds studied. The content of cyclodextrin in the background electrolyte was 25 m*M*; applied voltage, 20 kV, 2–35 μA. Other experimental conditions and symbols as in Fig. 2.

An increase in the pH of the BGE caused a decrease in the resolution for all the 2-APAs studied; at pH 5 complete enantiomeric resolution was obtained for all the compounds investigated whereas at pH 6 the resolution was lost ($R = 0$) for suprofen, indoprofen and ketoprofen but was satisfactory for the other compounds, and at pH 7 only ibuprofen was poorly resolved into its enantiomers. Based on our results, it appears that the optimum experimental conditions for the enantiomeric separation of the six 2-APAs can be obtained if the pH of the BGE is adjusted to 5. An increase in pH is not convenient for chiral resolution, probably owing to the higher dissociation of the carboxylic group and to the shorter migration time. The time spent by the analytes in the cavity of the CD is, of course, shortened with a decrease in resolution, and further, the dissociation of the carboxylic group will probably influence the stereoselective hydrogen bonds between this group and the substituents on the CD's rim.

As an example, Fig. 5 shows the electropherogram for the separation of ketoprofen, flurbiprofen, fenoprofen and ibuprofen into their enantiomers in a BGE at pH 5 containing 30 m*M* tri-OMe-β-CD.

### 3.2. Effect of the cyclodextrin type on the enantiomeric resolution

In order to verify the influence of the CD type on the resolution of the enantiomers of the 2-APAs, pH 5 was selected for the experiments and the BGE was supported with β-CD derivatives, namely $6^{A}$-methylamino-β-CD or heptakis-2,6-di-O-methyl-β-CD.

For methylated CDs, the substituent groups at positions 2, 3 and 6 are the same in all seven glucose molecules whereas in MeNH-β-CD all the substituents are of hydroxy type and only glucose (A) at position 6 is substituted with a methylamino group. The methylated CDs are not charged at the operating pH (5) whereas MeNH-β-CD is positively charged and thus moving towards the cathode (in the opposite direction to the analytes).

Both modified CDs were added to the BGE at concentrations of 2.5, 5, 10 and 20 m*M*. An increasing amount of the CDs cause a general

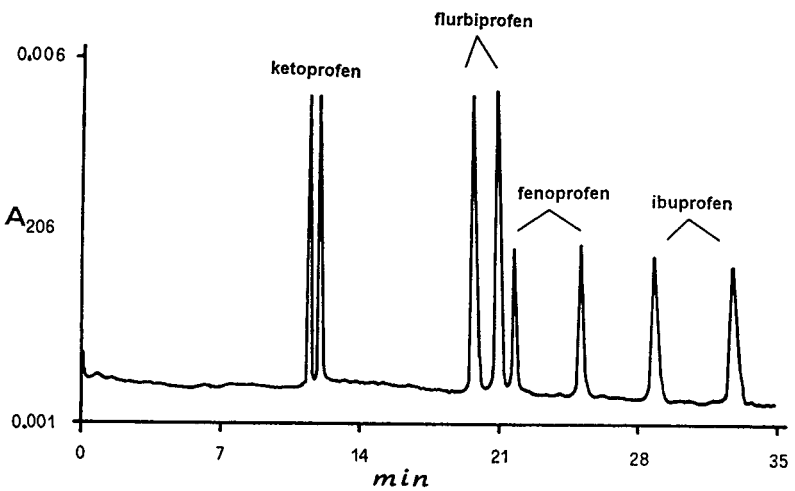


Fig. 5. Electropherogram of the enantiomeric separation of ibuprofen, fenoprofen, ketoprofen and flurbiprofen. Background electrolyte, 100 m*M* MES (pH 5) and 30 m*M* tri-O-methyl-β-CD; applied voltage, 20 kV, 6.6 μA; sampling: pressure, 10 psi s of a mixture of $10^{-4}$ *M* ibuprofen, $10^{-5}$ *M* fenoprofen, ketoprofen and flurbiprofen $5 \times 10^{-5}$ *M*. Other experimental conditions as in Fig. 2.

increase in the migration times for all the 2-APAs, but this was more evident for di-OMe- and MeNH-β-CD, showing a higher complexing effect of the former CD.

Table 1 shows the effect of the concentration of the two CDs on the resolution at pH 5.

Baseline resolution of the enantiomers was obtained for ibuprofen, suprofen and indoprofen whereas fenoprofen and flurbiprofen were poorly resolved and no resolution was achieved for ketoprofen when the BGE was supported with different amounts of MeNH-β-CD. An increase in the CD concentration increased the resolution for ibuprofen, suprofen and indoprofen and the best resolution was obtained for ibuprofen and suprofen at 20 m*M* ($R = 1.23$ and 1.12, respectively), whereas at 10 m*M* for indoprofen $R = 2.1$.

When di-OMe-β-CD was used as a chiral selector at pH 5, baseline enantiomeric resolution was obtained for ibuprofen and indoprofen; flurbiprofen, ketoprofen and suprofen were poorly resolved ($R < 0.5$) and fenoprofen was not resolved.

From these results, we can conclude that the positively charged CD, being useful for the enantiomeric separation of three of the six 2-APAs studied, showed a higher resolving power than di-OMe-β-CD but lower than tri-OMe-β-CD, except for suprofen. In fact, even relatively small amounts of positively charged CD (2.5–5 m*M* MeNH-β-CD) allowed the enantiomeric resolution of suprofen. The higher stereoselective effect of this modified CD in comparison with the methylated compound may be due to the charged group on the CD structure. In fact, the neutral CD acts as a quasi-stationary phase whereas the charged CD is moving in the opposite direction to the analytes, enhancing the complexation equilibria. Anyway, the inclusion–complexation power of the charged CD is lower than that of the methylated CDs. This behaviour is probably due to the structures of the CDs, in which the depth and the substituent groups on the rim play a very important role in inclusion–complexation. The depth of MeNH-β-CD cavity is probably similar to that of the β-CD (only one hydroxy group is substituted) and smaller than that of di-OMe-β-CD owing to the presence of methoxy groups on the rim, and thus the cavity of methylated CDs is more hydrophobic.

### 3.3. Effect of methanol on the resolution

The effect of the addition of methanol to the BGE on the enantiomeric resolution was studied for fenoprofen, ibuprofen, ketoprofen and flurbiprofen at pH 5. Experiments were performed at a low concentration of tri-OMe-β-CD (5 m*M*) where no or poor enantiomeric resolution was

Table 1
Effect of the amount of modified β-cyclodextrin on the enantiomeric resolution of profens

| Profen | Cyclodextrin (m*M*) | | | | | | | |
|---|---|---|---|---|---|---|---|---|
| | 2.5 | | 5 | | 10 | | 20 | |
| | $R_{\text{di-OMe}}$ | $R_{\text{MeNH}}$ | $R_{\text{di-OMe}}$ | $R_{\text{MeNH}}$ | $R_{\text{di-OMe}}$ | $R_{\text{MeNH}}$ | $R_{\text{di-OMe}}$ | $R_{\text{MeNH}}$ |
| Fenoprofen | 0 | <0.5 | 0 | <0.5 | 0 | <0.5 | 0 | <0.5 |
| Ibuprofen | 0.7 | <0.5 | 0.8 | 0.6 | 1.1 | 0.9 | 1.3 | 1.2 |
| Ketoprofen | 0 | 0 | 0 | 0 | 0 | 0 | <0.5 | 0 |
| Flurbiprofen | <0.5 | 0 | <0.5 | 0 | 0 | <0.5 | 0 | <0.5 |
| Suprofen | 0 | <0.5 | <0.5 | 0.8 | 0 | 0.9 | 0 | 1.1 |
| Indoprofen | 1.0 | 0.8 | 1.7 | 1.9 | 2.0 | 2.1 | 2.2 | 2.0 |

$R_{\text{di-OMe}}$ and $R_{\text{MeNH}}$ = resolution in presence of dimethylated and methylamino-β-cyclodextrin, respectively.

obtained and the methanol content in the BGE was chosen between 10 and 40% (v/v).

As expected, an increase in the methanol concentration in the BGE (containing the chiral selector) caused an increase in the migration times for the four 2-APAs. When 5 m*M* tri-OMe-β-CD was used in the absence of methanol we obtained enantiomeric resolution for fenoprofen and flurbiprofen ($R = 0.7$ and $<0.5$, respectively), whereas ibuprofen and ketoprofen showed no resolution. The addition of methanol did not influence the chiral resolution of ketoprofen and ibuprofen but slightly improved that for fenoprofen ($R = 0.82$ at 40% of methanol). In the absence of methanol, the flurbiprofen enantiomers were poorly separated, but baseline resolution was obtained by increasing the content of the organic additive in the BGE ($R = 1.4$ at 20% of methanol, increasing to 2.5 at 40%).

Fig. 6 shows the enantiomeric separation of racemic flurbiprofen with 5 m*M* tri-OMe-β-CD in the absence and presence of 10–40% (v/v) methanol.

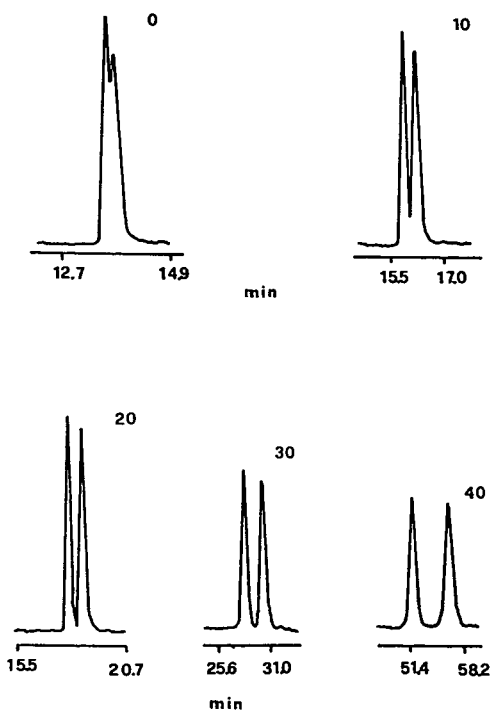


Fig. 6. Electropherograms of the enantiomeric separation of flurbiprofen in the absence and presence of an organic additive to the background electrolyte containing CD. Background electrolyte, 100 m*M* MES (pH 5) and 5 m*M* of tri-OMe-β-cyclodextrin and different concentrations of methanol (0–40%). Applied voltage, 20 kV, 6.6–3.5 μA.

### 3.4. *Qualitative analysis of pharmaceutical preparations*

Two samples containing about $10^{-4}$ *M* ibuprofen and ketoprofen were analysed using 50 m*M* MES (pH 5) supported with 20 and 30 m*M* tri-OMe-β-CD, respectively. The electropherograms showed the presence of the two enantiomers in both samples (results not shown), indicating that the two drugs are administered as racemic compounds. The presence of the two enantiomers was confirmed by spiking the two solutions with standard mixtures containing racemic ibuprofen and ketoprofen.

## 4. Conclusions

It has been demonstrated that capillary electrophoresis can be successfully used for the resolution of enantiomers of several 2-arylpropionic acid non-steroidal anti-inflammatory drugs when charged or uncharged cyclodextrin derivatives are added to the background electrolyte as a chiral selector. The chiral resolution is based on the inclusion–complexation between the CD used and the analytes, which causes selective retardation of enantiomers, allowing their separation. The tested modified cyclodextrin derivatives (heptakis-2,6-di-O-methyl-β-CD, heptakis-2,3,6-tri-O-methyl-β-CD and $6^{A}$-methylamino-β-CD) proved to be good complexing agents for the racemic compounds analysed and the most useful chiral selector was tri-OMe-β-CD. The chiral discrimination was influence by the CD type, its concentration, the pH of the BGE and the content of organic solvent.

Capillary electrophoresis can be considered as complementary to other analytical techniques, such as HPLC, for the separation of enantio-

mers. We can outline the following advantages: (i) the amounts of samples and separation buffer are much less than those used in HPLC (in general, nanolitre and microlitre volumes, respectively are used); (ii) usually the chiral selector is dissolved in the BGE and thus the use of expensive chiral columns is not required, (iii) relatively high efficiencies are obtained (more than 100 000 theoretical plates); (iv) the capillary is equilibrated in a few minutes and, owing to the use of small amounts of BGE, environmental pollution is reduced. The disadvantages of CE in comparison with HPLC are the lower sensitivity in terms of concentrations, the lower reproducibility and the smaller possibility of preparative applications.

## Acknowledgements

The authors thank Dr. Cecilia Bartolucci (Istituto di Strutturistica Chimica, CNR, Montelibretti, Italy) for providing some of standard enantiomers used in this study and Mr. M. Cristalli for technical assistance.

## References

[1] I.R. Innes and M. Nickersen, in L.S. Goodman and A. Gilman (Editors), *The Pharmacological Basis of Therapeutics*, Macmillan, New York, 1970, p. 477.
[2] A.J. Hutt and J. Caldwell, *J. Pharm. Pharmacol.*, 35 (1983) 693.
[3] N.P.E. Vermeulen and J.M. te Koppele, in I.W. Wainer (Editor), *Drug Stereochemistry*, Marcel Dekker, New York, 1993, p. 245.
[4] J. Debowski, D. Sybilska and J. Jurczak, *J. Chromatogr.*, 282 (1983) 83.
[5] T.J. Ward and D.W. Armstrong, *J. Liq. Chromatogr.*, 9 (1986) 407.
[6] G. Blaschke, *J. Liq. Chromatogr.*, 9 (1986) 341.
[7] E. Gil-Av, B. Feibush and R. Charles-Sigler, *Tetrahedron Lett.*, (1966) 1009.
[8] S. Terabe, H. Shibata and Y. Miyashita, *J. Chromatogr.*, 480 (1989) 403.
[9] A. Dobashi, T. Ono, S. Hara and J. Yamaguchi, *J. Chromatogr.*, 480 (1989) 413.
[10] P. Gozel, E. Gassmann, H. Michelsen and R.N. Zare, *Anal. Chem.*, 59 (1987) 44.
[11] W. Schutzner, M. Cristalli, M.G. Quaglia and S. Fanali, presented at the *5th International Symposium on HPCE, 25–28 January 1993, Orlando, FL.*
[12] R. Vespalec, V. Sustacek and P. Bocek, *J. Chromatogr.*, 638 (1993) 255.
[13] L. Valtcheva, J. Mohammed, G. Pettersson and S. Hjerten, *J. Chromatogr.*, 638 (1993) 263.
[14] T. Schmitt and H. Engelhardt, *Chromatographia*, 37 (1993) 475.
[15] C. Quang and M.G. Khaledi, *J. High Resolut. Chromatogr.*, 17 (1994) 99.
[16] A. Nardi, A. Eliseev, P. Bocek and S. Fanali, *J. Chromatogr.*, 638 (1993) 247.
[17] S. Fanali, in N.A. Guzman (Editor), *Capillary Electrophoresis Technology*, Marcel Dekker, New York, 1993, p. 731.
[18] R. Kuhn, F. Stoecklin and F. Erni, *Chromatographia*, 33 (1992) 32.
[19] J. Szejtli, *Cyclodextrins and their Inclusion Complexes*, Akadémiai Kiadó, Budapest, 1982, pp. 33–34.
[20] J. Szejtli, *Cyclodextrins and their Inclusion Complexes*, Akadémiai Kiadó, Budapest, 1982, pp. 74–93.
[21] K. Brune, G. Geisslinger and S. Menzel-Soglowek, *J. Clin. Pharmacol.*, 32 (1992) 944.
[22] S. Pedrazzini, W. Zanaboni-Muciacca, C. Sacchi and A. Forgione, *J. Chromatogr.*, 415 (1987) 214.
[23] J. Bojarski, *J. Liq. Chromatogr.*, 12 (1989) 2685.
[24] H.Y. Aboul-Enein and S.A. Bakr, *J. Liq. Chromatogr.*, 15 (1992) 1983.
[25] T.A.G. Noctor, G. Felix and I.W. Wainer, *Chromatographia*, 31 (1991) 55.
[26] M.D. Beeson and G. Vigh, *J. Chromatogr.*, 634 (1993) 197.
[27] N.H. Singh, F.N. Pasutto, R.T. Coutts and F. Jamali, *J. Chromatogr.*, 378 (1986) 125.
[28] Y.Y. Rawjee, D.U. Staerk and G. Vigh, *J. Chromatogr.*, 635 (1993) 291.
[29] Y.Y. Rawjee and G. Vigh, *Anal. Chem.*, 66 (1994) 619.
[30] A. D'Hulst and N. Verbeke, *J. Chromatogr.*, 608 (1992) 275.
[31] S. Hjertén, *J. Chromatogr.*, 347 (1985) 191.
[32] S. Fanali and P. Bocek, *Electrophoresis*, 11 (1990) 757.
[33] K. Harata, K. Uekama, T. Imai, F. Hirayama and M. Otagiri, *J. Inclus. Phenom.*, 6 (1988) 443.
[34] J. Snopek, I. Jelinek and E. Smolkova-Keulemansova, *J. Chromatogr.*, 411 (1987) 153.
[35] S. Fanali and M. Sinibaldi, *J. Chromatogr.*, 442 (1988) 371.

ELSEVIER

Journal of Chromatography A, 694 (1995) 307–313

JOURNAL OF CHROMATOGRAPHY A

# Ability of non-cyclic oligosaccharides to form molecular complexes and its use for chiral separation by capillary zone electrophoresis

Koji Kano*, Kenji Minami, Kazumi Horiguchi, Taizo Ishimura, Masahito Kodera

*Department of Molecular Science and Technology, Faculty of Engineering, Doshisha University, Tanabe-cho, Kyoto 610-03, Japan*

**Abstract**

The binding constants ($K$) for complexation of the phenyl acetates with linear $\alpha$-1,4-linked dextrins have been determined from the kinetics of the hydrolyses of the esters. The $K$ value tends to increase with increasing the number of the glucopyranose units, suggesting hydrophobic interaction as a binding force. The weak ability of the linear dextrins to form the molecular complexes makes it possible to separate the enantiomers of binaphthyl derivatives such as 1,1′-binaphthyl-2,2′-dicarboxylic acid, 1,1′-binaphthyl-2,2′-diyl hydrogenphosphate and 2,2′-dihydroxy-1,1′-binaphthyl-3,3′-dicarboxylic acid in their anionic forms. Hydrogen bonding as well as hydrophobic interaction is suggested as an essential force for enantioselective complexation between saccharide and anionic binaphthyl.

## 1. Introduction

Although cyclic oligosaccharides, cyclodextrins (CDs), are well known to include various organic compounds in their cyclic cavities [1], the ability of non-cyclic oligosaccharides to form molecular complexes has scarcely been recognized. However, judging from the fact that $\alpha$-1,4-linked linear polymer of glucose, amylose, forms complexes with various alcohols whose helical structures have been determined by X-ray analysis (see, for example, [2] and [3]), it is expected that linear $\alpha$-1,4-linked oligosaccharides such as maltohexaose ($G_6$) and/or maltoheptaose ($G_7$), which may have a turn of a dextrin helix [2], complex with organic compounds. We found that (4*Z*,15*Z*)-bilirubin-IX (BR) is bound to maltose ($G_2$), maltotriose ($G_3$) and $G_7$ to form chiral BR complexes through hydrogen bonding between the $CO_2^-$ groups of BR and the OH groups of linear $\alpha$-1,4-linked dextrin ($G_n$) [4]. Recently, the hydrophobic fluorescence probes such as 8-anilino-1-naphthalenesulfonate (ANS) and 6-toluidino-2-naphthalenesulfonate (TNS) form the molecular complexes with $G_n$ ($n = 4$–7) while the binding constants ($K$) are extremely small (1.8–27 $M^{-1}$) [5]. Meanwhile, CDs with many chiral centers can recognize the chiralities of their guest molecules [6]. Linear oligomers of glucose are also expected to act as guest molecules which discriminate between the enantiomers of the guest molecules. Although the studies on the molecular recognition by non-cyclic oligosaccharides seem to be very important in connection with the role of oligosaccharides at biological cell surfaces (see, for example, [7]),

* Corresponding author.

0021-9673/95/$09.50 
*SSDI* 0021-9673(94)00864-7

little attention has been paid to chiral recognition of non-cyclic oligosaccharides. The present study deals with the ability of $G_n$ ($n = 2$–7) to form molecular complexes and its use to separate the enantiomers of the binaphthyl derivatives such as 1,1′-binaphthyl-2,2′-dicarboxylic acid (BNC), 1,1′-binaphthyl-2,2′-diyl hydrogenphosphate (BNP), 2,2′-dihydroxy-1,1′-binaphthyl-3,3′-dicarboxylic acid (HBNC) and 1,1′-bi-2-naphthol (BN) by capillary zone electrophoresis (CZE) using $G_n$ as the chiral separators.

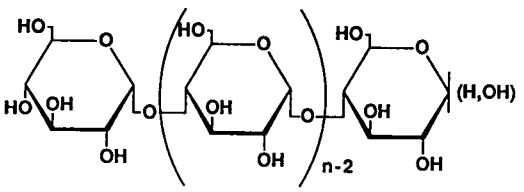


It is very important to know the ability of $G_n$ to form molecular complexes and to clarify the mechanisms of molecular complex formation of $G_n$. In general, however, it is very difficult to study the molecular complex formation of $G_n$ because of their very small $K$ values. Since the determination of small $K$ values by spectroscopic titrations is very difficult, we employed the kinetic method to evaluate the $K$ values for complexation of *p*-nitrophenyl acetate (PNPA) and *p*-carboxyphenyl acetate (PCPA) with $G_n$. Both PNPA and PCPA should be regarded as the probe molecules. The hydrolyses of the esters were carried out in aqueous alkaline solutions containing $G_n$. The results obtained in this work suggest a hydrophobic interaction between the ester and $G_n$. The weak ability of $G_n$ to form molecular complexes was applied to realize the optical resolution of the racemic binaphthyls using CZE. This may be the first case where the chiral recognition of the axial chiralities by non-cyclic oligosaccharides is proved.

## 2. Experimental

D-Glucose ($G_1$), $G_2$, $G_3$ (Nacalai), $G_4$, $G_5$, $G_6$ and $G_7$ (Hayashibara) were purchased and used without further purification. An antioxidant in $\alpha$- and $\beta$-CDs (Nacalai) commercially obtained was extracted with tetrahydrofuran (THF) using a Soxhlet extractor. PNPA (Nacalai) was recrystallyzed from aqueous ethanol. PCPA was prepared and purified according to the procedures described in the literature [8]. Optically active and racemic BNP and BN (Aldrich) were commercially obtained. The preparation of ( ± )-, (*S*)- and (*R*)-HBNCs were described before [9]. The hydrolyses of PNPA and PCPA were carried out using a UNISOKU stopped-flow apparatus with a multichannel spectrophotometer. The changes in absorbances of the phenolate ions were followed at 440 nm for PNPA and 295 nm for PCPA and the kinetic data were analyzed by a damping Gauss–Newton method (a non-linear least squares method) using a microcomputer.

The CZE experiments were performed with a Jasco capillary electrophoresis system CE-800 with a 300 mm (effective length) × 50 $\mu$m I.D. fused-silica capillary cartridge (non-coated). The capillary was filled with the buffer solution with $G_n$ and the sample in the same buffer solution was introduced into the capillary by applying the potential for 10 s. The electropherogram was taken at the same potential using a Jasco 875-CE UV–Vis detector.

The molecular mechanics–molecular dynamics (MM-MD) calculations were carried out using an AMBER program system (version 4, presented by P. Kollman, University of California at San Francisco, USA) on a COMTEC 4D RPC XS24Z R4000 workstation at 285.1–302.6 K for 10–11.8 ps. The calculations include the effects of water as a solvent. Before MM-MD calculations, the information of the charge of the glucopyranose was prepared by a MOPAC (version 6 developed by J.J.P. Stewart, US Airforce Academy, USA) calculation.

## 3. Results and discussion

### 3.1. Interaction between $G_n$ and esters

Spectroscopic titration using UV–Vis, fluorescence, circular dichroism or NMR spectroscopy is the most common way to determine the $K$ value. However, the spectroscopic titration can-

not be applied for most systems having very small $K$ values. In the present study, we used a kinetic method to evaluate the $K$ value for complexation of benzene derivatives with $G_n$. It is well known that CD accelerates the hydrolyses of phenyl acetates [1,10]. The hydrolysis of the ester catalyzed by saccharide is as follows:

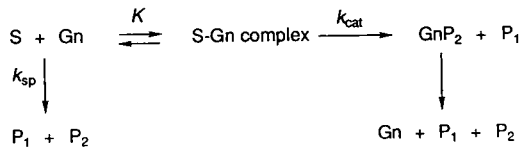


where S and $GnP_2$ represent the substrate (ester) and acylated $G_n$, respectively, and $k_{sp}$ and $k_{cat}$ are the pseudo first-order rate constant for the hydrolysis of the ester in the absence of $G_n$ and the first-order rate constant for the reaction of S–$G_n$ complex, respectively. In the case of CD, the dissociated secondary OH group of CD attacks to the carbonyl carbon of the ester to promote acyl transfer reaction. However, since the $pK_a$ of the secondary OH group of $G_n$ is much higher than that of CD, the nucleophilic attack of the dissociated OH group does not occur in the $G_n$-catalyzed hydrolysis under the present conditions. VanEtten et al. [11] reported the $G_1$-catalyzed hydrolyses of the phenyl acetates and assumed a hemiacetal alkoxide anion is an active species which attacks to the carbonyl group of the ester. The $K$ and $k_{cat}$ values can be evaluated from the Eadie-type plot [12]:

$$k_{obs} - k_{sp} = -(k_{obs} - k_{sp})/(K[G_n]) + k_{cat} - k_{sp} \quad (1)$$

The hydrolyses of PNPA were carried out in the pH 11.7 phosphate buffer (0.1 $M$) containing various amounts of $G_n$ at 25°C. The plot of $k_{obs}$ vs. $[G_n]$ is not linear for each saccharide (Fig. 1), indicating that the complexation between PNPA and $G_n$ occurs. Good linear relationship (correlation factor $r > 0.999$) between $(k_{obs} - k_{sp})$ and $(k_{obs} - k_{sp})/[G_n]$ provided $K$ and $k_{cat}$. The results are summarized in Table 1. In contrast with the CD-catalyzed hydrolyses, the $k_{cat}$ values are almost the same in the hydrolyses in the presence of various $G_n$ compounds. In the case of the PNPA–$\alpha$-CD complex, the active site (the dissociated secondary OH group of $\alpha$-CD) is located far from the carbonyl group of PNPA leading to smaller $k_{cat}$. Meanwhile, the PNPA molecule can alter its position in larger cavity of $\beta$-CD. The PNPA molecule may move freely in the PNPA–$G_n$ complex leading to relatively large and constant $k_{cat}$ in the $G_n$-catalyzed hydrolyses. Except for the $G_2$ complex, the $K$ value increases with increasing the number of the glucopyranose units of $G_n$. Similarly, very small $K$ values have been obtained in complexation of

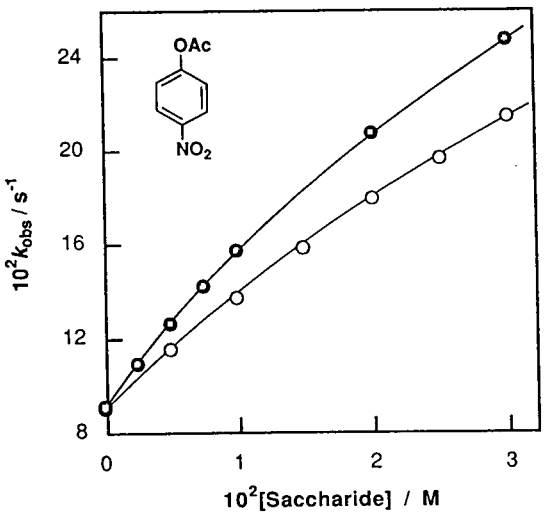


Fig. 1. Effects of the concentrations of $G_3$ (○) and $G_5$ (●) on $k_{obs}$ for hydrolyses of PNPA in 0.1 $M$ phosphate buffer at pH 11.7 and at 25°C.

Table 1
Linear dextrin-catalyzed hydrolyses of PNPA in 0.1 $M$ phosphate buffer at pH 11.7 and at 25°C

| Saccharide | $k_{obs}$ ($s^{-1}$) | $k_{cat}$ ($s^{-1}$) | $K$ ($M^{-1}$) |
|---|---|---|---|
| None | 0.09 | – | – |
| $G_1$ | 0.12 | 0.56 | 7.9 |
| $G_2$ | 0.14 | 0.48 | 13.4 |
| $G_3$ | 0.14 | 0.67 | 9.0 |
| $G_5$ | 0.15 | 0.60 | 14.2 |
| $G_7$ | 0.18 | 0.62 | 20.0 |
| $\alpha$-CD | 0.15 | 0.24 | 74.0 |
| $\beta$-CD | 0.49 | 0.76 | 147 |

The hydrolysis of PNPA (0.1 m$M$) was carried out in the phosphate buffer at pH 11.7 containing 0.01 $M$ saccharide.

$G_n$ with ANS or TNS [5]: the $K$ values for the TNS–$G_5$ and TNS–$G_7$ complexes being reported to be 1.9 and 27 $M^{-1}$, respectively.

The dissociated PCPA was chosen as another substrate which can interact with $G_n$ through hydrogen bonding between the $CO_2^-$ group of PCPA and the OH group of $G_n$. The results are shown in Table 2. In the case of $G_1$, a good linear relationship was observed between $k_{obs}$ and $[G_1]$, indicating that no complex of $G_1$ and PCPA is formed. The $k_{cat}$ value for each $G_n$ is much larger than those for $\alpha$- and $\beta$-CDs. Very small $k_{cat}$ for $\beta$-CD suggests the difference between the structures of the $\beta$-CD complexes of PNPA and PCPA. Similar to the case of PNPA, the $K$ value increases with increasing the number of the glucopyranose units of $G_n$ and no significant difference is found between the $K$ values for PNPA and PCPA. This may suggest that hydrogen bonding does not participate in complexation of PCPA and $G_n$. Our results are in good agreement with those obtained by Aoyama et al. [5] and indicate the hydrophobic nature of linear $\alpha$-1,4-linked dextrins by which the molecular complexes are formed. Recent studies on solubilization, Diels–Alder reactions and denaturation of protein also demonstrate that linear $\alpha$-1,4-linked dextrin shows an amphiphilic nature while only hydrophilic character is shown for $\beta$-1,4-linked glucoside cellulose and $\alpha$-1,4-linked dextran [13].

Table 2
Linear dextrin-catalyzed hydrolyses of PCPA in 0.1 $M$ phosphate buffer at pH 11.7 and at 25°C

| Saccharide | $k_{obs}$ ($s^{-1}$) | $k_{cat}$ ($s^{-1}$) | $K$ ($M^{-1}$) |
|---|---|---|---|
| None | 0.019 | – | – |
| $G_1$ | 0.022 | – | – |
| $G_2$ | 0.025 | 0.079 | 13.3 |
| $G_3$ | 0.026 | 0.078 | 15.5 |
| $G_5$ | 0.029 | 0.096 | 16.0 |
| $G_7$ | 0.032 | 0.094 | 21.0 |
| $\alpha$-CD | 0.025 | 0.044 | 29.2 |
| $\beta$-CD | 0.020 | 0.022 | 160 |

The hydrolysis of PNPA (0.1 m$M$) was carried out in the phosphate buffer at pH 11.7 containing 0.01 $M$ saccharide.

### 3.2. Chiral separation of binaphthyls by CZE using $G_n$ as separator

Rapid development has been achieved in chiral separation by HPLC [14] and CZE [15] using CDs as chiral separators. The enantiomers of amino acid derivatives [16–18] and drugs and related compounds [17,19–23] have been separated by CZE using $\alpha$-, $\beta$- and $\gamma$-CDs and their methylated derivatives. 5-Aminonaphthalene-2-sulfonic acid derivatives of monosaccharide enantiomers are also separated by CD CZE [24]. We also reported excellent separation of the enantiomers of BN, HBNC and BNC by CZE using heptakis(2,3,6-tri-*O*-methyl)-$\beta$-CD (TMe-$\beta$-CD) as a chiral additive in the running buffer electrolyte [9]. The present study on CZE reveals that linear dextrins ($G_n$) also discriminate between the enantiomers of the binaphthyl derivatives.

The electropherograms of BNC are shown in Fig. 2 and the numerical data are summarized in Table 3. The separation factor $\alpha$ is defined as

$$\alpha = (t_2 - t_0)/(t_1 - t_0) \quad (2)$$

where $t_1$ and $t_2$ represent the retention times of the first and second peaks, respectively, and $t_0$ is the retention time of the coexisting compound which does not interact with $G_n$. We used methanol (2%, v/v) to determine $t_0$. $G_n$ (0.4 $M$) in 0.04 $M$ carbonate buffer (pH 9–9.5) were used as the separators. Except for the case of $G_5$, baseline or partial separation of the enantiomers of BNC was achieved by CZE. In CZE using $G_2$, $G_3$ and $G_4$, the retention times of the (*S*)-enantiomer are shorter than those of the (*R*)-enantiomer. The enantiomers of BNC are partially resolved by $G_2$ ($\alpha = 1.02$) and baseline separation is realized by $G_3$ CZE ($\alpha = 1.10$). The retention times of the BNC enantiomers are close again in $G_4$ CZE ($\alpha = 1.09$) and no peaks separation occurs in the case of $G_5$ ($\alpha = 1.00$). The enantiomers of BNC are separated again by $G_6$ ($\alpha = 1.03$) and $G_7$ ($\alpha = 1.08$). In contrast with the cases of $G_2$, $G_3$ and $G_4$, the retention times of the (*S*)-enantiomer become longer than those of the (*R*)-enantiomer in CZE using $G_6$ and $G_7$. In these experiments, the currents were

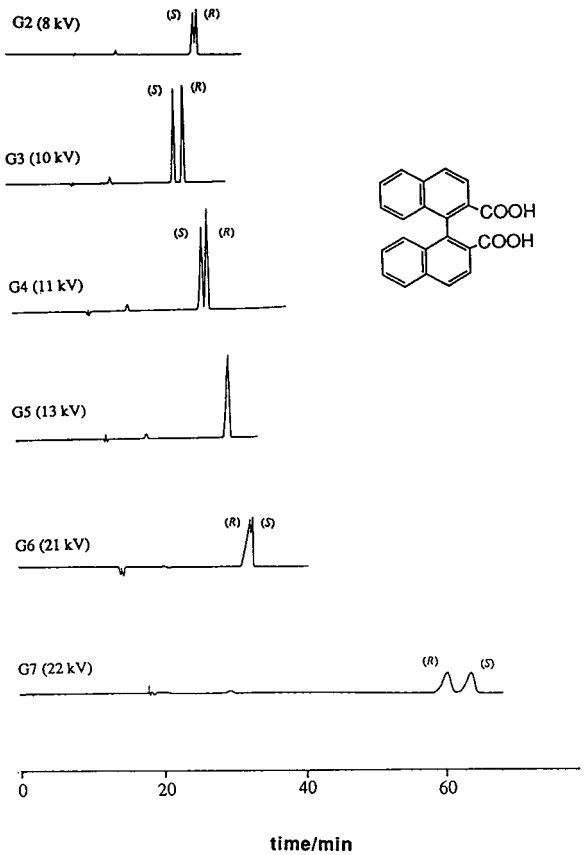


Fig. 2. Electropherograms of ( ± )-BNC (0.1 m$M$) obtained by CZE using 0.04 $M$ carbonate buffer (pH 9–9.5) containing $G_n$ (0.4 $M$); current 17–18 $\mu$A, detection wavelength 225 nm.

controlled to be 17–18 $\mu$A by changing applied voltages. Table 4 shows the results on CZE examined at constant voltage (10 kV). Essentially the same results were obtained. In CZE of BN, BNC, BNP and HBNC using TMe-$\beta$-CD or $\beta$-CD as the separator, the retention time of the enantiomer having a larger $K$ for complexation with CD is shorter than that of another enantiomer having a smaller $K$ [9]. Although we have not verified the correlation between the retention times of the enantiomers and the $K$ values for complexation of the enantiomers with $G_n$, the enantiomer having a shorter retention time seems to have a larger $K$. Therefore, it can be concluded that $G_3$ has the highest enantioselectivity amongst $G_2$, $G_3$ and $G_4$ which prefer the ($S$)-enantiomer of BNC as the guest and the ($S$)-selectivity is weakened and the ($R$)-selectivity is gradually enhanced with increasing the number of the glucopyranose units of the $G_n$. It is quite reasonable to assume that the macroscopic structure of $G_n$ as a polymer is preferable to complex with ($R$)-BNC while the microscopic structure of $G_n$ prefers the ($S$)-enantiomer of BNC.

In order to explain the effect of the chain length of $G_n$ on the chiral recognition of BNC, the MM-MD calculations were carried out for $G_n$ ($n = 2$–7) in water. The most stable structures derived from the calculations are shown in Fig. 3. As can be expected, a helical structure becomes remarkable as increasing the number of the glucopyranose units of $G_n$. The primary OH groups of $G_n$ of $n \geq 3$ are directed to the outside of the helix and the hydrophobic environment is constructed inside of the helix. One turn of the helix is prepared in $G_7$, which is in good agreement with the result of the X-ray analysis [2].

Table 3
Chiral separation of ( ± )-BNC (0.1 m$M$) by CZE at 17–18 $\mu$A using linear dextrins (0.4 $M$) as separators

| $G_n$ | Voltage (kV) | $t_0$ (min) | $t_1$ (min) | $t_2$ (min) | $\alpha$ |
|---|---|---|---|---|---|
| $G_2$ | 8 | 9.6 | 26.4 ($S$) | 26.8 ($R$) | 1.02 |
| $G_3$ | 10 | 9.2 | 23.6 ($S$) | 25.0 ($R$) | 1.10 |
| $G_4$ | 11 | 10.6 | 27.0 ($S$) | 27.9 ($R$) | 1.09 |
| $G_5$ | 13 | 12.0 | 29.8 ($S$) | 29.8 ($R$) | 1.00 |
| $G_6$ | 21 | 13.8 | 32.2 ($R$) | 32.7 ($S$) | 1.03 |
| $G_7$ | 22 | 17.8 | 60.3 ($R$) | 63.7 ($S$) | 1.08 |

The carbonate buffer (0.04 $M$) was used as a background electrolyte.

Table 4
Chiral separation of (±)-BNC (0.1 m*M*) by CZE at 10 kV using linear dextrins (0.4 *M*) as separators

| $G_n$ | Current ($\mu$A) | $t_0$ (min) | $t_1$ (min) | $t_2$ (min) | $\alpha$ |
|---|---|---|---|---|---|
| $G_2$ | 21 | 7.4 | 20.3 (*S*) | 20.6 (*R*) | 1.02 |
| $G_3$ | 17 | 9.2 | 23.6 (*S*) | 25.0 (*R*) | 1.10 |
| $G_4$ | 15 | 13.0 | 33.0 (*S*) | 34.0 (*R*) | 1.05 |
| $G_5$ | 13 | 16.4 | 40.8 (*S*) | 40.8 (*R*) | 1.00 |
| $G_6$ | 8 | 33.6 | 71.6 (*R*) | 72.5 (*S*) | 1.02 |

The carbonate buffer (0.04 *M*) was used as a background electrolyte.

The structures of $G_6$ and $G_7$ very much resemble those of $\alpha$- and $\beta$-CDs, respectively, though the catalyses of $G_6$ and $G_7$ for the hydrolyses of PNPA and PCPA are quite different from those of $\alpha$- and $\beta$-CDs. It is reasonable to assume that a hydrophobic environment is prepared inside of the helix of $G_n$ to which hydrophobic or amphiphilic compounds such as PNPA, PCPA and BNC are bound to form molecular complexes.

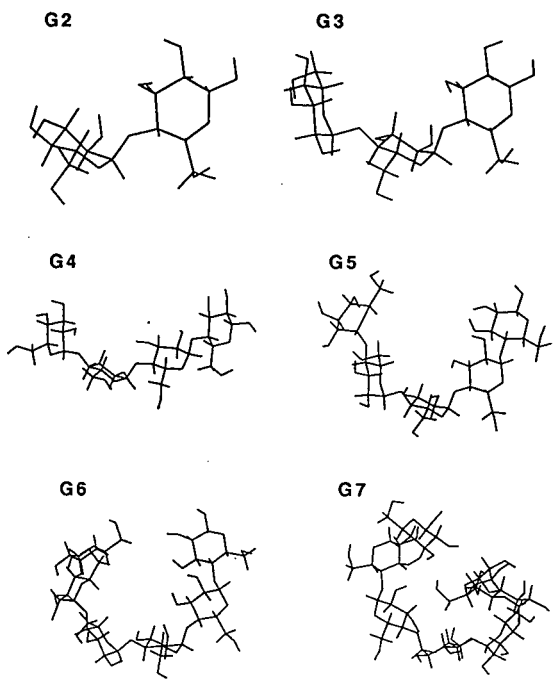


Fig. 3. Optimized structures of $G_n$ in water computed by the MM-MD calculations.

The fact that $G_n$ having larger $n$ forms more stable molecular complexes of the phenyl acetates can be interpreted in terms of the helical structure of $G_n$. In the previous paper [9], we reported that $\beta$-CD as well as TMe-$\beta$-CD prefers the (*R*)-enantiomer of BNC as the guest which is included in the cavity of CD. Pseudocyclic oligosaccharides such as $G_6$ and $G_7$ may recognize the chirality of BNC through the similar mechanism which is applied for CD.

The electropherograms of other (±)-binaphthyls are shown in Fig. 4. CZE was performed at 15 kV and 28 $\mu$A by using 0.4 *M* $G_2$ in the 0.04 *M* carbonate buffer at pH 9. The enantiomers of the anionic binaphthyls such as BNC, BNP and HBNC can be separated while no peak separation is achieved in the case of BN without charge. This seems to suggest the participation of hydrogen bonding between the anionic sample and the OH group(s) of $G_2$ in chiral recognition. Further study is now in progress to clarify the mechanism for chiral recognition by $G_n$.

## Acknowledgements

This work was supported by a Grant-in-Aid for Science Research on Priority Areas, "Asymmetric Synthesis of Chiral Molecules" (No. 05234229) from the Ministry of Education, Science and Culture, Japan. The authors are also indebted for the financial support in part by a Grant for Science Research from Doshisha University.

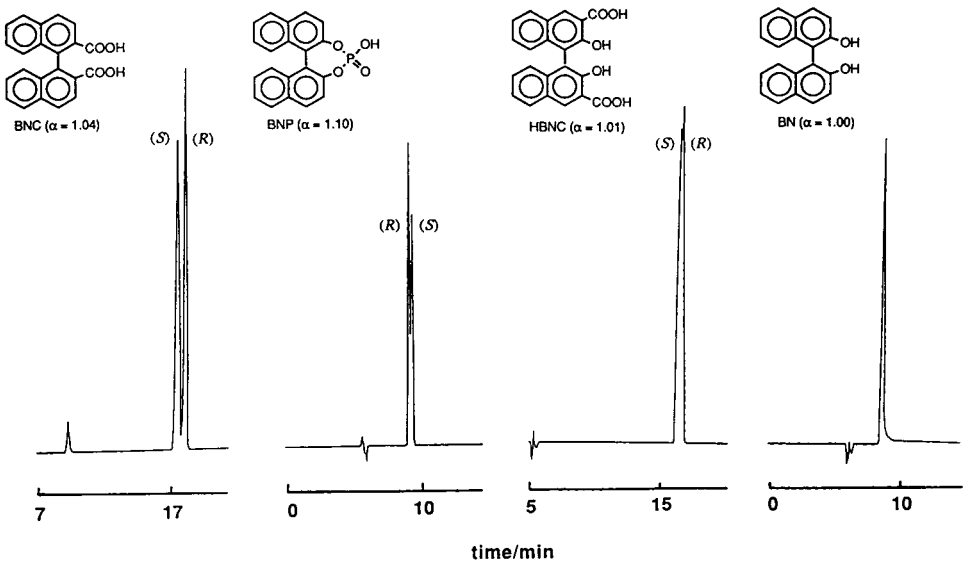


Fig. 4. Electropherograms of (±)-BNC, (±)-BNP, (±)-HBNC and (±)-BN (0.1 m*M*) obtained by CZE using 0.04 *M* carbonate buffer at pH 9.0 containing $G_2$ (0.4 *M*); applied voltage 15 kV, current 28 μA, detection wavelength 225 nm for BNC, 215 nm for BNP, 235 nm for HBNC, 227 nm for BN.

## References


[1] M.L. Bender and M. Komiyama, *Cyclodextrin Chemistry*, Springer, Berlin, 1978.
[2] R.E. Rundle and F.C. Edwards, *J. Am. Chem. Soc.*, 65 (1943) 2200.
[3] Y. Yamashita, *J. Polym. Sci., Part A*, 3 (1965) 3251.
[4] K. Kano, K. Yoshiyasu and S. Hashimoto, *J. Chem. Soc., Chem. Commun.*, (1988) 801.
[5] Y. Aoyama, J. Otsuki, Y. Nagai, K. Kobayashi and H. Toi, *Tetrahedron Lett.*, 33 (1992) 3775.
[6] K. Kano, in H. Dugas (Editor), *Bioorganic Chemistry Frontiers*, Vol. 3, Springer, Berlin, 1993, Ch. 1, p. 1.
[7] I. Eggens, B. Fenderson, T. Toyokuni, B. Dean, M. Stround and S. Hakomori, *J. Biol. Chem.*, 264 (1989) 9476.
[8] F.D. Chattaway, *J. Chem. Soc.*, (1931) 2495.
[9] K. Kano, Y. Tamiya, C. Otsuki, T. Shimomura, T. Ohno, O. Hayashida and Y. Murakami, *Supramolecular Chem.*, 2 (1993) 137.
[10] O.S. Tee, C. Mazza and X.-X. Du, *J. Org. Chem.*, 55 (1990) 3603; and references cited therein.
[11] R.L. VanEtten, J.F. Sebastian, G.A. Clowes and M.L. Bender, *J. Am. Chem. Soc.*, 89 (1967) 3242.
[12] G.S. Eadie, *J. Biol. Chem.*, 146 (1942) 85.
[13] D. Balasubramanian, B. Raman and C.S. Sundari, *J. Am. Chem. Soc.*, 115 (1993) 74.
[14] L. Coventry, in W.J. Lough (Editor), *Chiral Liquid Chromatography*, Blackie & Son, Glasgow, 1989, Ch. 8, p. 148.
[15] R. Kuhn and S. Hoffstetter-Kuhn, *Chromatographia*, 34 (1992) 505.
[16] A. Guttman, A. Paulus, A.S. Cohen, N. Grinberg and B.L. Karger, *J. Chromatogr.*, 448 (1988) 41.
[17] S. Fanali and P. Boček, *Electrophoresis*, 11 (1990) 760.
[18] M. Tanaka, S. Asano, M. Yoshinago, Y. Kawaguchi, T. Tetsumi and T. Shono, *J. Anal. Chem.*, 339 (1991) 63.
[19] S. Fanali, *J. Chromatogr.*, 474 (1989) 441.
[20] R. Kuhn, F. Stoecklin and F. Erni, *Chromatographia*, 33 (1992) 32.
[21] K.D. Altria, D.M. Goodall and M.M. Rogan, *Chromatographia*, 34 (1992) 19.
[22] I.D. Cruzado and G. Vigh, *J. Chromatogr.*, 608 (1992) 421.
[23] M.W.F. Nielen, *Anal. Chem.*, 65 (1993) 885.
[24] M. Stefansson and M. Novotny, *J. Am. Chem. Soc.*, 115 (1993) 11573.

Journal of Chromatography A

# NEWS SECTION

## INTERNATIONAL SYMPOSIUM ON MOLECULAR CHIRALITY, KYOTO, JAPAN, 24–27 MAY 1994

Fig.1. Professor K. Mosbach (University of Lund, Sweden) presents a lecture on "Molecular Imprinting", a novel concept of molecular recognition, for the younger active scientists at the workshop.

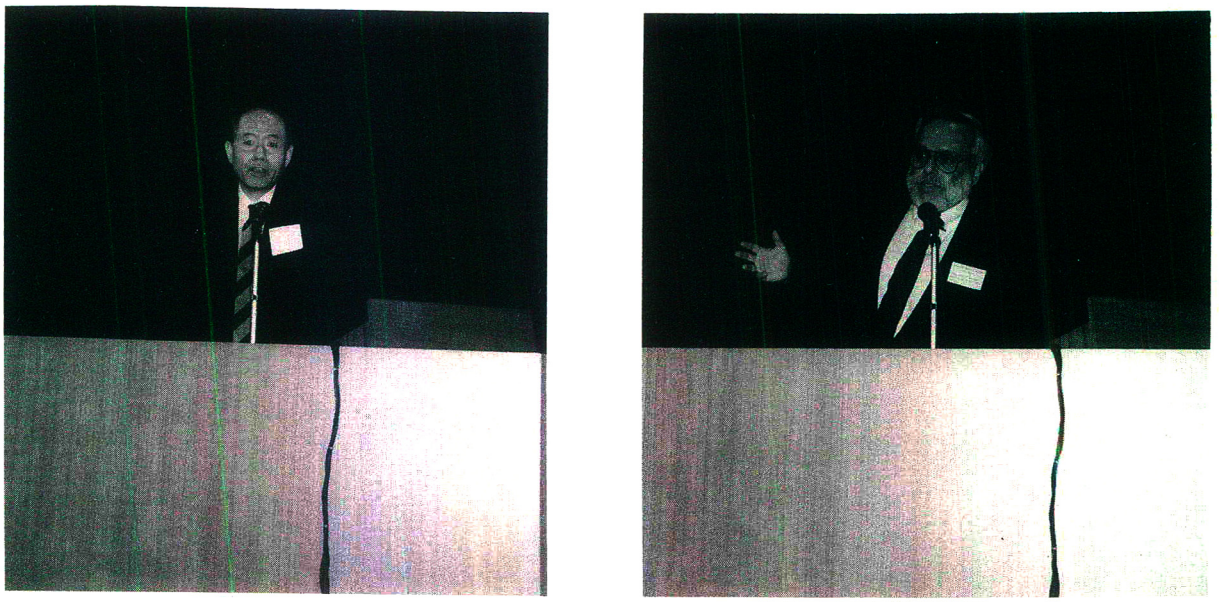

Fig. 2. (Left) Professor R. Noyori (Nagoya University, Japan) presents a lecture, entitled "Asymmetric Catalysis: Science and Opportunities". (Right) Professor K. Lipkowitz (Indiana University-Purdue University, IN, USA) presents a lecture regarding: "Supramolecular Chemistry for Proving Molecular Chirality".

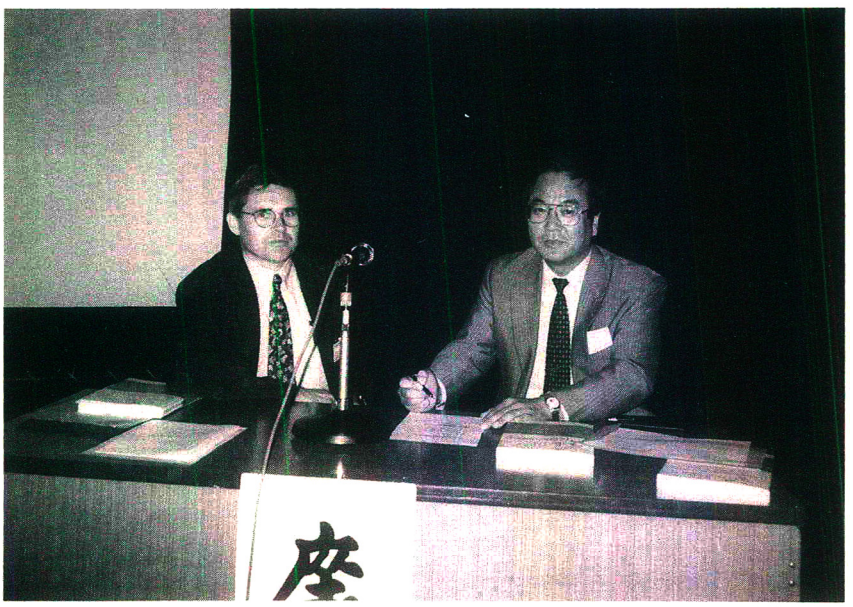

Fig. 3. Professors A. Collet (ENS Lyon, France) and K. Saigo (University of Tokyo, Japan) serve as chairmen to stimulate interactive discussions between presenter and audience.

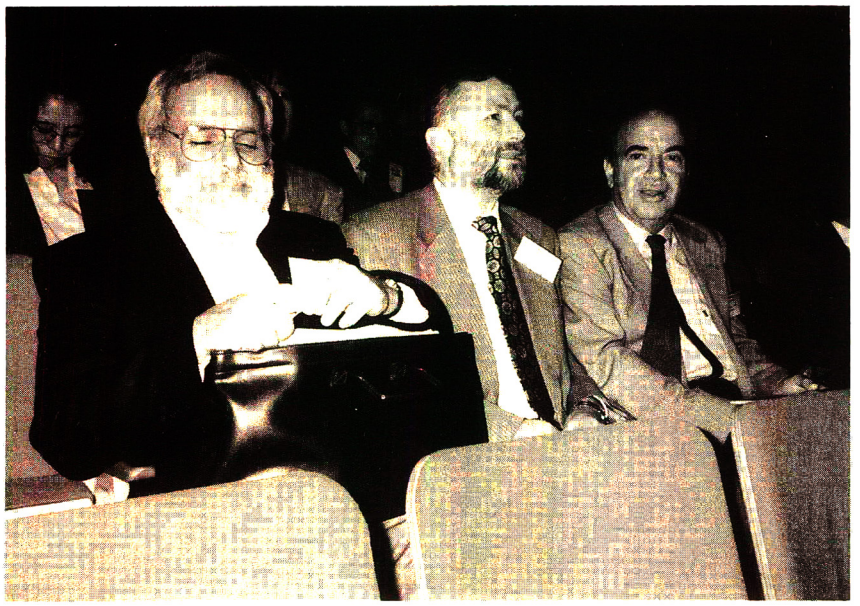

Fig. 4. Professors K. Lipkowitz, F. Gasparrini and D. Misiti (University "La Sapienza, Italy) (from left to right), in attendance at the lecture hall.

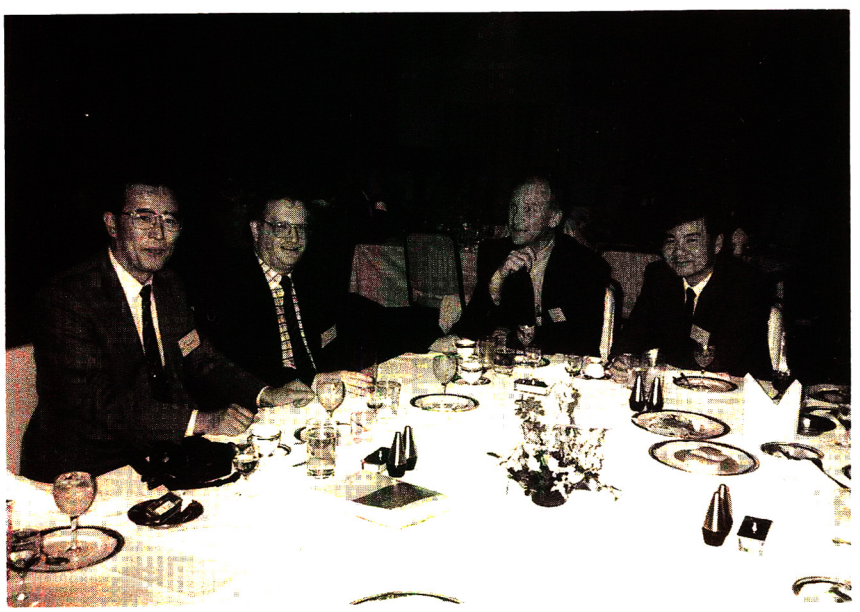

Fig. 5. Professors T. Nakagawa (University of Kyoto, Japan), A. Fell (University of Bradford, UK), W. Lindner (Karl-Franzens University, Austria) and S. Terabe (Himeji Institute of Technology, Japan) (left to right), exchange information at the board meeting.

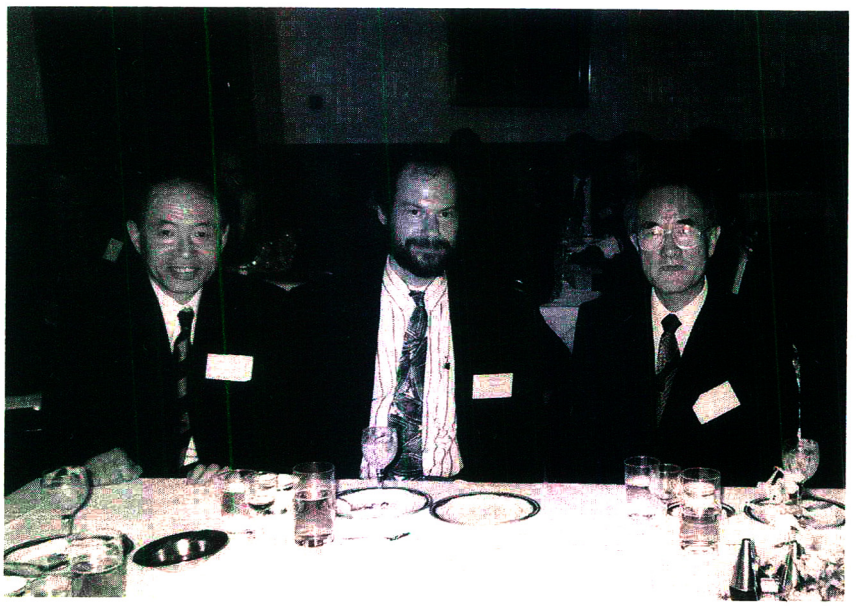

Fig. 6. Professor R. Noyori (Nagoya University, Japan), Dr. J. Blumenstein (FDA, USA), and Professor S. Hara (Tokyo College of Pharmacy, Japan) (left to right) having drinks and discussions at the board meeting.

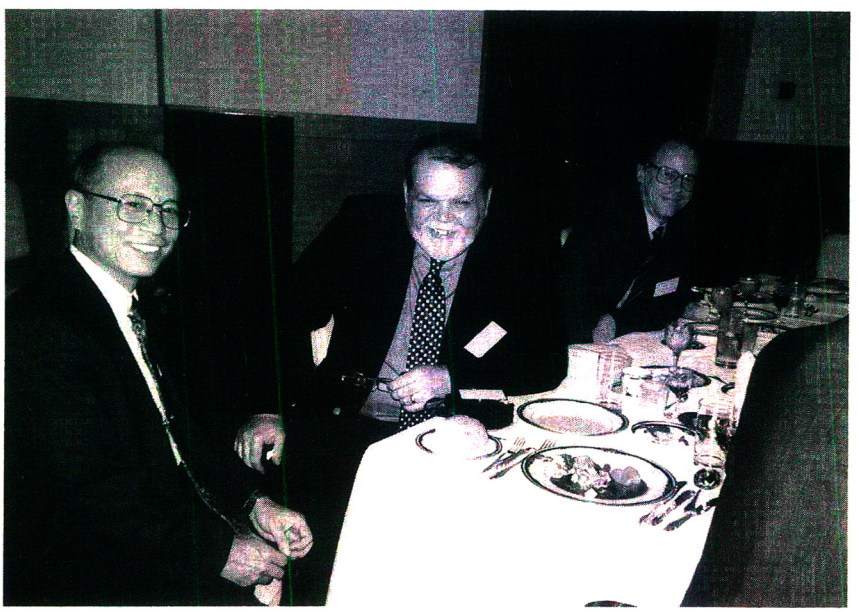

Fig. 7. Dr. K. Meguro (Takeda Chemical Industries, Japan), Professors J. Caldwell (St. Mary's Hospital Medical School, UK), and G. Tucker (University of Sheffield, UK) (left to right) exchange ideas at the board meeting.

**END OF SYMPOSIUM PAPERS**

# Hyphenated Techniques in Supercritical Fluid Chromatography and Extraction

Edited by **K. Jinno**

Journal of Chromatography Library Volume 53

This is the first book to focus on the latest developments in hyphenated techniques using supercritical fluids. The advantages of SFC in hyphenation with various detection modes, such as FTIR, MS, MPD and ICP and others are clearly featured throughout the book. Special attention is paid to coupling of SFE with GC or SFC.
In this edited volume, chapters are written by leading experts in the field. The book will be of interest to professionals in academia, as well as to those researchers working in an industrial environment, such as analytical instrumentation, pharmaceuticals, agriculture, food, petrochemicals and environmental.

**Contents:**




ELSEVIER SCIENCE B.V.


**© 1992 x + 334 pages Hardbound**
**Price: Dfl. 275.00 (US$ 157.25)**
**ISBNN0-444-88794-6**


*"...will be a good guide to the scope of successful applications of supercritical fluids and clearly demonstrates the ability of SFC to provide a wealth of information about analytes."*
**Chromatographia**

*"...a valuable new source of information describing the latest developments in SFC and SFE hyphenated techniques. The book is highly recommended for advanced undergraduate students and chromatographers."*
**LC-GC International**

**ORDER INFORMATION**

*For USA and Canada*
**ELSEVIER SCIENCE INC.**
P.O. Box 945
Madison Square Station
New York, NY 10160-0757
Fax: (212) 633 3880

*In all other countries*
**ELSEVIER SCIENCE B.V.**
P.O. Box 330
1000 AH Amsterdam
The Netherlands
Fax: (+31-20) 5862 845

*US$ prices are valid only for the USA & Canada and are subject to exchange rate fluctuations; in all other countries the Dutch guilder price (Dfl.) is definitive. Customers in the European Union should add the appropriate VAT rate applicable in their country to the price(s). Books are sent postfree if prepaid.*

# TrAC - Trends in Analytical Chemistry: Reference Edition

## Volume 13: 1994

### TrAC Compendium Series, Volume 13

*TrAC* provides a topical digest of current developments and new ideas in the analytical sciences. It does so in the form of broadly-based, easy-to-read scientific reviews, backed up by news and other features of interest to the international analytical chemistry community. The Reference Edition of *Trends in Analytical Chemistry (TrAC)* is a compilation of the archival material reprinted from the regular issues of the journal. For subscribers to the library edition of *TrAC*, the reference edition forms an integral part of the annual subscription, but for others it can be purchased individually. It provides informative and stimulating reading for all those who use analytical methods.

An extra supplement is included in this edition: TrAC Directory of Hyphenated Techniques.

- Containing approx. 400 V.I.P.s Worldwide
- Including Complete Addresses, Fax and Phone Numbers, and E-Mail Addresses (where available)
- Giving Many Techniques, Applications and Research Topics and Most Significant Publications in the area
- Providing an Extensive Subject Index

This directory forms an integral part of the 1994 subscription to the Library Edition and is also available as a separate publication.

***A selection of the contents.*** Recent advances in multidimensional gas chromatography (K.A. Krock, C.L. Wilkins). Modern multi-dimensional protein NMR spectroscopy. Parts I & II (E.R.P. Zuiderweg, S.R. Van Doren). Atmospheric-pressure-ionization mass spectrometry. Parts I &II (A.P. Bruins). Shpol'skii spectroscopy, a cryogenic high-resolution molecular fluorescence technique with a distinct potential in analytical chemistry (C. Gooijer *et al.*). Analytical applications of scanning tunneling microscopy (P.S. Weiss). Microwave-assisted process (MAP™) a new tool for the analytical laboratory (J.R.J. Paré *et al.*). The pigtailing approach to optical detection in capillary electrophoresis (A.E. Bruno *et al.*). Multivariate sensor arrays as industrial and environmental monitoring systems (W.P. Carey). Basic ion chemistry studies using a Fourier transform ion cyclotron resonance mass spectrometer (N.M.M. Nibbering). New horizons in gas chromatography: field applications of micro-miniaturized gas chromatographic techniques (E.B. Overton, K.R. Carney). Optimisation of indirect UV detection in capillary zone electrophoresis of low- molecular-mass anions (W. Buchberger *et al.*). Novel applications of near-infrared spectroscopy of water and aqueous solutions from physical chemistry to analytical chemistry (J. Lin, C.W. Brown). Surface water analysis (trace-organic contaminants) and EC regulations (M.-C. Hennion *et al.*). Interpretation and analysis of complex environmental data using chemometric methods (R.J. Wenning, G.A. Erickson). Author index. Subject index.


ELSEVIER
An imprint of Elsevier Science

**©1994 664 pages**
**Hardbound**
**Price: Dfl. 700.00 (US$400.00)**
**ISBN 0-444-82110-4**

## ORDER INFORMATION

**ELSEVIER SCIENCE B.V.**
P.O. Box 330
1000 AH Amsterdam
The Netherlands
Fax: +31 (20) 485 2845

For USA and Canada:
P.O. Box 945, New York
NY 10159-0945
Fax: +1 (212) 633 3680

*US$ prices are valid only for the USA & Canada and are subject to exchange rate fluctuations; in all other countries the Dutch guilder price (Dfl.) is definitive. Customers in the European Union should add the appropriate VAT rate applicable in their country to the price(s). Books are sent postfree if prepaid.*

## PUBLICATION SCHEDULE FOR THE 1995 SUBSCRIPTION

*Journal of Chromatography A* and *Journal of Chromatography B: Biomedical Applications*

| MONTH | 1994 | J | F | M | |
|---|---|---|---|---|---|
| Journal of Chromatography A | Vols. 683–688 | 689/1<br>689/2<br>690/1<br>690/2 | 691/1 + 2<br>692/1 + 2<br>693/1<br>693/2 | 694/1<br>694/2 | The publication schedule for further issues will be published later. |
| Bibliography Section | | | | 713/1 | |
| Journal of Chromatography B: Biomedical Applications | | 663/1<br>663/2 | 664/1<br>664/2 | 665/1<br>665/2 | |

## INFORMATION FOR AUTHORS

(Detailed *Instructions to Authors* were published in *J. Chromatogr. A*, Vol. 657, pp. 463–469. A free reprint can be obtained by application to the publisher, Elsevier Science B.V., P.O. Box 330, 1000 AH Amsterdam, Netherlands.)

**Types of Contributions.** The following types of papers are published: Regular research papers (full-length papers), Review articles, Short Communications and Discussions. Short Communications are usually descriptions of short investigations, or they can report minor technical improvements of previously published procedures; they reflect the same quality of research as full-length papers, but should preferably not exceed five printed pages. Discussions (one or two pages) should explain, amplify, correct or otherwise comment substantively upon an article recently published in the journal. For Review articles, see inside front cover under Submission of Papers.

**Submission.** Every paper must be accompanied by a letter from the senior author, stating that he/she is submitting the paper for publication in the *Journal of Chromatography A* or *B*.

**Manuscripts.** Manuscripts should be typed in **double spacing** on consecutively numbered pages of uniform size. The manuscript should be preceded by a sheet of manuscript paper carrying the title of the paper and the name and full postal address of the person to whom the proofs are to be sent. As a rule, papers should be divided into sections, headed by a caption (*e.g.*, Abstract, Introduction, Experimental, Results, Discussion, etc.). All illustrations, photographs, tables, etc., should be on separate sheets.

**Abstract.** All articles should have an abstract of 50–100 words which clearly and briefly indicates what is new, different and significant. No references should be given.

**Introduction.** Every paper must have a concise introduction mentioning what has been done before on the topic described, and stating clearly what is new in the paper now submitted.

**Experimental conditions** should preferably be given on a *separate* sheet, headed "Conditions". These conditions will, if appropriate, be printed in a block, directly following the heading "Experimental".

**Illustrations.** The figures should be submitted in a form suitable for reproduction, drawn in Indian ink on drawing or tracing paper. Each illustration should have a caption, all the *captions* being typed (with double spacing) together on a *separate sheet*. If structures are given in the text, the original drawings should be provided. Coloured illustrations are reproduced at the author's expense, the cost being determined by the number of pages and by the number of colours needed. The written permission of the author and publisher must be obtained for the use of any figure already published. Its source must be indicated in the legend.

**References.** References should be numbered in the order in which they are cited in the text, and listed in numerical sequence on a separate sheet at the end of the article. Please check a recent issue for the layout of the reference list. Abbreviations for the titles of journals should follow the system used by *Chemical Abstracts*. Articles not yet published should be given as "in press" (journal should be specified), "submitted for publication" (journal should be specified), "in preparation" or "personal communication".

Vols. 1–651 of the *Journal of Chromatography*; *Journal of Chromatography, Biomedical Applications* and *Journal of Chromatography, Symposium Volumes* should be cited as *J. Chromatogr.* From Vol. 652 on, *Journal of Chromatography A* (incl. Symposium Volumes) should be cited as *J. Chromatogr. A* and *Journal of Chromatography B: Biomedical Applications* as *J. Chromatogr. B*.

**Dispatch. Before sending the manuscript to the Editor please check that the envelope contains four copies of the paper complete with references, captions and figures. One of the sets of figures must be the originals suitable for direct reproduction. Please also ensure that permission to publish has been obtained from your institute.**

**Proofs.** One set of proofs will be sent to the author to be carefully checked for printer's errors. Corrections must be restricted to instances in which the proof is at variance with the manuscript.

**Reprints.** Fifty reprints will be supplied free of charge. Additional reprints can be ordered by the authors. An order form containing price quotations will be sent to the authors together with the proofs of their article.

# *Ovomucoid Bonded Column for Direct Chiral Separation*

# ULTRON ES-OVM

**Narrow-Bore Column ( 2.0 I.D. x 150 mm ) for Trace Analyses**
**Analytical Column ( 4.6 I.D. , 6.0 I.D. x 150 mm ) for Regular Analyses**
**Semi-Preparative Column (20.0 I.D. x 250 mm ) for Preparative Separation**

***Analysis of Trace FLURBIPROFEN in Metabolite with NARROW-BORE COLUMN***

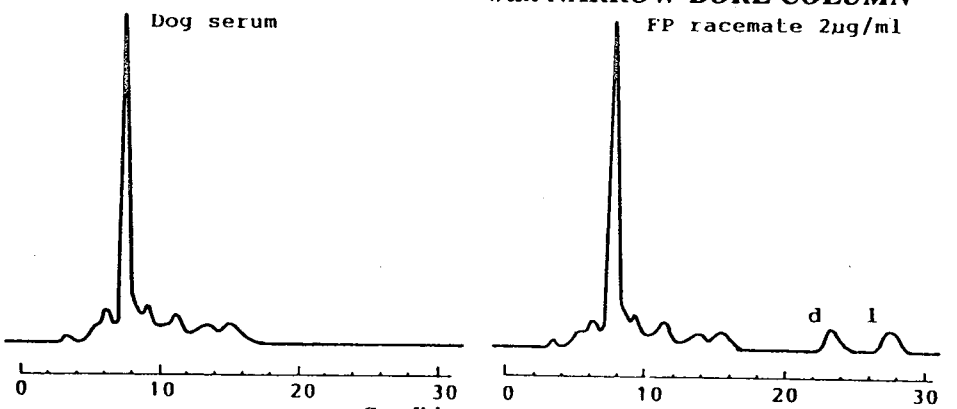


***Conditions***

Column: ULTRON ES-OVM(2.0I.D. x 150mm)
Mobile Phase: 20mMPhosphate Buffer(pH=3.0)/CH3CN =100/15
Flow Rate: 0.1ml/min
Temperature: 25°C
Injection: 5µl
Detection: UV- 247nm(0.05AUFS)

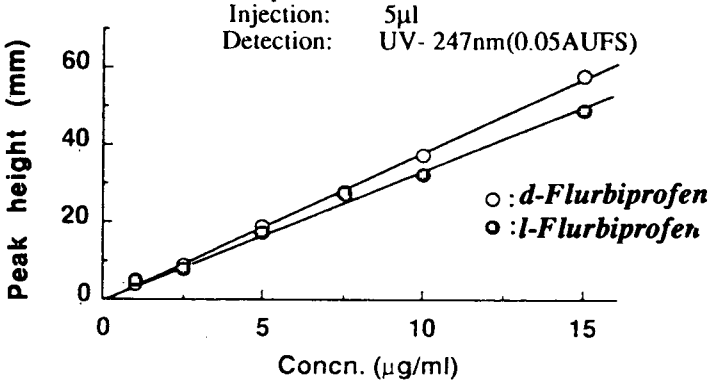


Calibration Curve for Each Enantiomer of Flurbiprofen


## SHINWA CHEMICAL INDUSTRIES, LTD.

**50 Kagekatsu-cho, Fushimi-ku, Kyoto 612, JAPAN**
**Phone:+81-75-621-2360 Fax:+81-75-602-2660**

**In the United States and Europe, please contact:**

## Rockland Technologies, Inc.

**538 First State Boulevard, Newport, DE 19804, U.S.A.**
**Phone: 302-633-5880 Fax: 302-633-5893**


**This product is licenced by Eisai Co., Ltd.**